EMERGING
INFECTIOUS DISEASES

EMERGING INFECTIOUS DISEASES

EDITOR-IN-CHIEF
D. Peter Drotman

EMERGING INFECTIOUS DISEASES®

Influenza October 2018

On the Cover

John Singer Sargent (1856–1925), *Interior of a Hospital Tent*, **1918** (detail). Watercolour over pencil on paper; 16 in × 21 in/39 cm × 53 cm. Imperial War Museums, © IWM ART 1611, Lambeth Road London SE1 6HZ

About the Cover p. 1968

L226Q
R140K
Receptor
S128N
A135V
A122P/T
K173E
K57R
E393K
N276D
I48T
E386A
V429I
A
L177I
M236I
E114K
V420M
Fusion peptide
D476N
S489R/N

1802

⊘DPDx

Diagnostic Assistance and Training in Laboratory Identification of Parasites

A free service of CDC available to laboratorians, pathologists, and other health professionals in the United States and abroad

Diagnosis from photographs of worms, histological sections, fecal, blood, and other specimen types

Expert diagnostic review

Formal diagnostic laboratory report

Submission of samples via secure file share

Visit the DPDx website for information on laboratory diagnosis, geographic distribution, clinical features, parasite life cycles, and training via Monthly Case Studies of parasitic diseases.

www.cdc.gov/dpdx
dpdx@cdc.gov

**U.S. Department of
Health and Human Services**
Centers for Disease
Control and Prevention

CS272346-DE

Human Pegivirus in Patients with Encephalitis of Unclear Etiology, Poland

Iwona Bukowska-Ośko, Karol Perlejewski, Agnieszka Pawełczyk, Małgorzata Rydzanicz,
Agnieszka Pollak, Marta Popiel, Kamila Caraballo Cortés, Marcin Paciorek, Andrzej Horban,
Tomasz Dzieciątkowski, Marek Radkowski, Tomasz Laskus

Medscape EDUCATION ACTIVITY

In support of improving patient care, this activity has been planned and implemented by Medscape, LLC and Emerging Infectious Diseases. Medscape, LLC is jointly accredited by the Accreditation Council for Continuing Medical Education (ACCME), the Accreditation Council for Pharmacy Education (ACPE), and the American Nurses Credentialing Center (ANCC), to provide continuing education for the healthcare team.

Medscape, LLC designates this Journal-based CME activity for a maximum of 1.00 ***AMA PRA Category 1 Credit(s)*™**. Physicians should claim only the credit commensurate with the extent of their participation in the activity.

All other clinicians completing this activity will be issued a certificate of participation. To participate in this journal CME activity: (1) review the learning objectives and author disclosures; (2) study the education content; (3) take the post-test with a 75% minimum passing score and complete the evaluation at http://www.medscape.org/journal/eid; and (4) view/print certificate. For CME questions, see page 1971.

Release date: September 14, 2018; Expiration date: September 14, 2019

Learning Objectives

Upon completion of this activity, participants will be able to:

- Describe evidence for human pegivirus (HPgV) infection in the central nervous system (CNS) among patients with encephalitis of unclear etiology, according to a case series
- Compare HPgV sequences in cerebrospinal fluid with those circulating in serum, according to a case series
- Determine clinical implications of evidence for HPgV infection in the CNS among patients with encephalitis of unclear etiology, according to a case series

CME Editor

Dana C. Dolan, BS, Copyeditor, Emerging Infectious Diseases. *Disclosure: Dana C. Dolan, BS, has disclosed no relevant financial relationships.*

CME Author

Laurie Barclay, MD, freelance writer and reviewer, Medscape, LLC. *Disclosure: Laurie Barclay, MD, has disclosed the following relevant financial relationships: owns stock, stock options, or bonds from Pfizer.*

Authors

Disclosures: ***Iwona Bukowska-Ośko, PhD; Karol Perlejewski, PhD; Agnieszka Pawełczyk, PhD; Małgorzata Rydzanicz, PhD; Agnieszka Pollak, PhD; Marta Popiel, PhD; Kamila Caraballo Cortés, PhD; Marcin Paciorek, PhD; Andrzej Horban, MD, PhD; Tomasz Dzieciątkowski, PhD; Marek Radkowski, MD, PhD;*** *and* ***Tomasz Laskus, MD, PhD,*** *have disclosed no relevant financial relationships.*

Human pegivirus (HPgV), previously called hepatitis G virus or GB virus C, is a lymphotropic virus with undefined pathology. Because many viruses from the family Flaviviridae, to which HPgV belongs, are neurotropic, we studied whether HPgV could infect the central nervous system. We tested serum and cerebrospinal fluid samples from 96 patients with a diagnosis of encephalitis for a variety of

pathogens by molecular methods and serology; we also tested for autoantibodies against neuronal antigens. We found HPgV in serum and cerebrospinal fluid from 3 patients who had encephalitis of unclear origin; that is, all the markers that had been tested were negative. Single-strand confirmation polymorphism and next-generation sequencing analysis revealed differences between the serum and cerebrospinal fluid–derived viral sequences, which is compatible with the presence of a separate HPgV compartment in the central nervous system. It is unclear whether HPgV was directly responsible for encephalitis in these patients.

Human pegivirus (HPgV) was originally described as a hepatitis virus by 2 independent groups of researchers and called GB virus C and hepatitis G virus (*1,2*). Whereas the infection was found to be common in patients with forms of chronic hepatitis, and particularly prevalent in patients with chronic hepatitis C infection, it is not associated with liver injury in the absence of concomitant infection with hepatitis C virus (HCV) or hepatitis B virus (HBV). Furthermore, the liver is not the primary replication site for this virus (*3,4*). This virus was recently renamed as pegivirus and assigned to a new genus (*Pegivirus*) within the family Flaviviridae (*5*).

Infection with HPgV is common worldwide; ≈5% of healthy blood donors in industrialized countries are viremic, whereas in some developing countries the prevalence of viremia among blood donors is ≈20% (*6*). There is evidence that HPgV is transmitted parenterally, sexually, and also vertically from mother to child (*7*). However, the high proportion of HPgV infection in apparently healthy blood donors and the general population suggests existence of nonparenteral routes. The reasons for the high prevalence of infection in developing countries are not entirely clear but could be related to overall poor hygienic conditions, as well as to the time of exposure. In sub-Saharan Africa, where HPgV is particularly common, this virus is transmitted mainly during childhood, which may facilitate the establishment of chronic infection (*7*). Because no association between HPgV and disease has been consistently identified, blood donors are not routinely screened for the virus.

Interest in the HPgV infection was revived when several studies identified its beneficial effect on the survival of HIV-infected persons (*8,9*); anti-HIV replication effects of HPgV were confirmed in vitro (*8*). Several in vivo and in vitro studies suggest that HPgV may directly interfere with HIV replication and affect host cell factors necessary for the HIV life cycle; specific mechanisms include modulation of cytokine and chemokine release and receptor expressions and lowering of T-cell activation and proliferation (*9*). However, infection with HPgV may not be totally benign; some studies found an association between infection and non-Hodgkin lymphoma (*10,11*), which could be the result of lowered immune activation.

Many viruses from the family Flaviviridae, most prominently arthropodborne viruses (arboviruses) such as West Nile virus (WNV) and tick-borne encephalitis virus (TBEV), are neurotropic and a prominent cause of encephalitis in Europe and North America (*12*). These factors raise the question whether HPgV could be neurotropic and whether it could be an etiologic agent in neuroinfections. Of note, despite substantial progress in diagnostics, the etiology of encephalitis remains unclear in 40%–80% of patients (*13,14*). A plethora of pathogens may cause encephalitis; many of these pathogens are rare and thus testing is not performed to identify them, and others have not yet been identified.

Three recent case reports described HPgV RNA in the human central nervous system (CNS), demonstrating that the virus can be present in the brain under certain circumstances (*15–17*). In the first study, viral sequences were detected postmortem in brain tissue from a patient with multiple sclerosis, not encephalitis (*15*). In the second study, the presence of HPgV might have been related to a severely compromised blood–brain barrier; the patient was HIV-positive and had cerebral toxoplasmosis and fungal encephalitis (*16*). Although the full-length virus was recovered from the patient's brain tissue, it is unclear which cells harbored the virus and it was possible that the actual source was blood. Furthermore, the association of HPgV with multiple sclerosis could not be established because the study was limited to a single case. In the third study, HPgV was detected in serum and CSF of a patient with a severe form of encephalitis of unclear origin (*17*). Of these 3 studies, none included comparison of serum- and CNS-derived virus. We conducted a study of 96 consecutive patients with diagnosis of encephalitis (*18*) in Poland during 2012–2015 to determine whether HPgV could be found in the CNS.

Materials and Methods

Patients and Routine Diagnostics

We prospectively enrolled patients with encephalitis at the Warsaw Hospital for Infectious Diseases (Warsaw, Poland) from June 2012 through July 2015. The details of this study were published previously (*18*). We defined encephalitis as an acute-onset illness with altered mental status, decreased level of consciousness, seizures, or focal neurologic signs, together with ≥1 abnormality of the CSF (leukocyte count ≥4 cells/mm^2 or protein level ≥40 mg/dL). We obtained written informed consent from all patients or from close relatives of patients unable to give

consent due to their condition. The Internal Review Board of the Medical University of Warsaw approved the study.

We collected CSF and serum samples from patients at admission (5–7 days after symptom onset) and kept them frozen at -80°C until analysis. We tested the samples from all 96 patients for the presence of 5′ untranslated region (UTR) HPgV RNA. We performed real-time quantitative PCR (qPCR) or real-time quantitative reverse transcription PCR (qRT-PCR) to detect human herpesvirus (HHV) 1 and 2, varicella zoster virus (VZV), cytomegalovirus (CMV), HHV-6, enteroviruses (coxsackievirus A9, A16, B2, B3, B4, B5; echovirus 5, 6, 9, 11, 18, 30; and enterovirus 71), TBEV, WNV, and human adenovirus (HAdV) in CSF samples. We used commercial serologic tests to test CSF and paired serum samples for HHV-1, HHV-2, VZV, TBEV, and WNV as described (18). We detected autoantibodies against neuronal surface antigens using the Autoimmune Encephalitis Mosaic 6 assay (Euroimmun AG, Luebeck, Germany).

HPgV 5′ UTR and E2 Amplification

We extracted total RNA with TRIzol LS (ThermoFisher Scientific, Waltham, MA, USA) from 400 µL of CSF or serum and suspended RNA in 20 µL of water, 5 µL of which was subsequently used for each amplification reaction. We amplified the HPgV 5′ UTR by nested reverse transcription PCR (RT-PCR) as described previously (19), resulting in 421 bp-length product; we amplified the E2 region following the RT-PCR protocol published by Smith et al. (20). The final product was 422 bp in length.

Single-Strand Conformation Polymorphism

We subjected the amplified PCR products to single-strand conformational polymorphism analysis, as described previously (21). In brief, we purified HPgV 5′ UTR and HPgV-E2 PCR products by using the Wizard PCR Preps DNA Purification System (Promega, Madison, WI, USA). We then subjected the products to thermal denaturation, ran them on nondenaturing 1% polyacrylamide gels at 400V in 25°C, fixed them with acetic acid, and stained them with silver stain.

Next-Generation Sequencing

We reamplified RT-PCR products with primers specifically designed for the Illumina MiSeq platform (Illumina, San Diego, CA, USA). Each primer contained the following: sequences complementary to the adapters on a flow cell; an 8-nt index sequence; sequences corresponding to the Illumina sequencing primers; and sequence-specific nested primers for the 5′ UTR and E2 region. Amplification of the 5′ UTR region included initial denaturation at 94°C for 5 min, 20 cycles of 94°C for 1 min, 58°C for 1 min, 72°C for 1 min, and final elongation at 72°C for 10 min. HPgV E2 amplification included denaturation at 94°C for 5 min followed by 20 cycles of 94°C for 18 s, 55°C for 20 s, 72°C for 90 s, and 1 cycle at 72°C for 10 min. We trimmed the libraries by using the LabChip XT apparatus (PerkinElmer, Waltham, Massachusetts, USA) with the DNA 300 Assay Kit (PerkinElmer); the range of fraction collection was 370–430 bp for 5′ UTR and 460–530 bp for E2.

We assessed the quality and average length of next-generation sequencing libraries by using Bioanalyzer (Agilent Technologies, Santa Clara, CA, USA). We equimolarly pooled the indexed samples and sequenced them on Illumina MiSeq with 301 bp-end reads according to the manufacturer's protocol.

Data Analysis

We trimmed raw reads using cutadapt version 1.2.1 (https://github.com/marcelm/cutadapt/); (22), then used FASTX-Toolkit (http://hannonlab.cshl.edu/fastx_toolkit/index.html) for additional processing. We removed all Phred quality score reads <20 using FASTQ/A Artifacts Filter and preprocessed the remaining reads (grouping, counting, and frequency arrangement) using R scripts (23). To diminish the contribution of false positive variants to genetic diversity, we applied the experimentally established sequencing error cutoff of 1.22%. Finally, we aligned remaining sequences and generated phylogenic trees with ClustalX version 2.0 (http://www.clustal.org/clustal2/) (24). We assessed nucleotide diversity per site and the number of substitutions with respect to the dominant serum sequence in each patient using DnaSP version 6.11.06 (25). We predicted the RNA secondary structures of the 5′ UTR using Mfold version 3.2 (http://unafold.rna.albany.edu/?q=mfold) (26), and searched for putative B cell epitopes within the E2 region using BepiPred-2.0 (http://www.cbs.dtu.dk/services/BepiPred/) (27).

Results

Four patients were positive for 5′ UTR HPgV RNA in serum, and 3 of these patients were also positive in CSF. We analyzed the samples from those 3 patients; their samples were collected at admission, which was 5–7 days after symptom onset. We diagnosed encephalitis of unclear origin for all 3 patients because they were negative for all the pathogens tested (Table 1). The small number of HPgV-infected patients did not allow for statistical analysis, but these patients were not strikingly different from other encephalitis patients. We initially suspected 1 patient, who had a severe illness with prolonged hospitalization, of having HHV infection, but tests did not confirm HHV. All 3 patients recovered without any neurologic sequelae.

We compared serum- and CSF-derived 5′ UTR and E2 amplicons from the 3 patients by single-strand conformational polymorphism analysis (Figure 1). Because this

Table 1. Comparison of clinical characteristics of 3 encephalitis patients infected with human pegivirus compared with patients with other forms of encephalitis, Poland, 2012–2015*

Characteristic	Encephalitis patients infected with pegivirus			Other encephalitis patients	
	Patient 1	Patient 2	Patient 3	Infectious cause identified, n = 41†	Unknown cause or autoimmune illness, n = 52‡
Male sex	No	No	Yes	30 (73)	23 (44)
Median age, y (range)	55	28	20	38 (19–85)	38 (20–82)
Pharmacological immunosuppression present	0	0	0	2 (5)	3 (6)
HIV positive	0	0	0	0	2 (4)
Cancer	0	0	0	6 (15)	1 (2)
Median length of hospital stay, d (range)	41	30	8	12 (5–97)	11.5 (6–79)
Fever >38°C	Yes	Yes	No	26 (63)	18 (35)
Headache	Yes	Yes	No	22 (54)	25 (48)
Altered mental status	Yes	Yes	No	36 (88)	47 (85)
Focal neurologic signs	No	No	Yes	9 (22)	10 (20)
Seizures	No	No	Yes	12 (29)	16 (31)
Stiff neck	No	No	No	7 (17)	12 (23)
CSF analysis					
Median leukocyte count, cells/mm² (range)	3	4	3	41 (1–1225)	18 (1–362)
Median protein level, g/L (range)	0.68	0.26	1.63	0.57 (0.16–3.21)	0.56 (0.11–3.33)
Death	0	0	0	1 (2.4)	0

*Values are no. (%) unless otherwise indicated. CSF, cerebrospinal fluid
†Identified infections were human herpesvirus 1 (n = 22), enterovirus (n = 6), varicella zoster virus (n = 5), tick-borne encephalitis virus (n = 6), and cytomegalovirus (n = 2).
‡All markers of viral infection were negative, but 5 patients had antibodies against N-methyl-D-aspartate receptor and a diagnosis of autoimmune encephalitis.

analysis suggested the presence of differences between the serum- and CSF-derived viral sequences in individual patients, we subjected all amplicons to next-generation sequencing. After filtering, the mean number of reads per sample was 70,759 (range 2,706–183,046) (Table 2).

When we compared 5′ UTR and E2 sequences phylogenetically, we found that serum- and CSF-derived sequences clustered together in individual patients; no sequence was found in multiple patients (Figure 2). Of note, we found several variants to be unique in the CSF compartment. These sequences comprised 2.28%–29.32% of all variants for 5′ UTR and 0%–41.78% of all variants for E2 (Table 2; Figure 3). Unique CSF-derived sequences were also present when we analyzed the E2 region on the amino acid level (Figure 4). The changes were serine to phenylalanine at aa position 508 in patient 2 and proline to leucine at position 572 in patient 3. Both changes were within the predicted B cell epitopes (aa 506–522 and 559–572).

We analyzed all 5′ UTR sequence variants to determine the predicted stability of their secondary RNA structure. We deemed the effect of variations minor because most were localized in the nonbasepaired parts (data not shown), and free energies of the hypothetical secondary structures were only occasionally and mildly affected (online Technical Appendix Figure, https://wwwnc.cdc.gov/EID/article/24/10/18-0161-Techapp1.pdf) (28).

Discussion

We detected HPgV sequences in CSF from 3/96 patients with encephalitis. We classified all 3 cases as encephalitis
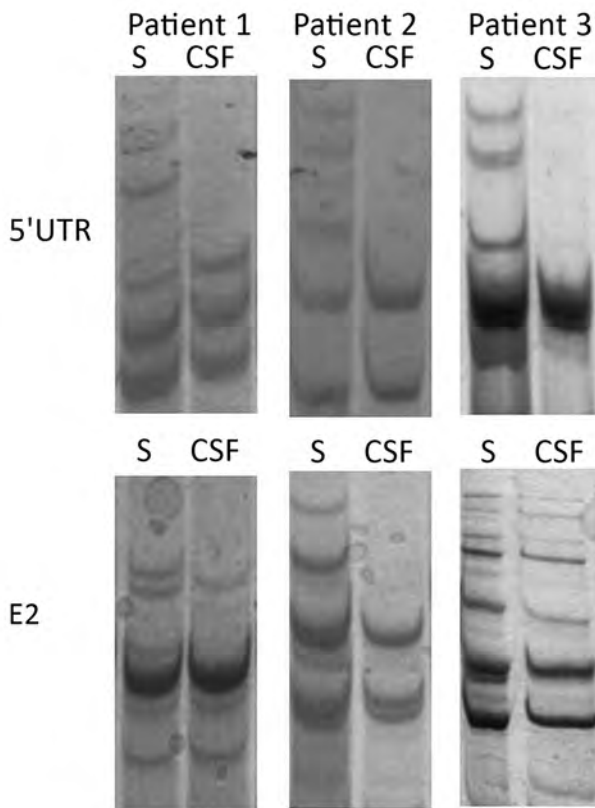
Figure 1. Single-strand conformation polymorphism analysis of 5′ UTR and E2 region human pegivirus amplicons from 3 patients with encephalitis of unclear origin, Poland, 2012–2015. CSF, cerebrospinal fluid; S, serum; UTR, untranslated region.

Table 2. 5 Human pegivirus variants in serum and cerebrospinal fluid in 3 patients with encephalitis of unknown origin, Poland, 2012–2015*

	Patient 1		Patient 2		Patient 3	
RNA region	Serum	CSF	Serum	CSF	Serum	CSF
5′ untranslated region						
No. reads before error cutoff	124,987	110,331	108,002	183,046	101,240	145,411
No. reads after error cutoff	61,783	57,668	49,075	109,061	55,328	75,998
No. nucleotide variants†	3	7	3	3	2	3
No. unique nucleotide variants in CSF†	–	5 (29.32)	–	1 (2.28)	–	1 (2.49)
No. nucleotide substitutions	2	7	2	2	1	2
Nucleotide diversity per site	0.004	0.007	0.004	0.004	0.003	0.004
E2 region						
No. reads before error cutoff	70,460	38,025	77,656	76,918	2,706	82,738
No. reads after error cutoff	26,720	20,619	26,558	42,609	453	34,887
No. nucleotide variants†	8	4	8	9	4	7
No. unique nucleotide variants in CSF†	–	0	–	5 (41.78)	–	3 (27.28)
No. nucleotide substitutions	4	2	5	5	2	3
Nucleotide diversity per site	0.007	0.004	0.006	0.007	0.004	0.005
No. amino acid variants†	2	2	2	5	2	4
No. unique amino acid variants in CSF†	–	0	–	3 (27.28)	–	2 (27.28)

*Numbers in parentheses are percentages. CSF, cerebrospinal fluid
†After applying the 1.22% sequencing error cutoff.

of unknown origin because they were negative for serologic and molecular markers of common CNS pathogens. Furthermore, we demonstrated that these viral sequences differed from those circulating in serum. The presence of viral RNA in CSF could be due to a compromised blood–brain barrier, which was possible in these patients with encephalitis. However, the presence of differences in circulating and CSF-derived sequences is more compatible with the existence of separate viral compartments and thus independent replication. Similar compartmentalization in which distinct blood and CNS viral populations indicate separately evolving populations has been described for other viruses, most prominently for HIV (*29*) but also for HCV (*30,31*) and human BK polyomavirus (*32*).
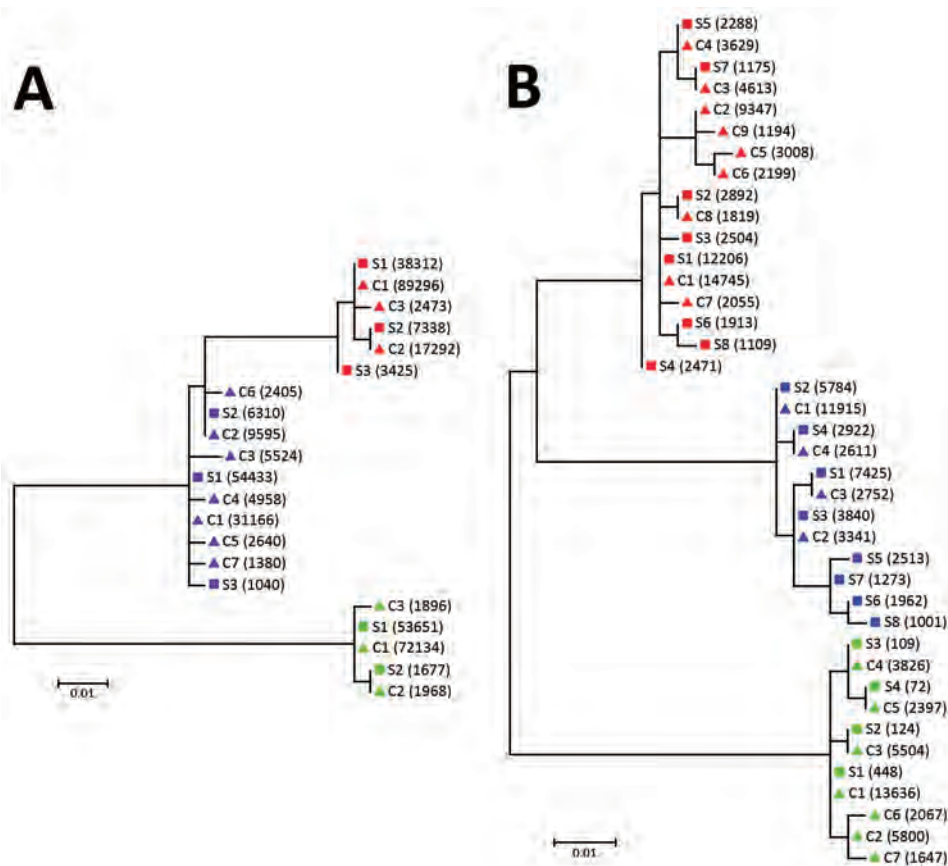
Figure 2. Phylogenetic analysis of A) 5′ UTR and B) E2 region sequences of human pegivirus from 3 patients with encephalitis of unclear origin, Poland, 2012–2015. Phylogenic trees were generated using ClustalX version 2.0 (http://www.clustal.org/clustal2/). Viral variant frequencies follow haplotype number. Red indicates patient 1; blue, patient 2; green, patient 3. Scale bars indicate number of nucleotide substitutions per site. C, cerebrospinal fluid; S, serum; UTR, untranslated region.
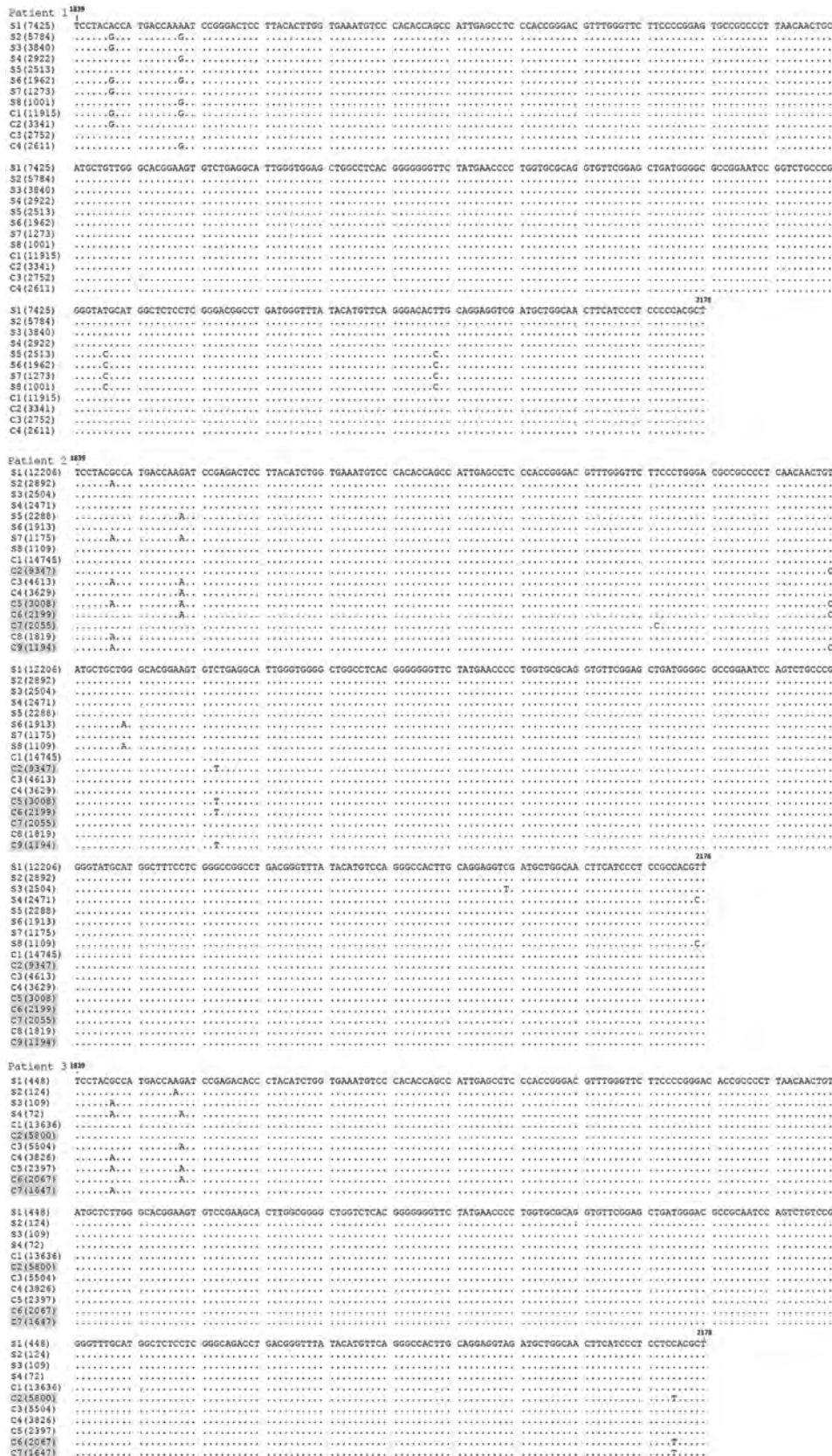
Figure 3. Comparison of E2 region human pegivirus sequences amplified from serum and cerebrospinal fluid from 3 patients with encephalitis of unclear origin, Poland, 2012–2015. Numbers in parentheses represent the number of reads representing a given sequence. Shading indicates sequences unique to cerebrospinal fluid. Nucleotide numbering follows the reference strain published by Linnen et al (2) (GenBank accession no. NC_001710.1). C, cerebrospinal fluid; S, serum.
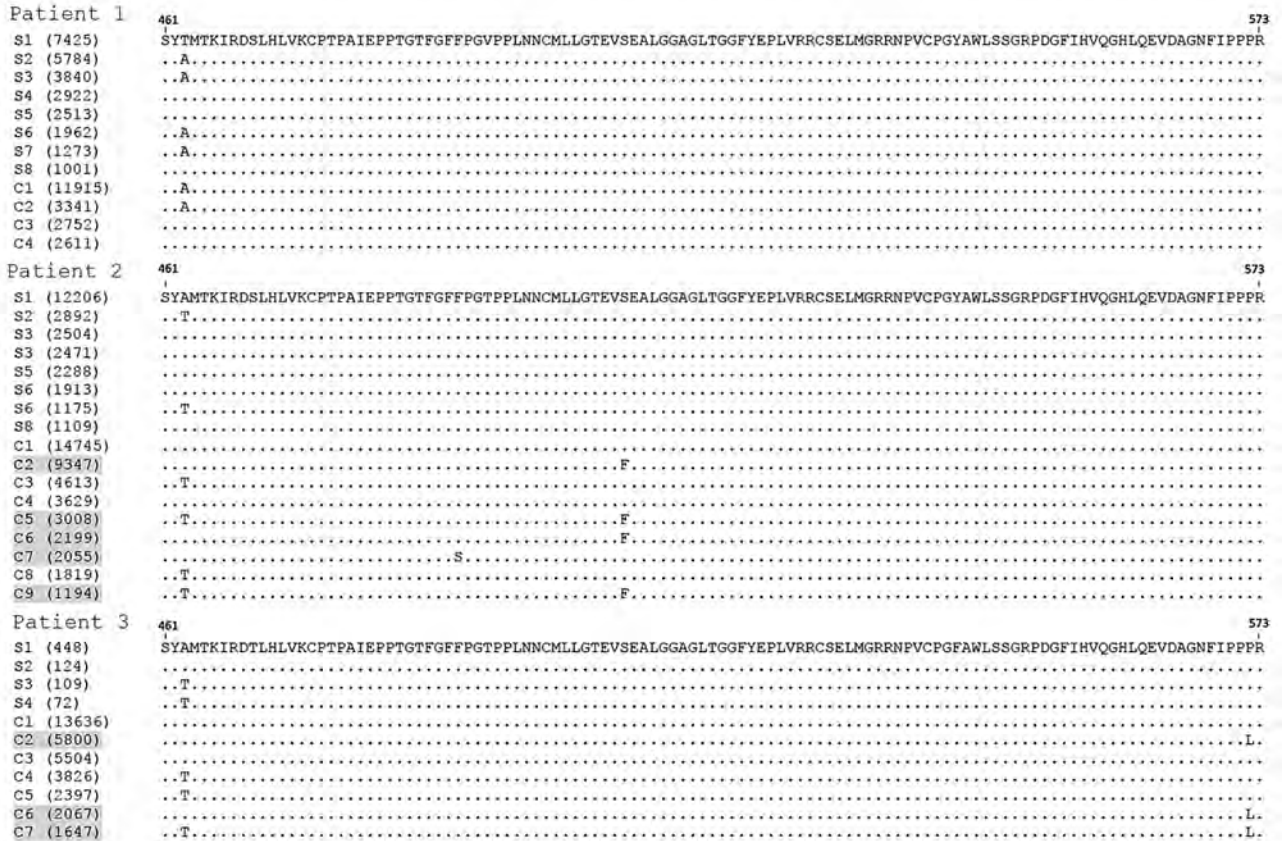
Figure 4. Comparison of amino acid composition of E2 region human pegivirus sequence variants amplified from serum and cerebrospinal fluid from 3 patients with encephalitis of unclear origin, Poland, 2012–2015. Numbers in parentheses represent the number of reads representing a given sequence. Shading indicates sequences unique to cerebrospinal fluid. C, cerebrospinal fluid; S, serum.

It is unclear how HPgV could access the CNS. Although initially HPgV was thought to be a hepatotropic virus, the viral negative strand, which is the putative replicative intermediate of the virus, was not detected in liver tissue (*3*); however, it was found in bone marrow and spleen (*33,34*). The virus is now considered lymphotropic because it can be detected at a low level in multiple lineages of peripheral leukocytes (*35,36*), and it has been speculated that the primary target could be a progenitor hematopoietic stem cell. The route for CNS access could be through infected leukocytes; all basic groups (T cells, B cells, macrophage/monocytes, and NK cells) have the ability to enter the brain under certain conditions (*37*). Certain monocyte family members are constantly replaced as part of normal physiology (*38,39*), while the entry of T cells and B cells depends largely on their activation state (*40,41*). Such a phenomenon related to trafficking of infected leukocytes through the blood–brain barrier has been long postulated for HIV-1 neuroinfection (*42*).

Whether HPgV was the causative factor of encephalitis in the patients we describe is not clear. Viral pathogens are typically present only transiently in CSF and this window could be easily missed, particularly when the spinal tap is done too late in the course of illness (*43*). If HPgV encephalitis exists, it could be a rare phenomenon. In a previous study of 17 encephalitis and aseptic meningitis cases of unknown cause, no CSF sample was positive (*44*). However, even infections with well-known neurotropic agents from the Flaviviridae family, such as WNV or TBEV, are usually subclinical or asymptomatic; clinical signs and symptoms develop only in 5%–30% of cases (*45,46*). Of note, in 2 of the cases we describe, the encephalitis was mild, and all 3 patients recovered without any neurologic sequelae. Obviously, the mere presence of a pathogen in the CNS in patients with encephalitis does not prove causality; for example, HCV sequences are commonly detected in brain and CSF of infected patients without any accompanying evidence of encephalitis (*29*). In our study, we detected HPgV sequences in CSF only in patients without an obvious cause of encephalitis and in none of the patients in whom a known pathogen was identified.

The identified 5′ UTR and E2 region sequence differences between CSF and serum compartments could have biological meaning. The 5′ UTR contains an internal ribosomal entry site that allows cap-independent viral translation (*28*). Such structures were identified within the 5′ UTR of the picornaviruses and were shown to interact with cellular proteins, thus affecting the host range of individual viruses (*47*). Research has also shown that, for HCV, translation efficiencies of brain-derived internal ribosomal entry site variants are generally lower than those found in serum, which could be a viral strategy favoring latency in the CNS (*31*). Taking this into consideration, we speculated that at least some of the 5′ UTR changes in the patients we report represent tissue-specific adjustment. Viral adaptive changes could be relatively small and yet make a huge difference; for example, it has been demonstrated for lymphocytic choriomeningitis virus in mice that variants differing by a single amino acid substitution are competitively selected either by the liver and spleen or by neurons (*48*).

On the amino acid level, we saw 2 unique E2 region changes in CSF variants compared with serum: in patient 2, serine was changed to phenylalanine at aa position 508, and in patient 3, proline was changed to leucine at position 572. Both were within regions predicted to contain B-cell epitopes, thus suggesting that they were the effect of immune pressure. Furthermore, the change in patient 3 was located in the region of E2 that was experimentally shown to contain a strong antigenic site and likely to be involved in cell binding or fusion (*49*).

RNA viruses in particular are characterized by a high degree of genetic heterogeneity; probably because the lack of proofreading 3′ 5′ exonuclease activity in viral RNA polymerases causes low fidelity. As a result, viruses circulate in the infected host as a population of closely related but nonidentical genomes, referred to as quasispecies (*50*). It is unclear whether the observed high HPgV variability developed in the patients we describe de novo after infection or if most or all variants were transmitted from the infecting host; both mechanisms could occur together. However, because viral transmission is typically accompanied by narrowing of the quasispecies spectrum (known as the bottleneck phenomenon), some extent of postinfection evolution is highly likely.

In summary, we detected HPgV sequences in the CSF of 3 patients with encephalitis of unclear origin, and these sequences from CSF differed from those circulating in serum. These findings are compatible with the presence of a separate viral compartment in the CNS. Determining if the pegivirus was responsible for encephalitis or if it was present along with another cause of encephalitis will require further research, including histopathological analysis.

About the Author

Dr. Bukowska-Ośko is a scientist in the Department of Immunopathology of Infectious and Parasitic Diseases at Medical University of Warsaw, Poland. Her primary research interests include molecular pathogenesis of hepatitis C, application of metagenomics in diagnostics of infectious diseases and brain infections.

References

1. Simons JN, Leary TP, Dawson GJ, Pilot-Matias TJ, Muerhoff AS, Schlauder GG, et al. Isolation of novel virus-like sequences associated with human hepatitis. Nat Med. 1995;1:564–9. http://dx.doi.org/10.1038/nm0695-564
2. Linnen J, Wages J Jr, Zhang-Keck ZY, Fry KE, Krawczynski KZ, Alter H, et al. Molecular cloning and disease association of hepatitis G virus: a transfusion-transmissible agent. Science. 1996;271:505–8. http://dx.doi.org/10.1126/science.271.5248.505
3. Laskus T, Radkowski M, Wang LF, Vargas H, Rakela J. Lack of evidence for hepatitis G virus replication in the livers of patients coinfected with hepatitis C and G viruses. J Virol. 1997; 71:7804–6.
4. Pessoa MG, Terrault NA, Detmer J, Kolberg J, Collins M, Hassoba HM, et al. Quantitation of hepatitis G and C viruses in the liver: evidence that hepatitis G virus is not hepatotropic. Hepatology. 1998;27:877–80. https://dx.doi.org/10.1002/hep.510270335
5. Adams MJ, King AM, Carstens EB. Ratification vote on taxonomic proposals to the International Committee on Taxonomy of Viruses (2013). Arch Virol. 2013;158:2023–30. http://dx.doi.org/10.1007/s00705-013-1688-5
6. Mohr EL, Stapleton JT. GB virus type C interactions with HIV: the role of envelope glycoproteins. J Viral Hepat. 2009;16:757–68. http://dx.doi.org/10.1111/j.1365-2893.2009.01194.x
7. Mphahlele MJ, Lau GK, Carman WF. HGV: the identification, biology and prevalence of an orphan virus. Liver. 1998;18:143–55. http://dx.doi.org/10.1111/j.1600-0676.1998.tb00142.x
8. Xiang J, Wünschmann S, Diekema DJ, Klinzman D, Patrick KD, George SL, et al. Effect of coinfection with GB virus C on survival among patients with HIV infection. N Engl J Med. 2001;345: 707–14. http://dx.doi.org/10.1056/NEJMoa003364
9. Bhattarai N, Stapleton JT. GB virus C: the good boy virus? Trends Microbiol. 2012;20:124–30. http://dx.doi.org/10.1016/j.tim.2012.01.004
10. Nakamura S, Takagi T, Matsuda T. Hepatitis G virus RNA in patients with B-cell non-Hodgkin's lymphoma. Br J Haematol. 1997;98:1051–2.
11. Krajden M, Yu A, Braybrook H, Lai AS, Mak A, Chow R, et al. GBV-C/hepatitis G virus infection and non-Hodgkin lymphoma: a case control study. Int J Cancer. 2010;126:2885–92.
12. Leyssen P, De Clercq E, Neyts J. Perspectives for the treatment of infections with Flaviviridae. Clin Microbiol Rev. 2000;13:67–82. http://dx.doi.org/10.1128/CMR.13.1.67-82.2000
13. Granerod J, Crowcroft NS. The epidemiology of acute encephalitis. Neuropsychol Rehabil. 2007;17:406–28. http://dx.doi.org/10.1080/09602010600989620
14. Granerod J, Tam CC, Crowcroft NS, Davies NW, Borchert M, Thomas SL. Challenge of the unknown. A systematic review of acute encephalitis in non-outbreak situations. Neurology. 2010; 75:924–32. http://dx.doi.org/10.1212/WNL.0b013e3181f11d65

15. Kriesel JD, Hobbs MR, Jones BB, Milash B, Nagra RM, Fischer KF. Deep sequencing for the detection of virus-like sequences in the brains of patients with multiple sclerosis: detection of GBV-C in human brain. PLoS One. 2012;7:e31886. http://dx.doi.org/10.1371/journal.pone.0031886

16. Liu Z, Zhang Y, Wei F, Xu M, Mou D, Zhang T, et al. Detection of GB virus C genomic sequence in the cerebrospinal fluid of a HIV-infected patient in China: a case report and literature review. Epidemiol Infect. 2016;144:106–12. http://dx.doi.org/10.1017/S0950268815001326

17. Fridholm H, Østergaard Sørensen L, Rosenstierne MW, Nielsen H, Sellebjerg F, Bengård Andersen Å, et al. Human pegivirus detected in a patient with severe encephalitis using a metagenomic pan-virus array. J Clin Virol. 2016;77:5–8. http://dx.doi.org/10.1016/j.jcv.2016.01.013

18. Popiel M, Perlejewski K, Bednarska A, Dzieciątkowski T, Paciorek M, Lipowski D, et al. Viral etiologies in adult patients with encephalitis in Poland: a prospective single center study. PLoS One. 2017;12:e0178481. http://dx.doi.org/10.1371/journal.pone.0178481

19. Laskus T, Radkowski M, Wang LF, Vargas H, Rakela J. Detection of hepatitis G virus replication sites by using highly strand-specific Tth-based reverse transcriptase PCR. J Virol. 1998;72:3072–5.

20. Smith DB, Basaras M, Frost S, Haydon D, Cuceanu N, Prescott L, et al. Phylogenetic analysis of GBV-C/hepatitis G virus. J Gen Virol. 2000;81:769–80. http://dx.doi.org/10.1099/0022-1317-81-3-769

21. Laskus T, Wilkinson J, Gallegos-Orozco JF, Radkowski M, Adair DM, Nowicki M, et al. Analysis of hepatitis C virus quasispecies transmission and evolution in patients infected through blood transfusion. Gastroenterology. 2004;127:764–76. http://dx.doi.org/10.1053/j.gastro.2004.06.005

22. Martin M. Cutadapt removes adapter sequences from high-throughput sequencing reads. EMBnet. 2011;17:10–2 2011. https://dx.doi.org/10.14806/ej.17.1.200

23. Hannon Laboratory. FastX Toolkit. 2015 [cited 2018 Jul 30]. http://hannonlab.cshl.edu/fastx_toolkit/index.html

24. Larkin MA, Blackshields G, Brown NP, Chenna R, McGettigan PA, McWilliam H, et al. Clustal W and Clustal X version 2.0. Bioinformatics. 2007;23:2947–8. http://dx.doi.org/10.1093/bioinformatics/btm404

25. Rozas J, Ferrer-Mata A, Sánchez-DelBarrio JC, Guirao-Rico S, Librado P, Ramos-Onsins SE, et al. DnaSP 6: DNA sequence polymorphism analysis of large data sets. Mol Biol Evol. 2017;34:3299–302. http://dx.doi.org/10.1093/molbev/msx248

26. Zuker M. Mfold web server for nucleic acid folding and hybridization prediction. Nucleic Acids Res. 2003;31:3406–15. http://dx.doi.org/10.1093/nar/gkg595

27. Jespersen MC, Peters B, Nielsen M, Marcatili P. BepiPred-2.0: improving sequence-based B-cell epitope prediction using conformational epitopes. Nucleic Acids Res. 2017;45(W1):W24–9. http://dx.doi.org/10.1093/nar/gkx346

28. Simons JN, Desai SM, Schultz DE, Lemon SM, Mushahwar IK. Translation initiation in GB viruses A and C: evidence for internal ribosome entry and implications for genome organization. J Virol. 1996;70:6126–35.

29. Bednar MM, Sturdevant CB, Tompkins LA, Arrildt KT, Dukhovlinova E, Kincer LP, et al. Compartmentalization, viral evolution, and viral latency of HIV in the CNS. Curr HIV/AIDS Rep. 2015;12:262–71. http://dx.doi.org/10.1007/s11904-015-0265-9

30. Radkowski M, Wilkinson J, Nowicki M, Adair D, Vargas H, Ingui C, et al. Search for hepatitis C virus negative-strand RNA sequences and analysis of viral sequences in the central nervous system: evidence of replication. J Virol. 2002;76:600–8. http://dx.doi.org/10.1128/JVI.76.2.600-608.2002

31. Forton DM, Karayiannis P, Mahmud N, Taylor-Robinson SD, Thomas HC. Identification of unique hepatitis C virus quasispecies in the central nervous system and comparative analysis of internal translational efficiency of brain, liver, and serum variants. J Virol. 2004;78:5170–83. http://dx.doi.org/10.1128/JVI.78.10.5170-5183.2004

32. Jørgensen GE, Hammarin AL, Bratt G, Grandien M, Flaegstad T, Johnsen JI. Identification of a unique BK virus variant in the CNS of a patient with AIDS. J Med Virol. 2003;70:14–9. http://dx.doi.org/10.1002/jmv.10370

33. Radkowski M, Kubicka J, Kisiel E, Cianciara J, Nowicki M, Rakela J, et al. Detection of active hepatitis C virus and hepatitis G virus/GB virus C replication in bone marrow in human subjects. Blood. 2000;95:3986–9.

34. Tucker TJ, Smuts HE, Eedes C, Knobel GD, Eickhaus P, Robson SC, et al. Evidence that the GBV-C/hepatitis G virus is primarily a lymphotropic virus. J Med Virol. 2000;61:52–8. http://dx.doi.org/10.1002/(SICI)1096-9071(200005)61:1<52::AID-JMV8>3.0.CO;2-L

35. Chivero ET, Bhattarai N, Rydze RT, Winters MA, Holodniy M, Stapleton JT. Human pegivirus RNA is found in multiple blood mononuclear cells in vivo and serum-derived viral RNA-containing particles are infectious in vitro. J Gen Virol. 2014;95:1307–19. http://dx.doi.org/10.1099/vir.0.063016-0

36. Chivero ET, Stapleton JT. Tropism of human pegivirus (formerly known as GB virus C/hepatitis G virus) and host immunomodulation: insights into a highly successful viral infection. J Gen Virol. 2015;96:1521–32. http://dx.doi.org/10.1099/vir.0.000086

37. Hickey WF. Leukocyte traffic in the central nervous system: the participants and their roles. Semin Immunol. 1999;11:125–37. http://dx.doi.org/10.1006/smim.1999.0168

38. Hickey WF, Vass K, Lassmann H. Bone marrow-derived elements in the central nervous system: an immunohistochemical and ultrastructural survey of rat chimeras. J Neuropathol Exp Neurol. 1992;51:246–56. http://dx.doi.org/10.1097/00005072-199205000-00002

39. Unger ER, Sung JH, Manivel JC, Chenggis ML, Blazar BR, Krivit W. Male donor-derived cells in the brains of female sex-mismatched bone marrow transplant recipients: a Y-chromosome specific in situ hybridization study. J Neuropathol Exp Neurol. 1993;52:460–70. http://dx.doi.org/10.1097/00005072-199309000-00004

40. Hickey WF, Hsu BL, Kimura H. T-lymphocyte entry into the central nervous system. J Neurosci Res. 1991;28:254–60. http://dx.doi.org/10.1002/jnr.490280213

41. Knopf PM, Harling-Berg CJ, Cserr HF, Basu D, Sirulnick EJ, Nolan SC, et al. Antigen-dependent intrathecal antibody synthesis in the normal rat brain: tissue entry and local retention of antigen-specific B cells. J Immunol. 1998; 161:692–701.

42. Zheng J, Gendelman HE. The HIV-1 associated dementia complex: a metabolic encephalopathy fueled by viral replication in mononuclear phagocytes. Curr Opin Neurol. 1997;10:319–26. http://dx.doi.org/10.1097/00019052-199708000-00007

43. Davies NW, Brown LJ, Gonde J, Irish D, Robinson RO, Swan AV, et al. Factors influencing PCR detection of viruses in cerebrospinal fluid of patients with suspected CNS infections. J Neurol Neurosurg Psychiatry. 2005;76:82–7. http://dx.doi.org/10.1136/jnnp.2004.045336

44. Radkowski M, Przyjalkowski W, Lipowski D, Wang LF, Laskus T. Lack of GB virus C/hepatitis G virus sequences in cerebrospinal fluid in patients with central nervous system infections. Scand J Infect Dis. 1998;30:539. http://dx.doi.org/10.1080/00365549850161647

45. Kaiser R. Tick-borne encephalitis: clinical findings and prognosis in adults. Wien Med Wochenschr. 2012;162:239–43. http://dx.doi.org/10.1007/s10354-012-0105-0

46. Růžek D, Dobler G, Donoso Mantke O. Tick-borne encephalitis: pathogenesis and clinical implications. Travel Med Infect Dis. 2010;8:223–32. http://dx.doi.org/10.1016/j.tmaid.2010.06.004

47. Agol VI. The 5′-untranslated region of picornaviral genomes. Adv Virus Res. 1991;40:103–80. http://dx.doi.org/10.1016/S0065-3527(08)60278-X

48. Dockter J, Evans CF, Tishon A, Oldstone MB. Competitive selection in vivo by a cell for one variant over another: implications for RNA virus quasispecies in vivo. J Virol. 1996;70:1799–803.

49. McLinden JH, Kaufman TM, Xiang J, Chang Q, Klinzman D, Engel AM, et al. Characterization of an immunodominant antigenic site on GB virus C glycoprotein E2 that is involved in cell binding. J Virol. 2006;80:12131–40. http://dx.doi.org/10.1128/JVI.01206-06

50. Domingo E, Sheldon J, Perales C. Viral quasispecies evolution. Microbiol Mol Biol Rev. 2012;76:159–216. http://dx.doi.org/10.1128/MMBR.05023-11

Address for correspondence: Karol Perlejewski, Medical University of Warsaw, Department of Immunopathology of Infectious and Parasitic Diseases, 3C Pawińskiego St, 02-106 Warsaw, Poland; email: kperlejewski@wum.edu.pl

April 2017: **Emerging Viruses**

- Biologic Evidence Required for Zika Disease Enhancements by Dengue Antibodies

- Neurologic Complications of Influenza B Virus Infection in Adults, Romania

- Implementation and Initial Analysis of a Laboratory-Based Weekly Biosurveillance System, Provence-Alpes-Côte d'Azur, France

- Transmission of Hepatitis A Virus through Combined Liver–Small Intestine–Pancreas Transplantation

- Influence of Referral Pathway on Ebola Virus Disease Case-Fatality Rate and Effect of Survival Selection Bias

- *Plasmodium malariae* Prevalence and *csp* Gene Diversity, Kenya, 2014 and 2015
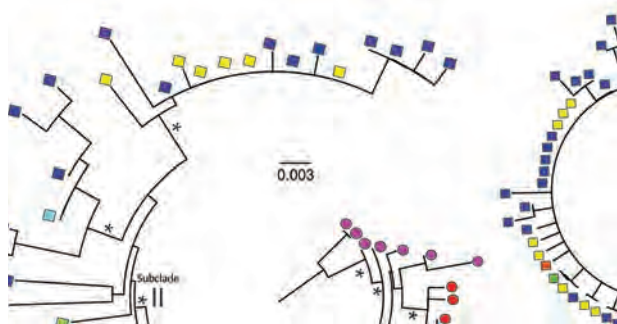
- Presence and Persistence of Zika Virus RNA in Semen, United Kingdom, 2016

- Three Divergent Subpopulations of the Malaria Parasite *Plasmodium knowlesi*

- Variation in *Aedes aegypti* Mosquito Competence for Zika Virus Transmission

- Outbreaks among Wild Birds and Domestic Poultry Caused by Reassorted Influenza A(H5N8) Clade 2.3.4.4 Viruses, Germany, 2016

- Highly Pathogenic Avian Influenza A(H5N8) Virus in Wild Migratory Birds, Qinghai Lake, China
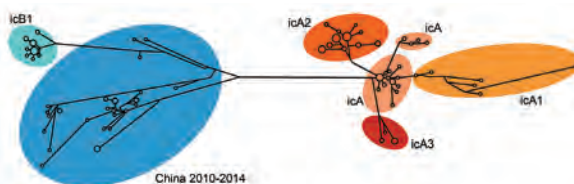
- Design Strategies for Efficient Arbovirus Surveillance

- Typhus Group Rickettsiosis, Texas, 2003–2013

- Detection and Molecular Characterization of Zoonotic Poxviruses Circulating in the Amazon Region of Colombia, 2014

- Reassortment of Influenza A Viruses in Wild Birds in Alaska before H5 Clade 2.3.4.4 Outbreaks

- Incidence and Characteristics of Scarlet Fever, South Korea, 2008–2015

- Markers of Disease Severity in Patients with Spanish Influenza in the Japanese Armed Forces, 1919–1920

- Molecular Identification of *Spirometra erinaceieuropaei* in Cases of Human Sparganosis, Hong Kong

- Zika Virus Seroprevalence, French Polynesia, 2014–2015

- Persistent Arthralgia Associated with Chikungunya Virus Outbreak, US Virgin Islands, December 2014–February 2016

- Assessing Sensitivity and Specificity of Surveillance Case Definitions for Zika Virus Disease

- Detection of Zika Virus in Desiccated Mosquitoes by Real-Time Reverse Transcription PCR and Plaque Assay

- Surveillance and Testing for Middle East Respiratory Syndrome Coronavirus, Saudi Arabia, April 2015–February 2016

EMERGING INFECTIOUS DISEASES

https://wwwnc.cdc.gov/eid/articles/issue/23/4/table-of-contents

Molecular Evolution, Diversity, and Adaptation of Influenza A(H7N9) Viruses in China

Jing Lu,[1] Jayna Raghwani,[1] Rhys Pryce, Thomas A. Bowden, Julien Thézé,
Shanqian Huang, Yingchao Song, Lirong Zou, Lijun Liang, Ru Bai, Yi Jing,
Pingping Zhou, Min Kang, Lina Yi, Jie Wu,[2] Oliver G. Pybus,[2] Changwen Ke[2]

The substantial increase in prevalence and emergence of antigenically divergent or highly pathogenic influenza A(H7N9) viruses during 2016–17 raises concerns about the epizootic potential of these viruses. We investigated the evolution and adaptation of H7N9 viruses by analyzing available data and newly generated virus sequences isolated in Guangdong Province, China, during 2015–2017. Phylogenetic analyses showed that circulating H7N9 viruses belong to distinct lineages with differing spatial distributions. Hemagglutination inhibition assays performed on serum samples from patients infected with these viruses identified 3 antigenic clusters for 16 strains of different virus lineages. We used ancestral sequence reconstruction to identify parallel amino acid changes on multiple separate lineages. We inferred that mutations in hemagglutinin occur primarily at sites involved in receptor recognition or antigenicity. Our results indicate that highly pathogenic strains likely emerged from viruses circulating in eastern Guangdong Province during March 2016 and are associated with a high rate of adaptive molecular evolution.

Since its first detection in March 2013, avian influenza A(H7N9) virus has caused 1,534 human infections that, as of November 30, 2017, had resulted in 608 deaths. Recurrent waves of human cases have been reported in 27 provinces in China, indicating sustained transmission of H7N9 viruses (*1*). Moreover, since its emergence, H7N9 virus has reassorted with influenza A(H9N2) viruses that co-circulate in China, resulting in an increasingly diverse array of virus genomes (*2–4*). The fifth influenza epidemic

wave (2016–17) was marked by a notable increase in the number of human cases (677 during September 2016–May 2017), making it the largest outbreak of influenza A(H7N9) since 2013. Moreover, geographic distribution of human cases suggests that H7N9 virus is now more widespread and that residences of patients have shifted gradually from urban to semiurban and rural areas (*1,5–7*). These epidemiologic observations have raised public health concerns.

Previous molecular surveillance studies suggested that H7N9 virus lineages originate in 2 densely populated areas, the Yangtze River Delta region in eastern China and the Pearl River Delta region in central Guangdong Province (*8*). Preliminary epidemiologic data suggested that most human infections in the current fifth epidemic wave were caused by viruses from the Yangtze River Delta region (*5*) (previously named lineage C viruses) (*3*). These viruses, in contrast to viruses from the Pearl River Delta region (previously named lineage B viruses) (*3*), appear to exhibit reduced cross-reactivity with existing candidate vaccine virus strains (*9*). Furthermore, a subset of lineage C isolates has also acquired a highly pathogenic (HP) phenotype (*5,10,11*).

These observations suggest that the increased epidemic activity of H7N9 viruses in China might be driven, at least in part, by ongoing virus evolution and adaptation. Decreased cross-reactivity and increased pathogenicity of some H7N9 viruses was discovered only recently (*9*), and the genetic diversity and evolution of the current fifth epidemic wave of these viruses are not yet well understood. Information necessary to clarify this situation includes geographic distribution of currently circulating H7N9 virus lineages, origin and genetic composition of newly emerged HP H7N9 viruses, and evolutionary and structural characterization of mutations associated with the fifth epidemic wave of these viruses.

We report 47 hemaglutinnin (HA) and 43 neuraminidase (NA) gene sequences of human-derived and poultry-derived H7N9 viruses that were isolated during 2015–2017 in Guangdong Province, China. We conducted structural and evolutionary analyses of these strains and characterized the evolution and emergence of currently circulating H7N9 viruses in China.

Materials and Methods

Ethics
This study was approved by the institutional ethics committee of the Center for Disease Control and Prevention of Guangdong Province. Written consent was obtained from patients or their guardian(s) when samples were collected. Patients were informed about the study before providing written consent, and data were anonymized for analysis.

Sample Collection
Samples from persons with suspected cases of influenza A(H7N9) were initially tested for avian influenza A virus in provincial clinics in Guangdong Province. Specimens with positive results were subsequently analyzed (12,13). For poultry-related samples, we obtained samples from locations where poultry were housed and processed (e.g., cages, feeding troughs, defeathering machines) (12). Respiratory specimens were collected from persons with suspected cases of influenza A(H7N9) by the Ministry of Health of China.

Sequence Alignment
For phylogenetic studies, we sequenced 47 HA and 41 NA sequences from 20 human samples and 28 poultry-related samples; all belonged to the fourth and fifth epidemic waves of influenza A(H7N9) (GISAID [https://www.gisaid.org/] accession nos. EPI866538–77, 972231–6, 972238–303, 974029, 974523, 974539–42, 997159–60, and 1171786–93). These new H7N9 sequences were combined with all available H7N9 gene sequences whose sampling dates and locations were known. Two gene sequence datasets were generated: H7, HA (n = 737) and N9, NA (n = 610). We constructed multiple sequence alignments by using ClustalW (14) and edited these sequences manually by using AliView (15).

Molecular Clock Phylogenetic Analysis
We estimated molecular clock phylogenies by using the Bayesian Markov Chain Monte Carlo approach implemented in BEAST version 1.8 (16) as described (4). We computed 4 independent Markov Chain Monte Carlo runs of 1.5×10^8 steps for each alignment and extracted a subset of 2,000 phylogenies from the posterior tree distribution, subsequently used as an empirical tree distribution for phylogeographic analyses (17). We computed maximum clade credibility trees for each dataset by using TreeAnnotator (16).

Phylogeographic Analysis of Influenza A(H7N9) Epidemic
We used the discrete phylogeographic method (18) implemented in BEAST to investigate spatial dynamics of H7N9 virus lineages from 6 regions in China as classified in a previous study (4). The 6 locations were eastern China (Anhui, Shanghai, Zhejiang, Jiangsu, and Shandong); central China (Jiangxi and Hunan); northern China (Beijing, Henan, Hebei, and Xinjiang); southeastern China (Fujian); central Guangdong Province (Guangzhou, Huizhou, Foshan, Dongguan, Zhongshan, Shenzhen, Jiangmen, Zhaoqing Yangjiang, Maoming, and Yunfu); and eastern Guangdong Province (Meizhou, Heyuan, Chaozhou, Jieyang, Shantou, Shanwei, and Shaoguan).

Because sporadic human cases detected in Malaysia and Taiwan were believed to have originated in China, we used available epidemiologic information to assign their location to the most likely source in China. Hong Kong and central Guangdong Province were treated as a single location because of their proximity to each other. We analyzed reported H7N9 virus infections and virus sequences (online Technical Appendix Table 1, https://wwwnc.cdc.gov/EID/article/24/10/17-1063-Techapp1.pdf). To estimate directionality of virus lineage movement, we used asymmetric continuous-time Markov chain phylogeographic model (19) and a Bayesian stochastic search variable selection procedure (18).

Inferring Phylogenetic Distribution of Amino Acid Changes
We investigated phylogenetic positions of amino acid changes among H7N9 virus isolates by using HA and NA maximum clade credibility trees. We estimated maximum posterior probability amino acid sequences for each internal node by using BEAST with a Jones–Taylor–Thornton amino acid substitution model (20), gamma-distributed among-site rate heterogeneity (21), and a strict molecular clock model. To infer amino acid substitutions along the trunk branches of the H7N9 phylogeny, we mapped amino acid changes onto internal branches by using a Java script (available on request). Trunk branches corresponded to internal branches that subtended >5 terminal nodes in the fifth influenza epidemic wave.

Structure-Based Mapping Analysis
We used the crystal structure of the HA (Protein Data Bank no. 4BSE) (22) and NA (Protein Data Bank no. 2C4L) glycoproteins from an influenza A(H7N9) virus to map amino acid changes identified by evolutionary analysis. We

performed residue mapping onto the H7 and N9 structures by using PyMol (*23*). We calculated solvent accessibility for trimeric hemagglutinin with the ligands removed by using ESPript (*24*) and identified receptor-binding residues by using CONTACT in CCP4 (*25*).

Positive Selection Analyses

To identify sites under positive selection, we used methods implemented in HyPhy (*26*) to estimate the dN/dS ratio of codons in HA. These methods included single-likelihood ancestor counting (*27*), fixed effects likelihood (*27*), mixed effects model of evolution (*28*), and the fast unconstrained Bayesian approximation approach (*29*).

Estimating Rates of Virus Molecular Adaptation

We estimated rates of adaptive substitution in H7N9 virus HA and NA genes by using an established population genetic method related to the McDonald-Kreitman test (*30,31*). We used a consensus of H7N9 first-wave sequences as an outgroup to estimate derived and ancestral mutational site frequencies in each subsequent wave. Specifically, we classified polymorphisms into 3 categories according to their frequency in the population (low, 0%–15%; intermediate, 15%–75%; and high, 75%–100%). We calculated the number of adaptive substitutions from the number of synonymous and nonsynonymous sites in each category and assessed statistical uncertainty by using a bootstrap approach (1,000 replicates) (*30,31*).

Serologic Analysis

We obtained serum samples from 4 patients with influenza A(H7N9) 2–3 weeks after clinical symptoms were observed. We performed hemagglutination inhibition assays by using different lineages of H7N9 viruses as antigens (online Technical Appendix). Three lineage C1 strains, 4 lineage C2 strains, 5 lineage B strains, and 4 HP strains were used as antigens (Table). We calculated serum titer for each H7N9 strain as the highest reciprocal serum dilution providing complete hemagglutination inhibition.

Results

Molecular Epidemiology of Viruses Isolated during 2013–2017

During 2013–2017, the influenza A(H7N9) virus epidemic lineage was geographically structured and classified into 3 major lineages, A, B, and C, in accordance with the lineage naming scheme used in a previous study (*3*). H7N9 virus has evolved in a clock-like manner (i.e., there is a strong linear relationship between genetic divergence and sampling time; correlation coefficient 0.95) (Figure 1). The estimated time to the most recent common ancestor (TMRCA) of H7N9 virus HA sequences is November 2012 (95% credible region October–December 2012). The corresponding molecular clock phylogeny for NA (online Technical Appendix Figure 1) also shows A–C lineages and has a similar estimated TMRCA of September 2012 (95% credible region July–October 2012). However, the topology of the NA phylogeny differs from that of HA, suggesting reassortment between HA and NA during emergence of the H7N9 virus epidemic lineage (Figure 2; online Technical Appendix Figure 1).

Different H7N9 virus lineages are associated with different epidemiologic patterns (Figures 2, 3). Specifically, most (86%, 32/37) lineage B viruses that were isolated during the fourth and fifth influenza epidemic waves descended from viruses circulating in central Guangdong Province during earlier epidemic seasons (Figure 2). In addition, lineage B viruses isolated from the fourth and fifth influenza waves

Table. Hemagglutination inhibition titers for serum samples from 4 patients infected with influenza A(H7N9) virus against reference H7N9 strains, China*

H7N9 strain	Date of collection	Clade	Titer by patient and H7N9 strain			
			P1, strain NA	P2, strain NA	P3, strain ZS29	P4, strain ST18
EPI972232/A/CZ009†	2017 Jan	C1	2,048	2,048	512	512
EPI972243/A/MZ011†	2017 Jan	C1	4,096	4,096	1,024	512
EPI1171792/A/ST18†	2017 Jan	C1	1,024	512	512	512
EPI656434/A/ST72	2015 Feb	C2	256	128	1024	128
EPI866569/A/ST021†	2016 Feb	C2	256	128	512	128
EPI656314/A/SW20	2015 Jan	C2	256	128	512	128
EPI1171791/A/SW33†	2015 Feb	C2	256	128	512	128
EPI972259/A/ZS201†	2016 Dec	B	256	128	512	128
EPI972234/A/FS10†	2017 Jan	B	256	256	512	128
EPI656054/A/ZS74	2014 Jan	B	512	256	512	128
EPI656038/A/ZS71	2014 Jan	B	256	256	512	128
EPI656014/A/GZ66	2014 Jan	B	512	256	512	64
EPI1171786/Env/YJ370†	2017 Sep	HP	64	64	512	64
EPI1171788/Env/YJ073†	2017 May	HP	64	64	512	64
EPI1171790/A/ZS29†	2017 Mar	HP	128	64	512	64
EPI919607/A/17SF003	2017 Jan	HP	256	64	512	128

*HP, highly pathogenic; NA, not available; P, patient no.
†Strains isolated and sequenced in this study.
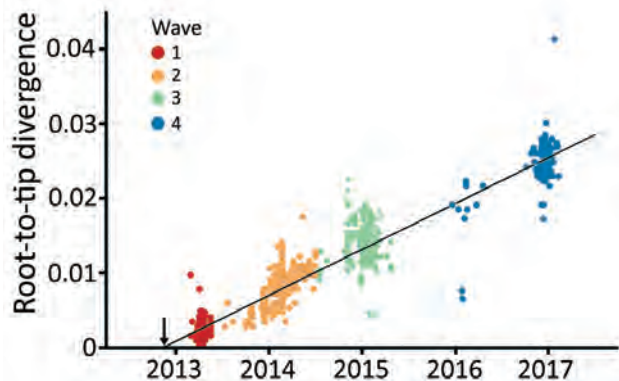
Figure 1. Regression of root-to-tip divergence estimated from hemagglutinin gene of influenza A(H7N9) viruses, China. Arrow indicates the time of the most recent common ancestor of the epidemic lineage.

were almost exclusively restricted to central (rather than eastern) Guangdong Province (Figures 2, 3). In contrast, viruses in eastern China, composed of 2 lineages (A and C) have been exported to and become dominant in multiple regions as the epidemic has progressed (*3*). These findings indicate a comparatively broader geographic dissemination (Figure 3; online Technical Appendix Figure 1).

The new isolates from eastern Guangdong Province, combined with isolates from eastern China (*1,5*), suggest that recent H7N9 virus activity is driven primarily by lineage C viruses (Figure 2). The estimated TMRCA of lineage C is December 2013 (95% highest posterior density October 2013–January 2014). For lineage C, we observed 2 clades (Figure 4). The larger of these clades (C1) circulates mainly in central and eastern China, and the smaller clade (C2) is found predominantly in eastern Guangdong Province. Clade C2 also includes recently identified HP viruses (Figures 1, 2, 4).

To investigate these HP viruses, we undertook retrospective screening of poultry-related samples collected in Guangdong Province during January 2016–February 2017 and identified 7 HP influenza virus isolates that belong to the HP cluster within C2 (Figure 2). These HP viruses also form a distinct cluster within lineage C viruses in the NA phylogeny (online Technical Appendix Figure 1). Our analyses indicated that the HP clade likely emerged from clade C2 viruses circulating in eastern Guangdong Province in 2016.

Adaptive Evolution in Virus C Lineage

We then investigated whether the increasing prevalence of lineage C viruses might be associated with virus adaptation. We combined ancestral sequence reconstruction of lineage B and C HA gene sequences (Figures 4, 5) by mapping residues that have undergone changes onto the crystal
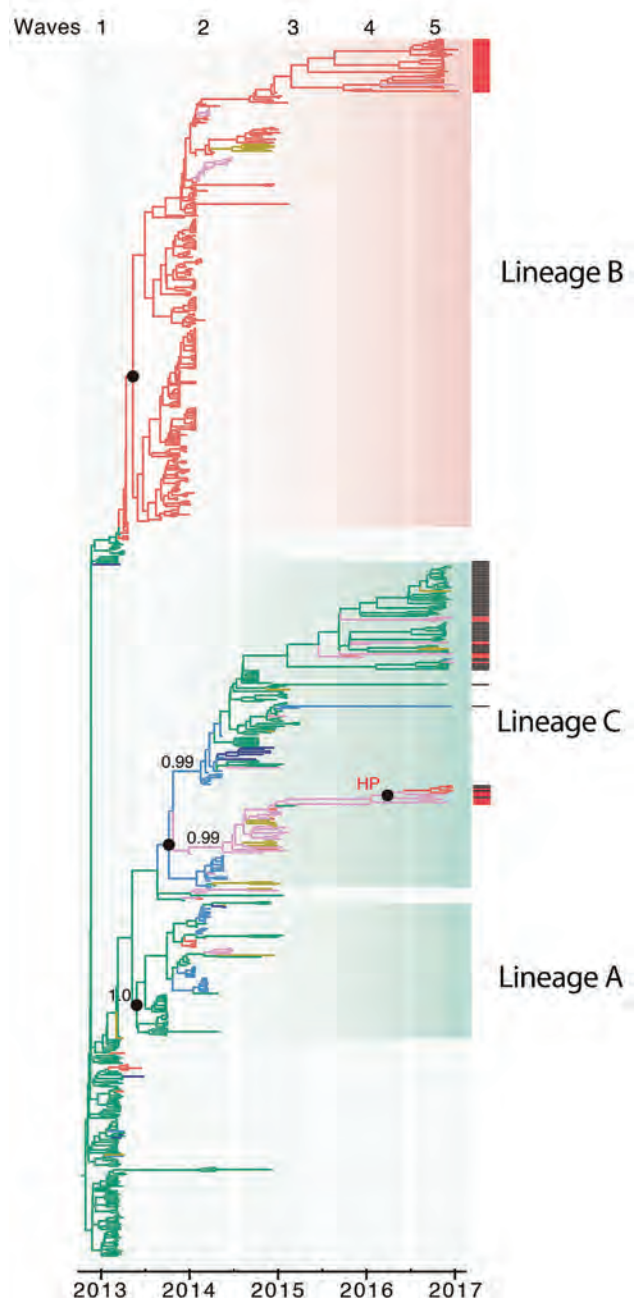
Figure 2. Genetic evolution and spatial spread of epidemic lineage of influenza A(H7N9) viruses, China, 2013–2017. Bayesian maximum clade credibility tree of the hemagglutinin gene is shown. Black bars to the right of the tree indicate sequences (from waves 4 and 5) from other studies (*1,5*), and red bars indicate sequences reported in this study from Guangdong Province. Branch colors indicate most probable ancestral locations of each branch. Three major lineages (A, B, and C) of H7N9 viruses were observed. Values along branches indicate bootstrap values. Black circles indicate posterior support >0.95. Location of posterior support is shown for selected clades. An H7N9 strain closely related to the highly pathogenic H7N9 virus cluster is indicated. HP, highly pathogenic.
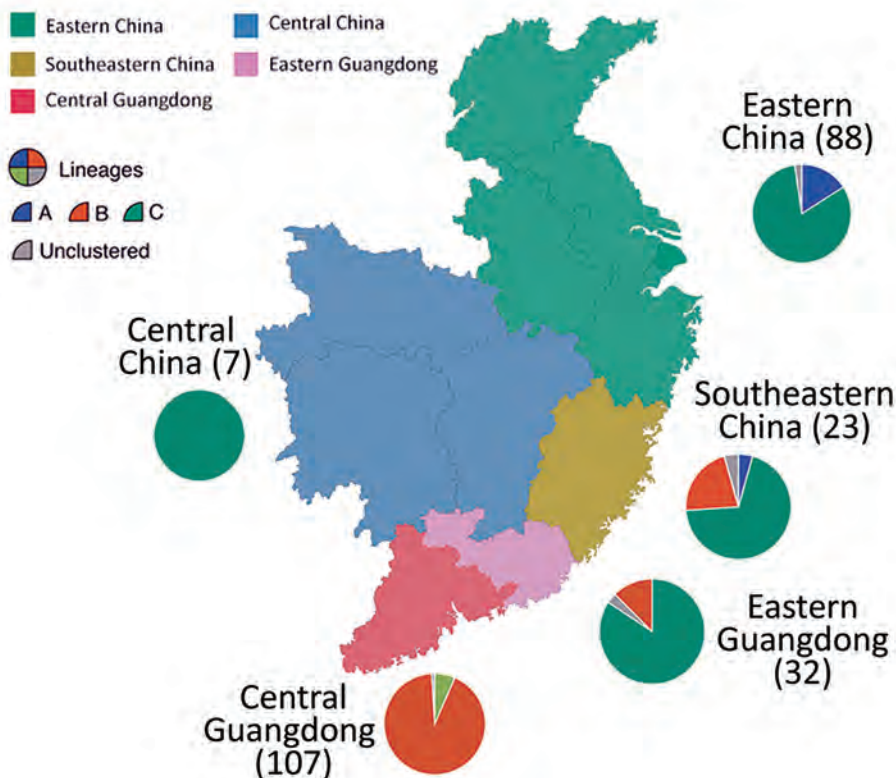
Figure 3. Geographic location and lineage classification of 374 influenza A(H7N9) human viruses, China. Values in parentheses indicate number of sequenced viruses from each region. Pie charts indicate approximate percentages of each virus lineage (A, B, C, or unclustered). Sequences from Xinjiang Province in northern China are not shown.

structure of the trimeric hemagglutinin. Our analysis identified several notable amino acid substitutions that occurred along the internal branches of lineage C viruses (Figure 4).

Around the time of the second influenza epidemic wave, ancestral viruses of lineage C acquired several amino acid changes in HA, specifically L177I, G386A, S489R, and S128N (based on H3 sequence numbering). Three of these mutations (G386A, S489R, and S128N) are located in solvent-accessible regions of HA (Figure 6; online Technical Appendix Table 2). Furthermore, S128N was found within the 130 loop and is proximal to the receptor surface (distance ≈20 Å) (Figure 6).

We found by evolutionary analysis that several HA sites acquired amino acid mutations independently in different phylogenetic clades. First, 4 mutations (A135V, L177I, M236I, and S489N) occurred independently along the trunk lineages that gave rise to the current lineage B and C viruses (Figure 5). Three of these mutations (A135V, M236I, and S489N) were observed only in the fourth and fifth influenza epidemic waves of lineage B (Figure 5). Second, comparison of the C1 and C2 clades also identified parallel amino acid changes within lineage C (A122T/P and M236I) (Figure 4).

The observation of parallel amino acid changes along those particular lineages (online Technical Appendix Tables 2, 3) that have persisted until the fifth influenza epidemic wave (i.e., parallel changes between lineages B

and C and between the C1 and C2 clades) is suggestive of convergent, adaptive molecular evolution. The parallel changes in lineage C (A122T/P and M236I) are estimated to be fully or partially solvent accessible and the A135V mutation is located at the receptor-binding site (Figure 6). One subclade of lineage B viruses appears to have acquired mutations A135V and S489N within the last 12 months (Figure 5). Therefore, we suggest that this subclade should be closely monitored in the future.

Within the C2 clade, we found that HA acquired 7 amino acid changes (I48T, A122P, K173E, L226Q, M236I, I326V, and E393K) on the internal branch immediately ancestral to the HP cluster. This internal branch represents a period of approximately 1 year (Figure 4). Although all of these changes appeared in residues with partial or full solvent accessibility, mutations K173E, L226Q, and I326V are particularly noteworthy because they have arisen at or near known antigenic, receptor-binding, and proteolytic cleavage sites, respectively (Figure 6). Furthermore, these mutations in the HP cluster also coincide with appearance of a 4-amino acid insertion (KRTA) near the HA1-HA2 proteolytic cleavage site (Figure 4). A subset of HA substitutions (at sites 57, 114, 140, 226, and 276) that occurred on the trunk branches of lineages B and C viruses was also found to be under positive selection on the basis of dN/dS ratios we estimated by using methods implemented in HyPhy (online Technical Appendix Table 4).
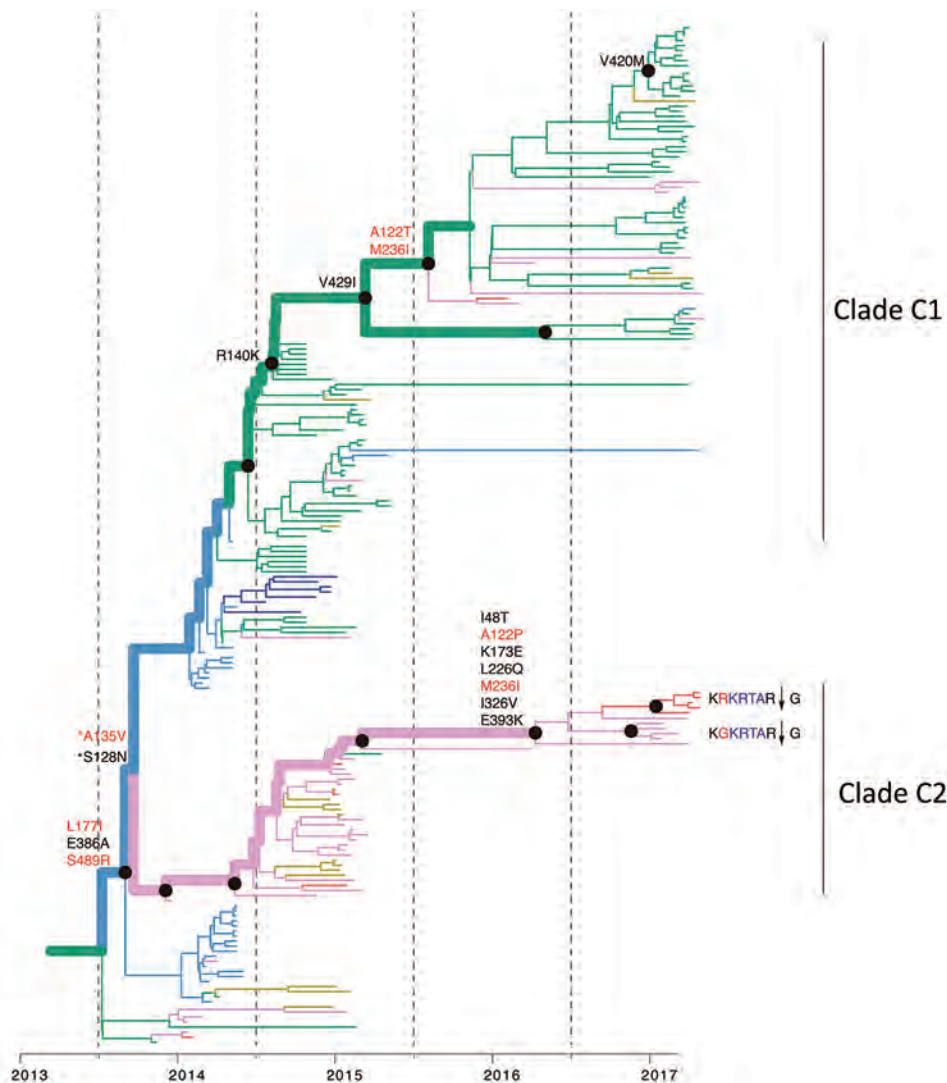
Figure 4. Reconstruction of amino acid changes along trunk of lineage B phylogenies of influenza A(H7N9) viruses, China. Maximum clade credibility tree of hemagglutinin gene sequences from lineage B is shown. Branches are colored according to geographic locations, as in Figure 3. Thicker lines indicate the trunk lineage leading up to the current fifth influenza epidemic wave. Amino acid changes along the trunk are indicated. Red branches indicate sites undergoing parallel amino acid changes across multiple lineages. Mutations correspond to H3 numbering scheme. *Indicates uncertainty about the phylogenetic position of the A135V and S128N mutations because branch posterior support is low.

We also investigated whether amino acid changes in the HA gene during emergence of influenza A(H7N9) virus have been driven by adaptive evolution similar to that observed for seasonal human influenza (*30*). We found evidence for adaptive evolution in HA genes of B and C virus lineages. We estimated that lineage B adapted at a rate of 0.80 (interquartile range [IQR] 0.21–0.95) adaptive substitutions across the whole HA gene per year and lineage A at a rate of 0.60 (IQR 0.10–1.18) adaptive substitutions per year. Within lineage C, the estimated adaptation rate of the C1 clade is ≈1.84 (IQR 1.09–2.14) adaptive substitutions per year and that for the C2 clade (which includes the HP cluster) is 3.12 (IQR 2.45–3.79) adaptive substitutions per year. These results indicate molecular adaptation across the whole H7N9 lineage and suggest that adaptation is faster in the 2 C clades than in the A and B lineages. Previous estimates of rates of adaptive substitution were 1.02 fixations per year in the whole HA gene for seasonal human

influenza A(H1N1) virus and 1.52 fixations per year in the whole HA gene for influenza A(H3N2) virus (*30*). In this context, the rate of adaptive evolution observed for lineage C here is notable and raises concern for ongoing evolution of these viruses.

Antigenic Properties

We collected serum samples from 4 patients infected with H7N9 virus during 2015 and 2017 (Table). For patients 3 and 4, the corresponding virus strains were isolated and sequenced. Phylogenetic analysis indicated that patient 3 was infected with clade C1 virus and that patient 4 was infected with HP virus. Hemagglutination inhibition results suggested the presence of 3 antigenic clusters among the 16 H7N9 virus strains selected. Serum samples from patients 1, 2, and 3 showed similar patterns, reacting robustly to clade C1 viruses and moderately to clade C2 and lineage B viruses but poorly to HP viruses. A serum sample from a
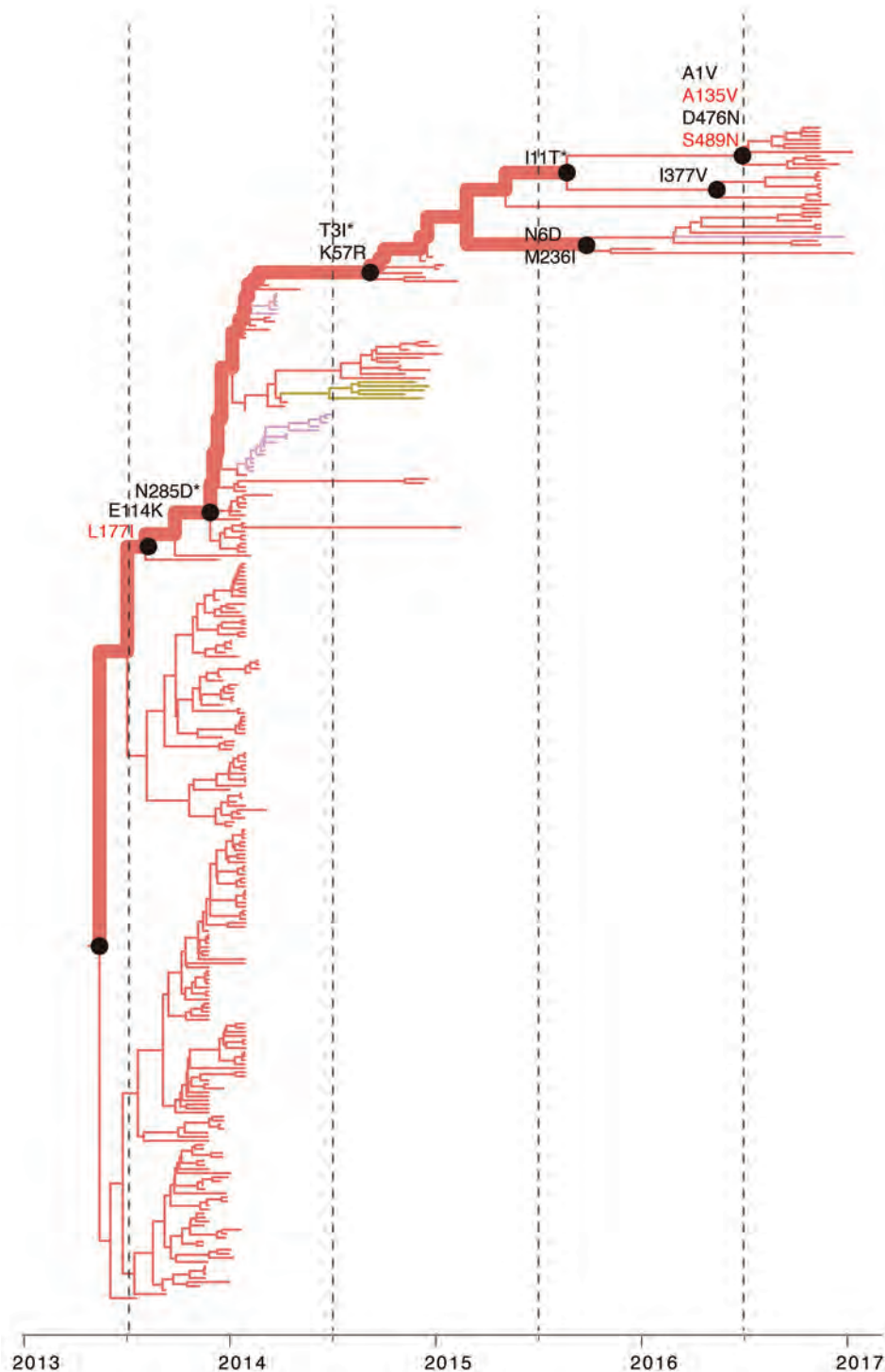
Figure 5. Reconstruction of amino acid changes along trunk of lineage C phylogenies of influenza A(H7N9) viruses, China. Maximum clade credibility tree of hemagglutinin gene sequences from lineage C is shown. Branches are colored according to geographic locations, as in Figure 3. Thicker lines indicate the trunk lineage leading up to the current fifth influenza epidemic wave. Amino acid changes along the trunk are indicated. Red branches indicate sites undergoing parallel amino acid changes across multiple lineages. Mutations correspond to H3 numbering scheme. *Mutation sites not present are numbered according to H7 numbering.

patient infected with an HP H7N9 virus appeared to react strongly to all H7N9 virus strains.

Discussion

Our results show that H7N9 viruses of lineage C, which were prevalent in the recent fifth influenza epidemic wave

in China, comprise 2 geographically distinct clades (C1 and C2) that have undergone adaptive evolution. Clade C1 is found primarily in eastern and central China and clade 2 in Guangdong Province, and both clades appear to have circulated in bird populations for ≈3 years. Our ancestral state reconstruction analysis provides crucial evidence that
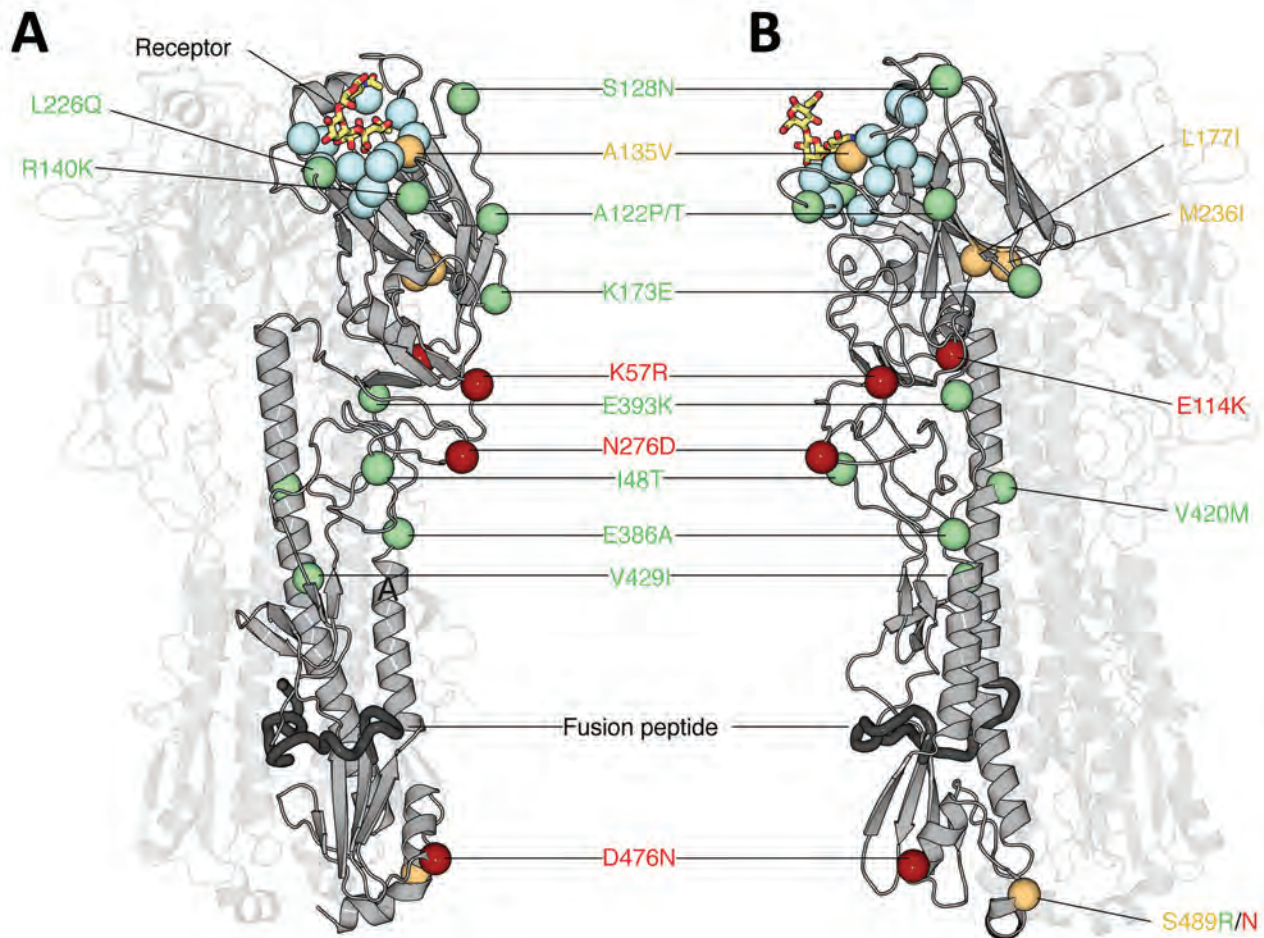
Figure 6. Structural analysis of amino acid changes in hemagglutinin in lineages B and C of influenza A(H7N9) viruses, China. Crystal structure of the homotrimeric H7 hemagglutinin bound to a human receptor analog (Protein Data Bank no. 4BSE) (*27*) (A) and rotated 90° counterclockwise (B) are shown. Two of the 3 protomers are displayed with high transparency to aid visualization. The carbon Cα positions of salient features are shown as spheres. Blue indicates receptor-binding residues, red indicates mutations in lineage B, green indicates mutations in lineage C, and orange indicates mutations in lineages B and C. Human receptor analog α2,6-SLN is shown as sticks colored according to constituent elements: carbon in orange, oxygen in red, and nitrogen in blue. Dark gray indicates the putative fusion peptide (*32*). Residues are numbered according to the H3 numbering system (online Technical Appendix Table 2, https://wwwnc.cdc.gov/EID/article/24/10/17-1063-Techapp1.pdf). A135 and L226 participate in receptor binding and thus are likely to modulate receptor specificity.

2 successful lineages of H7N9 viruses (lineages B and C) have experienced multiple parallel amino acid changes (Figures 4, 5), suggesting the possible action of convergent molecular evolution.

We also observed a higher rate of virus adaptation in eastern Guangdong Province (C2 clade compared with C1). Although clades C1 and C2 are phylogenetically closely related, serum from a clade C1 virus-infected patient has moderate reactivity with C2 strains from 2015–2016 and poor reactivity to the HP virus from 2016–2017. The higher adaptation rate and antigenic changes in clade C2 are of concern from a public health perspective. Introduction of HP avian influenza into domestic poultry might constitute a serious risk, as demonstrated by emergence of goose–Guangdong lineage HP

H5N1 viruses, which spilled back into wild birds and caused the longest global outbreak of HP avian influenza to date (*33*).

Parallel amino acid changes in clades C1 and C2 occurred at 2 sites in HA (122 and 236) (Figure 6). Furthermore, we observed 4 mutations that emerged independently in lineages B and C (sites 135, 177, 236, and 489). These results suggest adaptive convergent molecular evolution. Site 135 is located in the receptor-binding region and is near antigenic site A, as defined by Wiley et al. (*34*). Thus, the observed A135V mutation might modulate receptor affinity and contribute to immune escape (Figure 6), as observed in influenza A(H7N1) and A(H7N7) viruses (*35,36*).

Specifically, experimental studies indicate that threonine at position 135 in the HP H7N7 virus A/Netherlands/

219/2003 confers broad-scale resistance to neutralizing monoclonal antibodies against the earliest strain of H7N9 virus (A/Shanghai/02/2013) (*37*). Furthermore, the World Health Organization has reported that recent clade C1 viruses (but not those of lineage B) react less to postinfection ferret antiserum raised against the A/Anhui/1/2013 and A/Shanghai/2/2013-derived candidate vaccine strains (*9*). Consistent with this finding, we found that most clade C1 viruses isolated in 2015 have the A135V mutation. However, this mutation was only detected in a small proportion of recent lineage B viruses (Figure 5).

In this study, we performed a preliminary evaluation of the antigenicity of H7N9 viruses by using patient serum samples collected in 2015 and 2017. Without serum raised in response to early strains from 2013, we cannot discriminate antigenic change between strains from 2013 and those from 2017. However, the limited data we have indicate the presence of 3 antigenic clusters among the 4 phylogenetic clusters circulating during the fifth influenza epidemic wave (Table). HA1 positions 109–301 (H3 numbering) include the A–E antigenic epitopes, which are known to determine antigenicity of influenza A viruses (*34*). The amino acid changes responsible for the antigenic differences between clade C1 and other clades were located in antigenic site A (position 140, H3 numbering; online Technical Appendix Figure 2).

The mutation R140K has been observed in viruses isolated from ferrets experimentally infected with avian influenza A(H7N9) viruses and has been linked to antigenic drift of influenza A(H5N1) viruses (*38–40*). By comparing the sequences of the HP H7N9 virus cluster and other clade C2 viruses, we found a substitution in antigenic site E (position 173, H3 numbering) that could underlie antigenic change in HP H7N9 viruses (online Technical Appendix Figure 2). In future work, we aim to explore the roles of these substitutions in determining viral antigenicity in the context of H7N9 virus genomes by using reverse genetics.

HP H7N9 viruses belonging to lineage C2 were first detected in late 2016, but spread greatly in geographic range in early 2017 (*41*). Several mechanisms for the genesis of an HP virus from a low pathogenicity virus have been proposed, including transcription errors (*42*), stepwise amino acid substitutions (*43*), or recombination (*44*). For H7, emergence of HP viruses is attributed to nonhomologous recombination resulting in simultaneous insertion of several amino acids at the HA cleavage site. These insertions might be derived from host 28S rRNA sequence (*45*) or from other influenza gene segments, such as the matrix (*46*) and nucleoprotein genes (*44*). The 12-nt insert in the HP H7N9 virus strains is 100% identical to a region in the polymerase basic 1 gene in multiple avian influenza A viruses, including subtypes H3N2, H6N2, and H9N2, but is not present in the polymerase basic 1 gene of HP H7N9

virus. H9N2 virus is the most frequently detected avian influenza virus in chickens in China, and the detection rate of this subtype in environmental samples from live poultry markets is ≈20% during the influenza epidemic season (*13*). Therefore, co-infection with H7N9 and other avian influenza viruses, such as influenza A(H9N2) viruses, could, in theory, lead to insertion of a polybasic cleavage site by nonhomologous recombination.

Recent studies have shown that the HP H7N9 virus is more pathogenic in mice, and more thermally stable, than low pathogenicity A/Anhui/1/2013 virus (*47,48*). Current surveillance indicates that HP H7N9 viruses have spread to several provinces in China and are responsible for large influenza outbreaks in poultry in central and northern China that show high mortality rates (http://www.fao.org/ag/againfo/programmes/en/empres/ H7N9/situation_update.html). This finding raises the possibility of global dissemination of H7N9 viruses through migration of wild birds, in a manner similar to that observed for HP H5N1 viruses first identified in Guangdong Province (*32*). Although vaccination of poultry against H7N9 virus has now been implemented in some regions of China, virus adaptation and spatial distribution should be more closely monitored.

About the Author

Dr. Lu is a virologist at the Guangdong Provincial Center for Disease Control and Prevention, Guangzhou, China. His primary research interests are epidemiology, evolution, and transmission of viruses associated with emerging infectious diseases.

References

1. Xiang N, Li X, Ren R, Wang D, Zhou S, Greene CM, et al. Assessing change in avian influenza A(H7N9) virus infections during the fourth epidemic—China, September 2015–August 2016. MMWR Morb Mortal Wkly Rep. 2016;65:1390–4. http://dx.doi.org/10.15585/mmwr.mm6549a2

2. Cui L, Liu D, Shi W, Pan J, Qi X, Li X, et al. Dynamic reassortments and genetic heterogeneity of the human-infecting influenza A (H7N9) virus. Nat Commun. 2014;5:3142. http://dx.doi.org/10.1038/ncomms4142

3. Lam TT, Zhou B, Wang J, Chai Y, Shen Y, Chen X, et al. Dissemination, divergence and establishment of H7N9 influenza viruses in China. Nature. 2015;522:102–5. http://dx.doi.org/10.1038/nature14348

4. Wu J, Lu J, Faria NR, Zeng X, Song Y, Zou L, et al. Effect of live poultry market interventions on influenza A(H7N9) virus, Guangdong, China. Emerg Infect Dis. 2016;22:2104–12. http://dx.doi.org/10.3201/eid2212.160450

5. Iuliano AD, Jang Y, Jones J, Davis CT, Wentworth DE, Uyeki TM, et al. Increase in human infections with avian influenza A(H7N9) virus during the fifth epidemic—China, October 2016–February 2017. MMWR Morb Mortal Wkly Rep. 2017;66:254–5. http://dx.doi.org/10.15585/mmwr.mm6609e2

6. Wang X, Jiang H, Wu P, Uyeki TM, Feng L, Lai S, et al. Epidemiology of avian influenza A H7N9 virus in human beings across five epidemics in mainland China, 2013–17: an epidemiological study of laboratory-confirmed case series. Lancet Infect Dis. 2017;17:822–32. http://dx.doi.org/10.1016/S1473-3099(17)30323-7

7. Artois J, Jiang H, Wang X, Qin Y, Pearcy M, Lai S, et al. Changing geographic patterns and risk factors for avian influenza A(H7N9) infections in humans, China. Emerg Infect Dis. 2018;24:87–94. http://dx.doi.org/10.3201/eid2401.171393

8. Wang D, Yang L, Zhu W, Zhang Y, Zou S, Bo H, et al. Two outbreak sources of influenza A (H7N9) viruses have been established in China. J Virol. 2016;90:5561–73. http://dx.doi.org/10.1128/JVI.03173-15

9. Zhu W, Zhou J, Li Z, Yang L, Li X, Huang W, et al. Biological characterisation of the emerged highly pathogenic avian influenza (HPAI) A(H7N9) viruses in humans, in mainland China, 2016 to 2017. Euro Surveill. 2017;22:30533. http://dx.doi.org/10.2807/1560-7917.ES.2017.22.19.30533

10. Ke C, Mok CK, Zhu W, Zhou H, He J, Guan W, et al. Human infection with highly pathogenic avian influenza A(H7N9) virus, China. Emerg Infect Dis. 2017;23:1332–40. http://dx.doi.org/10.3201/eid2308.170600

11. Zhang F, Bi Y, Wang J, Wong G, Shi W, Hu F, et al. Human infections with recently-emerging highly pathogenic H7N9 avian influenza virus in China. J Infect. 2017;75:71–5. http://dx.doi.org/10.1016/j.jinf.2017.04.001

12. Ke C, Lu J, Wu J, Guan D, Zou L, Song T, et al. Circulation of reassortant influenza A(H7N9) viruses in poultry and humans, Guangdong Province, China, 2013. Emerg Infect Dis. 2014;20:2034–40. http://dx.doi.org/10.3201/eid2012.140765

13. Lu J, Wu J, Zeng X, Guan D, Zou L, Yi L, et al. Continuing reassortment leads to the genetic diversity of influenza virus H7N9 in Guangdong, China. J Virol. 2014;88:8297–306. http://dx.doi.org/10.1128/JVI.00630-14

14. Larkin MA, Blackshields G, Brown NP, Chenna R, McGettigan PA, McWilliam H, et al. Clustal W and Clustal X version 2.0. Bioinformatics. 2007;23:2947–8. http://dx.doi.org/10.1093/bioinformatics/btm404

15. Larsson A. AliView: a fast and lightweight alignment viewer and editor for large datasets. Bioinformatics. 2014;30:3276–8. http://dx.doi.org/10.1093/bioinformatics/btu531

16. Drummond AJ, Suchard MA, Xie D, Rambaut A. Bayesian phylogenetics with BEAUti and the BEAST 1.7. Mol Biol Evol. 2012;29:1969–73. http://dx.doi.org/10.1093/molbev/mss075

17. Lemey P, Rambaut A, Bedford T, Faria N, Bielejec F, Baele G, et al. Unifying viral genetics and human transportation data to predict the global transmission dynamics of human influenza H3N2. PLoS Pathog. 2014;10:e1003932. http://dx.doi.org/10.1371/journal.ppat.1003932

18. Lemey P, Rambaut A, Drummond AJ, Suchard MA. Bayesian phylogeography finds its roots. PLOS Comput Biol. 2009;5:e1000520. http://dx.doi.org/10.1371/journal.pcbi.1000520

19. Edwards CJ, Suchard MA, Lemey P, Welch JJ, Barnes I, Fulton TL, et al. Ancient hybridization and an Irish origin for the modern polar bear matriline. Curr Biol. 2011;21:1251–8. http://dx.doi.org/10.1016/j.cub.2011.05.058

20. Jones DT, Taylor WR, Thornton JM. The rapid generation of mutation data matrices from protein sequences. Comput Appl Biosci. 1992;8:275–82.

21. Yang Z. Among-site rate variation and its impact on phylogenetic analyses. Trends Ecol Evol. 1996;11:367–72. http://dx.doi.org/10.1016/0169-5347(96)10041-0

22. Xiong X, Martin SR, Haire LF, Wharton SA, Daniels RS, Bennett MS, et al. Receptor binding by an H7N9 influenza virus from humans. Nature. 2013;499:496–9. http://dx.doi.org/10.1038/nature12372

23. Schrödinger L. The PyMOL molecular graphics system. Version 1.8. New York: Schrödinger, LLC; 2015.

24. Gouet P, Courcelle E, Stuart DI, Métoz F. ESPript: analysis of multiple sequence alignments in PostScript. Bioinformatics. 1999;15:305–8. http://dx.doi.org/10.1093/bioinformatics/15.4.305

25. Winn MD, Ballard CC, Cowtan KD, Dodson EJ, Emsley P, Evans PR, et al. Overview of the CCP4 suite and current developments. Acta Crystallogr D Biol Crystallogr. 2011;67:235–42. http://dx.doi.org/10.1107/S0907444910045749

26. Pond SL, Frost SD, Muse SV. HyPhy: hypothesis testing using phylogenies. Bioinformatics. 2005;21:676–9. http://dx.doi.org/10.1093/bioinformatics/bti079

27. Kosakovsky Pond SL, Frost SD. Not so different after all: a comparison of methods for detecting amino acid sites under selection. Mol Biol Evol. 2005;22:1208–22. http://dx.doi.org/10.1093/molbev/msi105

28. Murrell B, Wertheim JO, Moola S, Weighill T, Scheffler K, Kosakovsky Pond SL. Detecting individual sites subject to episodic diversifying selection. PLoS Genet. 2012;8:e1002764. http://dx.doi.org/10.1371/journal.pgen.1002764

29. Murrell B, Moola S, Mabona A, Weighill T, Sheward D, Kosakovsky Pond SL, et al. FUBAR: a fast, unconstrained bayesian approximation for inferring selection. Mol Biol Evol. 2013;30:1196–205. http://dx.doi.org/10.1093/molbev/mst030

30. Bhatt S, Holmes EC, Pybus OG. The genomic rate of molecular adaptation of the human influenza A virus. Mol Biol Evol. 2011;28:2443–51. http://dx.doi.org/10.1093/molbev/msr044

31. Raghwani J, Bhatt S, Pybus OG. Faster adaptation in smaller populations: counterintuitive evolution of HIV during childhood infection. PLOS Comput Biol. 2016;12:e1004694. http://dx.doi.org/10.1371/journal.pcbi.1004694

32. Kapczynski DR, Pantin-Jackwood M, Guzman SG, Ricardez Y, Spackman E, Bertran K, et al. Characterization of the 2012 highly pathogenic avian influenza H7N3 virus isolated from poultry in an outbreak in Mexico: pathobiology and vaccine protection. J Virol. 2013;87:9086–96. http://dx.doi.org/10.1128/JVI.00666-13

33. Subbarao K, Klimov A, Katz J, Regnery H, Lim W, Hall H, et al. Characterization of an avian influenza A (H5N1) virus isolated from a child with a fatal respiratory illness. Science. 1998;279:393–6. http://dx.doi.org/10.1126/science.279.5349.393

34. Wiley DC, Wilson IA, Skehel JJ. Structural identification of the antibody-binding sites of Hong Kong influenza haemagglutinin and their involvement in antigenic variation. Nature. 1981;289:373–8. http://dx.doi.org/10.1038/289373a0

35. Monne I, Fusaro A, Nelson MI, Bonfanti L, Mulatti P, Hughes J, et al. Emergence of a highly pathogenic avian influenza virus from a low-pathogenic progenitor. J Virol. 2014;88:4375–88. http://dx.doi.org/10.1128/JVI.03181-13

36. de Wit E, Munster VJ, van Riel D, Beyer WE, Rimmelzwaan GF, Kuiken T, et al. Molecular determinants of adaptation of highly

pathogenic avian influenza H7N7 viruses to efficient replication in the human host. J Virol. 2010;84:1597–606. http://dx.doi.org/10.1128/JVI.01783-09

37. Schmeisser F, Vasudevan A, Verma S, Wang W, Alvarado E, Weiss C, et al. Antibodies to antigenic site A of influenza H7 hemagglutinin provide protection against H7N9 challenge. PLoS One. 2015;10:e0117108. http://dx.doi.org/10.1371/journal.pone.0117108

38. Belser JA, Gustin KM, Pearce MB, Maines TR, Zeng H, Pappas C, et al. Pathogenesis and transmission of avian influenza A (H7N9) virus in ferrets and mice. Nature. 2013;501:556–9. http://dx.doi.org/10.1038/nature12391

39. Cattoli G, Milani A, Temperton N, Zecchin B, Buratin A, Molesti E, et al. Antigenic drift in H5N1 avian influenza virus in poultry is driven by mutations in major antigenic sites of the hemagglutinin molecule analogous to those for human influenza virus. J Virol. 2011;85:8718–24. http://dx.doi.org/10.1128/JVI.02403-10

40. Xu L, Bao L, Deng W, Dong L, Zhu H, Chen T, et al. Novel avian-origin human influenza A(H7N9) can be transmitted between ferrets via respiratory droplets. J Infect Dis. 2014;209:551–6. http://dx.doi.org/10.1093/infdis/jit474

41. Yang L, Zhu W, Li X, Chen M, Wu J, Yu P, et al. Genesis and spread of newly emerged highly pathogenic H7N9 avian viruses in mainland China. J Virol. 2017;91:e01277-17. http://dx.doi.org/10.1128/JVI.01277-17

42. García M, Crawford JM, Latimer JW, Rivera-Cruz E, Perdue ML. Heterogeneity in the haemagglutinin gene and emergence of the highly pathogenic phenotype among recent H5N2 avian influenza viruses from Mexico. J Gen Virol. 1996;77:1493–504. http://dx.doi.org/10.1099/0022-1317-77-7-1493

43. Horimoto T, Rivera E, Pearson J, Senne D, Krauss S, Kawaoka Y, et al. Origin and molecular changes associated with emergence of a highly pathogenic H5N2 influenza virus in Mexico. Virology. 1995;213:223–30. http://dx.doi.org/10.1006/viro.1995.1562

44. Suarez DL, Senne DA, Banks J, Brown IH, Essen SC, Lee CW, et al. Recombination resulting in virulence shift in avian influenza outbreak, Chile. Emerg Infect Dis. 2004;10:693–9. http://dx.doi.org/10.3201/eid1004.030396

45. Kapczynski DR, Pantin-Jackwood M, Guzman SG, Ricardez Y, Spackman E, Bertran K, et al. Characterization of the 2012 highly pathogenic avian influenza H7N3 virus isolated from poultry in an outbreak in Mexico: pathobiology and vaccine protection. J Virol. 2013;87:9086–96. http://dx.doi.org/10.1128/JVI.00666-13

46. Pasick J, Handel K, Robinson J, Copps J, Ridd D, Hills K, et al. Intersegmental recombination between the haemagglutinin and matrix genes was responsible for the emergence of a highly pathogenic H7N3 avian influenza virus in British Columbia. J Gen Virol. 2005;86:727–31. http://dx.doi.org/10.1099/vir.0.80478-0

47. Shi J, Deng G, Kong H, Gu C, Ma S, Yin X, et al. H7N9 virulent mutants detected in chickens in China pose an increased threat to humans. Cell Res. 2017;27:1409–21. http://dx.doi.org/10.1038/cr.2017.129

48. Imai M, Watanabe T, Kiso M, Nakajima N, Yamayoshi S, Iwatsuki-Horimoto K, et al. A highly pathogenic avian H7N9 influenza virus isolated from a human is lethal in some ferrets infected via respiratory droplets. Cell Host Microbe. 2017;22:615–626.e8. http://dx.doi.org/10.1016/j.chom.2017.09.008

Address for correspondence: Changwen Ke or Jing Lu, Guangdong Provincial Center for Disease Control and Prevention, 160 Qunxian Rd, Dashi Town, Panyu District, Guangdong Province, Guangzhou 514300, China; email: kecw1965@aliyun.com or jimlu0331@gmail.com

Tuberculosis Treatment Monitoring by Video Directly Observed Therapy in 5 Health Districts, California, USA

Richard S. Garfein, Lin Liu, Jazmine Cuevas-Mota, Kelly Collins, Fatima Muñoz,
Donald G. Catanzaro, Kathleen Moser, Julie Higashi, Teeb Al-Samarrai, Paula Kriner,
Julie Vaishampayan, Javier Cepeda, Michelle A. Bulterys, Natasha K. Martin, Phillip Rios, Fredric Raab

We assessed video directly observed therapy (VDOT) for monitoring tuberculosis treatment in 5 health districts in California, USA, to compare adherence between 174 patients using VDOT and 159 patients using in-person directly observed therapy (DOT). Multivariable linear regression analyses identified participant-reported sociodemographics, risk behaviors, and treatment experience associated with adherence. Median participant age was 44 (range 18–87) years; 61% of participants were male. Median fraction of expected doses observed (FEDO) among VDOT participants was higher (93.0% [interquartile range (IQR) 83.4%–97.1%]) than among patients receiving DOT (66.4% [IQR 55.1%–89.3%]). Most participants (96%) would recommend VDOT to others; 90% preferred VDOT over DOT. Lower FEDO was independently associated with US or Mexico birth, shorter VDOT duration, finding VDOT difficult, frequently taking medications while away from home, and having video-recording problems (p<0.05). VDOT cost 32% (range 6%–46%) less than DOT. VDOT was feasible, acceptable, and achieved high adherence at lower cost than DOT.

Tuberculosis (TB) incidence rates in the United States increased slightly in 2015 after 20 years of decline (1). California has the third-highest TB incidence and the

Author affiliations: University of California San Diego, La Jolla, California, USA (R.S. Garfein, L. Liu, J. Cuevas-Mota, K. Collins, F. Muñoz, J. Cepeda, M.A. Bulterys, N.K. Martin, P. Rios, F. Raab); University of Arkansas, Fayetteville, Arkansas, USA (D.G. Catanzaro); San Diego County Health and Human Services Agency, San Diego, California, USA (K. Moser); San Francisco Department of Public Health, San Francisco, California, USA (J. Higashi); Santa Clara County Public Health Department, San Jose, California, USA (T. Al-Samarrai); Imperial County Public Health Department, El Centro, California, USA (P. Kriner); San Joaquin Public Health Services, Stockton, California, USA (J. Vaishampayan)

most TB cases in the United States (2). Although TB is treatable (3), poor medication adherence leads to ongoing transmission, disease progression, and development of drug-resistant strains. Treating drug-resistant TB requires longer regimens with costlier, more toxic, and less effective drugs, highlighting the need for reliable treatment adherence monitoring (4,5). Strict adherence has become increasingly important because new short-course and intermittent treatment regimens have lower tolerance for adherence gaps (6) and because preventing acquired resistance to new drugs developed to treat multidrug-resistant (MDR) and extensively drug-resistant TB is crucial for preserving gains made in this area (7).

Given the severe consequences of poor adherence, health agencies recommend directly observed therapy (DOT), a process in which healthcare workers or trusted designees watch patients swallow each medication dose (8–10). Although DOT is considered the preferred method for adherence monitoring by health agencies including the World Health Organization (11) and the US Centers for Disease Control and Prevention (12), varying degrees of effectiveness have been reported from delivery of DOT through home visits by DOT workers, patients visiting clinics, and trusted family or community members performing observations (13). Furthermore, the DOT process itself can hinder treatment because of its high cost, personnel requirements, potential for stigma, impact on patient income and mobility, and travel required by patients or healthcare workers (14).

These barriers to DOT prompted some US TB programs to use videoconferencing technology through videophones, computers, or smartphones to remotely observe patients swallowing pills (15,16). This live (synchronous) approach became known as video directly observed therapy (VDOT). Studies of synchronous VDOT indicate that patients adhere to their regimens and mostly prefer VDOT over in-person DOT and that VDOT saves TB programs

money by reducing travel and personnel costs (*17–19*). However, barriers such as limiting observation to business hours, network interruptions, and requirements of the Health Insurance Portability and Accountability Act (HIPAA) prompted development of smartphone applications to enable recorded (asynchronous) VDOT. A pilot study in Kenya provided the first published evidence of asynchronous VDOT's acceptance (*20*). Subsequently, the first study to systematically evaluate asynchronous VDOT among TB patients in San Diego, California, and Tijuana, Mexico, showed that patients and providers found VDOT to be feasible and acceptable, with >95% of expected doses observed, but lacked a comparison group (*21*). We assessed treatment adherence for patients using VDOT versus traditional DOT and evaluated adherence, feasibility, acceptability, and cost differences between urban and rural TB programs.

Methods

Design

We conducted a prospective, multisite, single-arm trial in which all participants had TB treatment monitored using asynchronous VDOT. As a comparator, medical record reviews provided adherence data from a sample of patients who were monitored using in-person DOT at the same clinics. All VDOT participants used DOT for the first 2 weeks or until medication tolerance was established (whichever was longer) before initiating VDOT. Participants continued using VDOT until treatment completion or their provider switched them back to DOT.

A University of California–San Diego Institutional Review Board approved this study, as did each participating health department. Study participation did not affect treatment prescribed by participants' physicians.

Population and Recruitment

The study population consisted of patients receiving DOT for active or suspected pulmonary TB in 3 urban (San Diego, San Francisco, Santa Clara) and 2 rural (San Joaquin, Imperial) California health jurisdictions. Patients ≥18 years of age with no plans to move from the jurisdiction before completing treatment and ≥30 days of treatment remaining were eligible. Patients with MDR TB were eligible; however, only 1.4% of California's TB patients had MDR TB (*22*).

TB program staff recruited patients sequentially during routine DOT visits. Research staff explained VDOT and study procedures to interested patients and obtained written informed consent. Asynchronous VDOT was available only to study participants; patients who declined participation continued treatment through DOT. In San Diego and Santa Clara counties, synchronous VDOT was also offered

to patients who were unsuitable for DOT. Two patients declined to participate before enrollment, and 5 who initially consented withdrew before starting VDOT.

Historical controls (n = 159) were group-matched by age, race or ethnicity, and sex from a random sample of patients at the 5 study sites to obtain estimates of adherence to in-person DOT. To avoid selection bias from using patients who were not offered VDOT, controls were selected from patients who completed TB treatment during the year before asynchronous VDOT introduction at each site.

VDOT Description

The VDOT application (Figure 1) enabled participants to record themselves swallowing each treatment dose and send videos for review by a DOT worker. Each recorded dose was automatically date- and time-stamped, encrypted, and uploaded to a secure server over a cellular or wireless network. Once the data were received by the server, the smartphone application deleted videos from the device to prevent unintentional disclosure of participant information and conserve device memory. Videos were stored on the smartphone in a manner that prevented viewing, editing, resending, or deleting them to protect participant privacy and ensure video fidelity. The asynchronous design allowed participants to take their medications regardless of network connectivity (e.g., while traveling) because videos uploaded automatically whenever cellular or WiFi connections were established. An application status screen allowed participants to see when videos were uploaded or pending. The system sent daily medication reminders by text message or email. Participants were loaned smartphones with cellular data plans to ensure that the application performed identically for all participants and avoided service outages.

TB program staff trained participants to use VDOT during routine clinic or home visits. As with DOT, whenever possible, participants were seen by staff who spoke their preferred language; otherwise, telephone-based translation services were used. Once participants demonstrated VDOT competency, they were given smartphones and instructed to record their next dose alone at the prescribed time. If the participant or DOT worker had concerns about the procedures, the DOT worker kept the phone and repeated the training during subsequent in-person DOT visits; thus, the number of training days could vary by participant. Participants also received a VDOT reference pamphlet. To minimize health risks, participants were instructed to call or visit their healthcare provider before taking medications when side effects occurred, rather than reporting side effects through videos. DOT workers regularly logged onto a password-protected website to view videos and document their observations. If expected videos were missing or videos did not clearly show participants ingesting medications, participants
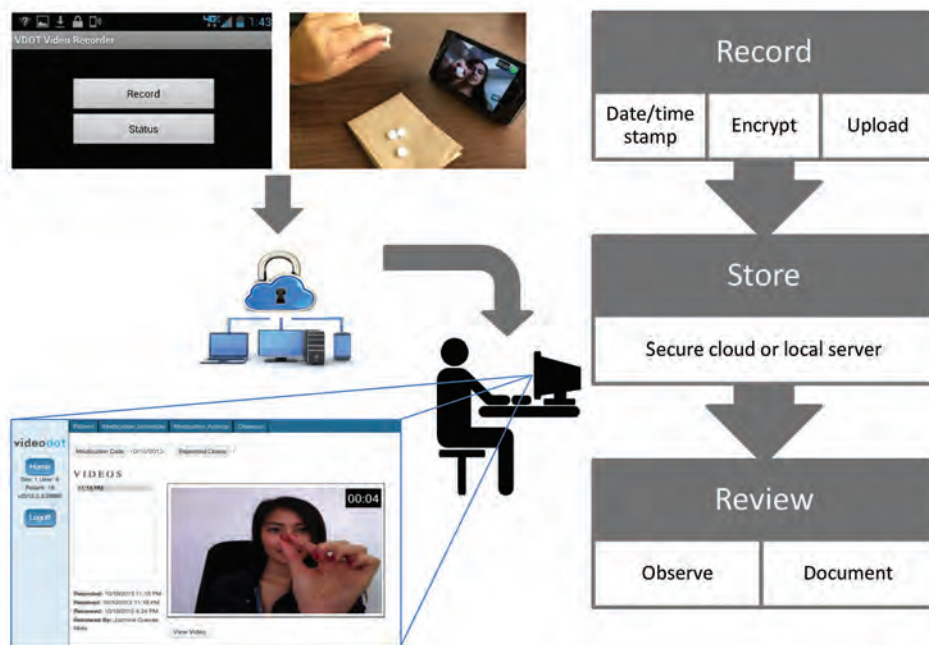
Figure 1. Schematic of asynchronous VDOT in a study assessing VDOT for monitoring tuberculosis treatment, 5 California health districts, 2015–2016. Patients use VDOT smartphone application to record a video of themselves ingesting their medications. After recording stops, the application encrypts the video and transfers it through a cellular or Wi-Fi connection to a server for storage and playback. On a routine basis, treatment monitors log into a secure website to view each video and document their observations. Missing videos or videos not showing complete dose ingestion trigger follow-up procedures to investigate missed doses and provide patient support as needed. VDOT, video directly observed therapy.

were contacted to identify problems and provide support as needed. Decisions about returning participants to DOT were made on a case-by-case basis rather than by using strict adherence-based criteria because some missed doses were unavoidable and requiring DOT for participants who could not meet in-person might adversely affect adherence. Routine medication refill and health monitoring visits occurred per standards of care.

Data Collection

We conducted brief (15–20 minute) baseline (before initiating VDOT) and follow-up (after ending VDOT) telephone interviews to assess sociodemographic variables, experience using mobile technology, TB history and risk factors, privacy concerns, and perceptions of TB treatment monitoring. Research staff, rather than care providers, conducted interviews to minimize response bias. Participants received $10 USD for each interview; no remuneration was paid for sending videos.

To measure treatment adherence among control patients, TB program staff reviewed their DOT records abstracting treatment start and end dates; DOT start and end dates; treatment outcome; and the number of doses expected, observed, and unobserved (i.e., self-administered, not taken, or treatment suspended). DOT was predominantly community-based and required staff travel; however, San Francisco also offered clinic-based DOT to patients who could conveniently access the clinic. Nonclinical personnel conducted most DOT visits; nurses also provided some DOT based on clinical needs and staffing considerations. Control patients were not interviewed.

VDOT versus DOT

Because VDOT was introduced after participants had initiated treatment using DOT, we calculated the fraction of expected doses observed (FEDO) while the patient was on VDOT as a measure of adherence. FEDO equals the number of observed doses divided by the sum of observed doses, missed doses, and self-administered doses. For each day that medication doses were expected, DOT workers documented whether they observed all, some, or no pills being ingested. For this analysis, doses were only considered observed if all pills were taken. If no video was received or ingestion of fewer than all pills was observed, the dose was considered missed, as were self-administered doses. Because weekend doses are not ordinarily observed in DOT, they were excluded from this calculation. FEDO was calculated for VDOT and control patients. Adherence (doses observed divided by total doses prescribed) was also computed for control patients because they used DOT throughout their treatment.

Cost Analysis

Employing a healthcare provider perspective, we used an ingredients-based, bottom-up approach (*23,24*) to estimate the average per-patient cost of a standard, Centers for Disease Control and Prevention–recommended (*3*), 6-month treatment regimen for drug-susceptible TB using DOT or VDOT. Because the likelihood of medication side effects differs between the intensive (56 daily doses) and continuation (126 daily doses) phases of treatment, costs were stratified by treatment phase and then summed to calculate the overall average patient treatment cost. Nurses from 4

sites completed a standardized questionnaire assessing personnel time, personnel salaries, and resources required to administer DOT and VDOT. Staff turnover precluded data collection from the fifth site. Completed questionnaires were discussed jointly by teleconference to ensure that all sites interpreted the questions and responded uniformly. Cost data were collected during March–June 2017 and presented in 2017 USD.

DOT personnel costs included time for patient contact, administrative tasks, and travel. VDOT personnel costs included time for community-based visits before initiating VDOT, patient VDOT training, administrative tasks, video observation, and follow-up when expected videos were not received. Some in-person observations also occurred among patients using VDOT because all patients received DOT for >2 weeks before starting VDOT and patients in San Francisco were observed in-person during weekly medication refill visits to the clinic. We converted annual salaries, including fringe benefits, into an hourly rate, assuming a 40-hour workweek. All personnel reported full-time employment. The total time for each DOT-related task (administrative, patient contact, and travel) needed to treat each patient was multiplied by the hourly rate and then summed for all personnel.

To calculate an overall per-patient travel cost, we multiplied the average number of miles per patient visit and total number of in-person visits by the current federal mileage reimbursement rate ($0.54 per mile). This approach conservatively estimated travel costs because it assumed that DOT workers used personal vehicles rather than costlier county-owned vehicles. Because DOT workers often visited multiple patients in a single outing rather than returning to the health department between each patient visit, we calculated the average number of miles per visit by dividing the average number of miles driven per day for DOT-related activities by the average number of in-person visits on any given day.

Corporate prices paid by the investigators for smartphones ($100) and service plans ($54/month) during the study were applied to all sites. An estimated VDOT application cost of $35/month/patient was applied on the basis of products commercially available at the time this article was written. Costs of antibiotics, laboratory tests, chest radiographs, and clinical examinations were excluded because they were assumed to be equivalent for VDOT and DOT.

Statistical Analysis

We used Kruskal-Wallis and Fisher exact tests to determine differences in sociodemographic characteristics, TB history, TB risk factors, and VDOT perception variables across study sites. We assessed associations between FEDO and independent variables by using Kruskal-Wallis tests (categorical variables), Wilcoxon rank sum tests (binary variables), and Spearman correlation coefficients (continuous variables). We used simple linear regression to identify factors associated with FEDO and considered significant variables ($p<0.15$) for inclusion in multivariable linear regression analysis. We used backward stepwise elimination to remove nonsignificant variables until only variables with $p<0.05$ remained in the final model and assessed normal assumption of residuals by using normal probability plot, and influential observations were assessed by residuals and Cook's distance. We performed Wilcoxon rank sum tests to compare FEDO between VDOT and DOT and used R statistical software (25) to conduct analyses.

Results

Participant Characteristics and VDOT Perceptions

Overall, 274 participants (248 urban and 26 rural) enrolled during October 2014–October 2015 contributed adherence and baseline interview data (Table 1). Median participant age was 44 (range 18–87) years; 61% were male, 57% were Asian, 30% were Hispanic or Latino, and 7% were white. Most (67%) were born in other countries (predominantly countries in Asia), followed by the United States (17%) and Mexico (16%). Education and income were low overall, but most participants had health insurance. Most participants (90%) owned cell phones; 72% owned smartphones. Substance use, other than smoking (42%), was uncommon, and no participants were homeless. Only race or ethnicity, education level, and country of birth differed across sites ($p<0.05$).

We obtained VDOT observation data from the 274 enrolled participants, 214 (78%) of whom completed follow-up interviews (Table 2). Twenty-seven percent of participants reported not sharing their VDOT experience with family members, and 66% did not share with others. Although 34% disclosed having concerns about being seen recording VDOT videos, only 8% failed to record >1 dose because of privacy concerns. At follow-up, only 2% of participants thought VDOT was less confidential than DOT, and 96% reported that VDOT was "very or somewhat easy to perform"; only 3% would choose DOT over VDOT if they had to repeat treatment, and 96% would recommend VDOT to other patients. Training VDOT procedures to participants took a median of 1 day across sites; 74% of participants required 1 day, whereas 4% needed ≥4 days (data not shown). Only 12 (4.4%) participants were returned to DOT before completing treatment because of poor adherence (n = 5), a lost or broken phone (n = 4), or technical or connectivity problems (n = 3).

FEDO by Treatment Monitoring Method

Study participants used VDOT a median of 5.4 months (interquartile range [IQR] 3.5–7.1 months), generating 42,211

Table 1. Baseline characteristics of patients participating in a study assessing VDOT for monitoring tuberculosis treatment, by site, 5 California health districts, 2015–2016*

Characteristic	Total	San Diego	San Francisco	Santa Clara	Imperial	San Joaquin	p value†
No. patients	272	99	99	49	10	15	
Age, y							
Mean (SD)	43.8 (16.5)	42.0 (16.9)	46.5 (15.5)	42.2 (16.2)	46.6 (22.0)	41.7 (16.1)	0.19
Range	18–87	18–87	24–86	21–83	21–69	21–76	
Education							
≤Primary school	26 (10)	10 (10)	12 (12)	3 (6)	1 (10)	0	0.02
High school	105 (39)	39 (40)	39 (40)	13 (27)	5 (50)	9 (60)	
Some college or technical school	67 (25)	25 (26)	17 (18)	15 (31)	4 (40)	6 (40)	
≥Bachelor's degree	71 (26)	24 (24)	29 (30)	18 (37)	0	0	
Sex							
M	167 (61)	59 (60)	61 (62)	34 (69)	5 (50)	8 (53)	0.65
F	105 (39)	40 (40)	38 (38)	15 (31)	5 (50)	7 (47)	
Race or ethnicity							
Asian	154 (57)	41 (41)	68 (69)	37 (76)	10 (10)	7 (47)	<0.001
Caucasian or white	19 (7)	7 (7)	7 (7)	1 (2)	0	4 (27)	
Hispanic or Latino	82 (30)	42 (42)	21 (21)	6 (12)	9 (90)	4 (27)	
Other‡	17 (6)	9 (9)	3 (3)	5 (10)	0	0	
Country of birth							
United States	47 (17)	22 (22)	9 (9)	4 (8)	4 (40)	8 (53)	<0.001
Mexico	44 (16)	26 (26)	7 (7)	5 (10)	5 (50)	1 (7)	
Other§	181 (67)	51 (52)	83 (84)	40 (82)	1 (10)	6 (40)	
Annual household income, USD							
<10,000	110 (44)	43 (46)	43 (47)	13 (29)	6 (55)	8 (57)	0.09
10,000–30,000	74 (30)	24 (28)	29 (32)	15 (33)	3 (27)	3 (21)	
30,000–50,000	26 (10)	13 (15)	9 (10)	2 (4)	0 (0)	2 (14)	
>50,000	39 (16)	10 (11)	11 (12)	15 (33)	2 (18)	1 (7)	
Had health insurance, yes vs. no	229 (85)	76 (78)	85 (86)	43 (90)	10 (91)	15 (100)	0.12
Owned cell phone, yes vs. no	247 (90)	90 (91)	92 (93)	44 (90)	9 (82)	12 (80)	0.33
Owned smartphone, yes vs. no	196 (72)	71 (72)	67 (68)	41 (84)	7 (64)	10 (67)	0.26
Homeless, yes vs. no¶	0	0	0	0	0	0	NA
Ever smoked cigarettes, yes vs. no	116 (42)	43 (43)	41 (41)	17 (35)	7 (64)	8 (53)	0.41
Marijuana use, yes vs. no¶	18 (7)	5 (5)	7 (7)	2 (4)	2 (18)	2 (13)	0.26
Noninjection drug use, yes vs. no¶	4 (1)	1 (1)	2 (2)	1 (2)	0	0	1
Ever injection drug use, yes vs. no	3 (1)	1 (1)	0	1 (2)	1 (9)	0	0.07

*Values are no. (%) participants unless otherwise indicated. VDOT, video directly observed therapy; NA, not applicable.
†p values based on Fisher exact test or Kruskal-Wallis test. Variable totals might not sum to column totals because of missing data.
‡Other race group includes African American (n = 3), American Indian (n = 2), Pacific Islander (n = 1), and mixed and other races (n = 11).
§Other countries were predominantly in Asia.
¶Referent period is the previous 6 months.

videos (Table 2). Median FEDO was 93.0% (IQR 83.4%–97.1%), compared with 66.4% (IQR 55.1%–89.3%) for control patients using only DOT (Figure 2). By contrast, median adherence was 100% (IQR 97.0%–100%) for control patients because of an unwavering commitment by TB program staff to ensure patients completed their treatment.

Correlates of FEDO

Median FEDO differed across individual sites (range 84.5%–96.1%; p<0.001); however, the extreme values occurred in the 2 rural sites (Table 2). Thus, FEDO did not differ between the combined urban and rural sites (92.8% vs. 94.2%; p = 0.51) in bivariate analysis (Table 3, https://wwwnc.cdc.gov/EID/article/24/10/18-0459-T3.htm). FEDO differed by race or ethnicity and country of birth, increased with longer VDOT use and higher annual income, and decreased with marijuana use in the prior 6 months. Participants who found VDOT more difficult, more often

took medications while away from home, more often had problems using the VDOT application, and more often had problems uploading videos because of poor network connectivity had lower FEDOs.

In multivariable analysis (Table 4), higher FEDO was independently associated with longer duration of VDOT use. Lower FEDO was associated with birth in Mexico or the United States compared with other countries; feeling VDOT was somewhat or very difficult compared with very easy; taking medication away from home most or every time compared with never; and having problems using VDOT more than half the time compared with "never."

VDOT versus DOT Costs

The estimated cost for monitoring a 6-month treatment regimen using VDOT (Table 5) varied by site (range $3,031–$3,911) and was 6%–46% cheaper than community-based

DOT (range $3,212–$5,788) across sites. Reduced personnel costs drove savings, which offset smartphone-related costs.

Discussion

VDOT was feasible and acceptable for monitoring TB medication ingestion in urban and rural California health districts. A higher proportion of expected doses was observed as scheduled among VDOT participants than among in-person DOT participants, resulting in shorter treatment duration.

Median FEDO for VDOT was lower than previously reported (95%) (21), possibly because the earlier study oversampled low-risk patients during the first trial of the VDOT application. Alternatively, the disparity could be attributable to our conservative approach to calculating

Table 2. Reported experiences of patients participating in a study assessing VDOT for monitoring tuberculosis treatment, by site, 5 California health districts, 2015–2016*

Characteristic	Total	Site					p value†
		San Diego	San Francisco	Santa Clara	Imperial	San Joaquin	
No. patients	274‡	100	99	49	11	15	
VDOT use							
Months on VDOT, median (IQR)	5.4 (3.5–7.1)	5.2 (3.2–6.3)	5.4 (3.5–7.3)	5.5 (4.1–8.1)	4.0 (2.1–5.6)	6.1 (4.4–7.7)	0.08
FEDO, median (SD), IQR	93.0 (13.5), 83–97	88.7 (15.1), 77–94	95.5 (11.8), 87–98	95.2 (10.3), 89–98	84.5 (20.0), 78–94	96.1 (7.9), 93–98	<0.001
No. patients in follow-up interviews	214	74	84	39	9	7	
Tuberculosis and treatment perceptions							
Did you share your VDOT experience with family members?							
Yes	156 (73)	55 (74)	55 (66)	30 (77)	9 (100)	6 (86)	0.18
No	58 (27)	19 (26)	29 (34)	9 (23)	0	1 (14)	
Did you share your VDOT experience with friends, neighbors, classmates, or coworkers?							
Yes	73 (34)	24 (32)	28 (33)	13 (33)	3 (33)	5 (71)	0.38
No	141 (66)	50 (68)	57 (67)	26 (67)	6 (67)	2 (29)	
Were you concerned someone would see you using the VDOT cell phone?							
Yes	73 (34)	19 (26)	34 (40)	15 (38)	4 (44)	1 (14)	0.23
No	141 (66)	55 (74)	51 (60)	24 (62)	5 (56)	6 (86)	
Did you ever fail to record a video because you were worried someone was watching you?							
Yes	18 (8)	7 (9)	9 (11)	2 (5)	0	0	0.87
No	196 (92)	67 (91)	76 (89)	37 (95)	9 (100)	7 (100)	
Confidentiality of VDOT vs. DOT?							
More	146 (70)	49 (67)	55 (66)	30 (77)	7 (78)	5 (83)	0.68
Less	5 (2)	2 (3)	1 (1)	2 (5)	0	0	
Same	59 (28)	22 (30)	27 (33)	7 (18)	2 (22)	1 (17)	
VDOT experience							
Overall, how easy/difficult did you find the VDOT process?							
Very easy	174 (81)	58 (78)	68 (79)	36 (92)	6 (67)	6 (86)	0.19
Somewhat easy	32 (15)	14 (19)	13 (15)	3 (8)	1 (11)	1 (14)	
Somewhat or very difficult	9 (4)	2 (3)	5 (6)	0	2 (22)	0	
If you had to redo tuberculosis treatment, would you choose VDOT or DOT?							
VDOT	192 (90)	67 (92)	75 (87)	35 (90)	9 (100)	6 (86)	
DOT	6 (3)	1 (1)	4 (5)	1 (3)	0	0	0.9
No preference	16 (7)	5 (7)	7 (8)	3 (8)	0	1 (14)	
Would you recommend VDOT to other tuberculosis patients?							
Yes	202 (96)	70 (95)	81 (96)	35 (97)	9 (100)	7 (100)	0.95
No	8 (4)	4 (5)	3 (4)	1 (3)	0	0	
How often did you take tuberculosis medication away from home?							
Never or rarely	120 (56)	39 (53)	54 (64)	19 (49)	5 (56)	3 (43)	0.36
Less than half or half the time	48 (22)	18 (24)	12 (14)	13 (33)	2 (22)	3 (43)	
Most of the time or every time	46 (21)	17 (23)	19 (22)	7 (18)	2 (22)	1 (14)	
How often did you have problems using the VDOT application?							
Never	82 (38)	24 (32)	41 (48)	16 (41)	1 (11)	0	0.06
Rarely	99 (46)	35 (47)	33 (39)	20 (51)	5 (56)	6 (86)	
Less than half the time	23 (11)	9 (12)	9 (11)	2 (5)	2 (22)	1 (14)	
Half the time or more	10 (5)	6 (8)	2 (2)	1 (3)	1 (11)	0	
How often did poor reception cause you problems uploading videos?							
Never	65 (31)	13 (18)	34 (40)	12 (31)	3 (33)	3 (43)	
Rarely	103 (49)	41 (56)	35 (42)	20 (51)	3 (33)	4 (57)	0.15
Less than half the time	24 (11)	11 (15)	7 (8)	3 (8)	3 (33)	0	
Half the time or more	20 (9)	8 (11)	8 (10)	4 (10)	0	0	

*Values are no. (%) participants unless otherwise indicated. DOT, directly observed therapy; FEDO, fraction of expected doses observed = number of complete doses observed via VDOT divided by the number of doses expected; IQR, interquartile range; VDOT, video directly observed therapy.
†p values based on Fisher exact test or Kruskal-Wallis test. Variable totals might not sum to column totals because of missing data.
‡Includes 2 participants who used VDOT but had missing baseline interview data.
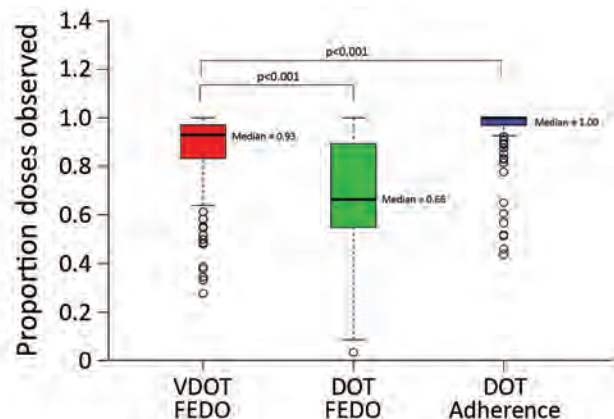
Figure 2. FEDO among patients monitored ingesting medication for tuberculosis by VDOT compared with FEDO and adherence for patients monitored using in-person DOT in a study assessing VDOT for monitoring tuberculosis treatment, 5 California health districts, 2015–2016. FEDO assessed by number of complete doses observed through VDOT divided by the number of doses expected. Adherence assessed by number of doses observed through DOT divided by the number of prescribed doses. Because missed or self-administered doses had to be rescheduled, the number of times a dose was expected could exceed the number of doses prescribed. DOT, directly observed therapy; FEDO, fraction of expected doses observed; VDOT, video directly observed therapy.

FEDO by only counting doses when all pills were taken and treating all doses as missed when a software error caused 5% of videos received to be unviewable. If unviewable videos and partial doses were counted as observed, FEDO in our study (median 96.4%, IQR 89%–99%) would have matched the prior study.

Defining eligibility criteria for VDOT a priori appears unnecessary. Despite efforts to define VDOT eligibility criteria using these data, only 1 variable known before treatment (country of birth) was associated with FEDO. DOT

studies similarly found few predictors of adherence (*26*). Initial concerns about older patients or those unfamiliar with smartphones having difficulty using VDOT were unfounded because these factors did not predict FEDO. Travel was also not problematic; study staff often reported that patients who traveled or had nontraditional work hours could adhere better after switching to VDOT. Monitoring anti-TB therapy involves ongoing communication, negotiation, and cooperation between patients and healthcare providers (*27*,*28*), and patient-centered care increased when patients had VDOT as an option. Other than ensuring that patients could tolerate their medications, operate the VDOT application, and access smartphones and service, no evidence was found to support requiring other eligibility criteria.

We observed an association between VDOT problems and lower FEDO, which was driven by only 10 participants who reported having problems half the time or more. Similarly, the association between FEDO and difficulty using VDOT resulted from 9 participants reporting that VDOT was somewhat or very difficult. However, most of these participants encountered the software error described previously, which lowered their FEDO and could explain why they felt VDOT was difficult. Lower FEDO among participants taking medications away from home most or every time could be attributable to difficulty finding a private location to make videos while away from home, which might have also made DOT difficult.

Unlike DOT or synchronous VDOT, asynchronous VDOT enabled patients to take medications outside normal business hours (e.g., at mealtimes or bedtime), which could minimize side effects and improve adherence (*16*). VDOT also allowed participants to fast during religious holidays, because medication doses could be observed at night after fasting ended. Avoiding intermittent dosing by allowing observations after hours and on weekends and holidays through VDOT could also improve treatment efficacy (*29*).

Table 4. Multivariable linear regression analysis of factors associated with FEDO among patients treated for tuberculosis, 5 California health districts, 2015–2016*

Characteristic	Beta coefficient	SE	p value
Months on VDOT (per month)	0.008	0.003	0.01
Country of birth (referent: other)			
Mexico	−0.095	0.022	<0.001
United States	−0.048	0.022	0.03
Perceived ease or difficulty of VDOT (referent: very easy)			
Somewhat easy	−0.003	0.024	0.90
Somewhat or very difficult	−0.130	0.042	0.002
Took medications while away from home (referent: never or rarely)			
Less than half or half the time	−0.004	0.020	0.83
Most of the time or always	−0.049	0.021	0.02
Had problems using the VDOT application (referent: never)			
Rarely	−0.001	0.018	0.97
Less than half the time	−0.040	0.029	0.16
More than half the time	−0.220	0.041	<0.001

*FEDO, fraction of expected doses observed = number of complete doses observed through VDOT divided by the number of doses expected; VDOT, video directly observed therapy.

Table 5. Average in-person DOT and VDOT costs per treatment course, by site, based on standard drug-susceptible tuberculosis treatment regimen consisting of 56 intensive-phase and 126 continuation-phase doses, 4 California health districts, 2015–2016*

Characteristic	San Diego	San Francisco	San Joaquin	Imperial
In-person DOT costs				
Personnel				
Administrative tasks	1,038	3,043	1,913	842
In-person patient contact	1,207	622	2,223	656
Travel	1,939	1,065	702	1,293
Total personnel (% of total)	4,185 (91)	4,729 (97)	4,838 (84)	2,791 (87)
Mileage (% of total)	364 (9)	158 (3)	950 (16)	421 (13)
Grand total	4,549	4,888	5,788	3,212
VDOT costs				
Personnel				
Administrative tasks	796	1,922	1,771	1,183
In-person patient contact	671	291	393	346
Watching videos	80	131	152	473
Other, e.g., training and follow-up	869	933	156	348
Total personnel (% of total)	2,526 (79)	3,277 (88)	2,472 (83)	2,350 (78)
Mileage (% of total)	20 (1)	0	31 (1)	46 (2)
Smartphone costs, device and service (% of total)	424 (13)	424 (7)	424 (8)	424 (14)
VDOT application service fee, $35/mo/patient (% of total)	210 (7)	210 (5)	210 (7)	210 (7)
Grand total	3,179	3,911	3,137	3,031
% Change for VDOT versus in-person DOT				
Personnel costs, %	−40	−31	−49	−16
Overall costs, %	−30	−20	−46	−6

*All values are USD unless otherwise indicated. Comparable data could not be obtained from the Santa Clara site because of staff turnover. DOT, directly observed therapy; VDOT, video directly observed therapy.

All sites, except 1, included participants with MDR TB (VDOT duration range 30–537 days) whose adherence was comparable to the cohort overall. Because MDR tuberculosis patients at times require dosing more than once daily, VDOT reduced stress on the TB programs and facilitated quicker return to daily activities for patients on these much longer regimens. Additionally, asynchronous VDOT does not require consistent network connectivity, making it useful for patients in remote areas.

Although asynchronous VDOT offers greater flexibility and reduces self-administered doses, DOT and synchronous VDOT might allow more frequent patient–provider interaction and facilitate patient support. However, asynchronous VDOT could improve case management efficiency by shifting the focus of in-person visits from treatment monitoring, perceived by patients as punitive (30,31), to patient care, support, and other key TB program activities such as contact tracing. The appropriate mix of remote monitoring and direct interaction to support patients throughout treatment remains to be determined with further research. Cost-effectiveness studies are also needed to inform policies around treatment monitoring.

TB risk factors were self-reported and could be underestimated if participants chose not to disclose stigmatized behaviors. Because no patients were homeless, we could not examine this risk factor. Three sites (Santa Clara, Imperial and San Joaquin) had never used asynchronous VDOT previously, potentially promoting conservative patient selection; however, their results were similar to sites with VDOT experience. In addition, San Francisco differed from the other sites by requiring weekly, rather than monthly, refill visits, which could have increased adherence; however, adherence was comparable across sites. Because providers could switch participants from VDOT back to DOT, observed FEDOs could have been skewed upward if nonadherent participants were removed from VDOT early. However, only 12 (4.3%) participants returned to DOT before completing treatment, of whom only 5 did so because of poor adherence. Removing these participants had little effect on FEDO overall. This study was conducted in a high-income country and might not reflect VDOT performance in low- and middle-income countries.

To our knowledge, our study is the largest prospective study of asynchronous VDOT to date. Patients with TB treatment monitored by VDOT had more expected medication doses observed than patients monitored using DOT. VDOT performed similarly in urban and rural health departments, with high observation rates and positive patient perceptions across sites. Although some participants returned to DOT, most were effectively monitored to completion by using VDOT. VDOT reduced TB-control program costs compared with DOT. Other than country of birth, patient characteristics did not predict adherence, suggesting that TB-control programs could offer VDOT broadly and provide additional support, or switch to DOT if adherence declines rather than restricting VDOT use to patients with prespecified characteristics. Asynchronous VDOT was found to be a cost-effective method of monitoring TB treatment in the United States; however, similar studies are needed in countries with high burdens of TB

and limited resources, where smartphone penetration and cultural acceptance of transmitting personal images over the Internet could differ.

About the Author

Dr. Garfein is an infectious disease epidemiologist at the USCD School of Medicine. His research focuses on the epidemiology and prevention of tuberculosis, HIV, and viral hepatitis among vulnerable populations. His research interests also include developing and evaluating interventions that support efforts to eliminate tuberculosis and other treatable diseases.

References

1. Salinas JL, Mindra G, Haddad MB, Pratt R, Price SF, Langer AJ. Leveling of tuberculosis incidence—United States, 2013-2015. MMWR Morb Mortal Wkly Rep. 2016;65:273–8. http://dx.doi.org/10.15585/mmwr.mm6511a2

2. Schmit KM, Wansaula Z, Pratt R, Price SF, Langer AJ. Tuberculosis - United States, 2016. MMWR Morb Mortal Wkly Rep. 2017;66:289–94. http://dx.doi.org/10.15585/mmwr.mm6611a2

3. Nahid P, Dorman SE, Alipanah N, Barry PM, Brozek JL, Cattamanchi A, et al. Official American Thoracic Society/Centers for Disease Control and Prevention/Infectious Diseases Society of America Clinical Practice Guidelines: Treatment of Drug-Susceptible Tuberculosis. Clin Infect Dis. 2016;63:e147–95. http://dx.doi.org/10.1093/cid/ciw376

4. Gandhi NR, Nunn P, Dheda K, Schaaf HS, Zignol M, van Soolingen D, et al. Multidrug-resistant and extensively drug-resistant tuberculosis: a threat to global control of tuberculosis. Lancet. 2010;375:1830–43. http://dx.doi.org/10.1016/S0140-6736(10)60410-2

5. Falzon D, Gandhi N, Migliori GB, Sotgiu G, Cox HS, Holtz TH, et al.; Collaborative Group for Meta-Analysis of Individual Patient Data in MDR-TB. Resistance to fluoroquinolones and second-line injectable drugs: impact on multidrug-resistant TB outcomes. Eur Respir J. 2013;42:156–68. http://dx.doi.org/10.1183/09031936.00134712

6. Mitnick CD, McGee B, Peloquin CA. Tuberculosis pharmacotherapy: strategies to optimize patient care. Expert Opin Pharmacother. 2009;10:381–401. http://dx.doi.org/10.1517/14656560802694564

7. Conradie F, Diacon A, Everitt D, Mendel C, Van Niekerk C, Howell P, et al. The NIX-TB trial of pretomanid, bedaquiline and linezolid to treat XDR-TB. Conference on Retroviruses and Opportunistic Infections; Seattle, Washington, USA; February 13–16, 2017 [cited 2018 Jul 27]. http://www.croiconference.org/sessions/nix-tb-trial-pretomanid-bedaquiline-and-linezolid-treat-xdr-tb

8. Frieden TR, Sbarbaro JA. Promoting adherence to treatment for tuberculosis: the importance of direct observation. World Hosp Health Serv. 2007;43:30–3.

9. Migliori GB, Zellweger JP, Abubakar I, Ibraim E, Caminero JA, De Vries G, et al. European union standards for tuberculosis care. Eur Respir J. 2012;39:807–19. http://dx.doi.org/10.1183/09031936.00203811

10. World Health Organization. Global tuberculosis control: a short update to the 2009 report [cited 2018 Jul 27]. http://www.who.int/iris/handle/10665/44241

11. World Health Organization. Multidrug and extensively drug-resistant TB (M/XDR-TB): 2010 global report on surveillance and response [cited 2018 Jul 27]. http://www.who.int/tb/features_archive/m_xdrtb_facts/en

12. Centers for Disease Control and Prevention. Treatment for TB disease [cited 2018 Jul 27]. https://www.cdc.gov/tb/topic/treatment/tbdisease.htm

13. Volmink J, Garner P. Directly observed therapy for treating tuberculosis. Cochrane Database Syst Rev. 2007;4:CD003343.

14. Pope DS, Chaisson RE. TB treatment: as simple as DOT? Int J Tuberc Lung Dis. 2003;7:611–5.

15. DeMaio J, Schwartz L, Cooley P, Tice A. The application of telemedicine technology to a directly observed therapy program for tuberculosis: a pilot project. Clin Infect Dis. 2001;33:2082–4. http://dx.doi.org/10.1086/324506

16. Wade VA, Karnon J, Eliott JA, Hiller JE. Home videophones improve direct observation in tuberculosis treatment: a mixed methods evaluation. PLoS One. 2012;7:e50155. http://dx.doi.org/10.1371/journal.pone.0050155

17. Mirsaeidi M, Farshidpour M, Banks-Tripp D, Hashmi S, Kujoth C, Schraufnagel D. Video directly observed therapy for treatment of tuberculosis is patient-oriented and cost-effective. Eur Respir J. 2015;46:871–4. http://dx.doi.org/10.1183/09031936.00011015

18. Center for Connected Health Policy. Using telehealth for directly observed therapy in treating tuberculosis [cited 2018 Jul 27]. http://www.cchpca.org/using-telehealth-directly-observed-therapy-treating-tuberculosis

19. Chuck C, Robinson E, Macaraig M, Alexander M, Burzynski J. Enhancing management of tuberculosis treatment with video directly observed therapy in New York City. Int J Tuberc Lung Dis. 2016;20:588–93. http://dx.doi.org/10.5588/ijtld.15.0738

20. Hoffman JA, Cunningham JR, Suleh AJ, Sundsmo A, Dekker D, Vago F, et al. Mobile direct observation treatment for tuberculosis patients: a technical feasibility pilot using mobile phones in Nairobi, Kenya. Am J Prev Med. 2010;39:78–80. http://dx.doi.org/10.1016/j.amepre.2010.02.018

21. Garfein RS, Collins K, Muñoz F, Moser K, Cerecer-Callu P, Raab F, et al. Feasibility of tuberculosis treatment monitoring by video directly observed therapy: a binational pilot study. Int J Tuberc Lung Dis. 2015;19:1057–64. http://dx.doi.org/10.5588/ijtld.14.0923

22. California Department of Public Health. Report on tuberculosis in California, 2016 [cited 2018 Jul 27]. https://www.cdph.ca.gov/Programs/CID/DCDC/CDPH%20Document%20Library/TBCB_Report_2016.pdf

23. Drummond MF, Sculpher MJ, Claxton K, Stoddart GL, Torrance GW. Methods for the economic evaluation of health care programmes. 4th ed. Oxford: Oxford University Press; 2015.

24. Chapko MK, Liu CF, Perkins M, Li YF, Fortney JC, Maciejewski ML. Equivalence of two healthcare costing methods: bottom-up and top-down. Health Econ. 2009;18:1188–201. http://dx.doi.org/10.1002/hec.1422

25. R Core Team. R: A language and environment for statistical computing [cited 2018 Jul 27]. https://www.R-project.org

26. Hirsch-Moverman Y, Daftary A, Franks J, Colson PW. Adherence to treatment for latent tuberculosis infection: systematic review of studies in the US and Canada. Int J Tuberc Lung Dis. 2008;12:1235–54.

27. Zhang H, Ehiri J, Yang H, Tang S, Li Y. Impact of community-based DOT on tuberculosis treatment outcomes: a systematic review and meta-analysis. PLoS One. 2016;11:e0147744. http://dx.doi.org/10.1371/journal.pone.0147744

28. Karumbi J, Garner P. Directly observed therapy for treating tuberculosis. Cochrane Database Syst Rev. 2015;5:CD003343.

29. Kasozi S, Clark J, Doi SA. Intermittent versus daily pulmonary tuberculosis treatment regimens: a meta-analysis. Clin Med Res. 2015;13:117–38. http://dx.doi.org/10.3121/cmr.2015.1272

30. Queiroz EM, De-La-Torre-Ugarte-Guanilo MC, Ferreira KR, Bertolozzi MR. Tuberculosis: limitations and strengths of directly observed treatment short-course. Rev Lat Am Enfermagem. 2012;20:369–77. http://dx.doi.org/10.1590/S0104-11692012000200021

31. Sagbakken M, Frich JC, Bjune GA, Porter JD. Ethical aspects of directly observed treatment for tuberculosis: a cross-cultural comparison. BMC Med Ethics. 2013;14:25. http://dx.doi.org/10.1186/1472-6939-14-25

Address for correspondence: Richard S. Garfein, University of California, San Diego, 9500 Gilman Dr, MC-0725, La Jolla, CA 92093-0507, USA; email: rgarfein@ucsd.edu

March 2017: **Tuberculosis and Mycobacteria**

https://wwwnc.cdc.gov/eid/articles/issue/23/3/table-of-contents

EMERGING INFECTIOUS DISEASES

Candida auris in Healthcare Facilities, New York, USA, 2013–2017

Eleanor Adams, Monica Quinn, Sharon Tsay, Eugenie Poirot, Sudha Chaturvedi, Karen Southwick, Jane Greenko, Rafael Fernandez, Alex Kallen, Snigdha Vallabhaneni, Valerie Haley, Brad Hutton, Debra Blog, Emily Lutterloh, Howard Zucker; *Candida auris* Investigation Workgroup[1]

Candida auris is an emerging yeast that causes healthcare-associated infections. It can be misidentified by laboratories and often is resistant to antifungal medications. We describe an outbreak of *C. auris* infections in healthcare facilities in New York City, New York, USA. The investigation included laboratory surveillance, record reviews, site visits, contact tracing with cultures, and environmental sampling. We identified 51 clinical case-patients and 61 screening case-patients. Epidemiologic links indicated a large, interconnected web of affected healthcare facilities throughout New York City. Of the 51 clinical case-patients, 23 (45%) died within 90 days and isolates were resistant to fluconazole for 50 (98%). Of screening cultures performed for 572 persons (1,136 total cultures), results were *C. auris* positive for 61 (11%) persons. Environmental cultures were positive for samples from 15 of 20 facilities. Colonization was frequently identified during contact investigations; environmental contamination was also common.

*C*andida auris is an emerging yeast that has caused healthcare-associated infections on multiple continents (*1–13*). The organism was first described in 2009 by Satoh et al. for a patient in Japan (*14*). In November 2016, Vallabhaneni et al. (*11*) reported cases in the United States. Identification of *C. auris* requires specialized laboratory techniques (*15–17*). It is often resistant to antifungal

medications (*18*), causes invasive infections (*1,4,5*) and outbreaks (*8,10*), and has become endemic to hospitals in some parts of the world (*2,5,6*). Therefore, its detection in New York, USA, healthcare facilities is concerning. We describe an ongoing outbreak of healthcare-associated *C. auris* cases involving multiple healthcare facilities in New York City (NYC), New York, USA, during 2013–2017.

Methods

Definitions and Data Analysis
We defined a case-patient as a person for whom a culture was positive for *C. auris*. Clinical cases are those for which the culture was obtained to diagnose or treat disease; screening cases are those for which the culture was obtained for surveillance purposes. We defined contacts as persons who had an epidemiologic link to a case-patient in place or time. We included clinical cases reported by April 30, 2017. Because surveillance cultures of contacts are performed after an associated clinical case is reported, we included surveillance cultures that were collected by June 26, 2017, and had final results available by July 19, 2017, which enabled us to better approximate the number of screening cases associated with clinical cases described herein. Data were analyzed by using SAS 9.4 (SAS Institute, Cary, NC, USA) and Excel 2016 (Microsoft, Redmond, WA, USA).

Case Finding and Investigation
In June 2016, the Centers for Disease Control and Prevention (CDC) issued an alert about *C. auris* (*19*), after which the New York State Department of Health (NYSDOH) issued an advisory (*20*) to inform healthcare facilities about the emerging pathogen and request that they notify NYSDOH of potential cases and forward suspected isolates to the New York state public health laboratory (Mycology Laboratory at Wadsworth Center, Albany, NY, USA). In November 2016, NYSDOH issued a

Author affiliations: New York State Department of Health, New Rochelle, New York, USA (E. Adams, K. Southwick); New York State Department of Health, Albany, New York, USA (M. Quinn, S. Chaturvedi, V. Haley, B. Hutton, D. Blog, E. Lutterloh, H. Zucker); Centers for Disease Control and Prevention, Atlanta, Georgia, USA (S. Tsay, E. Poirot, A. Kallen, S. Vallabhaneni); New York City Department of Health and Mental Hygiene, New York, New York, USA (E. Poirot); New York State Department of Health, Central Islip, New York, USA (J. Greenko); New York State Department of Health, New York (R. Fernandez); State University of New York at Albany School of Public Health, Albany, New York, USA (V. Haley, D. Blog, E. Lutterloh)

[1]Additional members of the workgroup are listed at the end of this article.

follow-up advisory (*21*) requesting that laboratories query their records for isolates of *C. auris* or species that could be confused with *C. auris*, such as *C. haemulonii*. Cases were also identified through active surveillance methods, including direct outreach to healthcare facilities and laboratories. Each clinical case was investigated through medical record reviews, contact tracing, and screening of contacts for colonization.

Contact Tracing

We obtained the names of persons who had resided in the same room as a case-patient in the 90 days before diagnosis for the case-patient. When close contacts could be located, we attempted to obtain samples for culture.

Surveillance and Infection Control Assessments

To emphasize the importance of detection, assist with infection control efforts, and conduct point prevalence surveys of facility contacts, we conducted site visits to facilities where transmission was suspected; our analysis included visits made through June 26, 2017. Initial point prevalence surveys included only a composite swab sample from the axilla and groin; subsequent surveys added a swab sample from the nares. For some persons, swab samples for surveillance cultures to identify persistent colonization were obtained and included samples from the axilla, groin, nares, rectum, wounds, and sites of noninvasive clinical infection. We also assessed key areas of healthcare infection control, including administrative support, hand hygiene, standard and transmission-based precautions, and environmental cleaning; we followed up with detailed assessments in specific areas as needed.

Environmental Investigation

Whenever possible, we obtained samples from the environments of facilities where case-patients were admitted or resided. We concentrated on surfaces that were frequently touched and on objects in case-patients' rooms.

Laboratory Techniques

To isolate *C. auris* from patient screening swab and environmental specimens, we used the method described by Welsh et al., with slight modification (*15*). In brief, we used the ESwab Culture and Transport system (Becton Dickinson, Franklin Lakes, NJ, USA) and placed the samples in 1 mL liquid Amies transport medium. Samples were vortexed for 30 s, after which 50 μL was plated on nonselective Sabouraud dextrose agar containing antibacterials (SDA-A), 50 μL was plated on selective media including SDA-A enriched with 10% salt (SDA-AS), and 200 μL was transferred to 5 mL of Sabouraud dextrose broth containing antibacterials and 10% salt (SDB-AS). Later, for more selective recovery of *C. auris* from surveillance samples,

we placed dulcitol, instead of dextrose, in the selective enrichment media.

We collected environmental samples by using sponge sticks (3M Health Care, St. Paul, MN, USA) and placed them in a zip-top bag containing 45 mL of phosphate-buffered saline (PBS) with 0.02% Tween 80. The bags were gently shaken for 1 min at 260 rpm in a Stomacher 400 Circulator (Laboratory Supply Network, Inc., Atkinson, NH, USA). The suspension without the sponge was poured in a 50-mL conical tube and centrifuged at 4,000 rpm for 5 min; supernatant was then decanted, leaving ≈3 mL of liquid in the bottom of the tube. We placed 50 μL of sponge suspension on different agar media and placed 1 mL of sponge suspension in 5 mL of SDB-AS broth, as we had done for patient swab samples.

Agar plates and broth tubes were incubated at 40°C for at least 2 weeks. To check for purity, we first streaked recovered yeast isolates on CHROMagar *Candida* medium (Difco; Becton Dickinson, Baltimore, MD, USA) and then subcultured them on SDA overnight and processed them for identification by matrix-assisted laser desorption/ionization time-of-flight (MALDI-TOF) mass spectrometry by using the standard ethanol–formic acid extraction procedure (*22*). Spectra were analyzed by using Flex Control 3.1 software (Bruker Daltonics, Inc., Billerica, MA, USA) and MALDI Biotyper OC version 3.1 (Bruker Daltonics, Bremen, Germany); per manufacturer's instructions, a score of ≥2.0 was used to identify *Candida* to the species level. The in-house MALDI-TOF database was enriched by adding spectra from several *C. auris* isolates from the current outbreak and by adding reference isolates from the CDC AR bank (https://www.cdc.gov/drugresistance/resistance-bank/index.html); their identity was confirmed by DNA sequencing. To check for purity, we streaked the clinical isolates of yeasts received from healthcare facilities onto CHROMagar *Candida* medium and used MALDI-TOF mass spectrometry for identification as described.

The MICs of azoles and echinocandins were determined by using broth microdilution with custom TREK frozen broth microdilution panels (catalog no. CML2F-CAN; Thermo Fisher Scientific, Marietta, OH, USA) (*23*). In brief, we prepared a suspension of *C. auris* at a concentration of 0.5×10^3 to 2.5×10^3 in RPMI–1640 medium (with glutamic acid and phenol red, and without bicarbonate; Sigma-Aldrich, St. Louis, MO, USA) and 0.2% glucose buffered to pH 7 with 0.165 mol/L 3-N morpholinepropanesulfonic acid (Sigma-Aldrich). We dispensed 100 μL *C. auris* inoculum into each well of the TREK plate. MICs of amphotericin B and 5-flucytosine were determined by Etest as recommended by the manufacturer (AB Biodisk; bioMérieux, Solna, Sweden) except that MICs were read at 24 h after incubation or until a confluent lawn of growth was seen. For Etests, the yeast inoculum was streaked on

RPMI medium containing 2% glucose and 1.5% agar, and then E-test strips were applied. *C. krusei* (ATCC 6258) and *C. parapsilosis* (ATCC 22019) were used as quality control strains. The TREK broth and Etest plates were incubated at 35°C and read visually after 24 hours. Because there are no established *C. auris*–specific susceptibility breakpoints, we used tentative breakpoints published by CDC (*16*).

Environmental surveillance samples (sponges) were also processed by real-time PCR (*24*). In brief, 1 mL of sponge liquid was washed twice with PBS containing 0.1% bovine serum albumin; as an inhibition control, pellet was resuspended in 50 μL PBS with 0.1% bovine serum albumin containing bicoid plasmid. Each sample went through freezing, heating, bead-beating, and centrifugation, and 5 μL of extracted DNA was tested in duplicate by real-time PCR. According to receiver operator characteristic curve analysis, a cycle threshold value of ≤38 was reported as positive and >38 was reported as negative. If PCR inhibition was observed, specimens were reported as inconclusive.

Results

Epidemiologic Investigation

We detected 51 clinical and 61 screening cases (Figure 1). All but 1 of the clinical cases from New York were diagnosed in NYC: 21 from 7 hospitals in Brooklyn, 16 from 3 hospitals and 1 private medical office in Queens, 12 from 5 hospitals and 1 long-term acute care hospital in Manhattan, and 1 from a hospital in the Bronx. One clinical case was identified in a western New York hospital in a patient who had recently been admitted to an involved Brooklyn hospital. Of the 51 clinical case-patients, 31 (61%) had resided in long-term care facilities (LTCFs) immediately before being admitted to the hospital in which their infection was diagnosed, and 19 of these 31 resided in skilled nursing

facilities with ventilator beds (VSNFs); 1 (2%) resided in a long-term acute care hospital; 5 (10%) had been transferred from another hospital; and 4 (8%) had traveled internationally within 5 years before diagnosis.

Exploration of epidemiologic links revealed a large, interconnected web of affected healthcare facilities throughout NYC (Figure 2). Determining the facility of acquisition of *C. auris* infection or colonization was difficult or impossible because of multiple healthcare exposures and because the incubation period is unknown.

Clinical Characteristics

The median age of clinical case-patients was 72 years (range 21–96 years); 26 (51%) were male. All patients had serious concurrent medical conditions; a substantial proportion required mechanical ventilation or central venous catheters or gastrostomy tubes (Table 1). Initial positive cultures were from blood (31/51, 61%), bile (3/51, 6%), urine (4/51, 8%), respiratory specimens (4/51, 8%), wounds (3/51, 6%), catheter tips (2/51, 4%), and 1 each from bone, ear, jejunal biopsy sample, and skin. The 30-day mortality rate was 14/51 (27%), and the 90-day rate was 23/51 (45%). For those with initial isolates from blood, the 30-day mortality rate was 12/31 (39%) and the 90-day rate was 18/31 (58%). The number of deaths attributable to *C. auris* infection is unknown.

Surveillance Cultures

As part of point prevalence surveys and contact investigations, we performed 1,136 screening cultures for *C. auris* colonization for 572 persons not known to be infected and who resided in or were admitted to 19 facilities (9 hospitals; 10 LTCFs, of which 7 were VSNFs), 4 healthcare workers, and 4 family members of 1 clinical case-patient. At least 1 culture was positive for *C. auris* for 61 (11%) persons at 12 (60%) facilities (5 hospitals and 7 LTCFs [including 5
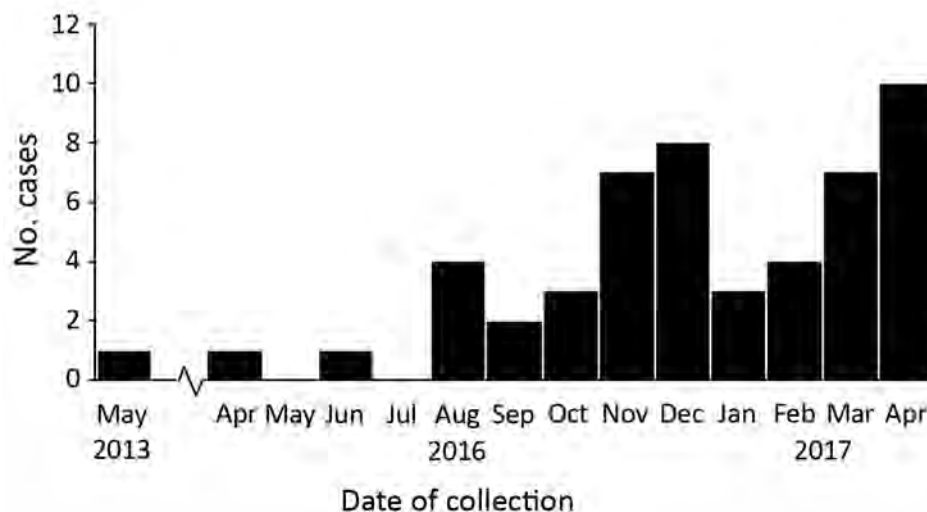
Figure 1. Number of confirmed clinical cases of *Candida auris* in New York, USA, May 2013–April 2017. Dates indicate the month that the first sample positive for *C. auris* was collected. The cases from May 2013, April 2016, and June 2016 were retrospectively identified after the June 2016 clinical alert from the Centers for Disease Control and Prevention was issued (*19*). The case from 2013, in a patient who had traveled to New York City from abroad for medical care, was probably a distinct importation with no further spread.

Figure 2. Epidemiologic links between healthcare facilities affected by *Candida auris*, New York, USA, 2013–2017. Arrows between facilities denote transfer of case-patients from one facility to the other within 90 days before collection date of first positive culture. Bold arrows indicate transfer of >1 case-patient. Bold boxes indicate hospitals; nonbold boxes indicate long-term care facilities; boxes with roofs indicate private residences. Numbers indicate numbers of clinical cases (C) and screening cases (S) at that facility. Screening cases are placed at the facility of diagnosis. Clinical cases are also shown at the facility of diagnosis unless the specimen was collected during the first week of admission at the diagnosing facility; in such situations, the cases are shown at the previous facility.
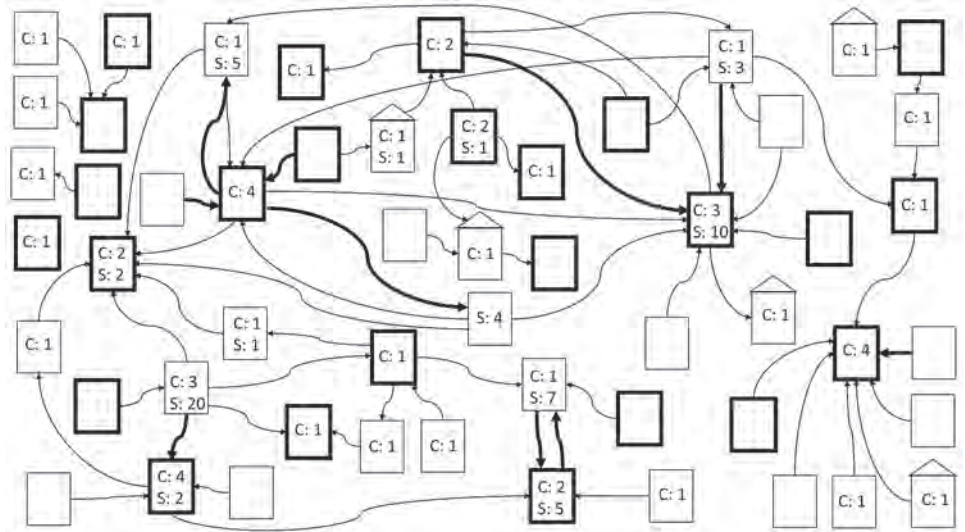
VSNFs]) and 1 family caregiver at a private residence. At the time of sample collection, 19 (31%) of these 61 persons were admitted to hospitals and 42 (67%) resided at LTCFs (40 [66%] at VSNFs). Culture results were positive for 13% of those who were tested while living at LTCFs and 8% of those in hospitals.

For 38 persons (clinical and screening case-patients), follow-up cultures were performed, either for clinical reasons or to determine whether they remained colonized. Long-term colonization was common (Figure 3).

Of 346 persons for whom nares and composite axilla–groin samples for culture were collected on the same day, results were positive for at least 1 site for 36 (10%).

Of these 36, results were positive for both sites for 14 (39%), at axilla–groin only for 13 (36%), and at nares only for 9 (25%).

Environmental Cultures and PCR

Of 781 environmental samples from 20 facilities (12 hospitals and 8 LTCFs [5 VSNFs]), 62 (8%) from 15 facilities (9 hospitals and 6 LTCFs [4 VSNFs]) were positive for *C. auris* by culture. In addition, 19 samples from 4 facilities were positive by PCR; culture results for 3 of these 4 facilities were also positive. Contamination of surfaces and objects in case-patients' rooms and mobile equipment outside the rooms was common (Table 2). High-yield items included

Table 1. Selected concurrent medical conditions and medical interventions for 51 persons with *Candida auris* infection, New York, USA, 2013–2017

Characteristic	No. (%) persons
Concurrent condition	
Respiratory insufficiency requiring support	33 (65)
Mechanical ventilation at time of diagnosis	17 (33)
Neurologic disease*	24 (47)
Diabetes	18 (35)
Malignancies	11 (22)
Colon cancer	5 (10)
End-stage renal disease	8 (16)
Hemodialysis	7 (14)
Kidney transplant	1 (2)
Decubitus ulcers	10 (20)
Otitis with complications	2 (4)
Medical interventions	
Hemodialysis	7 (14)
Central venous catheter within 7 d before first positive culture for *C. auris*	31 (61)
Gastrostomy tube at time of diagnosis	27 (53)
Receipt of systemic antifungal medication within 90 d before first culture positive for *C. auris*	25 (49)
Receipt of systemic antibiotics within 14 d before first culture positive for *C. auris*	42 (82)

*Includes seizure disorder (n = 8), cerebrovascular accident (n = 7), dementia (n = 4), anoxic brain injury (n = 3), spinal cord injury (n = 2), and 1 case each of Parkinson's disease, multiple sclerosis, Huntington's disease, Guillain-Barré syndrome, traumatic brain injury, pituitary tumor, and neuropathy.
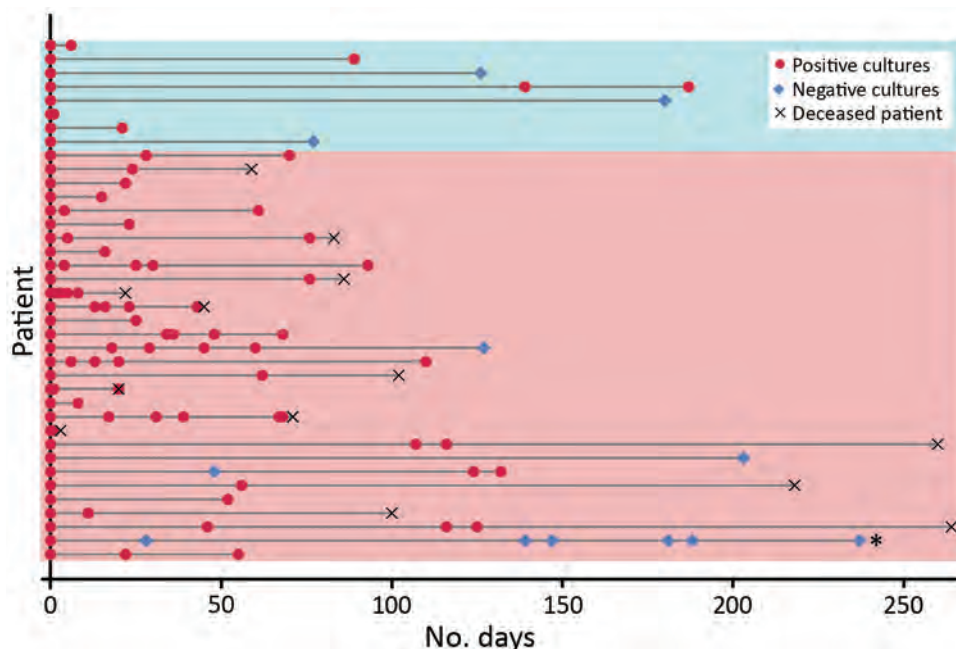
Figure 3. Long-term Candida auris colonization of clinical and screening case-patients, New York, USA, 2013–2017. Each patient for whom follow-up cultures were performed is represented by a horizontal line. The bottom 30 lines (pink shading) indicate clinical case-patients; the top 8 (blue shading) indicate screening case-patients. Follow-up cultures were collected from a variety of sites, typically axilla and groin and often nares, rectum, urine, and wounds. Persons were considered free of colonization with C. auris and eligible for removal of contact precautions when 2 sets of surveillance cultures at multiple sites, taken at least 1 week apart, were negative; only 1 person indicated on the figure (second from bottom) met this criterion.

bedrails, IV poles, beds, privacy and window curtains, windows, and floors.

Laboratory Identification of Clinical Isolates

From July 2016 through April 30, 2017, NYSDOH received 99 first isolates of a variety of yeasts from 99 persons, which clinical laboratories had sent for testing for *C. auris* (Table 3). Of those, 51 (52%) isolates were determined to be *C. auris* and represent the 51 clinical cases. Of the 99 isolates, 38 had been initially identified by the clinical laboratory as *C. haemulonii*, but NYSDOH determined 35 of those to be *C. auris*. Of 13 yeasts received with no identification, 11 were determined to be *C. auris*, and of 6 received with a preliminary identification of *C. auris*, 5 were confirmed as such.

Susceptibility to Antifungal Medications

Of 51 initial *C. auris* isolates recovered from clinical case-patients, 50 (98%) were resistant to fluconazole (Table 4) and 13 (25%) were resistant to fluconazole and amphotericin B. No initial isolates were resistant to echinocandins, although subsequent isolates obtained from 3 persons who had received an echinocandin acquired resistance to it. According to whole-genome sequencing at CDC, 50 (98%) of 51 isolates belonged to a South Asia clade (*25*); the other less related isolate was the only isolate susceptible to fluconazole.

Infection Control

Infection control assessments were conducted at 14 LTCFs and 12 hospitals affected by *C. auris*. Adherence to recommended infection control practices, such as implementation of contact precautions, varied. Specific observations were made in the areas of hand hygiene, contact precautions, use of personal protective equipment (PPE), and environmental cleaning and disinfection.

Hand hygiene problems included frequent suboptimal availability of alcohol-based hand sanitizers. Sanitizers were completely absent in 1 LTCF.

A common problem with implementation of contact precautions was ineffective signage. One facility had no signs or other effective systems to identify persons around whom contact precautions should be taken. Compliance with signs that consisted only of instructions to see the nurse before entering was poor. In one instance, a physician entered a room with such a sign and provided care without donning PPE; when questioned, he stated, "I don't see an isolation sign."

Problems with PPE use included lack of knowledge about which PPE was indicated, improper donning and doffing (e.g., gowns not covering shoulders or not being tied), and lack of availability of appropriate PPE. In 1 LTCF, PPE was locked in a closet; in another, the PPE carts were empty and staff were unable to locate supplies to replenish them; in a third, aprons were used instead of gowns.

Environmental cleaning and disinfection observations included use of household cleaners instead of Environmental Protection Agency–registered hospital-grade disinfectants (at some LTCFs), use of disinfectants without appropriate label claims, inadequate disinfection of shared equipment, and lack of knowledge of contact times.

Table 2. Environmental contamination with *Candida auris* in healthcare facilities, New York, USA, 2013–2017*

Category, object or surface	No. samples	Positive by culture, no. (%)	Positive by PCR and negative by culture, no. (%)	Negative by culture and PCR, no. (%)
Near-patient surfaces and objects in rooms				
Bedside/over bed table	44	2 (5)	2 (5)	40 (91)
Bed rail	49	7 (14)	5 (10)	37 (76)
TV remote/call button	36	2 (6)	2 (6)	32 (89)
IV poles	21	5 (24)	1 (5)	15 (71)
Bed	17	4 (24)	0	13 (77)
Privacy curtain	6	2 (33)	0	4 (67)
Miscellaneous other†	5	0	1 (20)	4 (80)
Total	178	22 (12)	11 (6)	145 (82)
Other surfaces and objects in rooms				
Door knob/handle	36	1 (3)	1 (3)	34 (94)
Sink	27	1 (4)	2 (7)	24 (89)
Window	22	3 (14)	1 (5)	18 (82)
Floor	17	4 (24)	0	13 (77)
Furniture	27	3 (11)	0	24 (89)
Window curtain	11	3 (27)	0	8 (73)
Light switch	9	0	0	9 (100)
Closet	6	0	0	6 (100)
Wall	4	1 (25)	0	3 (75)
Bathroom	4	1 (25)	0	3 (75)
Countertop	4	1 (25)	0	3 (75)
Toilet	4	0	0	4 (100)
Miscellaneous other‡	16	2 (13)	0	14 (88)
Total	187	20 (21)	4 (2)	163 (87)
Equipment in room				
Ventilator/respiratory equipment	12	1 (8)	0	11 (92)
Pump	4	0	0	4 (100)
Miscellaneous other§	19	4 (21)	0	15 (79)
Total	35	5 (14)	0	30 (86)
Equipment outside of room				
Clean supply cart	51	1 (2)	0	50 (98)
Ventilator/respiratory equipment	45	1 (2)	0	44 (98)
Vital sign machine	21	3 (14)	1 (5)	17 (81)
Normothermia system (e.g., Bair hugger)	20	1 (5)	0	19 (95)
Computer workstation	20	0	0	20 (100)
Thermometer	14	1 (7)	1 (7)	12 (86)
PPE/isolation cart/box	12	1 (8)	1 (8)	10 (83)
Lift/scale	11	2 (18)	0	9 (82)
Glucometer	11	0	0	11 (100)
Housekeeping cart	9	0	1 (11)	8 (89)
Dialysis equipment	7	1 (14)	0	6 (86)
Suction canister	6	1 (17)	0	5 (83)
Ultrasonography equipment	4	0	0	4 (100)
Miscellaneous other¶	29	1 (3)	0	28 (97)
Total	260	13 (5)	4 (2)	243 (94)

*A total of 660 samples were collected from surfaces, objects, and equipment in the rooms of *C. auris* case-patients and from mobile equipment outside the rooms on the affected nursing units. In addition, 62 samples from surfaces within the nursing units but outside the patient rooms and 23 samples from outside the affected nursing units were negative by culture and PCR. The location of 36 samples could not be ascertained; 2 were positive by culture. PPE, personal protective equipment; TV, television.
†PCR positive from light cord.
‡Cultures positive from handrail and phone.
§Cultures positive from glucometers (n = 2), vital signs machine, and stretcher.
¶Culture positive from bedpan flusher.

Discussion

This large, citywide, multiple-institution outbreak of *C. auris* infections is ongoing. As of February 2018, most confirmed clinical cases in the United States had been identified in New York, and case numbers continue to grow. The reasons for the preponderance of cases in New York are unknown; possibilities include a true higher prevalence from multiple introductions into this international port of entry, more complete detection from aggressive case finding, presence of a large interconnected network of healthcare facilities in NYC, or a combination of all 3 factors.

Transmission is ongoing in healthcare facilities, primarily among patients with extensive healthcare exposures. *C. auris* has been cultured from rooms and equipment in multiple facilities, and close contacts of case-patients have become colonized. Infection control lapses have probably amplified this process.

Table 3. Isolates received by the New York State public health laboratory, Wadsworth Center, Albany, NY, USA, from clinical laboratories for the purpose of identifying or excluding *Candida auris*, through April 30, 2017*

Organism, no. isolated	Clinical laboratories' identification system				Wadsworth Center identification using MALDI-TOF MS, no. isolates‡
	API	VITEK 2	VITEK MS†	Other	
Candida haemulonii, 38		36		1§	*C. auris*, 35
				1¶	*C. haemulonii*, 1; *Candida duobushaemulonii*, 1; *Candida glabrata*,1
No identification, 13	2	2	9		*C. auris*, 11 *C. glabrata*, 2
C. auris, 6				6§	*C. auris*, 5 *C. duobushaemulonii*, 1
Candida famata, 5	1	3		1#	*C. guilliermondii*, 1; *C. lusitaniae*, 1; *Candida parapsilosis*, 2; *Candida fermentati*, 1
Candida glabrata, 1		1			*C. glabrata*, 1
Candida guilliermondii, 1		1			*C. guilliermondii*, 1
Candida lusitaniae, 1		1			*C. lusitaniae*, 1
Candida sphaerica, 1		1			*Saccharomyces cerevisiae*, 1
Cryptococcus laurentii, 1		1			*Cryptococcus neoformans*, 1
C. neoformans, 1		1			*S. cerevisiae*, 1
C. famata/C. guilliermondii, 1		1			*C. parapsilosis*, 1
C. famata/C. parapsilosis, 1		1			*C. parapsilosis*, 1
C. famata/C. parapsilosis/Candida tropicalis, 1		1			*C. parapsilosis*, 1
Candida dubliniensis/C. haemulonii, 1		1			*C. glabrata*, 1
C. lusitaniae/Candida utiliz, 1			1		*C. lusitaniae*, 1
Candia sphaerica/Rhodotorula glutinis/Rhodotorula mucilaginosa/C. laurentii, 1		1			*C. parapsilosis*, 1
Zygosaccharomyces bailii/C. sake/C. famata/Candida lipolytica, 1		1			*C. glabrata*, 1
S. cerevisiae, 23	7	16			*S. cerevisiae*, 23
Trichosporon mucoides, 1		1			*T. mucoides*, 1

*API, bioMérieux, Inc., Durham, NC, USA; MALDI-TOF MS, Bruker Daltonics, Inc., Billerica, MA, USA; VITEK 2, bioMérieux, Durham, NC, USA; VITEK MS, bioMérieux, Solna, Sweden. MALDI-TOF, matrix-assisted laser desorption/ionization time-of-flight; MS, mass spectrometry.
†No *C. auris* entry.
‡Research use only library was expanded in-house by adding 10 *C. auris* isolates comprising clades I–IV (CDC-AR bank, https://www.cdc.gov/drugresistance/resistance-bank/index.html) and 8 *C. auris* isolates from New York in 2016 comprising clades I and II.
§MALDI-TOF MS, research use only library with 3 *C. auris* entries.
¶BD Phoenix Automated Microbiology System (BD Diagnostics, Sparks, MD, USA).
#RapID YEAST PLUS System (Thermo Fisher Scientific, Waltham, MA, USA).

Factors that contribute to transmission may include prolonged colonization of clinical and screening case-patients and environmental contamination. Persistent colonization of affected persons and the lack of an accepted decolonization regimen result in a large reservoir of persons carrying the organism. As Welsh et al. (*15*) demonstrated, *C. auris* can remain viable on inanimate surfaces for long periods, necessitating scrupulous environmental cleaning and disinfection. Affected patients frequently have extensive contact with multiple healthcare facilities, highlighting the value of careful and thorough communication at transfer.

The clinical cases in the New York outbreak are similar to clinical cases described elsewhere. Fungemia is a commonly reported clinical infection; 76% of infections reported in a series from Colombia (*9*) and 58% in a series from India (*4*) were bloodstream infections. These percentages are comparable to the findings from this New York series in which 61% of initial clinical isolates were from blood. Among medically fragile patients in NYC who had a history of extensive contact with healthcare facilities, clinicians should include *C. auris* in the differential diagnosis for patients with symptoms compatible with bloodstream infection.

Limitations of this investigation include the inability to determine where *C. auris* was acquired for most cases because of multiple healthcare exposures. Point prevalence surveys have not yet been conducted at all involved facilities. The best uses for and interpretation of PCR results are still being determined, especially when PCR is positive but culture result is negative. This investigation did not assess transmission in the community or outpatient settings; other investigators have described *C. auris* infections associated with an outpatient clinic (*12*).

Given the consequences of the development and spread of multidrug-resistant bacteria over the past several decades, the prospect of an endemic or epidemic multidrug-resistant yeast in US healthcare facilities is troubling. Data from other countries show that *C. auris* can become established within facilities. Chowdhary et al.

Table 4. Antifungal susceptibility data for first *Candida auris* isolates from 51 clinical cases, New York, USA, 2013–2017*

Antifungal	Tentative resistance breakpoint (*16*)	MIC$_{50}$†	MIC range†	No. (%) resistant
Fluconazole	$\geq$32	>256	8.00 to $\geq$256	50 (98)
Itraconazole	NA	0.500	0.25–1.00	NA
Voriconazole	NA	2.000	0.50–4.00	NA
Posaconazole	NA	0.250	0.12–0.50	NA
Isavuconazole	NA	0.500	0.25–2.00	NA
Caspofungin	$\geq$2	0.060	0.03–0.25	0
Micafungin	$\geq$4	0.120	0.06–0.25	0
Anidulafungin	$\geq$4	0.250	0.12–0.50	0
Amphotericin B	$\geq$2	1.500	0.50–4.00	15 (29)
Flucytosine	NA	0.125	0.125–0.25	NA

*NA, not available.
†MICs for azoles and echinocandins are defined as the lowest drug concentration that caused 50% growth inhibition compared with the drug-free controls; MICs for amphotericin B and flucytosine are defined as the lowest concentration at which there was 100% growth inhibition. MIC$_{50}$ was defined as the MIC at which $\geq$50% of the isolates of *C. auris* tested were inhibited.

(*2*) report that *C. auris* accounted for 5% of candidemia cases in a pediatric hospital and 30% in a tertiary general hospital in India. Chakrabarti et al. (*6*) report that *C. auris* was isolated from 19 of 27 intensive care units throughout India and accounted for 5.2% of *Candida* isolates from intensive care units. Okinda et al. (*26*) report that 38% of candidemia cases at a referral hospital in Africa were caused by *C. auris*, surpassing *C. albicans* cases (27%). Schelenz et al. (*10*) describe an outbreak in a London hospital that affected 50 patients.

Infection control lapses observed during site visits prompted NYSDOH leadership to conduct educational webinars for New York state clinicians and onsite infection control–focused reviews of all nonfederal hospitals and LTCFs in Brooklyn and Queens. NYSDOH also created a web page for healthcare personnel and the public (*27*). Intensive infection prevention and control efforts continue; the goals are delaying endemicity, preventing outbreaks within facilities, reducing transmission and geographic spread, and blunting the effect of *C. auris* in New York and the rest of the United States.

Additional members of the *Candida auris* Investigation Workgroup: Coralie Bucher, Richard L. Erazo, Rosalie Giardina, Janet Glowicz, Brendan R. Jackson, Ronald Jean Denis, Jillian Karr, Gale Liddell, Anastasia Litvintseva, Shawn R. Lockhart, Abimbola Ogundimu, Rutvik Patel, Maroya Walters, Rory Welsh, and YanChun Zhu.

About the Author

Dr. Adams is a public health physician with the NYSDOH, Metropolitan Area Regional Office, where she serves as the supervisor of the Healthcare Epidemiology and Infection Control Program, overseeing outbreak investigations in healthcare facilities in NYC, Long Island, and the Lower Hudson Valley.

References

1. Lee WG, Shin JH, Uh Y, Kang MG, Kim SH, Park KH, et al. First three reported cases of nosocomial fungemia caused by *Candida auris*. J Clin Microbiol. 2011;49:3139–42. http://dx.doi.org/10.1128/JCM.00319-11
2. Chowdhary A, Sharma C, Duggal S, Agarwal K, Prakash A, Singh PK, et al. New clonal strain of *Candida auris*, Delhi, India. Emerg Infect Dis. 2013;19:1670–3. http://dx.doi.org/10.3201/eid1910.130393
3. Sarma S, Kumar N, Sharma S, Govil D, Ali T, Mehta Y, et al. Candidemia caused by amphotericin B and fluconazole resistant *Candida auris*. Indian J Med Microbiol. 2013;31:90–1. http://dx.doi.org/10.4103/0255-0857.108746
4. Chowdhary A, Anil Kumar V, Sharma C, Prakash A, Agarwal K, Babu R, et al. Multidrug-resistant endemic clonal strain of *Candida auris* in India. Eur J Clin Microbiol Infect Dis. 2014;33:919–26. http://dx.doi.org/10.1007/s10096-013-2027-1
5. Magobo RE, Corcoran C, Seetharam S, Govender NP. *Candida auris*–associated candidemia, South Africa. Emerg Infect Dis. 2014;20:1250–1. http://dx.doi.org/10.3201/eid2007.131765
6. Chakrabarti A, Sood P, Rudramurthy SM, Chen S, Kaur H, Capoor M, et al. Incidence, characteristics and outcome of ICU-acquired candidemia in India. Intensive Care Med. 2015;41:285–95. http://dx.doi.org/10.1007/s00134-014-3603-2
7. Emara M, Ahmad S, Khan Z, Joseph L, Al-Obaid I, Purohit P, et al. *Candida auris* candidemia in Kuwait, 2014. Emerg Infect Dis. 2015;21:1091–2. http://dx.doi.org/10.3201/eid2106.150270
8. Calvo B, Melo ASA, Perozo-Mena A, Hernandez M, Francisco EC, Hagen F, et al. First report of *Candida auris* in America: clinical and microbiological aspects of 18 episodes of candidemia. J Infect. 2016;73:369–74. http://dx.doi.org/10.1016/j.jinf.2016.07.008
9. Morales-López SE, Parra-Giraldo CM, Ceballos-Garzón A, Martínez HP, Rodríguez GJ, Álvarez-Moreno CA, et al. Invasive infections with multidrug-resistant yeast *Candida auris*, Colombia. Emerg Infect Dis. 2017;23:162–4. http://dx.doi.org/10.3201/eid2301.161497
10. Schelenz S, Hagen F, Rhodes JL, Abdolrasouli A, Chowdhary A, Hall A, et al. First hospital outbreak of the globally emerging

Candida auris in a European hospital. Antimicrob Resist Infect Control. 2016;5:35. http://dx.doi.org/10.1186/s13756-016-0132-5

11. Vallabhaneni S, Kallen A, Tsay S, Chow N, Welsh R, Kerins J, et al.; MSD. Investigation of the first seven reported cases of *Candida auris*, a globally emerging invasive, multidrug-resistant fungus—United States, May 2013–August 2016. MMWR Morb Mortal Wkly Rep. 2016;65:1234–7. http://dx.doi.org/10.15585/mmwr.mm6544e1

12. Ben-Ami R, Berman J, Novikov A, Bash E, Shachor-Meyouhas Y, Zakin S, et al. Multidrug-resistant *Candida haemulonii* and *C. auris*, Tel Aviv, Israel. Emerg Infect Dis. 2017;23:195–203. http://dx.doi.org/10.3201/eid2302.161486

13. Ruiz Gaitán AC, Moret A, López Hontangas JL, Molina JM, Aleixandre López AI, Cabezas AH, et al. Nosocomial fungemia by *Candida auris*: first four reported cases in continental Europe. Rev Iberoam Micol. 2017;34:23–7. http://dx.doi.org/10.1016/j.riam.2016.11.002

14. Satoh K, Makimura K, Hasumi Y, Nishiyama Y, Uchida K, Yamaguchi H. *Candida auris* sp. nov., a novel ascomycetous yeast isolated from the external ear canal of an inpatient in a Japanese hospital. Microbiol Immunol. 2009;53:41–4. http://dx.doi.org/10.1111/j.1348-0421.2008.00083.x

15. Welsh RM, Bentz ML, Shams A, Houston H, Lyons A, Rose LJ, et al. Survival, persistence, and isolation of the emerging multidrug-resistant pathogenic yeast *Candida auris* on a plastic healthcare surface. J Clin Microbiol. 2017;55:2996–3005. http://dx.doi.org/10.1128/JCM.00921-17

16. Centers for Disease Control and Prevention. Recommendations for identification of *Candida auris* [cited 2017 Oct 18]. https://www.cdc.gov/fungal/diseases/candidiasis/recommendations.html

17. Mizusawa M, Miller H, Green R, Lee R, Durante M, Perkins R, et al. Can multidrug-resistant *Candida auris* be reliably identified in clinical microbiology laboratories? J Clin Microbiol. 2017;55:638–40. http://dx.doi.org/10.1128/JCM.02202-16

18. Lockhart SR, Etienne KA, Vallabhaneni S, Farooqi J, Chowdhary A, Govender NP, et al. Simultaneous emergence of multidrug resistant *Candida auris* on 3 continents confirmed by whole genome sequencing and epidemiological analyses. Clin Infect Dis. 2017;64:134–40. http://dx.doi.org/10.1093/cid/ciw691

19. Centers for Disease Control and Prevention. Clinical alert to U.S. healthcare facilities—June 2016. Global emergence of invasive infections caused by the multidrug-resistant yeast *Candida auris*

[cited 2017 Feb 28]. https://www.cdc.gov/fungal/diseases/candidiasis/candida-auris-alert.html

20. New York State Department of Health. Health advisory: alert to New York State healthcare facilities regarding the global emergence of invasive infections caused by the multidrug-resistant yeast *Candida auris* [cited 2017 Nov 24]. https://www.health.ny.gov/diseases/communicable/c_auris/docs/2016-08_candida_auris_advisory.pdf

21. New York State Department of Health. Health advisory: alert to New York State clinical laboratories: identification and reporting of suspected *Candida auris* isolates [cited 2017 Nov 24]. https://www.health.ny.gov/diseases/communicable/c_auris/docs/2016-11_candida_auris_advisory.pdf

22. Stevenson LG, Drake SK, Shea YR, Zelazny AM, Murray PR. Evaluation of matrix-assisted laser desorption ionization-time of flight mass spectrometry for identification of clinically important yeast species. J Clin Microbiol. 2010;48:3482–6. http://dx.doi.org/10.1128/JCM.00687-09

23. Clinical and Laboratory Standards Institute. M27–S4 reference method for broth dilution antifungal susceptibility testing of yeasts: fourth informational supplement. Wayne (PA): The Institute; 2012.

24. Leach L, Zhu Y, Chaturvedi S. Development and validation of a real-time PCR assay for rapid detection of *Candida auris* from surveillance samples. J Clin Microbiol. 2017;56:e01223-17. http://dx.doi.org/10.1128/JCM.01223-17

25. Tsay S, Welsh RM, Adams EH, Chow NA, Gade L, Berkow EL, et al. Notes from the field: ongoing transmission of *Candida auris* in health care facilities—United States, June 2016–May 2017. MMWR Morb Mortal Wkly Rep. 2017;66:514–5. http://dx.doi.org/10.15585/mmwr.mm6619a7

26. Okinda N, Kagotho E, Castanheira M, Njuguna A, Omuse G, Makau P, et al. Candidemia at a referral hospital in sub-Saharan Africa: emergence of *Candida auris* as a major pathogen. Poster presented at: European Congress of Clinical Microbiology and Infectious Diseases; 2014 May 10–13; Barcelona, Spain.

27. New York State Department of Health. Get the facts about *Candida auris* [cited 2017 Dec 28]. https://www.health.ny.gov/diseases/communicable/c_auris/

Address for correspondence: Emily Lutterloh, New York State Department of Health, Empire State Plaza, Corning Tower, Rm 523, Albany, NY 12237, USA; email: emily.lutterloh@health.ny.gov

Frequent Genetic Mismatch between Vaccine Strains and Circulating Seasonal Influenza Viruses, Hong Kong, China, 1996–2012

Martin C.W. Chan, Maggie H. Wang, Zigui Chen, David S.C. Hui, Angela K. Kwok,
Apple C.M. Yeung, Kun M. Liu, Yun Kit Yeoh, Nelson Lee,[1] Paul K.S. Chan

The World Health Organization selects influenza vaccine compositions biannually to cater to peaks in temperate regions. In tropical and subtropical regions, where influenza seasonality varies and epidemics can occur year-round, the choice of vaccine remains uncertain. Our 17-year molecular epidemiologic survey showed that most influenza A(H3N2) (9/11) and B (6/7) vaccine strains had circulated in East Asia >1 year before inclusion into vaccines. Northern Hemisphere vaccine strains and circulating strains in East Asia were closely matched in 7 (20.6%) of 34 seasons for H3N2 and 5 (14.7%) of 34 seasons for B. Southern Hemisphere vaccines also had a low probability of matching (H3N2, 14.7%; B, 11.1%). Strain drift among seasons was common (H3N2, 41.2%; B, 35.3%), and biannual vaccination strategy (Northern Hemisphere vaccines in November followed by Southern Hemisphere vaccines in May) did not improve matching. East Asia is an important contributor to influenza surveillance but often has mismatch between vaccine and contemporarily circulating strains.

Influenza is a major cause of illness and death worldwide. The human influenza virus spreads rapidly (average reproduction number of 1.28), typically infects 5%–10% of the population during seasonal epidemics, and results in 3–5 million cases of severe acute lower respiratory tract infection and ≈500,000 deaths per year globally (*1,2*). Continuous evolution of the single-stranded influenza virus results in antigenic drift of its surface proteins hemagglutinin (HA) and neuraminidase (*3,4*). Antigenic drift occurs on average 2–8 years in response to host immune selection pressure and is most frequently seen in influenza A(H3N2), followed by influenza B and influenza A(H1N1). Antigenic drift confers the virus an ability to escape immunity induced by previous infection or immunization (*5*).

Effectiveness of current influenza vaccines is predominantly determined by matching between vaccines and circulating strains (*6*). To achieve the best possible vaccine matching, the World Health Organization (WHO) has changed its recommended vaccine composition 12 times for influenza A(H3N2), 10 times for influenza B, and 6 times for influenza A(H1N1) since 1998 (*7*). WHO reviews influenza vaccine composition each February and September to provide timely recommendation for temperate regions of the Northern and Southern Hemispheres, respectively. Tropical and subtropical regions are expected to choose 1 of the 2 recommended vaccine compositions. However, influenza seasonality varies more in the tropics and subtropics, where epidemics can occur year-round. Moreover, a national policy on the choice and timing of vaccination is lacking in many tropical and subtropical countries, where 60% of the world's population resides (*8*).

We analyzed the 2 most frequently drifting influenza types, A(H3N2) and B, in Hong Kong during 1996–2012 to examine matching between vaccine strains and circulating field viruses to document the challenges faced in this region. We evaluated options on choosing the Northern or Southern Hemisphere vaccine compositions and the strategy of an annual or biannual vaccination.

Methods

Study Samples

We conducted a retrospective molecular epidemiologic study to analyze the HA sequences of influenza A(H3N2) and influenza B viruses that circulated during a 17-year period (1996–2012) in Hong Kong, a subtropical city in

East Asia (22°17′7.87″N, 114°9′27.68″E) with a high population density of 57,250 persons/km² in the most densely populated district, Kwun Tong (9). Hong Kong is an international hub. As recorded in 2011, Hong Kong received >34 million visitors from neighboring regions, including South and Southeast Asia, Taiwan, mainland China, and Macao, and an average of ≈650,000 cross-boundary trips between Hong Kong and mainland China were recorded daily (10,11). In this study, we used Hong Kong as a proxy to reflect the challenges faced in East Asia.

We focused on influenza A(H3N2) and influenza B, rather than A(H1N1), because changes in vaccine composition were more frequent for the former 2 viruses. Clinical specimens were derived from patients admitted to the Prince of Wales Hospital, which serves 9% (0.6 million) of Hong Kong's population (12). We sequenced an average of 30 influenza A(H3N2) and 30 influenza B clinical samples per year, except for 2009, when influenza A(H1N1)pdm09 predominated. Selection was prioritized for samples collected during different months to reveal the whole annual spectrum of circulating viruses.

Identifying Closest Vaccine Strains and Matched Seasons

We identified vaccine strain closest to each circulating virus on the basis of HA sequence analysis. We extracted viral RNA from specimens using the PureLink Viral RNA/DNA Mini kit (Thermo Fisher, Waltham, MA, USA). The full-length influenza A(H3N2) HA encoding region was amplified and Sanger sequenced according to our previously described method (13). Similarly, the full-length influenza B HA encoding region was amplified with primers FLUB-UNI9-HAF1 (5′-AGC AGA AGC AGA GCA TTT TYT AAT ATC-3′) and FLUB-HAR1 (5′-ACA AGC AAA CAA GYA CYA CAA YAA AG-3′) and Sanger sequenced. We downloaded ancestral influenza A(H3N2) and influenza B HA sequences from GenBank. Information about WHO-recommended vaccine strains and sequences were retrieved from the Influenza Research Database (14). When the recommendation included alternative vaccine strains, each of them was included for analysis.

We conducted neighbor-joining phylogenetic inference on the basis of the HA sequences using MEGA6 (15). Resulting trees were visualized using FigTree version 1.4.2. We then matched each circulating strain to a closest influenza A(H3N2) or influenza B vaccine strain based on pairwise protein sequence distances as calculated by the Poisson model (16). Circulating strains with equal distance to 2 vaccine strains were assigned to the vaccine recommended in an earlier year. Strains with distances >2 times the SD from the mean distance of all strains were regarded as outliers and thus had no closest vaccine strain assigned.

When the circulating viruses and their closest vaccine strain corresponded in time, the season was regarded as matched. On the other hand, when the circulating viruses coincided with vaccine strains from a previous season (e.g., circulating strain from 2012 matching vaccine strain from 2010), the season was regarded as not matched. This matching scheme was based on the rationale that WHO changes the influenza vaccine composition only when substantial antigenic drift has occurred, and suboptimal effectiveness would be expected for the previous vaccine compositions.

Seasonality and Protection Period

Unlike temperate regions, peak seasons of influenza in the subtropics are not restricted to winter months. Because previous studies have revealed a biannual pattern of influenza activity in Hong Kong and surrounding regions (12,17), we divided the surveyed 17-year period into 34 influenza seasons. We grouped calendar months under winter and summer influenza seasons on the basis of the average monthly number of hospital admissions of patients for whom influenza was laboratory confirmed that were recorded during the study period.

The Hong Kong Government Influenza Vaccination Programme recommends use of the Northern Hemisphere influenza vaccines and begins annual vaccination every November. Therefore, we defined the protection period of Northern Hemisphere vaccines as from November through October of the following year. Although Southern Hemisphere vaccines are not typically used in Hong Kong, for this analysis we regarded the protection period of these vaccines to be from May through April of the following year.

Results

During the 17-year study period, 8,011 persons with influenza A and 2,079 with influenza B were admitted to the Prince of Wales Hospital. Both infections exhibited 2 seasonal peaks in most years (Figure 1). Most influenza admissions occurred from late winter through early spring (late January through early March) and around summer (May–September), although the summer peak of influenza B varied more and was less prominent than that of influenza A. Based on this observed seasonality, we grouped circulating strains collected during November–April under the winter season and those collected during May–October under the summer season.

We successfully sequenced 502 influenza A(H3N2) and 481 influenza B samples covering all influenza seasons in the study period, except in 2009, when influenza A(H1N1)pdm09 dominated activity. In the phylogenetic analysis based on HA sequences, H3N2 virus exhibited a characteristic ladder-like tree topology suggesting continuous
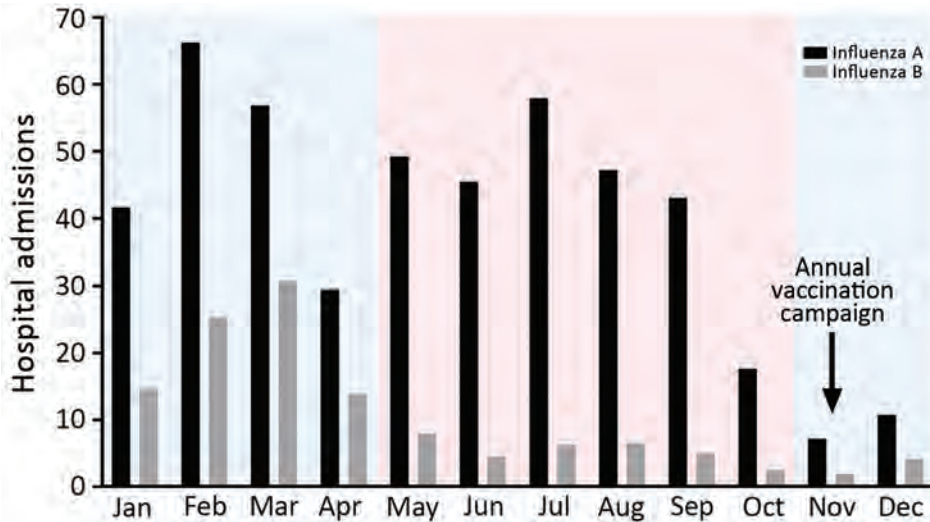
Figure 1. Seasonality of influenza A and B, Hong Kong, China, 1996–2012. The numbers of patients hospitalized with acute respiratory illnesses and who had laboratory-confirmed influenza were retrieved from a computerized laboratory information system at the microbiology department of a district general hospital that serves 9% (0.6 million) of Hong Kong's population. Pink indicates summer seasons; blue indicates winter seasons.

unidirectional evolution (Figure 2, panel A). Existing H3N2 variants circulated for a median of 2 years (range 1–4 years), with gaps between the winter and summer seasons, and became displaced rapidly by newly emerging variants. We observed a more complex tree topology for influenza B, where new lineages emerged from deep branches and evolved toward multiple directions (Figure 2, panel B). In addition, multiple influenza B variants co-circulated for a median of 6 years (range 2–15 years) before being displaced by new variants.

Of the 983 circulating strains examined, 8 (maximum 2 per season) influenza A(H3N2) and 12 (maximum 4 per season) influenza B viruses were regarded as far away from any vaccine strains recommended during the 17-year study period. The pairwise HA amino acid distances of these strains were more than twice the SD from the mean of the related clusters (online Technical Appendix Figures 1, 2, https://wwwnc.cdc.gov/EID/article/24/10/18-0652-Techapp1.pdf), and they were distant from all vaccine strains based on the phylogenetic tree topology.

Matching Between Circulating and Vaccine Strains

Influenza A(H3N2)

We assessed the temporal relationship between circulating H3N2 viruses collected in this study and their closest Northern Hemisphere vaccine strain based on HA amino acid sequence comparisons (Figure 3, panel A). Most Northern hemisphere vaccine-like strains (9/11) had circulated in Hong Kong for >1 year before WHO first recommended them for inclusion in the Northern Hemisphere vaccine. We found co-circulation of multiple strains in 17 (50.0%) of the 34 seasons. In 13 (38.2%) seasons, at least a portion of the circulating viruses were closely matched with the contemporary vaccine strain. However, in only 7

(20.6%) seasons, the closely matched portion accounted for the >50% of circulating viruses examined. A full match was achieved in only 2 (5.9%) seasons. We determined the proportion of circulating viruses that were genetically closely matched with vaccine strains based on HA amino acid sequence comparison (Table), which should not be taken as vaccine effectiveness because cross-protection between mismatched strains can occur.

We repeated the same analysis with respect to Southern Hemisphere vaccine strains. Similarly, most (8/11) Southern Hemisphere H3N2 virus vaccine strains had circulated in Hong Kong for >1 year before WHO first recommended them for inclusion in the Southern Hemisphere vaccine. A similar picture on matching was revealed (Figure 3, panel B). In 10 (29.4%) of the 34 seasons, at least a portion of the circulating viruses were closely matched with the contemporary vaccine strain. However, only in 5 (14.7%) seasons did the matched portion account for the >50% of circulating viruses examined.

Influenza B

We assessed the temporal relationship between circulating influenza B viruses and their closely matched Northern Hemisphere vaccine strains based on HA amino acid sequence comparisons (Figure 4, panel A). Most (6/7) of the Northern Hemisphere influenza B vaccine–like circulating strains had been found in Hong Kong >1 year before WHO first recommended them as vaccine strains. Co-circulation of multiple strains was found in 26 (76.5%) of the 34 seasons examined. In 15 (44.1%) seasons, at least some of the circulating viruses were closely matched with the contemporary Northern Hemisphere vaccine strain. However, in only 5 (14.7%) seasons did the matched portion account for the >50% of circulating viruses examined.

Analysis of Southern Hemisphere vaccine strains showed a similar result (Figure 4, panel B). Most (5/6) of the vaccine-like strains were found in Hong Kong >1 year before WHO first recommended them as vaccine strains. Again, we found matched strains in 14 (41.2%) seasons, but in only 4 (11.8%) seasons did the matched viruses account for the >50% of viruses examined.

Strain Drifting between Winter and Summer Seasons

Influenza A(H3N2)

In 7 of the 17 years (2002, 2003, 2004, 2005, 2007, 2009, and 2011), the predominant H3N2 virus strain in summer differed from that in the preceding winter. We further
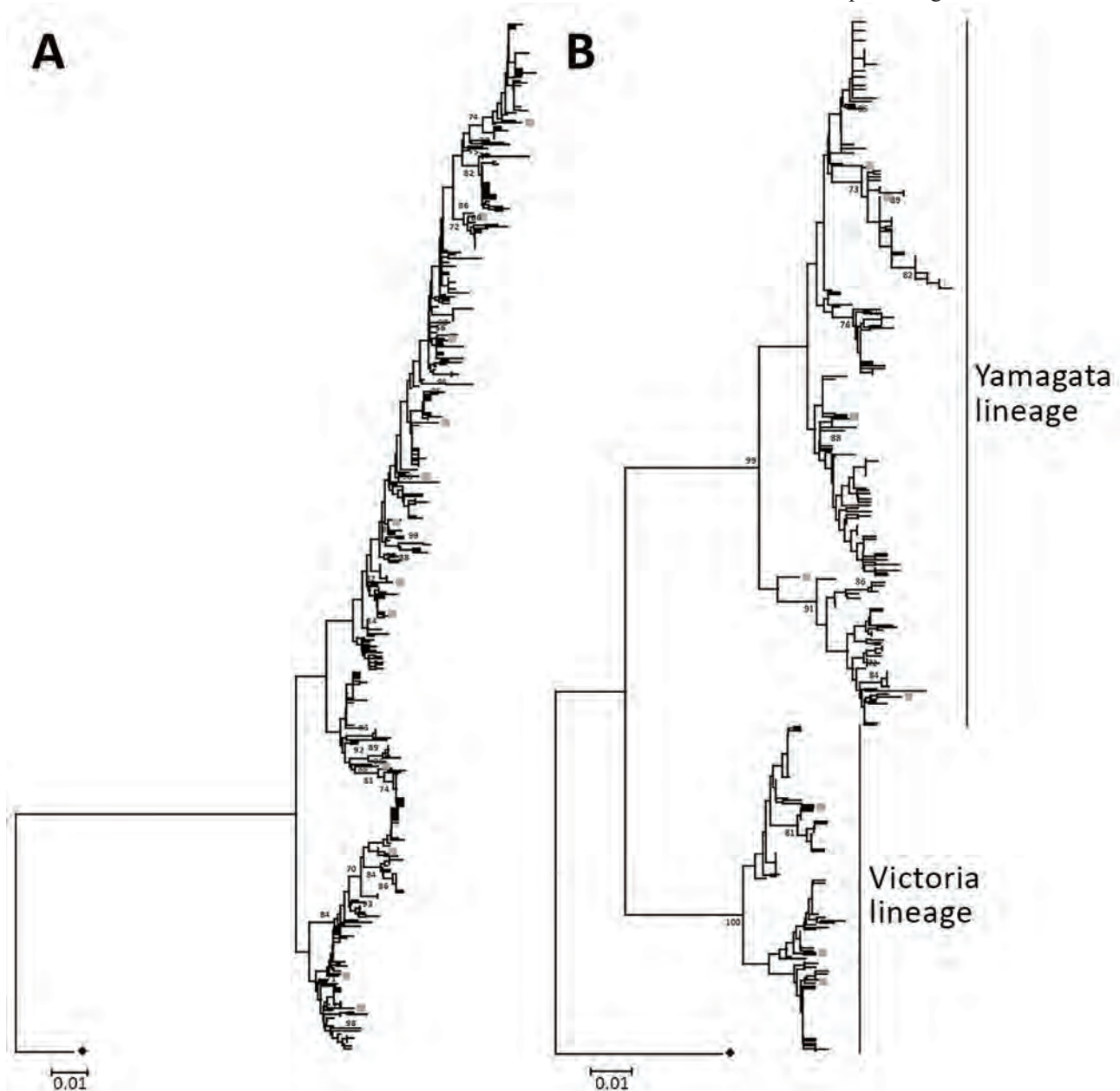
Figure 2. Neighbor-joining phylogenetic inference of near-complete hemagglutinin protein of influenza A(H3N2) (A) and influenza B (B), Hong Kong, China, 1996–2012. Pairwise protein sequence distances were calculated using a Poisson model. Triangles denote ancestral influenza strains: influenza A(H3N2), A/Hong Kong/1/1968, GenBank accession no. CY044261; influenza B, B/Lee/1940, accession no. CY115111. Gray squares denote recommended vaccine strains; for clarity, only those used in Figures 3 and 4 are shown. Bootstrap values >70% are shown at the respective nodes. All alignment positions containing gaps were omitted from the analysis. Trees were rooted to ancestral strains and drawn to scale. Scale bars indicate numbers of amino acid substitutions per position. GenBank accession numbers of hemagglutinin sequences of circulating strains collected in this study are shown in the online Technical Appendix Table (https://wwwnc.cdc.gov/EID/article/24/10/18-0652-Techapp1.pdf).

examined whether administration of an additional Southern Hemisphere vaccine at the beginning of summer (around May) could achieve better vaccine matching. In 5 of the 7 years, content of newly available Southern Hemisphere vaccines was identical to the preceding Northern Hemisphere vaccine composition. In 2004 and 2005, although another strain was chosen for the Southern Hemisphere vaccine, the new vaccine strain was not closely matched with circulating viruses at that time. These results suggested that additional administration of Southern Hemisphere vaccines at the beginning of summer would not have improved the immunity against the circulating H3N2 strains.

Influenza B

In 6 of the 17 years (2000, 2002, 2004, 2008, 2010, and 2011), a drift occurred in the predominant influenza B variant from winter to summer seasons. Similarly, we examined the value of an additional Southern Hemisphere vaccine administered at the beginning of summer and again found no benefit. In 5 of the 6 drift years, the newly recommended Southern Hemisphere vaccine composition was identical to the previous Northern Hemisphere vaccine. In 2008, although the Southern Hemisphere vaccine contained a new virus (Yamagata, B/Florida/4/2006) that closely matched the circulating viruses detected in the first half (winter season) of the same year, the circulating strain
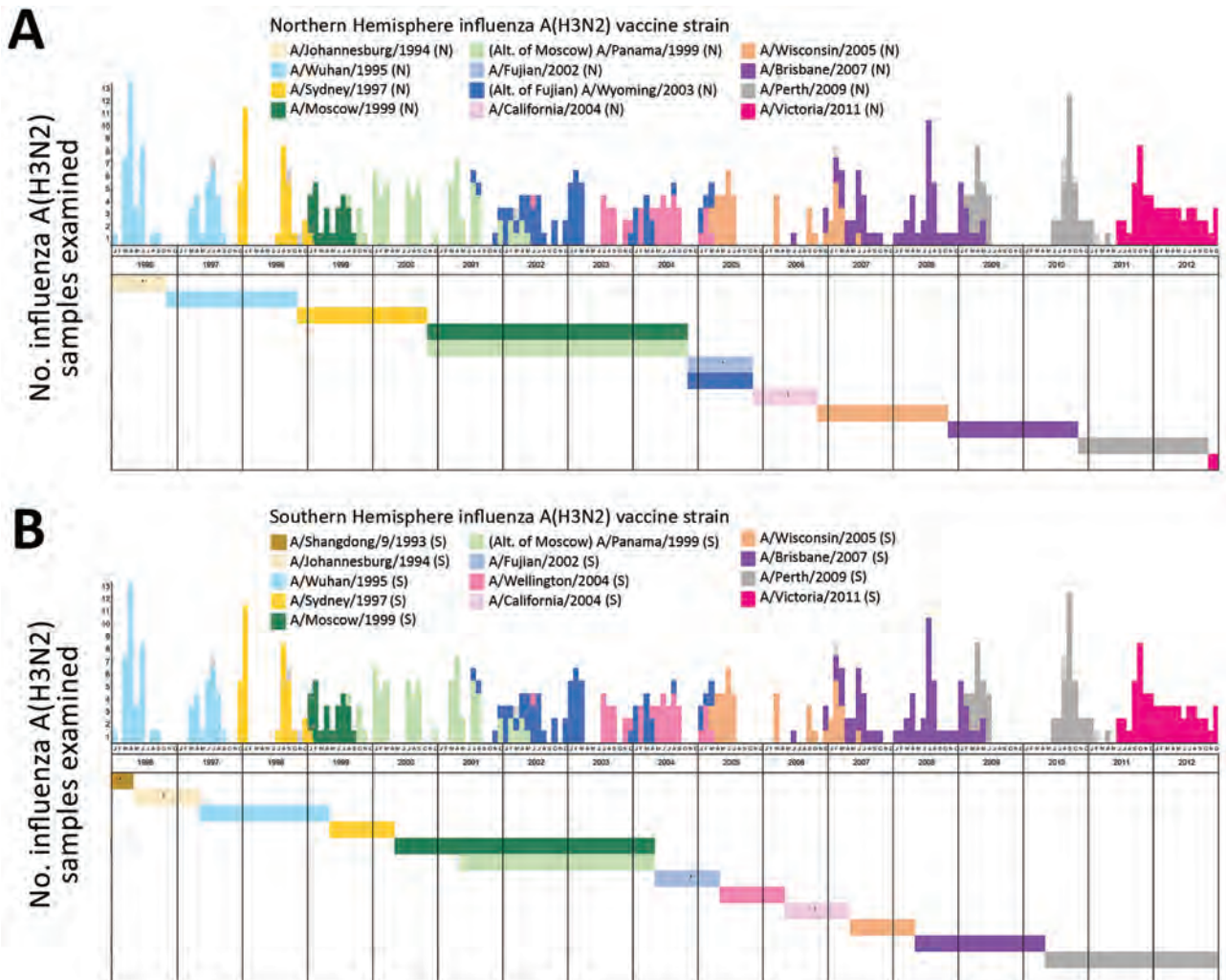
Figure 3. Matching between circulating and vaccine strains of influenza A(H3N2), Hong Kong, China, 1996–2012. Each circulating virus was assigned on the basis of full-length hemagglutinin amino acid distance and phylogenetic tree topology to the closest World Health Organization–recommended influenza A(H3N2) vaccine strain for Northern Hemisphere (A) and Southern Hemisphere (B) vaccines. Closely matched viruses are labeled with the same color. The circulating strains with no closest vaccine strain identified as defined in the Methods are indicated by dotted boxes. Horizontal color bars indicate the protection period of the corresponding vaccine strain. Asterisks indicate vaccine strains without closely matched circulating viruses. The protection period of Northern Hemisphere vaccines was defined as from November through the following October and of Southern Hemisphere vaccines from May through the following April. All the alternative vaccine strains were analyzed, and those with different results are shown.

Table. Proportion of circulating influenza viruses with HA amino acid sequences closely matched with vaccine strains, Hong Kong, China, 1996–2012*

Year, season	Influenza A(H3N2) vaccine strains, %†		Influenza B vaccine strains, %†	
	Northern Hemisphere	Southern Hemisphere	Northern Hemisphere	Southern Hemisphere
1996				
Winter	None‡	None‡	All§	All§
Summer	None‡	None‡	77.8	77.8
1997				
Winter	All§	None‡	14.7	None‡
Summer	94.4	94.4	None‡	None‡
1998				
Winter	None‡	None‡	None‡	None‡
Summer	None‡	None‡	None‡	None‡
1999				
Winter	18.8	None‡	6.3	6.3
Summer	None‡	None‡	None‡	None‡
2000				
Winter	None‡	None‡	None‡	None‡
Summer	None‡	None‡	None‡	None‡
2001				
Winter	All§¶	None‡	None‡	None‡
Summer	84.6¶	84.6¶	None‡	25.0
2002				
Winter	41.2¶	41.2¶	None‡	None‡
Summer	6.7	6.7	12.5	12.5
2003				
Winter	None‡	None‡	73.3	6.7
Summer	None‡	None‡	None‡	None‡
2004				
Winter	None‡	None‡	None‡	None‡
Summer	None‡	None‡	None‡	None‡
2005				
Winter	31.3#	None‡	29.4	None‡
Summer	None‡	None‡	12.5	12.5
2006				
Winter	None‡	None‡	None‡	None‡
Summer	None‡	None‡	None‡	90.0
2007				
Winter	52.4	None‡	9.1	9.1
Summer	6.7	6.7	None‡	None‡
2008				
Winter	None‡	None‡	22.2	22.2
Summer	None‡	All§	None‡	None‡
2009				
Winter	52.2	52.2	None‡	None‡
Summer**	22.2	22.2	None‡	None‡
2010				
Winter	None‡	None‡	66.7	None‡
Summer	None‡	92.9	26.7	26.7
2011				
Winter	87.5	87.5	64.3	64.3
Summer	None‡	None‡	37.5	37.5
2012				
Winter	None‡	None‡	31.0	31.0
Summer	None‡	None‡	None‡	None‡

*Calendar months belonging to winter or summer influenza seasons were based on the average number of cases admitted per month during the study period (Figure 1). Winter seasons were November of previous year through April of current year; influenza usually peaks in February and March. Summer seasons were May–October; influenza usually peaks in July and August. HA, hemagglutinin.
†Co-circulation of multiple strains with a certain percentage closely matched the contemporary vaccine strain based on HA amino acid sequence comparison.
‡None of the circulating viruses examined were closely matched with the contemporary vaccine strain based on HA amino acid sequence comparison.
§All circulating viruses examined were closely matched with the contemporary vaccine strain based on HA amino acid sequence comparison.
¶A/Panama/1999, an alternate to A/Moscow/99, closely matched the circulating strains of 2001 winter and summer seasons and 2002 winter season.
#The World Health Organization recommended 2 A(H3N2) vaccine strains for the Northern Hemisphere in 2005, one of which, A/Wyoming/2003, closely matched a portion of the viruses circulating during the 2005 winter season.
**Dominated by influenza A(H1N1)pdm09.

was soon replaced by another influenza B variant not covered in the recommended Southern Hemisphere vaccine.

Discussion

This study focused on the vaccine matching of influenza A(H3N2) and influenza B viruses because antigenic drift frequently occurs in these viruses, leading to changes in vaccine recommendation, more so than for influenza A(H1N1) virus (*7*). Antigenic characterization of influenza viruses, and thus the assessment of vaccine matching, has traditionally been based on hemagglutination inhibition (HI) assay. HI measures the ability of specific antibodies, typically reference ferret antiserum, to inhibit the binding of virus HA to receptors on erythrocytes. However, H3N2 virus variants from the past 3 decades have progressively displayed reduced avidity to erythrocytes of commonly used animal species, making the results of HI assays difficult to interpret (*8,18*). In this study, we analyzed the amino acid sequence of HA to infer vaccine matching because genetic and antigenic characteristics of influenza viruses display remarkable correspondence, and both carry a strong correlation with vaccine effectiveness (*19–21*). The molecular phylogenetic approach used enables direct analyses of viruses in clinical samples rather than relying on cell culture–propagated isolates. Furthermore, the molecular approach does not require influenza variant–specific antiserum and is more feasible for large-scale epidemiologic surveys. One caution in interpreting molecular results is
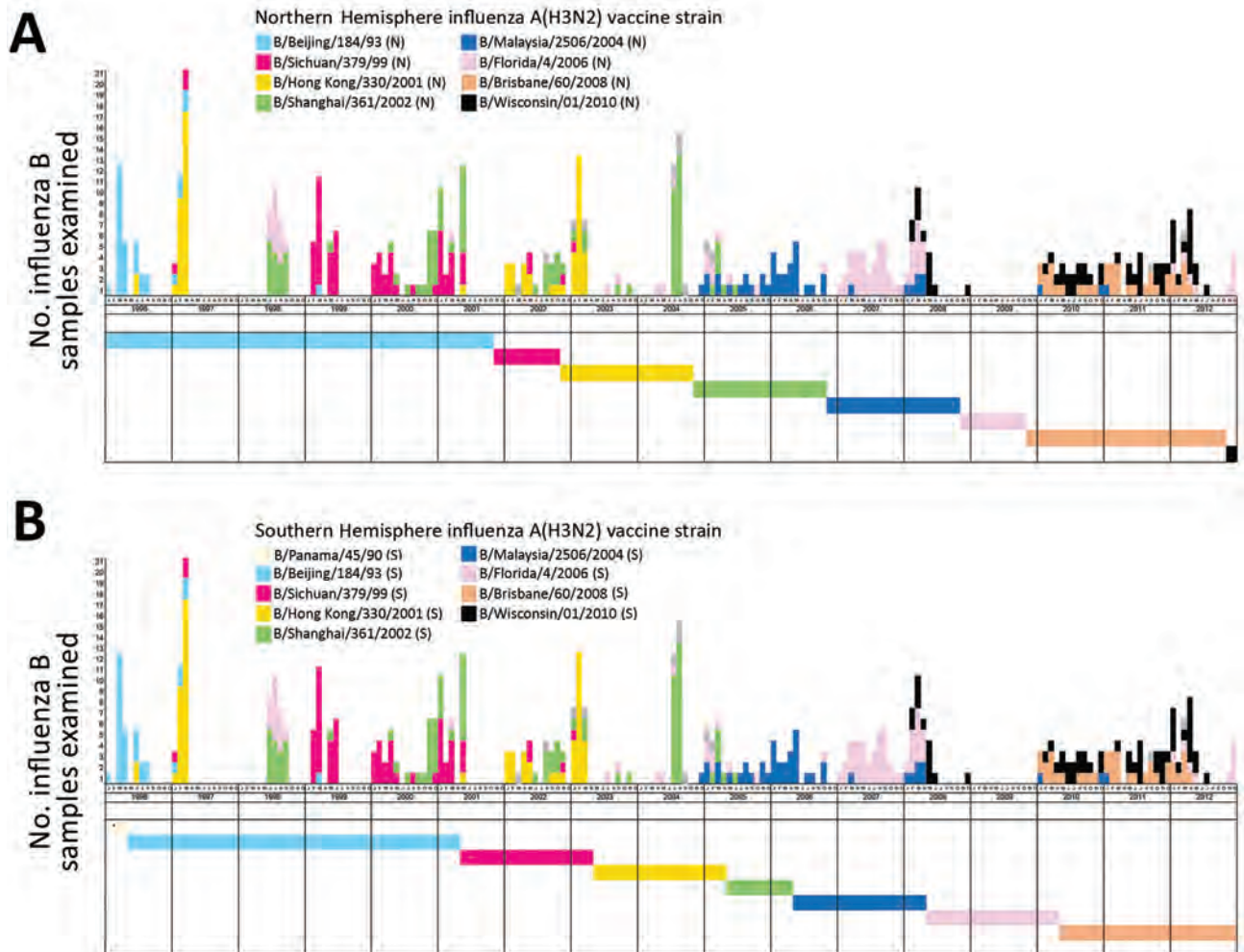
Figure 4. Matching between circulating and vaccine strains of influenza B, Hong Kong, China, 1996–2012. Each circulating virus was assigned on the basis of full-length hemagglutinin amino acid distances and phylogenetic tree topology to the closest World Health Organization–recommended influenza B vaccine strain for Northern Hemisphere (A) and Southern Hemisphere (B) vaccines. Closely matched viruses are labeled with the same color. The circulating strains with no closest vaccine strain identified as defined in the Methods are indicated by dotted boxes. Horizontal color bars indicate the protection period of the corresponding vaccine strain. Asterisks indicate vaccine strains without closely matched circulating viruses. The protection period of Northern Hemisphere (A) vaccines was defined as from November through the following October and of Southern Hemisphere (B) vaccines from May through the following April. All the alternative vaccine strains were analyzed, and those with different results are shown.

that influenza vaccines might still display cross-protection efficacy against circulating variants that are regarded as not closely matched to the vaccine strains based on genetic comparison. Nevertheless, our approach to define matching between vaccine and circulating strains would be sufficient to guide the selection of Northern and Southern Hemisphere vaccines and to inform the potential benefit of a biannual vaccination strategy using both Northern and Southern Hemisphere vaccines on the background of influenza epidemiology faced by subtropical countries.

Given the extensive amount of travel between Hong Kong and neighboring East Asia cities, we expect a substantial sharing of viruses detected in Hong Kong with the region. Although the proportion of infectious travelers is difficult to estimate, a study from Xiamen International Airport (Xiamen, China) in 2015–2016 found that ≈8/10,000 incoming travelers had influenza-like illness, of whom 21% tested positive for influenza (22). The fact that Hong Kong shares a similar, though not always synchronized, pool of influenza viruses with the neighboring East and Southeast Asian cities is supported by a study from Bahl et al. (23) and sequence information from Nextstrain (https://nextstrain.org). East and Southeast Asia are the sources of new genetic variants of H3N2 virus, which seed epidemics worldwide (24–28). In line with this, we demonstrated that most of the H3N2 virus strains selected for inclusion in influenza vaccines could be detected in East Asia >1 year before recommendation by WHO. Most of these newly emerged strains predominated for 2 years, covering 4 influenza seasons in this region. Although vaccine compositions were reviewed twice a year, when vaccines incorporating newly emerged strains were made available to the market, often another newly drifted influenza strain had become predominant in the region. Based on our analysis covering 17 years with 34 influenza seasons, the probability of a season having the contemporary vaccine closely matched with >50% of the circulating viruses was only 20.6%, and if we aimed at matching >70% of circulating viruses, the probability was further reduced to 14.7%. As reflected in a recent study on vaccine effectiveness against hospitalization among children in Hong Kong, efficacy against H3N2 virus was on average 36.6% (29).

Because Hong Kong, like many other subtropical cities, faces multiple influenza peaks annually, we raised the question whether Southern Hemisphere influenza vaccines would provide timely and better vaccine matching. However, we observed that most of the time composition of the Southern Hemisphere vaccine is the same as the preceding Northern Hemisphere vaccine and thus made no difference in vaccine matching. Furthermore, according to the current production schedule, Southern Hemisphere vaccines are made available in May, just after the period with highest influenza activity in Hong Kong (January–March).

Therefore, to administer influenza vaccine in May requires vaccines with efficacy lasting for almost 12 months, which is not a demonstrated property of current vaccines.

Given the comparable duration of winter and summer influenza seasons in Hong Kong, the next question was whether biannual vaccination with Northern and Southern Hemisphere vaccines administered before the winter and summer seasons, respectively, would improve immunity against circulating strains. In early 2015, Hong Kong faced a strong winter influenza peak associated with a newly drifted variant, influenza A(H3N2)/Switzerland, which was not incorporated into the Northern Hemisphere vaccine. In view of a possible strong summer peak, an ad hoc vaccination campaign was conducted in May using the newly available Southern Hemisphere vaccine that incorporated the new variant. However, willingness to accept the vaccine was low among healthcare professionals, and a major proportion expressed concern (30). Furthermore, in recent years, concern has surfaced that repeated influenza vaccination might negatively affect current vaccine effectiveness (31–33). Although a recent meta-analysis does not support such a claim (34), this possibility should not be ignored when considering biannual vaccination. Although the cost-effectiveness and feasibility of a biannual vaccination strategy is yet to be assessed, our analysis does not support that an additional vaccine before summer seasons can improve matching. We observed a substantial chance of drift in predominant influenza viruses from season to season (41.2% for H3N2 and 35.3% for influenza B), and the newly available Southern Hemisphere vaccines typically had the same strain composition as the preceding Northern Hemisphere vaccine or the updated Southern Hemisphere composition still did not achieve a close match with the then-circulating viruses.

East Asia and other subtropical regions face different challenges in achieving close vaccine matching for influenza A(H3N2) and influenza B. For H3N2 virus, the forthcoming predominant strain can be identified from a subtropical region–based surveillance network. The newly emerged strains usually predominate for 1–2 years, which cover 4 influenza seasons in this region. If recommendation on vaccine composition followed by manufacturing is accomplished within a few months, a close match can be achieved in the subsequent 2–3 seasons to provide the best possible vaccine effectiveness. This streamlined workflow should be practicable with current logistics and production provided that a sustainable market can be established in the region.

The challenge posed by influenza B is completely different. Although Bedford et al. suggested that East and Southeast Asia play limited roles in disseminating new variants of influenza B (24), we observed that most of the influenza B strains could be found in East Asia long

before they are selected as vaccine strains. East Asia is therefore also an important site for identifying emergent influenza B strains. However, co-circulation and multiple reintroductions of existing and emerging influenza strains complicate selection of vaccine strains. Incorporating both lineages of influenza B into the quadrivalent vaccine might be able to solve at least part of the problem. In either case, a next-generation influenza vaccine should be designed to provide broad cross-protection against different antigenic variants (*35*).

East Asia is an important contributor to the influenza virus surveillance program. However, vaccine strains incorporated in the Northern and Southern Hemisphere influenza vaccines frequently do not match the contemporary circulating viruses in this region. Even biannual vaccination is unlikely to improve vaccine matching. A specific strategy is urgently needed to select and produce influenza vaccines targeting the tropical and subtropical regions.

About the Author

Dr. Martin C.W. Chan is an assistant professor in the Department of Microbiology of the Chinese University of Hong Kong. His primary research interests are molecular epidemiology of acute viral infections, especially those caused by influenza viruses and noroviruses; use of metagenomic next-generation sequencing in clinical diagnostics; gut virome; and food virology.

References

1. Biggerstaff M, Cauchemez S, Reed C, Gambhir M, Finelli L. Estimates of the reproduction number for seasonal, pandemic, and zoonotic influenza: a systematic review of the literature. BMC Infect Dis. 2014;14:480. http://dx.doi.org/10.1186/1471-2334-14-480
2. World Health Organization. Influenza (seasonal). Fact sheet. 2016 [cited 2017 Jun 15]. http://www.who.int/mediacentre/factsheets/fs211/en/
3. Bennett JE, Dolin R, Blaser MJ. Mandell, Douglas, and Bennett's principles and practices of infectious diseases, 8th ed. Philadelphia: Elsevier; 2015.
4. Cox NJ, Subbarao K. Global epidemiology of influenza: past and present. Annu Rev Med. 2000;51:407–21. http://dx.doi.org/10.1146/annurev.med.51.1.407
5. Carrat F, Flahault A. Influenza vaccine: the challenge of antigenic drift. Vaccine. 2007;25:6852–62. http://dx.doi.org/10.1016/j.vaccine.2007.07.027
6. Houser K, Subbarao K. Influenza vaccines: challenges and solutions. Cell Host Microbe. 2015;17:295–300. http://dx.doi.org/10.1016/j.chom.2015.02.012
7. World Health Organization. WHO recommendations on the composition of influenza virus vaccines [cited 2017 Aug 10]. http://www.who.int/influenza/vaccines/virus/recommendations/en/
8. Hampson A, Barr I, Cox N, Donis RO, Siddhivinayak H, Jernigan D, et al. Improving the selection and development of influenza vaccine viruses—report of a WHO informal consultation on improving influenza vaccine virus selection, Hong Kong SAR, China, 18-20 November 2015. Vaccine. 2017;35:1104–9. http://dx.doi.org/10.1016/j.vaccine.2017.01.018
9. Kong H. Hong Kong: the facts [cited 2017 Sep 6]. https://www.gov.hk/en/about/abouthk/factsheets/docs/population.pdf
10. Census and Statistics Department, Government of the Hong Kong Special Administrative Region. Transport, communication and tourism. Cross-boundary travel survey 2015 [cited 2018 Jun 7]. https://www.censtatd.gov.hk/hkstat/sub/sp130.jsp?productCode=FA100267
11. Census and Statistics Department, Government of the Hong Kong Special Administrative Region. Transport, communication and tourism. Table E551: visitor arrivals by country/region of residence [cited 2018 Jun 7]. https://www.censtatd.gov.hk/hkstat/sub/sp130.jsp?productCode=D5600551
12. Chan PK, Tam WW, Lee TC, Hon KL, Lee N, Chan MC, et al. Hospitalization incidence, mortality, and seasonality of common respiratory viruses over a period of 15 years in a developed subtropical city. Medicine (Baltimore). 2015;94:e2024. http://dx.doi.org/10.1097/MD.0000000000002024
13. Tang JW, Ngai KL, Lam WY, Chan PK. Seasonality of influenza A(H3N2) virus: a Hong Kong perspective (1997–2006). PLoS One. 2008;3:e2768. http://dx.doi.org/10.1371/journal.pone.0002768
14. World Health Organization. Influenza Research Database. World Health Organization recommendations for composition of influenza vaccines [cited 2017 Aug 10]. https://www.fludb.org/brc/vaccineRecommend.spg?decorator=influenza
15. Tamura K, Stecher G, Peterson D, Filipski A, Kumar S. MEGA6: molecular evolutionary genetics analysis version 6.0. Mol Biol Evol. 2013;30:2725–9. http://dx.doi.org/10.1093/molbev/mst197
16. Zuckerkandl E, Pauling L. Evolutionary divergence and convergence in proteins. In: Bryson V, Vogel HJ, editors. Evolving genes and proteins. New York: Academic Press; 1965. p. 97–166.
17. Shu YL, Fang LQ, de Vlas SJ, Gao Y, Richardus JH, Cao WC. Dual seasonal patterns for influenza, China. Emerg Infect Dis. 2010;16:725–6. http://dx.doi.org/10.3201/eid1604.091578
18. Lin YP, Xiong X, Wharton SA, Martin SR, Coombs PJ, Vachieri SG, et al. Evolution of the receptor binding properties of the influenza A(H3N2) hemagglutinin. [Erratum in: Proc Natl Acad Sci U S A. 2013;110:2677. http://dx.doi.org/10.1073/pnas.1218841110]. Proc Natl Acad Sci U S A. 2012;109:21474–9.
19. Smith DJ, Lapedes AS, de Jong JC, Bestebroer TM, Rimmelzwaan GF, Osterhaus AD, et al. Mapping the antigenic and genetic evolution of influenza virus. Science. 2004;305:371–6. http://dx.doi.org/10.1126/science.1097211
20. Lee MS, Chen JS. Predicting antigenic variants of influenza A/H3N2 viruses. Emerg Infect Dis. 2004;10:1385–90. http://dx.doi.org/10.3201/eid1008.040107
21. Gupta V, Earl DJ, Deem MW. Quantifying influenza vaccine efficacy and antigenic distance. Vaccine. 2006;24:3881–8. http://dx.doi.org/10.1016/j.vaccine.2006.01.010
22. Chen J, Yang K, Zhang M, Shen C, Chen J, Wang G, et al. Rapid identification of imported influenza viruses at Xiamen International Airport via an active surveillance program. Clin Microbiol Infect. 2018;24:289–94. http://dx.doi.org/10.1016/j.cmi.2017.05.027
23. Bahl J, Nelson MI, Chan KH, Chen R, Vijaykrishna D, Halpin RA, et al. Temporally structured metapopulation dynamics and persistence of influenza A H3N2 virus in humans. Proc Natl Acad Sci U S A. 2011;108:19359–64. http://dx.doi.org/10.1073/pnas.1109314108
24. Bedford T, Riley S, Barr IG, Broor S, Chadha M, Cox NJ, et al. Global circulation patterns of seasonal influenza viruses vary with antigenic drift. Nature. 2015;523:217–20. http://dx.doi.org/10.1038/nature14460
25. Russell CA, Jones TC, Barr IG, Cox NJ, Garten RJ, Gregory V, et al. The global circulation of seasonal influenza A (H3N2) viruses. Science. 2008;320:340–6. http://dx.doi.org/10.1126/science.1154137

26. Lemey P, Rambaut A, Bedford T, Faria N, Bielejec F, Baele G, et al. Unifying viral genetics and human transportation data to predict the global transmission dynamics of human influenza H3N2. PLoS Pathog. 2014;10:e1003932. http://dx.doi.org/10.1371/journal.ppat.1003932

27. Bedford T, Cobey S, Beerli P, Pascual M. Global migration dynamics underlie evolution and persistence of human influenza A (H3N2). PLoS Pathog. 2010;6:e1000918. http://dx.doi.org/10.1371/journal.ppat.1000918

28. Chan J, Holmes A, Rabadan R. Network analysis of global influenza spread. PLOS Comput Biol. 2010;6:e1001005. http://dx.doi.org/10.1371/journal.pcbi.1001005

29. Cowling BJ, Chan KH, Feng S, Chan EL, Lo JY, Peiris JS, et al. The effectiveness of influenza vaccination in preventing hospitalizations in children in Hong Kong, 2009–2013. Vaccine. 2014;32:5278–84. http://dx.doi.org/10.1016/j.vaccine.2014.07.084

30. Wong MC, Nelson EA, Leung C, Lee N, Chan MC, Choi KW, et al. Ad hoc influenza vaccination during years of significant antigenic drift in a tropical city with 2 seasonal peaks: a cross-sectional survey among health care practitioners. Medicine (Baltimore). 2016;95:e3359. http://dx.doi.org/10.1097/MD.0000000000003359

31. Tam YH, Valkenburg SA, Perera RAPM, Wong JHF, Fang VJ, Ng TWY, et al. Immune responses to twice-annual influenza vaccination in older adults in Hong Kong. Clin Infect Dis. 2018;66:904–12. http://dx.doi.org/10.1093/cid/cix900

32. McLean HQ, Thompson MG, Sundaram ME, Meece JK, McClure DL, Friedrich TC, et al. Impact of repeated vaccination on vaccine effectiveness against influenza A(H3N2) and B during 8 seasons. Clin Infect Dis. 2014;59:1375–85. http://dx.doi.org/10.1093/cid/ciu680

33. Skowronski DM, Chambers C, Sabaiduc S, De Serres G, Winter AL, Dickinson JA, et al. A perfect storm: impact of genomic variation and serial vaccination on low influenza vaccine effectiveness during the 2014–2015 season. Clin Infect Dis. 2016;63:21–32. http://dx.doi.org/10.1093/cid/ciw176

34. Ramsay LC, Buchan SA, Stirling RG, Cowling BJ, Feng S, Kwong JC, et al. The impact of repeated vaccination on influenza vaccine effectiveness: a systematic review and meta-analysis. BMC Med. 2017;15:159. http://dx.doi.org/10.1186/s12916-017-0919-0

35. Pica N, Palese P. Toward a universal influenza virus vaccine: prospects and challenges. Annu Rev Med. 2013;64:189–202. http://dx.doi.org/10.1146/annurev-med-120611-145115

Address for correspondence: Paul K.S. Chan, The Chinese University of Hong Kong, Department of Microbiology, 1/F LCW Clinical Sciences Bldg., Prince of Wales Hospital,, Shatin, New Territories, Hong Kong Special Administrative Region, China; email: paulkschan@cuhk.edu.hk

etymologia revisited

Influenza
[in′′floo-en′zə]

Acute viral infection of the respiratory tract. From Latin *influentia*, "to flow into"; in medieval times, intangible fluid given off by stars was believed to affect humans. The Italian influenza referred to any disease outbreak thought to be influenced by stars. In 1743, what Italians called an *influenza di catarro* ("epidemic of catarrh") spread across Europe, and the disease came to be known in English as simply "influenza."

Sources: Dorland's illustrated medical dictionary. 30th ed. Philadelphia: Saunders; 2003 and Quinion M. World wide words. 1998 Jan 3 [cited 2005 Dec 5]. Available from http://www.worldwidewords.org/topicalwords/tw-inf1.htm

Originally published in January 2006

https://wwwnc.cdc.gov/eid/article/01/12/et-1201_article

Mapping *Histoplasma capsulatum* Exposure, United States

Amelia W. Maiga, Stephen Deppen, Beth Koontz Scaffidi, John Baddley,
Melinda C. Aldrich, Robert S. Dittus, Eric L. Grogan

Maps of *Histoplasma capsulatum* infection prevalence were created 50 years ago; since then, the environment, climate, and anthropogenic land use have changed drastically. Recent outbreaks of acute disease in Montana and Nebraska, USA, suggest shifts in geographic distribution, necessitating updated prevalence maps. To create a weighted overlay geographic suitability model for *Histoplasma*, we used a geographic information system to combine satellite imagery integrating land cover use (70%), distance to water (20%), and soil pH (10%). We used logistic regression modeling to compare our map with state-level histoplasmosis incidence data from a 5% sample from the Centers for Medicare and Medicaid Services. When compared with the state-based Centers data, the predictive accuracy of the suitability score–predicted states with high and mid-to-high histoplasmosis incidence was moderate. Preferred soil environments for *Histoplasma* have migrated into the upper Missouri River basin. Suitability score mapping may be applicable to other geographically specific infectious vectors.

Histoplasmosis is a regionally endemic mycosis caused by inhalation of the spores of the fungus *Histoplasma capsulatum* from the soil, leading occasionally to symptomatic disease and asymptomatic pulmonary nodules (*1*). Soils act as reservoirs for *Histoplasma*, especially where temperatures are 22°C–29°C and annual rainfall is 35–50 inches (*2*). According to a 1969 map by Edwards et al. of histoplasmin skin test reactivity among single-county-resident Navy recruits in the United States, *H. capsulatum* has been most prevalent in the Mississippi and Ohio River basins (*3*). Since then, much has changed with the environment, climate, and anthropogenic land use. Indeed, the advent of HIV/AIDS and the use of immunosuppressive medications for rheumatologic, dermatologic, and gastrointestinal conditions has unmasked areas of previously hidden histoplasmosis endemicity, nationally and globally (*4*). Recent outbreaks in Montana and Nebraska have led the Centers for Disease Control and Prevention to suggest that histoplasmosis is now endemic to these regions (*5,6*). State-level incidence rates of histoplasmosis among older patients also demonstrate a shift toward Nebraska and the northern Great Lakes area (*7*). In addition, a recent publication of surveillance data from 2011 through 2014 in 12 states suggests that histoplasmosis also occurs in Minnesota, Wisconsin, and Michigan, areas where histoplasmosis was not thought to be endemic (*8*).

Accurate maps of *H. capsulatum* prevalence assist in the early recognition, diagnosis, and treatment of acute infections. Pulmonary histoplasmosis may generate cancer-mimicking lung granulomas, causing false-positive radiographic images on high-resolution computed tomography and fluorodeoxyglucose positron emission tomography (FDG-PET) (*9–11*). Thus, an accurate understanding of the conditions for *H. capsulatum* is of practical epidemiologic and clinical value.

Edwards' 1969 survey of histoplasmosis endemicity is impractical to repeat now or in the foreseeable future (*3*). It would be prohibitively expensive to survey a sufficiently large sample of the population and, in our mobile society, nearly impossible to identify an appropriate number of lifetime-single-county residents who are representative of the broader population. Furthermore, the histoplasmin skin test is no longer available, and another approach is needed. Our study objective was to model known environmental factors preferred by *H. capsulatum* and produce a large-scale map to enable risk stratification of patients on the basis of their geographic history.

Materials and Methods

We created a site suitability model for *H. capsulatum* weighted by 3 environmental soil characteristics measured across the continental United States within a geographic information system (ArcGIS 10.3.1; ESRI, Redlands, CA, USA). Suitability scores ranged from 1 through 9 within each soil characteristic; higher scores signified more favorable conditions for *H. capsulatum*. Selection of raster datasets was based on known criteria for histoplasmosis

Author affiliations: Vanderbilt University Medical Center, Nashville, Tennessee, USA (A.W. Maiga, S. Deppen, M.C. Aldrich, R.S. Dittus, E.L. Grogan); Tennessee Valley Healthcare System Veterans Hospital, Nashville (A.W. Maiga, R.S. Dittus); Vanderbilt University, Nashville (B.K. Scaffidi); University of Alabama at Birmingham, Birmingham, Alabama, USA (J. Baddley)

behavior—land cover, water, and soil pH—because cultivation and anthropogenic land use increase the spread of *H. capsulatum* from the soil to the air (*1*).

Land Cover

We obtained land cover data from the 2006 National Land Cover Database (*12*). This publicly available dataset applies 16 classes of land cover or land use types over the conterminous United States at a spatial resolution of 30 × 30 meters. The risk for histoplasmosis growth is highest in areas of high soil humidity (e.g., near rivers), and soil moisture affects the temperature at which *H. capsulatum* can survive (*13–15*).

Distance from Water

Because no continuous flood risk map exists for the United States, we defined water presence by attributes extracted from the 2006 National Land Cover Database (e.g., open water, woody wetlands, or emergent herbaceous woodlands). Suitability for *H. capsulatum* was modeled to decrease with Euclidean distance from these water types across 9 equally distributed categories. Suitability scores ranged from a best-suited value of 9, which occurred from 0 through 222 meters, to a low value of 1, at ≥1,777 meters (Table). Open water was assumed to preclude presence of histoplasmosis.

Soil pH

We obtained soil pH raster data from the University of Wisconsin Atlas of the Biosphere, compiled by the International Geosphere-Biosphere Programme Global Soils Data Task in 1998 (*16*). Original data projection of the Environmental Systems Research Institute ArcView gridded format with a spatial resolution of 10,000 meters, or 10 km, was reclassified into 9 categories. The highest score of 9 was assigned to pH values near 7.4, the pH of normal lungs, the presumed ideal environment for the *H. capsulatum* exposure of interest. Decreasing pH values were modeled in a descending fashion to a score of 4 for pH >8 and a score of 1 for pH <4.5 (Table).

Mapping

We calculated the overall score for each ZIP code area as a weighted sum of assigned values from each of the 3 environmental factors. Each layer was preprocessed for analysis by mosaicking native coordinate systems across a common geographic coordinate system (World Geodetic System 1984, https://www.nga.mil/ProductsServices/Geodesyandgeophysics/Pages/WorldGeodeticSystem.aspx) and then clipping the data for each raster layer to the conterminous US border. Pixels for each layer were reclassified to a common scale of 1–9, ranging from least to most suitable for *H. capsulatum*. The unique map layers were then weighted and combined. Weighting was an iterative process to approximate the historical distribution of *Histoplasma* and recent histoplasmosis infection patterns, especially in the lower Mississippi River valley and, given the limitations of computational efficiency, to interpolate the final risk surface (*17*). The final suitability model included 3 layers of data: the 2006 National Land Cover Database with 16 classes of land cover or land use types (weighted 70%), Euclidean distance from the nearest open water source (20%), and soil pH (10%) (Table). A granular risk score was computed for each pixel. Next, the pixel values from the suitability map were extracted as points, and those points were joined to state and census tract polygons to provide a mean, median, and SD for exposure suitability scores aggregated to each spatial unit. To create a continuous exposure risk surface, we applied the inverse distance weights to interpolate a risk surface, which was then clipped to the US border.

We determined the 70%, 20%, and 10% weights through an iterative process based on Edwards' 1969 survey county-level data for a few states (Tennessee with high within-state variability, Mississippi and Kansas with low variability, and Florida as a coastal state). During the developmental phase of the suitability score, we compared different proportions with state-level Medicare data, but there were no better models. Because of the lack of granularity of the state data, our sensitivity analyses may not have been very informative for detecting minor differences in state prevalence.

Table. Scoring of 3 soil characteristics used for *Histoplasma* site suitability map*

Assigned value	Land cover class (70% weight)†	Meters from water (20% weight)	Soil pH (10% weight)
9	Cultivated crops, >20% vegetation	0–222	7.2–7.6
8	Pasture or hay, >20% vegetation	222–444	7.0–7.2 or 7.6–7.8
7	Open water, woody wetlands, >20% vegetation; or emergent herbaceous wetlands, >80% vegetation	444–666	6.7–7
6	Deciduous, evergreen or mixed forest, >20% vegetation	666–888	6.4–6.7 or 7.8–8.0
5	Dwarf scrub or shrub/scrub, >20% vegetation; or grassland used for grazing, >80% vegetation	888–1,110	6.0–6.4
4	Developed, open space such as lawns, <20% impervious	1,110–1,332	5.6–6.0 or >8
3	Developed, low and medium intensity, 20% to 79% impervious	1,332–1,555	5.1–5.6
2	Barren land such as rock, sand, or clay, <15% vegetation	1,555–1,777	≥4.5 and <5.1
1	Developed, high intensity, ≥80% impervious	1,777–1,999	<4.5

*A value of 9 represents the most suitable environment for *H. capsulatum*. The overall weighted score was calculated as follows: an area of evergreen forest, located 1,000 meters from water, with a soil pH of 7.7 would have a suitability score of (6 × 0.7) + (5 × 0.2) + (8 × 0.1) = 6.
†Excluded classes include perennial ice/snow and Alaska-only vegetation types.

Statistical Analyses

We summarized our data to the state level to permit comparison with previously published research (*7*). The reference standard was state-level histoplasmosis incidence data from a random 5% sample of the Centers for Medicare and Medicaid Services (CMS) claims data for 1999–2008 (*7*). Incident cases of endemic histoplasmosis required 1 inpatient claim or 2 outpatient claims over 7–90 days. We used 2 logistic regression models to assess the ability of our suitability histoplasmosis score to predict the binary outcome of correctly identifying states with high histoplasmosis incidence rates, defined as $\geq$5 cases/100,000 person-years, and states with mid-to-high incidence rates, defined as $\geq$3 cases/100,000 person-years. We generated the appropriate area under the receiver operator curves (AUCs) and calculated the Wilcoxon-Mann-Whitney test by using Stata version 12.0 (StataCorp LLC, College Station, TX, USA).

Results

Figure 1 depicts the granular suitability score map with mean scores by US ZIP code. The data and model are applicable to estimates of *Histoplasma* in soils east of the Rocky Mountains because of lack of suitable soil habitats and limits in data availability. We calculated suitability score estimates west of the Rocky Mountains, but many geographic blocks had no or limited water data and thus may overestimate *Histoplasma* suitability (e.g., distances >3,000 meters from substantial amounts of water may preclude the presence of *Histoplasma* irrespective of land use). Figure 2 compares the state-level suitability scores with 1999–2008 state-level incidence data from Baddley et al. (*7*). Our suitability score model identified the states with high and mid-to-high histoplasmosis incidence rates with AUCs of 0.72 and 0.74, respectively, when compared with state-based diagnosis rates among elderly persons during 1999–2008.

Discussion

Our histoplasmosis exposure suitability score predicted state-level histoplasmosis incidence rates from recent CMS data with an AUC $\geq$0.72. Our model confirms previous reports that preferred soil environments for *Histoplasma* have expanded into the upper Missouri River basin. This progression probably reflects changes in climate and human land use with increased cultivation in that region and urbanization of other regions of the country.

Our suitability score has limitations. We compared our score to state-level histoplasmosis incident cases as derived from administrative data and were thus unable to assess the validity of our score to predict disease incidence for a more granular geographic region. However, CMS is not likely to release county-level histoplasmosis infection rates because of the risk of identifying individual patients. The administrative data we used for our comparative analysis have their own limitations, namely reliance on codes from the International Classification of Disease, Ninth Revision
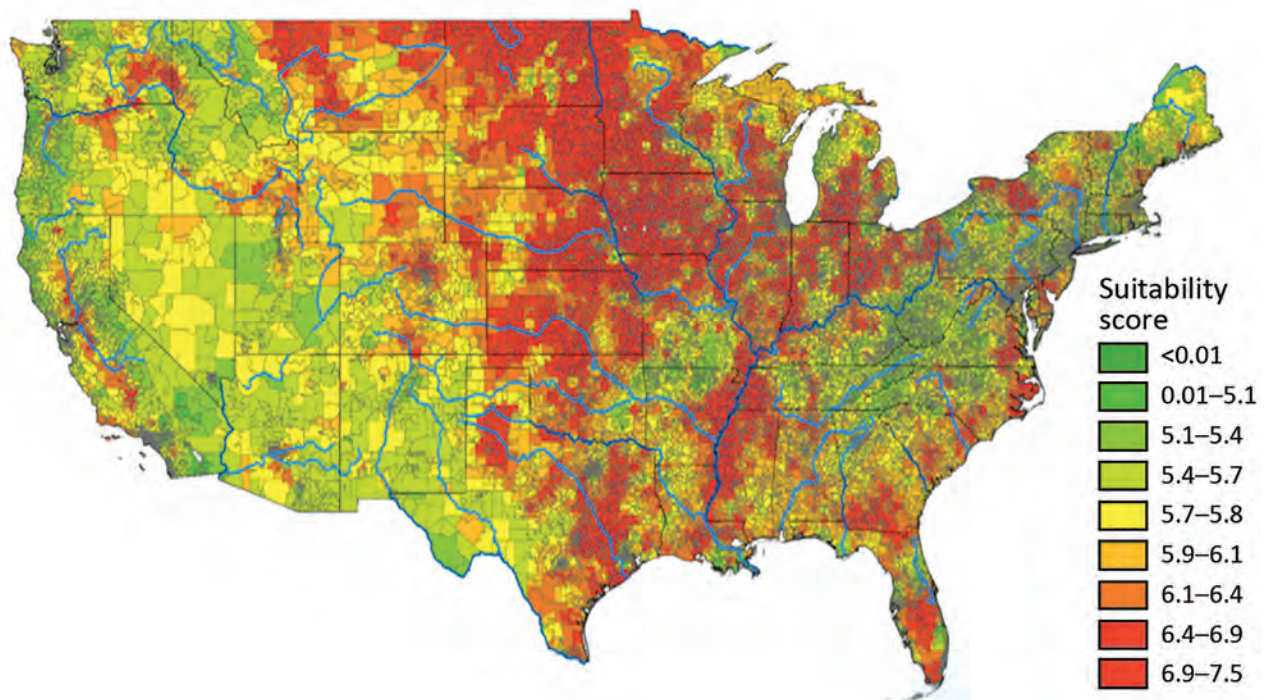
Figure 1. Mean *Histoplasma* site suitability score by US ZIP code. Red reflects greater histoplasmosis suitability; green reflects less suitability. The weighted mean score (Table) was calculated for each ZIP code. Data for geographic regions west of the Rocky Mountains are considered insufficient because of limited surface water data.
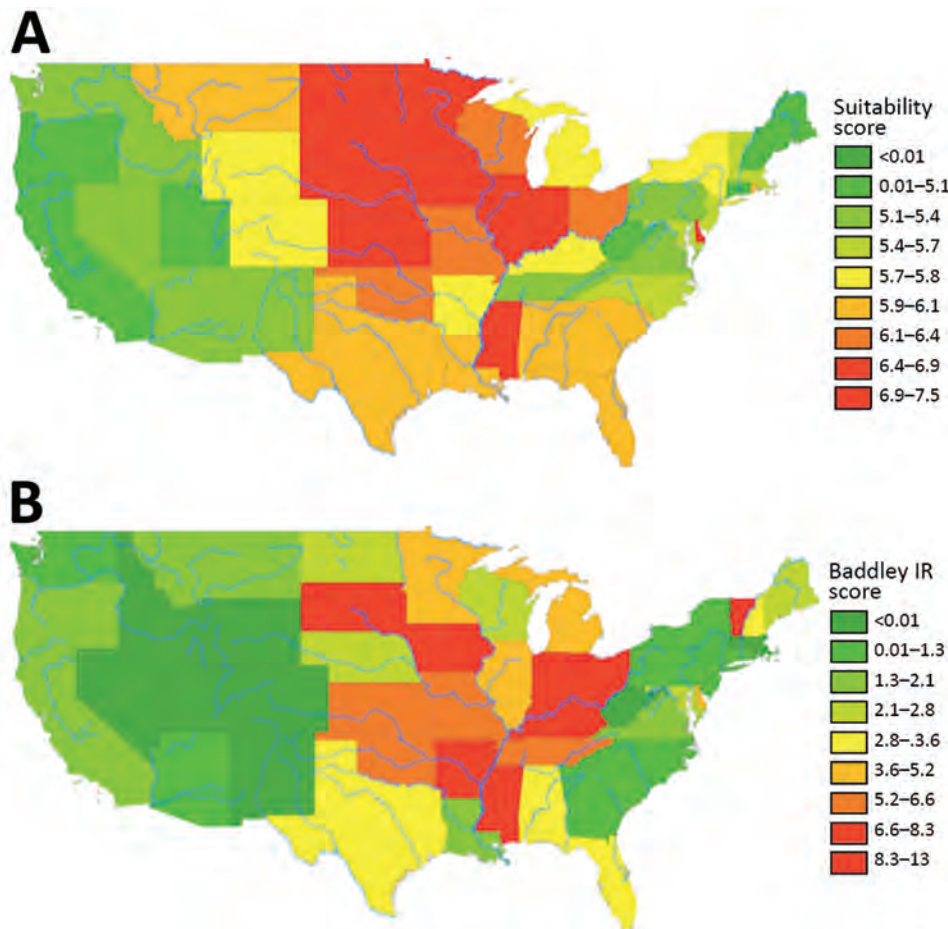
Figure 2. State-level suitability score compared with histoplasmosis incidence rates, United States. A) State-level suitability score map. B) State-level histoplasmosis incidence rates for 1999–2008 US Medicare and Medicaid data (no. cases/100,000 person-years).

Suitability score
- <0.01
- 0.01–5.1
- 5.1–5.4
- 5.4–5.7
- 5.7–5.8
- 5.9–6.1
- 6.1–6.4
- 6.4–6.9
- 6.9–7.5

Baddley IR score
- <0.01
- 0.01–1.3
- 1.3–2.1
- 2.1–2.8
- 2.8–.3.6
- 3.6–5.2
- 5.2–6.6
- 6.6–8.3
- 8.3–13

for histoplasmosis rate estimates, with unknown sensitivity and specificity.

We also did not include known specific vectors of histoplasmosis exposure (e.g., droppings in areas of bird or bat roosts). This exclusion is particularly relevant, given the microfocus concept that *Histoplasma* exist in small environmental foci, resulting in localized outbreaks or other exposures in non–histoplasmosis-endemic areas (*17,18*). It is also worth noting that the coarse resolution of the soil pH pixels limited the sensitivity of the weighted overlay result. Local studies that use soil pH from US Department of Agriculture data within each state at a smaller resolution may be preferred to upsampling the coarse International Geosphere-Biosphere Programme data. The accuracy of our approach should be confirmed with soil pH measurements. In addition, as with any aggregate measure, our score is subject to the ecologic fallacy, whereby inferences about individual risk are estimated by an overall estimate from the geographic region in which the person resides. This suitability score could be combined with occupational and residential histories to risk-stratify patients for fungal lung disease risk and to improve interpretation of chest images.

The accurate diagnosis of histoplasmosis is challenging and often requires a battery of antigen detection, serology, and histopathology studies (*19,20*). Serologic tests are imperfect and, although often specific, can have low sensitivity, particularly for immunosuppressed patients. Knowledge of the distribution of *H. capsulatum* exposure and histoplasmosis infection is also critical for the appropriate regional use of imaging to diagnose fungal lung disease in immunocompromised persons and persons with lung malignancies. Investigators have questioned the utility of FDG-PET for diagnosing lung nodules in regions where granulomatous disease is prevalent (*9,10,21*). A recent meta-analysis concluded that FDG-PET was less specific for diagnosing malignancy in populations where lung mycosis is endemic than in those where it is not (*11*).

In conclusion, we generated a detailed suitability map for *Histoplasma* exposure east of the Rocky Mountains, an approach that can be updated as land use changes. Our suitability map may provide a detailed prediction of the risk for acute histoplasmosis infection, including areas of new endemicity. Accurate mapping of *Histoplamosis* exposure may also aid in the interpretation of chest images, particularly in the context of lung cancer screening

programs (*22*). Future work might add elevation, soil moisture, water-holding capacity, and geologic data into the suitability model. Suitability score models have the potential to be applied to other infectious agents strongly associated with geographic-specific vectors, with the promise to inform healthcare and improve public health assessments and interventions.

About the Author

Dr. Maiga is a resident in General Surgery at Vanderbilt University Medical Center and a former Veterans Affairs Quality Scholar at the Tennessee Valley Healthcare System. Her research interests include clinician decision-making and predictive modeling, primarily related to lung cancer.

References

1. Christie A. Histoplasmosis and pulmonary calcification; geographic distribution. Am J Trop Med Hyg. 1951;31:742–52. http://dx.doi.org/10.4269/ajtmh.1951.s1-31.742
2. Sykes J, Taboada J. Histoplasmosis. In: Sykes J, editor. Canine and feline infectious disease. St. Louis: Elsevier Inc; 2014. p. 587–98.
3. Edwards LB, Acquaviva FA, Livesay VT, Cross FW, Palmer CE. An atlas of sensitivity to tuberculin, PPD-B, and histoplasmin in the United States. Am Rev Respir Dis. 1969;99(Suppl):1–132.
4. Bahr NC, Antinori S, Wheat LJ, Sarosi GA. Histoplasmosis infections worldwide: thinking outside of the Ohio River valley. Curr Trop Med Rep. 2015;2:70–80. http://dx.doi.org/10.1007/s40475-015-0044-0
5. Centers for Disease Control and Prevention. Histoplasmosis in a state where it is not known to be endemic—Montana, 2012–2013. MMWR Morb Mortal Wkly Rep; 2013:62:834–7.
6. Centers for Disease Control and Prevention. Outbreak of histoplasmosis among industrial plant workers—Nebraska, 2004. MMWR Morb Mortal Wkly Rep. 2004;53:1020–2.
7. Baddley JW, Winthrop KL, Patkar NM, Delzell E, Beukelman T, Xie F, et al. Geographic distribution of endemic fungal infections among older persons, United States. Emerg Infect Dis. 2011;17:1664–9. http://dx.doi.org/10.3201/eid1709.101987
8. Armstrong PA, Jackson BR, Haselow D, Fields V, Ireland M, Austin C, et al. Multistate epidemiology of histoplasmosis, United States, 2011–2014. Emerg Infect Dis. 2018;24:425–31. http://dx.doi.org/10.3201/eid2403.171258
9. Grogan E, Deppen SA, Ballman K, Andrade GM, Verdail FC, Aldrich MC, et al. Accuracy of FDG-PET to diagnose lung cancer in the ACOSOG Z4031 trial. Alliance for Clinical Trials in Oncology; 2012 June 29–July 1; Chicago, IL.
10. Deppen S, Putnam JB Jr, Andrade G, Speroff T, Nesbitt JC, Lambright ES, et al. Accuracy of FDG-PET to diagnose lung cancer in a region of endemic granulomatous disease. Ann Thorac Surg. 2011;92:428–33. http://dx.doi.org/10.1016/j.athoracsur.2011.02.052
11. Deppen SA, Blume JD, Kensinger CD, Morgan AM, Aldrich MC, Massion PP, et al. Accuracy of FDG-PET to diagnose lung cancer in areas with infectious lung disease: a meta-analysis. JAMA. 2014;312:1227–36. http://dx.doi.org/10.1001/jama.2014.11488
12. Fry J, Xian G, Jin S, Dewitz J, Homer C, Yang L, et al. Completion of the 2006 National Land Cover Database for the conterminous United States. Photogramm Eng Remote Sensing. 2011;77:858–64.
13. Mahvi TA. Factors governing the epidemiology of *Histoplasma capsulatum* in soil. Mycopathol Mycol Appl. 1970;41:167–76. http://dx.doi.org/10.1007/BF02051492
14. Goodman NL, Larsh HW. Environmental factors and growth of *Histoplasma capsulatum* in soil. Mycopathol Mycol Appl. 1967;33:145–56. http://dx.doi.org/10.1007/BF02053445
15. Menges RW, Furcolow ML, Larsh HW, Hinton A. Laboratory studies on histoplasmosis: I. The effect of humidity and temperature on the growth of *Histoplasma capsulatum*. J Infect Dis. 1952;90:67–70.
16. University of Wisconsin-Madison Center for Sustainability and the Global Environment. International Geosphere-Biosphere Programme-DIS. SoilData, version 0. A program for creating global soil-property databases, IGBP Global Soils Data Task, France. 1998 [cited 2018 Jul 22]. https://nelson.wisc.edu/sage/data-and-models/datasets.php
17. Benedict K, Mody RK. Epidemiology of histoplasmosis outbreaks, United States, 1938–2013. Emerg Infect Dis. 2016;22:370–8. http://dx.doi.org/10.3201/eid2203.151117
18. Randall JN, Donald S, Laurel R, Brian D, Sky RB, Elizabeth ES, et al. Histoplasmosis in Idaho and Montana, USA, 2012–2013. Emerg Infect Dis. 2015;21:1071–2. http://dx.doi.org/10.3201/eid2106.141367
19. McKinsey DS, McKinsey JP. Pulmonary histoplasmosis. Semin Respir Crit Care Med. 2011;32:735–44. http://dx.doi.org/10.1055/s-0031-1295721
20. Wheat LJ, Azar MM, Bahr NC, Spec A, Relich RF, Hage C. Histoplasmosis. Infect Dis Clin North Am. 2016;30:207–27. http://dx.doi.org/10.1016/j.idc.2015.10.009
21. Croft DR, Trapp J, Kernstine K, Kirchner P, Mullan B, Galvin J, et al. FDG-PET imaging and the diagnosis of non–small cell lung cancer in a region of high histoplasmosis prevalence. Lung Cancer. 2002;36:297–301. http://dx.doi.org/10.1016/S0169-5002(02)00023-5
22. Aberle DR, Adams AM, Berg CD, Black WC, Clapp JD, Fagerstrom RM, et al.; National Lung Screening Trial Research Team. Reduced lung-cancer mortality with low-dose computed tomographic screening. N Engl J Med. 2011;365:395–409. http://dx.doi.org/10.1056/NEJMoa1102873

Address for correspondence: Stephen Deppen, Department of Thoracic Surgery, 609 Oxford House, 1313 21st Ave S, Nashville, TN 37232, USA; email: steve.deppen@vanderbilt.edu

Transmission Dynamics of Highly Pathogenic Avian Influenza Virus A(H5Nx) Clade 2.3.4.4, North America, 2014–2015

Dong-Hun Lee,[1] Mia Kim Torchetti, Joseph Hicks, Mary Lea Killian, Justin Bahl, Mary Pantin-Jackwood, David E. Swayne

Eurasia highly pathogenic avian influenza virus (HPAIV) H5 clade 2.3.4.4 emerged in North America at the end of 2014 and caused outbreaks affecting >50 million poultry in the United States before eradication in June 2015. We investigated the underlying ecologic and epidemiologic processes associated with this viral spread by performing a comparative genomic study using 268 full-length genome sequences and data from outbreak investigations. Reassortant HPAIV H5N2 circulated in wild birds along the Pacific flyway before several spillover events transmitting the virus to poultry farms. Our analysis suggests that ≥3 separate introductions of HPAIV H5N2 into Midwest states occurred during March–June 2015; transmission to Midwest poultry farms from Pacific wild birds occurred ≈1.7–2.4 months before detection. Once established in poultry, the virus rapidly spread between turkey and chicken farms in neighboring states. Enhanced biosecurity is required to prevent the introduction and dissemination of HPAIV across the poultry industry.

Highly pathogenic avian influenza virus (HPAIV) A(H5N1) emerged in 1996 in Guangdong, China (A/goose/Guangdong/1/1996 [Gs/GD]), and has since caused outbreaks in poultry, infections in wild birds, and often fatal clinical cases in humans in >80 countries (1). In late autumn 2014, Gs/GD H5N8 clade 2.3.4.4 was reported in East Asia, Europe, and the west coast of North America (2,3). The timing and direction of this virus's dissemination, which coincided with waterfowl migration patterns, together with phylogenetic and geospatial data (3,4) support the hypothesis that Gs/GD H5N8 clade 2.3.4.4 was introduced into North America through the Beringian Crucible via intercontinental movement of migratory waterfowl (5,6).

In November and December 2014, novel reassortant H5N1, H5N2, and H5N8 viruses were detected in wild waterfowl along the Pacific flyway (2,7). Reassortant H5N2 virus was identified as the causative agent of influenza outbreaks in poultry farms in British Columbia, Canada, and among wild waterfowl in the northwestern United States (Video, https://wwwnc.cdc.gov/EID/article/24/10/17-1891-V1.htm) (8). This virus subsequently was the predominant strain during HPAIV outbreaks among poultry in the United States in 2015, particularly during March–June (9,10), and was detected in wild birds migrating along the Pacific, Central, and Mississippi flyways (11,12). The last reported virus detection related to the outbreak in the United States was in June 2015 from a Canada goose in Michigan. Despite increased surveillance efforts in the United States, HPAIV was rarely detected in wild bird populations during the latter half of 2015 and 2016 (13). In 2015, the virus was detected just 2 times by real-time reverse transcription PCR in mallards, once in July (from bird banding efforts in Utah) and once in November (from a hunter harvest in Oregon) (14). In 2016, H5N2 virus clade 2.3.4.4 was detected in 2 mallards sampled in Alaska and Montana, providing evidence for low-level maintenance of this virus in wild birds in northwestern North America (15,16). Despite disagreement about the role of flyways in limiting viral spread among wild birds (17,18), the rapid spatial diffusion and transmission of HPAIV in wild and domestic birds highlight the need to further investigate the processes involved in viral emergence and spread.

We sequenced and analyzed the full-length genome sequences of 249 H5N2 and 19 H5N8 HPAIVs collected during the 2014–2015 outbreaks in the United States. Viruses came from 32 wild birds, 7 raptors, 14 backyard poultry farms, and 196 commercial poultry sites. We used a molecular epidemiologic approach involving genome sequences and outbreak information to determine the evolution and spread patterns of these viruses.

[1]Current affiliation: University of Connecticut, Storrs, Connecticut, USA.

Materials and Methods

Genome Sequencing

The National Animal Health Laboratory Network conducts PCR testing for avian influenza in the United States, and per title 9, Code of Federal Regulations, nonnegative samples are forwarded to the National Veterinary Services Laboratories (Ames, Iowa, USA) for confirmation testing and genome sequencing. In December 2014, interagency wild bird surveillance started including testing for the HPAIV Gs/GD lineage in wild birds in the Pacific flyway, and by summer 2015, surveillance was further expanded to include testing for this virus in all flyways (19). In our study, we included all available wild bird (n = 32) and raptor (n = 7) viruses from these surveillance efforts and, for poultry, just 1 virus from each affected site with available samples (n = 210; 14/21 affected backyard sites, 196/211 affected commercial flocks) (20).

We extracted viral RNA from 249 H5N2-positive and 19 H5N8-positive oral or cloacal swab samples using MagMAX Viral RNA Isolation Kit (Ambion, Foster City, CA, USA). We synthesized complementary DNA and amplified all 8 segments by reverse transcription PCR using SuperScript III (Invitrogen, Carlsbad, CA, USA) (21). We conducted genome sequencing using the Ion Torrent PGM (Life Technologies, Waltham, MA, USA) or MiSeq (Illumina, San Diego, CA, USA) platforms as previously described (7,16). We assembled genome sequences using SeqMan NGen version 4 (http://www.dnastar.com/t-next-gen-seqman-ngen.aspx). We deposited nucleotide sequences in GenBank (online Technical Appendix Table 5, https://wwwnc.cdc.gov/EID/article/24/10/17-1891-Techapp1.pdf).

Maximum-Likelihood Phylogenetic Analysis of US HPAIV H5N2

Of the 265 H5N2 sequences analyzed, we retrieved the 16 viruses from Canada from the GISAID EpiFlu database (http://platform.gisaid.org) and sequenced the 249 viruses from the United States. In all, 32 viruses were from wild waterfowl in 10 states (Alaska, Idaho, Kansas, Kentucky, Michigan, Missouri, Montana, Oregon, Washington, Wyoming); 7 viruses were from captive and wild raptors in 5 states (Idaho, Minnesota, Missouri, Washington, Wisconsin); and 210 viruses were from backyard and commercial poultry farms in 13 states (Arkansas, Idaho, Iowa, Kansas, Minnesota, Missouri, Montana, Nebraska, North Dakota, Oregon, South Dakota, Washington, Wisconsin). Data from Minnesota (1 backyard farm, 99 commercial poultry farms, 1 wild bird) and Iowa (69 commercial poultry farms), where most commercial poultry were affected, predominated in this sample.

To demonstrate the phylogenetic organization of the HPAIV outbreak, we built a maximum-likelihood phylogenetic tree of the concatenated genome (all 8 genome segments) with RAxML version 8.0.0 (22) using default parameters and a general time-reversible model with gamma-distributed rate variation among sites. We divided the 265 H5N2 isolates into subgroups of related clusters by their bootstrap value (>70%) on maximum-likelihood phylogenetic analysis (23). To assess relatedness support, we performed rapid bootstrapping, with bootstrap convergence criterion yielding 1,000 bootstrap iterations. We illustrated the time series of outbreaks by subgroup and state using Tableau (https://www.tableau.com/).

Median-Joining Network Analysis

We concatenated all 8 genome segments of each virus isolate to generate a single alignment. We used these alignments to construct a phylogenetic network using the median-joining method implemented in program NETWORK version 5.0 (http://www.fluxus-engineering.com/sharenet_rn.htm) with epsilon set to 1 (24).

Ancestral State Reconstruction of Geographic Location and Host Type

To investigate virus transmission between host types over large spatial scales, we reconstructed the virus transmission history between states geographically using an ancestral state reconstruction approach with a Bayesian stochastic search variable selection to determine the most probable spatial and ecologic transmission history. For all phylogeographic analyses, we used an uncorrelated log-normal distribution relaxed-clock method with a Hasegawa, Kishino, and Yano nucleotide substitution model and Bayesian skyride coalescent prior.

Using a globally derived dataset (n = 127 taxa) of HPAIV hemagglutinin (HA) sequences from Asia, Europe, and North America, we tested whether the HPAIV H5 outbreak in North America resulted from a single virus introduction or multiple virus introductions into the bird population of North America. We then developed a more refined model to estimate viral diffusion and transmission between wild and domestic populations and assess the most likely route of spread. We incorporated HPAIV HA sequences from the US and Canada 2014–2015 outbreaks (11) into our discrete phylogenetic model. In this model, we defined geographic region and host type as discrete nominal categories. We categorized geographic region of virus collection by migratory flyway (Pacific, Central, Mississippi) and host type as chicken, turkey, wild bird, or backyard poultry. We estimated ancestral state transition rate and model parameters from a set of 5,000 empirical trees simulated from HPAIV H5 HA gene data collected throughout the outbreaks. For the discrete ancestral state model, we used a nonreversible continuous-time Markov chain model to estimate geographic and host transitions among wild and

domestic birds (*25*). We used Bayesian stochastic search variable selection to identify important transitions using a binary indicator (*I*) (*18,26,27*), enabling the calculation of Bayes factor with SPREAD version 1.0.6 (*28*). A transition was considered important when *I* was >0.5 and Bayes factor was >4.0 (*18,26*). We used the last 500 trees from each posterior distribution to construct heat maps representing the average number of transitions per month (online Technical Appendix).

Results

The highly pathogenic phenotype of viruses sequenced in this study were confirmed by presence of the polybasic amino acid motif at the HA cleavage site and through experimental infection of chickens by intravenous inoculation (online Technical Appendix). Analysis of globally circulating Gs/GD-lineage H5Nx clade 2.3.4.4 viruses showed a widespread distribution and confirmed that the lineage causing the outbreak in North America probably resulted from a single introduction (online Technical Appendix Table 2, Figure 1). During December 2014–March 2015, H5N2 was detected in poultry farms of British Columbia and in wild waterfowl and backyard poultry of states along the Pacific flyway (Figure 1). Subsequently, during March–June 2015, H5N2 predominated in poultry outbreaks in the Midwest.

We generated a maximum-likelihood phylogenetic tree and median-joining phylogenetic network of HPAIV H5N2 using 265 concatenated full-genome sequences (249 from the United States, 16 from Canada) to investigate the relatedness of isolates (Figure 2; online Technical Appendix

Figure 2). The H5N2 viruses formed 2 major genetic groups, group 1 and group 2 (includes subgroups 2a, 2b, 2c, 2d, 2e, and 2 nonclustered [2nc]), with maximum-likelihood phylogeny bootstrap proportions >75%. Group 1 contains 73 viruses from 11 US states and 2 Canada provinces across the Pacific (Alaska, Idaho, Montana, Oregon, and Washington, USA; British Columbia), Central (Kansas, South Dakota, and Wyoming, USA), and Mississippi (Arkansas, Minnesota, and Missouri, USA; Ontario, Canada) flyways (online Technical Appendix Figures 3, 4). Group 2 predominantly contained viruses isolated from poultry from states along the Mississippi flyway: 2a (n = 39; Iowa, Minnesota, Missouri, Wisconsin); 2b (n = 35; Minnesota); 2c (n = 11; Iowa, Minnesota); 2d (n = 4; Wisconsin); and 2e (n = 81; Iowa, Minnesota; Nebraska, South Dakota in Central flyway). Twenty-two 2nc viruses were detected in 6 states along the Central (North Dakota, South Dakota) and Mississippi (Kentucky, Michigan, Minnesota, Wisconsin) flyways.

Both group 1 and 2 viruses were found in wild birds and gallinaceous poultry (Figure 2; online Technical Appendix Figure 3). Wild birds infected with group 2 viruses were only infected with subgroup 2nc viruses. Group 1 viruses were recovered from all host types represented (28 wild birds, 5 raptors, 11 backyard poultry, 14 commercial poultry [1 chicken, 13 turkeys]). Subgroups 2c and 2d were found only in turkeys and had limited geographic spread. The remaining subgroups affected several hosts. Subgroup 2nc viruses were isolated from 6 wild birds, 13 commercial turkey sites, and 3 commercial chicken sites. Subgroup 2a was found in 2 backyard sites, 36 commercial turkey sites,
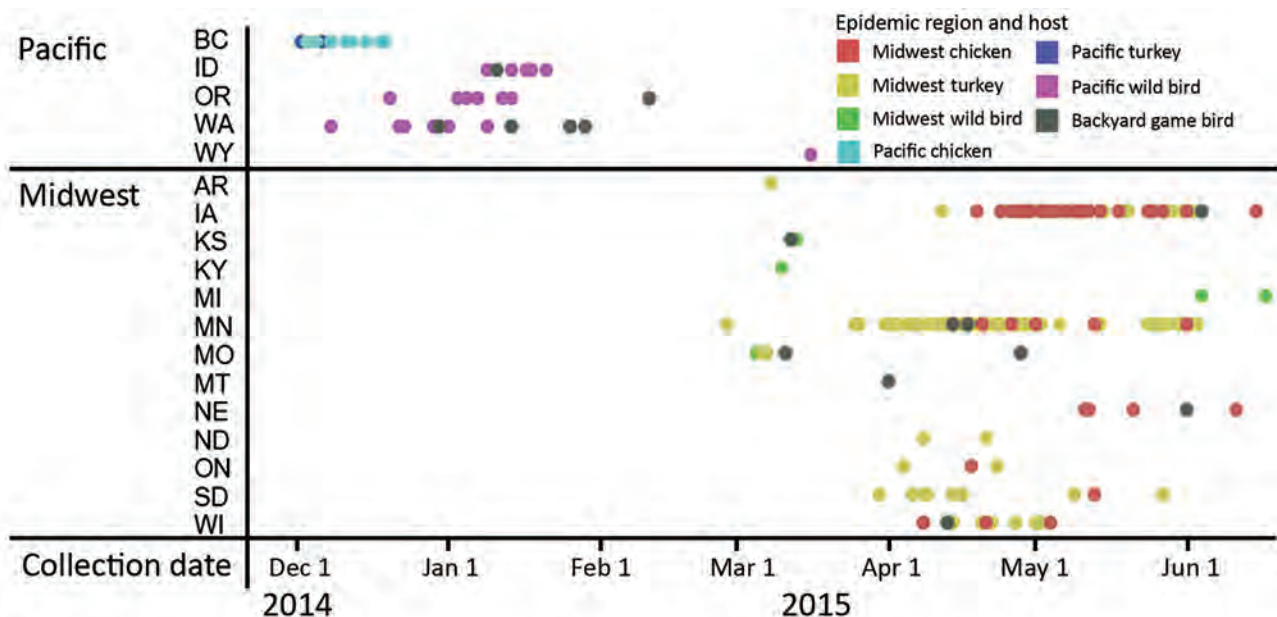
Figure 1. Time series of reassortant highly pathogenic avian influenza virus A(H5N2) distribution, by US state and Canada province, December 2014–June 2015. Virus region and host are indicated. BC, British Columbia, Canada; ON, Ontario, Canada.
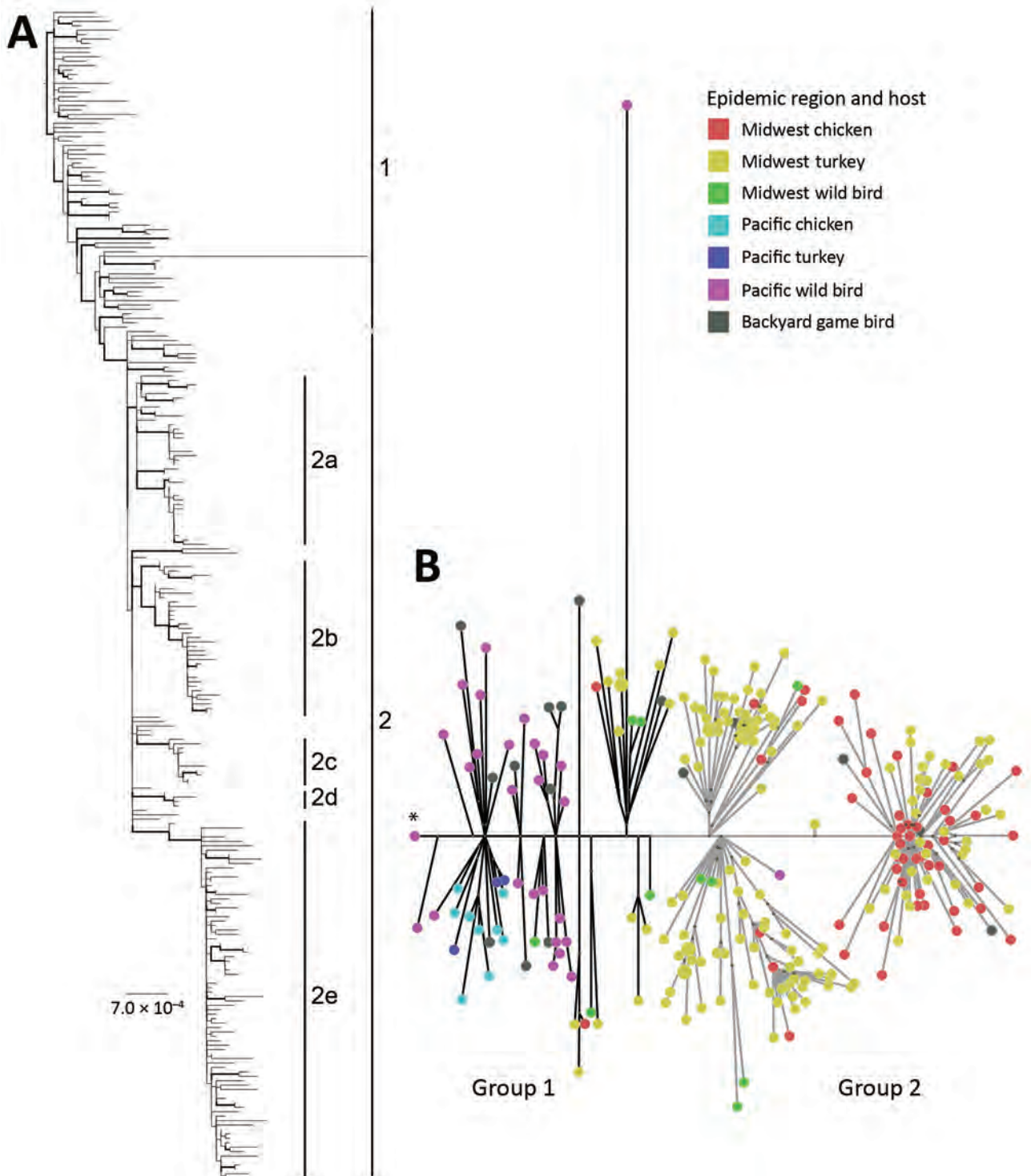
Figure 2. Genetic characterization of reassortant highly pathogenic avian influenza virus A(H5N2) clade 2.3.4.4, North America, 2014–2015. A) Maximum-likelihood phylogeny of concatenated complete genome sequences. Labels indicate genetic subgroups. Scale bar indicates nucleotide substitutions per site. The full version of the phylogenic tree is available in online Technical Appendix Figure 2 (https://wwwnc.cdc.gov/EID/article/24/10/17-1891-Techapp1.pdf). B) Median-joining phylogenetic network constructed by using concatenated complete genome sequences. This network includes the most parsimonious trees linking the sequences. Each unique sequence is represented by a circle sized relative to its frequency in the dataset. Virus region and host are indicated. *US index H5N2 virus (A/Northern_pintail/Washington/40964/2014).

and 1 commercial chicken site. Subgroup 2b predominantly affected commercial turkey sites (n = 32) and 3 commercial chicken flocks; subgroup 2e was recovered from 2 backyard, 36 commercial turkey, and 42 commercial chicken sites and 1 game bird flock. Genetic clustering of subgroups 2a, 2b, and 2e in maximum-likelihood analysis and the close genetic relatedness of Midwest poultry isolates in network analysis provide strong evidence for extensive interfarm transmission (Figure 2; online Technical Appendix Figure 2).
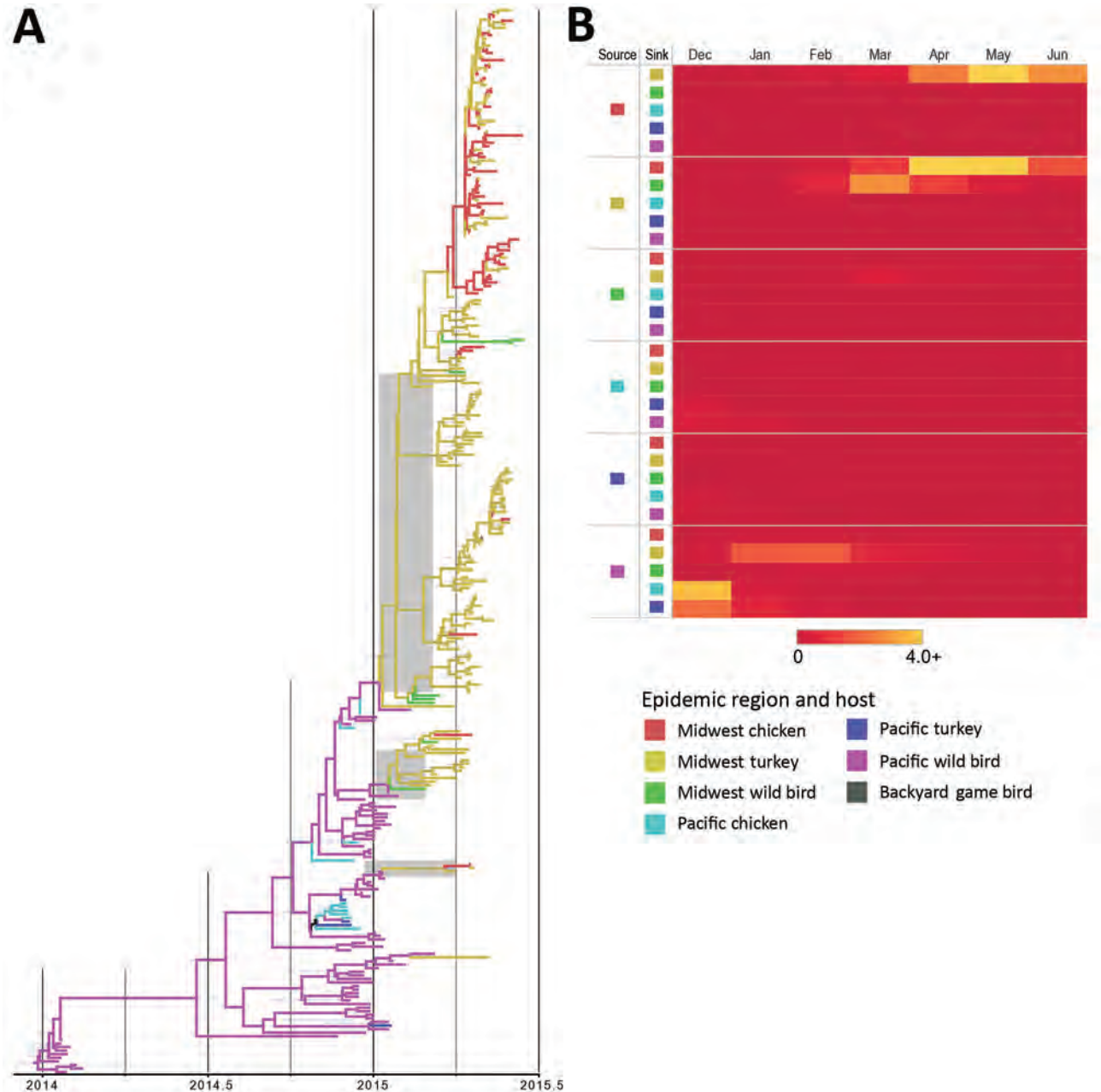
Figure 3. Phylogeographic reconstruction of source–sink dynamics of highly pathogenic avian influenza virus A(H5N2) outbreak, United States, 2014–2015. A) Phylogenetic tree of hemagglutinin gene of H5N2 isolates. The geographic region and host type were defined in the model as discrete nominal character states, and the number of state transitions at tree nodes was counted. The character states included in the phylogenetic model (Midwest chicken, Midwest turkey, Midwest wild bird, Pacific chicken, Pacific turkey, and Pacific wild bird) are indicated. Black nodes and branches represent an ancestral reconstruction that is highly uncertain, sharing equal probability between Pacific wild bird and Pacific turkey. The shaded boxes represent the time between the introduction of the virus into Midwest poultry populations and the first detection of the virus within the population. B) Heat map showing source–sink dynamics and average number of transitions per location per year (0–4.0).

Our phylogenetic analysis suggests that the outbreak in the Midwest was initiated through multiple independent HPAIV H5N2 introductions with group 1 viruses of wild bird origin (Figures 2, 3). To formally test the role of various host populations and elucidate the most likely route for viral spread in the United States, we integrated host type (wild birds, domestic chickens and turkeys, backyard poultry) into our geographic model. Our source–sink and phylogenetic network analyses suggest that the virus detected in the Midwest shares a common ancestor with the viruses detected in the Pacific flyway 1.7–2.4 months before the first detection in Midwest poultry facilities (Figure 3; online Technical Appendix Figure 5). Undetected infected hosts also could have migrated from the Pacific Coast through the Midwest, depositing infectious material on the US landscape, leading to the outbreaks in Midwest poultry populations. The virus subsequently rapidly transmitted between commercial turkey and chicken farms. The rapid rate of transmission suggests that underlying epidemiologic factors were driving the spread within and between farm systems.

Bayesian simulation results showed that turkey farms and chicken farms were equally supported as the source of infection of domestic flocks after establishment of the virus in Midwest US farms (Table). Although the discrete state transition rate from chicken farms to turkey farms was higher, this difference is likely an artifact of the substantially larger flocks found in chicken farms, which predominantly use layer houses. Our analysis showed high rates of transmission between turkey and chicken farms in the Midwest, probably confounding control efforts and contributing to the overall extent of the outbreak (Figure 3, panel B). No support exists for viral spread from Midwest wild birds to Midwest commercial farms, suggesting that this epidemiologic pathway likely did not play a role in the spread of the outbreak after the initial introduction into the Midwest (Table), which has further been supported by epidemiologic investigations (29). In addition, a transition from Midwest turkey to wild birds is supported by a high Bayes factor (4798.91) and posterior probability (0.999), suggesting HPAIV spillback from domestic poultry to wild birds at a low transition rate (Table).

We identified 14 common substitutions across the entire genome of HPAIV H5N2 when comparing with US index virus A/northern pintail/WA/40964/2014 (H5N2). These substitutions include 10 nonsynonymous substitutions in group 1 and 2 viruses (L386V and V649I in polymerase basic 2; L8F, N130T, and S157P in HA; R253K, E368K, and V412A in neuraminidase; Q78R in matrix 2; I176T in nonstructural protein 1) and 4 nonsynonymous substitutions in group 2 viruses (R215K in polymerase basic 1, A337V in polymerase acidic, N60H in nuclear export protein, K217T in nonstructural protein 1) (online Technical Appendix Table 3).

Discussion

Phylogenetic reconstruction of source–sink dynamics supports multiple independent introductions of HPAIV H5N8 into the United States during late 2014 from wild birds. Despite the frequent detection of HPAIV H5 in wild birds of the Pacific flyway up to February 2015 (30), only 2 commercial poultry and 1 backyard farm flocks became infected with HPAIV H5N8 and 7 backyard poultry flocks with HPAIV H5N2 in states along the Pacific flyway. No HPAIV H5N2 infections were found at commercial poultry sites in states along the Pacific flyway (31). In contrast with infrequent events in states along the Pacific flyway, 213 H5N2 events in commercial and backyard poultry were reported during March–June 2015 in the Midwest. Our analysis demonstrates extensive interfarm transmission of virus subgroups 2a, 2b, and 2e but not of group 1 viruses, which could also infect wild birds, suggesting a change in the epidemiologic processes driving viral spread. Although a national level–structured surveillance effort was not initiated until July 2015 (19), H5N2 detections were far less frequent in the Midwest than in the Pacific flyway, suggesting few H5N2-infected wild waterfowl were in the Central and Mississippi flyways during the outbreak period (32,33). Nonetheless, detection of H5N2 viruses from wild birds in the Midwest in early 2015 and our phylogenetic analysis suggest that the HPAIV H5N2 moved from the Pacific flyway to the Mississippi and Central flyways as early as January or February 2015, with subsequent interfarm transmission in and between states of the Midwest.

When performing the source–sink phylogenetic analysis, we made assumptions regarding sampling and population structure, which should be considered when interpreting results. For instance, sampling in this analysis is most likely biased toward commercial poultry because of the nature of HPAIV reporting. Oversampling of a specific population might lead to overestimation of that group as a sink to viral migration (34); however, a secondary simulation in which viral host characteristics were continuously randomized to observe the influence of sampling heterogeneity (35) revealed that sampling does not appear to bias the ancestral reconstruction in this data. Also, in the model, we included the complete random population mixing assumption, even though a structured coalescent approach might have helped limit bias introduced from ecologic barriers that structure wild and domestic bird populations; many of the HPAIV sequences from poultry hosts used in our study represented a single farm. No data were available regarding the size of farms, number of animals infected on those farms, or number of farms affected, all of which might further bias spatial diffusion parameter estimates in a structured coalescent analysis.

Table. Well-supported discrete trait viral transitions among chicken, turkey, and wild bird populations during highly pathogenic avian influenza virus H5 outbreak, Midwest and Pacific regions, USA, 2014–2015*

Transition from	Transition to	Bayes factor	Posterior probability	Mean transition rate
Midwest chicken	Midwest turkey	38,421.1688	1.0	5.0917
Midwest turkey	Midwest chicken	38,421.1688	1.0	1.8376
Midwest turkey	Midwest wild bird	4,798.9103	0.9991	0.8344
Pacific wild bird	Pacific chicken	464.3334	0.9909	0.8478
Pacific wild bird	Midwest turkey	227.2091	0.9816	0.8557
Pacific wild bird	Pacific turkey	201.2141	0.9792	0.5687
*Only the migrations supported by a Bayes factor >4 and posterior probability >0.5 are indicated.				

The hypothesis that HPAIV H5N2 was introduced into the Midwest through wild birds rather than poultry production channels is supported by epidemiologic evidence; during February 27–April 20, 2015, H5N2 virus was detected 17 times across 5 states and 16 counties in different hosts (wild bird, raptor, backyard flocks, turkey flocks), and epidemiologic links could not be found between Pacific Coast and Midwest farms for any virus subgroup. The widespread detection of the HPAIV H5 lineage in healthy wild birds (30), subclinical infection with high virus shedding, and transmission among mallard ducks experimentally infected with HPAIV H5N2 (36) support the hypothesis of HPAIV H5 dissemination to multiple states through wild waterfowl over a short period during wild aquatic bird migrations. For the outbreak in the Midwest (February–June 2015), events (infections with viruses of groups 1 and 2nc) detected early during the outbreak (February–April 2015) probably represent independent introductions, followed by limited secondary spread, and events (infections with viruses of subgroups 2a–e) detected later during the outbreak (April–June 2015) were largely caused by extensive interfarm transmission. Previous estimates of basic reproductive number and viral migration among host types in domestic and wild birds support our findings that HPAIV H5N2 rapidly spread between poultry facilities in the Midwest after the initial introduction of a virus of wild bird origin (37). Grear et al. showed that the H5N2 and H5N8 HPAIV outbreak did not encounter sufficient transmission barriers to prevent persistence when introduced to wild or domestic birds (37). Consistent with our data, Grear et al. concluded that once the HPAIV H5N2 entered the poultry production system in the Midwest, transmission was driven through poultry production–related mechanisms (37). That conclusion was based on evidence of a close phylogenetic distance among sequences from poultry facilities, relatively infrequent cross-species transmission, and a high estimated proportion of virus diversity in addition to the lack of detection of this lineage in reservoir hosts when using other surveillance data. Our Bayesian simulation also supports the high probability of 2-way transmission between poultry and wild bird populations.

The epidemiology of the HPAIV H5 detections and pathobiologic features suggest that the early H5N8 and H5N2 group 1 viruses detected in the United States were highly adapted to waterfowl and poorly adapted to chickens and turkeys (36,38–40). Index wild bird viruses [A/gyrfalcon/Washington/40188–6/2014 (H5N8), A/northern pintail/Washington/40964/2014 (H5N2)] required a high mean bird infectious dose of 50% (BID_{50}; $10^{5.7}$ EID_{50}) to infect chickens; directly inoculated and in-contact exposed survivors did not seroconvert (38). Increased virus adaptation to chickens and turkeys, specifically poultry, was observed among the H5N2 group 2 viruses and not the H5N2 group 1 viruses (39,40). In chickens, the BID_{50} of H5N2 group 2 viruses for poultry ($10^{3.2–3.6}$ EID_{50}) was lower than that of group 1 viruses for poultry ($10^{5.1}$ EID_{50}) and index wild birds ($10^{5.7}$ EID_{50}).

Examination of mutational frequencies and patterns showed common mutations among H5N2 subgroup 2a–e viruses fixed in the population during circulation in poultry. In particular, substitutions in the nucleoprotein amino acid 105 (M105V, M105I) were identified among H5N2 group 2 viruses from the United States and a virus isolate from a chicken in British Columbia (11) and has been suggested as a determinant for virus adaptation from ducks to chickens (41). Consistent with our previous study (39), we identified common substitutions (R215K polymerase basic 1, A337V polymerase acidic, N60H nuclear export protein, K217T nonstructural protein 1) in H5N2 group 2 viruses that increased infectivity and pathogenicity in chickens in comparison with group 1 viruses. In addition, we found substitution S157P at an antigenic site of the HA protein, which might affect the immunogenicity profile of the virus (42).

In summary, we analyzed the transmission dynamics of Asia-origin HPAIV H5 in the United States. The H5N8 virus came from East Asia, entered North America during the fall 2014 migration season (7), and spread rapidly along the wild bird flyways in the United States starting in December 2014. In the Pacific flyway, Eurasia H5N8 virus circulated in wild birds and disseminated to backyard and commercial poultry farms largely by point-source introductions; a single detection occurred in a backyard flock in Indiana outside the Pacific states. Furthermore, influenza A genome segments of the Eurasia H5N8 virus mixed with segments of the North America low pathogenicity avian influenza viruses, creating new reassortant HPAIVs H5N1, H5N2, and H5N8. For the reassortant H5N2 virus in the Midwest, our results strongly support introduction from the

Pacific flyway early in 2015, with ≥3 initial independent introductions and late events involving extensive secondary spread between poultry farms. These H5N8 and H5N2 viruses cause substantial illness and death in poultry but have, thus far, not been implicated in human infection. Mammalian studies in mice and ferrets suggest low public health risk (*43,44*).

During 2016–2017, HPAIV H5N8 clade 2.3.4.4 group B (Gochang-like) reemerged and caused outbreaks in wild birds and domestic poultry across Europe, Asia, and Africa (*45,46*). Enhanced biosecurity is required to prevent the introduction and dissemination of HPAIVs across the poultry industry; the role that human activity can play in viral spread via fomites should not be underestimated. Continued surveillance, virus characterization, and infectivity studies remain invaluable to monitoring the spread and evolution of these H5 viruses; such efforts could further the design of improved prevention strategies. Additional research is needed to decipher the potential mechanisms of virus introduction into poultry systems.

About the Author

Dr. Lee is a postdoctoral researcher at the Southeast Poultry Research Laboratory of the Agricultural Research Service, US Department of Agriculture, Athens, Georgia, USA. His research interests include molecular epidemiology and host–pathogen interactions of avian influenza viruses.

References

1. Lee DH, Bertran K, Kwon JH, Swayne DE. Evolution, global spread, and pathogenicity of highly pathogenic avian influenza H5Nx clade 2.3.4.4. J Vet Sci. 2017;18(S1):269–80. http://dx.doi.org/10.4142/jvs.2017.18.S1.269

2. Ip HS, Torchetti MK, Crespo R, Kohrs P, DeBruyn P, Mansfield KG, et al. Novel Eurasian highly pathogenic avian influenza A H5 viruses in wild birds, Washington, USA, 2014. Emerg Infect Dis. 2015;21:886–90. http://dx.doi.org/10.3201/eid2105.142020

3. Global Consortium for H5N8 and Related Influenza Viruses. Role for migratory wild birds in the global spread of avian influenza H5N8. Science. 2016;354:213–7. http://dx.doi.org/ 10.1126/science.aaf8852

4. Verhagen JH, Herfst S, Fouchier RAM. How a virus travels the world. Science. 2015;347:616–7. http://dx.doi.org/10.1126/ science.aaa6724

5. Lee DH, Torchetti MK, Winker K, Ip HS, Song CS, Swayne DE. Intercontinental spread of Asian-Origin H5N8 to North America through Beringia by migratory birds. J Virol. 2015;89:6521–4. http://dx.doi.org/10.1128/JVI.00728-15

6. Ramey AM, Reeves AB, TeSlaa JL, Nashold S, Donnelly T, Bahl J, et al. Evidence for common ancestry among viruses isolated from wild birds in Beringia and highly pathogenic intercontinental reassortant H5N1 and H5N2 influenza A viruses. Infect Genet Evol. 2016;40:176–85. http://dx.doi.org/10.1016/j.meegid.2016.02.035

7. Lee DH, Bahl J, Torchetti MK, Killian ML, Ip HS, DeLiberto TJ, et al. Highly pathogenic avian influenza viruses and generation of novel reassortants, United States, 2014–2015. Emerg Infect Dis. 2016;22:1283–5. http://dx.doi.org/10.3201/eid2207.160048

8. Pasick J, Berhane Y, Joseph T, Bowes V, Hisanaga T, Handel K, et al. Reassortant highly pathogenic influenza A H5N2 virus containing gene segments related to Eurasian H5N8 in British Columbia, Canada, 2014. Sci Rep. 2015;5:9484. http://dx.doi.org/ 10.1038/srep09484

9. US Department of Agriculture. HPAI 2014–2015 infected premises. 2016 Jun 8 [cited 2017 Nov 15]. https://www.aphis.usda.gov/ animal_health/animal_dis_spec/poultry/downloads/hpai-positive-premises-2014-2015.pdf

10. US Department of Agriculture. HPAI 2014/15 confirmed detections. 2015 [cited 2017 Nov 15]. https://www.aphis.usda.gov/ aphis/ourfocus/animalhealth/animal-disease-information/ avian-influenza-disease/sa_detections_by_states/hpai-2014-2015-confirmed-detections

11. Xu W, Berhane Y, Dubé C, Liang B, Pasick J, VanDomselaar G, et al. Epidemiological and evolutionary inference of the transmission network of the 2014 highly pathogenic avian influenza H5N2 outbreak in British Columbia, Canada. Sci Rep. 2016;6:30858. http://dx.doi.org/10.1038/srep30858

12. US Department of Agriculture. Wild bird positive highly pathogenic avian influenza cases in the United States. 2015 Sep 4 [cited 2017 Nov 15]. https://www.aphis.usda.gov/wildlife_damage/ downloads/WILD%20BIRD%20POSITIVE%20HIGHLY%20 PATHOGENIC%20AVIAN%20INFLUENZA%20CASES%20 IN%20THE%20UNITED%20STATES.pdf

13. Krauss S, Stallknecht DE, Slemons RD, Bowman AS, Poulson RL, Nolting JM, et al. The enigma of the apparent disappearance of Eurasian highly pathogenic H5 clade 2.3.4.4 influenza A viruses in North American waterfowl. Proc Natl Acad Sci U S A. 2016;113:9033–8. http://dx.doi.org/10.1073/pnas.1608853113

14. US Department of Agriculture. Wild bird positive highly pathogenic avian influenza cases in the United States. 2016 Jun 30 [cited 2017 Nov 15]. https://www.aphis.usda.gov/animal_health/ downloads/animal_diseases/ai/uspositivecases.pdf

15. US Department of Agriculture. Wild bird highly pathogenic avian influenza cases in the United States. 2017 Jul 7 [cited 2017 Nov 15]. https://www.aphis.usda.gov/animal_health/downloads/ animal_diseases/ai/uspositivecases17.pdf

16. Lee DH, Torchetti MK, Killian ML, DeLiberto TJ, Swayne DE. Reoccurrence of avian influenza A(H5N2) virus clade 2.3.4.4 in wild birds, Alaska, USA, 2016. Emerg Infect Dis. 2017;23:365–7. http://dx.doi.org/10.3201/eid2302.161616

17. Lam TT, Ip HS, Ghedin E, Wentworth DE, Halpin RA, Stockwell TB, et al. Migratory flyway and geographical distance are barriers to the gene flow of influenza virus among North American birds. Ecol Lett. 2012;15:24–33. http://dx.doi.org/ 10.1111/j.1461-0248.2011.01703.x

18. Bahl J, Krauss S, Kühnert D, Fourment M, Raven G, Pryor SP, et al. Influenza A virus migration and persistence in North American wild birds. PLoS Pathog. 2013;9:e1003570. http://dx.doi.org/10.1371/journal.ppat.1003570

19. US Department of Agriculture. Surveillance plan for highly pathogenic avian influenza in waterfowl in the United States, 2015 Jun [cited 2017 Nov 15] https://www.aphis.usda.gov/animal_health/downloads/animal_diseases/ai/2015-hpai-surveillance-plan.pdf

20. US Department of Agriculture. HPAI 2014–2015 infected premises. 2016 Jun 8 [cited 2017 Nov 15] https://www.aphis.usda.gov/animal_health/animal_dis_spec/poultry/downloads/hpai-positive-premises-2014-2015.pdf

21. Bowman AS, Sreevatsan S, Killian ML, Page SL, Nelson SW, Nolting JM, et al. Molecular evidence for interspecies transmission of H3N2pM/H3N2v influenza A viruses at an Ohio agricultural fair, July 2012. Emerg Microbes Infect. 2012;1:e33. http://dx.doi.org/10.1038/emi.2012.33

22. Stamatakis A. RAxML version 8: a tool for phylogenetic analysis and post-analysis of large phylogenies. Bioinformatics. 2014;30:1312–3. http://dx.doi.org/10.1093/bioinformatics/btu033

23. Hillis DM, Bull JJ. An empirical test of bootstrapping as a method for assessing confidence in phylogenetic analysis. Syst Biol. 1993;42:182–92. http://dx.doi.org/10.1093/sysbio/42.2.182

24. Bandelt HJ, Forster P, Röhl A. Median-joining networks for inferring intraspecific phylogenies. Mol Biol Evol. 1999;16:37–48. http://dx.doi.org/10.1093/oxfordjournals.molbev.a026036

25. Minin VN, Suchard MA. Counting labeled transitions in continuous-time Markov models of evolution. J Math Biol. 2008;56:391–412. http://dx.doi.org/10.1007/s00285-007-0120-8

26. Bahl J, Pham TT, Hill NJ, Hussein IT, Ma EJ, Easterday BC, et al. Ecosystem interactions underlie the spread of avian influenza A viruses with pandemic potential. PLoS Pathog. 2016;12:e1005620. http://dx.doi.org/10.1371/journal.ppat.1005620

27. Lemey P, Rambaut A, Drummond AJ, Suchard MA. Bayesian phylogeography finds its roots. PLOS Comput Biol. 2009;5:e1000520. http://dx.doi.org/10.1371/journal.pcbi.1000520

28. Bielejec F, Rambaut A, Suchard MA, Lemey P. SPREAD: spatial phylogenetic reconstruction of evolutionary dynamics. Bioinformatics. 2011;27:2910–2. http://dx.doi.org/10.1093/bioinformatics/btr481

29. US Department of Agriculture. Epidemiologic and other analyses of HPAI-affected poultry flocks: September 9, 2015 report. 2015 Sep 9 [cited 2017 Nov 15]. https://www.aphis.usda.gov/animal_health/animal_dis_spec/poultry/downloads/Epidemiologic-Analysis-Sept-2015.pdf

30. Bevins SN, Dusek RJ, White CL, Gidlewski T, Bodenstein B, Mansfield KG, et al. Widespread detection of highly pathogenic H5 influenza viruses in wild birds from the Pacific flyway of the United States. Sci Rep. 2016;6:28980. http://dx.doi.org/10.1038/srep28980

31. US Department of Agriculture. Final report for the 2014–2015 outbreak of highly pathogenic avian influenza (HPAI) in the United States. 2016 Aug 11 [cited 2017 Nov 15]. https://www.aphis.usda.gov/animal_health/emergency_management/downloads/hpai/2015-hpai-final-report.pdf

32. Jennelle CS, Carstensen M, Hildebrand EC, Cornicelli L, Wolf P, Grear DA, et al. Surveillance for highly pathogenic avian influenza virus in wild birds during outbreaks in domestic poultry, Minnesota, 2015. Emerg Infect Dis. 2016;22:1278–82. http://dx.doi.org/10.3201/eid2207.152032

33. Jennelle CS, Carstensen M, Hildebrand EC, Wolf PC, Grear DA, Ip HS, et al. Surveillance for highly pathogenic avian influenza in wild turkeys (*Meleagris gallopavo*) of Minnesota, USA during 2015 outbreaks in domestic poultry. J Wildl Dis. 2017;53:616–20. http://dx.doi.org/10.7589/2016-09-205

34. Frost SD, Pybus OG, Gog JR, Viboud C, Bonhoeffer S, Bedford T. Eight challenges in phylodynamic inference.

35. Edwards CJ, Suchard MA, Lemey P, Welch JJ, Barnes I, Fulton TL, et al. Ancient hybridization and an Irish origin for the modern polar bear matriline. Curr Biol. 2011;21:1251–8. http://dx.doi.org/10.1016/j.cub.2011.05.058

36. Pantin-Jackwood MJ, Costa-Hurtado M, Shepherd E, DeJesus E, Smith D, Spackman E, et al. Pathogenicity and transmission of H5 and H7 highly pathogenic avian influenza viruses in mallards. J Virol. 2016;90:9967–82. http://dx.doi.org/10.1128/JVI.01165-16

37. Grear DA, Hall JS, Dusek RJ, Ip HS. Inferring epidemiologic dynamics from viral evolution: 2014–2015 Eurasian/North American highly pathogenic avian influenza viruses exceed transmission threshold, $R_0 = 1$, in wild birds and poultry in North America. Evol Appl. 2018;11:547–57. http://dx.doi.org/10.1111/eva.12576

38. Bertran K, Swayne DE, Pantin-Jackwood MJ, Kapczynski DR, Spackman E, Suarez DL. Lack of chicken adaptation of newly emergent Eurasian H5N8 and reassortant H5N2 high pathogenicity avian influenza viruses in the U.S. is consistent with restricted poultry outbreaks in the Pacific flyway during 2014–2015. Virology. 2016;494:190–7. http://dx.doi.org/10.1016/j.virol.2016.04.019

39. DeJesus E, Costa-Hurtado M, Smith D, Lee DH, Spackman E, Kapczynski DR, et al. Changes in adaptation of H5N2 highly pathogenic avian influenza H5 clade 2.3.4.4 viruses in chickens and mallards. Virology. 2016;499:52–64. http://dx.doi.org/10.1016/j.virol.2016.08.036

40. Spackman E, Pantin-Jackwood MJ, Kapczynski DR, Swayne DE, Suarez DL. H5N2 highly pathogenic avian influenza viruses from the US 2014-2015 outbreak have an unusually long pre-clinical period in turkeys. BMC Vet Res. 2016;12:260. http://dx.doi.org/10.1186/s12917-016-0890-6

41. Tada T, Suzuki K, Sakurai Y, Kubo M, Okada H, Itoh T, et al. NP body domain and PB2 contribute to increased virulence of H5N1 highly pathogenic avian influenza viruses in chickens. J Virol. 2011;85:1834–46. http://dx.doi.org/10.1128/JVI.01648-10

42. Chen MW, Liao HY, Huang Y, Jan JT, Huang CC, Ren CT, et al. Broadly neutralizing DNA vaccine with specific mutation alters the antigenicity and sugar-binding activities of influenza hemagglutinin. Proc Natl Acad Sci U S A. 2011;108:3510–5. http://dx.doi.org/10.1073/pnas.1019744108

43. Pulit-Penaloza JA, Sun X, Creager HM, Zeng H, Belser JA, Maines TR, et al. Pathogenesis and transmission of novel highly pathogenic avian influenza H5N2 and H5N8 viruses in ferrets and mice. J Virol. 2015;89:10286–93. http://dx.doi.org/10.1128/JVI.01438-15

44. Kaplan BS, Russier M, Jeevan T, Marathe B, Govorkova EA, Russell CJ, et al. Novel highly pathogenic avian A(H5N2) and A(H5N8) influenza viruses of clade 2.3.4.4 from North America have limited capacity for replication and transmission in mammals. mSphere. 2016;1:e00003-16. http://dx.doi.org/10.1128/mSphere.00003-16

45. Pohlmann A, Starick E, Harder T, Grund C, Höper D, Globig A, et al. Outbreaks among wild birds and domestic poultry caused by reassorted influenza A(H5N8) clade 2.3.4.4 viruses, Germany, 2016. Emerg Infect Dis. 2017;23:633–6. http://dx.doi.org/10.3201/eid2304.161949

46. Lee DH, Sharshov K, Swayne DE, Kurskaya O, Sobolev I, Kabilov M, et al. Novel reassortant clade 2.3.4.4 avian influenza A(H5N8) virus in wild aquatic birds, Russia, 2016. Emerg Infect Dis. 2017;23:359–60. http://dx.doi.org/10.3201/eid2302.161252

Epidemics. 2015;10:88–92. http://dx.doi.org/10.1016/j.epidem.2014.09.001

Address for correspondence: David E. Swayne, Southeast Poultry Research Laboratory, US Department of Agriculture, Agricultural Research Service, 934 College Station Rd, Athens, GA 30605, USA; email: david.swayne@ars.usda.gov

etymologia

Hemagglutinin [heʹmə-glooʹtĭ-nin] and Neuraminidase [noorʹə-minʹĭ-dās]

Ronnie Henry

In 1941, virologist George K. Hirst discovered that adding influenza virus to red blood cells (erythrocytes) in a test tube caused the cells to agglutinate, mediated by one of the virus surface glycoproteins, hemagglutinin (from the Greek *haima*, "blood," + Latin *gluten*, "glue"). Alfred Gottschalk later showed that hemagglutinin binds virus to host cells by attaching to sialic acids (from the Greek *sialon*, "saliva") on carbohydrate side chains of cell-surface glycoproteins and glycolipids. The other influenza virus surface protein, neuraminidase (referring to brain lipids from which it was first derived), is a virus receptor-destroying enzyme that removes its substrate, sialic acids, from infected cell surfaces so that newly made progeny viruses are released to infect additional cells. At present, 18 hemagglutinin subtypes (H1–H18) and 11 neuraminidase subtypes (N1–N11) are recognized.
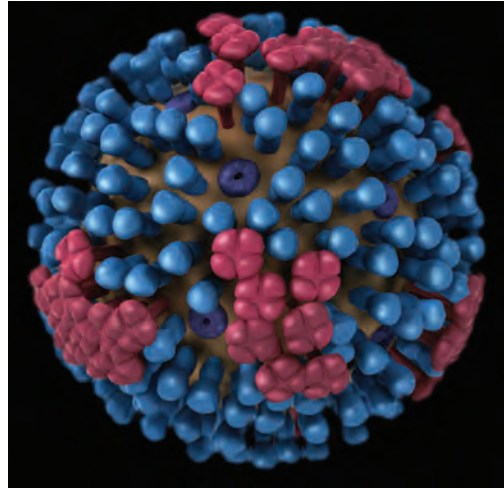
Figure. Image of influenza virus showing hemagglutinin (blue) and neuraminidase (red) proteins on the surface of the virus. Content source: Centers for Disease Control and Prevention, National Center for Immunization and Respiratory Diseases (NCIRD).

Sources
1. Gottschalk A. The chemistry and biology of sialic acids and related substances. London: Cambridge University Press; 1960.
2. Hirst GK. The agglutination of red cells by allantoic fluid of chick embryos infected with influenza virus. Science. 1941;94:22–3. http://dx.doi.org/10.1126/science.94.2427.22
3. Hirst GK. Adsorption of influenza hemagglutinins and virus by red blood cells. J Exp Med. 1942;76:195–209. http://dx.doi.org/10.1084/jem.76.2.195

Address for correspondence: Ronnie Henry, Centers for Disease Control and Prevention, 1600 Clifton Rd NE, Mailstop E03, Atlanta, GA 30329-4027, USA; email: boq3@cdc.gov

Zika Virus Infection during Pregnancy and Effects on Early Childhood Development, French Polynesia, 2013–2016

Lorenzo Subissi, Timothée Dub, Marianne Besnard, Teheipuaura Mariteragi-Helle,
Tuxuan Nhan, Delphine Lutringer-Magnin, Philippe Barboza, Céline Gurry,
Pauline Brindel, Eric J. Nilles, David Baud, Angela Merianos, Didier Musso,
Judith R. Glynn, Gilles Dupuis, Van-Mai Cao-Lormeau,[1] Marine Giard,[1] Henri-Pierre Mallet[1]

Congenital Zika virus syndrome consists of a large spectrum of neurologic abnormalities seen in infants infected with Zika virus in utero. However, little is known about the effects of Zika virus intrauterine infection on the neurocognitive development of children born without birth defects. Using a case-control study design, we investigated the temporal association of a cluster of congenital defects with Zika virus infection. In a nested study, we also assessed the early childhood development of children recruited in the initial study as controls who were born without known birth defects,. We found evidence for an association of congenital defects with both maternal Zika virus seropositivity (time of infection unknown) and symptomatic Zika virus infection during pregnancy. Although the early childhood development assessment found no excess burden of developmental delay associated with maternal Zika virus infection, larger, longer-term studies are needed.

Zika virus is a mosquito-vectored flavivirus first isolated in 1947 in the Zika forest in Uganda (*1*). For the next 60 years, Zika virus was considered to cause sporadic and mild

Author affiliations: World Health Organization, Geneva, Switzerland (L. Subissi, P. Barboza, C. Gurry, P. Brindel); Institut Pasteur, Paris, France (T. Dub); French Polynesia Hospital Center, Pirae, French Polynesia (M. Besnard, D. Lutringer-Magnin); Institut Louis Malardé, Papeete, French Polynesia (T. Mariteragi-Helle, T. Nhan, D. Musso, V.-M. Cao-Lormeau); Brigham and Women's Hospital and Harvard Humanitarian Initiative, Boston, Massachusetts, USA (E.J. Nilles); World Health Organization, Manila, Philippines (E.J. Nilles, A. Merianos); University Hospital, Lausanne, Switzerland (D. Baud); Aix Marseille University, IRD, AP-HM, SSA, VITROME, IHU-Méditerranée Infection, Marseille, France (D. Musso); London School of Hygiene & Tropical Medicine, London, UK (J.R. Glynn); University of Québec, Montreal, Québec, Canada (G. Dupuis); Centre de Liaison sur l'Intervention et la Prévention Psychosociales, Montreal (G. Dupuis); Bureau de Veille Sanitaire, Direction de la Santé, Papeete (M. Giard, H.-P. Mallet)

infection in humans (*2*). In 2007, Zika virus emerged in the Western Pacific island of Yap, Federated States of Micronesia (*3*). In 2013, Zika virus emerged in French Polynesia, causing a large outbreak (>30,000 clinical cases estimated during October 2013–April 2014) before spreading rapidly to other Pacific Islands (*4*–*6*). Zika virus emerged in Brazil in 2015 and spread to most of the Americas in 2016 (*7*).

Like some other members of the family *Flaviviridae*, such as West Nile virus and Japanese encephalitis virus, Zika virus is neurotropic (*8*). The link between Zika virus and neurologic disorders such as Guillain-Barré syndrome in adults and microcephaly in newborns is now established (*9*–*15*). Of 84 countries or territories with active autochthonous transmission of Zika virus (as of March 2017), 23 have reported an increase in incidence of Guillain-Barré syndrome, and 31 have reported patients with microcephaly, central nervous system (CNS) malformations, or both potentially associated with Zika virus infection (*16*). After the French Polynesia Zika virus outbreak, health authorities reported an unusual increase in microcephaly and other rare CNS abnormalities of unknown etiology, including corpus callosum or septal agenesis, spina bifida, and brainstem dysfunction (*17*).

Zika virus may be associated with multiple congenital abnormalities (*18*–*20*). The malformations and dysfunctions caused by Zika virus infection during pregnancy are known as congenital Zika syndrome (CZS), but the anatomic, functional, and neurocognitive impairments associated with in utero Zika virus infection have not been precisely defined (*21*). Characterizing the factors contributing to neurocognitive deficits in children born to mothers infected with Zika virus during pregnancy but without overt anatomic malformations, and quantifying the risk of neurocognitive dysfunction, may have major, substantive clinical and public health implications.

[1]These authors contributed equally to this article.

We report 2 linked studies conducted in French Polynesia: a retrospective case-control study to determine whether the unusual cluster of CNS congenital defects during and after the Zika virus outbreak in French Polynesia was associated with maternal Zika virus infection, and a cross-sectional study to identify neurocognitive deficits in young children without known birth defects born to mothers who were pregnant during the outbreak. Both studies were powered on the case-control study.

Methods

Study Design and Population

Case-Control Study

The case-patient definition was any fetus or neonate with a CNS congenital defect of unexplained etiology and a maternal gestational period that overlapped the extended Zika virus circulation period (June 1, 2013–August 31, 2014) by ≥1 weeks (17). Unexplained etiology meant that most commonly suspected etiologies (toxoplasmosis, other, rubella, cytomegalovirus, and herpes [TORCH] infections and genetics) were excluded. We identified cases and controls among fetuses and newborns from the Centre Hospitalier de Polynésie Française in Pirae, French Polynesia, where 60% of all deliveries in this country occur. We identified eligible fetuses from pregnancy terminations using the medical records of the prenatal diagnosis center and eligible newborns from a previously reported case series of congenital cerebral malformations and dysfunctions (17) and from the in-hospital discharge records of the neonatology ward and the neonatal intensive care unit. We matched each case-patient to 5 controls by age of the mother at pregnancy (±5 y) and date of conception (date of mother's last prepregnancy menstrual period ±14 d). We selected the controls randomly from hospital birth records. For logistical reasons, only women residing in Tahiti or Moorea, the 2 most populated and accessible islands, were invited to participate as controls.

Cross-Sectional Study

Because a rate of ≈50% Zika virus seropositive mothers was expected in the control group of the case-control study, an additional cross-sectional study was designed to assess whether Zika virus infection in the mother was associated with delayed or abnormal early childhood development (ECD) in the child. Two nurses were trained to conduct anthropometric and neurocognitive testing. ECD was then compared between children with seropositive or seronegative mothers.

Data Collection

During January–August 2016, mothers of case-patients and controls completed a face-to-face questionnaire on social and economic characteristics, clinical data, and environmental factors, including exposure to chemicals (alcohol, tobacco, drugs, or deltamethrin pesticide spraying) during pregnancy. We retrieved information on seroconversion for *Toxoplasma gondii* and rubella virus during pregnancy from medical files; information on cytomegalovirus (CMV) seroconversion was available for case-patients only. We assessed exposure to deltamethrin by spatiotemporally linking outdoor spraying by the vector control teams with the mother's residence address during pregnancy. We stratified maternal socioeconomic status as low, medium, or high, adapting from the 4-factor Hollingshead scale (22). Gestational age was estimated by each mother's primary obstetrician, using last menstrual period and first-trimester ultrasound measurements for each mother.

Laboratory Testing

We detected anti–Zika virus and anti–dengue virus (DENV) neutralizing antibodies in serum from mothers of the case-patients and the controls by using seroneutralization tests, as previously described (9,23). We incubated serial 2-fold dilutions (from 1:10 to 1:1,280) of each serum sample, previously heat inactivated, for 1 h with strains of Zika virus, DENV-1, DENV-2, DENV-3, or DENV-4. We then inoculated the serum–virus mixtures onto Vero cells and incubated then for 5–7 d. We used ELISA to show the presence of nonneutralized replicative virus in inoculated cells; the reciprocal serum dilution corresponding to the last well showing neutralization activity was the 50% neutralization antibody titer for that serum sample (23,24). We determined Zika virus infection in mothers by detection of anti–Zika virus neutralizing antibodies (NAb) in serum collected 20–35 months after the expected beginning date of pregnancy. We defined mothers for whom the anti–Zika virus NAb titer was ≥20 as seropositive and those with a titer <20 as seronegative.

Assessment of Physical and Developmental Status of Children

We used 4 anthropometric indicators for children's developmental status: weight for age, height for age, weight for height, and head circumference for age. We calculated Z scores (number of SDs of a value above or below the mean) using WHO Anthro software (25). We calculated birth anthropometric indicators (Z scores for weight, height, and head circumference) using INTERGROWTH-21st project software (26). We used the French version of the Child Development Assessment Scale, kindly provided by the Centre for Liaison on Intervention and Prevention in the Psychosocial Area, Canada (http://www.ged-cdas.ca), to assess ECD. The Child Development Assessment Scale, which is available in French and is well correlated with the Bayley scale 3rd edition (27), consists of questions and

observations adapted to children 0–5 years of age and has been validated for use by nonspecialized health or education professionals (Vézina N. Elaboration and validation of the Child Development Assessment Scale, 0–5 years [thesis]. Québec City (QC, Canada): Université du Québec; 2005). The scale is divided into 3 domains: socioemotional; cognitive, including language; and motor. In each domain, children are classified as adequate (no development issues), question (development to be monitored), or problem (specialized pediatric testing required).

Exposures, Outcomes, and Statistical Analysis

We used 2 measures of exposure: maternal Zika virus seropositivity, a binary variable (yes/no) based on serology results; and reported Zika virus infection, a categorical variable, which used information reported by the mothers (Zika-like illness during or outside pregnancy), associated with serology results, and divided into symptomatic infection during pregnancy; asymptomatic infection, timing unknown; and no infection (seronegative mothers) and symptomatic infection when not pregnant. Zika-like illness corresponded to a clinical diagnosis of Zika virus disease or a recalled infectious episode characterized by rash, fever, or both associated with $\geq$2 of the following symptoms: conjunctivitis, arthralgia, myalgia, or limb edema.

Case-Control Study

We performed a conditional logistic regression analysis to assess whether CNS congenital defect was associated with the 2 measures of exposure: maternal Zika virus seropositivity and reported Zika virus infection. We conducted a univariate analysis using all identified potential maternal risk factors and confounders (reported chikungunya infection, use of medical or recreational drugs, exposure to deltamethrin during pregnancy, age, socioeconomic status, history of miscarriage and/or termination of pregnancy), as well as parity and history of congenital defects in the family. Variables at p<0.2 in the univariate analysis were further tested by multivariate conditional logistic regression and were retained in the final model if p<0.1. When data sparsity did not allow adjustment for more variables, we retained only those at p<0.05; we grouped maternal middle and high socioeconomic status categories together and compared them with low socioeconomic status. We used a Wilcoxon signed-rank test to compare means between cases and controls and Pearson χ^2 test to compare categorical variables. We estimated the association between CNS congenital defects and maternal Zika virus infection by matched crude and adjusted odds ratios (ORs) with 95% CIs. We maximized the study power for the case-control study, for which we aimed to include all eligible cases (n = 25), and we chose a control–case ratio of 5:1 to have 98.5% power to detect a bilateral (α = 5%) significant difference,

assuming 50% of controls (28) and $\geq$90% of cases (9) were seropositive for Zika virus. The case-control study protocol was approved by the French Polynesia Ethics Committee on February 2, 2016.

Cross-Sectional Study

The main outcome was a binary variable derived from the results of the Child Development Assessment Scale (no abnormal development vs. abnormal development). We performed a multivariate logistic regression analysis to assess the associations of ECD with maternal Zika virus seropositivity and reported Zika virus infection. We used the same method as described in the preceding section, with breastfeeding as an additional risk factor/confounder. We performed statistical analyses using Stata version 13.0 (StataCorp LLC, College Station, TX, USA). For the comparison between the French-speaking Canadian children (n = 269) and the sample of our cross-sectional study (n = 107), we had a power of 80% to detect an effect size d = 0.32 at α = 0.05. The observed effect size (Cohen d) for the cognitive domain is 0.31, and 0.2 for the motor dimension. For the affective dimension, the effect size (ϕ coefficient) is 0.03.

The cross-sectional study on ECD among controls was approved on June 3, 2016. We obtained written informed consent from all mothers.

Results

Case-Control Study

We identified 26 case-patients; 1 case-patient was later found to have a congenital defect with genetic etiology and thus was no longer eligible and was excluded from the analysis, along with the related 5 controls. The mother of 1 child with microcephaly, already described by Besnard et al. (17), as well as the mothers of 2 newborns retrospectively identified with other CNS abnormalities, declined to participate in the study. Another child's mother was lost to follow-up (Figure 1). Thus, a total of 21 case-patients (84% of those invited) and 102 controls (94%) were enrolled in the case-control study.

We recruited 5 controls per case-patient for all but 2 case-patients; because of the tight matching and the lack of suitable controls, 1 case-patient had 4 matched controls and 1 case-patient had 3. All controls and 17 case-patients were from Tahiti or Moorea (Figure 2).

Of the 21 case-patients, 7 had microcephaly, 5 had brainstem dysfunction of the neonate characterized by an inability to suck and swallow, and 9 had other CNS congenital defects (Table 1). Moreover, 6 had ventriculomegaly and 3 had arthrogryposis. Several case-patients had $\geq$1 CNS abnormality. For 10 case-patients, pregnancy resulted in termination; of the remaining 11 newborns, 7 were still alive as of July 2017 (Table 1). Seven of the 11 newborns
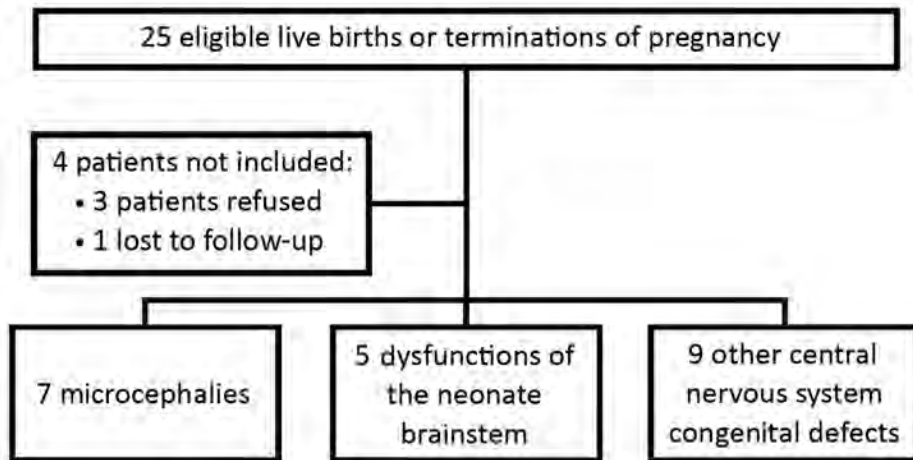
Figure 1. Flowchart for the recruitment of eligible cases for study of Zika virus infection during pregnancy and effects on early childhood development, French Polynesia, 2013–2016.

had complete imaging, ophthalmoscopy, evoked otoacoustic emissions, and neuroclinical follow-up.

Maternal toxoplasma serology was positive for 48% (10/21) of the case-patients and 60% (61/102) of the controls; seroconversion occurred during pregnancy for 1 control. Rubella serology was positive for 81% (17/21) of the case-patients and 94% (96/102) of the controls; no seroconversion occurred in any group. We performed maternal CMV serologic testing for 86% (18/21) of the case-patients: 2 were positive without signs of recent seroconversion, but further testing for CMV in amniotic fluid was negative (*17*). All study participants were seronegative for *Treponema pallidum*. The mother of 1 case-patient was known to be seropositive for HIV before the start of the pregnancy.

The gestational periods of fetuses and infants enrolled in the study started during June 2013–August 2014, and the infants were born during February 2014–May 2015. Median maternal age at conception was 27 years for case-patients and 28 years for controls. Case-patients and controls did not differ significantly in terms of fetal gender, ethnicity, and maternal socioeconomic status. Excluding the cases that ended in termination of pregnancy, gestational age at birth did not differ significantly between case-patients and controls (Table 2).

Figure 2. Geographic distribution of eligible cases for study of Zika virus infection during pregnancy and effects on early childhood development, French Polynesia, 2013–2016. Black text indicates islands with ≥1 case (number of cases from each island is in parentheses); gray text indicates names of archipelagoes. Inset shows the location of French Polynesia in the Pacific Ocean. Data source: GADM version 2.8 (https://gadm.org/download_country_v2.html). Map production: World Health Organization Health Emergencies Programme.

Table 1. Main and secondary diagnoses for 21 case-patients recruited in case-control study of Zika virus infection during pregnancy and effects on early childhood development, French Polynesia, 2013–2016

Diagnoses	No. (%)	Pregnancy termination	Live births	Child alive,* n = 7
Main diagnoses				
Microcephaly	7 (33)	4	3	1
Brainstem dysfunction of the neonate	5 (24)	0	5	3
Other CNS congenital defects	9 (43)	6	3	3
Septal and/or corpus callosum agenesis	3 (14)	1	2	2
Intraventricular hemorrhage	1 (5)	0	1	1
Cerebral hemorrhage and placental calcifications	1 (5)	1	1	0
Polymalformative syndrome	2 (10)	2	0	0
Complete or sacral spina bifida	2 (10)	2	0	0
Secondary diagnoses				
Ventriculomegaly	6 (29)	4	2	2
Arthrogryposis	3 (14)	3	0	0
*As of July 2017.				

Maternal Zika virus seroprevalence was 95% among case-patients and 76% among controls (p = 0.07). We classified mothers of 38% of case-patients and 17% of controls as having had symptomatic Zika virus infection during pregnancy and mothers of 57% of case-patients and 60% of controls as having had asymptomatic infection (timing unknown, p = 0.07; Table 3). Of mothers who reported symptomatic Zika virus infection during pregnancy, for case-patients, 88% (7/8) reported it in the first trimester and 12% (1/8) in the second trimester, whereas for controls, 71% (12/17) reported it in the first trimester and 29% (5/17) in the second or third trimester. Compared with those with no evidence of Zika virus infection during pregnancy, the matched crude OR for CNS congenital defects and maternal Zika virus seropositivity was 6.02, and for CNS congenital defects and symptomatic Zika virus infection during pregnancy, the matched crude OR was 6.79. After adjustment for maternal socioeconomic status, these ORs were 7.07 for the first group (95% CI 0.86–58.3; likelihood ratio test p = 0.02), and 7.19 for the second (95% CI 1.39–37.2; likelihood ratio test p = 0.04). Further adjustment for other potential confounders made no difference to the results. Before and after adjustment for confounders, asymptomatic Zika virus infection (timing unknown) was not associated with CNS congenital defects (Table 3).

Cross-Sectional Study of Early Childhood Development

More than 1.5 years after the end of the Zika virus outbreak, during June–August 2016, we enrolled 107 children (median age 23 months) in a cross-sectional study and assessed them using the Childhood Development Assessment Scale. Of these children, 44 (41%) were girls, 17 (16%) were born prematurely, and 12 (11%) were classified as having low birthweight (<2,500 g). Except for 1 low birth length baby, anthropometry at birth was within reference range; at the time of evaluation, none of the children was underweight, had low length for age, had low weight for length, or had

microcephaly (online Technical Appendix Table 1, https://wwwnc.cdc.gov/EID/article/24/10/17-2079-Techapp1.pdf).

We noted evidence for a difference between mean scores of the study participants and the reference population (French-speaking Canadian children) only for the cognitive domain (p = 0.001) (online Technical Appendix Table 2). Neurocognitive testing using the Childhood Development Assessment Scale was normal for 93% of the children in the socioemotional domain, 64% in the cognitive domain, and 76% in the motor domain (online Technical Appendix Tables 3, 4). We found no evidence for a detrimental effect of maternal Zika virus seropositivity or reported Zika virus infection on ECD in children born without birth defects (Table 4). The weak univariate association of deltamethrin exposure during pregnancy with ECD delays was not significant after adjustment for confounders. Low maternal socioeconomic status (adjusted odds ratio [aOR] 5.28, 95% CI 1.96–14.2) and not breast-feeding (aOR 4.00, 95% CI 1.06–15.1) were associated with abnormal ECD.

Discussion

We report a case-control study assessing the role of Zika virus infection in CNS malformations, including, but not limited to, microcephaly, in newborns and fetuses whose gestation occurred during the Zika virus outbreak in French Polynesia during 2013–2014. We also report a population-based developmental assessment of children born without birth defects after a Zika virus outbreak.

At the time of the outbreak in French Polynesia, risks associated with reported Zika virus infection were unknown. Four years later, 1 case-control study from Brazil provided evidence that Zika virus infection during pregnancy is associated with microcephaly, and a few cohort studies described Zika virus–associated adverse pregnancy outcomes (11,14,18). Given widespread Zika virus transmission in the Western Hemisphere, clarifying the full spectrum of CZS is a critical public health priority. We conducted our study as part of the World Health Organization (WHO) effort in leading a multicountry

Table 2. Characteristics and comparison of case-patients and controls in study of Zika virus infection during pregnancy and early childhood development, French Polynesia, 2013–2016*

Characteristics	Cases, n = 21	Controls, n = 102	p value†
Mother's age at pregnancy, median (IQR)	26.8 (22.1–35.7)	27.8 (22.2–33.7)	NA
15–24	8 (38)	37 (36)	NA
25–34	7 (33)	43 (42)	NA
>35	6 (29)	22 (22)	NA
Estimated pregnancy start date, median (IQR)	2013 Dec 11 (2013 Oct 23–2014 May 9)	2013 Dec 8 (2013 Oct 16–2014 May 16)	
January–September 2013	4 (19)	19 (19)	NA
October 2013–December 2014	9 (43)	43 (42)	
January–April 2014	2 (9)	10 (10)	
May–August 2014	6 (29)	30 (29)	
Maternal socioeconomic status			
Low	9 (43)	34 (34)	0.52
Middle	4 (19)	31 (31)	
High	8 (38)	36 (36)	
Child's birthweight, g	n = 11	n = 100	
<1,500	0	2 (2)	
1,500–2,500	3 (27)	9 (9)	
>2,500	8 (73)	89 (89)	
Child's sex			
F	10 (48)	42 (41)	0.64
M	11 (52)	60 (59)	
Child's ethnicity			
Polynesian	14 (74)	61 (71)	0.56
Caucasian	2 (11)	2 (2)	
Mixed/other	3 (16)	23 (27)	
Pregnancy outcome			
Termination of pregnancy	10 (48)	NA	NA
Gestational age at termination of pregnancy, median (IQR)	25.5 (23–29)	NA	NA
Live birth	11 (52)	102 (100)	NA
Gestational age at child's birth, median (IQR)	39 (36–40)	39 (38–40)	0.23
Term, >37 weeks	8 (73)	85 (83)	
Premature, 27–36 weeks	3 (27)	17 (17)	
Mother's past infection with dengue viruses			
DENV-1 seropositivity	17 (81)	88 (87)	0.50
DENV-2 seropositivity	12 (57)	50 (50)	0.54
DENV-3 seropositivity	16 (76)	78 (77)	0.99
DENV-4 seropositivity	10 (48)	52 (51)	0.74
Other risk factors/confounders			
Family history of congenital abnormalities	6 (29)	24 (25)	0.84
Drug use during pregnancy‡	9 (45)	34 (33)	0.23
Deltamethrin outdoor spraying during pregnancy	10 (48)	50 (51)	0.73

*Values are no. (%) except as indicated. IQR, interquartile range; NA, not applicable.
†Likelihood ratio using conditional logistic regression.
‡Cannabis, cocaine, alcohol, or tobacco.

coordinated approach to data sharing, surveillance, and research to establish the spectrum of CNS abnormalities attributable to CZS (*29*).

We found evidence that maternal Zika virus seropositivity, with or without reported Zika-like illness during pregnancy, was associated with 7-fold increased odds of congenital CNS defects. Zika virus seroprevalence in the control mothers in the study was 76%, higher than the 49% prevalence detected in the general population of French Polynesia (*28*). Such a difference may exist because the previous Zika virus serosurvey was conducted on a representative subset of the general population, with a median age of 43 years, involving both female and male participants, whereas our study involved only pregnant women, with a median age of 28 years.

Several studies have clearly shown unequal rates of Zika virus infection in men and women, possibly as a consequence of sexual transmission of Zika virus (*30,31*). Pregnant women may be more susceptible to Zika virus infection than nonpregnant women of the same age because of the immune tolerance induced by the pregnancy to tolerate paternal antigens (*32*). All the mothers of fetuses or children with microcephaly and other CNS congenital defects were seropositive, whereas 80% (4/5) of the mothers of newborns with brainstem dysfunction were seropositive, compared with 78% (18/23) of their matched controls (matched crude OR 1.05, 95% CI 0.10–11.4). Although no association was found, this finding is inconclusive because the study had little power to perform subgroup analysis by congenital CNS defect. Excluding microcephaly, only

Table 3. Crude and adjusted OR for congenital central nervous system abnormalities and maternal Zika virus infection status, French Polynesia, 2013–2016*

Exposures	Case-patients, no. (%)	Controls, no. (%)	Matched crude OR (95% CI)	Matched adjusted OR† (95% CI)	LRT p value
Zika virus seropositivity	20 (95)	78 (76)	6.02 (0.77–47.1)	7.07 (0.86–58.3)	0.02
Reported Zika virus infection					
No infection during pregnancy‡	1 (5)	24 (24)	1	1	0.04
Asymptomatic (timing unknown)§	12 (57)	61 (60)	2.05 (0.54–7.80)	1.93 (0.47–7.96)	
Symptomatic during pregnancy¶	8 (38)	17 (17)	6.79 (1.36–33.8)	7.19 (1.39–37.2)	

*LRT, likelihood ratio test; NA, not applicable; OR, odds ratio.
†Adjusted for maternal socioeconomic status.
‡Seronegative mothers and seropositive mothers who reported Zika-like illness outside pregnancy.
§Seropositive mothers who did not report Zika-like illness during or outside pregnancy.
¶Seropositive mothers who reported Zika-like illness during pregnancy.

multicountry studies or meta-analyses can give a clear answer on the causal link between Zika virus and each reported rare CNS congenital defect (*33,34*).

Within the nested cross-sectional study, we assessed control children only on anthropometry and ECD. Both eye and hearing abnormalities have been described in children with CZS; we were unable to test for such abnormalities and cannot infer any conclusion about their burden among children born without diagnosed birth defects in French Polynesia (*35–37*).

Our cross-sectional study did not provide evidence that maternal Zika virus seropositivity or symptomatic Zika virus infection during pregnancy were associated with unusual developmental delay in children born without birth defects (Table 4; online Technical Appendix Table 4).

Known risk factors for developmental delay (low maternal socioeconomic status and lack of breast-feeding) were associated with abnormal childhood development in this study. This result supports the validity of our findings and suggests that if reported Zika virus infection was frequently associated with delayed ECD, we would have likely detected it. However, this study lacked power to detect rare outcomes or minor developmental differences: only 17 control mothers had clear evidence of Zika virus infection with symptoms during pregnancy.

The difference in the cognitive development score in children in French Polynesia compared with children in Canada (online Technical Appendix Table 2) is likely to be the result of confounding factors such as socioeconomic status or other population differences; for

Table 4. Crude and adjusted odds ratios for maternal Zika virus infection and other risk factors and early childhood development, French Polynesia, 2013–2016*

Risk factors	Early childhood development				
	Adequate in all domains, no. (%)	Question or problem in ≥1 domain, no. (%)	Adequate in all domains versus question or problem in ≥1 domain		
			Crude OR (95% CI)	Adjusted OR (95% CI)	LRT p value
Zika virus seropositivity, n = 107					
No	13 (50)	13 (50)	1	1	0.07
Yes	46 (57)	35 (43)	0.76 (0.31–1.84)	0.35 (0.11–1.13)†	
Reported Zika infection, n = 107					
No infection during pregnancy‡	19 (56)	15 (44)	1	1	0.19
Asymptomatic, timing unknown§	30 (54)	26 (46)	1.09 (0.47–2.59)	0.51 (0.16–1.58)†	
Symptomatic during pregnancy¶	10 (59)	7 (41)	0.89 (0.27–2.88)	0.58 (0.14–2.51)†	
Deltamethrin outdoor spraying during pregnancy, n = 104					
No	34 (69)	15 (31)	1	1	0.07
Yes	24 (44)	31 (56)	2.92 (1.30–6.57)	2.69 (0.92–7.84)#	
Maternal socioeconomic status,** n = 106					
Middle and high	47 (66)	24 (34)	1	1	<0.001
Low	11 (31)	24 (69)	4.27 (1.80–10.2)	5.28 (1.96–14.2)††	
Breast-feeding,** n = 106					
Yes, including artificial feeding	52 (57)	39 (43)	1	1	0.03
No	6 (40)	9 (60)	2.00 (0.66–6.09)	4.00 (1.06–15.1)‡‡	

*LRT, likelihood ratio test; OR, odds ratio.
†Adjusted for deltamethrin outdoor spraying during pregnancy, maternal socioeconomic status, breastfeeding, and date of pregnancy start (divided into 4 categories based on risk of exposure to Zika virus; see Table 2).
‡Seronegative mothers and seropositive mothers who reported Zika-like illness outside pregnancy.
§Seropositive mothers who did not report Zika-like illness during or outside pregnancy.
¶Seropositive mothers who reported Zika-like illness during pregnancy.
#Adjusted for ZIKV seropositivity (main exposure), maternal socioeconomic status, breastfeeding, and date of pregnancy start.
**No interaction (test for interaction p = 0.26) and no multicolinearity were detected for maternal socioeconomic status and breastfeeding.
††Adjusted for ZIKV seropositivity (main exposure), deltamethrin outdoor spraying during pregnancy, breastfeeding, and date of pregnancy start.
‡‡Adjusted for ZIKV seropositivity (main exposure), deltamethrin outdoor spraying during pregnancy, maternal socioeconomic status, and date of pregnancy start.

example, the cognitive scale include items that may be influenced by the cultural context. Furthermore, children in Canada were recruited in Quebec's public network of kindergartens, which have programs to stimulate children's development.

The main limitation of our study is the low number of cases (n = 21), which makes the study underpowered to detect a strong association between maternal Zika virus seropositivity and birth defects, as illustrated by the 95% CI crossing the null value. Another limitation is how the exposure was assessed. We used maternal Zika virus seropositivity as a proxy for Zika virus infection during pregnancy, but it is probable that some women were infected with Zika virus outside the gestational period. However, misclassification of mothers, which is likely to be nondifferential assuming they were infected during pregnancy when, in fact, they were infected outside the gestational period, would weaken any association between fetal CNS abnormalities and Zika virus seroconversion. We adjusted for the rapid variations in exposure over a short time by matching controls to cases by date of conception.

Our second measure of exposure, reported Zika virus infection, includes a rough estimate of time of infection (outside or during pregnancy), based on serology data combined with recalled information. This measure may be susceptible to recall bias, because mothers of case-patients are more likely to recall Zika-like illness during pregnancy. However, serology data were compatible with recalled information for both cases and controls (only 1 of 26 mothers who reported Zika-like illness during pregnancy was seronegative). Because of the geographic spread of French Polynesia and the lack of funding, controls could not be residents of any island other than Tahiti or Moorea, which contain >70% of the overall population. We also excluded private hospitals, where 40% of deliveries occur. Therefore, it is likely that socioeconomic status confounded the associations, which is why we adjusted for maternal socioeconomic status in the analysis.

Our study confirms the association between maternal Zika virus infection and CNS congenital defects. Among children with no known congenital defects, we found no evidence that congenital Zika virus infection had a major negative effect on the early stages of childhood development. Because the first large Zika virus outbreak occurred in French Polynesia about 2 years before the Zika outbreaks in Latin America, children exposed to Zika in utero in French Polynesia are now older than those in other countries, but it may still be early to detect subtle developmental delays. Although our data are encouraging, systematic in-depth assessment of childhood development in larger cohorts of exposed children, and at older ages, is needed to detect potential developmental and learning delays.

About the Author

Dr. Subissi is a microbiologist and epidemiologist with a strong interest in epidemic-prone RNA viruses. He has worked as WHO consultant for the World Health Organization in epidemic contexts such as Ebola in Guinea, yellow fever in Angola, and Zika in French overseas territories.

References

1. Dick GWA, Kitchen SF, Haddow AJ. Zika virus. I. Isolations and serological specificity. Trans R Soc Trop Med Hyg. 1952;46:509–20. http://dx.doi.org/10.1016/0035-9203(52)90042-4
2. Baud D, Gubler DJ, Schaub B, Lanteri MC, Musso D. An update on Zika virus infection. Lancet. 2017;390:2099–109. http://dx.doi.org/10.1016/S0140-6736(17)31450-2
3. Duffy MR, Chen T-H, Hancock WT, Powers AM, Kool JL, Lanciotti RS, et al. Zika virus outbreak on Yap Island, Federated States of Micronesia. N Engl J Med. 2009;360:2536–43. http://dx.doi.org/10.1056/NEJMoa0805715
4. Cao-Lormeau V-M, Roche C, Teissier A, Robin E, Berry A-L, Mallet H-P, et al. Zika virus, French Polynesia, South Pacific, 2013. Emerg Infect Dis. 2014;20:1060. http://dx.doi.org/10.3201/eid2011.141380
5. Musso D, Bossin H, Mallet HP, Besnard M, Broult J, Baudouin L, et al. Zika virus in French Polynesia 2013–14: anatomy of a completed outbreak. Lancet Infect Dis. 2018;18:e172–82. http://dx.doi.org/10.1016/S1473-3099(17)30446-2
6. Musso D, Cao-Lormeau VM, Gubler DJ. Zika virus: following the path of dengue and chikungunya? Lancet. 2015;386:243–4. http://dx.doi.org/10.1016/S0140-6736(15)61273-9
7. Faria NR, Quick J, Claro IM, Thézé J, de Jesus JG, Giovanetti M, et al. Establishment and cryptic transmission of Zika virus in Brazil and the Americas. Nature. 2017;546:406–10. http://dx.doi.org/10.1038/nature22401
8. Tang H, Hammack C, Ogden SC, Wen Z, Qian X, Li Y, et al. Zika virus infects human cortical neural progenitors and attenuates their growth. Cell Stem Cell. 2016;18:587–90. http://dx.doi.org/10.1016/j.stem.2016.02.016
9. Cao-Lormeau V-M, Blake A, Mons S, Lastère S, Roche C, Vanhomwegen J, et al. Guillain-Barré syndrome outbreak associated with Zika virus infection in French Polynesia:

a case-control study. Lancet. 2016;387:1531–9. http://dx.doi.org/10.1016/S0140-6736(16)00562-6

10. Schuler-Faccini L, Ribeiro EM, Feitosa IML, Horovitz DDG, Cavalcanti DP, Pessoa A, et al.; Brazilian Medical Genetics Society–Zika Embryopathy Task Force. Possible association between Zika virus infection and microcephaly—Brazil, 2015. MMWR Morb Mortal Wkly Rep. 2016;65:59–62. http://dx.doi.org/10.15585/mmwr.mm6503e2

11. de Araújo TVB, Ximenes RAA, Miranda-Filho DB, Souza WV, Montarroyos UR, de Melo APL, et al.; investigators from the Microcephaly Epidemic Research Group; Brazilian Ministry of Health; Pan American Health Organization; Instituto de Medicina Integral Professor Fernando Figueira; State Health Department of Pernambuco. Association between microcephaly, Zika virus infection, and other risk factors in Brazil: final report of a case-control study. Lancet Infect Dis. 2018;18:328–36. http://dx.doi.org/10.1016/S1473-3099(17)30727-2

12. Cauchemez S, Besnard M, Bompard P, Dub T, Guillemette-Artur P, Eyrolle-Guignot D, et al. Association between Zika virus and microcephaly in French Polynesia, 2013–15: a retrospective study. Lancet. 2016;387:2125–32. http://dx.doi.org/10.1016/S0140-6736(16)00651-6

13. Rasmussen SA, Jamieson DJ, Honein MA, Petersen LR. Zika virus and birth defects—reviewing the evidence for causality. N Engl J Med. 2016;374:1981–7. http://dx.doi.org/10.1056/NEJMsr1604338

14. Honein MA, Dawson AL, Petersen EE, Jones AM, Lee EH, Yazdy MM, et al.; US Zika Pregnancy Registry Collaboration. Birth defects among fetuses and infants of US women with evidence of possible Zika virus infection during pregnancy. JAMA. 2017;317:59–68. http://dx.doi.org/10.1001/jama.2016.19006

15. Parra B, Lizarazo J, Jiménez-Arango JA, Zea-Vera AF, González-Manrique G, Vargas J, et al. Guillain-Barré syndrome associated with Zika virus infection in Colombia. N Engl J Med. 2016;375:1513–23. http://dx.doi.org/10.1056/NEJMoa1605564

16. World Health Organization. Zika situation report. 2017 [cited 2018 Mar 28]. http://www.who.int/emergencies/zika-virus/situation-report/10-march-2017/en/

17. Besnard M, Eyrolle-Guignot D, Guillemette-Artur P, Lastère S, Bost-Bezeaud F, Marcelis L, et al. Congenital cerebral malformations and dysfunction in fetuses and newborns following the 2013 to 2014 Zika virus epidemic in French Polynesia. Euro Surveill. 2016;21:30181. http://dx.doi.org/10.2807/1560-7917.ES.2016.21.13.30181

18. Brasil P, Pereira JP Jr, Moreira ME, Ribeiro Nogueira RM, Damasceno L, Wakimoto M, et al. Zika virus infection in pregnant women in Rio de Janeiro. N Engl J Med. 2016;375:2321–34. http://dx.doi.org/10.1056/NEJMoa1602412

19. Schwartz DA. The origins and emergence of Zika virus, the newest TORCH infection: what's old is new again. Arch Pathol Lab Med. 2017;141:18–25. http://dx.doi.org/10.5858/arpa.2016-0429-ED

20. Moore CA, Staples JE, Dobyns WB, Pessoa A, Ventura CV, Fonseca EB, et al. Characterizing the pattern of anomalies in congenital Zika syndrome for pediatric clinicians. JAMA Pediatr. 2017;171:288–95. http://dx.doi.org/10.1001/jamapediatrics.2016.3982

21. Kapogiannis BG, Chakhtoura N, Hazra R, Spong CY. Bridging knowledge gaps to understand how Zika virus exposure and infection affect child development. JAMA Pediatr. 2017;171:478–85. http://dx.doi.org/10.1001/jamapediatrics.2017.0002

22. Hollingshead AB. Four factor index of social status. New Haven (CT, USA): Yale University Department of Psychology; 1975

23. Aubry M, Teissier A, Huart M, Merceron S, Vanhomwegen J, Mapotoeke M, et al. Seroprevalence of dengue and chikungunya virus antibodies, French Polynesia, 2014–2015. Emerg Infect Dis. 2018;24:558–61. http://dx.doi.org/10.3201/eid2403.171149

24. Aubry M, Richard V, Green J, Broult J, Musso D. Inactivation of Zika virus in plasma with amotosalen and ultraviolet A illumination. Transfusion. 2016;56:33–40. http://dx.doi.org/10.1111/trf.13271

25. de Onis M, Garza C, Victora CG, Onyango AW, Frongillo EA, Martines J. The WHO Multicentre Growth Reference Study: planning, study design, and methodology. Food Nutr Bull. 2004;25(Suppl):S15–26. http://dx.doi.org/10.1177/15648265040251S103

26. Cheikh Ismail L, Knight HE, Bhutta Z, Chumlea WC; International Fetal and Newborn Growth Consortium for the 21st Century. Anthropometric protocols for the construction of new international fetal and newborn growth standards: the INTERGROWTH-21st Project. BJOG. 2013;120(Suppl 2):42–7. http://dx.doi.org/10.1111/1471-0528.12125

27. Bayley N. Bayley scales of infant and toddler development, 3rd edition. London: Pearson; 2005.</bok>

28. Aubry M, Teissier A, Huart M, Merceron S, Vanhomwegen J, Roche C, et al. Zika virus seroprevalence, French Polynesia, 2014–2015. Emerg Infect Dis. 2017;23:669–72. http://dx.doi.org/10.3201/eid2304.161549

29. Costello A, Dua T, Duran P, Gülmezoglu M, Oladapo OT, Perea W, et al. Defining the syndrome associated with congenital Zika virus infection. Bull World Health Organ. 2016;94:406–406A. http://dx.doi.org/10.2471/BLT.16.176990

30. Coelho FC, Durovni B, Saraceni V, Lemos C, Codeco CT, Camargo S, et al. Higher incidence of Zika in adult women than adult men in Rio de Janeiro suggests a significant contribution of sexual transmission from men to women. Int J Infect Dis. 2016;51:128–32. http://dx.doi.org/10.1016/j.ijid.2016.08.023

31. Lozier M, Adams L, Febo MF, Torres-Aponte J, Bello-Pagan M, Ryff KR, et al. Incidence of Zika virus disease by age and sex—Puerto Rico, November 1, 2015–October 20, 2016. MMWR Morb Mortal Wkly Rep. 2016;65:1219–23. http://dx.doi.org/10.15585/mmwr.mm6544a4

32. King NJC, Teixeira MM, Mahalingam S. Zika virus: mechanisms of infection during pregnancy. Trends Microbiol. 2017;25:701–2. http://dx.doi.org/10.1016/j.tim.2017.05.005

33. Baud D, Gérardin P, Merriam A, Alves MP, Musso D, Genton B, et al. Harness shared data in international Zika registry. BMJ. 2016;355:i5319. http://dx.doi.org/10.1136/bmj.i5319

34. Panchaud A, Vouga M, Musso D, Baud D. An international registry for women exposed to Zika virus during pregnancy: time for answers. Lancet Infect Dis. 2016;16:995–6. http://dx.doi.org/10.1016/S1473-3099(16)30255-9

35. Ventura CV, Maia M, Travassos SB, Martins TT, Patriota F, Nunes ME, et al. Risk factors associated with the ophthalmoscopic findings identified in infants with presumed Zika virus congenital infection. JAMA Ophthalmol. 2016;134:912–8. http://dx.doi.org/10.1001/jamaophthalmol.2016.1784

36. Leal MC, Muniz LF, Ferreira TSA, Santos CM, Almeida LC, Van Der Linden V, et al. Hearing loss in infants with microcephaly and evidence of congenital Zika virus infection—Brazil, November 2015–May 2016. MMWR Morb Mortal Wkly Rep. 2016;65:917–9. http://dx.doi.org/10.15585/mmwr.mm6534e3

37. de Paula Freitas B, de Oliveira Dias JR, Prazeres J, Sacramento GA, Ko AI, Maia M, et al. Ocular findings in infants with microcephaly associated with presumed Zika virus congenital infection in Salvador, Brazil. JAMA Ophthalmol. 2016;134:529–35. http://dx.doi.org/10.1001/jamaophthalmol.2016.0267

Address for correspondence: Marine Giard, Bureau de Veille Sanitaire, Direction de la Santé, BP 611, 98713 Papeete, French Polynesia; email: marine.giard@sante.gov.pf

Evaluation of Effectiveness of a Community-Based Intervention for Control of Dengue Virus Vector, Ouagadougou, Burkina Faso

Samiratou Ouédraogo, Tarik Benmarhnia, Emmanuel Bonnet,
Paul-André Somé, Ahmed S. Barro, Yamba Kafando, Diloma Dieudonné Soma,
Roch K. Dabiré, Diane Saré, Florence Fournet, Valéry Ridde

We evaluated the effectiveness of a community-based intervention for dengue vector control in Ouagadougou, the capital city of Burkina Faso. Households in the intervention (n = 287) and control (n = 289) neighborhoods were randomly sampled and the outcomes collected before the intervention (October 2015) and after the intervention (October 2016). The intervention reduced residents' exposure to dengue vector bites (vector saliva biomarker difference −0.08 [95% CI −0.11 to −0.04]). The pupae index declined in the intervention neighborhood (from 162.14 to 99.03) and increased in the control neighborhood (from 218.72 to 255.67). Residents in the intervention neighborhood were less likely to associate dengue with malaria (risk ratio 0.70 [95% CI 0.58–0.84]) and had increased knowledge about dengue symptoms (risk ratio 1.44 [95% CI 1.22–1.69]). Our study showed that well-planned, evidence/community-based interventions that control exposure to dengue vectors are feasible and effective in urban settings in Africa that have limited resources.

Since 2010, dengue outbreaks have been detected repeatedly in several countries in sub-Saharan Africa (1–4). The resurgence of dengue outbreaks in the region might be explained by factors such as urbanization, globalization, lack of effective mosquito control, and climate change (5,6). Dengue virus (DENV) belongs to the *Flaviviridae* family and has 4 serotypes (DENV-1 to DENV-4) (7) that cause human disease through transmission by infected female mosquitoes, mainly *Aedes* mosquitoes. These mosquitoes have fully adapted to urban settings, where crowded human populations live in close proximity to large mosquito populations (8). Although DENV-2 has been reported most frequently, all 4 DENV serotypes are circulating in Africa (9). *Ae. aegypti* was found to be the main species in urban settings (10). Future climate projections indicate considerable potential for shifting establishment of *Ae. aegypti* mosquitoes in all regions of the world and especially in Africa (11). However, dengue continues to be a neglected disease in this region, often eclipsed by the substantial burden of malaria (12). Dengue infection is usually not included among the differential diagnoses of acute febrile illness (13).

The World Health Organization (WHO) has stated that effective vector control measures are critical to achieving and sustaining reduction of disease attributable to dengue (14). Common dengue vector control measures, which are typically community-driven in tandem with health promotion campaigns, include use of insecticide-treated materials (15) or water storage tanks (16) and elimination of breeding sites or use of larvicides (17). The environment can be modified to deprive mosquito vectors of favorable breeding sites. A growing body of evidence indicates that changes in these conditions have led to alterations in the prevalence, spread, geographic range, and control of many infections transmitted by these vectors (14). Many community-level interventions have been conducted in Asia and Latin America (18); overall, the results suggest that these interventions led to a reduction of vector densities. However, we did not find any reports about community-based interventions (CBIs) aimed at controlling the dengue vector in Africa, nor did Bowman et al. (18) in a recent systematic review.

Our study describes an evaluation of the effectiveness of a CBI for dengue vector control in a neighborhood of Ouagadougou, the capital city of Burkina Faso (*19*). We chose this city because dengue outbreaks were detected in Ouagadougou in 2013 (*12*). DENV-2 has been endemic for more than 30 years in the country, and 3 serotypes (DENV-1, DENV-2, and DENV-3) have been identified (*12,20,21*), leading to the occurrence of more severe cases often not captured by the relatively weak surveillance system, which has resulted in underreporting (*22*) and a lack of national coordinate response activities.

Population and Methods

Study Site and Participants

The study was conducted in 2 comparable neighborhoods of Ouagadougou, Tampouy and Juvenat, selected from a total of 5 areas in the city (online Technical Appendix Figure 1, https://wwwnc.cdc.gov/EID/article/24/10/18-0069-Techapp1.pdf). Both neighborhoods' socioeconomic profiles are highly diverse (*23*) and include wealthy households in modern concrete individual houses with running water and electricity, households with a modest standard of living, and poor people living in fairly small houses in the same compound, sometimes without basic amenities. We defined a household as a person or a group of persons with the same head of household, living in a housing unit, who provide themselves with food or other essentials for living; in Burkina Faso, 1, 2, or more households living in different housing units sometimes share the same compound.

Tampouy (Figure 1), located in the northwest of Ouagadougou, was randomly chosen to receive the intervention, whereas Juvenat, on the east side of the city, was selected as the control neighborhood. In 2015, we estimated that 4,264 households were located within a 1-km radius around the primary healthcare center in Tampouy. In the similarly delimited area in the control neighborhood of Juvenat, we identified 3,294 households. We chose a 1-km radius to reduce the probability of contamination between the control and intervention areas while also having a sufficient number of households for the study. The number of households in the area were estimated by using data from Burkina Faso's National Institute of Statistics and Demography and data collected through very high spatial resolution satellite imagery, which also enabled the distinction of dwellings from other types of buildings. To measure the study outcomes, we used the geographic coordinates of households to randomly sample without replacement 287 households in Tampouy and 289 households in Juvenat. In this study, we considered a compound as a delimited living space where ≥1 household was found.

Intervention Design

The CBI occurred during June–early October 2016. Because this period is the rainy season, it is also the peak dengue transmission period (*24*).

We used an ecohealth intervention approach that consists of a pesticide-free dengue vector control (*25*). The theoretical approach to creating the communication materials is described in online Technical Appendix Figure 2. The intervention neighborhood received a behavior change intervention structured around 3 components (online Technical Appendix Table 1). The intervention design is based on selected effective CBIs in controlling dengue vector (*25–28*) through a participatory process with community leaders. Selected community members, leaders, and a community theatrical troupe received training on dengue prevention. These community members then organized community activities and served as educators.

Key messages addressed WHO recommendations for identifying *Ae. aegypti* mosquito breeding sites and dengue transmission, symptoms, management, and prevention (*14*). Education materials created through the participatory process included posters created by workshop participants, which were then professionally drawn by a local artist, and a theater piece illustrating the key messages: 1) how dengue is transmitted, its symptoms, and how it differs from malaria; 2) timely use of health services; and 3) how to prevent dengue and strategies to identify and control *Ae. aegypti* mosquito breeding sites.

Community leaders were identified by community members. They included those responsible for places of worship (e.g., churches and mosques), representatives of community associations, and community health workers collaborating with the primary healthcare center. Participation in the intervention was voluntary. Community leaders invited members to participate in the intervention, and an announcer was hired to travel with a loudspeaker along every street in the intervention neighborhood to invite everyone. Interested persons attended communication and education activities, including community theater, which involved a play, interaction of the actors with the audience, and a question and answer session, as well as community clean-up activities conducted in the public spaces. The intervention also included door-to-door visits, school education, and self-awareness assessment sessions that involved education with messages intended to raise student awareness of dengue and provide information on the disease by using posters. These events were followed by a poster drawing competition among all students, illustrating the key messages they had learned about dengue.

In the control area, no communication activities were carried out for dengue awareness and control. The risk of cross-contamination between the 2 sites was low because the control area was located >12 km from the intervention area.

All intervention activities were coordinated by 5 researchers with experience in implementation of CBIs and 5 experienced entomologists and conducted by 17 community members and theater actors with experience conducting CBIs, recruited and trained for the intervention, and 7 community representatives (e.g., traditional chiefs, religious leaders, and local association heads) for a peer review and follow-up of the activities. An evaluation of the
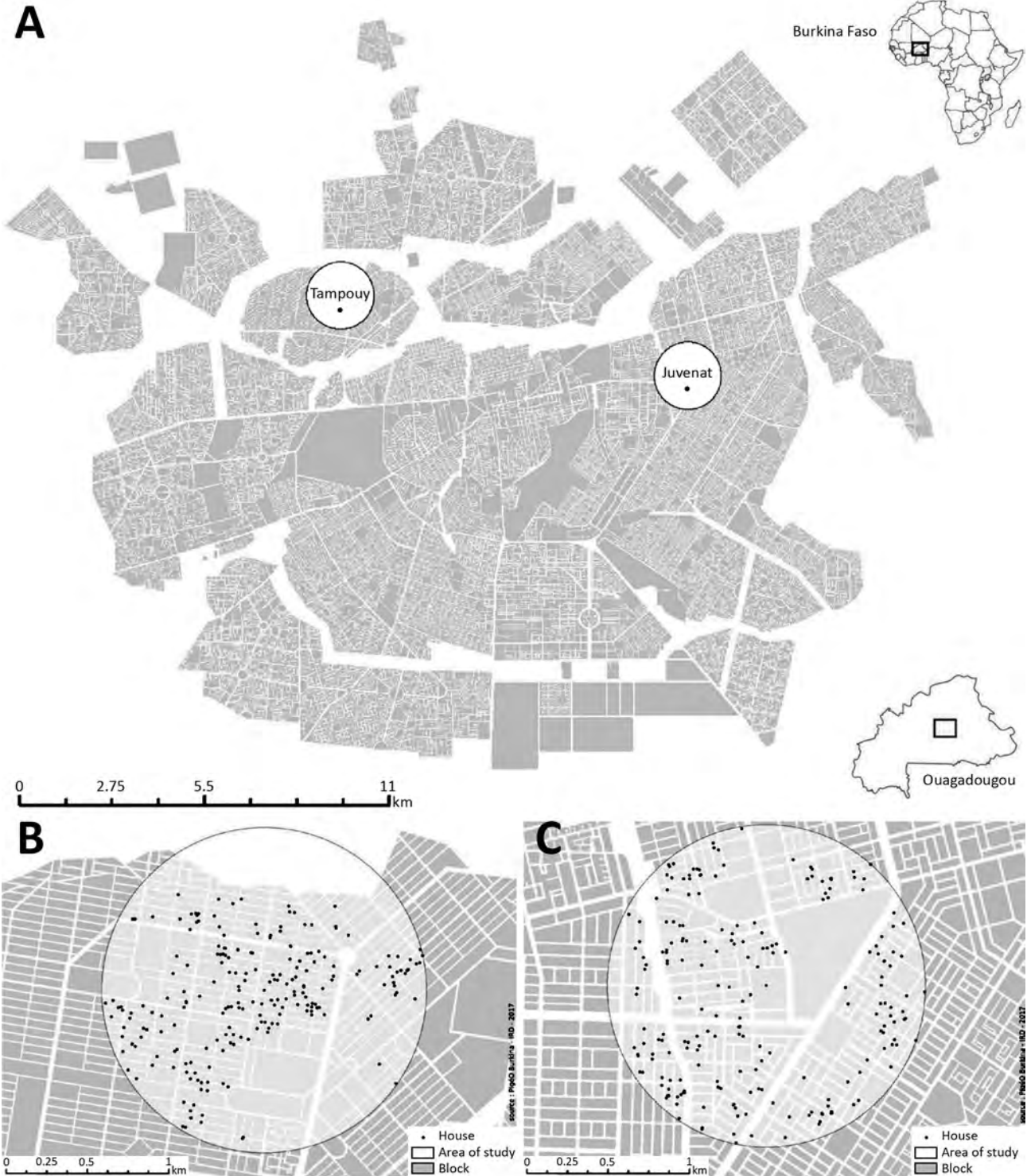
Figure 1. Intervention and control areas for an evaluation of a community-based intervention for dengue vector control conducted in Ouagadougou, Burkina Faso, June–October 2016. A) Ouagadougou overview; inset shows location of Ouagadougou in Burkina Faso. B) Tampouy (intervention neighborhood). C) Juvenat (control neighborhood).

intervention design and implementation processes showed that most of the activities had been carried out as planned with only minor modifications (online Technical Appendix Table 1).

Outcomes

Before the intervention, in late October 2015, we performed a baseline data collection in the control and intervention neighborhoods. We collected the same data in late October 2016 in both neighborhoods (after the intervention and during the peak dengue transmission period for 2016) to assess the effectiveness of the intervention. The primary outcomes (serologic and entomologic data) were collected at the compound level and the secondary outcomes (data on knowledge, attitudes, and practices) at the household level, given that in our study neighborhood we found ≥2 households living in the same compound (29). The residents of the compound are exposed to the same population of mosquitoes. However, depending on their age, education level, and sanitation habits, individual households might have different levels of knowledge and attitudes about dengue and its prevention.

Primary Outcomes (Continuous Variables)

Immunologic Biomarkers

Evidence of compound residents' exposure to *Ae. aegypti* mosquito bites was used to measure the population's exposure to mosquito bites. In each compound, 2 residents (1 child and 1 adult) present at the time of data collection were randomly sampled to provide blood drops for an *Ae. aegypti* mosquito saliva biomarker test. ELISA was performed on these standardized dried blood spots, and results were expressed as ΔOD (optical density), defined as the level of IgG to Nterm-34 kDa peptide. These ΔOD values were calculated according to the formula $\Delta OD = ODx - 2ODn$, where ODx represents the mean of individual OD values in antigen wells and ODn the OD value in a well with no antigen (30). The measurement of immunologic response to *Ae. aegypti* mosquito saliva in human populations has been documented as a relevant tool to assess a host's level of exposure to *Ae. aegypti* mosquito bites and the risk for vectorborne disease (31).

Entomologic Data

In the compound where blood samples were collected, interviewers were asked to identify all *Ae. aegypti* mosquito breeding sites with water and to collect and count all the larvae and pupae from the containers. The water was poured out of the containers only at the endline survey, and residents were advised to avoid these kinds of containers. Standard entomologic indices included the *Ae. aegypti* mosquito house index (compounds with larvae or pupae

× 100 compounds examined), container index (containers with larvae or pupae × 100 containers examined), Breteau index (containers with larvae or pupae per 100 compounds examined), and pupae index (pupae per 100 compounds examined) (31). These indices were generated at the neighborhood level.

Secondary Outcomes

The secondary outcomes were self-reported knowledge, attitudes, and practices (categoric variables), collected during a face-to-face interview with an adult household respondent.

Knowledge about dengue was assessed by asking "Can you list diseases that include fever as a symptom?"; "Have you ever heard of dengue?"; "Is dengue a form of malaria?"; and "Is dengue dangerous?" Knowledge about dengue's mode of transmission was assessed by asking "Is dengue transmitted by the same mosquito as malaria?" Attitudes and practices for preventing dengue fever and diseases causing fever were assessed by asking "Do you store water in containers?"; "Do you cover your water containers?"; and "Do you use bed nets?"

All data were collected by trained interviewers who did not participate in the intervention. Each neighborhood had its own interview team at baseline and endline, and the interviewers' work was supervised by the research team. The questionnaire was administered using the free Open Data Kit software (https://opendatakit.org).

Verbal consent was obtained from the respondents to the household questionnaire and from those who provided a blood sample. For children providing samples, at least 1 parent provided consent.

Statistical Analysis

We used a propensity score (PS) stratification approach to estimate the effect of the intervention on the outcomes of interest while ensuring that covariate balance was achieved between intervention and control groups (32). After estimating the PS for the control and the intervention groups (online Technical Appendix Figure 3), we excluded compounds and households with a PS outside of the overlapping intervention–control zone of the PS distribution. To obtain the optimal stratification setting while keeping a good covariate balance, we stratified the distribution of PS by using a 5-quantile approach, as recommended previously (32). This approach enabled exchangeability between intervention and control groups by ensuring that neighborhoods within a specific propensity score strata were compared. We modeled the propensity of receiving the intervention by using a logistic regression model that included the following covariates as independent variables: the number of households; sets of bedding in the compound and residents in the compound; the status of the person who provided the blood sample (adult or child); the household or households

wealth index quintile (1 being the poorest and 5 the richest); and the questionnaire respondent characteristics such as status (head of the household, lady of the household, or other responsible adult), sex (male or female), and a variable that specified the respondent's self-reported reading ability (cannot read, can read, or can read with difficulties).

To estimate the effect of the intervention on the changes in outcomes in each specific household, we used linear regression models (with a fixed effect for the PS strata) for continuous outcomes. For binary outcomes, we used Poisson regression models with robust variance (with a fixed effect for the PS strata) (33). Using a modified Poisson model (i.e., with robust variance) has been shown to be a good alternative to logistic regression, especially when the outcome prevalence is not small. The Poisson model also gives the risk for the exposed group (not the odds ratio, as in logistic regression). Analyses were conducted by using Stata 14.2 (StataCorp LLC, College Station, TX, USA).

Serologic analysis was performed by using GraphPad Prism5 software (San Diego, CA, USA) (30). The descriptions of the covariates, data analysis, and results are provided in online Technical Appendix Figure 4.

Results

Baseline and Endline Data
The number of compounds and households randomly sampled, those who completed the study at baseline and endline, and the numbers included in the data analyses are detailed in Figure 2. We summarized the characteristics of the compounds at baseline (2015) and endline (2016) (online Technical Appendix Table 2). In the control neighborhood, among households for which responses to the questions were obtained at baseline, heads of household were more likely to be the respondents to the questionnaire (88/161 [54.66%]) than in the intervention neighborhood (31/176 [17.61%]) and were less likely to be female (78/158 [49.37%]) than in the intervention neighborhood (130/173 [75.14%]). The respondents had lower reading ability in the intervention neighborhood; 108 (62.79%) of 172 respondents could read, compared with 133 (84.71%) of 157 in the control neighborhood.

Outcomes and Estimation
We summarized residents' immunologic response to *Ae. aegypti* mosquito bites in the intervention and control neighborhoods (online Technical Appendix Table 3). The raw propensity score mean (± SD) was 0.50 (± 0.13) for all observations. For intervention neighborhood observations, PS was 0.53 (± 0.10); for control neighborhood observations, PS was 0.47 (± 0.15). After stratification, the within-strata differences in the PSs between intervention and control observations ranged from 0.01 to 0.03.

At baseline, residents showed higher exposure to *Ae. aegypti* mosquito bites in the intervention neighborhood (ΔOD mean [± SD] 0.17 [± 0.10]) than the control neighborhood (ΔOD 0.13 [± 0.06]). At endline, residents from the intervention neighborhood showed lower exposure to *Ae. aegypti* mosquito bites (ΔOD 0.18 [± 0.08]) than the control neighborhood (ΔOD 0.20 [± 0.12]). The regression analysis on residents' immunologic response showed that the intervention reduced exposure to *Ae. aegypti* mosquito bites (coefficient –0.08 [95% CI –0.11 to –0.04]).

In Tampouy, the container index decreased in the intervention neighborhood (from 17.56% to 14.43%) and increased in the control neighborhood (30.41% to 35.91%), similar to what was observed for the pupae index (decreasing from 162.14 to 99.03 in the intervention and increasing from 218.72 to 255.67 in the control neighborhood). A greater decrease was observed in the house index in the intervention neighborhood (from 32.04% to 21.36%) compared with the control neighborhood (from 33.00% to 31.53%) as well as in the Breteau index (from 40.77% to 27.67% in the intervention neighborhood compared with 54.19% to 48.28% in the control neighborhood (Figure 3; online Technical Appendix Table 3). However, the regression models did not show an effect of the intervention on the absolute number of *Ae. aegypti* mosquito breeding sites or on the number of preimaginal stages of vector (larvae and pupae) at the compound level.

The households that received the intervention increased their knowledge of dengue (risk ratio [RR] 1.13 [95% CI 1.01–1.27]) and disease symptoms (RR 1.44 [95% CI 1.22–1.69]) and were less likely to associate dengue with malaria (RR 0.70 [95% CI 0.58–0.84]). Respondents self-reported that they had increased their actions against mosquitoes (RR 1.42 [95% CI 1.29–1.57]) and used more bed nets (RR 1.31 [95% CI 1.22–1.42]).

Discussion
Our study assessed the effectiveness of a CBI for dengue vector control in Ouagadougou, Burkina Faso. This evidence-based intervention was developed with local stakeholders, adapted to the community, and implemented following an ecohealth approach (26).

In Tampouy, the intervention reduced residents' exposure to *Ae. aegypti* mosquito bites and container and pupae indices, whereas these indices increased in Juvenat, the control neighborhood. House and Breteau indices also had a greater reduction in the intervention neighborhood. Knowledge about dengue was very limited at baseline in both the intervention and control neighborhoods. Respondents in the intervention neighborhood had increased knowledge about dengue and actions to control mosquitoes, a first step in the process of dengue vector control activities. In the control neighborhood, limited knowledge of dengue transmission, prevention, and treatment resulted in poorer
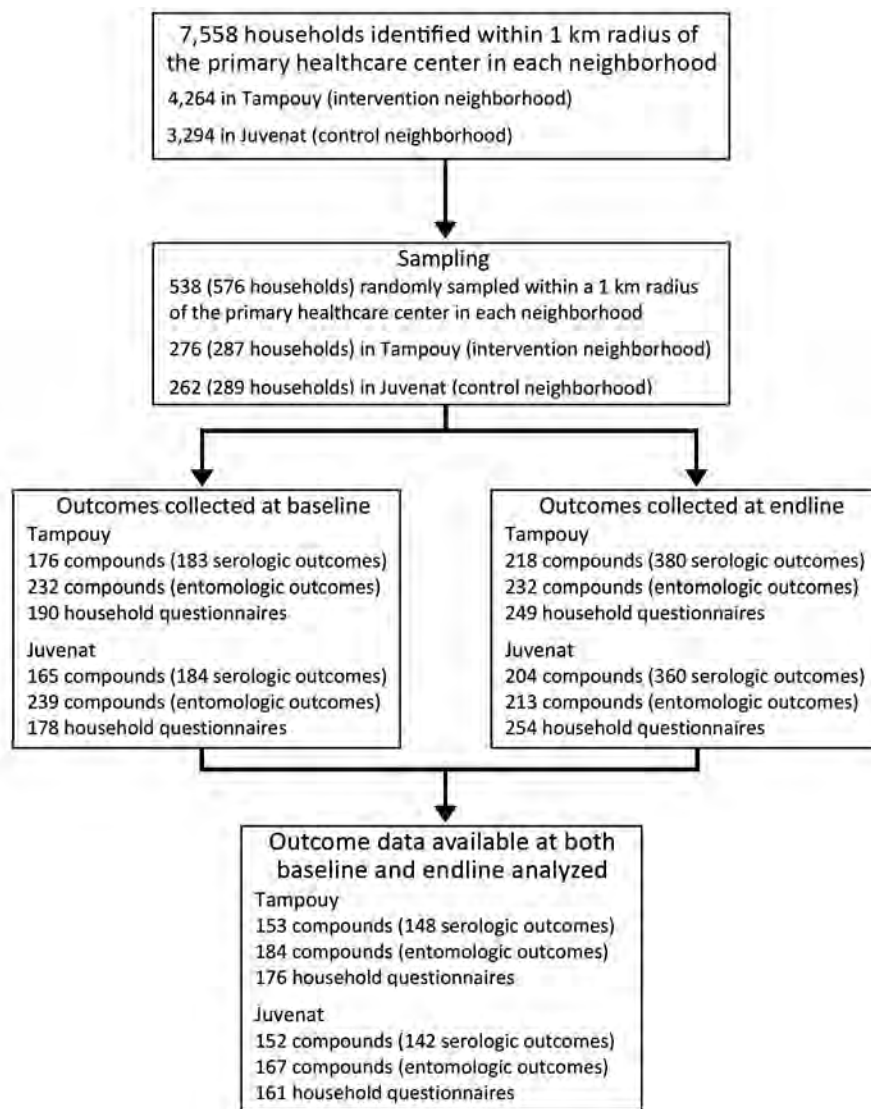
Figure 2. Flowchart for identification of compounds and households for a community-based intervention for dengue vector control conducted in Ouagadougou, Burkina Faso, June–October 2016.

protective practices against dengue vector. These results are in line with those from previous studies performed in Asia and Latin America (*26–28,34,35*).

In both the intervention and control neighborhoods, the entomologic indices were high at baseline, which might be the case for the entire city. Residents might not be aware of the conditions or factors that can exacerbate the presence of dengue vectors. Moreover, a real need exists to characterize *Ae. aegypti* mosquito breeding sites in Ouagadougou so they can be specifically targeted through education and vector control activities. Entomologic studies are also needed to clarify the ecologic aspects of the *Ae. aegypti* mosquito; strengthened disease surveillance is also needed because persons can be bitten by mosquitoes outside of the home. An integrated surveillance system (i.e., addressing epidemiology and entomology) allows for data triangulation, which should lead to better vector control planning.

We did not find an effect of the intervention on the number of *Ae. aegypti* breeding sites or the number of larvae and pupae found in compounds. Water stored for a long time became stagnant and a potential *Ae. aegypti* mosquito breeding site. Residents in the intervention neighborhood might have adopted measures to protect themselves from *Ae. aegypti* mosquito bites, which is confirmed by the reduction in the immunologic biomarkers; however, they might have developed the habit of pouring out or covering water containers. Moreover, the interviewers knew the intervention status of the neighborhoods, which could have led to potential reporting bias and might be seen as a limitation of the study. However, the results of the serologic biomarkers and the household questionnaires showed that any potential bias was minimal.

Persons' health beliefs and their dengue-related knowledge, attitudes, and practices are likely to shape
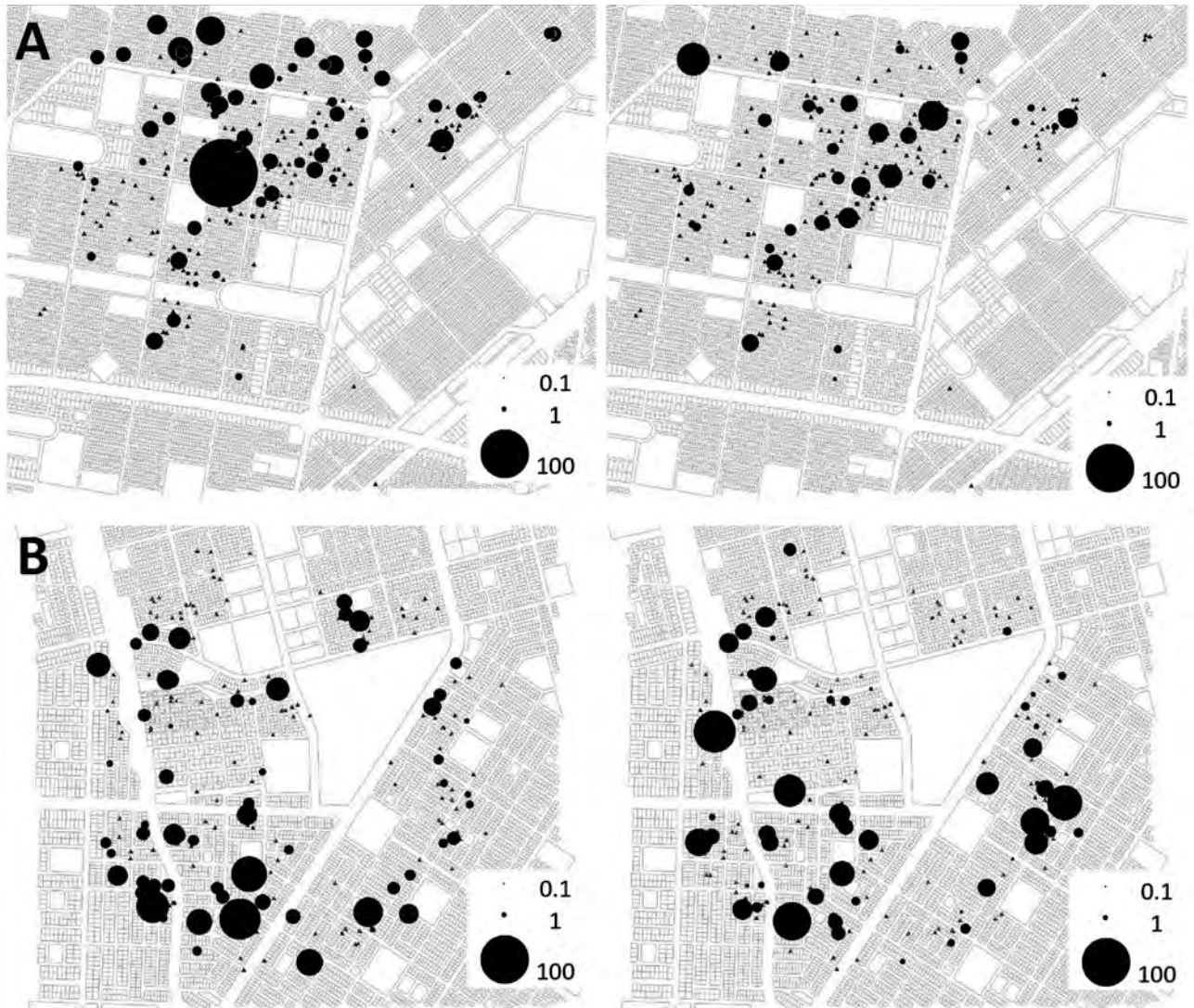
Figure 3. *Aedes aegypti* larvae and pupae per resident (black dots) in the compounds of (A) intervention neighborhood (Tampouy) and (B) control neighborhood (Juvenat) at baseline (left) and endline (right) of an evaluation of a community-based intervention for dengue vector control conducted in Ouagadougou, Burkina Faso, June–October 2016.

their healthcare practices and behaviors (*36*). The success of dengue prevention and mosquito control efforts in the community relies on the effectiveness of initiatives to educate the public about dengue and how it spreads, how the general public can control *Ae. aegypti* mosquito breeding sites, and how to improve household environmental sanitation through sustained modification of human behavior (*37*).

According to Stahl et al. (*38*), preventing dengue outbreaks is much cheaper than paying for the consequences of an outbreak. Burkina Faso is experiencing an alarming increase in dengue cases and the dengue vector population during raining seasons. The spread of the vector is associated with climate change, globalization, and rapid urbanization (*39*); however, many other major diseases

can also be transmitted by the mosquito vectors of dengue (e.g., yellow fever, chikungunya, and Zika) (*5*). WHO has recommended that any country in the dengue belt with *Ae. aegypti* mosquitoes should be vigilant about the spread of Zika virus (*40*). Understanding which interventions are effective in what context is needed to prevent new diseases that could be established with competent vectors and to control current diseases. Now that the favorable environmental conditions for Zika vector spread have been confirmed to exist in Africa, complacency is not an option (*41*).

Considerable enthusiasm exists for novel vector control approaches to prevent diseases transmitted by *Ae. aegypti* mosquitoes, including 1) release of mosquitoes infected with a strain of *Wolbachia* spp. bacteria; 2) release of large

numbers of sterile male vectors; 3) use of mosquitoes engineered to carry a lethal gene; and 4) use of pyriproxyfen, a powerful synthetic analog of mosquito juvenile hormone (*42*). An effective prevention and control strategy against *Aedes* mosquito–borne diseases in tropical urban settings includes a strong community effort in social mobilization and communication, along with use of new technologies that combine enhanced mosquito control with effective vaccines and improved diagnosis and clinical management, including the use of antivirals and therapeutic antibodies (*43*).

In sub-Saharan Africa, the promotion of health literacy is critical to active and informed participation in health promotion and disease prevention (*44*); it is one component that can facilitate or be a barrier to a health education and communication intervention for dengue vector control. Public health authorities should sustain their education and communication efforts and the budget for such efforts not only when an outbreak is ongoing. Communities must be reminded of when to carry out the actions, how to properly carry out the recommended behaviors, and what the benefits are to carrying them out. To achieve sustained behavior changes in dengue vector control, continuous communication and interaction between governmental agencies and the communities is essential.

Acknowledgments

About the Author

Dr. Ouédraogo is a postdoctoral researcher at the University of Montreal Public Health Research Institute. Her research focuses on evaluating public health programs and interventions.

References

1. Centers for Disease Control and Prevention. Ongoing dengue epidemic—Angola, June 2013. MMWR Morb Mortal Wkly Rep. 2013;62:504–7.
2. Eldin C, Gautret P, Nougairede A, Sentis M, Ninove L, Saidani N, et al. Identification of dengue type 2 virus in febrile travellers returning from Burkina Faso to France, related to an ongoing outbreak, October to November 2016. Euro Surveill. 2016;21:30425. http://dx.doi.org/10.2807/1560-7917.ES.2016.21.50.30425
3. Gautret P, Botelho-Nevers E, Charrel RN, Parola P. Dengue virus infections in travellers returning from Benin to France, July–August 2010. Euro Surveill. 2010;15:19657.
4. Gautret P, Simon F, Hervius Askling H, Bouchaud O, Leparc-Goffart I, Ninove L, et al.; EuroTravNet. Dengue type 3 virus infections in European travellers returning from the Comoros and Zanzibar, February–April 2010. Euro Surveill. 2010;15:19541.
5. Gubler DJ. Dengue, urbanization and globalization: the unholy trinity of the 21st century. Trop Med Health. 2011;39(Suppl):3–11. http://dx.doi.org/10.2149/tmh.2011-S05
6. Ebi KL, Nealon J. Dengue in a changing climate. Environ Res. 2016;151:115–23. http://dx.doi.org/10.1016/j.envres.2016.07.026
7. Yacoub S, Mongkolsapaya J, Screaton G. Recent advances in understanding dengue. F1000Res. 2016;5:5.
8. Gubler DJ, Clark GG. Dengue/dengue hemorrhagic fever: the emergence of a global health problem. Emerg Infect Dis. 1995;1:55–7. http://dx.doi.org/10.3201/eid0102.952004
9. Jaenisch T, Junghanss T, Wills B, Brady OJ, Eckerle I, Farlow A, et al.; Dengue in Africa Study Group. Dengue expansion in Africa—not recognized or not happening? Emerg Infect Dis. 2014;20. http://dx.doi.org/10.3201/eid2010.140487
10. Zahouli JB, Utzinger J, Adja MA, Müller P, Malone D, Tano Y, et al. Oviposition ecology and species composition of *Aedes* spp. and *Aedes aegypti* dynamics in variously urbanized settings in arbovirus foci in southeastern Côte d'Ivoire. Parasit Vectors. 2016;9:523. http://dx.doi.org/10.1186/s13071-016-1778-9
11. Wu X, Lu Y, Zhou S, Chen L, Xu B. Impact of climate change on human infectious diseases: empirical evidence and human adaptation. Environ Int. 2016;86:14–23. http://dx.doi.org/10.1016/j.envint.2015.09.007
12. Ridde V, Agier I, Bonnet E, Carabali M, Dabiré KR, Fournet F, et al. Presence of three dengue serotypes in Ouagadougou (Burkina Faso): research and public health implications. Infect Dis Poverty. 2016;5:23. http://dx.doi.org/10.1186/s40249-016-0120-2
13. Wilairatana P, Tangpukdee N, Krudsood S. Misdiagnosis of malaria in malaria-dengue endemic area. Trop Med Surg. 2014;2:e119. http://dx.doi.org/10.4172/2329-9088.1000e119
14. World Health Organization. Global strategy for dengue prevention and control 2012–2020 [cited 2017 Nov 27]. http://apps.who.int/iris/bitstream/10665/75303/1/9789241504034_eng.pdf?ua=1
15. Manrique-Saide P, Che-Mendoza A, Barrera-Perez M, Guillermo-May G, Herrera-Bojorquez J, Dzul-Manzanilla F, et al. Use of insecticide-treated house screens to reduce infestations of dengue virus vectors, Mexico. Emerg Infect Dis. 2015;21:308–11. http://dx.doi.org/10.3201/eid2102.140533
16. Kusumawathie PH, Yapabandarab AM, Jayasooriya GA, Walisinghe C. Effectiveness of net covers on water storage tanks for the control of dengue vectors in Sri Lanka. J Vector Borne Dis. 2009;46:160–3.

17. Farajollahi A, Healy SP, Unlu I, Gaugler R, Fonseca DM. Effectiveness of ultra-low volume nighttime applications of an adulticide against diurnal *Aedes albopictus*, a critical vector of dengue and chikungunya viruses. PLoS One. 2012;7:e49181. http://dx.doi.org/10.1371/journal.pone.0049181

18. Bowman LR, Donegan S, McCall PJ. Is dengue vector control deficient in effectiveness or evidence?: systematic review and meta-analysis. PLoS Negl Trop Dis. 2016;10:e0004551. http://dx.doi.org/10.1371/journal.pntd.0004551

19. United Nations Department of Economic and Social Affairs Population Division. 2014 revision of the World Urbanization Prospects [cited 2017 Nov 27]. http://www.un.org/en/development/desa/publications/2014-revision-world-urbanization-prospects.html

20. Baronti C, Piorkowski G, Touret F, Charrel R, de Lamballerie X, Nougairede A. Complete coding sequences of two dengue virus type 2 strains isolated from an outbreak in Burkina Faso in 2016. Genome Announc. 2017;5:e00209–17. http://dx.doi.org/10.1128/genomeA.00209-17

21. Tarnagda Z, Cissé A, Bicaba BW, Diagbouga S, Sagna T, Ilboudo AK, et al. Dengue fever in Burkina Faso, 2016. Emerg Infect Dis. 2018;24:170–2. http://dx.doi.org/10.3201/eid2401.170973

22. World Health Organization. Dengue fever—Burkina Faso. Disease outbreak news [cited 2018 Jun 4]. http://www.who.int/csr/don/6-november-2017-dengue-burkina-faso

23. Observatoire des Populations de Ouagadougou. Rapport scientifique sur la caractérisation sociologique des quartiers de l'OPO (Juin 2013)—Projet Wellcome Trust 2008–2013, Axe Qualitatif [cited 2017 Dec 1]. http://www.issp02.issp.bf/opo/Publications/Rapport-scientifique-juin2013-Caracterisation-des-quartiers-Axe-qualite.pdf

24. Yaro S, Carabali M, Lim J, Dahourou D, Kagone ST, Nikiema TJ, et al. Burden of dengue in children and adults of Ouagadougou, Burkina Faso [cited 2017 Nov 27]. http://www.equitesante.org/equiteburkina/recherche-lutte-contre-dengue

25. Arunachalam N, Tyagi BK, Samuel M, Krishnamoorthi R, Manavalan R, Tewari SC, et al. Community-based control of *Aedes aegypti* by adoption of eco-health methods in Chennai City, India. Pathog Glob Health. 2012;106:488–96. http://dx.doi.org/10.1179/2047773212Y.0000000056

26. Toledo Romani ME, Vanlerberghe V, Perez D, Lefevre P, Ceballos E, Bandera D, et al. Achieving sustainability of community-based dengue control in Santiago de Cuba. Soc Sci Med. 2007;64:976–88. http://dx.doi.org/10.1016/j.socscimed.2006.10.033

27. Vanlerberghe V, Toledo ME, Rodríguez M, Gomez D, Baly A, Benitez JR, et al. Community involvement in dengue vector control: cluster randomised trial. BMJ. 2009;338:b1959.

28. Kay B, Vu SN. New strategy against *Aedes aegypti* in Vietnam. Lancet. 2005;365:613–7.

29. Randall S, Coast E, Antoine P, Compaore N, Dial F-B, Fanghanel A, et al. UN census "households" and local interpretations in Africa since Independence. SAGE Open. 2015;5:18. http://dx.doi.org/10.1177/2158244015589353

30. Elanga Ndille E, Doucoure S, Damien G, Mouchet F, Drame PM, Cornelie S, et al. First attempt to validate human IgG antibody response to Nterm-34kDa salivary peptide as biomarker for evaluating exposure to *Aedes aegypti* bites.

PLoS Negl Trop Dis. 2012;6:e1905. http://dx.doi.org/10.1371/journal.pntd.0001905

31. World Health Organization. Dengue control: vector surveillance [cited 2017 Nov 27]. http://www.who.int/denguecontrol/monitoring/vector_surveillance

32. Linden A. A comparison of approaches for stratifying on the propensity score to reduce bias. J Eval Clin Pract. 2017;23:690–6. http://dx.doi.org/10.1111/jep.12701

33. Zou G. A modified poisson regression approach to prospective studies with binary data. Am J Epidemiol. 2004;159:702–6. http://dx.doi.org/10.1093/aje/kwh090

34. Caprara A, Lima JW, Peixoto AC, Motta CM, Nobre JM, Sommerfeld J, et al. Entomological impact and social participation in dengue control: a cluster randomized trial in Fortaleza, Brazil. Trans R Soc Trop Med Hyg. 2015;109:99–105. http://dx.doi.org/10.1093/trstmh/tru187

35. Andersson N, Nava-Aguilera E, Arosteguí J, Morales-Perez A, Suazo-Laguna H, Legorreta-Soberanis J, et al. Evidence based community mobilization for dengue prevention in Nicaragua and Mexico (Camino Verde, the Green Way): cluster randomized controlled trial. BMJ. 2015;351:h3267. http://dx.doi.org/10.1136/bmj.h3267

36. Wong LP, Shakir SM, Atefi N, AbuBakar S. Factors affecting dengue prevention practices: nationwide survey of the Malaysian public. PLoS One. 2015;10:e0122890. http://dx.doi.org/10.1371/journal.pone.0122890

37. Artwanichakul K, Thiengkamol N, Thiengkamol T. Structural model of dengue fever prevention and control behavior. Eur J Soil Sci. 2012;32:485.

38. Stahl HC, Butenschoen VM, Tran HT, Gozzer E, Skewes R, Mahendradhata Y, et al. Cost of dengue outbreaks: literature review and country case studies. BMC Public Health. 2013;13:1048. http://dx.doi.org/10.1186/1471-2458-13-1048

39. Xu L, Stige LC, Chan KS, Zhou J, Yang J, Sang S, et al. Climate variation drives dengue dynamics. Proc Natl Acad Sci U S A. 2017;114:113–8. http://dx.doi.org/10.1073/pnas.1618558114

40. Gulland A. WHO urges countries in dengue belt to look out for Zika. BMJ. 2016;352:i595. http://dx.doi.org/10.1136/bmj.i595

41. Meda N, Salinas S, Kagoné T, Simonin Y, Van de Perre P. Zika virus epidemic: Africa should not be neglected. Lancet. 2016;388:337–8. http://dx.doi.org/10.1016/S0140-6736(16)31103-5

42. von Seidlein L, Kekulé AS, Strickman D. Novel vector control approaches: the future for prevention of Zika virus transmission? PLoS Med. 2017;14:e1002219. http://dx.doi.org/10.1371/journal.pmed.1002219

43. Gubler DJ. Emerging vector-borne flavivirus diseases: are vaccines the solution? Expert Rev Vaccines. 2011;10:563–5. http://dx.doi.org/10.1586/erv.11.35

44. Barry MM, D'Eath M, Sixsmith J. Interventions for improving population health literacy: insights from a rapid review of the evidence. J Health Commun. 2013;18:1507–22. http://dx.doi.org/10.1080/10810730.2013.840699

Address for correspondence: Samiratou Ouédraogo, University of Montreal Public Health Research Institute (IRSPUM), 7101 Avenue du Parc, 3rd Fl, Montréal, QC H3N 1X9, Canada; email: samioued@yahoo.fr

Evaluation of Nowcasting for Detecting and Predicting Local Influenza Epidemics, Sweden, 2009–2014

Armin Spreco, Olle Eriksson, Örjan Dahlström, Benjamin John Cowling, Toomas Timpka

The growing availability of big data in healthcare and public health opens possibilities for infectious disease control in local settings. We prospectively evaluated a method for integrated local detection and prediction (nowcasting) of influenza epidemics over 5 years, using the total population in Östergötland County, Sweden. We used routine health information system data on influenza-diagnosis cases and syndromic telenursing data for July 2009–June 2014 to evaluate epidemic detection, peak-timing prediction, and peak-intensity prediction. Detection performance was satisfactory throughout the period, except for the 2011–12 influenza A(H3N2) season, which followed a season with influenza B and pandemic influenza A(H1N1) pdm09 virus activity. Peak-timing prediction performance was satisfactory for the 4 influenza seasons but not the pandemic. Peak-intensity levels were correctly categorized for the pandemic and 2 of 4 influenza seasons. We recommend using versions of this method modified with regard to local use context for further evaluations using standard methods.

Although the seasonal variations in influenza incidence among nations and global regions are well described (*1*), the duration and intensity of influenza epidemics in local communities have been less well monitored and understood. The rapidly growing availability of big data from diagnostic and prediagnostic (syndromic) sources in healthcare and public health settings opens new possibilities for increasing the granularity in infectious disease control (*2,3*). However, development of outbreak models and efficient use of the information produced by prediction models in public health response decision-making remain challenging. This observation was recently highlighted

by the Congress of the United States request that the Government Accountability Office gather information on validation of emerging infectious disease model predictions (https://energycommerce.house.gov/wp-content/uploads/2017/11/20171109GAO.pdf).

We previously reported the design of a nowcasting method (detection of influenza epidemics and short-term predictions) for local-level application in the northwestern region of the world (*4*). In other fields, such as meteorology, nowcasting methods represent standard tools for warning the public against dangerous high-impact events (*5*). The rationale for developing this novel method was to inform the planning of local responses and adjustments of healthcare capacities. Many such adjustments are planned and performed locally, at county and municipality levels. In Sweden, for instance, the hospital bed capacity is habitually overextended; on average, 103 patients occupy 100 regular hospital bed units (*6*). It is therefore important that an influenza epidemic is noticed early at the local level to make time for implementation of adjustments (e.g., freeing hospital beds by removing from the waiting list those patients scheduled for elective interventions).

We performed a prospective 5-year evaluation of local influenza nowcasting by using routine health information system data. The evaluation period included 1 pandemic (2009) and 4 winter influenza seasons (Figure). The nowcasting method is based on mathematical modeling of epidemic curves generated from historic local data (*4*). Nowcasting comprises 3 functions: detection of the local start of the epidemic, prediction of peak timing, and prediction of peak intensity.

Methods

We used an open cohort design based on the total population (n = 445,000) in Östergötland County, Sweden. We used prospective data from July 1, 2009, through June 30, 2014, from 2 sources in the countywide health information system: clinical influenza-diagnosis cases recorded by physicians and syndromic chief complaint data from a
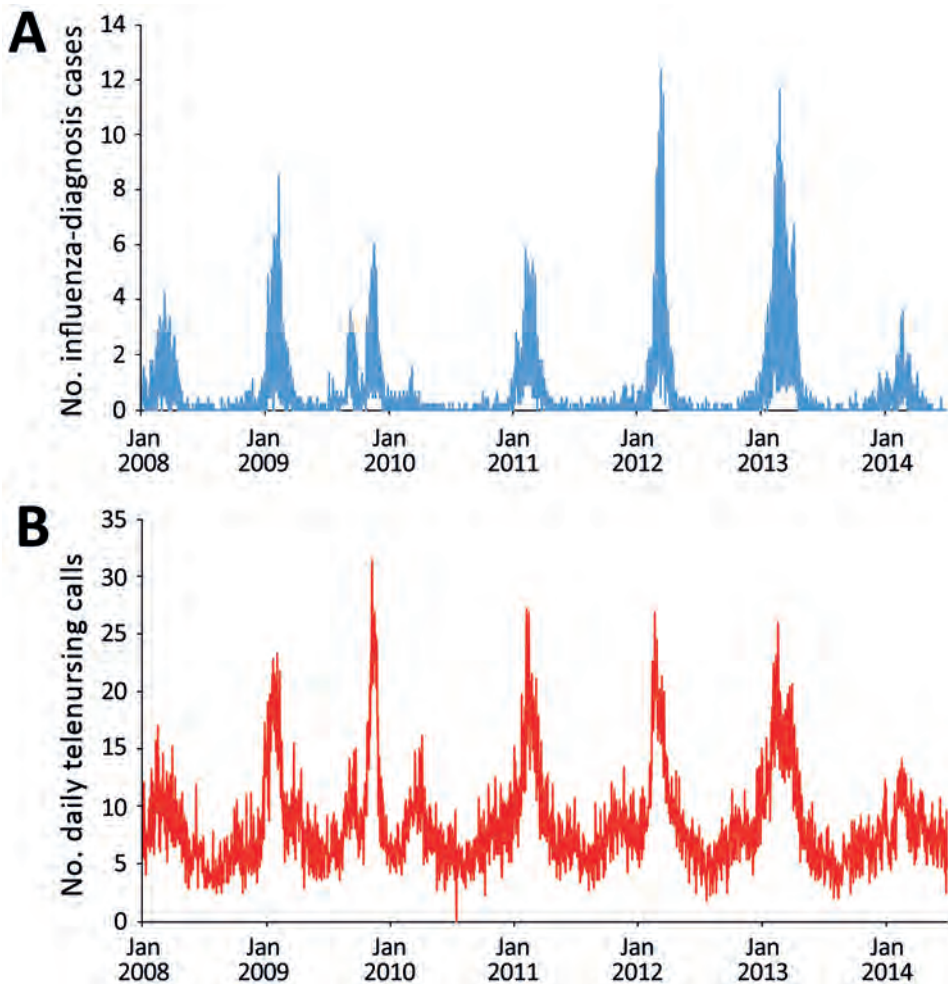
Figure. Data used for evaluation of nowcasting for detection and prediction of local influenza epidemics, Östergötland County, Sweden, January 1, 2008, through June 30, 2014. A) Unadjusted daily numbers of influenza-diagnosis cases per 100,000 population. B) Unadjusted daily telenursing calls because of fever (child and adult) per 100,000 population.

telenursing service (*4*). The influenza-diagnosis case data were used for detection of the local start of the epidemic and prediction of its peak intensity; the syndromic data were used for prediction of the peak timing. Timeliness was used as a performance metric for detection of the local start of the epidemic and the peak-timing prediction; the correct identification of intensity category on a 5-grade scale was used for peak-intensity prediction. The study design was approved by the Regional Research Ethics Board in Linköping (no. 2012/104–31).

Definitions

We identified influenza cases by using codes from the International Classification of Diseases, 10th Revision, for influenza (J10.0, J10.1, J10.8, J11.0, J11.1, J11.8) (*7*) as recorded in the local electronic health data repository. We identified influenza-related telenursing call cases by using the chief complaint codes associated with influenza symptoms (dyspnea, fever [child and adult], cough [child and adult], sore throat, lethargy, syncope, dizziness, and headache [child and adult]).

The intensity level for the start of a local epidemic (i.e., the endpoint for the detection function) was set to 6.3 influenza-diagnosis cases/100,000 population recorded during a floating 7-day period in the countywide health information system (*3*). A recent comparison of influenza intensity levels in Europe estimated a similar definition (6.4 influenza-diagnosis cases/wk/100,000 population) for the 2008–09 winter influenza season in Sweden (*8*). Peak timing was defined as the date when the highest number of influenza-diagnosis cases were documented in the countywide electronic patient record. Peak intensity was defined as the number of influenza-diagnosis cases that had been documented on that date.

The detection threshold was adjusted to situations when extended simmering of influenza-related activity appears before an epidemic. Such simmering was associated with exceptionally mild winter influenza seasons and pandemics. Preepidemic simmering before winter influenza seasons was defined as occurring when the period between increased influenza incidence above baseline and the start of the epidemic is prolonged (*4*). The upper

threshold for the baseline was set to 3.2 influenza-diagnosis cases/100,000 population during a floating 7-day period (i.e., half of the defined start-of-epidemic intensity level). If the baseline threshold was surpassed for a period 3 times longer than the average period before previous epidemics without exceeding the start-of-epidemic level (i.e., 6.3 influenza-diagnosis cases/100,000 population during a floating 7-day period), preepidemic simmering was considered to have occurred. Preepidemic simmering in association with a pandemic was defined as that ensuing from the date of a World Health Organization pandemic alert. We determined all definitions and adjustments before using the method for detection and prediction.

Method Application

Technical details concerning the 3 functions of nowcasting are provided in online Technical Appendix 1 (https://wwwnc.cdc.gov/EID/article/24/10/17-1940-Techapp1.pdf). The programming code for the analyses is provided in online Technical Appendix 2 (https://wwwnc.cdc.gov/EID/article/24/10/17-1940-Techapp2.pdf).

To calibrate the detection component of the nowcasting method, we retrospectively determined weekday effects on recording of influenza-diagnosis cases and a baseline alarm threshold by using learning data. These data were collected from January 1, 2008, through June 30, 2009, including the 2 winter influenza seasons 2007–08 and 2008–09. To determine weekday effects, we used data from the entire learning data collection period. To determine the initial alerting threshold, we used only data from the winter influenza season in 2008–09. The 2007–08 winter influenza season could not be used for this purpose because collection of learning data had already started. Throughout the study period, the calibration data were updated after every winter influenza season (i.e., no updates after the 2009 pandemic outbreak). The detection algorithm was thus applied to the next epidemic by using the revised threshold determined in the updated learning dataset. We identified 2 exceptional situations: pandemic settings and winter influenza seasons that simmered before they started (4). In these situations, the alarm threshold is doubled. Accordingly, following the World Health Organization pandemic alert (9), the alarm threshold was doubled for the 2009 season. Before the 2010–11 winter influenza season, the threshold was reset to the regular level. No updates were performed because the set of learning data remained the same (i.e., it contained data from the 2008–09 winter influenza season). For the 2011–12 winter influenza season, we updated the threshold by using learning data from the 2008–09 and 2010–11 winter influenza seasons. For the 2012–13 winter influenza season, we updated the threshold by using learning data from the 2008–09, 2010–11, and 2011–12 winter influenza seasons. For the 2013–14 winter influenza season, we again updated the alerting threshold by using learning data from the previous winter influenza seasons (2008–09, 2010–11, 2011–12, and 2012–13). However, because this winter influenza season simmered before it started, the threshold was doubled before the detection method was applied. The weekday effects were assumed to be relatively constant over time in the local detection analyses and therefore were not updated after every winter influenza season.

We also used the set of learning data from the winter influenza seasons in 2007–08 and 2008–09 to initially calibrate the first component of the local prediction module. The dataset was used to decide the grouping of chief complaints with the largest correlation strength and longest lead time between influenza-diagnosis data and telenursing data (10,11). The best performing telenursing chief complaint was fever (child and adult), and the most favorable lead time was 14 days. When the peak timing had been determined, the second component of the local prediction module was applied to influenza-diagnosis data from the corresponding epidemics to find the peak intensity on the predicted peak day (4). Regarding weekday effects on local prediction, the same calculation was applied and the same grouping of chief complaints and lead time were used throughout the study.

Metrics and Interpretations

For trustworthiness of the nowcasting method in local healthcare planning, we set the maximum acceptable timeliness error for detection and peak timing predictions to 1.5 weeks. Method performance was defined to be excellent if the absolute value of the timeliness error was ≤3 days, good if it was 4–7 days, acceptable if it was 8–11 days, and poor if it was ≥12 days. For peak intensity predictions, we used the epidemic threshold and intensity level categories (nonepidemic, low, medium, high, and very high) identified for Sweden in a study involving 28 European countries (8) (Table 1). If the predicted peak intensity fell into the same category as the actual peak intensity, the prediction was considered successful; otherwise, it was considered unsuccessful.

Results

Local Detection

The detection component of the local nowcasting method showed good performance during the 2009 pandemic of influenza A(H1N1)pdm09 (pH1N1) virus (Table 2), alerting for the local influenza epidemic 5 days after it actually started. For the 2010–11 winter influenza season with influenza B and pH1N1 viruses circulating, the local detection performance was also good; the alarm was raised 5 days after the start of the local epidemic. During the 2011–12 winter influenza season, with influenza A(H3N2) virus

Table 1. Epidemic intensity categories used to interpret performance measurements in evaluation of nowcasting for detection and prediction of local influenza epidemics, Sweden, 2009–2014*

Intensity level	Threshold, cases/d/100,000 population					
	2008–09	2009 pandemic	2010–11	2011–12	2012–13	2013–14
Nonepidemic	<0.9	<0.9	<0.9	<1.0	<1.2	<1.2
Low	0.9	0.9	0.9	1.0	1.2	1.2
Medium	2.4	2.5	2.5	2.5	2.8	2.9
High	5.5	5.4	5.4	5.2	5.6	5.5
Very high	7.9	7.5	7.5	7.1	7.7	7.4

*Based on (8).

activity only, detection performance was poor. During that season, the alarm was raised 15 days before the actual local epidemic started. During the 2012–13 and 2013–14 winter influenza seasons, with influenza A(H3N2), influenza B, and pH1N1 viruses circulating, the local detection performance was excellent; alarms were raised 3 days before the 2012–13 epidemic started and 3 days after the 2013–14 epidemic started.

Local Prediction

For the 2009 influenza pandemic, performance of the local peak-timing prediction was poor, but the peak-intensity level was correctly categorized (medium intensity epidemic) (Table 3). For the 2010–11 winter influenza season, with influenza B and pH1N1 viruses circulating, the local peak-timing prediction was excellent and the peak intensity was successfully predicted to the correct category (medium intensity). For the 2011–12 winter influenza seasons with influenza A(H3N2) virus circulating and the 2012–13 winter season with influenza A(H3N2), influenza B, and pH1N1 viruses circulating, the local peak-timing predictions were good. The local peak-intensity predictions were successful for the 2012–13 winter influenza season, correctly categorizing it to a very high intensity level and unsuccessful for the 2011–12 season, categorizing it as a medium intensity epidemic when it actually developed into a very high-intensity epidemic. For the 2013–14 winter influenza season, with influenza B and pH1N1 viruses circulating and a simmering start, the local peak-timing prediction was acceptable, but the local peak intensity was wrongly predicted to be at the nonepidemic level when the winter influenza season actually reached a medium intensity level.

Discussion

In this prospective 5-year evaluation of a method for local nowcasting of influenza epidemics that used routine health information system data, we identified aspects that were satisfactory and identified areas where improvements are needed. The detection function displayed satisfactory performance throughout the evaluation period, except for the 2011–12 winter influenza season, in which influenza A(H3N2) virus circulated after a season with influenza B and pH1N1 virus activity. Peak-timing prediction performance was satisfactory for the 4 winter influenza seasons but not for the 2009 pandemic. In addition, the method categorized the local peak-intensity levels correctly for the 2009 pandemic and for 2 of the winter influenza seasons, but it was unsuccessful at forecasting the very high peak intensity of the 2011–12 season and the medium peak intensity of the 2013–14 season, which was preceded by a simmering phase.

The results indicate that securing the availability of a new data source is only the first step toward using the data stream in routine surveillance. The syndromic data source used for the big data stream in this study was subjected to rigorous restructuring and maintenance. Nonetheless, not all parameters associated with the syndromic data stream were regularly updated. For the peak-timing predictions made by using telenursing data, we assumed that increases in telenursing activity precede influenza diagnoses by 14 days. Although this assumption is grounded (10,11), the interval may change over time and thereby influence influenza predictions. Using the constant interval estimate, we estimated the influenza diagnosis peaks for the 2011–12 and 2012–13 winter influenza seasons 1 week before and 1 week after the actual influenza-diagnosis peaks. In

Table 2. Performance of the detection algorithm displayed with alert thresholds updated by using data from previous winter influenza seasons in evaluation of nowcasting for detection and prediction of local influenza epidemics, Sweden, 2009–2014*

Influenza virus activity	Updated threshold, cases/d/100,000 population	Timeliness†	Interpretation
2009 pH1N1‡	0.424	−5	Good
2010–11 B and pH1N1	0.212	−5	Good
2011–12 A(H3N2)	0.207	15	Poor
2012–13 A(H3N2), B, and pH1N1	0.242	3	Excellent
2013–14 A(H3N2), B, and pH1N1‡	0.481	−3	Excellent

*pH1N1, pandemic influenza A(H1N1)pdm09 virus.
†Positive value means that the algorithm issued an alarm before the local epidemic had started; negative value means that the alarm was raised after the start of the epidemic.
‡The threshold was doubled because of a pandemic alert or observation of a period of simmering influenza activity.

Table 3. Performance of peak-timing and peak-intensity predictions from evaluation of nowcasting for detection and prediction of local influenza epidemics, Sweden, 2009–2014*

Influenza virus active	Time-of-peak predictions†				Peak intensity predictions		
	Date when prediction made	Time to peak, d	Prediction error	Interpretation	Category (cases/d/100,000 population)		Interpretation
					Predicted	Factual	
2009 pH1N1	2009 Sep 27	8	−28	Poor	Medium (3.3)	Medium (2.9)	Successful
2010–11 B and pH1N1	2011 Feb 11	10	0	Excellent	Medium (4.5)	Medium (4.9)	Successful
2011–12 A(H3N2)	2012 Feb 25	9	7	Good	Medium (4.5)	Very high (12.4)	Unsuccessful
2012–13 A(H3N2), B, and pH1N1	2013 Feb 22	10	−7	Good	Very high (10.1)	Very high (11.7)	Successful
2013–14 A(H3N2), B, and pH1N1	2014 Feb 17	8	−8	Acceptable	Nonepidemic (1.0)	Medium (3.4)	Unsuccessful

*pH1N1, pandemic influenza A(H1N1)pdm09 virus.
†Positive value means that the peak was predicted to be reached before the actual peak occurred; negative value means that the peak was predicted to be reached after the actual peak occurred.

other words, the basic prediction method may have been more accurate at predicting the peak timing than the results of this study show. In the setting of our study, the performance was most likely decreased by the assumption that telenursing precedes influenza diagnosis by 14 days is applicable to all situations. Althouse et al. reported that methods underpinning the use of big data sources (e.g., search query logs) need regular upkeep to maintain their accuracy (*12*). In future versions of nowcasting methods, regular updates and syndromic sources that are more stable than telenursing data (regarding time lag to influenza diagnosis data) may become available and can be used to improve the peak-timing predictions.

Influenza forecasting is methodologically challenging (*13,14*), and only a few prospective evaluations have transparently reported algorithms and study designs. In the first Centers for Disease Control and Prevention (CDC) challenge, a prospective study of state-of-the-art methods in which 4 aspects of influenza epidemics (start week, peak week, peak percentage, and duration) were forecasted by using routine data (*15*), none of the evaluated methods showed satisfactory performance for all aspects. Similarly, in the second CDC challenge, in which 3 aspects of influenza epidemics (start week, peak week, and peak intensity) were forecasted by using 7 methods, none of the evaluated methods displayed satisfactory performance (*16*). These challenge studies have substantially helped to widen the understanding of the difficulties of forecasting different aspects of influenza epidemics. In our study, the detection and peak-intensity prediction functions of the local nowcasting method underperformed during the 2011–12 winter influenza season. One reason for the observed underperformance may be that the data from preceding seasons used to generate local epidemic curves were insufficient for modeling the between-seasons drift in the immunity status of the population in relation to the circulating influenza strain. In other words, the present parameters used to compute

epidemic curves were deficient when large drifts in population immunity with corresponding changes in virus dissemination patterns occurred. For instance, the epidemic phase of the influenza A(H3N2) season in 2011–12 may not have started with virus spread among the young persons in the community as it had during previous seasons (*17,18*). It has been suggested that including virologic information (i.e., influenza virus type and subtype) as model parameters may improve the predictive accuracy of mathematical models (*19*). We contend also that, for local influenza detection and prediction, historical accounts of the circulating influenza virus types should be considered for inclusion in the statistical models and suggest adding information about the population age structure. However, such model extensions must also be paralleled by securing a continuous supply of the corresponding data in the local settings where the models are to be used.

This study has strengths and weaknesses that need to be considered when interpreting the results. The main strength of the study is that it prospectively evaluates an integrated influenza nowcasting method in a local community. On the basis of experiences from previous studies (*4,15,16,20*), we considered timeliness to be the most valid general evaluation metric for our purposes. To be able to accurately support adjustments of local healthcare capacity, we used daily data for the evaluations. In the CDC challenge studies (*15,16*), forecasts of the start and peak timing of an epidemic were based on weekly data and considered accurate if they occurred within 1 week of the actual timing of each component. Therefore, we consider the limits used for evaluating detection and the peak-timing predictions in this study to be at least as strict as those in the CDC challenge. Regarding the prediction of peak intensity, we considered a forecast to be accurate if it predicted the peak intensity to be the correct peak-intensity category as defined by Vega et al. (*8*), who calculated the thresholds for each of these categories for every winter influenza season by applying

the moving epidemic method (*21*) on 5–10 previously occurring seasons. Hence, we consider these categories to be reliable. A longer prospective evaluation period would have increased the possibility of drawing valid conclusions concerning the outcome of the evaluation, and it would be preferable to have corresponding local data from other cities or regions (*22*). Evaluating our nowcasting method for epidemics from several other regions would enable conclusions to be drawn about the generalizability of the method.

We contend that methods for local nowcasting of influenza epidemics based on routine health information system data have potential for general dissemination and use. Future versions of the nowcasting model will be gradually extended with information on population age distribution and on current and previously circulating influenza types. Such extensions need to be paralleled by securing a routine supply of data to the added parameters in local health information systems. We recommend using versions of the nowcasting method modified with regard to their local use context for further evaluations with standard measures.

About the Author

Dr. Spreco is a researcher in the field of syndromic surveillance at Linköping University, Sweden. His main research focus is on evaluation and development of algorithms for detection and prediction of infectious diseases.

References

1. Polansky LS, Outin-Blenman S, Moen AC. Improved global capacity for influenza surveillance. Emerg Infect Dis. 2016;22:993–1001. http://dx.doi.org/10.3201/eid2206.151521
2. Shaman J, Karspeck A, Yang W, Tamerius J, Lipsitch M. Real-time influenza forecasts during the 2012-2013 season. Nat Commun. 2013;4:2837. http://dx.doi.org/10.1038/ncomms3837
3. Riley RD, Ensor J, Snell KI, Debray TP, Altman DG, Moons KG, et al. External validation of clinical prediction models using big datasets from e-health records or IPD meta-analysis: opportunities and challenges. BMJ. 2016;353:i3140. http://dx.doi.org/10.1136/bmj.i3140
4. Spreco A, Eriksson O, Dahlström Ö, Cowling BJ, Timpka T. Integrated detection and prediction of influenza activity for real-time surveillance: algorithm design. J Med Internet Res. 2017; 19:e211. http://dx.doi.org/10.2196/jmir.7101
5. Bližňák V, Sokol Z, Zacharov P. Nowcasting of deep convective clouds and heavy precipitation: comparison study between NWP model simulation and extrapolation. Atmos Res. 2017;184:24–34. http://dx.doi.org/10.1016/j.atmosres.2016.10.003
6. Sveriges Kommuner och Landsting. Ingen på sjukhus i onödan. No one in hospital unnecessarily [in Swedish]. Stockholm: Sveriges Kommuner och Landsting; 2016.
7. World Health Organization. International statistical classification of diseases and related health problems. 10th Revision, vol. 2. Geneva: The Organization; 2010.
8. Vega T, Lozano JE, Meerhoff T, Snacken R, Beauté J, Jorgensen P, et al. Influenza surveillance in Europe: comparing intensity levels calculated using the moving epidemic method. Influenza Other Respi Viruses. 2015;9:234–46. http://dx.doi.org/10.1111/irv.12330
9. World Health Organization. Influenza A(H1N1) [cited 2017 Jan 15]. http://www.who.int/mediacentre/news/statements/2009/h1n1_20090429/en/
10. Timpka T, Spreco A, Dahlström Ö, Eriksson O, Gursky E, Ekberg J, et al. Performance of eHealth data sources in local influenza surveillance: a 5-year open cohort study. J Med Internet Res. 2014;16:e116. http://dx.doi.org/10.2196/jmir.3099
11. Timpka T, Spreco A, Eriksson O, Dahlström Ö, Gursky EA, Strömgren M, et al. Predictive performance of telenursing complaints in influenza surveillance: a prospective cohort study in Sweden. Euro Surveill. 2014;19:46. http://dx.doi.org/10.2807/1560-7917.ES2014.19.46.20966
12. Althouse BM, Scarpino SV, Meyers LA, Ayers JW, Bargsten M, Baumbach J, et al. Enhancing disease surveillance with novel data streams: challenges and opportunities. EPJ Data Sci. 2015;4:pii:17. http://dx.doi.org/10.1140/epjds/s13688-015-0054-0
13. Chretien JP, George D, Shaman J, Chitale RA, McKenzie FE. Influenza forecasting in human populations: a scoping review. PLoS One. 2014;9:e94130. http://dx.doi.org/10.1371/journal.pone.0094130
14. Lazer D, Kennedy R, King G, Vespignani A. Big data. The parable of Google Flu: traps in big data analysis. Science. 2014;343:1203–5. http://dx.doi.org/10.1126/science.1248506
15. Biggerstaff M, Alper D, Dredze M, Fox S, Fung IC, Hickmann KS, et al.; Influenza Forecasting Contest Working Group. Results from the Centers for Disease Control and Prevention's predict the 2013–2014 influenza season challenge. BMC Infect Dis. 2016;16:357. http://dx.doi.org/10.1186/s12879-016-1669-x
16. Biggerstaff M, Johansson M, Alper D, Brooks LC, Chakraborty P, Farrow DC, et al. Results from the second year of a collaborative effort to forecast influenza seasons in the United States. Epidemics. 2018 Feb 24;pii:S1755–4365(17)30088–9. Epub ahead of print [cited 2018 Jun 14].10.1016/j.epidem.2018.02.003
17. Schanzer D, Vachon J, Pelletier L. Age-specific differences in influenza A epidemic curves: do children drive the spread of influenza epidemics? Am J Epidemiol. 2011;174:109–17. http://dx.doi.org/10.1093/aje/kwr037
18. Timpka T, Eriksson O, Spreco A, Gursky EA, Strömgren M, Holm E, et al. Age as a determinant for dissemination of seasonal and pandemic influenza: an open cohort study of influenza outbreaks in Östergötland County, Sweden. PLoS One. 2012;7:e31746. http://dx.doi.org/10.1371/journal.pone.0031746
19. Moniz L, Buczak AL, Baugher B, Guven E, Chretien JP. Predicting influenza with dynamical methods. BMC Med Inform Decis Mak. 2016;16:134. http://dx.doi.org/10.1186/s12911-016-0371-7
20. Cowling BJ, Wong IO, Ho LM, Riley S, Leung GM. Methods for monitoring influenza surveillance data. Int J Epidemiol. 2006;35:1314–21. http://dx.doi.org/10.1093/ije/dyl162
21. Vega T, Lozano JE, Meerhoff T, Snacken R, Mott J, Ortiz de Lejarazu R, et al. Influenza surveillance in Europe: establishing epidemic thresholds by the moving epidemic method. Influenza Other Respir Viruses. 2013;7:546–58. http://dx.doi.org/10.1111/j.1750-2659.2012.00422.x
22. Moss R, Zarebski A, Dawson P, McCaw JM. Retrospective forecasting of the 2010-2014 Melbourne influenza seasons using multiple surveillance systems. Epidemiol Infect. 2017;145:156–69. http://dx.doi.org/10.1017/S0950268816002053

Address for correspondence: Armin Spreco, Linköping University, Division of Social Medicine, Department of Medical and Health Sciences, Faculty of Health Sciences, SE-581 83 Linköping, Sweden; email: armin.spreco@liu.se

Rapid Increase in Carriage Rates of *Enterobacteriaceae* Producing Extended-Spectrum β-Lactamases in Healthy Preschool Children, Sweden

Johan Kaarme, Hilde Riedel, Wesley Schaal, Hong Yin, Tryggve Nevéus, Åsa Melhus

By collecting and analyzing diapers, we identified a >6-fold increase in carriage of extended-spectrum β-lactamase (ESBL)–producing *Enterobacteriaceae* for healthy preschool children in Sweden (p<0.0001). For 6 of the 50 participating preschools, the carriage rate was ≥40%. We analyzed samples from 334 children and found 56 containing ≥1 ESBL producer. The prevalence in the study population increased from 2.6% in 2010 to 16.8% in 2016 (p<0.0001), and for 6 of the 50 participating preschools, the carriage rate was ≥40%. Furthermore, 58% of the ESBL producers were multidrug resistant, and transmission of ESBL-producing and non–ESBL-producing strains was observed at several of the preschools. Toddlers appear to be major carriers of ESBL producers in Sweden.

The rapid dispersion of multidrug-resistant bacteria is considered one of the main threats to global public health (*1*), and it shows no sign of abating. Members of the family *Enterobacteriaceae* harboring extended-spectrum β-lactamases (ESBLs) are playing a major role in this development. These bacteria have spread quickly worldwide as a result of their mobile genetic elements or clonal dissemination (*2*), and the resulting infections have become a clinical challenge. Consequently, illnesses and deaths caused by these bacteria and related healthcare costs have increased (*3,4*).

Transferable enzymes of the ESBL type have been reported since the early 1980s (*5*). These enzymes confer resistance to penicillins, cephalosporins, and monobactams, but not to cephamycins or carbapenems, and are inhibited by β-lactam inhibitors (*6*). Their prevalence is steadily increasing. During the past 2 decades, CTX-M type enzymes have become the most predominant, followed by

the previously dominating SHV and TEM types (*2*). The dissemination of ESBL producers of the CTX-M type is problematic because co-resistance to other major classes of antimicrobial drugs is frequent (*7*). The European Centre for Disease Prevention and Control has declared that the increasing prevalence of ESBLs in invasive isolates in Europe is particularly worrisome (*8*).

Most studies on ESBL producers have focused on hospitalized and adult patients, some have explored the prevalence for healthy persons, and even fewer included children (*8–10*). In 2010, we conducted a study on fecal carriage of ESBL-producing *Enterobacteriaceae* for healthy preschool children in Sweden and reported a prevalence of 2.6% (*11*). Recent studies conducted in other countries have indicated diversified but sometimes high prevalence and spread of ESBL producers, in which daycare centers have been suggested to constitute possible reservoirs (*12,13*).

The primary purpose of this follow-up study was to investigate whether the prevalence of ESBL producers had increased in our community-based pediatric population during the past 6 years. In addition, we explored whether our previous indications of transmission of ESBL producers between children in preschools could be confirmed.

Materials and Methods

Settings and Study Design
During August 2016, we conducted a prospective follow-up study in Uppsala, Sweden. All 71 municipal preschools in the central parts of the city were invited to participate. In 2015, a total of 80% of all children 1–5 years of age in Uppsala County attended preschool. Of these children, 74% were enrolled in municipal preschools (mean 16.7 children in each group). The remaining children attended private preschools or other child care providers or stayed at home (*14*). Most attendees spent 6–8 hour/workday in the preschools.

Authors affiliations: Uppsala University, Uppsala (J. Kaarme, H. Riedel, W. Schaal, T. Nevéus, Å. Melhus); Falu Hospital, Falun, Sweden (H. Yin)

Before the study was conducted, an advisory statement was obtained from the Regional Ethics Committee that established diapers as biologic waste. Therefore, no ethics consent was needed. Information about the study was thereafter sent to the directors of the participating preschools for further distribution to the staff and parents. In preschools in which staff and parents gave their verbal consent, 1 diaper/child was collected the morning after defecation. The time span from defecation to processing of the samples was 16–25 hours. Each diaper was marked with the age of the child to avoid duplicates. Approximately 1 month later, we revisited the preschools and collected environmental samples from water traps of washbasins, toilet flush buttons, and lunch tables.

Statistics on antimicrobial drug consumption in Uppsala County were provided by the Swedish Strategic Programme for the Rational Use of Antimicrobial Agents and Surveillance of Resistance (https://isim.ku.dk/staff/vip/?pure=en%2Fpublications%2Fstrama-the-swedish-strategic-programme-for-the-rational-use-of-antimicrobial-agents-and-surveillance-of-resistance(95ae88b0-93b5-11dd-86a6-000ea68e967b).html). Information for prescriptions of antimicrobial drugs used in Uppsala County and drug requisitions to Uppsala University Hospital in 2015 was also provided by this program.

Bacteria and Media

After collection, diapers were transported to the Department of Clinical Microbiology at Uppsala University Hospital. Stool was streaked onto MacConkey agar plates (Acumedia, Lansing, MI, USA) containing a cefotaxime disc (5 µg; Oxoid Ltd., Basingstoke, UK). Stool was also inoculated into 2 tubes containing Luria–Bertani broth (Becton, Dickinson and Co., Sparks, MD, USA) supplemented with cefpodoxime (5 µg/mL) or ertapenem (1.25 µg/mL) (Oxoid Ltd.). After incubation at 37°C for 24 hours, we semiquantified growth in the inhibition zones on MacConkey agar plates as follows: light, 1–10 CFU; moderate, 11–100 CFU; and heavy, >100 CFU. The broth was plated onto cysteine–lactose electrolyte-deficient agar plates (Becton, Dickinson and Co.) that contained cefotaxime (5 µg) and ceftazidime (10 µg) discs for selection of ESBL producers and imipenem (10 µg) and ceftazidime (10 µg) discs for selection of carbapenemase producers. We identified colonies growing in the inhibition zones after 24 hours of incubation to the species level by using matrix-assisted laser desorption/time-of-flight mass spectrometry.

Environmental samples were collected with cotton swabs and inoculated on site into Luria–Bertani broth. Subsequent handling was identical with that for fecal isolates.

Antimicrobial Drug Susceptibility Testing

We determined antimicrobial drug susceptibility for all isolates that showed growth in the inhibition zones of cefotaxime, ceftazidime, or imipenem by using the disc diffusion method and breakpoints recommended by the European Committee on Antimicrobial Susceptibility Testing (15). We tested mecillinam, amoxicillin/clavulanic acid, piperacillin/tazobactam, cefoxitin, cefotaxime, ceftazidime, cefepime, aztreonam, meropenem, gentamicin, tobramycin, amikacin, nalidixic acid, ciprofloxacin, trimethoprim, cotrimoxazole, nitrofurantoin, and tigecycline. We defined multidrug resistance as resistance to ≥2 antimicrobial drug classes, in addition to resistance to cephalosporins, penicillins, and monobactams.

We performed phenotypic confirmation of ESBL production as described (16). Isolates resistant to cephalosporins but not inhibited by clavulanic acid or cefoxitin were tested by using a multiplex PCR described by Pérez-Pérez and Hanson to detect plasmid-mediated AmpC (17).

Repetitive Element Palindromic PCR

To explore genetic relatedness between *Escherichia coli* isolates from the same preschool, we performed a previously described repetitive element palindromic PCR (rep-PCR) (11) with a slight modification: only primer ERIC2 (5′-AAGTAAGTGACTGGGGTGAGCG-3′) was used. We analyzed 86 isolates from 18 preschools with the largest number of diapers with susceptible *E. coli*. A total of 45 isolates from 13 preschools were ESBL producers; the remaining 41 isolates were fully susceptible to cephalosporins and meropenem. We collected these susceptible isolates from 4 preschools that had no ESBL-positive isolates (n = 6, n = 12, n = 6, and n = 10) and 1 preschool with 1 ESBL-positive isolate (n = 7). These isolates were included as controls to determine whether transmission occurred between children independent of ESBL production.

Whole-Genome Sequencing

To determine ESBL types and genetic relatedness, we subjected 43 ESBL-producing *E. coli* isolates from 25 preschools to whole-genome sequencing. Isolates representative of each DNA pattern determined by the rep-PCR were chosen for each preschool. For confirmation of the performance of the rep-PCR, all ESBL producers from 2 preschools (n = 3 and n = 4) and all ESBL producers from 2 children (n = 2 and n = 2) were also completely sequenced.

We prepared DNA by using the MagAttract DNA mini M48 Kit (QIAGEN, Solna, Sweden) and the BioRobot M48 (GenoVision, West Chester, PA, USA). We sequenced genomes of selected isolates by using IonTorrent (Life Technologies, Carlsbad, CA, USA) and a read length of 400 bp, according to the manufacturer's instructions. We assembled reads into a draft genome using the AssemblerSPAdes Plugin in TorrentSuite Version 4.2 (Thermo Fisher Scientific, Waltham, MA, USA) and the recommended settings

of Life Technologies. We constructed databases for each of the assembled genomes (*18*). Sequence data were edited by using the Emboss suite (*19*) and the *E. coli* Multilocus Sequence Typing website (*20*).

We aligned whole-genome sequences with a common reference sequence (GenBank accession no. NC_010473.1) by using ABACAS (*21*) with gaps omitted. These sequences were separated by strain type according to multilocus sequence typing. Within each strain type, differences between samples were further refined by counting the number of single-nucleotide polymorphisms (SNPs) between each pair. SNP determination was performed by using MUMmer (*22*).

Statistical Analysis

We used the 2-tailed Fisher exact test to compare groups. Differences were considered significant if p≤0.05.

Results

Study Population

A total of 58 (82%) of 71 municipal preschools agreed to participate in the study; the preschools were evenly distributed across the city. Four of the preschools were excluded because of no delivery of diapers on the day of collection, and 4 others were excluded because of a sudden relocation of children after a fire, making it impossible to follow the epidemiology. Thus, of the 71 invited municipal preschools, 50 (70%) delivered samples that were included in the study.

The number of diapers collected from each preschool ranged from 1 to 18 (median 6 diapers/preschool). The collection yielded 334 stool samples and 204 environmental samples. The age range of participating children was 13–45 months (median 25 months) (Figure 1); 8 samples had no information about the age of the child.

Cefotaxime-Resistant Isolates

Of 334 children, we found 67 (20.1%) from 32 preschools who had cefotaxim-resistant *Enterobacteriaceae* isolates in their stool. Of these 67 children, 56 (16.8%) had ≥1 ESBL producer (Figure 2) and 15 (4.5%) had ≥1 AmpC producer. We isolated 62 ESBL-producing and 15 AmpC-producing *Enterobacteriaceae* strains.

The number of carriers of ESBL-producing isolates from a single preschool ranged from 1 to 7, yielding a carriage rate of 0%–80% for the included preschools. For 6 of the preschools, the carriage rate was ≥40%, and in 18 preschools, none of the children were ESBL carriers. The median detection rate for the preschools was 13% positive samples.

Most (n = 47) of the ESBL-positive children had 1 ESBL producer, but 5 children had 2 ESBL-producing strains at the same time, either 2 *E. coli* strains (n = 3) or a combination of *E. coli* and *Klebsiella pneumoniae* (n = 2). For 4 children, both ESBL- and AmpC-type enzymes were detected. One child had 2 ESBL producers (*E. coli* and *K. pneumoniae*) and 1 AmpC producer (CITM-positive *E. coli*).

Eleven children had only an AmpC-producing isolate. Thus, the total number of detected cefotaxime-resistant AmpC-producing *Enterobacteriaceae* isolates was 15 (4.5%). These isolates had the following species distribution: *E. coli* (n = 7), *Enterobacter cloacae* (n = 6), *Citrobacter freundii* (n = 1), and *Citrobacter brakii* (n = 1). For the *E. coli* isolates, plasmid-mediated resistance predominated; 4 isolates were DHAM positive and 1 isolate was CITM positive.

Thirty (69.8%) of the 43 fully sequenced ESBL-producing *E. coli* isolates harbored CTX-M-15, five had CTX-M-14 or CTX-M-14–like β-lactamases, four had CTX-M-55, three had CTX-M-57, and one had CTX-M-27. Eleven of the isolates harbored concomitant TEM enzymes: four had TEM-2, two had TEM-55, two had TEM-56, two had TEM-109, and one had TEM-4.
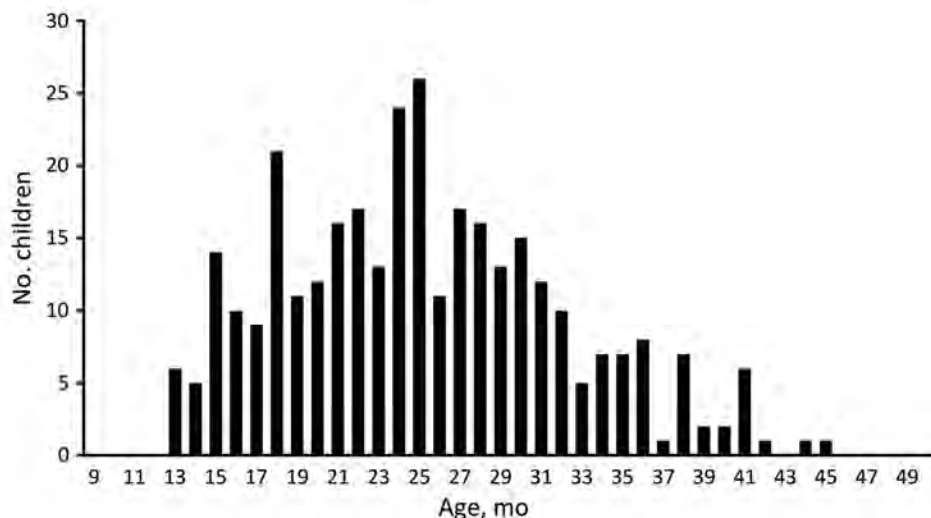
Figure 1. Age distribution of healthy preschool children in study of rapid increase in carriage rates of *Enterobacteriaceae* producing extended-spectrum β-lactamases, Sweden.

Figure 2. Age distribution of extended-spectrum β-lactamase carriers in study of rapid increase in carriage rates of *Enterobacteriaceae* producing extended-spectrum β-lactamases, Sweden.

The 3 most common multilocus sequence types (STs) for the ESBL producers for which whole-genome sequencing was performed were ST131 (n = 11, 25.6%), followed by ST10 and ST354 (both n = 5, 11.6%). ST131 was present in 9 preschools, ST10 in 4, and ST354 in 3. Other STs represented were ST38 or the clonal complex containing ST58, ST127, ST155, ST328, ST349, ST362, ST450, ST602, ST998, ST1423, ST1634, ST2064, ST3877, and ST6448.

The 204 environmental samples yielded only 1 AmpC-producing *E. coli* isolate from a washbasin in 1 of the diaper-changing rooms of 1 preschool. This preschool had 3 fecal samples with ESBL/AmpC production, which was unrelated to the AmpC-producing *E. coli*.

Transmission of *E. coli* Isolates
We detected identical strains in both preschools with and without ESBL producers. If there were 2–3 ESBL-positive children in a preschool, they, as a rule, had the same strain.

With increasing numbers of ESBL-positive children in a school, the likelihood increased for >1 strain being involved. In the preschool that had the highest total number of ESBL-positive children (n = 7), 4 ESBL strains were identified, of which 3 were *E. coli*. All *E. coli* strains had been transmitted to 1 or 2 additional children, but the ESBL-positive *K. pneumoniae* strain was detected in only 1 child. We found no correlation between the quantity of growth in the inhibition zone of cefotaxime and the tendency to spread.

The 3 most common STs were further analyzed to rule out transmission between preschools. ST10 isolates were unambiguously different (SNPs 1,200–15,000). ST38 isolates were generally more closely related than were ST10 isolates but were insufficient to support direct transmission. The closest pair of STs showed a difference of ≈300 SNPs. The most frequent ST group, ST131, held several moderately to closely related isolates. Three isolates formed the closest group (SNPs <45). Another group of 3 isolates was moderately related to the other 3 samples and to each other (SNPs ≈100–350). The remaining isolates formed a separate group with SNPs >400.

In preschools that had susceptible *E. coli* strains, ≤2 children had the same strain, and ≤3 strains were present in the same children. Only 1 preschool showed no spread of *E. coli* strains between the children. In this preschool, there were no children who had ESBL producers.

Antimicrobial Drug Resistance
Thirty-six (58%) of the 62 ESBL-producing isolates and 3 (20%) of the 15 AmpC-producing isolates were multidrug resistant. For ESBL producers, the most frequent drug resistance was resistance to trimethoprim (71.7%) or cotrimoxazole (65.0%), followed by the quinolones (nalidixic acid 68.3% and ciprofloxacin 35%) (Figure 3). For AmpC-positive
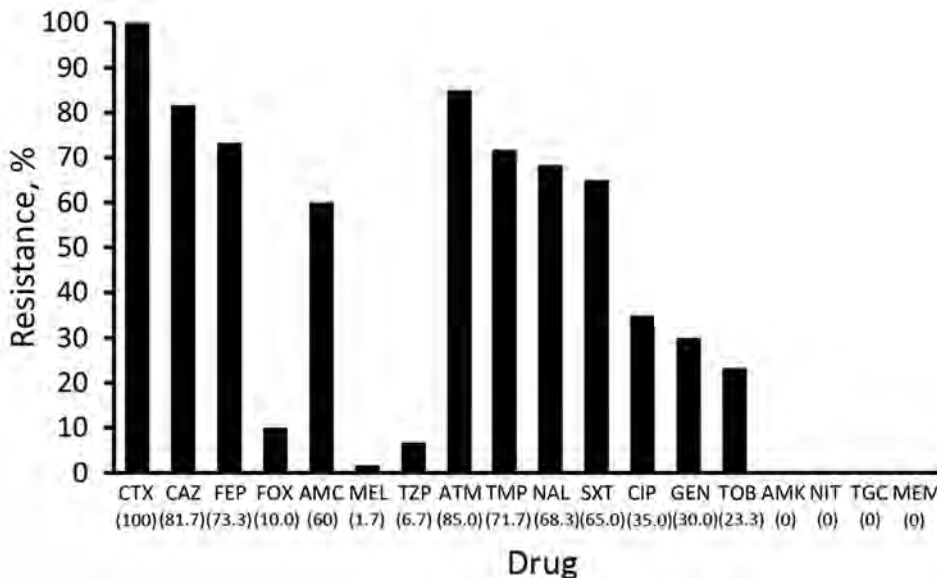
Figure 3. Antimicrobial drug resistance for extended-spectrum β-lactamase–producing *Enterobacteriaceae* isolates from 62 healthy preschool children, Sweden. Values in parentheses along the x-axis are percentages. AMC, amoxicillin/clavulanic acid; AMK, amikacin; ATM, aztreonam; CAZ, ceftazidime; CIP, ciprofloxacin, CTX, cefotaxime; FEP, cefepime; FOX, cefoxitin; GEN, gentamicin; MEL, mecillinam; MEM, meropenem; NAL, nalidixic acid; NIT, nitrofurantoin; SXT, sulfamethoxazole/trimethoprim; TGC, tigecycline; TOB, tobramycin; TZP, piperacillin/tazobactam; TMP, trimethoprim.
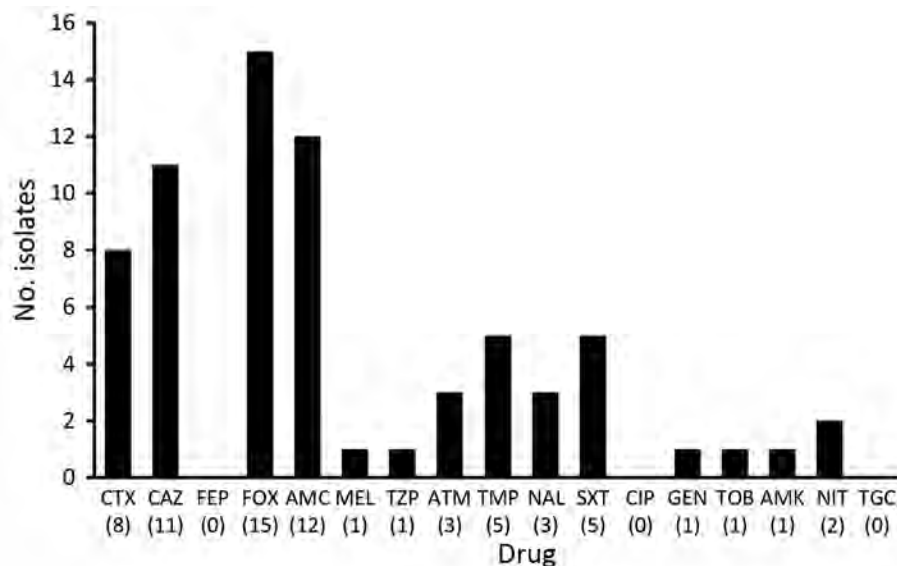
Figure 4. Antimicrobial drug resistance for AmpC-producing *Enterobacteriaceae* isolates from 15 healthy preschool children, Sweden. Values in parentheses along the x-axis are percentages. AMC, amoxicillin/clavulanic acid; AMK, amikacin; ATM, aztreonam; CAZ, ceftazidime; CIP, ciprofloxacin, CTX, cefotaxime; FEP, cefepime; FOX, cefoxitin; GEN, gentamicin, MEL, mecillinam; NAL, nalidixic acid; NIT, nitrofurantoin; SXT, sulfamethoxazole/trimethoprim; TGC, tigecycline; TOB, tobramycin; TZP, piperacillin/tazobactam; TMP, trimethoprim.

isolates, the pattern was similar but the overall resistance rates were lower, with the exception of nitrofurantoin (Figure 4).

Consumption of Antimicrobial Drugs

Uppsala County had the second highest number of prescriptions and sales on hospital requisitions in Sweden in 2015: a total of 13.9 defined daily doses/1,000 person-days. Of these doses, 4.87 defined daily doses/1,000 person-days were prescribed to children <1–17 years of age and 5.58 defined daily doses/1,000 person-days to children 1–5 years of age. Most (93.5%) of the antimicrobial drugs were prescribed for outpatients. The most commonly used drug by children was penicillin V, followed by amoxicillin with or without clavulanic acid and flucloxacillin (Table).

Discussion

We investigated the carriage rate of ESBL producers in healthy preschool children and whether preschools might serve as a reservoir for ESBL producers in Sweden. We analyzed 334 stool samples, and results showed that the prevalence of ESBL-producing *Enterobacteriaceae* was 16.8% in the study population, which was a >6-fold increase compared with findings of the study we conducted in 2010 in the same setting and with identical handling of samples (*11*). Such a rapid increase of ESBL producers in a country with a low level of endemicity, and within a relatively infection-prone group with few treatment options, is worrisome, especially because 58% of the isolates were multidrug resistant. A similar increase, but on a lower level (from 4.8% to 10.2%), has been reported for healthy children in France during 2010–2015 (*23*).

Studies on fecal carriage of cefotaxime-resistant *Enterobacteriaceae* for healthy adults have shown widely divergent results, from a few percent up to >90% carriage, and with a pronounced geographic variation (*24*). A recent study in Sweden on elderly persons living in their own homes showed an ESBL prevalence of 8.7% (*25*), which was almost half the prevalence we found in our study.

There are few comparable studies on carriage rates of ESBL producers for healthy children. Pallecchi et al. reported an increase from 0.1% to 1.7% for children in Bolivia and Peru during 2002–2005 (*26*), and a study in Portugal reported a prevalence of 2.7% for healthy children during 2007 (*27*). Subsequent studies from the Netherlands, France, Spain, Laos, Lebanon, and Germany have reported carriage rates of 4.6%–49.6%; the highest prevalences were 24.8% for preschool children in Laos and 49.6% for healthy infants in Lebanon (*12,23,28–32*).

The prevalence of ESBL producers varied between preschools in this study (0%–80%, median 13% positive samples). Preschools with high prevalences were found in all parts of Uppsala, Sweden, as was transmission of ESBL producers in children. However, transmission was not exclusive for ESBL producers. Cephalosporin-susceptible *E. coli* strains were transmitted in all but 1 of the investigated preschools, which indicated that prerequisites for spread of ESBL producers were present.

Attendance at preschools and daycare centers has been shown to increase the risk for transmission of microbes and gastrointestinal infections (*33,34*). Furthermore, a recent study in the Netherlands reported an increased risk for colonization with ESBL producers in household members if the children attend daycare centers (*35*). However, Birgy et al. reported an inverse relationship (*23*). All participating preschools had uniformly high standards of hygiene, although we did not study compliance with hygiene guidelines. Close contacts, crowding, difficulty in complying with basic hygiene routines, and a high likelihood for exposure to antimicrobial drugs, especially third-generation

Table. Antimicrobial drug use for children <1–17 years of age, Uppsala County, Sweden, 2015*

Drug	DDD/1,000 person-days
Phenoxymethylpenicillin	2.44
Amoxicillin	0.59
Flucloxacillin	0.56
Amoxicillin/clavulanic acid	0.20
Trimethoprim/sulfamethoxazole	0.18
Cefadroxil	0.16
Erythromycin	0.13
Pivmecillinam	0.08
Clindamycin	0.06
Ceftibuten	0.06
Nitrofurantoin	0.05
Azithromycin	0.05
Ciprofloxacin	0.05
Cloxacillin	0.03
Meropenem	0.02
Cefotaxime	0.02
Metronidazole	0.02
Benzylpenicillin	0.01
Vancomycin	0.01
Piperacillin/tazobactam	0.01

*The following drugs had DDD values <0.01/1,000 person-days: coxycycline, ampicillin, cefuroxime, ceftazidime, ceftriaxone, ertapenem, imipenem, ceftaroline fosamil, tobramycin, gentamicin, moxifloxacin, colistin, daptomycin, rifampin, retapamulin, and fusidic acid. DDD, defined daily dose.

cephalosporins, for young children (for whom prescriptions in Uppsala are comparably high in Sweden, but still low in comparison with international standards) make it plausible that preschools could act as reservoirs or even hotspots for ESBL producers. To our knowledge, only 3 studies have addressed this hypothesis, but results were somewhat contradictory (*11,23,30*). No larger changes in antimicrobial drug use were detected in the population included in this study during 2010–2016. In addition, we believe that it is less likely that selective pressure is the explanation for the higher prevalence.

With the exception of 1 AmpC-producing *E. coli* that had no close genetic relatedness with isolates from the children, no other cephalosporin-resistant isolate was identified in the environment. Therefore, it is more likely that the transmission route was person-to-person, rather than spread from environmental sources. Nevertheless, none of the strains was ESBL producing or transmitted among >3 children in a preschool. The most common ESBL-producing *E. coli* strain in the study was ST131 (*36*). Like all more frequent STs that were present in >1 preschool, the most SNPs were in the hundreds or thousands. Therefore, a common source of these strains does not appear likely, except for the 3 ST131 isolates.

Studies have confirmed a relationship between ESBL carriage and foreign travel (especially to Southeast Asia), geographic location, recent use of antimicrobial drugs, close contact with ESBL carriers, hospital care, or residency in nursing homes (*2,25*). Once colonized, presence of ESBL producers can have a long duration. Barreto Miranda et al. reported that 25% of travelers from Germany still carried ESBL producers after 6 months (*37*). In addition, carriage for as long as 5 years appears to be possible (*38*). However, it is not yet known how long carriage can persist in children or if it differs from carriage in adults.

The fact that our samples were collected anonymously is a major limitation because we could not evaluate risk factors such as antimicrobial drugs, hospital care, international travel, siblings, and family conditions. However, because our objectives were to explore the overall prevalence and possible transmission between attendees, underlying causes for the increase were beyond the scope of the study, but investigating these causes would be of interest in a future study. The fact that fecal and environmental samples were collected 1 month after collection of diapers is also a limitation. However, detection of ESBL-positive children, no change in routines, and a low isolation frequency for multidrug resistance makes environmental spread less likely.

In conclusion, the prevalence of ESBL-producing *Enterobacteriaceae* was explored for preschool children in Sweden. Results showed that 16.8% of the children carried ESBL producers, which was the highest prevalence ever recorded in Sweden. Toddlers appear to be major carriers for ESBL producers, and preschools might act as hotspots for these bacteria.

About the Author

Dr. Kaarme is a pediatrician at Uppsala University Children's Hospital, Uppsala, Sweden. His research interests are antimicrobial drug resistance and microbiota.

References

1. World Health Organization. Factsheet, October 2015 [cited 2016 Aug 27]. http://www.who.int/mediacentre/factsheets/antibiotic-resistance/en/
2. Woerther PL, Burdet C, Chachaty E, Andremont A. Trends in human fecal carriage of extended-spectrum β-lactamases in the community: toward the globalization of CTX-M. Clin Microbiol Rev. 2013;26:744–58. http://dx.doi.org/10.1128/CMR.00023-13

3. Pitout JD. Infections with extended-spectrum β-lactamase-producing *Enterobacteriaceae*: changing epidemiology and drug treatment choices. Drugs. 2010;70:313–33. http://dx.doi.org/10.2165/11533040-000000000-00000

4. Slama TG. Gram-negative antibiotic resistance: there is a price to pay. Crit Care. 2008;12(Suppl 4):S4. http://dx.doi.org/10.1186/cc6820

5. Livermore DM. Defining an extended-spectrum β-lactamase. Clin Microbiol Infect. 2008;14(Suppl 1):3–10. http://dx.doi.org/10.1111/j.1469-0691.2007.01857.x

6. Bush K, Jacoby GA. Updated functional classification of β-lactamases. Antimicrob Agents Chemother. 2010;54:969–76. http://dx.doi.org/10.1128/AAC.01009-09

7. Logan LK, Braykov NP, Weinstein RA, Laxminarayan R; CDC Epicenters Prevention Program. Extended-spectrum β-lactamase–producing and third-generation cephalosporin-resistant *Enterobacteriaceae* in children: trends in the United States, 1999–2011. J Pediatric Infect Dis Soc. 2014;3:320–8. http://dx.doi.org/10.1093/jpids/piu010

8. European Centre for Disease Prevention and Control. Report, 2014 [cited 2016 Aug 27]. http://ecdc.europa.eu/en/publications/publications/antimicrobial-resistance-europe-2014.pdf

9. Lübbert C, Straube L, Stein C, Makarewicz O, Schubert S, Mössner J, et al. Colonization with extended-spectrum β-lactamase-producing and carbapenemase-producing *Enterobacteriaceae* in international travelers returning to Germany. Int J Med Microbiol. 2015;305:148–56. http://dx.doi.org/10.1016/j.ijmm.2014.12.001

10. Kantele A, Lääveri T, Mero S, Vilkman K, Pakkanen SH, Ollgren J, et al. Antimicrobials increase travelers' risk of colonization by extended-spectrum β-lactamase–producing *Enterobacteriaceae*. Clin Infect Dis. 2015;60:837–46. http://dx.doi.org/10.1093/cid/ciu957

11. Kaarme J, Molin Y, Olsen B, Melhus A. Prevalence of extended-spectrum β-lactamase–producing *Enterobacteriaceae* in healthy Swedish preschool children. Acta Paediatr. 2013;102:655–60. http://dx.doi.org/10.1111/apa.12206

12. Koningstein M, Leenen MA, Mughini-Gras L, Scholts RM, van Huisstede-Vlaanderen KW, Enserink R, et al. Prevalence and risk factors for colonization with extended-spectrum cephalosporin-resistant *Escherichia coli* in children attending daycare centers: a cohort study in the Netherlands. J Pediatric Infect Dis Soc. 2015;4:e93–9.

13. Murray TS, Peaper DR. The contribution of extended-spectrum β-lactamases to multidrug-resistant infections in children. Curr Opin Pediatr. 2015;27:124–31. http://dx.doi.org/10.1097/MOP.0000000000000182

14. The Swedish National Agency for Education. (Skolverket). Statistics, 2015 [cited 2016 Aug 27]. http://www.jmftal.artisan.se/databas.aspx#tab-1

15. The European Committee on Antimicrobial Susceptibility Testing. Breakpoint tables for interpretation of MICs and zone diameters. Version 6.0, 2016 [cited 2016 Oct 12]. http://www.eucast.org

16. Carter MW, Oakton KJ, Warner M, Livermore DM. Detection of extended-spectrum β-lactamases in klebsiellae with the Oxoid combination disk method. J Clin Microbiol. 2000;38:4228–32.

17. Pérez-Pérez FJ, Hanson ND. Detection of plasmid-mediated AmpC β-lactamase genes in clinical isolates by using multiplex PCR. J Clin Microbiol. 2002;40:2153–62. http://dx.doi.org/10.1128/JCM.40.6.2153-2162.2002

18. Altschul SF, Gish W, Miller W, Myers EW, Lipman DJ. Basic local alignment search tool. J Mol Biol. 1990;215:403–10. http://dx.doi.org/10.1016/S0022-2836(05)80360-2

19. The European Molecular Biology Open Software Suite (EMBOSS) [cited 2016 Nov 7]. http://emboss.sourceforge.net

20. University of Warwick. MLST databases [cited 2016 Nov 7]. http://mlst.warwick.ac.uk/mlst/dbs/Ecoli

21. Assefa S, Keane TM, Otto TD, Newbold C, Berriman M. ABACAS: algorithm-based automatic contiguation of assembled sequences. Bioinformatics. 2009;25:1968–9. http://dx.doi.org/10.1093/bioinformatics/btp347

22. Kurtz S, Phillippy A, Delcher AL, Smoot M, Shumway M, Antonescu C, et al. Versatile and open software for comparing large genomes. Genome Biol. 2004;5:R12. http://dx.doi.org/10.1186/gb-2004-5-2-r12

23. Birgy A, Levy C, Bidet P, Thollot F, Derkx V, Béchet S, et al. ESBL-producing *Escherichia coli* ST131 versus non-ST131: evolution and risk factors of carriage among French children in the community between 2010 and 2015. J Antimicrob Chemother. 2016;71:2949–56. http://dx.doi.org/10.1093/jac/dkw219

24. Ruppé E, Armand-Lefèvre L, Estellat C, Consigny PH, El Mniai A, Boussadia Y, et al. High rate of acquisition but short duration of carriage of multidrug-resistant *Enterobacteriaceae* after travel to the tropics. Clin Infect Dis. 2015;61:593–600. http://dx.doi.org/10.1093/cid/civ333

25. Blom A, Ahl J, Månsson F, Resman F, Tham J. The prevalence of ESBL-producing *Enterobacteriaceae* in a nursing home setting compared with elderly living at home: a cross-sectional comparison. BMC Infect Dis. 2016;16:111. http://dx.doi.org/10.1186/s12879-016-1430-5

26. Pallecchi L, Bartoloni A, Fiorelli C, Mantella A, Di Maggio T, Gamboa H, et al. Rapid dissemination and diversity of CTX-M extended-spectrum β-lactamase genes in commensal *Escherichia coli* isolates from healthy children from low-resource settings in Latin America. Antimicrob Agents Chemother. 2007;51:2720–5. http://dx.doi.org/10.1128/AAC.00026-07

27. Guimarães B, Barreto A, Radhouani H, Figueiredo N, Gaspar E, Rodrigues J, et al. Genetic detection of extended-spectrum β-lactamase-containing *Escherichia coli* isolates and vancomycin-resistant enterococci in fecal samples of healthy children. Microb Drug Resist. 2009;15:211–6. http://dx.doi.org/10.1089/mdr.2009.0910

28. Fernández-Reyes M, Vicente D, Gomariz M, Esnal O, Landa J, Oñate E, et al. High rate of fecal carriage of extended-spectrum-β-lactamase-producing *Escherichia coli* in healthy children in Gipuzkoa, northern Spain. Antimicrob Agents Chemother. 2014;58:1822–4. http://dx.doi.org/10.1128/AAC.01503-13

29. Hijazi SM, Fawzi MA, Ali FM, Abd El Galil KH. Prevalence and characterization of extended-spectrum β-lactamases producing *Enterobacteriaceae* in healthy children and associated risk factors. Ann Clin Microbiol Antimicrob. 2016;15:3. http://dx.doi.org/10.1186/s12941-016-0121-9

30. Stoesser N, Xayaheuang S, Vongsouvath M, Phommasone K, Elliott I, Del Ojo Elias C, et al. Colonization with *Enterobacteriaceae* producing ESBLs in children attending pre-school childcare facilities in the Lao People's Democratic Republic. J Antimicrob Chemother. 2015;70:1893–7.

31. Harries M, Dreesman J, Rettenbacher-Riefler S, Mertens E. Faecal carriage of extended-spectrum β-lactamase-producing *Enterobacteriaceae* and Shiga toxin-producing *Escherichia coli* in asymptomatic nursery children in Lower Saxony (Germany), 2014. Epidemiol Infect. 2016;Sep 9:1–9.

32. Hijazi SM, Fawzi MA, Ali FM, Abd El Galil KH. Multidrug-resistant ESBL-producing *Enterobacteriaceae* and associated risk factors in community infants in Lebanon. J Infect Dev Ctries. 2016;10:947–55. http://dx.doi.org/10.3855/jidc.7593

33. Heusinkveld M, Mughini-Gras L, Pijnacker R, Vennema H, Scholts R, van Huissede-Vlaanderen KW, et al. Potential causative agents of acute gastroenteritis in households with preschool children: prevalence, risk factors, clinical relevance and household transmission. Eur J Clin Microbiol Infect Dis. 2016;35:1691–700. http://dx.doi.org/10.1007/s10096-016-2714-9

34. Pijnacker R, Mughini-Gras L, Vennema H, Enserink R, Van den Wijngaard CC, Kortbeek T, et al. Characteristics of child daycare centres associated with clustering of major enteropathogens. Epidemiol Infect. 2016;144:2527–39. http://dx.doi.org/10.1017/S0950268816001011

35. Van den Bunt G, Liakopoulos A, Mevius DJ, et al. ESBL/AmpC-producing *Enterobacteriaceae* in households with children of preschool age: prevalence, risk factors and co-carriage. J Antimicrob Chemother. 2016; epub ahead of print.

36. Pitout JD, DeVinney R. *Escherichia coli* ST131: a multidrug-resistant clone primed for global domination. F1000 Res. 2017;6:6. http://dx.doi.org/10.12688/f1000research.10609.1

37. Barreto Miranda I, Ignatius R, Pfüller R, Friedrich-Jänicke B, Steiner F, Paland M, et al. High carriage rate of ESBL-producing *Enterobacteriaceae* at presentation and follow-up among travellers with gastrointestinal complaints returning from India and Southeast Asia. J Travel Med. 2016;23:tav024. http://dx.doi.org/10.1093/jtm/tav024

38. Brolund A. Overview of ESBL-producing *Enterobacteriaceae* from a Nordic perspective. Infect Ecol Epidemiol. 2014;4:4. http://dx.doi.org/10.3402/iee.v4.24555

Address for correspondence: Johan Kaarme, Uppsala University Children's Hospital, SE-751 85 Uppsala, Sweden; email: jkaarme@hotmail.com

September 2016: **Antimicrobial Resistance**

- Co-Infections in Visceral Pentastomiasis, Democratic Republic of the Congo

- Multistate US Outbreak of Rapidly Growing Mycobacterial Infections Associated with Medical Tourism to the Dominican Republic, 2013–2014

- Virulence and Evolution of West Nile Virus, Australia, 1960–2012

- Phylogeographic Evidence for 2 Genetically Distinct Zoonotic *Plasmodium knowlesi* Parasites, Malaysia
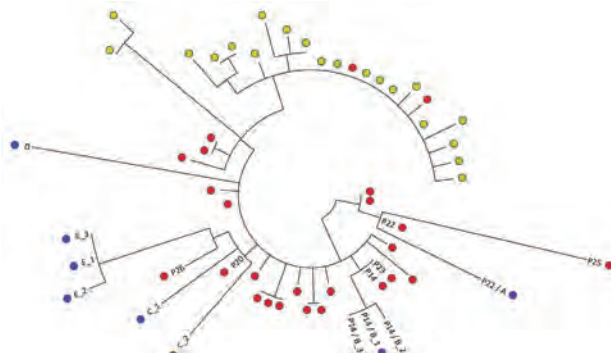
- Hemolysis after Oral Artemisinin Combination Therapy for Uncomplicated *Plasmodium falciparum* Malaria

- Enterovirus D68 Infection in Children with Acute Flaccid Myelitis, Colorado, USA, 2014

- Middle East Respiratory Syndrome Coronavirus Transmission in Extended Family, Saudi Arabia, 2014

- Exposure-Specific and Age-Specific Attack Rates for Ebola Virus Disease in Ebola-Affected Households, Sierra Leone

- Outbreak of *Achromobacter xylosoxidans* and *Ochrobactrum anthropi* Infections after Prostate Biopsies, France, 2014

- Human Babesiosis, Bolivia, 2013

- Assessment of Community Event–Based Surveillance for Ebola Virus Disease, Sierra Leone, 2015

- Probable Rabies Virus Transmission through Organ Transplantation, China, 2015

- Cutaneous Melioidosis Cluster Caused by Contaminated Wound Irrigation Fluid

- Possible Role of Fish and Frogs as Paratenic Hosts of *Dracunculus medinensis*, Chad

- Time Lags between Exanthematous Illness Attributed to Zika Virus, Guillain-Barré Syndrome, and Microcephaly, Salvador, Brazil

- Use of Unamplified RNA/cDNA–Hybrid Nanopore Sequencing for Rapid Detection and Characterization of RNA Viruses
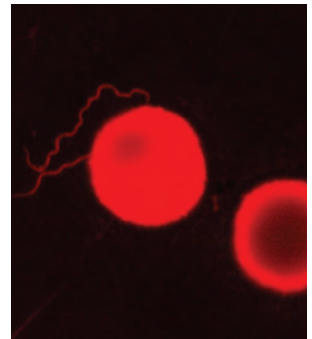
- Importation of Hybrid Human-Associated *Trypanosoma cruzi* Strains of Southern South American Origin, Colombia

- Lyssavirus in Indian Flying Foxes, Sri Lanka

- Survival and Growth of *Orientia tsutsugamushi* in Conventional Hemocultures

EMERGING INFECTIOUS DISEASES

https://wwwnc.cdc.gov/eid/articles/issue/22/9/table-of-contents

Influenza Transmission
Dynamics in Urban Households, Managua, Nicaragua, 2012–2014

Aubree Gordon, Tim K. Tsang, Benjamin J. Cowling, Guillermina Kuan, Sergio Ojeda,
Nery Sanchez, Lionel Gresh, Roger Lopez, Angel Balmaseda, Eva Harris

Author affiliations: University of Michigan, Ann Arbor, Michigan, USA (A. Gordon); The University of Hong Kong, Hong Kong, China (T.K. Tsang, B.J. Cowling); Ministry of Health, Managua, Nicaragua (G. Kuan, R. Lopez, A. Balmaseda); Sustainable Sciences Institute, Managua (S. Ojeda, N. Sanchez, L. Gresh); University of California, Berkeley, California, USA (E. Harris)

During August 2012–November 2014, we conducted a case ascertainment study to investigate household transmission of influenza virus in Managua, Nicaragua. We collected up to 5 respiratory swab samples from each of 536 household contacts of 133 influenza virus–infected persons and assessed for evidence of influenza virus transmission. The overall risk for influenza virus infection of household contacts was 15.7% (95% CI 12.7%–19.0%).

Oseltamivir treatment of index patients did not appear to reduce household transmission. The mean serial interval for within-household transmission was 3.1 (95% CI 1.6–8.4) days. We found the transmissibility of influenza B virus to be higher than that of influenza A virus among children. Compared with households with <4 household contacts, those with ≥4 household contacts appeared to have a reduced risk for infection. Further research is needed to model household influenza virus transmission and design interventions for these settings.

Influenza virus is a respiratory pathogen of major medical and public health concern, causing an estimated 3–5 million cases of severe illness and 250,000–500,000 deaths annually worldwide (1). Households provide a convenient and valuable setting for studying the transmission of influenza virus (2–5). Several studies in high-income country settings suggest that the rate of influenza virus transmission in the household is several-fold higher than that in the community (3,4). In a study conducted in Vietnam, 26% of influenza virus infections were acquired in the household (6). The influence of household transmission on influenza epidemics has led to an increased interest in household-based interventions (7–11). However, in low-income and low-middle–income countries, where nearly half the world's population lives, household influenza transmission has not been well studied. Moreover, estimates of the serial interval (i.e., time between index case and symptom onset in secondary infection) are limited to pandemic influenza in nonhousehold settings (6,12–15). Therefore, a more thorough investigation of household transmission is essential for the development of effective household-based interventions for the control of pandemic and interpandemic influenza in these settings.

Demographic factors that have been found to influence influenza transmission include the size of the household, age of the index patient, and age of contacts (4,6,16–19). Both household size and population demographics differ dramatically between industrialized and developing country settings. In Nicaragua, persons from several generations often live in the same household, leading to large household sizes by high-income country standards. In addition, in 2014, ≈32% of the population of Nicaragua was <15 years of age, whereas in other countries where influenza household transmission studies have been conducted, 12% 23% of the population was estimated to be in this age range (5,6,20–22).

To investigate influenza transmission in households, we performed a case ascertainment study of influenza in urban households in Managua, Nicaragua. We used an individual-based hazard model to characterize transmission dynamics within households and estimate factors affecting influenza transmission.

Materials and Methods

Study Subjects

Index influenza cases were identified at the Health Center Sócrates Flores Vivas, a primary care facility in Managua, Nicaragua, run by the Ministry of Health of Nicaragua. Index patients were eligible for enrollment if a) they had influenza-like illness, defined as fever or feverishness with cough, sore throat, or runny nose; 2) their symptom onset, defined as the earliest day with influenza-like illness, was within the previous 48 hours; 3) they were positive for influenza by rapid antigen test or reverse transcription PCR (RT-PCR); 4) no household members had had symptoms of influenza-like illness in the previous 2 weeks; and 5) they lived with ≥1 additional person. After index case enrollment, we conducted a household visit to enroll patient household contacts, collect initial respiratory and blood samples, and administer questionnaires to the household and individual household members. We defined a household as a group of persons living together who shared a kitchen and ≥1 meal a day. We visited households 4 additional times (every 2–3 days) to collect respiratory samples and daily symptom information, and we collected the final blood sample 30–45 days after index case enrollment.

This study was approved by the institutional review boards at the Ministry of Health of Nicaragua, the University of Michigan (Ann Arbor, Michigan, USA), and the University of California, Berkeley (Berkeley, California, USA). Consent to participate was obtained from all adult participants, and parental permission was obtained for all children. Assent was obtained for children ≥6 years of age.

Laboratory Methods

We stored nasal and throat swab samples at 4°C–8°C and transported them to the National Virology Laboratory (Managua, Nicaragua) within 12 hours. We tested all samples for influenza on an ABI 7500 Fast PCR platform (Applied Biosystems, Foster City, CA, USA) following validated protocols from the US Centers for Disease Control and Prevention (Atlanta, GA, USA).

Statistical Analysis

We characterized influenza transmission dynamics within households and the effects of factors affecting transmission using an individual-based hazard model (5,17). In the model, the risk for RT-PCR–confirmed infection among household contacts depended on the time from symptom onset of other infected persons in the household. The hazard (λ) of infection of person j at time t from an infected household member i, with symptom onset t_i is $\lambda_{i\circledast j}(t) = \lambda_n \times S_j$, where λ_n is the baseline hazard of household transmission and S_j is the factors affecting transmissibility.

The distribution of the serial interval was a discretized Weibull distribution (*23*), with probability mass function

$$f_i(t) = \exp\left(-\left(\frac{t}{\gamma}\right)^\alpha\right) - \exp\left(-\left(\frac{t+1}{\gamma}\right)^\alpha\right), t > t_i,$$

where t is the number of days after symptom onset of the index patient, α is the shape, and γ is the scale parameter for the distribution. The model used to estimate the distribution included infection of household contacts by persons inside the household (index cases [i.e., secondary infections] and other infected household members [i.e., tertiary infections]) and outside the household (i.e., community infections). The hazard of infection from the community was assumed to be constant over the duration of the follow-up: $\lambda_{j,c}(t) = \psi$, where ψ is the baseline community risk (*5*). Therefore, the hazard of infection for a person j at day t is $\lambda_j(t) = \lambda_{j,c}(t) + \mathring{a}_i \lambda_{i \circledast j}(t)$, and the summation involves the infected household contacts of person j only.

In the transmission model, age group ($\leq$18 years vs. >18 years) and vaccination status of the household contacts were factors that might affect the susceptibility of household contacts to infection (*5,17*). In addition, we accounted for the possible differences in transmission related to the different influenza virus types [influenza A(H1N1), influenza A(H3N2), and influenza B]; treatment (with vs. without oseltamivir) of index case; index patient age group (children $\leq$5 years of age vs. older children and adults); and household sizes, hereafter denoted as the preliminary analysis. In addition to these factors, we further explored the differences in the relative susceptibilities of children and adults to influenza types A and B, which was represented by an interaction of age and influenza types in the model. We considered this analysis the main analysis (online Technical Appendix, https://wwwnc.cdc.gov/EID/article/24/10/16-1258-Techapp1.pdf).

We fitted this model into a Bayesian framework, constructed a Markov chain Monte Carlo algorithm, and estimated parameters (*24*). We used conditional likelihood in the statistical model to account for the study design feature that no household contacts had symptom onset at or before the day of index case enrollment (online Technical Appendix). To evaluate model adequacy, we conducted a simulation study with the model to compare the estimated and observed risks of groups with different characteristics (online Technical Appendix). We performed statistical analyses with R version 3.1.1 (https://cran.r-project.org/) and MATLAB version 7.8.0 (https://www.mathworks.com/products/matlab.html).

Results

During August 2012–November 2014, a total of 168 potential index patients consented to participate in the study. We excluded 6 households with multiple index cases, 5 households with influenza virus infections of mixed subtypes, and 24 households with index cases that were initially positive for influenza by rapid antigen test but not confirmed positive by RT-PCR. In total, 133 households with index cases of influenza virus infection confirmed by RT-PCR were included in our analysis (Figure 1). At the initial visit, 541 household contacts were present, and 536 (99%) were enrolled. A total of 2,285 respiratory samples were collected from household contacts (mean 4.3 respiratory samples/contact). Of the 356 household contacts, 84 (15.7%, 95% CI 12.7%–19.0%) had RT-PCR–confirmed influenza virus infections (Table 1). Of these, 21 (25%) did not exhibit symptoms. Influenza transmission was observed in 52 (39%) households. Of the households with influenza transmission, 34 had 1 contact with an RT-PCR–confirmed influenza virus infection, 10 had 2 contacts, and 8 had $\geq$3 contacts. Most index cases (76%) were managed with oseltamivir. The average age of index patients was 6.6 (range 0–45) years, and the average age of household contacts was 24.2 (range 0–87) years. Mean household size was 5.0 (range 2–17) members. Among household contacts, the overall observed risk for influenza A(H1N1) virus infection was 13.4% (9/67, 95% CI 6.3%–24.0%), influenza A(H3N2) virus 14.3% (46/322, 95% CI 10.7%–18.6%), and influenza B virus 19.7% (29/147, 95% CI 13.6%–27.1%).

In the preliminary analysis, we adjusted for age group of household contacts, vaccination history, index patient age group, index case treatment status, and household contact number but did not include the interaction of age group of household contacts and influenza type and subtype. In this analysis, we found that household contacts of index patients with RT-PCR–confirmed influenza B virus infections were more likely to get infected than those of index patients with influenza A(H3N2) virus infections (relative infectivity 1.71, 95% CI 1.08–2.80) or influenza A(H1N1) virus infections (relative infectivity 1.56, 95% CI 0.75–3.43).

In the main model, we included the interaction of age group of household contacts and influenza type, which
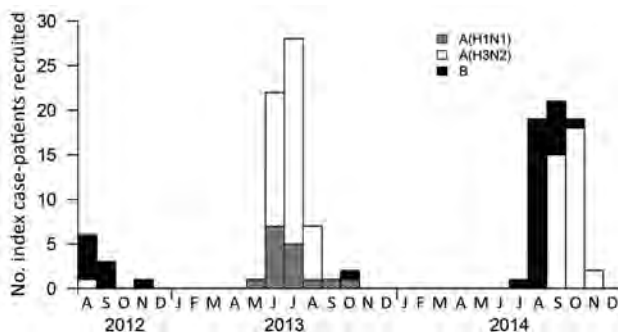
Figure 1. Timeline of enrollment of index cases of PCR-confirmed monoinfections of seasonal influenza A(H1N1) virus, influenza A(H3N2) virus, or influenza B virus, Managua, Nicaragua, August 2012–November 2014. Only the index cases included in the final analysis are shown.

Table 1. Characteristics of influenza virus–infected index cases-patients and household contacts, Managua, Nicaragua, August 2012–November 2014*

Characteristic	Influenza type, no./total (%)			Total, no. (%)
	A(H1N1)	A(H3N2)	B	
Index patients	16	80	37	133
Age, y				
≤5	10 (63)	52 (65)	15 (41)	77 (58)
6–18	5 (31)	23 (29)	21 (57)	49 (37)
>18	1 (6)	5 (6)	1 (3)	7 (5)
Sex				
F	6 (38)	36 (45)	17 (46)	59 (44)
M	10 (63)	44 (55)	20 (54)	74 (56)
Prior vaccination				
Yes	1 (6)	2 (3)	3 (8)	6 (5)
No	15 (94)	78 (98)	34 (92)	127 (95)
Oseltamivir treatment				
Yes	16 (100)	53 (66)	32 (86)	101 (76)
No	0	27 (34)	5 (14)	32 (24)
No. household contacts				
1–3	6 (38)	44 (55)	23 (62)	73 (55)
4–5	5 (31)	19 (24)	6 (16)	30 (23)
>5	5 (31)	17 (21)	8 (22)	30 (23)
No. secondary cases in household				
0	10 (63)	54 (68)	17 (46)	81 (61)
1	4 (25)	16 (20)	14 (38)	34 (26)
2	1 (6)	4 (5)	5 (14)	10 (8)
>2	1 (6)	6 (8)	1 (3)	8 (6)
Household contacts	67	322	147	536
Age, y				
≤18	30 (45)	147 (46)	64 (44)	241 (45)
>18	37 (55)	175 (54)	83 (56)	295 (55)
Sex				
F	46 (69)	202 (63)	94 (64)	342 (64)
M	21 (31)	120 (37)	53 (36)	194 (36)
Prior vaccination				
Yes	3 (4)	9 (3)	20 (14)	32 (6)
No	64 (96)	313 (97)	127 (86)	504 (94)
With confirmed infection				
Overall	9/67 (13)	46/322 (14)	29/147 (20)	84/536 (16)
≤18 y†	3/30 (10)	33/147 (22)	21/64 (33)	57/241 (24)
>18 y†	6/37 (16)	13/175 (7)	8/83 (10)	27/295 (9)
No. confirmed infections without reported symptoms				
Overall	2/9 (22)	15/46 (33)	4/29 (14)	21/84 (25)
≤18 y†	2/3 (67)	11/33 (33)	3/21 (14)	16/57 (28)
>18 y†	0/6	4/13 (31)	1/8 (13)	5/27 (19)

*Not all percentages add up to 100% because of rounding.
†The denominator is the number of infected household contacts in the corresponding age group.

accounted for the difference in relative susceptibility between children and adults for influenza A and influenza B. Using this model, we found no differences in risk for infection between influenza A(H3N2) virus and influenza A(H1N1) virus or influenza B virus (Table 2). This finding suggested that the observed increased susceptibility to infection with influenza B virus could be explained by an interaction between age of household contacts and influenza type; in other words, child contacts were more susceptible to infection with influenza B virus than influenza A virus, and among adult contacts, the risk for infection with influenza A virus was similar to the risk for infection with influenza B virus.

We estimated that child household contacts (≤18 years of age) were more susceptible to RT-PCR–confirmed influenza A virus infection than adult contacts (>18 years of age) (relative susceptibility 2.26, 95% CI 1.38–3.88),

and child contacts were more susceptible to RT-PCR–confirmed influenza B virus infection than adult contacts (relative susceptibility 4.47, 95% CI 2.05–11.02). Because there were only 7 adult index patients (Table 1), we could not explore potential differences in infectivity of child versus adult cases. However, we did explore relative infectivity of younger children (≤5 years of age) versus older children and adults; the estimated relative infectivity of younger children was 1.55 (95% CI 0.98–2.45) (Table 2).

We found no statistically significant association between oseltamivir treatment of index patients and risk for infection among household contacts (risk ratio 0.69, 95% CI 0.42–1.12). We estimated vaccine effectiveness among vaccinated household contacts as 54% (95% CI -32% to 89%). Household contacts of index patients having ≥4 household contacts had ≈30% 40% lower risk for infection than those

Table 2. Factors affecting influenza transmission in urban households, Managua, Nicaragua, August 2012–November 2014

Characteristics	Risk ratio (95% CI)
Influenza type	
A(H3N2)	Referent
A(H1N1)	1.18 (0.5–2.42)
B	0.96 (0.4–2.15)
Age of household contact, y	
>18	Referent
≤18 for influenza A	2.26 (1.38–3.88)
≤18 for influenza B	4.47 (2.05–11.02)
Prior vaccination of household contact	
No	Referent
Yes	0.46 (0.11–1.32)
Age of index patient, y	
≤5	Referent
>5	1.55 (0.98–2.45)
Oseltamivir treatment of index case	
No	Referent
Yes	0.69 (0.42–1.12)
No. household contacts	
1–3	Referent
4–5	0.60 (0.30–1.10)
>5	0.69 (0.37–1.18)

of index patients having <4 household members, but this difference was not statistically significant (Table 2; online Technical Appendix Table). We estimated that the mean

serial interval for within-household transmission was 3.1 (95% CI 1.6–8.4) days (SD 2.0 [95% CI 0.4–10.8] days).

We performed simulation studies to assess the adequacy of our model (Figure 2). The median estimated risks for infection among groups from the 10,000 simulated household epidemics were close to the risks observed, suggesting our model provided a reasonable fit of the data.

Discussion

We describe the results from a case ascertainment study of influenza transmission in urban households of Nicaragua. In this setting, we found the mean serial interval for within-household influenza transmission to be 3.1 days. We further observed an overall risk for RT-PCR–confirmed influenza virus infection of ≈16% among household contacts of index patients with RT-PCR–confirmed influenza virus infections, despite high oseltamivir treatment of index patients (76%).

We found evidence that influenza B virus was more transmissible than influenza A virus, which was explainable by higher transmissibility of this virus among children (Table 2). As expected, children were more susceptible to influenza A and influenza B than adults in our study, presumably because of lower levels of preexisting immunity
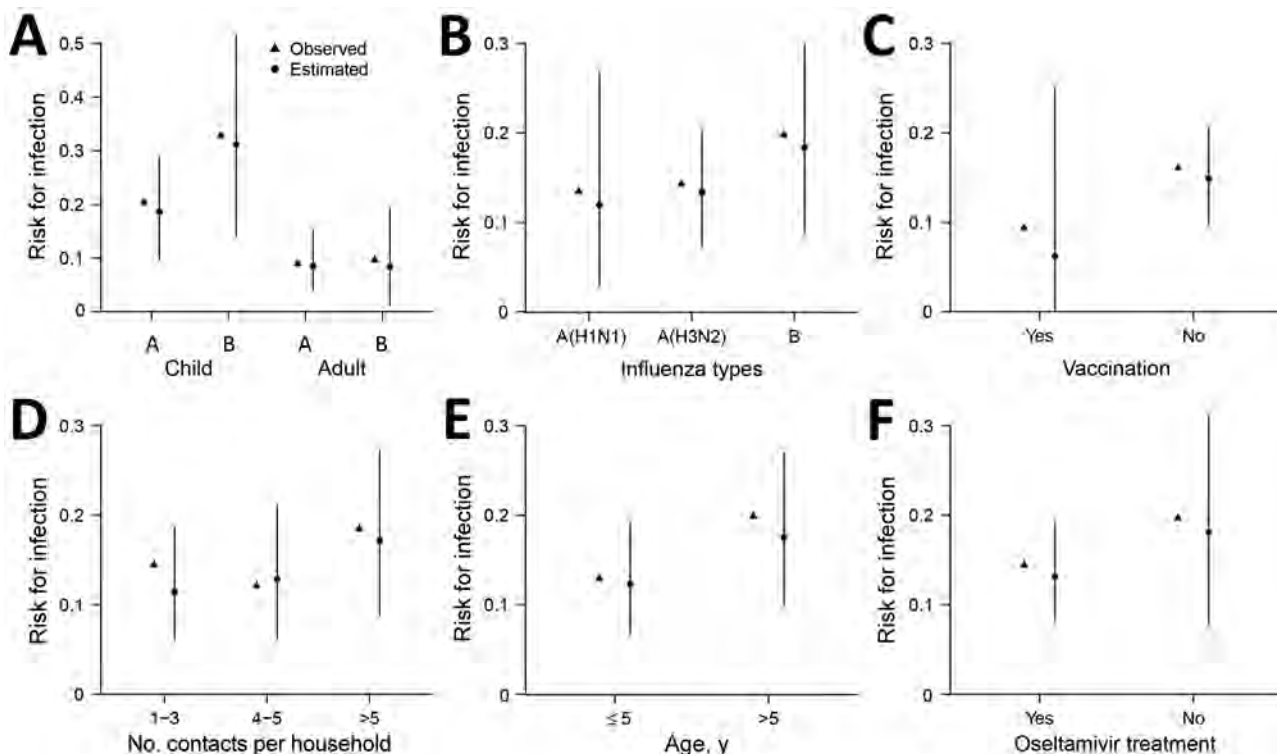
Figure 2. Observed and estimated risks for influenza virus infection of household contacts of index patients with reverse transcription PCR–confirmed influenza virus infections, by characteristic, Managua, Nicaragua, August 2012–November 2014. We estimated risk for infection by performing simulations using a multivariate model fitted to the collected data. Estimates represent 10,000 simulated epidemics in households with a structure that matched exactly that of the observed household. Points indicate medians, and bars represent the 2.5%–97.5% ranges of those 10,000 simulations. Risks for infection are shown for A) child and adult household contacts with influenza A virus infection or influenza B virus infection; B) virus type and subtype; C) vaccinated and nonvaccinated household contacts; D) household contact number; E) age group; and F) household contacts of index patients who were and were not treated with oseltamivir.

and different contact patterns (*25*). This finding is consistent with those of other studies (*4,6,16,17*). However, a large randomized controlled trial in households in Thailand did not observe significant differences between children and adults in risk for influenza virus infection (*10*).

We did not detect a significant effect for oseltamivir treatment of index patients on influenza transmissibility. This observation is consistent with several other household transmission studies that have found that oseltamivir treatment decreases the infectious period but does not have a statistically significant effect on the secondary attack rate of laboratory-confirmed influenza (*19,26,27*). However, other studies have shown a reduction in household transmission from index patients treated with oseltamivir (*28,29*). In a review, about half of household transmission studies reported a significant association between index case oseltamivir treatment and reduction in transmission in households, suggesting this issue is still unresolved (*30*). On the other hand, our study might be underpowered to detect this association, considering that 76% of the index patients were treated with oseltamivir.

We did not observe that vaccination had a significant effect on influenza transmission in the household. However, the proportion of contacts vaccinated in this study was low (5%), and thus, the study was underpowered to detect vaccine effectiveness in this population.

We did not find a statistically significant association between risk of acquiring an infection and number of household contacts, although the point estimate suggests that the risk for infection among household contacts of index patients with ≥4 household contacts was 30%–40% lower than those of index patients with <4 household contacts. This association has also been reported in other studies. The absence of this association in a study might indicate insufficient sample size (*4–6*).

We estimated the mean serial interval for influenza in households in Nicaragua to be 3.1 days. This estimate is similar to those found in other settings, such as Hong Kong, where the mean serial interval estimate for influenza A was 3.2–3.6 days (*16,21,22*); Thailand, where the estimate was 3.3–3.7 days, depending on the type and subtype of influenza (*31*); and Michigan, where the mean serial interval reported was 3.2 days (*32*). In a review of influenza A(H1N1) pdm09 virus transmission, the mean serial interval was estimated to be 2.6 days (*33*).

A major strength of our study was the collection of up to 5 respiratory samples from each household contact, regardless of whether they had symptoms, for 9–12 days after index case identification. However, our study has several limitations, the most notable being that we enrolled index influenza cases only among persons seeking medical care. This aspect of the study design could have biased the study toward sicker than average index patients, which could have inflated our influenza transmission estimate. Also, because adults tend to seek treatment later in their illnesses than children and enrollment was limited to index patients who sought treatment ≤2 days after symptom onset, our study was overrepresented by index cases in children. This enrollment criterion could have also led to an increase in the intensity of transmission and shortened the observed serial interval of transmission (*4*). Last, not enough adult index cases were enrolled to examine whether child index cases might be more infectious than adult index cases.

In summary, in this household transmission study of influenza in Managua, Nicaragua, we observed a high secondary attack rate of influenza and a serial interval within the range of those observed in high-income country settings. Our findings extend the relatively limited knowledge available regarding influenza transmission in low-middle–income countries. Further research is needed to investigate how household conditions affect influenza transmission and to design household-based interventions in these settings.

About the Author

Dr. Gordon is an assistant professor at the University of Michigan, Ann Arbor, Michigan, USA. Her research interests are the areas of infectious disease epidemiology and global health, with a focus on influenza burden and transmission.

References

1. World Health Organization. Influenza (seasonal). 2018 Jan 31 [cited 2016 Jul 28]. http://www.who.int/mediacentre/factsheets/fs211/en/
2. Longini IM Jr, Koopman JS, Haber M, Cotsonis GA. Statistical inference for infectious diseases. Risk-specific household and community transmission parameters. Am J Epidemiol.

1988;128:845–59. http://dx.doi.org/10.1093/oxfordjournals. aje.a115038

3. Longini IM Jr, Koopman JS, Monto AS, Fox JP. Estimating household and community transmission parameters for influenza. Am J Epidemiol. 1982;115:736–51. http://dx.doi.org/10.1093/oxfordjournals.aje.a113356

4. Cauchemez S, Carrat F, Viboud C, Valleron AJ, Boëlle PY. A Bayesian MCMC approach to study transmission of influenza: application to household longitudinal data. Stat Med. 2004;23:3469–87. http://dx.doi.org/10.1002/sim.1912

5. Cauchemez S, Donnelly CA, Reed C, Ghani AC, Fraser C, Kent CK, et al. Household transmission of 2009 pandemic influenza A (H1N1) virus in the United States. N Engl J Med. 2009;361:2619–27. http://dx.doi.org/10.1056/NEJMoa0905498

6. Cauchemez S, Ferguson NM, Fox A, Mai Q, Thanh T, Thai PQ, et al. Determinants of influenza transmission in South East Asia: insights from a household cohort study in Vietnam. PLoS Pathog. 2014;10:e1004310. http://dx.doi.org/10.1371/journal.ppat.1004310

7. Wu JT, Riley S, Fraser C, Leung GM. Reducing the impact of the next influenza pandemic using household-based public health interventions. PLoS Med. 2006;3:e361. http://dx.doi.org/10.1371/journal.pmed.0030361

8. Cowling BJ, Chan KH, Fang VJ, Cheng CK, Fung RO, Wai W, et al. Facemasks and hand hygiene to prevent influenza transmission in households: a cluster randomized trial. Ann Intern Med. 2009;151:437–46. http://dx.doi.org/10.7326/0003-4819-151-7-200910060-00142

9. Ng S, Cowling BJ, Fang VJ, Chan KH, Ip DK, Cheng CK, et al. Effects of oseltamivir treatment on duration of clinical illness and viral shedding and household transmission of influenza virus. Clin Infect Dis. 2010;50:707–14. http://dx.doi.org/10.1086/650458

10. Simmerman JM, Suntarattiwong P, Levy J, Jarman RG, Kaewchana S, Gibbons RV, et al. Findings from a household randomized controlled trial of hand washing and face masks to reduce influenza transmission in Bangkok, Thailand. Influenza Other Respi Viruses. 2011;5:256–67. http://dx.doi.org/10.1111/j.1750-2659.2011.00205.x

11. MacIntyre CR, Cauchemez S, Dwyer DE, Seale H, Cheung P, Browne G, et al. Face mask use and control of respiratory virus transmission in households. Emerg Infect Dis. 2009;15:233–41. http://dx.doi.org/10.3201/eid1502.081166

12. Thai PQ, Mai Q, Welkers MR, Hang NK, Thanh T, Dung VT, et al. Pandemic H1N1 virus transmission and shedding dynamics in index case households of a prospective Vietnamese cohort. J Infect. 2014;68:581–90. http://dx.doi.org/10.1016/j.jinf.2014.01.008

13. Andayi F, Crepey P, Kieffer A, Salez N, Abdo AA, Carrat F, et al. Determinants of individuals' risks to 2009 pandemic influenza virus infection at household level amongst Djibouti city residents— a CoPanFlu cross-sectional study. Virol J. 2014;11:13. http://dx.doi.org/10.1186/1743-422X-11-13

14. Kieffer A, Paboriboune P, Crépey P, Flaissier B, Souvong V, Steenkeste N, et al. 2009 A(H1N1) seroconversion rates and risk factors among the general population in Vientiane Capital, Laos. PLoS One. 2013;8:e61909. http://dx.doi.org/10.1371/journal.pone.0061909

15. Asiedu-Bekoe F, Adu DA, Offei A. Mass oseltamivir prophylaxis halts pandemic influenza A H1N1 2009 outbreak in a secondary school in Ashanti Region, Ghana. Ghana Med J. 2012;46:219–24.

16. Lau MS, Cowling BJ, Cook AR, Riley S. Inferring influenza dynamics and control in households. Proc Natl Acad Sci U S A. 2015;112:9094–9. http://dx.doi.org/10.1073/pnas.1423339112

17. Tsang TK, Cauchemez S, Perera RA, Freeman G, Fang VJ, Ip DK, et al. Association between antibody titers and protection against influenza virus infection within households. J Infect Dis. 2014;210:684–92. http://dx.doi.org/10.1093/infdis/jiu186

18. Hirotsu N, Wada K, Oshitani H. Risk factors of household transmission of pandemic (H1N1) 2009 among patients treated with antivirals: a prospective study at a primary clinic in Japan. PLoS One. 2012;7:e31519. http://dx.doi.org/10.1371/journal.pone.0031519

19. Nishiura H, Oshitani H. Household transmission of influenza (H1N1-2009) in Japan: age-specificity and reduction of household transmission risk by zanamivir treatment. J Int Med Res. 2011;39:619–28. http://dx.doi.org/10.1177/147323001103900231

20. The World Bank. Population ages 0–14 (% of total). 2017 [cited 2015 Jul 23]. http://data.worldbank.org/indicator/SP.POP.0014.TO.ZS

21. Cowling BJ, Chan KH, Fang VJ, Lau LLH, So HC, Fung ROP, et al. Comparative epidemiology of pandemic and seasonal influenza A in households. N Engl J Med. 2010;362:2175–84. http://dx.doi.org/10.1056/NEJMoa0911530

22. Cowling BJ, Fang VJ, Riley S, Malik Peiris JS, Leung GM. Estimation of the serial interval of influenza. Epidemiology. 2009;20:344–7. http://dx.doi.org/10.1097/EDE.0b013e31819d1092

23. Cauchemez S, Donnelly CA, Reed C, Ghani AC, Fraser C, Kent CK, et al. Household transmission of 2009 pandemic influenza A (H1N1) virus in the United States. N Engl J Med. 2009;361:2619–27. http://dx.doi.org/10.1056/NEJMoa0905498

24. Gilks WR, Richardson S, Spiegelhalter DJ. Markov chain Monte Carlo in practice. Interdisciplinary statistics. London: Chapman & Hall; 1995.

25. Mossong J, Hens N, Jit M, Beutels P, Auranen K, Mikolajczyk R, et al. Social contacts and mixing patterns relevant to the spread of infectious diseases. PLoS Med. 2008;5:e74. http://dx.doi.org/10.1371/journal.pmed.0050074

26. Fry AM, Goswami D, Nahar K, Sharmin AT, Rahman M, Gubareva L, et al. Effects of oseltamivir treatment of index patients with influenza on secondary household illness in an urban setting in Bangladesh: secondary analysis of a randomised, placebo-controlled trial. Lancet Infect Dis. 2015;15:654–62. http://dx.doi.org/10.1016/S1473-3099(15)70041-1

27. Ng S, Cowling BJ, Fang VJ, Chan KH, Ip DKM, Cheng CKY, et al. Effects of oseltamivir treatment on duration of clinical illness and viral shedding and household transmission of influenza virus. Clin Infect Dis. 2010;50:707–14. http://dx.doi.org/10.1086/650458

28. Halloran ME, Hayden FG, Yang Y, Longini IM Jr, Monto AS. Antiviral effects on influenza viral transmission and pathogenicity: observations from household-based trials. Am J Epidemiol. 2007;165:212–21. http://dx.doi.org/10.1093/aje/kwj362

29. Teh B, Olsen K, Black J, Cheng AC, Aboltins C, Bull K, et al. Impact of swine influenza and quarantine measures on patients and households during the H1N1/09 pandemic. Scand J Infect Dis. 2012;44:289–96. http://dx.doi.org/10.3109/00365548.2011.631572

30. Tsang TK, Lau LLH, Cauchemez S, Cowling BJ. Household transmission of influenza virus. Trends Microbiol. 2016;24:123–33. http://dx.doi.org/10.1016/j.tim.2015.10.012

31. Levy JW, Cowling BJ, Simmerman JM, Olsen SJ, Fang VJ, Suntarattiwong P, et al. The serial intervals of seasonal and pandemic influenza viruses in households in Bangkok, Thailand. Am J Epidemiol. 2013;177:1443–51. http://dx.doi.org/10.1093/aje/kws402

32. Petrie JG, Ohmit SE, Cowling BJ, Johnson E, Cross RT, Malosh RE, et al. Influenza transmission in a cohort of households with children: 2010-2011. PLoS One. 2013;8:e75339. http://dx.doi.org/10.1371/journal.pone.0075339

33. Boëlle PY, Ansart S, Cori A, Valleron AJ. Transmission parameters of the A/H1N1 (2009) influenza virus pandemic: a review. Influenza Other Respi Viruses. 2011;5:306–16. http://dx.doi.org/10.1111/j.1750-2659.2011.00234.x

Address for correspondence: Aubree Gordon, University of Michigan, Epidemiology, 1415 Washington Heights, Ann Arbor, MI 48109, USA; email: gordonal@umich.edu

Non-*cyp51A* Azole-Resistant *Aspergillus fumigatus* Isolates with Mutation in HMG-CoA Reductase

Daisuke Hagiwara,[1] Teppei Arai,[1] Hiroki Takahashi, Yoko Kusuya, Akira Watanabe, Katsuhiko Kamei

The recent increase in azole-resistant *Aspergillus fumigatus* is a global concern. Identifying the mutations that confer azole resistance is essential for developing novel methods for prompt diagnosis and effective drug treatment. We screened *A. fumigatus* clinical isolates for novel mutations conferring azole resistance. We compared the genomic sequences of susceptible and resistant isolates without mutations in *cyp51A* (non-*cyp51A*) and found mutations in *hmg1* and *erg6* involved in ergosterol biosynthesis. We also found the novel mutations in these genes in azole-resistant isolates with different genetic backgrounds. The resistant isolates with mutations in *hmg1* showed increased intracellular ergosterol levels compared with susceptible isolates. This finding supports the concept that the ergosterol level is a determinant for resistance to any class of azoles. Multiple isolates with increased resistance to azole possessed a mutation in *hmg1*, indicating that this mutation is widely present in non-*cyp51A* azole-resistant *A. fumigatus*.

*A*spergillus fumigatus is known as an opportunistic pathogen of fungal infection and causes a high mortality rate among immunosuppressed patients (*1,2*). Azole drugs are considered the first-line therapy in various diseases of aspergillosis. The recent increase of azole drug–resistant *A. fumigatus* is a major limitation of therapeutic strategies in clinical settings and a concern throughout the world (*3*). Most azole-resistant strains harbor a mutation in the *cyp51A* gene, encoding a target protein for azole drugs (*4*). The point-mutated Cyp51A has lower binding affinity to azole drugs, causing azole resistance in these strains (*5*). The amino acid substitution in Cyp51A protein is thought to occur during azole therapy inside hosts. In addition, 34 bp or 46 bp of tandem repeats in the promoter region of *cyp51A* cause azole resistance (*6*). The high incidence of such tandem repeat–type resistant strains is alarming (*7*), and it

Author affiliations: University of Tsukuba, Tsukuba, Japan (D. Hagiwara); Chiba University, Chiba City, Japan (D. Hagiwara, T. Arai, H. Takahashi, Y. Kusuya, A. Watanabe, K. Kamei)

is widely accepted that the tandem repeat–type resistant mechanism is derived from exposure to azole fungicides in the environment (*8*). Whereas such *cyp51A*-related azole-resistant strains have been reported frequently in the past 10 years, strains without any mutation in the *cyp51A* gene showing low susceptibility to azole drugs have, to some extent, been isolated (*9*). Which mutation leads to azole resistance has thus far been determined in only a few non-*cyp51A* azole-resistant strains. For a deeper and broader understanding of the molecular mechanisms underlying resistance to antifungal drugs, the non-*cyp51A* azole-resistant strains have become the focus of attention.

The *cdr1B* gene, encoding an ABC transporter, plays a role in azole resistance. Deletion of the gene resulted in azole-sensitive phenotypes (*10*), and an azole-resistant strain with constitutive expression of *cdr1B* has been isolated from a patient (*11*). The expression of *cdr1B* is dependent on AtrR, a recently characterized transcriptional factor (*12*), but the reason for the constitutive expression remains unclear. A strain showing azole resistance with a mutation (P88L) in the *hapE* gene has also been isolated; the mutation was discovered by genome comparison between azole-resistant strains and corresponding susceptible strains (*13*). A recent study showed that HapE forms a CCAAT binding complex, which plays a role in the negative regulation of *cyp51A* expression. The amino acid substitution in HapE (P88L) resulted in increased *cyp51A* expression and consequent azole resistance (*14*).

These studies provided convincing evidence of the roles of Cdr1B and HapE in azole adaptation in *A. fumigatus*. However, each of these mutations has been reported only once in clinical isolates. Furthermore, a large portion of the non-*cyp51A* azole-resistant *A. fumigatus* strains have yet to be investigated to determine which genes and mutations could be responsible for azole resistance. To fill a gap in our understanding of the mechanism for azole resistance in the non-*cyp51A* strains, we searched for mutations in a

series of isolates derived from a single patient in Japan who had chronic pulmonary aspergillosis (CPA) and isolates from other patients with and without azole resistance.

Materials and Methods

A. fumigatus Strains

All clinical isolates used in this study were preserved at Chiba University Medical Mycology Research Center (Chiba City, Japan). We obtained 19 isolates from a patient at hospital C who had CPA (Tables 1, 2), 3 isolates (IFM 63768, IFM 63666, and IFM 63772) from another CPA patient at hospital C on different days, and additional isolates from 3 other patients with CPA at different hospitals (IFM 62140 at hospital K, IFM 64258 at hospital I, and IFM 64303 at hospital T). We also obtained 16 azole-susceptible clinical isolates (Table 3) from respiratory samples (sputa, pleural effusion, lung tissues, or bronchoalveolar fluids) or pus from a subcutaneous abscess from patients with aspergillosis in various hospitals in Japan.

Microsatellite Genotyping

For genotyping, we PCR amplified and sequenced 6 loci of ≈400 bp from all of the isolates as described previously (15). We counted the repeat numbers of each region (2A, 2B, 2C, 3A, 3B, 3C, 4A, 4B, and 4C) from the sequence.

Antifungal Susceptibility Testing

We performed antifungal susceptibility testing as described previously (16). In brief, we performed tests in triplicate using amphotericin B (AMPH), itraconazole (ITCZ), voriconazole (VRCZ), and posaconazole (PSCZ) in RPMI 1640 medium (pH 7.0) at 35°C, according to the Clinical and Laboratory Standards Institute reference method for broth microdilution (https://clsi.org/standards/products/microbiology/documents/m38), with partial modifications using the dried plate for antifungal susceptibility testing (Eiken Chemicals, Tokyo, Japan).

Sequencing *cyp51A*, *erg6*, and *hmg1* Genes

To detect mutations in *cyp51A*, *erg6*, and *hmg1* genes, we performed PCR amplification and sequenced these regions using appropriately designed primers (online Technical Appendix Table 1, https://wwwnc.cdc.gov/EID/article/24/10/18-0730-Techapp1.pdf). We performed sequence variant detection by comparison with reference sequences from GenBank and Fungi DB (http://fungidb.org/fungidb/) (GenBank accession no. AF338659 for *cyp51A*, Fungi DB accession nos. AFUB_020770 for *hmg1*, and AFUB_099400 for *erg6*).

Whole-Genome Sequencing

We performed whole-genome sequencing by using next-generation methods as described previously (15). In brief, we extracted genome DNA from overnight-cultured mycelia by DNeasy Plant Mini Kit (QIAGEN, Hilden, Germany) or by phenol-chloroform extraction and Nucleobond AXG column (TaKaRa, Kusatsu, Japan) with Nucleobond Buffer Set III (TaKaRa). For analyzing IFM 60814 and IFM 63240, we prepared a fragmented DNA library by using a Nextera DNA sample preparation kit according to the manufacturer's instructions (Illumina, San Diego, CA). The mean length of the libraries was 376–674 bp. We performed sequencing in a paired-end 2 × 150 bp mode on a MiSeq system (Illumina). For analyzing IFM 63666 and IFM 63768, we prepared a fragmented DNA library using KAPA HyperPlus Library Preparation Kit (Kapa Biosystems, Wilmington, MA) according to the manufacturer's

Table 1. Number of short tandem repeats in *Aspergillus fumigatus* isolates from a single patient in Japan*

Isolate IFM no.	Date isolated (isolate set)	Short tandem repeats								
		2A	2B	2C	3A	3B	3C	4A	4B	4C
60814	2011 Sep (1st)	21	20	16	39	13	24	10	12	8
62916	2014 Sep (2nd)	21	20	16	39	13	24	10	12	8
63240	2014 Nov (3rd)	21	20	16	39	13	25	10	12	8
63241		21	20	16	39	13	25	10	12	8
63242		21	20	16	39	13	25	10	12	8
63243		21	20	16	39	13	25	10	12	8
63248	2015 Jan (4th)	21	20	16	39	13	24	10	12	8
63249		21	20	16	39	13	25	10	12	8
63537	2015 Jul (5th)	21	20	16	39	13	24	10	12	8
63594	2015 Sep (6th)	21	20	16	39	13	24	10	12	8
63595		21	20	16	39	13	24	10	12	8
63596		21	20	16	39	13	24	10	12	8
63711	2015 Dec (7th)	21	20	16	39	13	24	10	12	8
63712		21	20	16	39	13	24	10	12	8
63713		21	20	16	39	13	24	10	12	8
63714		21	20	16	39	13	24	10	12	8
64138	2016 Apr (8th)	21	20	16	39	13	24	10	12	8
64139		21	20	16	39	13	24	10	12	8
64173	2016 May (9th)	21	20	16	39	13	24	10	12	8

*IFM, Institute of Food Microbiology (now Medical Mycology Research Center), Chiba University, Chiba City, Japan.

Table 2. Characteristics of *Aspergillus fumigatus* isolates from a single patient in Japan*

Isolate IFM no.	Date isolated (isolate set)	MCFG MEC, mg/L	MIC, mg/L				Gene with mutation		
			AMPH	ITCZ	VRCZ	PSCZ	*Cyp51*	*Hmg1*	*Erg6*
60814	2001 Sep (1st)	<0.015	0.5	0.5	0.5	1	–	–	–
62916	2014 Sep (2nd)	<0.015	0.5	>8	>8	8	G448S	S269F	E49K
63240	2014 Nov (3rd)	<0.015	1	>8	>8	4	–	S269F	A350T
63241		<0.015	0.5	>8	>8	8	–	S269F	A350T
63242		<0.015	1	>8	>8	8	–	S269F	A350T
63243		<0.015	1	>8	>8	8	–	S269F	A350T
63248	Jan 2015 (4th)	ND	ND	ND	ND	ND	–	S269F	E49K
63249		<0.015	1	4	8	8	G448S	S269F	E49K
63537	2015 Jul (5th)	<0.015	1	>8	8	8	–	S269F	A350T
63594	2015 Sep (6th)	<0.015	1	>8	>8	8	–	S269F	A350T
63595		<0.015	1	>8	>8	>8	G448S	S269F	E49K
63596		<0.015	1	>8	>8	8	–	S269F	A350T
63711	2015 Dec (7th)	ND	ND	ND	ND	ND	–	S269F	E49K
63712		ND	ND	ND	ND	ND	G448S	S269F	E49K
63713		ND	ND	ND	ND	ND	G448S	S269F	E49K
63714		<0.015	1	>8	8	4	–	S269F	E49K
64138	2016 Apr (8th)	ND	ND	ND	ND	ND	–	S269F	E49K
64139		ND	ND	ND	ND	ND	G448S	S269F	E49K
64173	2016 May (9th)	<0.015	0.5	>8	8	4	–	S269F	A350T

*AMPH, amphotericin B; IFM, Institute of Food Microbiology (now Medical Mycology Research Center), Chiba University, Chiba City, Japan; ITCZ, itraconazole; MCFG, micafungin; MEC, minimal effective concentration; ND, not determined; PSCZ, posaconazole; VRCZ, voriconazole; –, no mutation.

instructions. We performed sequencing in a paired-end 2 × 300 bp mode on a MiSeq system (Illumina).

Single-Nucleotide Variant Detection

To search for single-nucleotide polymorphisms (SNPs) between IFM 60814, the first isolate obtained, and IFM 63240–63243, the third set of isolates, we performed read-mapping and SNP detection using CLC Genomics Workbench (CLC bio, Aarhus, Denmark). In brief, we trimmed the reads from each isolate and mapped them to the Af293 reference genome. By comparing them with the Af293 sequence, we detected sites with SNPs in IFM 60814, IFM 63240, IFM 63241, IFM 63242, and IFM 63243. We also compared the sets of varied sites between IFM 60814 and IFM 63240–63243. We considered the unique sites common in IFM 63240–63243 to be the SNPs between the first isolate and the third set of isolates.

We cleaned the read datasets of IFM 63666 and IFM 63768 using Trimmomatic version 0.33 (*17*). We trimmed reads to generate de novo assembly of the draft genome of IFM 63666 using Platanus version 1.2. 4 with default parameters (*18*). We performed annotation of all predicted open reading frames of the draft genome using AUGUSTUS version 2.5.5 (*19*). For nucleotide differences between IFM 63666 and IFM 63768, we mapped the trimmed reads of IFM 63768 to the draft genome of IFM 63666 using SMALT version 0.7.6 (http://www.sanger.ac.uk/science/tools/smalt-0). We identified SNPs using SAMtools version 0.1.19–44428cd (*20*) and filtered with ≥10-fold coverage, ≥30 mapping quality, and 75% consensus using in-house scripts (*21,22*). We annotated the functional effect of SNPs with SnpEff version 4.11 (*23*).

Table 3. Characteristics of azole-susceptible isolates of *Aspergillus fumigatus* in Japan*

Isolate IFM no.	MCFG MEC, mg/L	MIC, mg/L			Gene with mutation		Short tandem repeats					
		AMPH	ITCZ	VRCZ	*hmg1*	*erg6*	3A	3B	3C	4A	4B	4C
49435	≤0.015	1	0.25	0.25	–	–	52	17	20	10	11	11
50268	≤0.015	0.5	0.25	0.125	–	–	14	10	11	13	9	10
50669	≤0.015	1	0.5	0.25	–	–	12	18	20	16	9	5
50999	≤0.015	1	0.5	0.5	–	–	33	12	37	11	9	5
51748	≤0.015	0.5	0.125	0.125	–	–	26	11	29	25	10	8
51977	≤0.015	1	0.25	0.25	–	–	25	9	7	12	11	17
57130	≤0.015	1	0.25	0.125	–	–	47	21	19	10	11	5
58402	≤0.015	1	0.5	0.5	–	–	27	10	5	9	9	5
60065	≤0.015	1	1	0.5	–	–	15	17	17	17	16	10
60516	≤0.015	1	1	1	–	–	22	11	7	16	11	8
60901	≤0.015	1	0.5	0.5	H564Y	–	23	28	21	8	11	10
61572	≤0.015	1	0.5	0.5	–	–	59	19	7	10	14	8
61960	≤0.015	1	0.5	0.5	–	–	27	11	35	10	9	10
62674	≤0.015	1	1	2	–	–	35	10	14	16	10	10
62709	≤0.015	1	0.5	0.5	–	–	38	18	7	10	14	9
62821	≤0.015	1	0.5	0.25	–	–	37	14	7	10	11	10

*AMPH, amphotericin B; IFM, Institute of Food Microbiology (now Medical Mycology Research Center), Chiba University, Chiba City, Japan; ITCZ, itraconazole; MCFG, Micafungin; MEC, minimal effective concentration; VRCZ, voriconazole; –, no mutation.

Growth Test for Ergosterol-Related Inhibitors

We performed disk diffusion assay using the protocol described by Qiao et al. (24). We spread a 200-µL suspension (1 × 10⁶ conidia/mL) of each of the tested isolates uniformly onto YGA (glucose 2%, yeast extract 0.5%, agar 2%, trace element). We impregnated blank paper disks 8 mm in diameter with 2.5 µg amphotericin B, 100 µg nystatin, or 40 µg lovastatin and placed the disks onto the center of the inoculated agar plates. We incubated the plates at 37°C and measured the diameters of the zones of inhibition 48 hours later. We performed each assay 3 times and calculated the mean diameter.

Ergosterol Quantification

We conducted total ergosterol extraction using the protocol described by Arthington-Skaggs et al. and Alcazar-Fuolietal (25,26). We cultured A. fumigatus isolates for 20 h in glucose minimal medium. We harvested mycelia by filtration, washed them with sterile water, and then dried and weighed them. We added 3 mL of 25% alcoholic potassium hydroxide solution to dried mycelia and mixed for 1 min, then incubated the mixture in an 80°C water bath for 1 h. After incubation, we added water and 3 mL of pentane and mixed for 3 min. We transferred the upper pentane layer to a clean glass tube for evaporation. We dissolved the dried samples in 1 mL of methanol and filtered it through a 0.22-µm pore size membrane filter. We analyzed ergosterol content using the Shimadzu LC-20A system (Shimadzu, Kyoto, Japan) with COSMOSIL 5C¹⁸-MS-II column (4.6 mm ID × 100 mm; Nacalai Tesque, Kyoto, Japan). We established a flow rate of 1 mL/min of acetonitrile to water (95:5 vol/vol). We used peak areas and heights recorded at a 254-nm wavelength in an RF-20Axs (Shimadzu) for quantification, expressing total ergosterol concentration as µg ergosterol per mg fungal dry weight. We repeated each experiment ≥3 times.

Construction of Mutant Erg6, Hmg1, and Cyp51A Expressed Strains

To construct transformants expressing erg6, hmg1, or cyp51A with the mutation, we cloned the alleles using the shuttle vector pPTR I (Takara Bio, Otsu, Japan) and GeneArt Seamless Cloning and Assembly Kit (Invitrogen, Tokyo, Japan). Primers used for the cloning are listed in online Technical Appendix Table 2. We used genome DNAs of IFM 60814 (for wild-type [WT] gene) and IFM 63240 (for mutated allele) as templates to clone the alleles. The resultant plasmids were pPTRI-erg6ᵂᵀ, pPTRI-hmg1ᵂᵀ, pPTRI-cyp51Aᵂᵀ, pPTRI-erg6ᴬ³⁵⁰ᵀ, pPTRI-hmg1ˢ²⁶⁹ᶠ, and pPTRI-cyp51Aᴳ⁴⁴⁸ˢ, which we used for transformation of isolate IFM 60814. After selection with pyrithiamine, we verified the sequences of each gene of the candidate transformants by Sanger sequencing.

Results

Multiazole Resistant Strains from a Single Patient

We recovered a total of 19 A. fumigatus isolates from 1 patient on 9 testing dates during September 2011–May 2016 (Tables 1, 2). Microsatellite analysis showed almost identical short tandem repeats across the isolates, derived from a genetically clonal background. The patient started treatment with VRCZ after the first isolation of A. fumigatus in September 2011. Whereas the first isolate (IFM 60814) was susceptible to antifungal drugs including ITCZ, VRCZ, and PSCZ, later isolates showed resistance to the azoles (MICs: ITCZ, 4 to >8; VRCZ, 8 to >8; PSCZ, 4 to >8). By sequencing the cyp51A gene, we found amino acid substitution G448S IFM 62916 (second isolation date), IFM63248 (fourth isolation date), IFM63595 (sixth isolation date), IFM63712 (seventh isolation date), IFM63713 (seventh isolation date), and IFM64139 (eighth isolation date). These isolates were most likely resistant to VRCZ as a result of the G448S mutation, which has been reported to confer VRCZ resistance in A. fumigatus. However, the multiazole resistance mechanism in the isolates with no G448S mutation remained unknown. The growth of isolate IFM 62916 was markedly impaired with glucose minimal medium and potato dextrose agar, whereas the isolates from the third isolation date also showed a moderately delayed growth compared with those of the first strain (online Technical Appendix Figure 1).

Genome-Wide Sequence Comparison of Azole-Susceptible and Azole-Resistant Isolates

To gain insight into the multiazole resistance mechanism in the non-cyp51A strains, we sequenced the genomes of the isolates from the first (IFM 60814) and third (IFM 63240–63243) testing dates by next-generation sequencing. Compared with IFM 60814, IFM 63240–63243 commonly showed 7 nonsynonymous mutations, including 6 SNPs (4 amino acid substitutions and 2 nonsense mutations, which generate termination codon) and a 1-bp deletion resulting in a frame shift of the protein (online Technical Appendix Table 2). The 6 genes with mutations included erg6, encoding sterol 24-C-methyltransferase and hmg1, encoding hydroxymethylglutaryl-CoA (HMG-CoA) reductase. The mutation of erg6 (A350T) resided in a Sterol_MT_C domain (PF08498) in the C-terminus, whereas the mutation of hmg1 (S269F) was located at the beginning of the sterol-sensing domain (PF12349) (online Technical Appendix Figure 2). Because both of these genes are functionally related to the ergosterol biosynthesis pathway, we assumed that these mutations affect ergosterol biosynthesis and the consequential azole resistance in the strains.

We examined the rest of the isolates from the patient for mutations in the hmg1 and erg6 genes. Despite the presence

of A350T, we identified E49K in the *erg6* gene in several isolates, whereas Hmg1 S269F existed in all isolates tested (Tables 1, 2). These results indicate that all of the isolates showing multiazole resistance had mutations in both *hmg1* and *erg6* genes, regardless of the mutation in *cyp51A* gene.

Different Ergosterol Levels in Multiazole-Resistant Isolates

We investigated the phenotypes associated with the ergosterol biosynthesis pathway in IFM 63240, a representative of the isolate from the third testing day. Disk diffusion assay showed that this isolate was more sensitive to polyene drugs, amphotericin B, and nystatin, suggesting that ergosterol production might be differentially regulated (Figure 1). The ergosterol content in the cells, measured by HPLC, showed significant increase (p = 0.0145) in the third set of isolates compared with the first isolate (Figure 2, panel A). At the same time, we found no differences between the first and third isolates regarding sensitivity to terbinafine, which interferes with the early stage of ergosterol biosynthesis, and fenpropimorph, which inhibits ergosterol biosynthesis (data not shown). Of note, the isolate from the third set showed increased sensitivity to lovastatin, an inhibitor of HMG-CoA reductase (Figure 1).
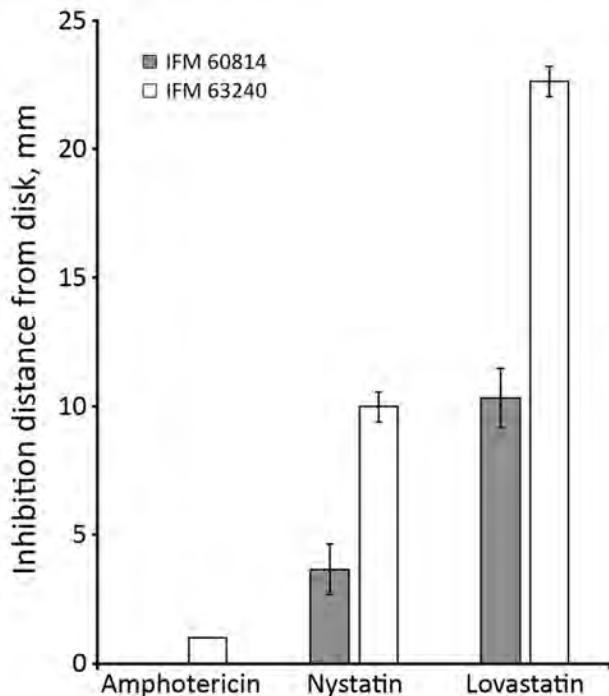
Figure 1. Growth inhibition by lovastatin and polyene drugs in azole-susceptible and azole-resistant *Aspergillus fumigatus* isolates from a patient in Japan. Growth inhibition tests were conducted by disk assay. IFM 60814 is a susceptible isolate identified on the first date of testing; IFM 63240 is a resistant isolate identified on the third date of testing, with mutations in *hmg1*. The results of repeated experiments are expressed as mean ± SD (error bars).
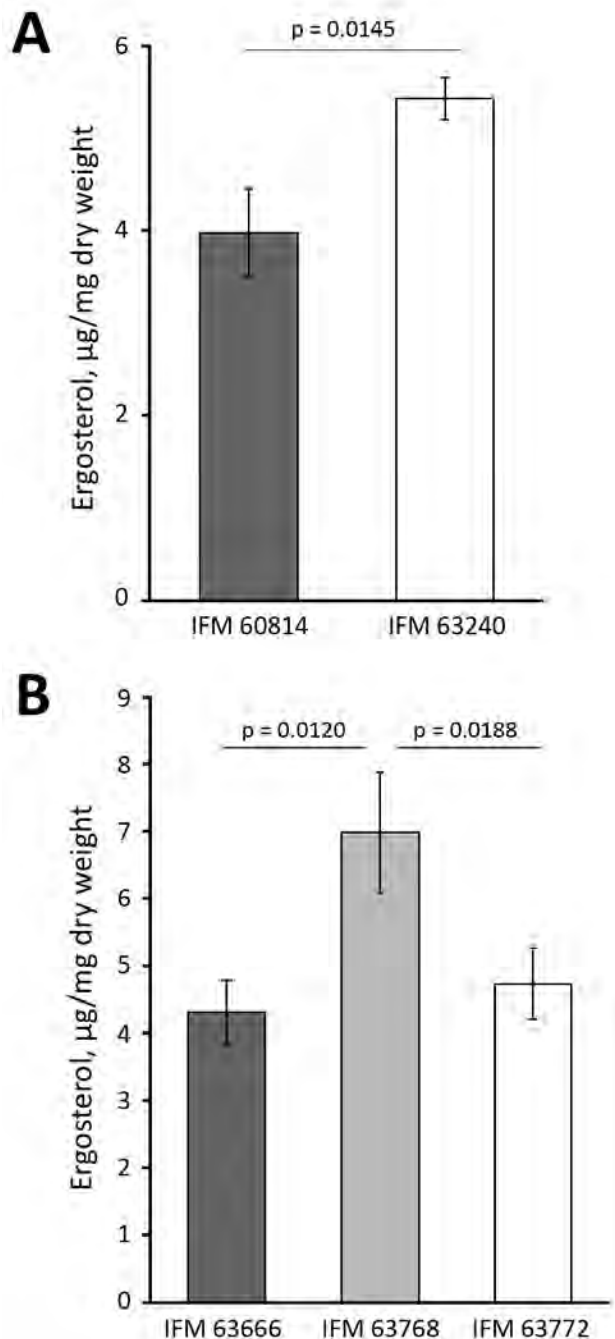
Figure 2. Total ergosterol content of azole-susceptible and azole-resistant *Aspergillus fumigatus* isolates in Japan. Ergosterol was quantified in the sets of IFM 60814, a susceptible isolate identified on the first date of testing, and IFM 63420, a resistant isolate identified on the third date of testing, both from 1 patient (A); and IFM 63666, IFM 63768, and IFM 63772, all isolated from other patients in the same hospital (B). The results of repeated experiments are expressed as mean ± SD (error bars). The significance of total ergosterol content was determined by the Student *t*-test (unpaired, unequal variance). A p value <0.05 was considered significant.

Evaluation of Mutant *erg6* and *hmg1* by Transformation

Considering the different level of ergosterol biosynthesis in the third set of isolates, we wanted to determine whether the mutation in *erg6* and/or *hmg1* genes was responsible for the phenotypes (i.e., sensitivity to polyenes and resistance to azoles). To address this question, we constructed the isolates carrying these mutant alleles as well as the corresponding wild-type gene by introducing *erg6*^{A350T} or *hmg1*^{S269F} into the first strain (hereafter designated as 1st+*erg6*^{A350T} and 1st+*hmg1*^{S269F}). These mutant alleles were ectopically expressed in the transformed strains. We also constructed the strain carrying *cyp51A*^{G448S} (1st+*cyp51A*^{G448S}) for verification of the role of the mutation in azole resistance as previously reported (*27*). The MICs for azoles were determined in these strains (Table 4), showing that introducing *erg6*^{A350T} or *hmg1*^{S269F} did not affect susceptibility to azoles, whereas the *cyp51A*^{G448S} conferred resistance to VRCZ.

Mutations in *erg6* and *hmg1* in Other Non-*cyp51A* Azole-Resistant Isolates

We studied whether the other non-*cyp51A* azole-resistant isolates possess mutations in *erg6* or *hmg1*. Over the past decade, we have collected clinical azole-resistant *A. fumigatus* strains in Japan: 4 non-*cyp51A* azole-resistant isolates (IFM 62140, IFM 64258, IFM 64303, and IFM 63768) showing a VRCZ MIC of ≥8 (Table 5). Each isolate was from a patient who had a history of treatment with VRCZ before isolation. Although IFM 64303 has no mutations in *erg6* and *hmg1* genes, the other 3 isolates possessed different mutations in *erg6* and/or *hmg1*. IFM 62140 had *erg6*^{A75S} and *hmg1*$^{F261\_del}$, IFM 63768 had *hmg1*^{S269Y}, and IFM 64258 had *erg6*^{V206A} and *hmg1*^{F390Y}, which were different from the pattern observed in IFM 63240. These results suggested a potential link between azole resistance and the mutations in *erg6* and *hmg1* genes. Notably, IFM 63768 and IFM 63240 had a mutation in Hmg1 at S269 in which serine was substituted by different amino acids (i.e., Hmg1^{S269Y} and Hmg1^{S269F}). To investigate the possibility that such mutations are just frequently occurring polymorphisms we sequenced *erg6* and *hmg1* in 16 azole-susceptible isolates. We did not find mutation in *erg6*, although 1 of the 16 isolates, IFM 60901, had a *hmg1*^{H564Y} mutation (Table 3). We did not find the mutations *hmg1*$^{S269F/Y}$, *hmg1*$^{F261\_del}$, and *hmg1*^{F390Y} in the azole-susceptible isolates. These results

suggest that the mutations in *erg6* and *hmg1* found in the azole-resistant isolates are not mere polymorphisms in *A. fumigatus* but can be implicated in azole resistance.

Comparing Genome Sequences of Non-*cyp51A* Azole-Resistant Isolate and Corresponding Isolates

In our collection, an azole-susceptible isolate (IFM 63666) was isolated 2 months before isolation of azole-resistant IFM 63768 (*hmg1*^{S269Y}) from the same patient. The 2 isolates shared the same short tandem repeats, indicating a clonal lineage. We then sequenced the genomes of IFM 63768 and IFM 63666. Comparing the genome sequences, we discovered only 1 nonsynonymous mutation other than *hmg1*^{S269Y} in IFM 63768, which was I395M in Afu4g04290 encoding a putative histone H4 deacetylase protein. Although we could not see the effect of the mutation in Afu4g04290, this result supported the possibility that Hmg1^{S269Y} is the determinant for azole resistance in this isolate. We compared ergosterol levels in the cells between IFM63768 and IFM 63666 and found an increased amount in IFM 63768 with *hmg1*^{S269Y} (Figure 2, panel B). We isolated IFM 63772 from the same patient in addition to these isolates, and it showed moderate resistance to VRCZ, resistance to PSCZ, and no mutations in *erg6* and *hmg1* (Table 5). The amount of ergosterol in IFM 63772 was comparable to that of IFM 63666 (Figure 2, panel B).

Discussion

The emergence of drug-resistant fungal strains has been on the rise in recent years, leading to a serious situation. Azole-resistant strains occurring during the course of therapy have been increasingly reported all over the world since the early discovery of an ITCZ-resistant strain (*5*). Some studies have shown that there are many azole-resistant *A. fumigatus* strains without mutation in *cyp51A* gene, and the molecular mechanisms underlying resistance in the strains remain unstudied (*28–30*). This finding indicates that many unclear molecular mechanisms related to azole resistance still exist.

In this study, we screened novel mutations conferring resistance by comparing the genomic sequences of susceptible and resistant strains isolated from the same patient. We found mutations in *hmg1* and *erg6*, encoding enzymes Hmg1 and Erg6, respectively, which are involved in

Table 4. Antifungal susceptibility test of mutants of *erg6* and *hmg1* from *Aspergillus fumigatus* isolates in Japan by transformation*

Strain	Genotype	MCFG MEC, mg/L	MIC, mg/L				
			AMPH	ITCZ	VRCZ	MCZ	PSCZ
1st+*erg6*^{WT}	*cyp51A, erg6, +erg6*^{WT}, *hmg1*	<0.015	2	1	1–2	2	1–4
1st+*erg6*^{A350T}	*cyp51A, erg6, +erg6*^{A350T}, *hmg1*	<0.015	2	1	0.5–1	2	4
1st+*hmg1*^{WT}	*cyp51A, erg6, hmg1, +hmg1*^{WT}	<0.015	2	1	1	2	1–4
1st+*hmg1*^{S269F}	*cyp51A, erg6, hmg1, +hmg1*^{S269F}	<0.015	1–2	0.5–1	0.5	1–2	2–4
1st+*cyp51A*^{WT}	*cyp51A, +cyp51A*^{WT}, *erg6, hmg1*	<0.015	1–2	1	1–2	2–4	0.25–4
1st+*cyp51A*^{G448S}	*cyp51A, +cyp51A*^{G448S}, *erg6, hmg1*	<0.015	1–2	4	>8	4	4

*AMPH, amphotericin B; ITCZ, itraconazole; MCFG, micafungin; MEC, minimal effective concentration; MCZ, miconazole; ND, not determined; PSCZ, posaconazole; STR, short tandem repeats; VRCZ, voriconazole.

Table 5. Characteristics of *Aspergillus fumigatus* isolates from different patients in Japan*

Isolate IFM no.	Hospital	MCFG MEC, mg/L	MIC, mg/L				Gene with mutation			STRs					
			AMPH	ITCZ	VRCZ	PSCZ	cyp51A	hmg1	erg6	3A	3B	3C	4A	4B	4C
62140	K	<0.015	2	4	8	2	–	F261_del	A75S	42	11	14	13	9	8
64258	I	<0.015	1	4	8	4	–	F390Y	V206A	26	14	17	5	11	10
64303	T	<0.015	2	2	8	–	–	–	–	34	18	22	10	11	11
63666	C	<0.015	1	1	2	1	–	–	–	29	13	15	10	9	5
63768	C	<0.015	1	8	>8	8	–	S269Y	–	29	13	15	10	9	5
63772	C	<0.015	1	2	4	8	–	–	–	29	13	15	10	9	5

*AMPH, amphotericin B; IFM, Institute of Food Microbiology (now Medical Mycology Research Center), Chiba University, Chiba City, Japan; ITCZ, itraconazole; MCFG, micafungin; MEC, minimal effective concentration; PSCZ, posaconazole; STRs, short tandem repeats; VRCZ, voriconazole; –, no mutation.

ergosterol biosynthesis. Hmg1 is a HMG-CoA reductase that catalyzes reduction of HMG-CoA to mevalonic acid and acts as a rate-limiting enzyme in ergosterol biosynthesis. *Erg6* encodes sterol methyltransferase, which catalyzes the conversion of lanosterol to eburicol in *A. fumigatus* (*26*). The mutations of *hmg1* we discovered were located in the sterol-sensing domain (SSD), responsible for the function of this enzyme. Thus, the mutation ($hmg1^{S269F}$) might affect ergosterol biosynthesis efficiency. In fact, ergosterol levels in the strain bearing $hmg1^{S269F}$ or $hmg1^{S269Y}$ were increased, which led us to presume that such mutations altered the activity of Hmg1 and resulted in hyperaccumulation of ergosterol in the cells. Although further clarification is needed, one possibility is that larger amounts of azole drugs are required to inhibit growth of the cells with an increased level of ergosterol. Among the non-*cyp51A* azole-resistant strains we studied, all the strains bearing mutation in *hmg1* showed resistance to multiple azoles. This finding also supported the idea that the ergosterol level is a determinant for the resistance against any class of azoles.

Because Hmg1 acts as a rate-limiting enzyme, we investigated the phenotypes associated with ergosterol biosynthesis in the *hmg1* mutated strain. Polyene drugs such as amphotericin B and nystatin bind to ergosterol in the plasma membrane, leading to cell death by promoting membrane leakage. Of note, the strain with mutation in Hmg1 was more sensitive to these polyene drugs, compared with the strains without the mutation, likely because the azole-resistant strain has more ergosterol in the cell membrane, and polyene can increasingly access ergosterol and damage the membrane. We also found that the azole-resistant strain with Hmg1 mutation had increased susceptibility to lovastatin. Lovastatin is a competitive inhibitor of Hmg1, so the mutation may have increased the affinity to lovastatin. However, clarification for this will still be required in future studies.

Mutation of *hmg1* has been reported in experiments designed to produce azole-resistant strains in the laboratory (*31*). In this study, the mutation in *hmg1* was identified in clinical azole-resistant isolates. The mutation was discovered in several isolates with different genetic backgrounds, which strongly suggested the importance of the mutation in azole resistance.

To analyze functions of the amino acid substitutions in Cyp51A, Hmg1, and Erg6 identified here, mutant alleles ($cyp51A^{G448S}$, $hmg1^{S269F}$, and $erg6^{A350T}$) were ectopically expressed in susceptible strains. Introducing mutated $cyp51A^{G448S}$ conferred azole resistance in the host strain even in the presence of wild-type *cyp51A*. On the other hand, mutations in *hmg1* and *erg6* did not confer azole resistance when the wild type was present. The amino acid substitution of Hmg1 is present in SSD, which is a conserved motif of membrane proteins involved in sterol sensing and acts on feedback regulation of the enzymatic reaction (*32*). Therefore, the mutated Hmg1 may be impaired in the feedback regulation. In the strain expressing $hmg1^{S269F}$, it is considered that wild-type *hmg1* can receive feedback inhibition, and thus the strain did not accumulate ergosterol and did not alter azole susceptibility. All mutations of *hmg1* found in this study are present in SSD, suggesting that mutations in SSD are important for conferring azole resistance.

In this study, we discovered novel genetic changes related to azole resistance. Several non-*cyp51*A azole-resistant clinical isolates harbor the mutation in *hmg1*, which suggested that this possible resistance mechanism is prevalent in non-*cyp51A* strains. We proposed that multiazole drug resistance is imparted by a mutation in a protein other than the target protein of azole drugs. Future elucidation of the molecular mechanism of the *hmg1* mutation will lead to a more complete understanding of the azole resistance mechanism in *A. fumigatus*.

About the Author

Dr. Hagiwara is an associate professor with the Faculty of Life and Environmental Sciences, University of Tsukuba, Japan. His research interests include azole drug resistance mechanism and fungal secondary metabolite. Dr. Arai is research assistant professor with the Medical Mycology Research Center, Chiba University, Japan. His research interests include azole drug resistance mechanism, resistance gene detection method, and fungal secondary metabolite.

References

1. Shao PL, Huang LM, Hsueh PR. Recent advances and challenges in the treatment of invasive fungal infections. Int J Antimicrob Agents. 2007;30:487–95. http://dx.doi.org/10.1016/j.ijantimicag.2007.07.019

2. Meis JF, Chowdhary A, Rhodes JL, Fisher MC, Verweij PE. Clinical implications of globally emerging azole resistance in *Aspergillus fumigatus*. Philos Trans R Soc B. 2016;371:20150460. http://dx.doi.org/10.1098/rstb.2015.0460

3. Chowdhary A, Sharma C, Meis JF. Azole-resistant aspergillosis: epidemiology, molecular mechanisms, and treatment. J Infect Dis. 2017; 216: S436–S444. https://doi.org/10.1093/infdis/jix210

4. Hagiwara D, Watanabe A, Kamei K, Goldman GH. Epidemiological and genomic landscape of azole resistance mechanisms in *Aspergillus* fungi. Front Microbiol. 2016;7:1382. http://dx.doi.org/10.3389/fmicb.2016.01382

5. Warrilow AG, Parker JE, Price CL, Nes WD, Kelly SL, Kelly DE. In vitro biochemical study of cyp51-mediated azole resistance in *Aspergillus fumigatu*s. Antimicrob Agents Chemother. 2015;59:7771–8. http://dx.doi.org/10.1128/AAC.01806-15

6. Chowdhary A, Kathuria S, Xu J, Meis JF. Emergence of azole-resistant *aspergillus fumigatus* strains due to agricultural azole use creates an increasing threat to human health. PLoS Pathog. 2013;9:e1003633. http://dx.doi.org/10.1371/journal.ppat.1003633

7. Fuhren J, Voskuil WS, Boel CH, Haas PJ, Hagen F, Meis JF, et al. High prevalence of azole resistance in *Aspergillus fumigatus* isolates from high-risk patients. J Antimicrob Chemother. 2015;70:2894–8. http://dx.doi.org/10.1093/jac/dkv177

8. Snelders E, van der Lee HA, Kuijpers J, Rijs AJ, Varga J, Samson RA, et al. Emergence of azole resistance in *Aspergillus fumigatus* and spread of a single resistance mechanism. PLoS Med. 2008;5:e219. http://dx.doi.org/10.1371/journal.pmed.0050219

9. Vermeulen E, Lagrou K, Verweij PE. Azole resistance in *Aspergillus fumigatus*: a growing public health concern. Curr Opin Infect Dis. 2013;26:493–500. http://dx.doi.org/10.1097/QCO.0000000000000005

10. Paul S, Diekema D, Moye-Rowley WS. Contributions of *Aspergillus fumigatus* ATP-binding cassette transporter proteins to drug resistance and virulence. Eukaryot Cell. 2013;12:1619–28. http://dx.doi.org/10.1128/EC.00171-13

11. Fraczek MG, Bromley M, Buied A, Moore CB, Rajendran R, Rautemaa R, et al. The cdr1B efflux transporter is associated with non-cyp51a-mediated itraconazole resistance in *Aspergillus fumigatus*. J Antimicrob Chemother. 2013;68:1486–96. http://dx.doi.org/10.1093/jac/dkt075

12. Hagiwara D, Miura D, Shimizu K, Paul S, Ohba A, Gonoi T, et al. A novel zn2-cys6 transcription factor atrr plays a key role in an azole resistance mechanism of *Aspergillus fumigatus* by co-regulating *cyp51A* and *cdr1B* expressions. PLoS Pathog. 2017;13:e1006096. http://dx.doi.org/10.1371/journal.ppat.1006096

13. Camps SM, Dutilh BE, Arendrup MC, Rijs AJ, Snelders E, Huynen MA, et al. Discovery of a *hapE* mutation that causes azole resistance in *Aspergillus fumigatus* through whole genome sequencing and sexual crossing. PLoS One. 2012;7:e50034. http://dx.doi.org/10.1371/journal.pone.0050034

14. Gsaller F, Hortschansky P, Furukawa T, Carr PD, Rash B, Capilla J, et al. Sterol biosynthesis and azole tolerance is governed by the opposing actions of SrbA and the CCAAT binding complex. PLoS Pathog. 2016;12:e1005775. http://dx.doi.org/10.1371/journal.ppat.1005775

15. Hagiwara D, Takahashi H, Watanabe A, Takahashi-Nakaguchi A, Kawamoto S, Kamei K, et al. Whole-genome comparison of *Aspergillus fumigatus* strains serially isolated from patients with aspergillosis. J Clin Microbiol. 2014;52:4202–9. http://dx.doi.org/10.1128/JCM.01105-14

16. Hagiwara D, Watanabe A, Kamei K. Sensitisation of an azole-resistant *Aspergillus fumigatus* strain containing the Cyp51A-related mutation by deleting the SrbA gene. Sci Rep. 2016; 6:38833. http://dx.doi.org/10.1038/srep38833

17. Bolger AM, Lohse M, Usadel B. Trimmomatic: a flexible trimmer for Illumina sequence data. Bioinformatics. 2014;30:2114–20. http://dx.doi.org/10.1093/bioinformatics/btu170

18. Kajitani R, Toshimoto K, Noguchi H, Toyoda A, Ogura Y, Okuno M, et al. Efficient de novo assembly of highly heterozygous genomes from whole-genome shotgun short reads. Genome Res. 2014;24:1384–95. http://dx.doi.org/10.1101/gr.170720.113

19. Stanke M, Morgenstern B. AUGUSTUS: a web server for gene prediction in eukaryotes that allows user-defined constraints. Nucleic Acids Res. 2005;33(Web Server):W465–W467. http://dx.doi.org/10.1093/nar/gki458

20. Li H, Handsaker B, Wysoker A, Fennell T, Ruan J, Homer N, et al.; 1000 Genome Project Data Processing Subgroup. The sequence alignment/map format and SAMtools. Bioinformatics. 2009;25:2078–9. http://dx.doi.org/10.1093/bioinformatics/btp352

21. Suzuki S, Horinouchi T, Furusawa C. Prediction of antibiotic resistance by gene expression profiles. Nat Commun. 2014; 5:5792. http://dx.doi.org/10.1038/ncomms6792

22. Tenaillon O, Rodríguez-Verdugo A, Gaut RL, McDonald P, Bennett AF, Long AD, et al. The molecular diversity of adaptive convergence. Science. 2012;335:457–61. http://dx.doi.org/ 10.1126/science.1212986

23. Cingolani P, Platts A, Wang L, Coon M, Nguyen T, Wang L, et al. A program for annotating and predicting the effects of single nucleotide polymorphisms, SnpEff. Fly (Austin). 2012;6:80–92. http://dx.doi.org/10.4161/fly.19695

24. Qiao J, Kontoyiannis DP, Wan Z, Li R, Liu W. Antifungal activity of statins against *Aspergillus* species. Med Mycol. 2007;45:589–93. http://dx.doi.org/10.1080/13693780701397673

25. Arthington-Skaggs BA, Warnock DW, Morrison CJ. Quantitation of Candida albicans ergosterol content improves the correlation between in vitro antifungal susceptibility test results and in vivo outcome after fluconazole treatment in a murine model of invasive candidiasis. Antimicrob Agents Chemother. 2000;44:2081–5. http://dx.doi.org/10.1128/AAC.44.8.2081-2085.2000

26. Alcazar-Fuoli L, Mellado E, Garcia-Effron G, Lopez JF, Grimalt JO, Cuenca-Estrella JM, et al. Ergosterol biosynthesis pathway in Aspergillus fumigatus. Steroids. 2008;73:339–47. http://dx.doi.org/10.1016/j.steroids.2007.11.005

27. Krishnan Natean S, Wu W, Cutright JL, Chandrasekar PH. In vitro–in vivo correlation of voriconazole resistance due to G448S mutation (cyp51A gene) in Aspergillus fumigatus. Diagn Microbiol Infect Dis. 2012;74:272–277.

28. Chowdhary A, Sharma C, Hagen F, Meis JF. Exploring azole antifungal drug resistance in Aspergillus fumigatus with special reference to resistance mechanisms. Future Microbiol. 2014; 9:697–711. http://dx.doi.org/10.2217/fmb.14.27

29. Moye-Rowley WS. Multiple mechanisms contribute to the development of clinically significant azole resistance in *Aspergillus fumigatus*. Front Microbiol. 2015;6:70. http://dx.doi.org/10.3389/fmicb.2015.00070

30. Wei X, Chen P, Gao R, Li Y, Zhang A, Liu F, et al. Screening and characterization of a non-cyp51A mutation in an *Aspergillus fumigatus* cox10 strain conferring azole resistance.

Antimicrob Agents Chemother. 2016;61:pii: e02101-16. http://dx.doi.org//10.1128/AAC.02101-16

31. Zhang J, van den Heuvel J, Debets AJM, Verweij PE, Melchers WJG, Zwaan BJ, et al. Evolution of cross-resistance to medical triazoles in Aspergillus fumigatus through selection pressure of environmental fungicides. Proc Biol Sci. 2017; 284:20170635. http://dx/doi.org/10.1098/rspb.2017.0635

32. Theesfeld CL, Pourmand D, Davis T, Garza RM, Hampton RY. The sterol-sensing domain (SSD) directly mediates signal-regulated endoplasmic reticulum-associated degradation (ERAD) of 3-hydroxy-3-methylglutaryl (HMG)-CoA reductase isozyme Hmg2. J Biol Chem. 2011;286:26298–307. http://dx.doi.org/10.1074/jbc.M111.244798

Address for correspondence: Akira Watanabe, Chiba University, Medical Mycology Research Center, 1-8-1 Inohana, Chuo-ku, Chiba City, Chiba, Japan; email: fewata@faculty.chiba-u.jp

Follow the EID journal on Twitter and get the most current information from Emerging Infectious Diseases.

Multilocus Sequence Typing of *Mycoplasma pneumoniae*, Japan, 2002–2016

Mariko Ando,[1] Miyuki Morozumi,[1] Yoko Adachi, Kimiko Ubukata, Satoshi Iwata

In Japan, *Mycoplasma pneumoniae* resistance to macrolides is high. To compare sequence types (STs) of susceptible and resistant isolates, we performed multilocus sequence typing for 417 isolates obtained in Japan during 2002–2016. The most prevalent ST overall was ST3, for macrolide-resistant was ST19, and for macrolide-susceptible were ST14 and ST7.

Macrolide-resistant *Mycoplasma pneumoniae* was first isolated in Japan in 2000 (*1*). Macrolide-resistant *M. pneumoniae* is highly prevalent in Asia and has been reported from several parts of the world (*2–7*). During a 2011–2012 outbreak in Japan, the resistance rate was as high as 90% (*8*). Molecular typing methods have been developed for *M. pneumoniae* and include multilocus variable-number tandem-repeat analysis (MLVA), P1 typing, and others (*9*). In recent years, multilocus sequence typing (MLST) involving molecular analysis of 7–8 housekeeping genes has been applied to various bacterial pathogens (*10,11*). In 2014, MLST for *M. pneumoniae* was devised by Brown et al. (*12*). Using this MLST method for *M. pneumoniae*, we compared sequence types (STs) of macrolide-susceptible and macrolide-resistant *M. pneumoniae* isolates from Japan and examined their evolutionary relationships. As is commonly performed for this pathogen, we also typed the P1 adhesin gene.

The Study

Using the random function of Excel 2010 (Microsoft, Redmond, CA, USA), we randomly selected 417 *M. pneumoniae* isolates (372 from children, 45 from adults) from 1,084 isolates obtained from patients throughout Japan who had had pneumonia or bronchitis during 2002–2016. Samples were not collected in 2014. The strains were isolated from clinical samples sent from 31 medical institutions in Japan to the Department of Infectious Diseases at Keio University School of Medicine in Tokyo. Of these strains, 232 (55.6%) were macrolide-susceptible *M. pneumoniae* and 185 (44.4%) were macrolide-resistant *M. pneumoniae* that

Author affiliations: Keio University School of Medicine, Tokyo, Japan (M. Ando, M. Morozumi, Y. Adachi, K. Ubukata, S. Iwata); National Cancer Center Hospital, Tokyo (S. Iwata)

had 23S rRNA point mutations. According to *M. pneumoniae* numbering, these mutations were A2063G (n = 163), A2063T (n = 10), A2064G (n = 10), A2063C (n = 1), or C2617A (n = 1). We used microdilution methods with pleuropneumonia-like organism broth (Difco, Detroit, MI, USA) to determine MICs for 6 antimicrobial agents against these strains of macrolide-susceptible and macrolide-resistant *M. pneumoniae* (Table 1).

For MLST analysis, we sequenced 8 housekeeping genes (*ppa*, *pgm*, *gyrB*, *gmk*, *glyA*, *atpA*, *arcC*, and *adk*) in each strain by using the 8 primer sets described in the MLST database (https://pubmlst.org/mpneumoniae/) (*12*). New alleles and STs were registered in the *M. pneumoniae* MLST database. To determine relationships between STs, we conducted clonal complex (CC) analysis by using eBURST version 3.1 (http://eburst.mlst.net/v3/mlst_datasets/). Frequency analysis was performed with the Fisher exact test.

Typing of the P1 adhesin gene in *M. pneumoniae* was performed as previously described (*13*). After PCR, the purified DNA products were treated with a restriction enzyme (*Hae*III) for 1 hour. The standard stains M129 (ATCC 29342) and FH (ATCC 15531) were used as controls.

Among macrolide-susceptible *M. pneumoniae* isolates, the most prevalent STs were ST3 (52.6%), ST14 (28.4%), and ST7 (6.9%) (Figure 1). Among macrolide-resistant isolates, the most prevalent ST was also ST3 (74.6%), but the next most prevalent were ST19 (11.4%) and ST14 (4.9%). ST7 was more prevalent in macrolide-susceptible than in macrolide-resistant isolates (p = 0.008); ST19 was more prevalent in macrolide-resistant isolates (p<0.001). Although ST14 was prevalent among macrolide-susceptible *M. pneumoniae*, it also was represented among macrolide-resistant *M. pneumoniae*, associated with the 23S rRNA mutation A2064G. We did not identify any differences in ST frequencies between isolates from children and adults or between areas in Japan.

When we compared the relationship between year of strain isolation and ST (Table 2), ST3 accounted for most macrolide-susceptible *M. pneumoniae*, but ST14 also was present in every year; in other words, 2 STs were consistently common among macrolide-susceptible

---

[1]These authors contributed equally to this article.

Table 1. Antimicrobial activity of 6 antimicrobial agents against 417 *Mycoplasma pneumoniae* strains, Japan, 2002–2016*

Antimicrobial agent and *M. pneumoniae* macrolide-resistance level	MIC, µg/mL†		
	50%	90%	Range
Clarithromycin			
Susceptible	0.0039	0.0078	0.00195 to 0.031
Resistant	64	>64	0.5 to >64
Azithromycin			
Susceptible	0.00049	0.00098	0.00012 to 0.00195
Resistant	64	64	0.031 to >64
Minocycline			
Susceptible	0.5	1	0.031 to 1
Resistant	0.25	1	0.063 to 1
Doxycycline			
Susceptible	0.5	0.5	0.063 to 0.5
Resistant	0.25	0.5	0.125 to 0.5
Levofloxacin			
Susceptible	0.5	1	0.125 to 1
Resistant	0.5	1	0.5 to 1
Tosufloxacin			
Susceptible	0.5	0.5	0.25 to 1
Resistant	0.5	0.5	0.25 to 2

*Macrolide-susceptible *M. pneumoniae* = 232; macrolide-resistant *M. pneumoniae* = 185.
†MIC ranges for macrolides were 16 to >64 µg/mL for A2063G (n = 163) and A2064G (n = 10) and >64 µg/mL for A2063C (n = 1). MIC for azithromycin was affected by the mutations A2063T (1–4 µg/mL) (n = 10) and C2617A (0.031 µg/mL) (n = 1). MIC for clarithromycin was affected by C2617A (0.5 µg/mL). MICs for quinolone and tetracycline in both macrolide-susceptible and macrolide-resistant *M. pneumoniae* were almost the same.

M. pneumoniae. In 2016, infection with macrolide-susceptible *M. pneumoniae,* especially ST7 and ST14, was epidemic. Among macrolide-resistant isolates, most were ST3. Although ST3 was identified more frequently in macrolide-susceptible isolates during 2002–2006, its identification in macrolide-resistant isolates has increased rapidly since then, and macrolide-resistant ST3 became more common in 2008. ST19 has been identified since the *M. pneumoniae* epidemic in 2006.

Data showing the relationship between CC and STs according to eBURST (Figure 2) include the 417 strains in this study and 62 strains registered to the MLST database from other countries. Of the 2 CC clusters, the center of CC1 was ST3, from which new STs including ST19 and ST17 arose with ≥1 alleles mutated. CC1 appears

more frequently in macrolide-resistant *M. pneumoniae* (p<0.001). The center of CC2 was ST2, and almost all strains in Japan belonged to ST7 and ST14. ST22 did not belong to either CC1 or CC2, but 5 of 8 of its alleles were identical to those of CC1. In certain areas of Japan, ST22 has emerged in macrolide-resistant and macrolide-susceptible *M. pneumoniae*.

P1 typing analysis indicated that *M. pneumoniae* STs belonging to CC1 and ST22 were type 1, and STs belong to CC2 were type 2. ST14 and ST15 were type 2a, which is a subtype of P1 type 2.

Conclusions
Molecular analysis by MLST is conducted commonly for various bacterial pathogens worldwide but not for
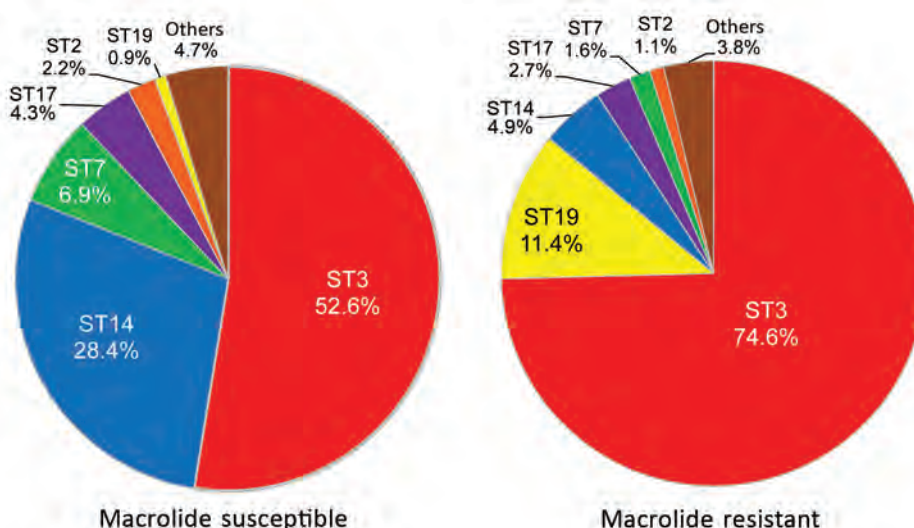
Figure 1. Multilocus sequence typing results for 232 macrolide-susceptible and 185 macrolide-resistant *Mycoplasma pneumoniae* isolates, Japan, 2002–2016. Ten STs were identified for macrolide-susceptible and 12 STs for macrolide-resistant *M. pneumoniae*. ST, sequence type.

Table 2. Relationship between year isolated and ST among 232 macrolide-susceptible and 185 macrolide-resistant *Mycoplasma pneumonia* isolates, Japan, 2002–2016*

| | Macrolide-susceptible *M. pneumoniae* | | | | | | | | Macrolide-resistant *M. pneumoniae* | | | | | | | | |
| | CC1 | | | CC2 | | | Other | | CC1 | | | CC2 | | | Other | | |
Year	ST 3	ST 17	ST 19	ST 2	ST 7	ST 14	ST	Subtotal	ST 3	ST 17	ST 19	ST 2	ST 7	ST 14	ST	Subtotal	Total
2002	8			3	3	10	3	27						2		2	29
2003	13				3	2	1	19	3			2				5	24
2004	13					2	2	17	4					1		5	22
2005	12				1	3		16	3						1	4	20
2006	24	2		1		3	2	32	15		5				2	22	54
2007	10	4		1		8		23	12		7					19	42
2008	7	1				7		15	15	2				1		18	33
2009	8					2		10	12		1					13	23
2010	4		1			2	3	10	8		4				1	13	23
2011	5	1				1		7	13		2			3	1	19	26
2012	8		1			2		11	16	3	2					21	32
2013	3	1						4						1		1	5
2015	2				1	5		8	25							25	33
2016	5	1			8	19		33	12				3	1	2	18	51
Total	122	10	2	5	16	66	11	232	138	5	21	2	3	9	7	185	417
%	52.6	4.3	0.9	2.2	6.9	28.4	4.7	100	74.6	2.7	11.4	1.1	1.6	4.9	3.8	100	

*CC, clonal complex; ST, sequence type.

M. pneumoniae. We identified differences in STs between macrolide-susceptible and macrolide-resistant *M. pneumoniae* in Japan. Of the STs noted among isolates from 4 countries (the United Kingdom, the United States, China, and France), ST3 and ST14 were identified often in Japan, but other STs were not identified in Japan (Figure 2). During 1977–2011, the most prevalent *M. pneumoniae* STs in England and Wales were ST2, ST3, ST4, and ST11 (*14*). In this respect, STs reported from Japan show patterns quite different from those from other countries. The most prevalent STs in Japan were ST3, ST14, ST19, and ST7. In particular, ST3 of macrolide-susceptible *M. pneumoniae* was the most prevalent during 2002–2006, the early

period of our surveillance, but ST3 of macrolide-resistant *M. pneumoniae*, with a point mutation of A2063G in the 23S rRNA gene, increased rapidly since an outbreak of *M. pneumoniae* infection in 2006, and macrolide-resistant *M. pneumoniae* became most common after 2008. This change toward resistance occurred in parallel with increased use of macrolides in children. ST14 and ST7 were more prevalent among macrolide-susceptible than macrolide-resistant *M. pneumoniae*; ST19 was prevalent among macrolide-resistant *M. pneumoniae*.

We detected 2 types of the P1 adhesin gene, types 1 and 2 (which includes 2a), and analyzed them in terms of STs. Recent studies have identified various subtypes
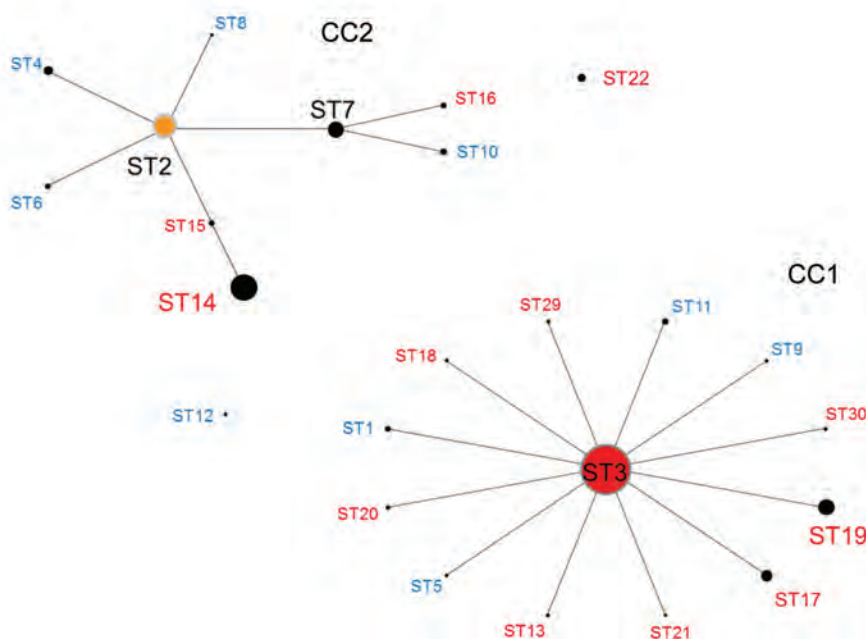
Figure 2. Relationship between CC and ST for *Mycoplasma pneumoniae* isolates by eBURST version 3.1 analysis (http://eburst.mlst.net/v3/mlst_datasets/). Data included 417 strains from Japan, 2002–2016, and 62 strains isolated from the United Kingdom, the United States, China, and France. For all isolates, 24 STs were identified. The size of each circle is proportional to the number of isolates for each ST. Red indicates isolates detected in Japan only; blue indicates isolates detected in the United Kingdom, the United States, China, and France but not Japan; black indicates isolates detected in all 5 countries. CC, clonal complex; ST, sequence type.

through comprehensive genomic comparisons (*15*). Similar to the results of MLST, P1 gene types have shown diversification. We did not conduct MLVA in this study, but a previous study found CC1 and CC2 to differ in MLVA type: CC1 contained MLVA type 4572, and CC2 contained MLVA types 3662 and 3562 (*12*).

In summary, macrolide-resistant *M. pneumoniae* are emerging and increasing. Surveillance of macrolide-resistant *M. pneumoniae* based on molecular epidemiology, including STs and P1 adhesion gene identifications, are necessary to clarify worldwide trends and address public health concerns.

About the Authors

Ms. Ando is a graduate student in the Department of Infectious Diseases, Keio University School of Medicine. Dr. Morozumi is an assistant professor at Keio University School of Medicine; her research interests include molecular epidemiology as well as severe infections caused by *Streptococcus agalactiae* and *M. pneumoniae*.

References

1. Okazaki N, Narita M, Yamada S, Izumikawa K, Umetsu M, Kenri T, et al. Characteristics of macrolide-resistant *Mycoplasma pneumoniae* strains isolated from patients and induced with erythromycin in vitro. Microbiol Immunol. 2001;45:617–20. http://dx.doi.org/10.1111/j.1348-0421.2001.tb01293.x
2. Averbuch D, Hidalgo-Grass C, Moses AE, Engelhard D, Nir-Paz R. Macrolide resistance in *Mycoplasma pneumoniae*, Israel, 2010. Emerg Infect Dis. 2011;17:1079–82. http://dx.doi.org/10.3201/eid1706.101558
3. Eshaghi A, Memari N, Tang P, Olsha R, Farrell DJ, Low DE, et al. Macrolide-resistant *Mycoplasma pneumoniae* in humans, Ontario, Canada, 2010–2011. Emerg Infect Dis. 2013;19:19. http://dx.doi.org/10.3201/eid1909.121466
4. Li X, Atkinson TP, Hagood J, Makris C, Duffy LB, Waites KB. Emerging macrolide resistance in *Mycoplasma pneumoniae* in children: detection and characterization of resistant isolates. Pediatr Infect Dis J. 2009;28:693–6. http://dx.doi.org/10.1097/INF.0b013e31819e3f7a
5. Morozumi M, Iwata S, Hasegawa K, Chiba N, Takayanagi R, Matsubara K, et al.; Acute Respiratory Diseases Study Group.
Increased macrolide resistance of *Mycoplasma pneumoniae* in pediatric patients with community-acquired pneumonia. Antimicrob Agents Chemother. 2008;52:348–50. http://dx.doi.org/10.1128/AAC.00779-07
6. Pereyre S, Charron A, Renaudin H, Bébéar C, Bébéar CM. First report of macrolide-resistant strains and description of a novel nucleotide sequence variation in the P1 adhesin gene in *Mycoplasma pneumoniae* clinical strains isolated in France over 12 years. J Clin Microbiol. 2007;45:3534–9. http://dx.doi.org/10.1128/JCM.01345-07
7. Zhao F, Liu G, Wu J, Cao B, Tao X, He L, et al. Surveillance of macrolide-resistant *Mycoplasma pneumoniae* in Beijing, China, from 2008 to 2012. Antimicrob Agents Chemother. 2013;57:1521–3. http://dx.doi.org/10.1128/AAC.02060-12
8. Okada T, Morozumi M, Tajima T, Hasegawa M, Sakata H, Ohnari S, et al. Rapid effectiveness of minocycline or doxycycline against macrolide-resistant *Mycoplasma pneumoniae* infection in a 2011 outbreak among Japanese children. Clin Infect Dis. 2012;55:1642–9. http://dx.doi.org/10.1093/cid/cis784
9. Brown RJ, Spiller BO, Chalker VJ. Molecular typing of *Mycoplasma pneumoniae*: where do we stand? Future Microbiol. 2015;10:1793–5. http://dx.doi.org/10.2217/fmb.15.96
10. Enright MC, Spratt BG. Multilocus sequence typing. Trends Microbiol. 1999;7:482–7. http://dx.doi.org/10.1016/S0966-842X(99)01609-1
11. Skaare D, Anthonisen IL, Caugant DA, Jenkins A, Steinbakk M, Strand L, et al. Multilocus sequence typing and *ftsI* sequencing: a powerful tool for surveillance of penicillin-binding protein 3-mediated beta-lactam resistance in nontypeable *Haemophilus influenzae*. BMC Microbiol. 2014;20;14:131. http://dx.doi.org/10.1186/1471-2180-14-131
12. Brown RJ, Holden MTG, Spiller OB, Chalker VJ. Development of a multilocus sequence typing scheme for molecular typing of *Mycoplasma pneumoniae*. J Clin Microbiol. 2015;53:3195–203. http://dx.doi.org/10.1128/JCM.01301-15
13. Kenri T, Taniguchi R, Sasaki Y, Okazaki N, Narita M, Izumikawa K, et al. Identification of a new variable sequence in the P1 cytadhesin gene of *Mycoplasma pneumoniae*: evidence for the generation of antigenic variation by DNA recombination between repetitive sequences. Infect Immun. 1999;67:4557–62.
14. Brown RJ, Nguipdop-Djomo P, Zhao H, Stanford E, Spiller OB, Chalker VJ. *Mycoplasma pneumoniae* epidemiology in England and Wales: a national perspective. Front Microbiol. 2016;7:157. http://dx.doi.org/10.3389/fmicb.2016.00157
15. Diaz MH, Desai HP, Morrison SS, Benitez AJ, Wolff BJ, Caravas J, et al. Comprehensive bioinformatics analysis of *Mycoplasma pneumoniae* genomes to investigate underlying population structure and type-specific determinants. PLoS One. 2017;14:12.

Address for correspondence: Satoshi Iwata, Keio University School of Medicine, Department of Infectious Diseases, 35 Shinanomachi, Shinjuku-ku, Tokyo 160-8582, Japan; and National Cancer Center Hospital, Department of Infectious Diseases, 5-1-1 Tsukiji, Chuo-ku, Tokyo 104-0045, Japan; email: siwata@a8.keio.jp

Emerging Enteroviruses Causing Hand, Foot and Mouth Disease, China, 2010–2016

Yu Li,[1] Zhaorui Chang,[1] Peng Wu,[1]
Qiaohong Liao, Fengfeng Liu, Yaming Zheng,
Li Luo, Yonghong Zhou, Qi Chen,
Shuanbao Yu, Chun Guo, Zhenhua Chen,
Lu Long, Shanlu Zhao, Bingyi Yang,
Hongjie Yu,[2] Benjamin J. Cowling

Coxsackievirus A6 emerged as one of the predominant causative agents of hand, foot and mouth disease epidemics in many provinces of China in 2013 and 2015. This virus strain accounted for 25.9% of mild and 15.2% of severe cases in 2013 and 25.8% of mild and 16.9% of severe cases in 2015.

Hand, foot and mouth disease (HFMD) is a common childhood infectious disease caused by enteroviruses (*1*). In China, HFMD cases must be reported to the Notifiable Infectious Diseases Reporting Information System. Apart from clinical and demographic information, case notifications also include etiologic results, if available, classified into 3 categories: enterovirus A71 (EV-A71), coxsackievirus (CV) A16, and other enteroviruses. However, not all cases have etiologic results, the Notifiable Infectious Diseases Reporting Information System (NIDRIS) does not indicate cases that tested negative for enteroviruses, and testing methods vary among hospitals (*2*). To capture more information on the etiologic spectrum of HFMD in China, a laboratory surveillance network has been established in provincial-level centers for disease control and prevention (CDCs). EV-A71 and CV-A16 were previously believed to be the main causative viruses for HFMD in Asia, but several studies have suggested that other enteroviruses appear

to be increasing since 2008 (*3–9*). Nevertheless, these past studies in China could not provide an overview at the national level because of limitations in geographic locations or study settings; furthermore, none of them systematically examined proportions of specific enteroviruses testing positive among tested HFMD cases. We analyzed data from this laboratory network to examine causative pathogens of HFMD cases and epidemiologic differences associated with various pathogens.

The Study

Since June 2009, clinical specimens must be collected from all severe HFMD cases, and the first 5 reported mild cases (case classification criteria in the online Technical Appendix, https://wwwnc.cdc.gov/EID/article/24/10/17-1953-Techapp1.pdf) in each county of China every month and are tested for enteroviruses at local CDCs using PCR (online Technical Appendix) (*10*). Test results are characterized as negative for enterovirus or positive for EV-A71, CV-A16, or other enteroviruses. For specimens testing positive for other enteroviruses, further serotyping is not conducted as a routine practice, but some local CDCs with more laboratory capacity may select a subset of these specimens to test on the serotype at their own discretion, especially when the proportion of other enteroviruses detected was relatively high.

We collected individual laboratory data during January 2010–December 2016 from 23 provincial CDCs (online Technical Appendix Figure 1). In these provinces, HFMD case notifications accounted for 88.4% of HFMD cases notified in China overall. We analyzed virus serotypes in combination with sex, age, and clinical severity of each case. The dataset includes 693,580 individual illness episodes in the 23 provinces; 7,632–59,507 (median 31,317) episodes per province were reported. Clinical samples were collected from each illness onset, including throat swabs (374,685; 54.0%), feces (153,947; 22.2%), rectal swabs (129,837; 18.7%), and other specimens (35,111; 5.1%) such as vesicular or cerebrospinal fluid.
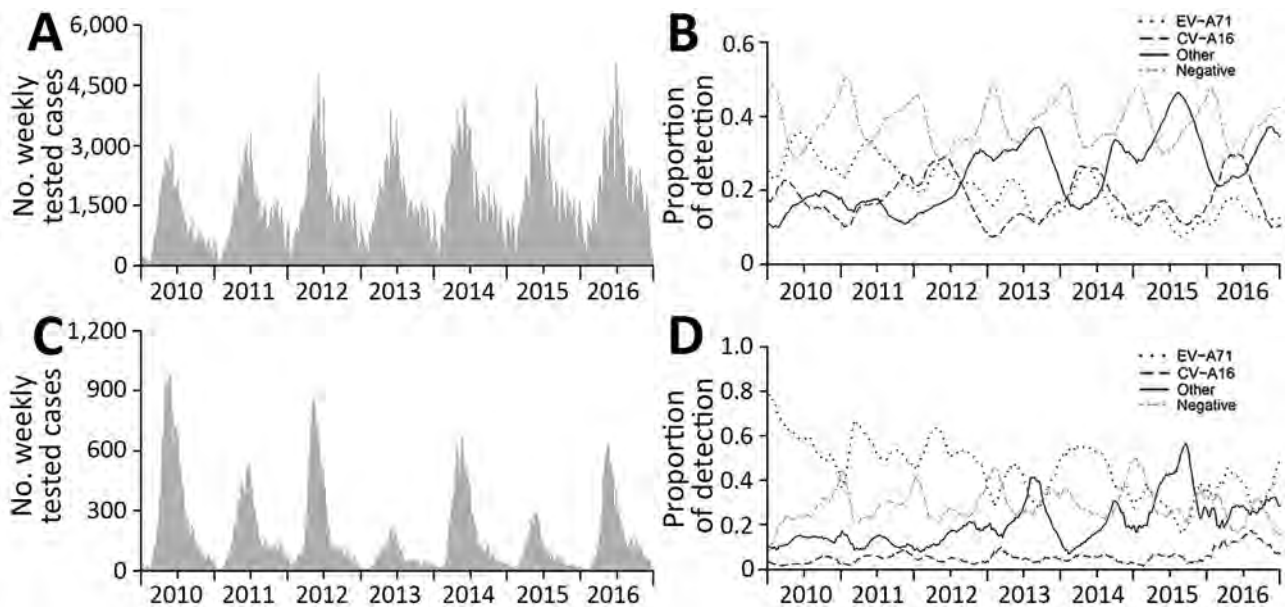
Weekly proportions of positive enteroviruses (1 – enterovirus-negative specimens divided by all specimens collected for testing) were generally lower in mild cases

Author affiliations: Chinese Center for Disease Control and Prevention. Beijing, China (Y. Li, Z. Chang, Q. Liao, F. Liu, Y. Zheng, L. Luo, S. Yu, H. Yu); The University of Hong Kong, Hong Kong, China (Y. Li, P. Wu, B. Yang, B.J. Cowling); Fudan University, Shanghai, China (Y. Zhou, H. Yu); Hubei Center for Disease Prevention and Control, Wuhan, China (Q. Chen); Huazhong University of Science and Technology, Wuhan, China (C. Guo); Chengdu Center for Disease Prevention and Control, Chengdu, China (Z. Chen); Sichuan University, Chengdu, China (L. Long); Hunan Center for Disease Prevention and Control, Changsha, China (S. Zhao)

[1]These authors contributed equally to this article.

[2]Current affiliation: Fudan University School of Public Health, Shanghai, China.

Figure 1. Weekly proportions of enteroviruses detection by serotype among hand, foot and mouth disease cases, January 2010–December 2016, China: A) number of tested mild cases; B) proportions of serotypes among mild cases C) number of tested severe cases; D) proportions of serotypes among severe cases.

Table. Serotypes of non–EV-A71 and non–CV-A16 enteroviruses among HFMD cases, by clinical severity, 2013 and 2015, China*

	2013, no. (%)		2015, no. (%)	
Test result	Mild, n = 87,226	Severe, n = 3,837	Mild, n = 99,461	Severe, n = 4,712
EV negative	32,801 (37.60)	1,100 (28.67)	35,167 (35.36)	1,273 (27.02)
EV-A71	15,503 (17.77)	1,557 (40.58)	11,800 (11.86)	1,352 (28.69)
CV-A16	10,811 (12.39)	197 (5.13)	13,959 (14.03)	265 (5.62)
Other enteroviruses	28,111 (32.23)	983 (25.62)	38,535 (38.74)	1,822 (38.67)
Further serotyping of other enteroviruses				
Total	Mild, n = 3,260†	Severe, n = 42‡	Mild, n = 2,474§	Severe, n = 71¶
CV-A6	2,620 (80.37)	28 (66.67)	1,471 (59.46)	31 (43.70)
CV-A10	176 (5.40)	4 (9.52)	104 (4.20)	#
CV-A2	22 (0.67)	1 (2.38)	5 (0.20)	#
CV-A5	9 (0.28)	1 (2.38)	2 (0.08)	#
CV-A4	2 (0.06)	#	9 (0.36)	#
ECV-6	9 (0.28)	#	#	#
CV-B4	13 (0.4)	#	#	#
ECV-25	8 (0.25)	#	#	#
CV-A12	5 (0.15)	#	#	#
CV-B5	5 (0.15)	#	#	#
CV-B2	4 (0.12)	#	1 (0.04)	#
ECV-7	4 (0.12)	#	#	#
ECV-9	3 (0.09)	#	#	#
CV-A8	1 (0.03)	#	3 (0.12)	#
CV-A14	2 (0.06)	#	#	#
CV-A21	2 (0.06)	#	#	#
ECV-12	2 (0.06)	#	#	#
CV-B1	2 (0.06)	#	#	#
ECV-30	1 (0.03)	#	1 (0.04)	#
Other	6 (0.18)**	#	#	#
Untyped	364 (11.37)	8 (19.05)	878 (35.49)	40 (56.34)

*CV, coxsackievirus; ECV, echovirus; EV, enterovirus.
†Results are based on data from Beijing, Fujian, Guangdong, Guangxi, Heilongjiang, Henan, Hubei, Jiangsu, Jilin, Shanxi, Sichuan, Shandong, Tianjin, Xinjiang, and Yunnan provinces.
‡Results are based on data from Fujian, Guangdong, Guangxi, Henan, and Shanxi provinces.
§Results are based on data from Beijing, Fujian, Guangxi, Heilongjiang, Jiangsu, Sichuan, Tianjin, and Zhejiang provinces.
¶Results are based on data from Guangdong and Jiangsu provinces.
#The serotypes were not detected, but might be included in the untyped specimens because of laboratory capacity restrictions.
**Other serotypes include CV-A20, CV-A24, ECV-1, ECV-96, Polio1, and Polio2, with 1 of each serotype detected.

(median 62.4%, range 42.0%–74.0%) than in severe cases (median 73.1%, range 27.3%–100%) and showed seasonal variations: peaks in April–May and low levels in December–January (Figure 1). The highest weekly proportion of EV-A71 detections among mild cases was 37.7% in 2010; a decreasing trend was observed thereafter. EV-A71 vaccine probably had little effect on the change in EV-A71 detections because it was not available until March 2016 and was not included in the routine vaccination program. In contrast, weekly proportions of detection of other enteroviruses generally increased with time, reaching a maximum of 48.4% in 2015. The proportion of cases positive for CV-A16 was relatively stable at ≈20% across the years, following a similar temporal trend to that of EV-A71. However, detections of different serotypes of enteroviruses generally demonstrated a similar temporal pattern among severe cases as among mild cases, except that the proportion of CV-A16 was relatively low, fluctuating at ≈5% across the period (Figure 1). Proportions of detection generally declined with age for other enteroviruses, whereas EV-A71 and CV-A16 showed an increasing trend with age, particularly in mild cases (online Technical Appendix Figure 2).

EV-A71 and CV-A16 predominated in 2010–2012, 2014, and 2016, but other enteroviruses were predominant in 2013 and 2015. In those 2 years, further serotyping on other enteroviruses was widely conducted (Table). In 2013, a total of 3,260 (11.6% of 28,111 specimens positive for other enteroviruses) specimens collected from mild cases and 42 (4.3% of 983) specimens collected from severe cases underwent further serotyping; in 2015, a total of 2,474 (6.4% of 38,535) specimens collected from mild cases and 71 (3.9% of 1,822) specimens collected from severe cases underwent further serotyping. The serotyping results showed that, of mild cases infected with other enteroviruses, 80% in 2013 and 59% in 2015 were infected with CV-A6; for severe cases, 67% in 2013 and 44% in 2015 were infected with CV-A6. By multiplying the proportion of other enteroviruses by the proportion of CV-A6 among other enteroviruses, we estimated that CV-A6 accounted for 25.9% of mild cases and 15.2% of severe cases in 2013 and 25.8% of mild cases and 16.9% of severe cases in 2015. This result at the national level supports regional and subregional studies in China (3–9), suggesting that CV-A6 emerged as a main causative agent of HFMD in 2013 and 2015, but detections of CV-A6 were still low in some provinces of southwestern and northeastern China (Figure 2; online Technical Appendix Figure 3). D3 is the predominant subgenotype for CV-A6 (11). During the same period, CV-A10 accounted for 4.2%–9.5% of other enteroviruses. Serotypes other than CV-A6 and CV-A10, including CV-A2, CV-A5, CV-A4, CV-B4, echovirus 6 and -25, and others, accounted for a small proportion (0.03%–2.4%) of specimens tested for further serotyping.

These rare serotypes could possibly become prevalent in the future because of accumulative immunity to the prevalent enteroviruses, the potential replacement effect induced by vaccination programs against predominant enteroviruses, or both. One limitation of serotyping results of other enteroviruses is that they tend to reflect those of areas with more intensive HFMD transmission, because local CDCs generally select areas where the most cases are detected for further serotyping.

We found that detection proportions of other enteroviruses were generally negatively associated with that of EV-A71 in mild and severe cases (Pearson correlation coefficient –0.73 for mild cases and –0.70 for severe cases) and CV-A16 in mild cases (Pearson correlation coefficient –0.52) (Figure 1). This result might indicate competitive interactions between other enteroviruses and EV-A71 or CV-A16, which should be considered when evaluating the effect of introducing a new enterovirus vaccine, especially when the proportion of other enteroviruses is increasing. The epidemiologic modeling study suggested that cross-protection between EV-A71 and CV-A16 exists for nearly 7 weeks, on average, in the context of natural infections (12). However, vaccine trials reported that monovalent EV-A71 vaccine failed to protect against CV-A16–associated HFMD (13). Similarly, whether cross protection exists between EV-A71 and other enteroviruses, such as CV-A6 and CV-A10, remains poorly understood to date, although limited studies have been more indicative of a lack of cross protection between EV-A71 and coxsackieviruses including CV-A6 (14,15).

Conclusions

Data from national laboratory network surveillance of HFMD in China show that detection of enteroviruses other than EV-71 and CV-A16 has been increasing in both mild and severe cases and that CV-A6 has been emerging as another predominant serotype recently, but not in every province. Serotyping of individual enteroviruses apart from currently tested EV-71 and CV-A16 is suggested for routine virologic surveillance. Further studies may be needed to investigate potential cross immunity between EV-A71 and other enteroviruses such as CV-A6, CV-A10, and others.
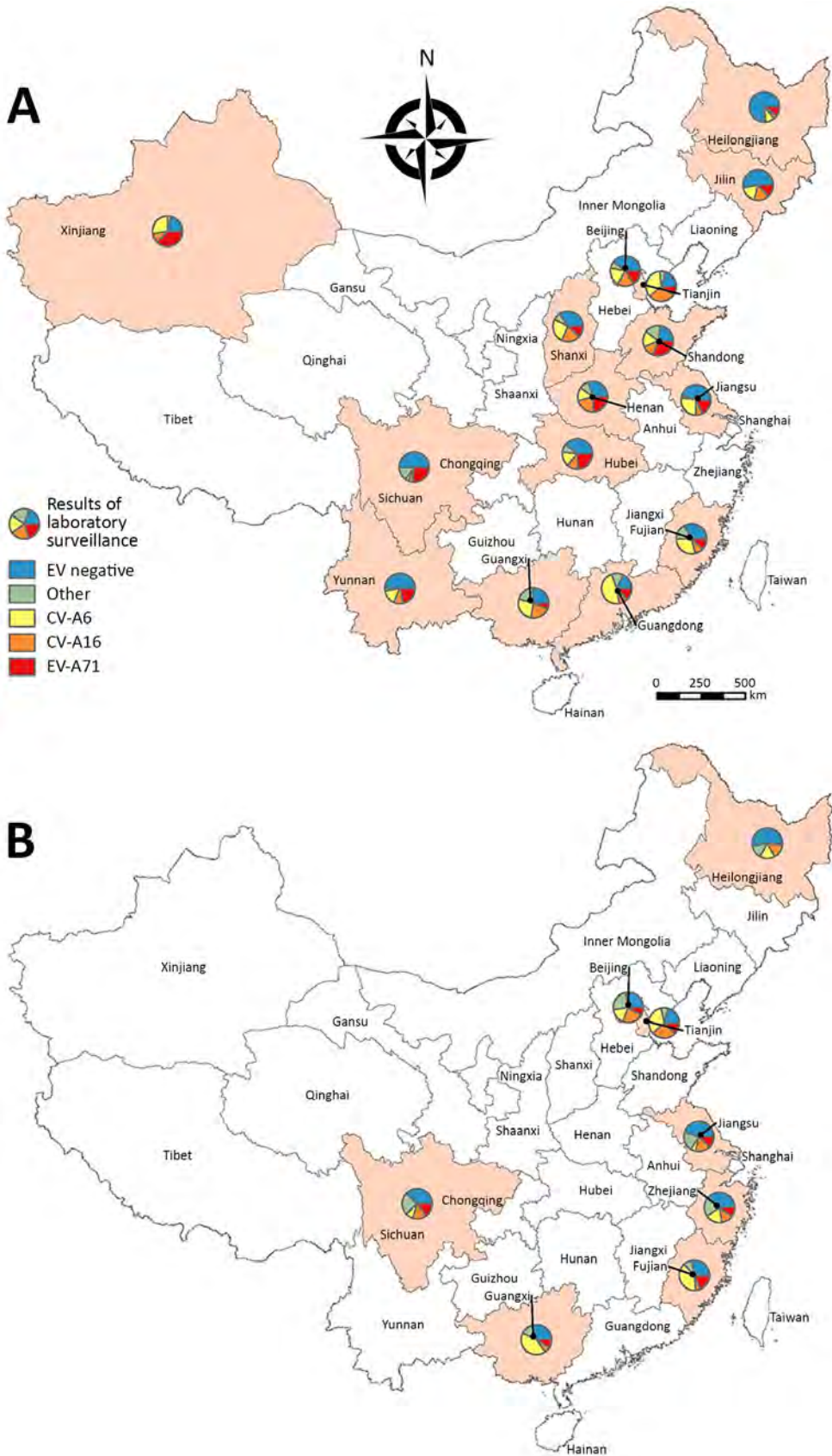
Figure 2. Estimated yearly detection proportions of CV-A6, EV-A71, CV-A16, and other enteroviruses among mild hand, foot and mouth disease cases by province in China: A) 2013; B) 2015. CV, coxsackievirus; EV, enterovirus.

About the Author

Dr. Li is a doctoral candidate at the School of Public Health, the University of Hong Kong. His primary research interests include epidemiology and transmission dynamics of zoonotic and vectorborne diseases, and hand, foot and mouth disease.

References

1. Aswathyraj S, Arunkumar G, Alidjinou EK, Hober D. Hand, foot and mouth disease (HFMD): emerging epidemiology and the need for a vaccine strategy. Med Microbiol Immunol (Berl). 2016;205:397–407. http://dx.doi.org/10.1007/s00430-016-0465-y
2. Yang B, Liu F, Liao Q, Wu P, Chang Z, Huang J, et al. Epidemiology of hand, foot and mouth disease in China, 2008 to 2015 prior to the introduction of EV-A71 vaccine. Euro Surveill. 2017;22. http://dx.doi.org/10.2807/1560-7917.ES.2017.22.50.16-00824
3. Hongyan G, Chengjie M, Qiaozhi Y, Wenhao H, Juan L, Lin P, et al. Hand, foot and mouth disease caused by coxsackievirus A6, Beijing, 2013. Pediatr Infect Dis J. 2014;33:1302–3. http://dx.doi.org/10.1097/INF.0000000000000467
4. Li JS, Dong XG, Qin M, Feng HR, Yang JY, Li RX, et al. Outbreak of hand, foot, and mouth disease caused by coxsackievirus A6 in a Juku in Fengtai District, Beijing, China, 2015. Springerplus. 2016;5:1650. http://dx.doi.org/10.1186/s40064-016-3307-x
5. Xia Y, Shan J, Ji H, Zhang J, Yang H, Shen Q, et al. Study of the epidemiology and etiological characteristics of hand, foot, and mouth disease in Suzhou City, East China, 2011–2014. Arch Virol. 2016;161:1933–43. http://dx.doi.org/10.1007/s00705-016-2878-8
6. Zeng H, Lu J, Zheng H, Yi L, Guo X, Liu L, et al. The epidemiological study of coxsackievirus A6 revealing hand, foot and mouth disease epidemic patterns in Guangdong, China. Sci Rep. 2015;5:10550. http://dx.doi.org/10.1038/srep10550
7. Weng Y, Chen W, He W, Huang M, Zhu Y, Yan Y. Serotyping and genetic characterization of hand, foot, and mouth disease (HFMD) –associated enteroviruses of non-EV71 and non-CVA16 circulating in Fujian, China, 2011–2015. Med Sci Monit. 2017;23:2508–18. http://dx.doi.org/10.12659/MSM.901364
8. Li Y, Bao H, Zhang X, Zhai M, Bao X, Wang D, et al. Epidemiological and genetic analysis concerning the non-enterovirus 71 and non-coxsackievirus A16 causative agents related to hand, foot and mouth disease in Anyang city, Henan Province, China, from 2011 to 2015. J Med Virol. 2017;89: 1749–58. http://dx.doi.org/10.1002/jmv.24847
9. Bian L, Wang Y, Yao X, Mao Q, Xu M, Liang Z. Coxsackievirus A6: a new emerging pathogen causing hand, foot and mouth disease outbreaks worldwide. Expert Rev Anti Infect Ther. 2015; 13:1061–71. http://dx.doi.org/10.1586/14787210.2015.1058156
10. Xing W, Liao Q, Viboud C, Zhang J, Sun J, Wu JT, et al. Hand, foot, and mouth disease in China, 2008–12: an epidemiological study. Lancet Infect Dis. 2014;14:308–18. http://dx.doi.org/10.1016/S1473-3099(13)70342-6
11. Song Y, Zhang Y, Ji T, Gu X, Yang Q, Zhu S, et al. Persistent circulation of coxsackievirus A6 of genotype D3 in mainland of China between 2008 and 2015. Sci Rep. 2017;7:5491. http://dx.doi.org/10.1038/s41598-017-05618-0
12. Takahashi S, Liao Q, Van Boeckel TP, Xing W, Sun J, Hsiao VY, et al. Hand, foot, and mouth disease in China: modeling epidemic dynamics of enterovirus serotypes and implications for vaccination. PLoS Med. 2016;13:e1001958. http://dx.doi.org/10.1371/journal.pmed.1001958
13. Zhu FC, Meng FY, Li JX, Li XL, Mao QY, Tao H, et al. Efficacy, safety, and immunology of an inactivated alum-adjuvant enterovirus 71 vaccine in children in China: a multicentre, randomised, double-blind, placebo-controlled, phase 3 trial. Lancet. 2013;381:2024–32. http://dx.doi.org/10.1016/S0140-6736(13)61049-1
14. Liu CC, Guo MS, Wu SR, Lin HY, Yang YT, Liu WC, et al. Immunological and biochemical characterizations of coxsackievirus A6 and A10 viral particles. Antiviral Res. 2016;129:58–66. http://dx.doi.org/10.1016/j.antiviral.2016.02.008
15. Lin Y, Wen K, Pan Y, Wang Y, Che X, Wang B. Cross-reactivity of anti-EV71 IgM and neutralizing antibody in series sera of patients infected with enterovirus 71 and coxsackievirus A 16. J Immunoassay Immunochem. 2011;32:233–43. http://dx.doi.org/10.1080/15321819.2011.559297

Address for correspondence: Hongjie Yu, School of Public Health, Fudan University, Key Laboratory of Public Health Safety, Ministry of Education, 130 Dong'an Rd, Xuhui District, Shanghai 200032, China; email: cfetpyhj@vip.sina.com

Cronobacter spp. in Common Breast Milk Substitutes, Bogotá, Colombia

**Maria del Rocío Morato-Rodríguez,
Daniel Velandia-Rodríguez, Sandra Castañeda,
Milton Crosby, Herbert Vera**

In Bogotá, Colombia, a large number of babies are fed with breast milk substitutes made from corn and plantain starch. We found 34.3% of tested samples to be contaminated with *Cronobacter* spp.; *C. sakazakii* was the most recovered species. Our findings underscore the risk for contamination of breast milk substitutes.

*C*ronobacter spp. is a group of emerging foodborne opportunistic pathogenic microorganisms that can cause deadly disease in neonates, children, older adults, and immunocompromised persons, including meningitis, septicemia, and necrotizing enterocolitis in neonates and infants (*1*). The presence of *Cronobacter* spp. is widespread in dry foods. Occurrence is higher in infant milk formula (IMF) because some species of *Cronobacter* are able to tolerate different types of stress in IMF; for example, *C. sakazakii* is able to survive up to 2 years in IMF, which increases the possibility for baby foods to become reservoirs, given that milk increases the cultivability and recovery of *C. sakazakii* in dry environments (*2*).

In Colombia, according to the 2010 Nutritional Situation Survey (ENSIN, for its acronym in Spanish), breast-feeding supplementation is gradually made from birth, starting at 27% in the first months until 76% at 9 months of age (*3*). These data suggest that a large number of children can start the intake of supplementary foods, most likely in the form of bottle-feeding (*3*). IMFs are not sterile products; pathogenic microorganisms such as *Salmonella* spp. and *Cronobacter* spp. can be recovered from them (*4*).

At the local level in Colombia, the most common IMF substitutes used are corn and plantain starches. The main reason for their use is the high cost of imported foods (*5*). The microbiologic quality of these foods is important because they are given to breast-fed infants or children <1

year of age, who are vulnerable to infections. However, unlike IMFs, little attention has been paid to the contamination of IMF substitutes with *Cronobacter* spp.

The Study

We collected information on starch brands and consumption preferences from the stores where starch products were sold. We sampled city districts with the highest frequency of consumption (i.e., >1×/wk). The sampling was distributed per percentage weight according to city district and starch composition. We collected 36 samples of corn starch, 53 samples of plantain starch, and 13 samples of other starches (N = 102 samples)

According to the evaluation conducted after enactment of the current baby food regulations in Colombia (*6*), product noncompliance was most often attributable to the presence of coliforms, which were detected in 23.5% (24/102) of samples. Coliforms were detected in 50% (12/24) of plantain starch samples, 12.5% (3/24) of other starch samples, and 0% (0/24) of corn starch samples. For the detection of *Cronobacter* spp., we used the ISO 22964:2006 method, by which we were able to recover isolates from 35 (34.3%) samples. However, recovery was already improved in the new ISO 22964:2017 version, which is desirable because *Cronobacter* spp. have been found at levels of <1 UFC/100 g of IMFs (*7*).
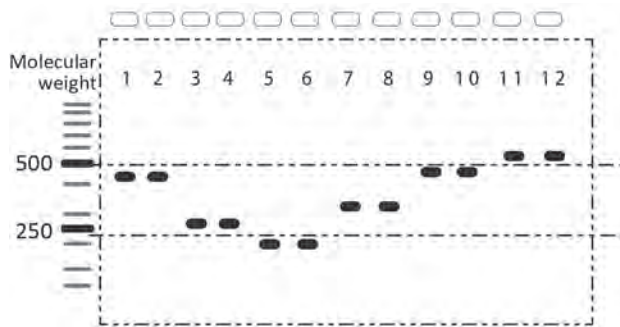
We differentiated *Cronobacter* spp. species by using PCR *cgcA* enzyme (*8*) (Platinum Blue PCR Super Mix; Invitrogen, Carlsbad, CA, USA). We then improved specificity and reduced the amplification of nonspecified fragments (Figure 1).

Of the 102 samples, 34.3% (35/102) were positive for *Cronobacter* spp. (26.5% [27/35] of plantain starch samples, 7.8% [8/35] of other starch samples, and 0% of corn starch samples). The *Cronobacter* species identified were *C. sakazakii* (74% [26/35] of isolates), *C. malonaticus* (14% [5/35] of isolates), and *C. dublinensis* (11% [4/35] of isolates) (Figure 2).

The 34.3% *Cronobacter* spp. prevalence was similar to that reported in plant derivatives (e.g., 20.1% [*9*] and 31.3% [*10*]) and in cereals (63%) (*11*). Prevalence in processed and other foods has ranged from 3% to 30% (*12*). Although the greatest number of positive isolates was recovered from plantain starches, no information on *Cronobacter* spp. in plantain matrixes is available.

Figure 1. Individual evaluation of multiplex PCR primers used to differentiate 6 species of *Cronobacter* in a study of *Cronobacter* spp. in common breast milk substitutes, Bogotá, Colombia, 2016. Lanes were used as guides for calculating the molecular weight of each band.

Conclusions

From the point of view of microbiologic quality, the presence of coliform bacteria and pathogens shows the risk of contamination of IMF substitutes. For *Cronobacter* spp., the international standard is a total absence in IMF (*13*). The most recovered species in the samples we tested was *C. sakazakii*, which is the species associated with the highest number of disease cases reported in neonates and whose sequence type 4 is already known to be associated with severe cases of meningitis (*14*). The PCR method we used enabled greater coverage compared with the traditional method because the identification of the species is confirmed in a single analytical run, thus speeding up the subsequent public health response and providing valuable information for epidemiologic surveillance.

In Bogotá, no cases of foodborne diseases related to the presence of *Cronobacter* spp. have been reported. However, *Cronobacter* are not subject to mandatory reporting in Colombia because no active surveillance of this pathogen exists, and the medical community lacks information about the pathogen. It is important to characterize and document the presence of *Cronobacter* spp. in different foods to assess the risk to which children <1 year of age and breast-fed infants are exposed and to identify the connection between diseases like meningitis and the consumption of contaminated baby foods produced locally. Some measures have been proposed to mitigate this risk. It is vital to indicate on the starch packaging that starch must be reconstituted in water at ≥70°C for ≥1 minute before consumption, and starch leftovers must be refrigerated to minimize the risk for contamination with *Cronobacter* spp. (*15*). In addition, the World Health Organization–Codex Alimentarius Code of Hygiene

Figure 2. Species of C*ronobacter* recovered from corn, plantain, and other starches in a study of *Cronobacter* spp. in common breast milk substitutes, Bogotá, Colombia, 2016.

Practices provides guidelines for governments, industries, and consumers to support and teach caregivers about safe preparation of starches (*13*). Our findings must lead to an in-depth review of the current regulations for baby foods in Colombia and a modification of Bogotá's System of Inspection, Surveillance, and Control so that this system can be more preventive and responsive in ensuring the health of citizens.
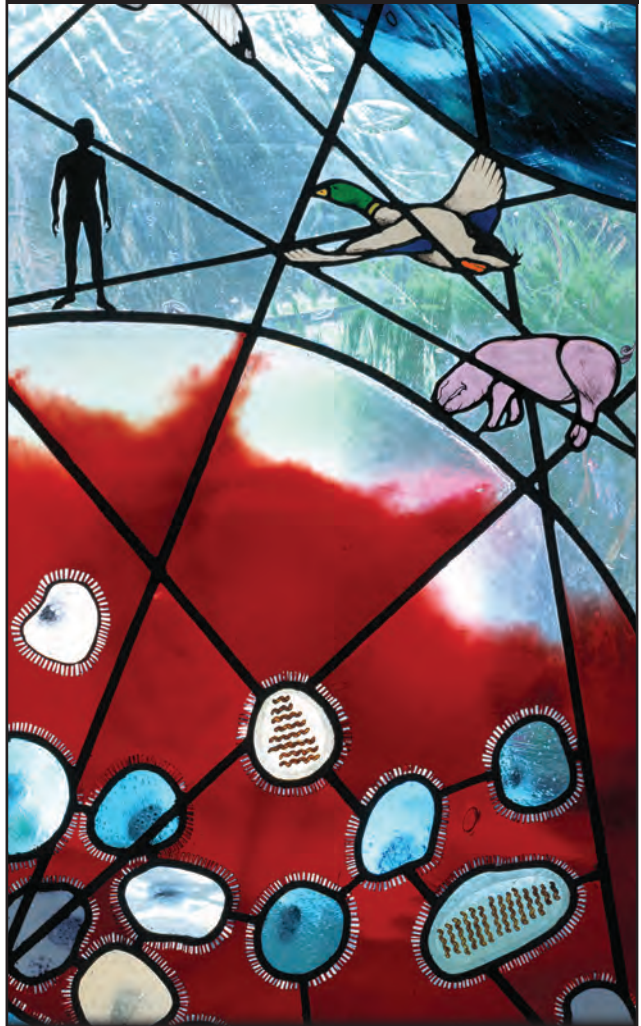
About the Author

Ms. Rocío Morato-Rodríguez is a microbiologist at the Public Health Laboratory of Bogotá. Her primary research interests include issues related to food safety, quality assurance, and risk assessment.

References

1. Odeyemi OA, Sani NA. The prevention of *Cronobacter* infections in hospital neonatal intensive care units. J Infect Public Health. 2016;9:110–2. http://dx.doi.org/10.1016/j.jiph.2015.06.012

2. Hu S, Yu Y, Xiao X. Stress resistance, detection and disinfection of *Cronobacter* spp. in dairy products: a review. Food Control. 2018;85:400–15. http://dx.doi.org/10.1016/j.foodcont.2017.10.014

3. Ministerio de la Protección Social Instituto Nacional de Salud IC de BF. Encuesta Nacional de la Situación Nutricional en Colombia (ENSIN) 2010. Bogotá (Colombia): Ministerio de la Protección Social Bogota; 2010. p. 513

4. Bejarano-Roncancio JJ, Castillo-Quiroga YM. Major microbiological contaminants in infant milk formulas 1 [in Spanish]. CienciaU-AT. 2013;25:42–8. http://dx.doi.org/10.29059/cienciauat.v7i2.19

5. Yao K, N'guessan KF, Zinzendorf NY, Kouassi KA, Kouassi KC, Loukou YG, et al. Isolation and characterization of *Cronobacter* spp. from indigenous infant flours sold in public health care centres within Abidjan, Côte d'Ivoire. Food Control. 2016;62:224–30. http://dx.doi.org/10.1016/j.foodcont.2015.10.041

6. Ministerio de Salud, Ministerio de la Protección Social Colombia. Resolución número 11488 de 1984 [cited 2015 Aug 18]. p. 107–19. https://www.icbf.gov.co/cargues/avance/docs/resolucion_minsalud_r1148884.htm

7. Gičová A, Orieškova M, Oslanecová L, Drahovská H, Kaclíková E. Identification and characterization of *Cronobacter* strains isolated from powdered infant foods. Lett Appl Microbiol. 2014;58:242–7. http://dx.doi.org/10.1111/lam.12179

8. Carter L, Lindsey LA, Grim CJ, Sathyamoorthy V, Jarvis KG, Gopinath G, et al. Multiplex PCR assay targeting a diguanylate cyclase-encoding gene, *cgcA*, to differentiate species within the genus *Cronobacter*. Appl Environ Microbiol. 2013;79:734–7. http://dx.doi.org/10.1128/AEM.02898-12

9. Sani NA, Odeyemi OA. Occurrence and prevalence of *Cronobacter* spp. in plant and animal derived food sources: a systematic review and meta-analysis [cited 2016 Oct 12]. http://www.springerplus.com/content/4/1/545

10. Turcovský I, Kuniková K, Drahovská H, Kaclíková E. Biochemical and molecular characterization of *Cronobacter* spp. (formerly *Enterobacter sakazakii*) isolated from foods. Antonie van Leeuwenhoek. 2011;99:257–69. http://dx.doi.org/10.1007/s10482-010-9484-7

11. Lou X, Si G, Yu H, Qi J, Liu T, Fang Z. Possible reservoir and routes of transmission of *Cronobacter* (*Enterobacter sakazakii*) via wheat flour. Food Control. 2014;43:258–62. http://dx.doi.org/10.1016/j.foodcont.2014.03.029

12. Parra J, Oliveras L, Rodriguez A, Riffo F, Jackson E, Forsythe S. Risk of *Cronobacter Sakazakii* contamination in powdered milk for infant nutrition [in Spanish]. Rev Chil Nutr. 2015;42:83–9.

13. Codex Alimentarius Commission. Code of hygiene practice for powdered preparations for infants and young children [in Spanish]. CAC/RCP 66–2008 [cited 2016 Apr 25]. http://www.msp.gub.uy/sites/default/files/archivos_adjuntos/CXP_066s%20%282%292009.pdf

14. Jaradat ZW, Al Mousa W, Elbetieha A, Al Nabulsi A, Tall BD. *Cronobacter* spp.—opportunistic food-borne pathogens. A review of their virulence and environmental-adaptive traits. J Med Microbiol. 2014;63:1023–37. http://dx.doi.org/10.1099/jmm.0.073742-0

15. Yang H-Y, Kim S-K, Choi S-Y, You D-H, Lee S-C, Bang W-S, et al. Effect of acid, desiccation and heat stresses on the viability of *Cronobacter sakazakii* during rehydration of powdered infant formula and in simulated gastric fluid. Food Control. 2015;50:336–41. http://dx.doi.org/10.1016/j.foodcont.2014.09.012

Address for correspondence: María del Rocío Morato-Rodríguez, Secretaria Distrital de Salud de Bogota, Cra 32 #12-81 Bogotá, Código 111611, Colombia; email: mrmorato@saludcapital.gov.co or mrmorator@unal.edu.co

Effectiveness of Whole, Inactivated, Low Pathogenicity Influenza A(H7N9) Vaccine against Antigenically Distinct, Highly Pathogenic H7N9 Virus

Masato Hatta, Gongxun Zhong, Shiho Chiba, Tiago J.S. Lopes, Gabriele Neumann, Yoshihiro Kawaoka

The recent emergence of highly pathogenic influenza A(H7N9) variants poses a great risk to humans. We show that ferrets vaccinated with low pathogenicity H7N9 virus vaccine do not develop severe symptoms after infection with an antigenically distinct, highly pathogenic H7N9 virus. These results demonstrate the protective benefits of this H7N9 vaccine.

Low pathogenicity influenza A(H7N9) viruses, which cause mild or asymptomatic disease in poultry, have caused ≥1,564 human infections since March 2013, with a case-fatality rate of ≈40% (1–5). Recently, highly pathogenic H7N9 viruses, characterized by multiple basic amino acids at the cleavage site of their hemagglutinin (HA) protein, have emerged. More than 750 cases of human H7N9 infections in 2017 (6) and the emergence of highly pathogenic H7N9 viruses emphasize the need for effective vaccines against low pathogenicity and highly pathogenic H7N9 viruses. We examined whether a World Health Organization (WHO) candidate vaccine based on a low pathogenicity H7N9 influenza virus would protect ferrets against an antigenically distinct, highly pathogenic H7N9 influenza virus.

The Study

We generated a recombinant virus (HK125–HYPR8) that possesses the HA and neuraminidase (NA) genes of a low pathogenicity WHO-recommended H7N9 candidate vaccine virus (A/Hong Kong/125/2017 [7]) and the remaining genes from a high-yield A/Puerto Rico/8/34 (PR8) vaccine backbone virus (8). The HK125–HYPR8 virus was inactivated with β-propiolactone and purified through sucrose gradient ultracentrifugation.

We vaccinated 5-month-old female ferrets (6 per group) that were serologically negative for currently circulating human influenza viruses with 15 μg of HA of inactivated whole HK125–HYPR8 virions without adjuvant (Group 1) or mixed at a 1:1 ratio with AddaVax adjuvant (InvivoGen, San Diego, CA, USA), a squalene-based oil-in-water nanoemulsion similar to MF59 (9) (group 2); control animals received phosphate-buffered saline (group 3) or adjuvant (group 4) (Figure 1, panel A). All animals were vaccinated intramuscularly in both hind legs twice, 28 days apart.

Twenty-eight days after the second immunization, we intranasally challenged ferrets with 10^6 PFUs of highly pathogenic H7N9 rGD/3-NA294R virus (a neuraminidase inhibitor–sensitive subpopulation of highly pathogenic A/Guangdong/17SF003/2016 H7N9 virus) (10). These vaccine and challenge viruses belong to the Yangtze River Delta lineage of H7N9 viruses, which is responsible for recent infections of humans with highly pathogenic H7N9 viruses (6). However, A/Hong Kong/125/2017 and the A/Guangdong/17SF003/2016 challenge virus differ antigenically (11) (online Technical Appendix Table 1, https://wwwnc.cdc.gov/EID/article/24/10/18-0403-Techapp1.pdf).

We monitored clinical signs, body weight, and body temperature daily for 14 days and collected throat and nasal swab specimens every day until day 7 postchallenge. On day 4 postchallenge, we euthanized 3 ferrets from each group and collected organs (lung, trachea, nasal turbinates, olfactory bulbs, and brain tissues pooled from anterior and posterior brain sections) for virus titration. We conducted statistical analysis of hemagglutinin inhibition (HI) titers, virus titers in swab and organ samples, and bodyweight and temperature changes among groups (online Technical Appendix Tables 2–21). We defined statistical significance as p<0.05.

After 1 immunization, HI titers were significantly lower in the ferrets immunized with nonadjuvanted HK125–HYPR8 vaccine than in those immunized with AddaVax-adjuvanted HK125–HYPR8 vaccine (p = 0.038; Figure 1, panel B; online Technical Appendix Table 2); however, after 2 immunizations, ferrets vaccinated with or without adjuvant (groups 1 and 2) developed high HI titers against HK125–HYPR8 virus. Vaccination with HK125–PR8 vaccine did not elicit measurable HI titers against the rGD/3-NA294R challenge virus after the first immunization but elicited reasonably high titers after the second immunization (Figure 1, panel B). After challenge with highly pathogenic H7N9 virus,

Author affiliations: University of Wisconsin–Madison, Madison, Wisconsin, USA (M. Hatta, G. Zhong, S. Chiba, T.J.S. Lopes, G. Neumann, Y. Kawaoka); University of Tokyo, Tokyo, Japan (Y. Kawaoka)

nonvaccinated ferrets (groups 3 and 4) became lethargic, experienced diarrhea, and lost appetite and bodyweight on days 2–6 postinfection (online Technical Appendix Figure), whereas vaccinated ferrets showed no noticeable symptoms. In addition, nonvaccinated ferrets demonstrated statistically higher body temperature than vaccinated ferrets on days 1, 2, 3, 5, and 6 postchallenge (online Technical Appendix Figure, Table 5). One ferret in group 3 and 2 ferrets in group 4 had to be euthanized on days 6–8 postinfection (Figure 1, panel C) because of severe symptoms (neurologic signs or inability to remain upright). In contrast, none of the vaccinated ferrets had any symptoms, indicating a protective effect of the low pathogenicity H7N9 vaccine against the challenge virus.

Analysis of throat and nasal swab samples demonstrated replication of highly pathogenic challenge virus in all ferrets (Figure 2, panel A). However, virus titers started to decline in vaccinated ferrets by day 3 postchallenge, and the

infection was resolved by day 5 postchallenge; in contrast, nonvaccinated ferrets continued to shed high titers of challenge virus 4–7 days postchallenge. The virus titers in nasal swab samples on days 1, 3, 4, 5, 6, and 7 postchallenge and those in throat swab samples on days 1–7 postchallenge from nonvaccinated ferrets were significantly higher than those in vaccinated ferrets (online Technical Appendix Table 10). Thus, vaccination with HK125–HYPR8 virus led to reduced replication of the challenge virus in the upper respiratory tract of infected ferrets.

On day 4 postinfection, we euthanized 3 animals per group and determined virus titers in organs. We also assessed virus titers in organs of ferrets that were euthanized because of severe disease symptoms. In nonvaccinated ferrets, we detected high titers of virus in respiratory organs; in addition, we recovered virus from the olfactory bulbs or pooled samples from anterior and posterior sections of
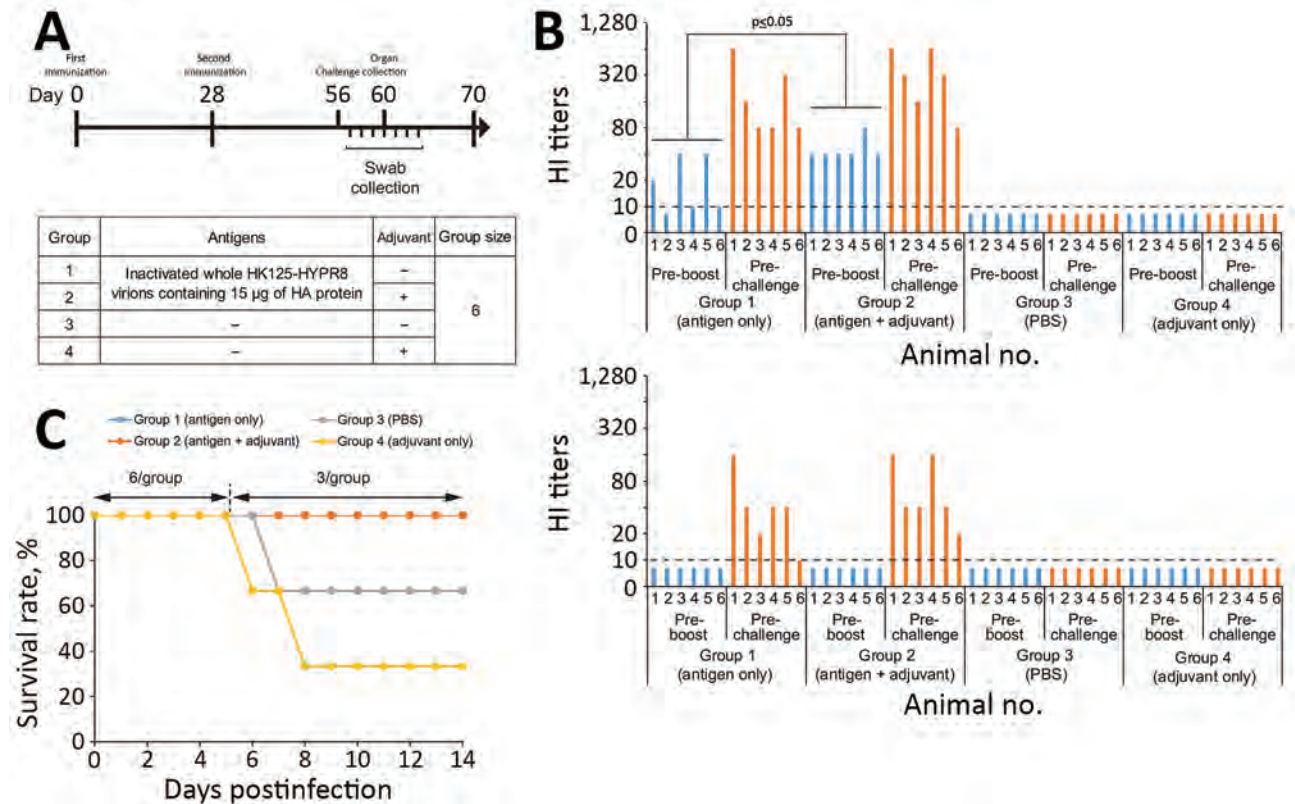
Figure 1. Study design, HI titers after vaccination, and survival rates of vaccinated and nonvaccinated ferrets challenged with highly pathogenic influenza A(H7N9) virus. A) Study design. Six ferrets per group were immunized with inactivated whole HK125–HYPR8 virions containing 15 μg of HA protein without (group 1) or with adjuvant (group 2); control animals were vaccinated with PBS (group 3) or adjuvant (group 4). Animals were vaccinated intramuscularly twice 28 days apart. Twenty-eight days after the second immunization, ferrets were challenged with highly pathogenic H7N9 rGD/3-NA294R virus. Throat and nasal swab specimens were collected on days 1–7 postchallenge; 3 animals per group were euthanized on day 4 postchallenge to assess virus titers in organs. B) HI titers after vaccination. HI assays were performed against HK125–HYPR8 (upper panel) and rGD/3-NA294R (lower panel) with ferret sera collected before the second immunization (preboost) and before challenge (prechallenge). Statistical significance was determined as described in the online Technical Appendix (https://wwwnc.cdc.gov/EID/article/24/10/18-0403-Techapp1.pdf). C) Survival rates. Survival was monitored for 14 days after challenge. Because 3 ferrets were euthanized on day 4 postchallenge for organ sampling, the survival rate was calculated on the basis of a group size of n = 3 thereafter. HA, hemagglutinin; HI, hemagglutination inhibition; PBS, phosphate-buffered saline.

the brains of 7 of the 9 animals tested (Figure 2, panel B). In vaccinated ferrets, we detected virus in the nasal turbinates of 4 of 6 animals and in the olfactory bulbs of 2 of 6 animals. We recovered no virus from the tracheas, lungs, or pooled samples from anterior and posterior brain sections (Figure 2, panel B), indicating that vaccination with HK125–HYPR8 prevented challenge virus replication in the lower respiratory organs.

Conclusions

We report the effectiveness of a whole, inactivated, low pathogenicity H7N9 vaccine against an antigenically distinct, highly pathogenic H7N9 virus in a ferret model. Vaccination prevented challenge virus replication in the lower respiratory organs, led to faster virus clearance in the upper respiratory organs, and prevented severe disease and death in ferrets, although the HI titers against the rGD/3-NA294R
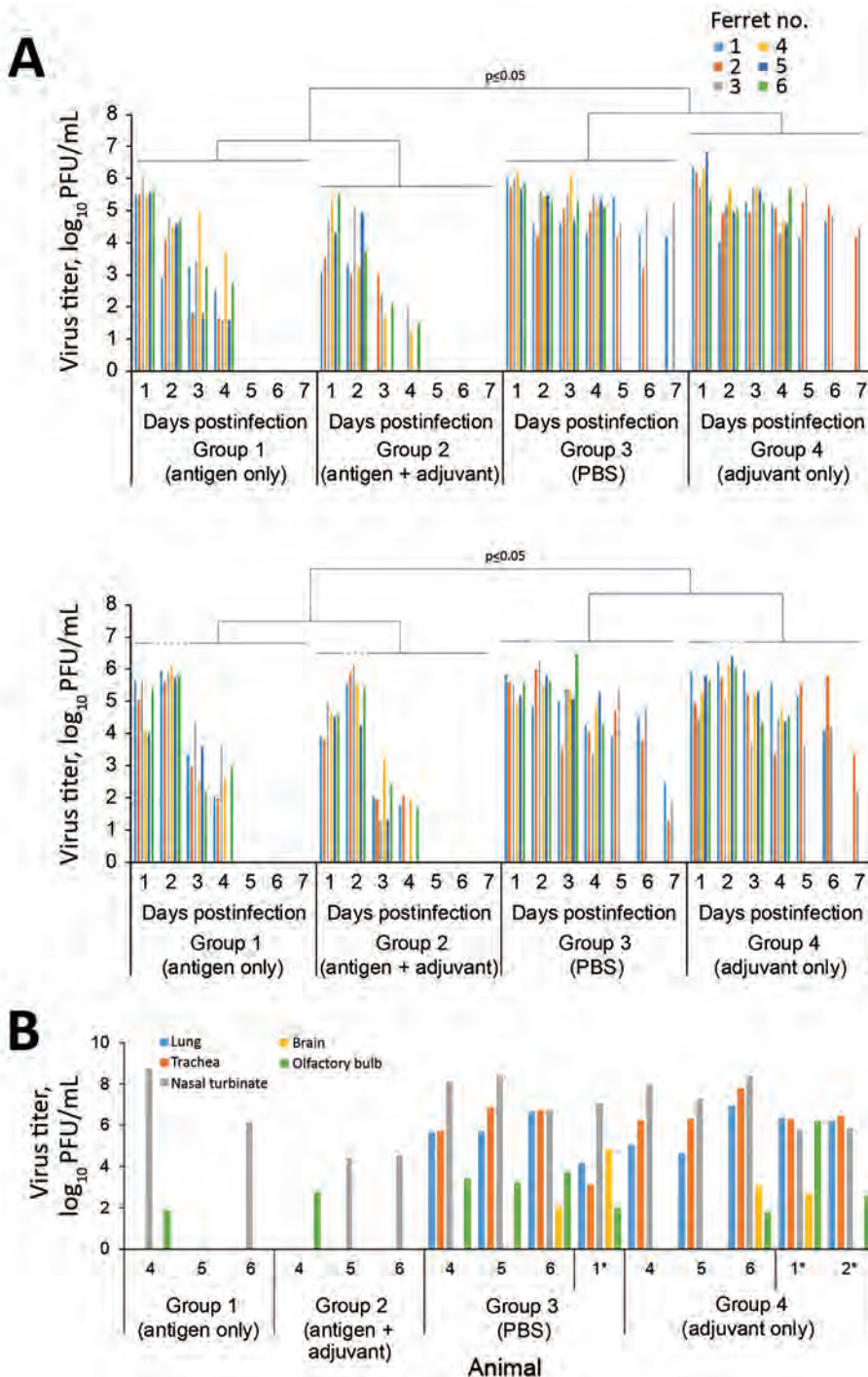
Figure 2. Virus titers in throat and nasal swab specimens and in the organs of vaccinated and nonvaccinated ferrets challenged with highly pathogenic influenza A(H7N9) virus. A) Virus titers in swab samples. Throat and nasal swabs were collected on days 1–7 postchallenge. Virus titers were determined based on plaque assays in MDCK cells. Statistical significance was determined as described in the online Technical Appendix (https://wwwnc.cdc.gov/EID/article/24/10/18-0403-Techapp1.pdf). B) Three ferrets from each group were euthanized on day 4 postchallenge for virus titration in the indicated organs. We also assessed virus titers in organs of ferrets that were euthanized because of severe symptoms (*). Virus titers were determined based on plaque assays in MDCK cells. Numbers along baseline indicate animal number. PBS, phosphate-buffered saline.

challenge virus were lower than those against the HK125–HYPR8 vaccine virus. Statistical analyses demonstrated that HI titers against the HK125–HYPR8 vaccine virus after the first immunization were significantly higher (p = 0.038) in animals immunized with adjuvanted vaccine compared with animals immunized with nonadjuvanted vaccine (Figure 1, panel B; online Technical Appendix Table 2). Bodyweight changes after challenge were significantly milder (p = 0.0132–0.0489 on days 4–10, 12, and 13) in ferrets immunized with adjuvanted vaccine than in those vaccinated with nonadjuvanted vaccine. In addition, virus titers in nasal swabs on days 3 and 4 postchallenge (p = 0.0052 on day 3; p = 0.0163 on day 4) and in throat swabs on days 1, 3, and 4 (p = 0.0047 on day 1; p = 0.0003 on days 3 and 4) in ferrets immunized with nonadjuvanted vaccine were significantly higher than in those ferrets immunized with adjuvanted vaccine (online Technical Appendix Tables 9, 11), suggesting superior efficacy with Addavax.

Previously, WHO selected several low pathogenicity H7N9 candidate vaccine viruses, including A/Hong Kong/125/2017 (7). With the emergence of highly pathogenic H7N9 viruses that are antigenically distinct from previously circulating H7N9 viruses, WHO has updated its recommendations, and a candidate vaccine virus for highly pathogenic H7N9 viruses is now available (12). We tested whether in the event of a large-scale outbreak of highly pathogenic H7N9 viruses, candidate vaccine viruses to antigenically distinct H7N9 viruses might serve as a first line of defense. Our results in ferrets indicate the potential of a whole, inactivated vaccine based on a low pathogenicity H7N9 virus to prevent severe disease with fatal outcome after infection with an antigenically distinct, highly pathogenic H7N9 virus.

About the Author

Dr. Hatta is a senior scientist at the Influenza Research Institute at the University of Wisconsin–Madison. His research focuses on identifying the molecular determinants of influenza virus pathogenicity, with particular emphasis on the pathogenicity of highly pathogenic influenza viruses.

References

1. Centers for Disease Control and Prevention (CDC). Asian lineage avian influenza A (H7N9) virus [cited 2018 Feb 28]. https://www.cdc.gov/flu/avianflu/h7n9-virus.htm
2. Shen Y, Lu H. Global concern regarding the fifth epidemic of human infection with avian influenza A (H7N9) virus in China. Biosci Trends. 2017;11:120–1. http://dx.doi.org/10.5582/bst.2017.01040
3. Wang X, Jiang H, Wu P, Uyeki TM, Feng L, Lai S, et al. Epidemiology of avian influenza A H7N9 virus in human beings across five epidemics in mainland China, 2013–17: an epidemiological study of laboratory-confirmed case series. Lancet Infect Dis. 2017;17:822–32. http://dx.doi.org/10.1016/S1473-3099(17)30323-7
4. Zhou L, Ren R, Yang L, Bao C, Wu J, Wang D, et al. Sudden increase in human infection with avian influenza A(H7N9) virus in China, September–December 2016. Western Pac Surveill Response J. 2017;8:6–14. http://dx.doi.org/10.5365/wpsar.2017.8.1.001
5. Iuliano AD, Jang Y, Jones J, Davis CT, Wentworth DE, Uyeki TM, et al. Increase in human infections with avian influenza A(H7N9) virus during the fifth epidemic—China, October 2016–February 2017. MMWR Morb Mortal Wkly Rep. 2017;66:254–5. http://dx.doi.org/10.15585/mmwr.mm6609e2
6. Centre for Health Protection (Hong Kong). Avian influenza report, volume 13, number 42 [cited 2017 Dec 29]. http://www.chp.gov.hk/files/pdf/2017_avian_influenza_report_vol13_wk42.pdf
7. World Health Organization. Summary of status of development and availability of avian influenza A(H7N9) candidate vaccine viruses and potency testing reagents [cited 2017 Sep 28]. http://www.who.int/influenza/vaccines/virus/candidates_reagents/summary_a_h7n9_cvv_20170928.pdf?ua=1
8. Ping J, Lopes TJ, Nidom CA, Ghedin E, Macken CA, Fitch A, et al. Development of high-yield influenza A virus vaccine viruses. Nat Commun. 2015;6:8148. http://dx.doi.org/10.1038/ncomms9148
9. Ott G, Radhakrishnan R, Fang J-H, Hora M. The adjuvant MF59: a 10-year perspective. In: O'Hagan DT, editor. Vaccine adjuvants: preparation methods and research protocols. Totowa (NJ): Springer New York; 2000. p. 211–28.
10. Imai M, Watanabe T, Kiso M, Nakajima N, Yamayoshi S, Iwatsuki-Horimoto K, et al. A highly pathogenic avian H7N9 influenza virus isolated from a human is lethal in some ferrets infected via respiratory droplets. Cell Host Microbe. 2017;22:615–626.e8. http://dx.doi.org/10.1016/j.chom.2017.09.008
11. Zoonotic influenza viruses: antigenic and genetic characteristics and development of candidate vaccine viruses for pandemic preparedness [in French]. Wkly Epidemiol Rec. 2017;92:129–44.
12. World Health Organization. Summary of status of development and availability of avian influenza A(H7N9) candidate vaccine viruses and potency testing reagents [cited 2018 Mar 5]. http://www.who.int/influenza/vaccines/virus/candidates_reagents/summary_a_h7n9_cvv_20180305.pdf?ua=1

Address for correspondence: Yoshihiro Kawaoka, University of Wisconsin–Madison, Influenza Research Institute, Department of Pathobiological Sciences, School of Veterinary Medicine, 575 Science Dr, Madison, WI 53711, USA; email: yoshihiro.kawaoka@wisc.edu

Two Community Clusters of Legionnaires' Disease Directly Linked to a Biologic Wastewater Treatment Plant, the Netherlands

Anna D. Loenenbach, Christian Beulens, Sjoerd M. Euser, Jeroen P.G. van Leuken, Ben Bom, Wim van der Hoek, Ana Maria de Roda Husman, Wilhelmina L.M. Ruijs, Alvin A. Bartels, Ariene Rietveld, Jeroen W. den Boer, Petra S. Brandsema

A biologic wastewater treatment plant was identified as a common source for 2 consecutive Legionnaires' disease clusters in the Netherlands in 2016 and 2017. Sequence typing and transmission modeling indicated direct and long-distance transmission of *Legionella*, indicating this source type should also be investigated in sporadic Legionnaires' disease cases.

In autumn 2016, six reported cases of Legionnaires' disease (LD) were linked to the town of Boxtel, the Netherlands. In the second half of 2017, eight more cases were identified among residents of the town. During 2003–2015, only 1 non–travel-related LD case was reported in Boxtel. In 2016 and 2017, the cases were investigated to determine if they were linked to a common source. We describe the epidemiologic, environmental, and microbiologic investigation of these 2 *Legionella* clusters.

The Study

We defined cases as *Legionella* pneumonia in a person with illness meeting the European Union case definition (*1*) who resided in or visited Boxtel 2–14 days before disease onset during 2016–2017. The 2016 cluster (cluster 1) consisted of 4 residents and 2 nonresidents who work in the industrial

Author affiliations: European Centre for Disease Prevention and Control, Stockholm, Sweden (A.D. Loenenbach); National Institute for Public Health and the Environment, Bilthoven, the Netherlands (A.D. Loenenbach, J.P.G. van Leuken, B. Bom, W. van der Hoek, A.M. de Roda Husman, W.L.M. Ruijs, A.A. Bartels, P.S. Brandsema); Municipal Health Service Hart voor Brabant, 's-Hertogenbosch, Tilburg, the Netherlands (C. Beulens, A. Rietveld); Regional Public Health Laboratory Kennemerland, Haarlem, the Netherlands (S.M. Euser, J.W. den Boer); Utrecht University, Utrecht, the Netherlands (A.M. de Roda Husman)

area of Boxtel. The onset of disease symptoms ranged from October 28 to December 11, 2016. During July 10–November 3, 2017, seven more cases (all in Boxtel residents) occurred (cluster 2) (Figure 1). Further investigation identified another case, in a person who visited Boxtel 5 days before symptom onset.

The median age of the 14 patients was 72 years (range 51–93 years); 8 patients (57%) were male (Table 1). All 14 patients were hospitalized, 7 (50%) were smokers, and 11 (79%) had co-morbid conditions.

Patient interviews did not identify any common exposure, and none of the case-patients had recently traveled abroad. Mapping cases based on the patients' residential postal code and prevailing wind direction (mainly southwest during individual incubation times [https://www.knmi.nl]) indicated that the source could be within the industrial area of Boxtel.

In November 2016, environmental samples were collected at several potential sources, including a fountain and 5 wet cooling towers (WCT) (Table 2). However, no *Legionella* were detected in these samples. The emergence of new LD cases in 2017 led to the reexamination of these locations, along with identification of additional potential sources, including a biologic wastewater treatment plant (BWTP) in the industrial area. The installation, which was transformed into a BWTP for energy production in summer 2015, consisted of 3 ponds with different degrees of aeration. All ponds tested positive for *L. pneumophila* (Table 2). Because the BWTP effluent drains to the municipal wastewater treatment plant (MWTP), located in the northwest of Boxtel, and discharges onto the Dommel River after treatment, these locations were also sampled. Subsequently, 2 air scrubbers near the BWTP were tested, and air above the BWTP was sampled.

All 14 cases were confirmed by urine antigen testing (Table 1). Clinical and environmental isolates were genotyped by using sequence-based typing (SBT), as previously described (*2*,*3*), and compared with the European Working Group for *Legionella* Infectious Sequence-Based Typing Database (http://www.hpa-bioinformatics.org.uk/legionella/legionella_sbt/php/sbt_homepage.php). An identical sequence type (ST), ST1646, was found in 5 patients (2 in cluster 1 and 3 in cluster 2) (Figure 1). Two other sequence types were found for 2 patients in cluster 1 (Table 1). SBT of the environmental

Figure 1. Legionnaires' disease cases, by sequence type and week of disease onset, Boxtel, the Netherlands, October 2016–December 2017. BWTP, biologic wastewater treatment plant; ST, sequence type.

isolates from the BWTP, the MWTP, and the river also identified ST1646. This sequence type was also detected in isolates from air sampled above the BWTP pond with the most aeration. *Legionella* was not detected in the other sampled locations (Table 2).

We used a transmission model for rapid detection of potential environmental sources of airborne pathogens in outbreak investigations (*4,5*), which was used for *Legionella* for the first time and applied to the data collected for the outbreak investigation in Boxtel. The model calculated a measure of risk (MR) based on

patients' residential addresses in Boxtel, date of illness onset, and population density. Locations with the highest MR values (hotspots) are likely to contain the actual infection source. The model identified 1 hotspot, located in the southwest of the industrial area, ≈650 m from the BWTP (Figure 2).

To prevent further *Legionella* transmission by aerosols, 2 temporary tents were erected successively to cover the 2 aerated ponds, 1 in December 2017 and the other in January 2018. A permanent solution for covering both aeration ponds is under exploration. After the

Table 1. Characteristics of 14 case-patients in 2 community clusters of Legionnaires' disease directly linked to a biologic wastewater treatment plant, Boxtel, the Netherlands, October 2016–December 2017*

Characteristic	No. (%)		
	Cluster 1, n = 6	Cluster 2, n = 8	Clusters 1 and 2, N = 14
Patient characteristics			
Median age >72 y			5 (35.7)
Sex			8 (57.1)
M			8 (57.1)
F			6 (42.9)
Smoking			7 (50.0)
Co-morbid conditions			11 (78.6)
Hospital admission			14 (100)
ICU admission			
Death			0
Diagnostic results			
Legionella culture performed			6 (42.9)
LP sg1 culture positive			5 (35.7)
Urine antigen test positive			14 (100)
LP PCR positive			4†
Typing results			
ST1646	2 (33.3)	3 (37.5)	5 (35.7)
Non-ST1646‡	2 (33.3)	0	2 (14.3)
No isolate	2 (33.3)	5 (62.5)	7 (50.0)

*Sources: National Notification Database Osiris; Database National Reference Laboratory for *Legionella*, Haarlem, the Netherlands. ICU, intensive-care unit; LP, *Legionella pneumophila*; ST, sequence type.
†Number of PCR tests performed is not available; only number of tests with positive results known.
‡Obtained through nested PCR with direct sequence-based typing.

Table 2. Results of environmental samples taken during investigation of 2 community clusters of Legionnaires' disease directly linked to a biologic wastewater treatment plant, Boxtel, the Netherlands, October 2016–December 2017*

Location of samples	Sampling date, wk/y	CFU/L	*Legionella pneumophila* serogroup	ST
Water samples†				
BWTP				
Pond 1 (low aeration)	48/2017	2.0×10^6	sg1	‡
	50/2017	5.6×10^7	sg1	ST1646
Pond 2 (no aeration)	48/2017	7.1×10^8	sg1	ST1646
	50/2017	19.2×10^8	sg1	ST1646
Pond 3 (high aeration)	48/2017	15.0×10^8	sg1	ST1646
	50/2017	22.6×10^8	sg1	‡
Municipal wastewater treatment plant				
Influent	39/2017	1.0×10^5	sg1	ST1646
Pond	39/2017	2×10^3	sg1	ST1646
River midstream	39/2017	2×10^3	sg1	ST1646
Riverside	39/2017	2×10^4	sg1	ST1646
Fountain, city center	50/2016	Negative		
	39/2017	Negative		
WCTs and air scrubbers next to BWTP, industrial area				
	50/2016	Negative		
	39/2017	Negative		
	48/2017	Negative		
4 WCTs, industrial area	50/2016	Negative		
5 WCTs, industrial area	39/2017	Negative		
Misting device, industrial area	39/2017	Negative		
Other environmental samples†				
Biologic wastewater treatment plant				
Air sample inside pond 3 tent	50/2017	Positive	sg1	‡
Swab inner surface pond 3 tent	50/2017	Positive	sg1	ST1646

*Source: Database National Reference Laboratory for *Legionella*, Haarlem, the Netherlands. BWTP, biologic wastewater treatment plant; sg, serogroup; ST, sequence type; WCT, wet cooling tower.
†Water samples were analyzed with an accredited in-house developed method based on ISO 11731:2017, with an additional step of acid treatment. Air samples were collected using a SASS 2300 air sampler (Research International, Seattle, WA, USA) and analyzed with an accredited in-house developed method based on ISO 11731:2017.
‡Sequence type profile was incomplete because of technical problems experienced during *mompS* typing; however, for all 6 available alleles, results were in accordance with the ST1646 profile (*flaA*, 2; *pile*, 10; *asd*, 14; *Mip*, 10; *mompS*, not available; *proA*, 4; *neuA*, 11).

detection of *Legionella* in the BWTP effluent, a sludge filter defect was identified and repaired. Resampling of the effluent was negative for *Legionella*, indicating that the risk for ongoing contamination of the MWTP and river were reduced.

Discussion

The LD outbreak in Boxtel occurred in 2 distinct small clusters, rather than a more typical single cluster of cases in a short period. However, the increased LD incidence in the town compared with historical values and the matching sequencing results of clinical isolates suggested a common source for both clusters.

The sequence type ST1646, found in 5 patient isolates and in the environmental samples, identified the BWTP as the most likely source for both LD clusters. Since 2013, this rare sequence type has been detected in 7 other cases in the same region and 2 cases elsewhere in the Netherlands (*3*). ST1646 has not previously been detected in environmental samples (*3*). We were unable to epidemiologically link the other ST1646 cases to Boxtel.

The transmission models outcome, which posited a single hotspot near the BWTP, offers further support

for the BWTP as the putative source of infection. The distance of the hotspot, at ≈650 m, is well within the range of a possible source calculated with this model in a previous study (*5*).

Two other clinical strains from cluster 1 were not found in any environmental sample. However, the aeration ponds might have harbored different genotypes. Detection of multiple genotypes causing LD cases from exposure to a single water treatment plant has been previously described (*6*).

BWTPs have been identified as the source of previous LD outbreaks (*6–10*). Several risk factors for amplification and transmission of *Legionella* were present in the Boxtel BWTP: a water temperature around 35°C, nutrient-rich water, and aerosol formation through aeration.

Documented outbreaks associated with BWTPs have involved an additional disseminator, such as a WCT or river, in the dissemination of contaminated aerosols, usually marked by a sudden increase in cases. In this outbreak, we assume direct dispersion of bacteria from the BWTP ponds to the patients, which could explain the sporadic nature of the epidemic curve, with 0–2 cases per week spread over 2 periods of 8–16 weeks.
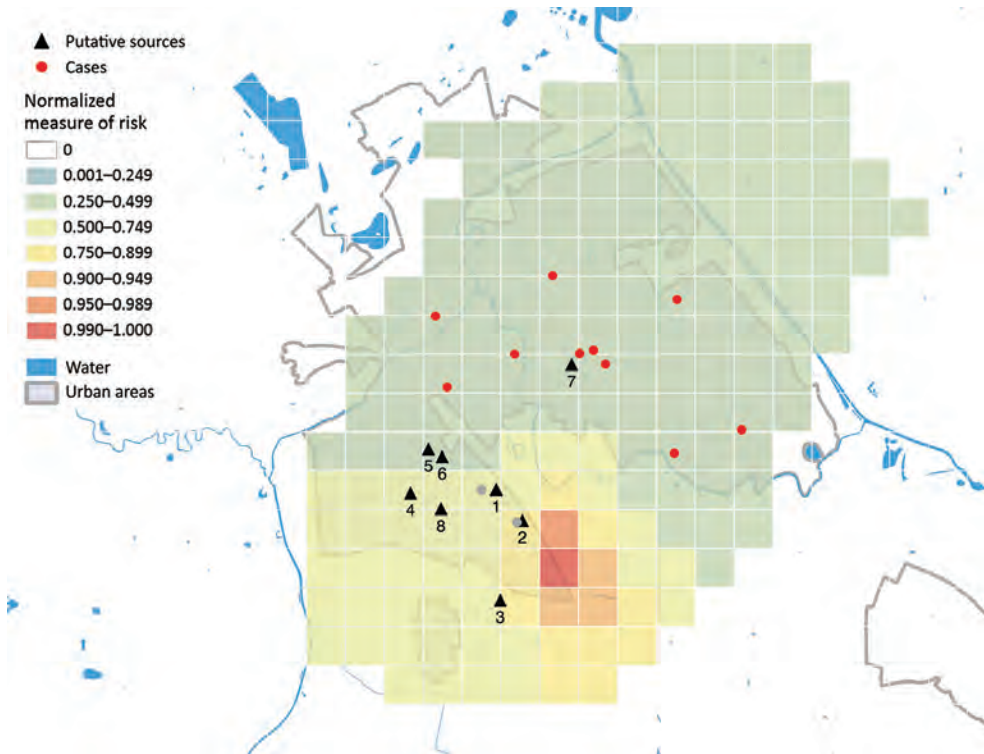
Figure 2. Map of the norrmalized measure of risk for Legionnaires' disease, Boxtel, the Netherlands, October 2016–December 2017. Results are based on case-patients living in Boxtel who constituted the clusters occurring in 2016 and 2017 (n = 11). Red dots indicate the residential address (postal code) of case-patients. A hotspot is an area with a measure of risk ≥0.9. Gray dots indicate Legionnaires' disease cases in nonresidents; these cases are not included in the model. Black triangles indicate the putative sources: 1, biologic wastewater treatment plant (industrial area); 2, wet cooling tower next to the biologic waste water treatment plant (industrial area); 3–6, wet cooling towers (industrial area); 7, fountain (city center); 8, misting device (industrial area).

Transmission from WCTs has been described as occurring at a distance of up to 12 km (*11*), whereas direct aerosol dispersal from BWTPs has been detected at a distance of up to 300 m (*8*). In this outbreak, the assumed bacteria transmission from the BWTP ponds to the patients occurred over a distance of ≥1.6 km. Transmission directly from the elevated aeration ponds is plausible with prevailing wind direction. However, we cannot exclude the possibility that WCTs, air scrubbers, or both in the vicinity of the BWTP disseminated *L. pneumophila*–containing aerosols, although test results for these installations were negative.

Although incidence of community-acquired LD has increased in the Netherlands since 2013 (*12*), infection sources are rarely found (*13*). Because our results indicate direct dispersal over a large distance of ≥1.6 km, further investigations should consider nontraditional *Legionella* sources, like BWTPs, as possible sources for sporadic LD cases.

The aeration ponds in Boxtel were covered, but whether this measure is sufficient to mitigate all exposure risks involved with this type of installation is still unclear. Because biologic aeration ponds are increasingly used in modern (energy-producing) wastewater treatment installations in the Netherlands, more evaluation is required for the potential health risks associated with BWTPs.

About the Author

Ms. Loenenbach is a fellow at the European Programme for Intervention Epidemiology Training and is based at the National Institute for Public Health and Environment, the Netherlands. Her primary research interests include infectious disease epidemiology, social anthropology, and gender studies.
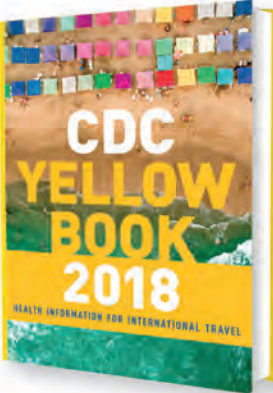
References

1. European Centre for Disease Prevention and Control. European Legionnaires' Disease Surveillance Network (ELDSNet)—operating procedures for the surveillance of travel-associated Legionnaires' disease in the EU/EEA. Stockholm: European Centre for Disease Prevention and Control; 2017.
2. Ratzow S, Gaia V, Helbig JH, Fry NK, Lück PC. Addition of *neuA*, the gene encoding N-acylneuraminate cytidylyl transferase, increases the discriminatory ability of the consensus sequence-based scheme for typing *Legionella pneumophila* serogroup 1 strains. J Clin Microbiol. 2007;45:1965–8. http://dx.doi.org/10.1128/JCM.00261-07
3. Gaia V, Fry NK, Afshar B, Lück PC, Meugnier H, Etienne J, et al. Consensus sequence-based scheme for epidemiological typing of clinical and environmental isolates of *Legionella pneumophila.* J Clin Microbiol. 2005;43:2047–52. http://dx.doi.org/10.1128/JCM.43.5.2047-2052.2005
4. Schimmer B, Ter Schegget R, Wegdam M, Züchner L, de Bruin A, Schneeberger PM, et al. The use of a geographic information system to identify a dairy goat farm as the most likely source of an urban Q-fever outbreak. BMC Infect Dis. 2010;10:69. http://dx.doi.org/10.1186/1471-2334-10-69
5. van Leuken JP, Havelaar AH, van der Hoek W, Ladbury GA, Hackert VH, Swart AN. A model for the early identification of sources of airborne pathogens in an outdoor environment. PLoS One. 2013;8:e80412. http://dx.doi.org/10.1371/journal.pone.0080412
6. Kusnetsov J, Neuvonen LK, Korpio T, Uldum SA, Mentula S, Putus T, et al. Two Legionnaires' disease cases associated with industrial waste water treatment plants: a case report. BMC Infect Dis. 2010;10:343. http://dx.doi.org/10.1186/1471-2334-10-343
7. Blatny JM, Reif BA, Skogan G, Andreassen O, Høiby EA, Ask E, et al. Tracking airborne *Legionella* and *Legionella pneumophila* at a biological treatment plant. Environ Sci Technol. 2008;42:7360–7. http://dx.doi.org/10.1021/es800306m
8. Olsen JS, Aarskaug T, Thrane I, Pourcel C, Ask E, Johansen G, et al. Alternative routes for dissemination of *Legionella pneumophila* causing three outbreaks in Norway. Environ Sci Technol. 2010;44:8712–7. http://dx.doi.org/10.1021/es1007774
9. Nygård K, Werner-Johansen Ø, Rønsen S, Caugant DA, Simonsen Ø, Kanestrøm A, et al. An outbreak of legionnaires disease caused by long-distance spread from an industrial air scrubber in Sarpsborg, Norway. Clin Infect Dis. 2008;46:61–9. http://dx.doi.org/10.1086/524016
10. van Heijnsbergen E, Schalk JA, Euser SM, Brandsema PS, den Boer JW, de Roda Husman AM. Confirmed and potential sources of *Legionella* reviewed. Environ Sci Technol. 2015;49:4797–815. http://dx.doi.org/10.1021/acs.est.5b00142
11. Walser SM, Gerstner DG, Brenner B, Höller C, Liebl B, Herr CE. Assessing the environmental health relevance of cooling towers—a systematic review of legionellosis outbreaks. Int J Hyg Environ Health. 2014;217:145–54. http://dx.doi.org/10.1016/j.ijheh.2013.08.002
12. Rijksinstituut voor Volksgezondheid en Milieu. *Legionella* webpagina [in Dutch] [cited 2018 Jul 5]. https://www.rivm.nl/Onderwerpen/L/Legionella/Legionella_webpagina1
13. Den Boer JW, Euser SM, Brandsema P, Reijnen L, Bruin JP. Results from the National *Legionella* Outbreak Detection Program, the Netherlands, 2002-2012. Emerg Infect Dis. 2015;21:1167–73. http://dx.doi.org/10.3201/eid2107.141130

Address for correspondence: Anna D. Loenenbach, Rijksinstituut voor Volksgezondheid en Milieu Antonie van Leeuwenhoeklaan 9, 3721 MA Bilthoven, Bilthoven 3720 BA, the Netherlands; email: aloenenbach@gmail.com

Rapid Spread of Pneumococcal Nonvaccine Serotype 7C Previously Associated with Vaccine Serotype 19F, England and Wales

Ashley Makwana, Shamez N. Ladhani,
Georgia Kapatai, Ella Campion,
Norman K. Fry, Carmen Sheppard

We observed a sudden and rapid increase in rare invasive pneumococcal disease serotype 7C, from an annual average of 3 cases during 2000–01 through 2015–16 to 29 cases in 2016–17. The increase was caused almost entirely by clonal expansion of sequence type 177, previously associated with vaccine serotype 19F.

The bacterium *Streptococcus pneumoniae* is a major global cause of meningitis, septicemia, and pneumonia and is associated with high rates of illness and death. In September 2006, the childhood immunization program in the United Kingdom introduced PCV7, a pneumococcal conjugate vaccine against the 7 most common serotypes causing invasive pneumococcal disease (IPD) in children; a 13-valent PCV replaced it in April 2010 (*1*). Both vaccines have been associated with rapid and widespread declines in IPD across all age groups and, despite an increase in other disease from non-PCV serotypes, overall IPD rates have dropped by 56% and have remained lower than prevaccine rates (*1*).

In England and Wales, Public Health England (PHE) conducts enhanced national surveillance for IPD (*1*). National Health Service laboratories routinely report clinically significant infections to PHE and submit invasive isolates to the PHE National Reference Laboratory for serotyping (*2*). We observed an unusual increase in invasive isolates serotyped as 7C early in 2017 that continued into the 2017–18 epidemiologic year. We analyzed the epidemiology, clinical characteristics, genetic epidemiology, and outcomes of serotype 7C IPD since 2000–01 in England and Wales.

The Study

We performed whole-genome sequencing (WGS) on 44 of 66 invasive 7C isolates collected during July 2005–June

2017, as well as 37 of 42 isolates collected during July 2017–January 31, 2018. We used previously published methods for WGS analysis (*3,4*). We used Bowtie version 2 (*5*) to map WGS reads to sequences for 1,689 antimicrobial-resistant genes in the ARG-ANNOT database (*6*). We used PBP typing to predict β-lactam resistance (*7*). Using MEGA7 (*8*), we drew a neighbor-joining tree (*9*) based on single-nucleotide polymorphism (SNP) alignments, as previously described (*10*). We included PHE data available on the European Nucleotide Archive (https://www.ebi.ac.uk/ena) (online Technical Appendix Table, https://wwwnc.cdc.gov/EID/article/24/10/18-0114-Techapp1.pdf) and used a non–sequence type (ST) 177 serotype 19F (Taiwan 19F-14; GenBank accession no. NC_012469.1) as a reference sequence. We did not identify and remove recombination events in the WGS alignment before constructing the phylogeny. Data on antimicrobial drug susceptibility testing performed according to British Society for Antimicrobial Chemotherapy guidelines (*11*) were available on a subset of isolates.

From epidemiologic year 2000–01 through 2015–16, a total of 84,305 laboratory-confirmed IPD episodes occurred in England and Wales, including 51 serotype 7C IPD cases; an annual average of 3 cases (range 1–6) were confirmed. In 2016–17, a total of 29 cases were confirmed, compared to 5, 4, and 4 in the previous 3 years (2013–14, 2014–15, and 2015–16, respectively); an additional 42 cases were confirmed during the first 7 months of the 2017–18 epidemiologic year (Figure 1, panel A). We found no evidence of geographic or temporal clustering of cases. Cases were diagnosed across all age groups and especially in those ≥65 years of age (84/122, 68.9%), including 38 cases in the 65–79 age group and 46 cases in persons ≥80 years of age. Of the 80 cases (93.8%) diagnosed from 2000–01 through 2016–17, a total of 75 included bacteremia and 5 meningitis (in patients ages 1 month, 5 months, 6 months, 30 years, and 48 years).

All isolates were cultured from blood or cerebrospinal fluid. Case-fatality ratio (CFR) was 25% (20/80) and increased with age: 12.5% (1/8) in children <15 years of age, 0 in the 15–44-year age group, 23% (3/13) in the 45–64-year age group, 25% (6/24) in the 65–79-year age group, and 37% (10/27) in the ≥80-year age group. CFR in the oldest 2 age groups was similar to the CFR for other serotypes
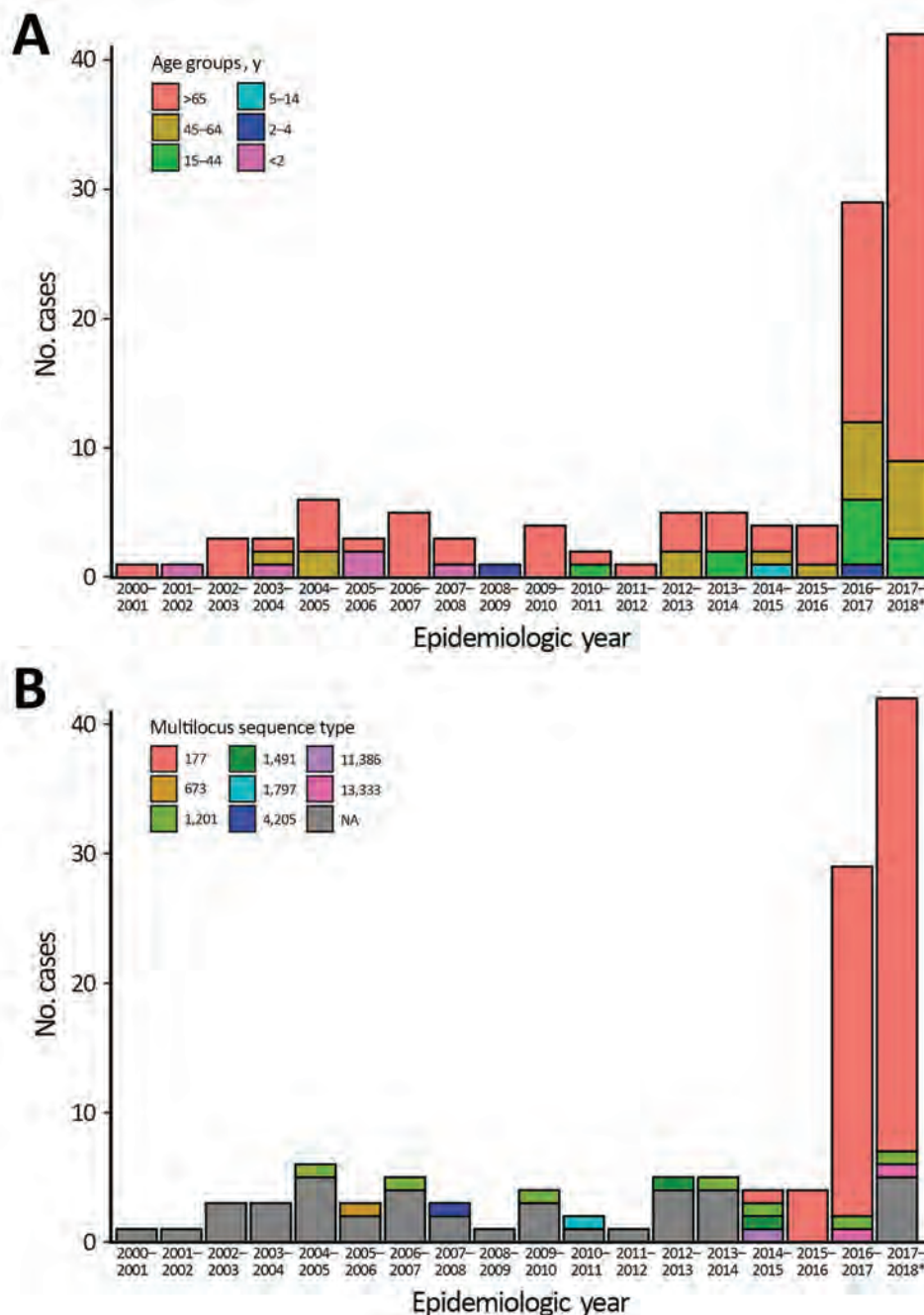
Figure 1. Cases of invasive pneumococcal disease (IPD) caused by serotype 7C between epidemiologic years 2000–01 and 2016–17 and an additional 42 cases reported July 1, 2017, through January 31, 2018, by (A) age group and (B) MLST sequence type, England and Wales. Surveillance is not complete for the 2017–18 epidemiologic year; figure shows only cases for the 7 months indicated. NA indicates missing sequence data.

in those age groups (23% for the 65–79-year age group and 40% for the ≥80-year age group).

The first serotype 7C isolate associated with ST177 appeared in 2012–13 and again in 2014–15, followed by all 4 cases in 2015–16 and 27/29 cases in 2016–17 (Figure 1, panel B). During July 2017–January 2018, a total of 35/37 sequenced 7C isolates were associated with ST177. A review of available PHE MLST data showed that ST177 was also associated with serotypes 19F (MLST derived for 25 isolates during 2002–2015) and 24F (MLST derived for 13 isolates during 2014–15).

We generated the neighbor-joining tree (Figure 2) following SNP analyses on 59 isolates, using MEGA7 using isolate Taiwan 19F-14. The tree shows that 7C-ST177 isolates had a more recent common ancestor with serotypes 19F and 24F belonging to ST177 than with non-ST177 7C isolates (except the single isolate belonging to ST11386, a single-locus variant [SLV] of ST177). The 7C-ST177

isolates were closely related, with <100 SNPs between them. We found >6,000 SNPs separating the 7C-ST177 and the non-ST177 serotype 7C (except 1 SLV of ST177 with <100 SNP distance from the ST177 isolates).

We did not detect any antimicrobial drug resistance determinants or PBP types suggesting β-lactam nonsusceptibility in the genomes of any ST177 7C isolates. MIC data were available on 13 serotype 7C isolates but only 2 were ST177; both were fully susceptible to all antimicrobial drugs tested.

Conclusions

In England and Wales, the recent increase in IPD due to the nonvaccine serotype 7C was associated with clonal expansion of ST177. Previously, this serotype was associated with vaccine serotype 19F, although we also observed serotype 24F isolates with this ST in later years. Nearly all the increase occurred in older adults, with no evidence of change in clinical presentation or CFR when compared with the other serotypes causing IPD in the same age groups. The age-related CFRs observed in our cohort are consistent with those from other industrialized countries with established PCV programs (*12*).

Additional WGS data from historical serotypes 19F and 24F isolates may help determine whether this 7C-ST177 arose from capsular switching, which appears likely given the rapid expansion of this clone. It is also possible that the increase in serotype 24F IPD after PCV13 replaced PCV7 may be attributable to ST177 (*1*), although we did not investigate this in our study. IPD cases due to serotype 24F have increased in children (from 3 to 28 cases), adults (from 7 to 71 cases), and older adults (from 14 to 84 cases) since PCV13 implementation (*1*).

ST177 has been associated with serotype 19F, with 39/42 isolates submitted to the PubMLST isolates database associated with this serotype (https://pubmlst.org/spneumoniae/). In England and Wales, ST177 was represented exclusively by serotype 19F in elderly patients before PCV7 introduction (*13*). Because serotypes 19F and 24F are common causes of IPD, we were unable to sequence all invasive isolates. The clonal expansion of 7C-ST177 could be a consequence of natural fluctuation of nonvaccine serotypes caused by negative frequency selection (*14*). Although ST177 is the ST of the globally disseminated Portugal 19F-21 Pneumococcal Molecular Epidemiology Network clone that is multidrug resistant (*15*), we did not identify resistance determinants in any of the 7C-ST177 isolates we studied.

In summary, serotype 7C remains a rare cause of IPD in England and Wales but is linked to a sudden, rapid increase in cases of IPD because of clonal expansion of ST177, previously associated with vaccine serotype 19F. We encourage other countries to monitor pneumococcal surveillance programs for evidence of similar increases.

Figure 2. Neighbor-joining tree following single-nucleotide polymorphism analyses on 59 pneumococcal isolates collected in England and Wales during July 2005–June 2017. The percentage of replicate trees in which the associated taxa clustered together in the bootstrap test (1,000 replicates) is shown next to the branch junctions. All positions with <90% site coverage were eliminated. Missing data and ambiguous bases were allowed at any position. There were a total of 20,359 variant positions in the final dataset. Red nodes represent ST177 isolates; green node, an isolate with SLV of ST177; black nodes, non-ST177 isolates. Squares represent 7C serotype; triangles, 24F serotype; and circles 19F serotype. The open circle represents the Taiwan 19F-14 reference sequence (GenBank accession no. NC_012469.1). Scale bar shows the number of nucleotide substitutions represented by branch length. ST, sequence type.

About the Author

Mr. Makwana is an epidemiologic analyst at Public Health England in London. He is involved in the enhanced national surveillance of invasive pneumococcal disease in England and Wales, with a particular interest in the direct and indirect population impact of conjugate vaccines on prevention of invasive bacterial infections.

References

1. Waight PA, Andrews NJ, Ladhani SN, Sheppard CL, Slack MP, Miller E. Effect of the 13-valent pneumococcal conjugate vaccine on invasive pneumococcal disease in England and Wales 4 years after its introduction: an observational cohort study. Lancet Infect Dis. 2015;15:535–43. http://dx.doi.org/10.1016/S1473-3099(15)70044-7
2. Lund E, Henrichsen J. Laboratory diagnosis, serology and epidemiology of *Streptococcus pneumoniae*. In: Bergan T, Norris JR, editors. Methods in microbiology. 12th edition. London, New York, San Francisco: Academic Press; 1978. p. 241–62.
3. Kapatai G, Sheppard CL, Al-Shahib A, Litt DJ, Underwood AP, Harrison TG, et al. Whole genome sequencing of *Streptococcus pneumoniae*: development, evaluation, and verification of targets for serogroup and serotype prediction using an automated pipeline. PeerJ. 2016;4:e2477. http://dx.doi.org/10.7717/peerj.2477
4. Tewolde R, Dallman T, Schaefer U, Sheppard CL, Ashton P, Pichon B, et al. MOST: a modified MLST typing tool based on short read sequencing. PeerJ. 2016;4:e2308. http://dx.doi.org/10.7717/peerj.2308
5. Langmead B. Aligning short sequencing reads with Bowtie. Curr Protoc Bioinform. 2010;32: 11.7.1–11.7.14.
6. Gupta SK, Padmanabhan BR, Diene SM, Lopez-Rojas R, Kempf M, Landraud L, et al. ARG-ANNOT, a new bioinformatic tool to discover antibiotic resistance genes in bacterial genomes. Antimicrob Agents Chemother. 2014;58:212–20. http://dx.doi.org/10.1128/AAC.01310-13
7. Li Y, Metcalf BJ, Chochua S, Li Z, Gertz RE Jr, Walker H, et al. Penicillin-binding protein transpeptidase signatures for tracking and predicting β-lactam resistance levels in *Streptococcus pneumoniae*. MBio. 2016;7:e00756-16. http://dx.doi.org/10.1128/mBio.00756-16
8. Kumar S, Stecher G, Tamura K. MEGA7: Molecular Evolutionary Genetics Analysis version 7.0 for bigger datasets. Mol Biol Evol. 2016;33:1870–4. http://dx.doi.org/10.1093/molbev/msw054
9. Saitou N, Nei M. The neighbor-joining method: a new method for reconstructing phylogenetic trees. Mol Biol Evol. 1987;4:406–25.
10. Kapatai G, Sheppard CL, Troxler LJ, Litt DJ, Furrer J, Hilty M, et al. Pneumococcal 23B molecular subtype identified using whole genome sequencing. Genome Biol Evol. 2017;9:2145–58. http://dx.doi.org/10.1093/gbe/evx092
11. A guide to sensitivity testing. Report of the Working Party on Antibiotic Sensitivity Testing of the British Society for Antimicrobial Chemotherapy. J Antimicrob Chemother. 1991;27 Suppl D:1–50.
12. Marrie TJ, Tyrrell GJ, Majumdar SR, Eurich DT. Effect of age on the manifestations and outcomes of invasive pneumococcal disease in adults. Am J Med. 2018;131:100.e1–100.e7.
13. Pichon B, Bennett HV, Efstratiou A, Slack MP, George RC. Genetic characteristics of pneumococcal disease in elderly patients before introducing the pneumococcal conjugate vaccine. Epidemiol Infect. 2009;137:1049–56. http://dx.doi.org/10.1017/S0950268808001787
14. Corander J, Fraser C, Gutmann MU, Arnold B, Hanage WP, Bentley SD, et al. Frequency-dependent selection in vaccine-associated pneumococcal population dynamics. Nat Ecol Evol. 2017; 1:1950–1960.
15. Sá-Leão R, Tomasz A, Sanches IS, Brito-Avô A, Vilhelmsson SE, Kristinsson KG, et al. Carriage of internationally spread clones of *Streptococcus pneumoniae* with unusual drug resistance patterns in children attending day care centers in Lisbon, Portugal. J Infect Dis. 2000;182:1153–60. http://dx.doi.org/10.1086/315813

Address for correspondence: Ashley Makwana, Public Health England's National Infection Service, Immunisation, Hepatitis, and Blood Safety Department, 61 Colindale Ave, London, NW9 5EQ, UK; email: Ashley.Makwana@phe.gov.uk

Acute Encephalitis with Atypical Presentation of Rubella in Family Cluster, India

Sumit D. Bharadwaj,[1] Rima R. Sahay,[1] Pragya D. Yadav, Sara Dhanawade, Atanu Basu, Virendra K. Meena, Suji George, Rekha Damle, Gajanan N. Sapkal

We report 3 atypical rubella cases in a family cluster in India. The index case-patient showed only mild febrile illness, whereas the other 2 patients showed acute encephalitis and died of the disease. We confirmed rubella in the index and third cases using next-generation sequencing and IgM.

Rubella is usually considered a mild viral infection. Approximately 25%–50% of infections are asymptomatic (*1*). Differential diagnosis of viral acute encephalitis syndrome (AES) caused by rubella, herpes simplex virus, measles, varicella zoster virus, and Epstein–Barr virus infections can be accomplished through the unique presentation of rash in each case. Rubella typically presents as fever with rash and is mostly diagnosed clinically, but rubella leading to fatal AES is rare (1/6,000 cases) (*2*). A cluster of rubella-associated encephalitis has been reported from Japan (*3*) and rubella encephalitis without rash from Tunisia (*4*).

We report on rubella in 3 unvaccinated siblings in India. We investigated this family cluster at the request of the treating physician in August 2017, on the eighth day postinfection of the index case-patient.

The Study

The affected family belonged to a lower-middle-income group in a village in Maharashtra, India. The father worked as a ward attendant at a hospital, and the mother was a homemaker. There were 3 children in the family; the index rubella case-patient was a 7-year-old girl, who recovered following a mild febrile illness. The 2 other siblings, an 8-year-old girl and a 2-year-old boy, died of acute encephalitis within 4 days of onset of disease (Figure). No history of similar illness in the neighborhood, travel history, or visitors were reported. There was also no history of consumption of fruits or accidental ingestion of any toxic drugs or pesticides

Author affiliations: National Institute of Virology, Pune, India (S.D. Bharadwaj, R.R. Sahay, P.D. Yadav, A. Basu, V.K. Meena, S. George, R. Damle, G.N. Sapkal); Bharati Vidyapeeth Deemed University Medical College and Hospital, Sangli, India (S. Dhanawade)

before symptom onset. Nutritional status for all children was normal for height, weight, and body mass index.

The index case-patient developed a low-grade intermittent fever; her temperature rose in the evening. The fever subsided within 2 days after the patient took acetaminophen. She had not been immunized against rubella. Her throat was uncongested and there were no rashes or mucocutaneous lesions. Systematic examination revealed no abnormalities. Biochemical tests were normal. Tests for dengue virus and malarial parasites were negative. The child recovered without any sequelae. The investigating team examined her on the eighth day following onset of symptoms.

Two days following onset of illness in the index case-patient, her 8-year-old sister developed a high-grade fever and eye pain. There was no history of rash or mucocutaneous lesions. On day 2 of her illness, she had multiple episodes of convulsions with nonprojectile vomiting and was admitted to a hospital. On day 3, she was put on a mechanical ventilator, but she died that day. The cause of death was cardiorespiratory failure with meningoencephalitis due to intractable seizures. This child had not been immunized for rubella; no clinical samples were available to test.

One day after the onset of fever in the second patient, her 2-year-old brother developed a mild fever with no rash or mucocutaneous lesions. His intermittent fever subsided after he took acetaminophen. Two days later, he developed a high-grade fever with convulsions and nonprojectile vomiting. He became semiconscious, with decerebrated rigidity. He became comatose and was put on mechanical ventilation on day 4 of his illness. Plantar reflex was absent, and deep tendon reflexes were diminished. No cardiovascular system abnormality was noted. His chest was clear, with no wheeze or stridor. Abdominal examination revealed no notable organomegaly. The child received antimicrobial drugs, phenytoin, mannitol, and acyclovir. He died on day 5 of his illness. Details from the medical records for the second and third case-patients are provided in online Technical Appendix 1 Table 1 (https://wwwnc.cdc.gov/EID/article/24/10/18-0053-Techapp1.pdf).
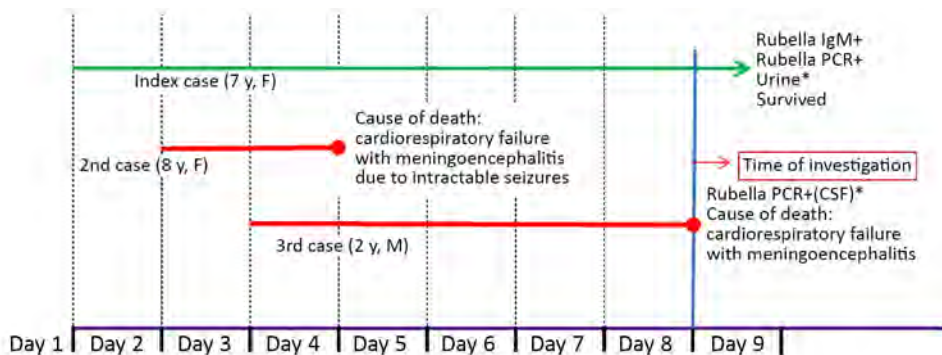
We tested serum and urine samples from the index case-patient and serum, urine, and cerebrospinal fluid (CSF) samples from the third case-patient for Japanese encephalitis virus (*5*), West Nile virus (*6*), Chandipura virus (*7*), and enteroviruses (*8*) using real-time quantitative reverse

---

Figure. Timeline of clinical events for 3 siblings infected with rubella and encephalitis, India. *Negative for Japanese encephalitis virus, Chandipura virus, dengue virus, West Nile virus, enterovirus, and herpes simplex virus. CSF, cerebrospinal fluid.

transcription PCR (qRT-PCR); for dengue, chikungunya, and Zika viruses using CDC Trioplex qRT-PCR; and for rubella using RT-PCR (*9*). We further used quantitative PCR to test for varicella zoster virus DNA (*10*) and PCR for herpes simplex virus 1 (Genekam Biotechnology, Duisburg, Germany, No. K091). We also tested samples for rubella IgM and IgG using a Siemens Healthcare Kit (Siemens, Erlangen, Germany). We extracted RNA and DNA using a QIAAmp total nucleic acid extraction kit (QIAGEN, Hilden, Germany).

We obtained a rubella nested PCR product of 185 bases from a CSF sample from the third case-patient; no amplification was obtained from serum and urine, so we used the CSF sample for next-generation sequencing (*11*).We tested serum samples from close contacts of the index and third case-patients for the presence of rubella IgM and IgG (Table 1; online Technical Appendix 2, https://wwwnc.cdc.gov/EID/article/24/10/18-0053-Techapp2.xlsx). We prepared the RNA library following the defined protocol (*12*) using

a TruSeq Stranded mRNA Library preparation kit (Illumina, San Diego, CA, USA); quantified it using a KAPA Library Quantification Kit (Roche, Indianapolis, IN, USA); and loaded it on an Illumina Miniseq NGS platform. We imported raw RNA data of 147 MB in CLC Genomics Workbench software (QIAGEN) for further analysis. We assembled the RNA data using de novo and reference assembly methods and obtained 1.9 million reads with an average length of 138 bp. From the total read, 0.57% mapped to the reference genome (GenBank accession no. JN635296) with an average length of 123 bp. De novo assembly of reads gave 86 contigs with an average length of 1,281 bp. Reference mapping led to a ≈8 kb region (4.5 kb of nonstructural protein [NSP], 3 kb of structural protein [SP], and 0.5 kb in both NSP and SP regions) that was broken intermittently (GenBank accession nos. MG987207.1 for NSP and MG987208.1 for SP) (online Technical Appendix 1 Figure 1). We used a 732-bp E1 gene sequence to identify the rubella genotype (online Technical

Table 1. Laboratory investigations and results of the clinical samples of close contacts of case-patients with rubella and encephalitis in a family cluster in India

NIV no.*	Specimen	Contact relationship to index and third case-patients	Age, y/sex	Contact with case-patients	Anti-rubella IgM ELISA	Anti-rubella IgG ELISA
1730348	Serum	Father	40/M	All 3	Equivocal	Positive
1730348-2	Serum	Father	40/M	All 3	Equivocal	Positive
1730358	Serum	Mother	27/F	All 3	Negative	Positive
1730358-2	Serum	Mother	27/F	All 3	Negative	Positive
1730362	Serum	Physician	38/F	Index, 3rd	Negative	Positive
1730365	Serum	Physician	32/F	Index, 3rd	Negative	Positive
1730367	Serum	Physician	25/F	Index, 3rd	Negative	Positive
1730371	Serum	Physician	26/F	Index, 3rd	Negative	Positive
1730382	Serum	Physician	26/F	Index, 3rd	Negative	Positive
1730411	Serum	Physician	25/F	Index, 3rd	Negative	Positive
1730389	Serum	Physician	26/F	Index, 3rd	Negative	Positive
1730391	Serum	Nursing staff	22/F	Index, 3rd	Positive	Positive
1730394	Serum	Nursing staff	25/F	Index, 3rd	Negative	Positive
1730396	Serum	Nursing staff	29/F	Index, 3rd	Negative	Equivocal
1730398	Serum	Paternal uncle 1	33/M	Index, 3rd	Negative	Positive
1730374	Serum	Paternal aunt 1	25/F	Index, 3rd	Negative	Positive
1730933	Serum	Paternal uncle 2	34/M	Index, 3rd	Negative	Positive
1730936	Serum	Cousin	11/M	Index, 3rd	Negative	Positive
1730939	Serum	Cousin	8/M	Index, 3rd	Negative	Negative
1730941	Serum	Paternal aunt 2	21/F	Index, 3rd	Negative	Positive
1730944	Serum	Grandfather	70/M	Index, 3rd	Negative	Positive
1730948	Serum	Grandmother	65/F	Index, 3rd	Negative	Positive
1730950	Serum	Paternal aunt 2	26/F	Index, 3rd	Negative	Positive

*NIV, National Institue of Virology.

Table 2. Rubella virus variability with respect to Indian strain BAS*†

	Intragroup variability, %	
Genotype	Nucleotide	Amino acid
GI	6–9	1–2
GII	2–8	0–1
GIIA	8	0–1
GIIB	2–3	0–1
GIIC	7	0–2
NIV E1 gene	3	1

*GenBank accession no. AF039134.
†NIV, National Institue of Virology.

Appendix 1 Figure 1). The phylogenetic tree that we constructed revealed that this virus belongs to rubella genotype 2B (Table 2; online Technical Appendix 1 Figure 2).

Conclusions

Rubella encephalitis without identification of typical rubella rash is rarely reported. In the cluster we describe, the parents were asymptomatic and positive for anti-rubella IgG when tested on the eighth day from the onset of symptoms in the index case-patient. The rubella IgM equivocal status of the father suggests that he could be a possible source of infection to the family. His occupation as a hospital ward attendant also indicates a possibility of infection either through respiratory secretions or by contact with an infectious agent on his body or on items carried to and from his workplace. In rubella, neurologic symptoms most often occur 1–6 days after the onset of the exanthem (*13*). In this cluster, rapid disease progression meant the second and third case-patients died within 4 days of illness onset. The index case-patient tested positive for rubella IgM on the eighth day postinfection and the third case-patient tested positive for rubella IgM on the fifth day postinfection, but their specimens were negative for IgG, suggesting that the children were not immunized and had not had any past rubella infection. A serum sample from the index case-patient from the 14th day postinfection was IgG positive. Through epidemiologic linkage, the causative agent in the second case may be similar to that for the other cases.

In conclusion, rubella encephalitis can present without rash. Rubella virus infection should be considered in the differential diagnosis of AES in unvaccinated children.

Acknowledgments

About the Author

Dr. Bhardwaj and Dr. Sahay are medical scientists at the National Institute of Virology, Pune, India, and are trained in clinical and field epidemiology. Their research areas include respiratory illness of viral origin and emerging and reemerging viral infections as well as clinical and epidemiological investigation of disease outbreaks.

References

1. Prober CG. Central nervous system infections. In: Behrman RE, Kliegman RM, Jenson HB, editors. Nelson textbook of pediatrics. Philadelphia: W.B. Saunders, 2004. p. 2038–47.
2. Paret G, Bilori B, Vardi A, Barzilay A, Barzilay Z. [Rubella encephalitis]. Harefuah. 1993;125:410–1, 447.
3. Ishikawa T, Asano Y, Morishima T, Nagashima M, Sobue G, Watanabe K, et al. Epidemiology of acute childhood encephalitis: Aichi Prefecture, Japan, 1984–90. Brain Dev. 1993;15:192–7. https://dx.doi.org/10.1016/0387-7604(93)90064-F
4. Chaari A, Bahloul M, Berrajah L, Ben Kahla S, Gharbi N, Karray H, et al. Childhood rubella encephalitis: diagnosis, management, and outcome. J Child Neurol. 2014;29:49–53. http://dx.doi.org/10.1177/0883073812469443
5. Sapkal GN, Wairagkar NS, Ayachit VM, Bondre VP, Gore MM. Detection and isolation of Japanese encephalitis virus from blood clots collected during the acute phase of infection. Am J Trop Med Hyg. 2007;77:1139–45. https://dx.doi.org/10.4269/ajtmh.2007.77.1139
6. Anukumar B, Sapkal GN, Tandale BV, Balasubramanian R, Gangale D. West Nile encephalitis outbreak in Kerala, India, 2011. J Clin Virol. 2014;61:152–5. http://dx.doi.org/10.1016/j.jcv.2014.06.003
7. Rao BL, Basu A, Wairagkar NS, Gore MM, Arankalle VA, Thakare JP, et al. A large outbreak of acute encephalitis with high fatality rate in children in Andhra Pradesh, India, in 2003, associated with Chandipura virus. Lancet. 2004;364:869–74. http://dx.doi.org/10.1016/S0140-6736(04)16982-1
8. Sapkal GN, Bondre VP, Fulmali PV, Patil P, Gopalkrishna V, Dadhania V, et al. Enteroviruses in patients with acute encephalitis, Uttar Pradesh, India. Emerg Infect Dis. 2009;15:295–8. https://dx.doi.org/10.3201/eid1502.080865
9. Bosma TJ, Corbett KM, O'Shea S, Banatvala JE, Best JM. PCR for detection of rubella virus RNA in clinical samples. J Clin Microbiol. 1995;33:1075–9.
10. Weidmann M, Meyer-König U, Hufert FT. Rapid detection of herpes simplex virus and varicella-zoster virus infections by real-time PCR. J Clin Microbiol. 2003;41:1565–8. http://dx.doi.org/10.1128/JCM.41.4.1565-1568.2003
11. World Health Organization. Standardization of the nomenclature for genetic characteristics of wild- type rubella viruses [cited 2017 Sep 13]. http://www.who.int/immunization/monitoring_surveillance/burden/laboratory/Rubella_nomemclature_report.pdf?ua=1
12. Yadav PD, Albariño CG, Nyayanit DA, Guerrero L, Jenks MH, Sarkale P, et al. Equine encephalosis virus in India, 2008. Emerg Infect Dis. 2018;24:898–901. http://dx.doi.org/10.3201/eid2405.171844
13. Rantala H, Uhari M. Occurrence of childhood encephalitis: a population-based study. Pediatr Infect Dis J. 1989;8:426–30. http://dx.doi.org/10.1097/00006454-198907000-00004

Address for correspondence: Gajanan N. Sapkal, National Institute of Virology, Pune, 20-A, Dr. Ambedkar Road, Pune (Maharashtra), Pin 411001, India; email: gajanansapkalniv@gmail.com

Influenza C Virus in Cattle with Respiratory Disease, United States, 2016–2018

Hewei Zhang, Elizabeth Porter, Molly Lohman,
Nanyan Lu, Lalitha Peddireddi, Gregg Hanzlicek,
Douglas Marthaler, Xuming Liu, Jianfa Bai

We identified influenza C virus (ICV) in samples from US cattle with bovine respiratory disease through real-time PCR testing and sequencing. Bovine ICV isolates had high nucleotide identities (≈98%) with each other and were closely related to human ICV strains (≈95%). Further research is needed to determine bovine ICV's zoonotic potential.

Influenza viruses are contagious zoonotic pathogens that belong to the *Orthomyxoviridae* family, which consists of 4 genera: *Alphainfluenzavirus* (influenza A virus), *Betainfluenzavirus* (influenza B virus), *Gammainfluenzavirus* (influenza C virus [ICV]), and *Deltainfluenzavirus* (influenza D virus) (*1*–*4*). Classification of influenza viruses is based on the antigenic differences in the nucleoprotein and matrix protein and supported by intergenic homologies of 20%–30% and intragenic homologies >85% (*3*).

The most common influenza pathogen is influenza A virus, which can infect humans, pigs, cattle, birds, as well as other animals (*2*,*4*). ICV was first identified in humans in 1947. This group of influenza viruses was initially thought to exclusively infect humans until isolates were identified in pigs in China (*5*,*6*) and Japan (*7*). Antigenic and genetic analyses suggest that ICV might transmit between humans and pigs in nature (*8*); however, interspecies transmission has not been confirmed experimentally. In 2011, an influenza C–like virus was identified in swine and cattle in the United States (*9*); this virus was initially proposed to be an ICV subtype but was later identified as influenza D virus (*3*) because the virus had ≈50% overall amino acid identity with human ICV strains, a level of divergence similar to that between influenza A and influenza B viruses.

Although influenza viruses of other genera can infect cattle, the potential for ICV infection in cattle has not been previously investigated. The objective of this study

Author affiliations: Chinese Academy of Agricultural Sciences, Institute of Special Economic Animal and Plant Sciences, Changchun, China (H. Zhang); Kansas State University Veterinary Diagnostic Laboratory, Manhattan, Kansas, USA (H. Zhang, E. Porter, M. Lohman, N. Lu, L. Peddireddi, G. Hanzlicek, D. Marthaler, X. Liu, J. Bai)

was to determine if ICV can be found in specimens from cattle with bovine respiratory disease and, if so, determine the prevalence.

The Study

Bovine respiratory disease complex (BRDC) is one of the most common causes of death in livestock in US feedlots and feedlots worldwide (*10*). During October 2016–January 2018, we collected 1,525 samples (mainly nasal swab and lung tissue specimens) from cattle in the Midwest of the United States and submitted them to Kansas State Veterinary Diagnostic Laboratory (Manhattan, Kansas, USA) for BRDC diagnostic testing. We screened samples for ICV by real-time reverse transcription PCR, as well as for 10 other BRDC-associated pathogens (*Mannheimia haemolytica*, *Pasteurella multocida*, *Histophilus somni*, *Bibersteinia trehalosi*, *Mycoplasma bovis*, bovine viral diarrhea virus, bovine respiratory syncytial virus, bovine respiratory coronavirus, bovine herpesvirus 1, and influenza D virus; online Technical Appendix, https://wwwnc.cdc.gov/EID/article/24/10/18-0589-Techapp1.pdf). We sequenced a 590-bp fragment of the matrix gene from 12 ICV-positive samples (GenBank accession nos. MH421865–73; online Technical Appendix Table) to confirm the PCR results and perform a phylogenetic analysis. We selected 1 isolate (C/bovine/Montana/12/2016) for complete genome sequencing (GenBank accession nos. MH348113–9).

Of 1,525 samples, 64 (4.20%) were positive for ICV: 38 samples with a cycle threshold (C_t) <36 and 26 with a C_t 36–39. The most common pathogens were bovine respiratory coronavirus (34.98%), *M. bovis* (32.27%), and *M. haemolytica* (17.04%). The remaining BRDC pathogens were present but less prevalent: *P. multocida* (13.42%), *H. somni* (12.58%), influenza D virus (11.93%), bovine respiratory syncytial virus (9.19%), bovine viral diarrhea virus (7.05%), *B. trehalosi* (3.47%), and bovine herpesvirus 1 (2.95%).

Co-infections with ≥1 pathogen are common in BRDC cases. ICV-positive samples were also found to be positive for ≥1 bovine respiratory disease pathogen (n = 12, Table 1), the most common being *M. bovis* (9/12), followed by *H. somni* (7/12), and *M. haemolytica* (6/12). Among the ICV-positive samples, ICV12 was strongly positive (C_t 15.81); this sample was also positive for *M. haemolytica* and *P. multocida*, both bacterial pathogens commonly associated with secondary infections. Other BRDC pathogens associated

Table 1. Cycle thresholds for ICV and other bovine respiratory pathogens in 12 ICV strong positive samples from cattle with respiratory disease, United States, October 2016–January 2018*

ID no.	State	ICV	BVDV	BHV-1	BRSV	BCoV	IDV	*Mycoplasma bovis*	*Mannheimia haemolytica*	*Pasteurella multocida*	*Histophilus somni*	*Bibersteinia trehalosi*
ICV1†	TX	29.95	–	–	–	–	36.77	39.41	–	–	–	–
ICV2†	OK	23.92	–	–	–	–	24.25	29.17	31.30	–	31.32	–
ICV3†	OK	21.02	–	–	38.93	27.00	29.15	31.40	NT	NT	NT	NT
ICV4‡	OK	29.98	–	–	–	–	–	24.54	31.33	–	31.05	–
ICV5†	MO	24.47	–	34.98	–	–	–	30.12	–	28.00	24.40	34.00
ICV6†	CO	26.91	–	–	–	–	–	30.25	32.78	29.60	30.00	35.00
ICV12†	MT	15.81	–	–	–	–	–	–	22.87	25.70	–	–
ICV16‡	NE	27.18	16.44	–	–	–	–	28.47	–	–	–	–
ICV18†	MN	30.58	–	–	–	–	–	–	35.06	–	–	–
ICV20‡	KS	27.92	–	–	–	–	–	–	–	–	23.49	–
ICV21‡	KS	26.72	–	–	35.59	–	–	25.67	30.95	–	28.47	–
ICV22†	MT	25.08	–	–	–	–	20.24	35.58	–	–	35.64	–

*BCoV, bovine respiratory corona virus; BHV-1, bovine herpesvirus 1; BRSV, bovine respiratory syncytial virus; BVDV, bovine viral diarrhea virus; ICV, influenza C virus; ID, identification; IDV, influenza D virus; NT, not tested (sample used up); –, negative.
†Nasal swab sample used in analysis.
‡Lung sample used in analysis.

with secondary infections (*M. bovis*, bovine viral diarrhea virus, and *H. somni*) were also detected in samples ICV4, ICV16, ICV18, and ICV20 (*11–13*). These results suggest that ICV is associated with bovine respiratory disease in cattle.

We further evaluated 12 strong positive (C_t<31) samples by sequencing a 590-bp fragment of their matrix gene. Alignment of the partial matrix gene sequences indicated that the isolates in 3 samples (ICV2, ICV3, and ICV4) obtained from different cattle on the same farm in Oklahoma were identical. Because these 3 influenza viruses were most likely the same strain, the virus in just 1 sample (ICV2) was used for phylogenetic analysis. The matrix gene sequence in sample ICV5 from Missouri (GenBank accession no. MH421866) was identical to that in ICV6 from Colorado (GenBank accession no. MH421867).

Phylogenetic analysis indicated that the bovine ICV isolates are closely related to the porcine and human ICV isolates, and the bovine ICV isolates are more closely related to each other (Table 2; Figure). The bovine ICV isolates' partial matrix gene sequences shared high nucleotide identities (≈98%). For both partial matrix gene sequences and the whole genome sequence (7 segments), the nucleotide identity between bovine and human isolates was ≈95%. The full genome sequence of C/bovine/Montana/12/2016

from sample ICV12 had high nucleotide identity to C/Mississippi/80 (and several other human ICV strains), with an overall identity of 97.1%. Nucleotide identities between these 2 isolates were also high for each gene: 97.0% for polymerase basic 2, 97.7% for polymerase basic 1, 97.5% for polymerase 3, 96.2% for hemagglutinin esterase, 96.8% for nucleoprotein, 96.8% for matrix, and 97.6% for nonstructural protein. The only porcine ICV isolate available was more closely related to human (≈98% identity) isolates than bovine (≈95% identity) isolates; the porcine ICV isolate had nearly the same identity that the human ICV isolates had among each other (Table 2).

The phylogenetic tree of the partial matrix gene sequences (Figure) further demonstrates the relationship between bovine and human ICV isolates. All bovine ICVs formed a separate clade on the phylogenetic tree, with a 99% bootstrap value. Of the 195 partial matrix gene sequences from human ICVs, the 10 corresponding sequences from bovine ICVs had the highest identities (average 96.70%) to those from C/Mississippi/80 (GenBank no. AB000720.1), C/Nara/82 (GenBank no. AB000723), and C/Kyoto/41/82 (GenBank no. AB000724) and the lowest identities (average 94.21%) to those from C/Yamagata/30/2014 (GenBank no. LC123874) and C/Yamagata/32/2014 (GenBank no. LC123875).

Table 2. Average nucleotide identities among bovine, porcine, and human ICV strains, United States*

Gene sequence	Bovine ICV, %	Human ICV, %	Bovine ICV vs. human ICV, %	Bovine ICV vs. porcine ICV, %	Human ICV vs. porcine ICV, %
Matrix, partial	98.43	98.47	95.54	96.06	98.84
Polymerase basic 2	NA	97.76	94.97	95.00	98.34
Polymerase basic 1, full length	NA	97.59	94.69	94.70	98.08
Polymerase 3	NA	97.79	96.36	95.50	97.31
Hemagglutinin esterase	NA	95.44	90.83	91.10	95.97
Nucleoprotein	NA	97.67	95.48	95.30	97.85
Matrix, complete	NA	98.33	95.51	95.80	98.82
Nonstructural protein	NA	98.32	95.67	95.80	98.36
Entire genome		97.56	94.79	94.74	97.82

*ICV, influenza C virus; NA, not applicable.
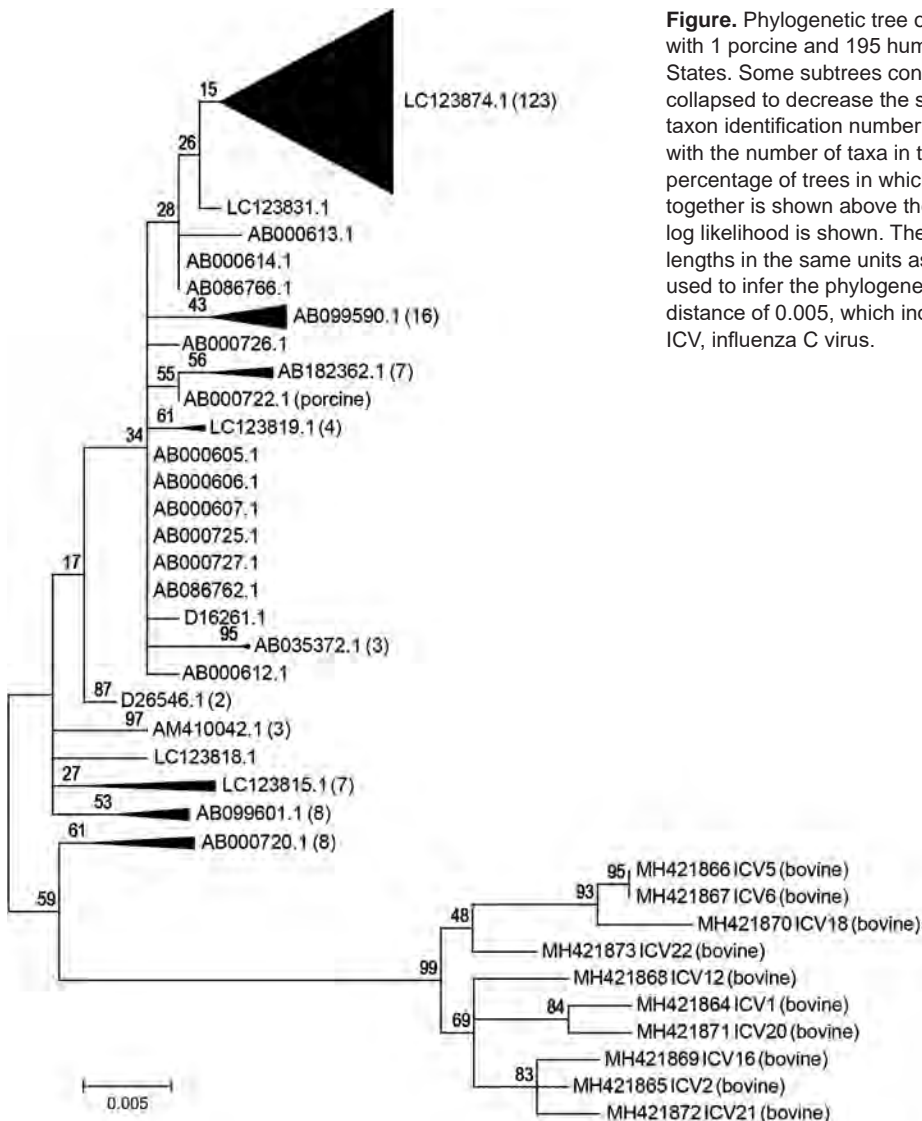
Figure. Phylogenetic tree of 10 bovine ICV isolates compared with 1 porcine and 195 human ICV isolates (not labeled), United States. Some subtrees containing only human isolates were collapsed to decrease the size of the image. A representative taxon identification number for each collapsed subtree is shown with the number of taxa in the subtree in parentheses. The percentage of trees in which the associated taxa clustered together is shown above the branches. The tree with the highest log likelihood is shown. The tree is drawn to scale, with branch lengths in the same units as those of the evolutionary distances used to infer the phylogenetic tree. Scale bar indicates the relative distance of 0.005, which indicates a 0.5% sequence difference. ICV, influenza C virus.

Conclusions

This study confirms the presence of ICV in US cattle with clinical signs of bovine respiratory disease. Although interspecies transmission of influenza viruses occurs between humans and other animals, we do not have data that indicates ICV is a zoonotic pathogen. However, the full genome sequence of C/bovine/Montana/12/2016 has 97.1% nucleotide identity with the human isolate C/Mississippi/80, which is within the range of average identities among human isolates. More detailed investigations are needed to confirm if ICV is involved in bovine respiratory disease, to characterize the relationship between bovine and human ICV strains, and to determine the zoonotic potential of bovine ICV isolates to cause human disease.

About the Author

Mr. Zhang is a joint doctoral student candidate at the Chinese Academy of Agricultural Sciences in Changchun, China, and Kansas State University in Manhattan, Kansas, USA. His research interests are the development and validation of molecular diagnostic assays for animal and zoonotic pathogens.

References

1. King AMQ, Lefkowitz EJ, Mushegian AR, Adams MJ, Dutilh BE, Gorbalenya AE, et al. Changes to taxonomy and the International Code of Virus Classification and Nomenclature ratified by the International Committee on Taxonomy of Viruses (2018). Arch Virol. 2018. http://dx.doi.org/10.1007/s00705-018-3847-1
2. Spickler AR. Influenza. Flu, grippe, avian influenza, grippe aviaire, fowl plaque, swine influenza, hog flu, pig flu, equine influenza, canine influenza. 2016 [cited 2018 Mar 8]. http://www.cfsph.iastate.edu/Factsheets/pdfs/influenza.pdf

3. Hause BM, Collin EA, Liu R, Huang B, Sheng Z, Lu W, et al. Characterization of a novel influenza virus in cattle and swine: proposal for a new genus in the *Orthomyxoviridae* family. MBio. 2014;5:e00031-14. http://dx.doi.org/10.1128/mBio.00031-14

4. Vemula SV, Zhao J, Liu J, Wang X, Biswas S, Hewlett I. Current approaches for diagnosis of influenza virus infections in humans. Viruses. 2016;8:96. http://dx.doi.org/10.3390/v8040096

5. Guo YJ, Jin FG, Wang P, Wang M, Zhu JM. Isolation of influenza C virus from pigs and experimental infection of pigs with influenza C virus. J Gen Virol. 1983;64:177–82. http://dx.doi.org/10.1099/0022-1317-64-1-177

6. Yuanji G, Desselberger U. Genome analysis of influenza C viruses isolated in 1981/82 from pigs in China. J Gen Virol. 1984;65:1857–72. http://dx.doi.org/10.1099/0022-1317-65-11-1857

7. Yamaoka M, Hotta H, Itoh M, Homma M. Prevalence of antibody to influenza C virus among pigs in Hyogo Prefecture, Japan. J Gen Virol. 1991;72:711–4. http://dx.doi.org/10.1099/0022-1317-72-3-711

8. Kimura H, Abiko C, Peng G, Muraki Y, Sugawara K, Hongo S, et al. Interspecies transmission of influenza C virus between humans and pigs. Virus Res. 1997;48:71–9. http://dx.doi.org/10.1016/S0168-1702(96)01427-X

9. Hause BM, Ducatez M, Collin EA, Ran Z, Liu R, Sheng Z, et al. Isolation of a novel swine influenza virus from Oklahoma in 2011 which is distantly related to human influenza C viruses.

PLoS Pathog. 2013;9:e1003176. http://dx.doi.org/10.1371/journal.ppat.1003176

10. US Department of Agriculture. Cattle and calves nonpredator death loss in the United States, 2010. 2011 [cited 2018 Mar 8]. https://www.aphis.usda.gov/animal_health/nahms/general/downloads/cattle_calves_nonpred_2010.pdf

11. Gabinaitiene A, Siugzdaite J, Zilinskas H, Siugzda R, Petkevicius S. *Mycoplasma bovis* and bacterial pathogens in the bovine respiratory tract. Vet Med (Praha). 2011;56:28–34. http://dx.doi.org/10.17221/1572-VETMED

12. Bielefeldt-Ohmann H. The pathologies of bovine viral diarrhea virus infection. A window on the pathogenesis. Vet Clin North Am Food Anim Pract. 1995;11:447–76. http://dx.doi.org/10.1016/S0749-0720(15)30461-8

13. Basqueira NS, Martin CC, dos Reis Costa JF, Okuda LH, Pituco ME, Batista CF, et al. Bovine respiratory disease (BRD) complex as a signal for bovine viral diarrhea virus (BVDV) presence in the herd. Acta Sci Vet. 2017;45:1434.

Address for correspondence: Jianfa Bai or Xuming Liu, Kansas State University, Veterinary Diagnostic Laboratory, College of Veterinary Medicine, 2005 Research Park Cir, Manhattan, KS 66502, USA; email: jbai@vet.ksu.edu or xmliu@vet.ksu.edu

April 2014: **Coronaviruses and Influenza Viruses**

- Distribution of Pandemic Influenza Vaccine and Reporting of Doses Administered, New York, New York, USA

- Regional Variation in Travel-related Illness acquired in Africa, March 1997–May 2011

- Active Surveillance for Avian Influenza Virus, Egypt, 2010–2012

- Antibodies against MERS Coronavirus in Dromedaries, United Arab Emirates, 2003 and 2013

- Novel Betacoronavirus in Dromedaries of the Middle East, 2013

- Rotavirus Surveillance in Urban and Rural Areas of Niger, April 2010–March 2012

- Large Outbreak of *Cryptosporidium hominis* Infection Transmitted through the Public Water Supply, Sweden

- Efficiency of Points of Dispensing for Influenza A(H1N1) pdm09 Vaccination, Los Angeles County, California, USA, 2009

- Underdiagnosis of Foodborne Hepatitis A, the Netherlands, 2008–2010

- Travel-associated Antimicrobial Drug–Resistant Nontyphoidal Salmonellae, 2004–2009

- Ciprofloxacin Resistance and Gonorrhea Incidence Rates in 17 Cities, United States, 1991–2006

- Contact Investigation for Imported Case of Middle East Respiratory Syndrome, Germany

- Rapid Increase in Pertactin-deficient *Bordetella pertussis* Isolates, Australia

- *Gnathostoma* spp. in Live Asian Swamp Eels (*Monopterus* spp.) from Food Markets and Wild Populations, United States

- Epidemic of Mumps among Vaccinated Persons, the Netherlands, 2009–2012

- High Rates of Antimicrobial Drug Resistance Gene Acquisition after International Travel, the Netherlands

- Characteristics of Patients Infected with Norovirus GII.4 Sydney 2012, Hong Kong, China

- Pathology of US Porcine Epidemic Diarrhea Virus Strain PC21A in Gnotobiotic Pigs

- Cetacean Morbillivirus in Coastal Indo-Pacific Bottlenose Dolphins, Western Australia

EMERGING INFECTIOUS DISEASES

https://wwwnc.cdc.gov/eid/articles/issue/20/4/table-of-contents
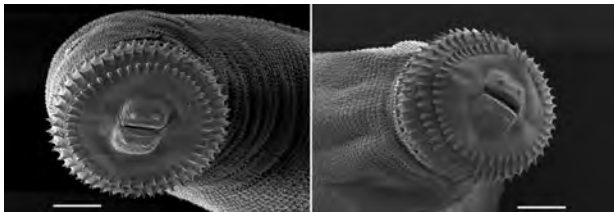
Simple Estimates for Local Prevalence of Latent Tuberculosis Infection, United States, 2011–2015

**Maryam B. Haddad, Kala M. Raz,
Timothy L. Lash, Andrew N. Hill,
J. Steve Kammerer, Carla A. Winston,
Kenneth G. Castro, Neel R. Gandhi,
Thomas R. Navin**

We used tuberculosis genotyping results to derive estimates of prevalence of latent tuberculosis infection in the United States. We estimated <1% prevalence in 1,981 US counties, 1%–<3% in 785 counties, and ≥3% in 377 counties. This method for estimating prevalence could be applied in any jurisdiction with an established tuberculosis surveillance system.

Approximately 25% of the world's population is latently infected with *Mycobacterium tuberculosis*. Latent tuberculosis infection (LTBI) is an asymptomatic equilibrium between the immune response of the host and the infectious process. Although not infectious, LTBI can be activated years later as infectious tuberculosis (TB), which is why diagnosing and treating LTBI in high-risk populations is a key component of the World Health Organization End TB Strategy (*1–4*).

Most countries have established systems for surveillance of active TB. Public health interventions to control TB include timely detection and treatment of active cases and prompt investigations of persons with recent contact with someone who has infectious TB. However, few jurisdictions have estimates of local LTBI prevalence. Having such estimates could help direct TB prevention efforts for persons with the highest risk for infection, highest risk for progression to TB, and greatest benefit from treatment to prevent progression (*2–4*). We describe a simple method that uses genotyping results from active TB cases to derive a population estimate of untreated LTBI prevalence for any jurisdiction.

The Study

The US National TB Surveillance System contains 48,955 verified TB cases for 2011–2015. In the subset of 37,723 (77.1%) cases that were confirmed by culture, 36,104 (95.7%) had an *M. tuberculosis* isolate genotyped by the National TB Genotyping Service by using spacer oligonucleotide typing and 24-locus mycobacterial interspersed repetitive unit–variable number tandem repeat methods. The 50 US states and the District of Columbia are divided into 3,143 local jurisdictions (typically called counties). We used the US Census 2010 population denominator, annual TB incidence averaged during 2008–2015, and 2 assumptions for each county to derive an estimated prevalence of LTBI among residents.

For the 1,360 counties with no genotyped TB cases, which corresponded to 8% of the US population, we estimated local LTBI prevalence as <1%. For other counties, we assumed that all genotyped TB cases not attributed to recent *M. tuberculosis* transmission arose from preexisting LTBI (i.e., were reactivation TB). We used the previously field-validated plausible source-case method (*5–7*) to attribute cases to recent transmission (i.e., plausible source case within 10 miles within previous 2 years having infectious TB and a matching genotype result) for the District of Columbia and 49 US states. All cases diagnosed in non–US-born persons within 100 days of entry into the United States were excluded because the presumption was that these persons did not represent infection acquired in the United States. Because some cases in Oklahoma were missing geographic identifiers for identifying the 10-mile radius, a modification for these cases in this analysis was that the plausible source case could have occurred anywhere in the same county. Our second assumption was that the same recent transmission versus reactivation TB proportions for genotyped cases would apply to nongenotyped TB cases in each county (*8*).

Based on the estimate of Shea et al. (*8*) of ≈0.084 cases of reactivation TB/100 person-years among US residents with LTBI, we applied a uniform population-level 0.10% annual risk for progression to active disease to derive an estimated number of county residents with LTBI. As sensitivity analyses, we examined how LTBI prevalence estimates would decrease with a higher 0.14% uniform annual risk and how estimates would increase with a lower 0.06% uniform annual risk. We present estimates as uncertainty limits and provide the formula and examples of this method (Table 1).

Table 1. Formula and examples of method for estimating prevalence of latent TB infection, United States, 2011–2015*

Variable	a	b	c	d	e	f	g	h
Jurisdiction	Population	Average annual no. active TB cases	Proportion of TB cases attributed to recent transmission	Annual no. cases attributed to reactivation TB	Estimated no. infected residents if 0.10% annual risk for progression	Estimated prevalence of infection if 0.10% annual risk for progression, %	Sensitivity analysis for estimated prevalence of latent infection, %	
							Lower uncertainty limit based on 0.14% annual risk for progression	Upper uncertainty limit based on 0.06% annual risk for progression
Example X	Any size	0	NA	0	NA	<1	NA	NA
Example Y	150,000	1	0	1	1,000	0.7	0.5	1.1
Example Z	2,000,000	50	0.2	40	40,000	2.0	1.4	3.3

*Let a = jurisdiction population, b = average annual no. TB cases in that jurisdiction, and c = proportion of TB cases attributed to recent transmission (i.e., [1 − c] = proportion attributed to latent TB infection). Then if b = 0, d = 0, and f <1%, otherwise d = b × (1 − c) and e = d/0.0010 if one assumes a 0.10% annual risk and f = e/a (×100 to express as a percentage) or (d/0.0014/a for lower uncertainty limit and h = d/0.0006/a for upper uncertainty limit. NA, not applicable; TB, tuberculosis.

We estimated that 3.1% (uncertainty limits 2.2%–5.2% based on higher or lower risk progression assumptions) of the US population, corresponding to 8.9 (6.3–14.8) million persons, were latently infected with *M. tuberculosis* during 2011–2015. County-level estimates varied widely: estimated LTBI prevalence of <1% in 1,981 counties, 1% –<3% in 785 counties, and ≥3% in 377 counties (Figure). As defined by the US Census Bureau Small Area Income and Poverty Estimates,

poverty in >20% of the population was a characteristic of 146 (72%) of the 202 rural counties and 62 (35%) of the 175 metropolitan counties that had an estimated LTBI prevalence >3% (Table 2).

Conclusions

Preventing TB is a growing focus of TB control strategies in the United States and internationally. As governments, public health departments, and private sector partners
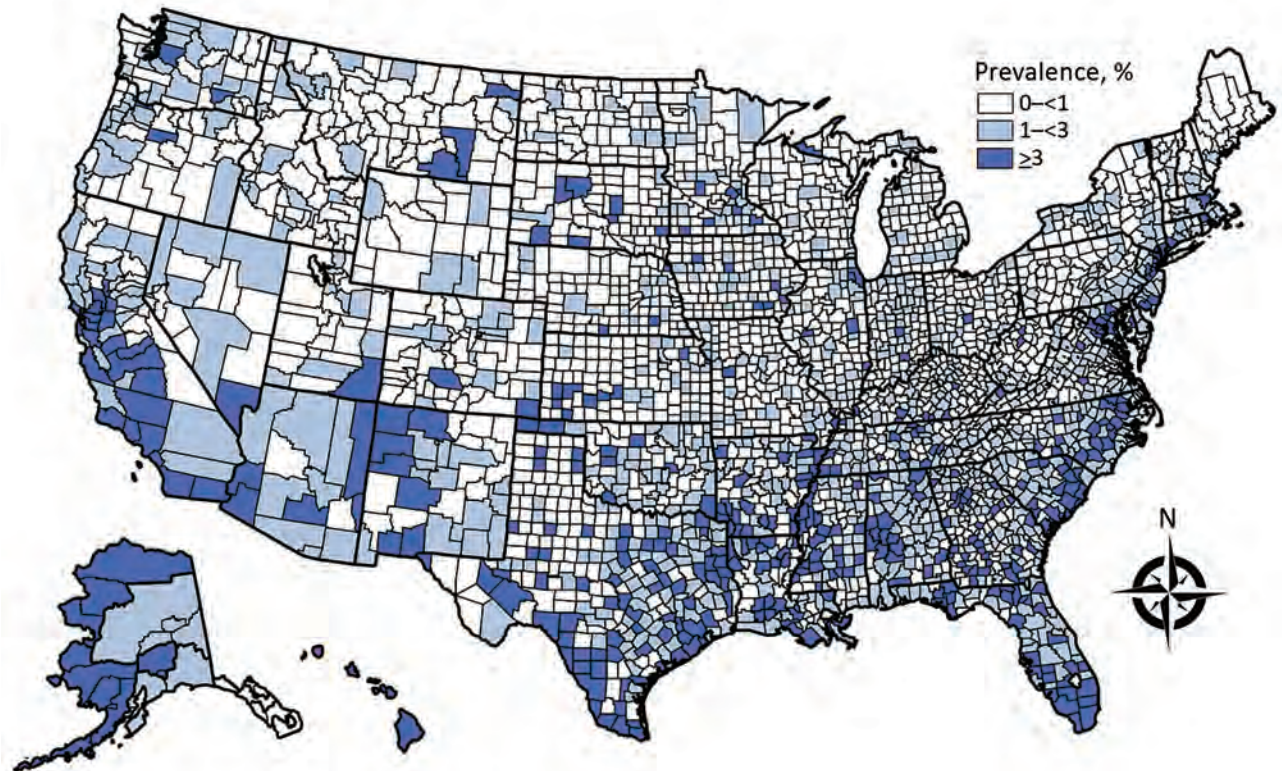
Figure. Estimated prevalence of latent tuberculosis infection, by county, United States, as derived from genotyped cases of tuberculosis reported to the US National Tuberculosis Surveillance System, 2011–2015. County equivalents (i.e., Alaska boroughs, District of Columbia, Louisiana parishes, and Virginia independent cities) are also shown. A modified method for analyzing data for Oklahoma is found in the text. Prevalence estimates for Alaska are aggregated by region.

Table 2. Characteristics of 1,976 rural and 1,167 metropolitan counties, by estimated prevalence of latent TB infection, United States, 2011–2015*

	1,976 rural counties			1,167 metropolitan counties		
Characteristic	1,454 with estimated prevalence <1%	320 with estimated prevalence 1%–<3%	202 with estimated prevalence ≥3%	527 with estimated prevalence <1%	465 with estimated prevalence 1%–<3%	175 with estimated prevalence ≥3%
US Census 2010 data						
Combined population of counties	28,727,127	11,750,121	5,816,158	37,414,210	115,341,399	109,697,523
Median county population, rounded to thousands	13,000	32,000	23,000	38,000	144,000	291,000
Estimated prevalence of *Mycobacterium tuberculosis* infection						
Estimated no. infected in all counties	126,140	191,707	329,547	212,563	2,300,435	5,772,136
Estimated median no. infected/county	0	500	1,112	124	2,376	12,388
County population living in poverty, %†						
<10	95 (7)	13 (4)	2 (1)	112 (21)	63 (14)	25 (14)
10–15.5	564 (39)	78 (24)	29 (14)	221 (42)	171 (37)	30 (17)
15.6–19.9	378 (26)	95 (30)	25 (12)	124 (24)	144 (31)	58 (33)
≥20	417 (29)	134 (42)	146 (72)	70 (13)	87 (19)	62 (35)
Race/ethnic group in county with largest no. active TB cases reported						
Black non-Hispanic	81 (15)	42 (13)	60 (30)	45 (14)	86 (18)	57 (33)
White non-Hispanic	241 (45)	109 (34)	34 (17)	142 (44)	110 (24)	17 (10)
Hispanic	74 (14)	58 (18)	60 (30)	25 (8)	82 (18)	43 (25)
Alaska Native/Native American or Pacific Islander	36 (7)	14 (4)	15 (7)	8 (2)	8 (2)	3 (2)
Asian	43 (8)	24 (8)	8 (4)	48 (14)	118 (25)	46 (26)
No predominant race/ethnic group	979 (67)	73 (23)	24 (12)	259 (49)	61 (13)	9 (5)

*Values are no. (%) unless otherwise noted. County equivalents (i.e., Alaska boroughs, District of Columbia, Louisiana parishes, and Virginia independent cities) are also shown. US Department of Agriculture 2013 Rural–Urban Continuum Codes were dichotomized (i.e., codes 4–9 were considered rural and codes 0–3 were considered metropolitan).
†County all-ages poverty level in 2011 as determined by US Census Bureau Small Area Income and Poverty Estimates.

intensify TB prevention activities, having a tool to understand local variations in LTBI prevalence could help prioritize resources (*2–4*).

We used routinely collected TB surveillance and genotyping data to derive untreated LTBI prevalence estimates for all US counties. This method was designed to be simple (Table 1). By excluding the contribution of any TB cases attributed to recent transmission, our estimates disregard the comparatively smaller number of recent infections and instead draw attention to more longstanding LTBI prevalence. Because time since initial *M. tuberculosis* infection was unknown, a uniform population-level 0.10% annual risk for progression to active disease was assumed. Changing that uniform risk to 0.14% would have decreased the number of counties with an estimated LTBI prevalence ≥3% to 113 counties. A change to 0.06% would have increased the number of counties with an estimated LTBI prevalence ≥3% to 516 counties.

A more sophisticated approach to estimate local longstanding LTBI prevalence might consider individual characteristics and differentiate risk for progression based on HIV status, age group, and possibly geographic region, place of birth, and recent migration (*8*). For example, a person receiving a TB diagnosis soon after arrival in a county would increase the LTBI prevalence estimates for that county, even if the TB was caused by an infection that had been acquired in another jurisdiction.

Conversely, our overall estimate that 2.2%–5.2% of the US population is infected is similar to estimates from the 2011–2012 National Health and Nutrition Examination Survey (*9*).

For the United States, the last published nationwide county-level estimates of LTBI prevalence are based on 1958–1965 data, when 275,558 men 17–21 years of age who had lived their entire lives in 1 county were examined as they entered the US Navy (*10*). Men from poor counties in the southwestern United States and the Appalachian Mountains were more likely to have positive tuberculin skin test results (*10*). Compared with estimates from 5 decades ago, our estimates show a more diffuse pattern of higher LTBI prevalence counties (Figure). However, poverty remains a frequent characteristic of counties that we estimated as having a higher LTBI prevalence.

This method has limitations. We applied the proportion of genotyped TB cases in the county estimated to arise from preexisting LTBI to all nongenotyped TB cases in that county, which could overestimate the prevalence of LTBI in counties with many pediatric TB cases, which tend to be more difficult to confirm by culture techniques (i.e., cannot be genotyped), yet are sentinel events for recent transmission. Conversely, the genotyping methods used during 2011–2015 might have overestimated recent TB infections (i.e., underestimated LTBI prevalence) in certain localities with longstanding genotyping clusters;

this limitation should decrease as the National TB Genotyping Service transitions to universal whole-genome sequencing in 2018.

This method also has several advantages. It could be applied in jurisdictions without TB genotyping services, given an assumption or range of assumptions about the proportion of active TB cases arising from LTBI in the jurisdiction. Rather than relying on costly and imperfect LTBI screening methods, its starting point is verified cases of TB that are already routinely reported to established TB surveillance systems. If deemed applicable, an adjustment for underreported TB cases could be made. In addition, these cases represent infected persons who have the greatest risk for progression to active TB and are the populations most likely to benefit from interventions to prevent TB in the future.

Acknowledgments

About the Author

Ms. Haddad is an epidemiologist at the National Center for HIV/AIDS, Viral Hepatitis, STD, and TB Prevention, Centers for Disease Control and Prevention, and a doctoral candidate at Emory University, Atlanta, GA. Her research interests include the history and social determinants of tuberculosis in North America.

References

1. Houben RM, Dodd PJ. The global burden of latent tuberculosis infection: a re-estimation using mathematical modelling. PLoS Med. 2016;13:e1002152. http://dx.doi.org/10.1371/journal.pmed.1002152
2. World Health Organization. Latent TB infection: updated and consolidated guidelines for programmatic management. Geneva: The Organization; 2018.
3. Bibbins-Domingo K, Grossman DC, Curry SJ, Bauman L, Davidson KW, Epling JW Jr, et al.; US Preventive Services Task Force. Screening for latent tuberculosis infection in adults: US Preventive Services Task Force recommendation statement. JAMA. 2016;316:962–9. http://dx.doi.org/10.1001/jama.2016.11046
4. Taylor Z, Nolan CM, Blumberg HM; American Thoracic Society; Centers for Disease Control and Prevention; Infectious Diseases Society of America. Controlling tuberculosis in the United States. Recommendations from the American Thoracic Society, CDC, and the Infectious Diseases Society of America. MMWR Recomm Rep. 2005;54:1–81.
5. France AM, Grant J, Kammerer JS, Navin TR. A field-validated approach using surveillance and genotyping data to estimate tuberculosis attributable to recent transmission in the United States. Am J Epidemiol. 2015;182:799–807. http://dx.doi.org/10.1093/aje/kwv121
6. Yuen CM, Kammerer JS, Marks K, Navin TR, France AM. Recent transmission of tuberculosis— United States, 2011–2014. PLoS One. 2016;11:e0153728. http://dx.doi.org/10.1371/journal.pone.0153728
7. Centers for Disease Control and Prevention. Reported tuberculosis in the United States, 2016. Atlanta: The Centers; 2017.
8. Shea KM, Kammerer JS, Winston CA, Navin TR, Horsburgh CR Jr. Estimated rate of reactivation of latent tuberculosis infection in the United States, overall and by population subgroup. Am J Epidemiol. 2014;179:216–25. http://dx.doi.org/10.1093/aje/kwt246
9. Miramontes R, Hill AN, Yelk Woodruff RS, Lambert LA, Navin TR, Castro KG, et al. Tuberculosis infection in the United States: prevalence estimates from the National Health and Nutrition Examination Survey, 2011–2012. PLoS One. 2015;10:e0140881. http://dx.doi.org/10.1371/journal.pone.0140881
10. Edwards LB, Acquaviva FA, Livesay VT, Cross FW, Palmer CE. An atlas of sensitivity to tuberculin, PPD-B, and histoplasmin in the United States. Am Rev Respir Dis. 1969;99(Suppl):1–132.

Address for correspondence: Maryam B. Haddad, Centers for Disease Control and Prevention, 1600 Clifton Rd NE, Mailstop US12-4, Atlanta, GA 30329–4027, USA; email: mhaddad@cdc.gov

Invasive Pneumococcal Disease in Refugee Children, Germany

Stephanie Perniciaro, Matthias Imöhl, Mark van der Linden

Refugee children in Germany are not routinely given a pneumococcal conjugate vaccine. Cases of invasive pneumococcal disease (IPD) in 21 refugee children were compared with those in 405 Germany-born children for 3 pneumococcal seasons. Refugee children had significantly higher odds of vaccine-type IPD and multidrug-resistant IPD than did Germany-born children.

Germany has taken in >1 million refugees since 2015 (1), more than one third of whom were children <18 years of age (2). Invasive pneumococcal disease (IPD) is a major cause of childhood death, especially in resource-poor environments (3). Conflict settings are associated with outbreaks of vaccine-preventable diseases for reasons ranging from poor sanitation in refugee holding areas to the rapid movement of refugees, which, in turn, allows for a similarly rapid spread of disease and the interruption of immunization services because of the lack of personnel (4).

Of the 10 most frequent countries of origin for refugees arriving in Germany in 2017 (Syria, Iraq, Afghanistan, Turkey, Iran, Nigeria, Eritrea, Russia, Somalia, and Albania), 6 have a national vaccination program that includes pneumococcal conjugate vaccines (PCVs) (5); however, because of the crisis conditions facing those who fled, timely infant vaccination is unlikely (4). Vaccine-preventable disease outbreaks have been reported in refugee housing facilities in Germany (6,7), and most of these cases have originated after arrival in Germany. The vaccination program for newly arrived refugees does not include PCVs (8).

Since 1997, the German National Reference Center for Streptococci (GNRCS) has been collecting bacterial isolates from IPD cases in children occurring throughout Germany. We compared IPD isolates received from known refugee children residing in Germany to IPD isolates from Germany-born children for the 2014–15, 2015–16, and 2016–17 pneumococcal seasons.

Author affiliation: University Hospital RWTH Aachen, Aachen, Germany

The Study

In this retrospective, unmatched case-control study, we considered all 514 isolates from children (<16 years of age) with IPD in the GNRCS collection isolated during July 1, 2014–June 30, 2017, for inclusion in the analysis. We defined a case of IPD as *Streptococcus pneumoniae* (identified by optochin sensitivity and bile solubility) isolated from a normally sterile site. For the analysis, case isolates were from refugee children with IPD, and control isolates were from Germany-born children with IPD. Refugee status was documented by GNRCS personnel in conjunction with determining vaccination status, as described elsewhere (9). Because identification of refugee status was tied to the determination of vaccination status, all children with an unknown vaccination status were excluded.

We determined serotype by using Neufeld's Quellung reaction and antimicrobial drug resistance by MIC testing, as previously described (10). Antimicrobial drug resistance was defined by the Clinical and Laboratory Standards Institute 2015 breakpoints (11).

We calculated odds ratios (ORs) and 95% CIs with R software version 3.4.0 (https://www.r-project.org/foundation) using Firth's bias-reduced logistic regression and adjusted for age and sex using the logistf package (12). We assigned statistical significance to ORs for which the 95% CI did not exceed 1. Variables considered in the analysis were age, sex, vaccination status, and refugee status of the patient, as well as the serotype and antimicrobial drug resistance profile of the isolate.

During July 1, 2014–June 30, 2017, the GNRCS received 21 IPD isolates from known refugee children (Table). The average age of infection in refugee children was 3 years. Of these cases, 11 (44%) had an unknown clinical diagnosis (6 isolates were from blood, 2 from cerebrospinal fluid, 3 from other exudates), 4 (19%) were from meningitis, 3 (14%) were from sepsis, and 3 (14%) were from pneumonia. Thirteen refugee children, all of whom were unvaccinated, had vaccine-type IPD (62% overall; 2014–15, 67%; 2015–16, 67%; 2016–17, 50%). Only 2 refugee children, both with non–vaccine-type IPD, had been vaccinated with 13-valent PCV, both with only 1 dose, after arrival in Germany.

We determined vaccination status for 405 isolates from Germany-born children (Table). The average age at the time of infection was 2 years. Fifty-four children (13%) had pneumonia, 88 (22%) had sepsis, 130 (32%) had meningitis, and 133 cases (33%) had an unknown or other

Table. Invasive pneumococcal disease in refugee children and German-born children, July 1, 2014–June 30, 2017*

IPD season	No. patients	Mean patient age, y	No. (%) patients				
			Unvaccinated	PCV13 vaccinated	VT serotype	Non-VT serotype	Resistant to >3 classes of antimicrobial drugs
Refugee children in Germany							
2014–15	3	1	3 (100)	0	2 (67)	1 (33)	1 (33)
2015–16	12	3	10 (83)	2 (17)	8 (67)	4 (33)	4 (33)
2016–17	6	5	5 (83)	0	3 (50)	3 (50)	3 (50)
Total	21	3	18 (86)	2 (9)	13 (62)	8 (38)	8 (38)
Germany-born children							
2014–15	107	2	19 (18)	73 (68)	28 (26)	79 (74)	5 (5)
2015–16	122	2	21 (17)	86 (70)	19 (16)	103 (84)	1 (0.8)
2016–17	176	3	45 (26)	117 (66)	28 (16)	148 (84)	4 (2)
Total	405	2	85 (21)	276 (68)	75 (19)	330 (81)	10 (2)

*VT serotypes are 4, 6B, 9V, 14, 18C, 19F, 23F, 1, 5, 7F, 3, 6A, and 19A. Antimicrobial drug resistance is determined according to the 2015 breakpoints of the Clinical and Laboratory Standards Institute (*11*). IPD, invasive pneumococcal disease; PCV13, 13-valent pneumococcal conjugate vaccine; VT, vaccine type.

diagnosis. Seventy-five cases in this group were vaccine-type IPD (19% overall; 2014–15, 26%; 2015–16, 16%; 2016–17, 16%). Refugee children had significantly higher odds of contracting vaccine-type IPD (OR 6.60, 95% CI 2.73–16.84) over the study period.

Eight isolates (38% overall; 2014–15, 33%; 2015–16, 33%; 2016–17, 50%) from refugee children were resistant to ≥3 classes of antimicrobial drugs, compared with 10 isolates (2% overall; 2014–15, 4%; 2015–16, 1%; 2016–17, 2%) from Germany-born children. Refugee children had significantly higher odds (OR 23.84, 95% CI 7.98–72.73) of contracting antimicrobial-resistant IPD over the study period. Five vaccine-type isolates (38% overall; 2014–15, 50%; 2015–16, 25%; 2016–17, 67%) from refugees were resistant to ≥3 of antimicrobial drugs, compared with 5 vaccine-type isolates (7% overall; 2014–15, 11%; 2015–16, 5%; 2016–17, 4%) from Germany-born children. Among vaccine-type IPD cases, refugee children were significantly more likely (OR 8.82, 95% CI 2.13–40.10) to have antimicrobial drug–resistant infections.

IPD incidence estimates are shown in online Technical Appendix Table 1 (https://wwwnc.cdc.gov/EID/article/24/10/18-0253-Techapp1.pdf). For single-season ORs, the CIs were often wide, and the sample sizes in refugee children were low (2014–15, n = 3; 2015–16, n = 12; 2016–17, n = 6). These ORs are shown in online Technical Appendix Table 2 and should be interpreted cautiously.

Conclusions

Refugee children in Germany are at greater risk of contracting vaccine-type IPD, antimicrobial drug–resistant IPD, and antibiotic-resistant vaccine-type IPD. As such, a PCV program for refugee children may be worth considering in Germany. Vaccination in newly arrived refugees presents an opportunity to cost-effectively, safely, and humanely protect a vulnerable population from negative health outcomes resulting from vaccine-preventable diseases (*13*). Given that children in Germany with insecure residence status are twice as likely to be incompletely vaccinated (*2*),

a PCV program for refugee children in Germany might require additional follow-up measures to ensure consistency and provide sufficient protection, particularly because PCV dosing in Germany-born children with IPD has been lax (*9*). A PCV program could help reduce antimicrobial drug–resistant pneumococcal infections, the carriage of resistant strains (*14*), overall antimicrobial drug use, and the prevalence of resistance genes within the pneumococcal population (*15*).

The IPD case numbers from refugees are low, but the proportion of vaccine-type isolates and antimicrobial drug–resistant isolates from refugee children are nevertheless much higher than those of Germany-born children. Children of unknown vaccination status (n = 109) were excluded from the analysis; because of the small sample sizes, if even 1 additional child with vaccine-type IPD per year was a refugee, the effects we describe would be magnified (online Technical Appendix Table 3).

The risk of vaccine-type IPD is low among fully vaccinated children in Germany. However, among unvaccinated and undervaccinated children, a reintroduction of vaccine-type pneumococci may result in increased risk of pneumococcal disease. Without intervention, refugee children may continue to constitute a special risk group for vaccine-type IPD and antimicrobial drug–resistant IPD in Germany. Fully immunizing these children against vaccine-type IPDs may help reduce the risk for IPD illness and death in Germany.

About the Author

Mrs. Perniciaro is a doctoral candidate at the German National Reference Center for Streptococci, University Hospital RWTH Aachen. Her interests include invasive pneumococcal disease epidemiology and pneumococcal conjugate vaccine effectiveness.

References

1. Razum OS, Saß A-C, Bozorgmehr K. Gesundheitliche Versorgung von Geflüchteten: Herausforderungen und Lösungsansätze. Bundesgesundheitsblatt. 2016;59:543–4. http://dx.doi.org/10.1007/s00103-016-2344-5

2. Wenner J, Razum O, Schenk L, Ellert U, Bozorgmehr K. Gesundheit von Kindern und Jugendlichen aus Familien mit ungesichertem Aufenthaltsstatus im Vergleich zu Kindern mit und ohne Migrationshintergrund: Auswertung der KiGGS-Daten 2003–06. Bundesgesundheitsblatt. 2016;59:627–35. http://dx.doi.org/10.1007/s00103-016-2338-3

3. O'Brien KL, Wolfson LJ, Watt JP, Henkle E, Deloria-Knoll M, McCall N, et al.; Hib and Pneumococcal Global Burden of Disease Study Team. Burden of disease caused by *Streptococcus pneumoniae* in children younger than 5 years: global estimates. Lancet. 2009;374:893–902. http://dx.doi.org/10.1016/S0140-6736(09)61204-6

4. Nnadi CE, Etsano A, Uba B, Ohuabunwo C, Melton M, wa Nganda G, et al. Approaches to vaccination among populations in areas of conflict. J Infect Dis. 2017;216(S1):368–72. http://dx.doi.org/10.1093/infdis/jix175

5. World Health Organization. WHO vaccine-preventable diseases: monitoring system. 2017 global summary [cited 2017 Sept 20]. http://apps.who.int/immunization_monitoring/globalsummary/schedules

6. Grote U, Schleenvoigt BT, Happle C, Dopfer C, Wetzke M, Ahrenstorf G, et al. Norovirus outbreaks in German refugee camps in 2015. Z Gastroenterol. 2017;55:997–1003. http://dx.doi.org/10.1055/s-0043-109701

7. Kühne AG, Gilsdorf A. Ausbrüche von Infektionskrankheiten in Gemeinschaftsunterkünften für Asylsuchende 2004–2014 in Deutschland. Bundesgesundheitsblatt. 2016;59:570–7. http://dx.doi.org/10.1007/s00103-016-2332-9

8. Robert Koch Institut. Konzept zur Umsetzung frühzeitiger Impfungen bei Asylsuchenden nach Ankunft in Deutschland. Epidemiologisches Bulletin. 2015;41:439–48. http://dx.doi.org/10.17886/EpiBull-2015-011.4

9. van der Linden M, Falkenhorst G, Perniciaro S, Fitzner C, Imöhl M. Effectiveness of pneumococcal conjugate vaccines (PCV7 and PCV13) against invasive pneumococcal disease among children under two years of age in Germany. PLoS One. 2016;11:e0161257. http://dx.doi.org/10.1371/journal.pone.0161257

10. Imöhl M, Reinert RR, van der Linden M. Antibiotic susceptibility rates of invasive pneumococci before and after the introduction of pneumococcal conjugate vaccination in Germany. Int J Med Microbiol. 2015;305:776–83. http://dx.doi.org/10.1016/j.ijmm.2015.08.031

11. Clinical and Laboratory Standards Institute. Performance standards for antimicrobial susceptibility testing: twenty-fifth informational supplement (M100-S25). Wayne (PA): The Institute; 2015.

12. Heinze G. A comparative investigation of methods for logistic regression with separated or nearly separated data. Stat Med. 2006;25:4216–26. http://dx.doi.org/10.1002/sim.2687

13. Pavlopoulou IDT, Tanaka M, Dikaloti S, Samoli E, Nisianakis P, Boleti OD, et al. Clinical and laboratory evaluation of new immigrant and refugee children arriving in Greece. BMC Pediatr. 2017;17:132. http://dx.doi.org/10.1186/s12887-017-0888-7

14. Hampton LM, Farley MM, Schaffner W, Thomas A, Reingold A, Harrison LH, et al. Prevention of antibiotic-nonsusceptible *Streptococcus pneumoniae* with conjugate vaccines. J Infect Dis. 2012;205:401–11. http://dx.doi.org/10.1093/infdis/jir755

15. Grijalva CG. Decrease in antibiotic use, an added benefit of PCVs. Lancet Infect Dis. 2014;14:175–7. http://dx.doi.org/10.1016/S1473-3099(13)70356-6

Address for correspondence: Stephanie Perniciaro, German National Reference Center for Streptococci, Department of Medical Microbiology, RWTH Aachen University Hospital, Pauwelsstraße 30, 52074 Aachen Germany; email: sperniciaro@ukaachen.de
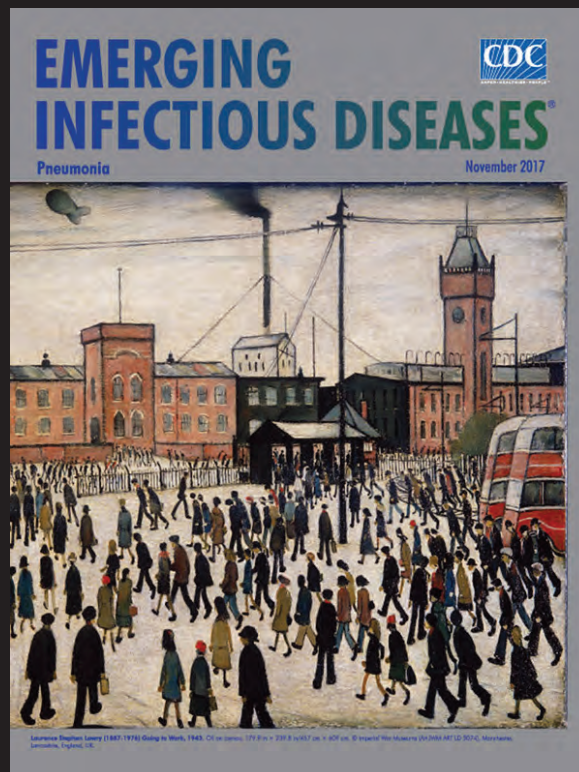
Mycobacterium caprae Infection in Captive Borneo Elephant, Japan

Shiomi Yoshida, Satomi Suga, Satoshi Ishikawa, Yasuhiko Mukai, Kazunari Tsuyuguchi, Yoshikazu Inoue, Taro Yamamoto, Takayuki Wada

In 2016, disseminated tuberculosis caused by *Mycobacterium caprae* was diagnosed in a captive Borneo elephant in Japan. The bacterium was initially identified from clinical isolates. An isolate collected during a relapse showed isoniazid monoresistance and a codon 315 *katG* mutation.

Elephants are susceptible to infection by some members of the *Mycobacterium tuberculosis* complex (MTBC) (*1*). The MTBC comprises several genetically homogeneous species that have a wide range of hosts and can cause tuberculosis in humans and in animals. Infection in elephants is presumed to originate from human caretakers who have tuberculosis; however, transmission between elephants or from other animals is also possible (*2–4*).

Phylogenetic events during the divergence of MTBC species are represented within the genomes of MTBC species (*5*). Whole-genome sequencing has shown that single-nucleotide polymorphism (SNP) microevolution occurs in MTBC strains in the host.

We describe mycobacterial infection in an elephant that was caused by a relatively uncommon species of MTBC. *M. caprae* infection, a species of the MTBC, was diagnosed in a captive Borneo elephant (*Elephas maximus borneensis*) that was brought directly from Borneo island after being orphaned.

The Study

In February 2016, an ≈17-year-old female Borneo elephant in the Fukuyama Zoo (Fukuyama, Japan) had low-grade fever (99.9°F), anorexia, progressive weight loss, and cough with sputum. The elephant had been housed alone in a

Author affiliations: Nagasaki University Graduate School of Biomedical Sciences, Nagasaki, Japan (S. Yoshida); National Hospital Organization Kinki-chuo Chest Medical Center Clinical Research Center, Sakai, Japan (S. Yoshida, K. Tsuyuguchi, Y. Inoue); Fukuyama Zoo, Fukuyama, Japan (S. Suga, S. Ishikawa, Y. Mukai); Nagasaki University Institute of Tropical Medicine, Nagasaki (T. Yamamoto, T. Wada); Nagasaki University School of Tropical Medicine and Global Health, Nagasaki (T. Wada)

facility with a roofed room and an open-air enclosure and had no contact with other animals. She was seropositive by Chembio DPP VetTB Assay for Elephants (Chembio Diagnostic Systems, Inc., Medford, NY, USA), which detects antibodies to CFP10/ESAT-6 and MPB83 antigens (*6,7*).

Submitted specimens to the National Hospital Organization Kinki-chuo Chest Medical Center (Sakai, Japan) were sputum, feces, urine, and vaginal discharge recovered from the floor. Acid-fast bacilli were visualized on Ziehl-Neelsen staining performed according to standard methods (*8*). Isolates with smooth to greasy, domed, nonchromogenic colonies were recovered from all submitted samples using both 7H11 agar and MGIT broth (Becton Dickinson, Fukushima, Japan) and identified as MTBC using loop-mediated isothermal amplification (Eiken Chemical, Tokyo, Japan) and TaqMan PCR (Roche Diagnostics, Tokyo, Japan) (*9*).

A single colony was sequenced using MiSeq (Illumina, Inc., Tokyo, Japan). Raw reads were trimmed by base quality and were mapped to the *M. tuberculosis* reference genome, H37Rv (GenBank accession no. CP003248). The initial isolate, EPDC01, was characterized by the presence and absence of genomic regions of difference, the mutation (G to A) of $oxyR^{285}$ and *M. caprae*–specific SNPs in *lepA* (*10*) (Table 1, https://wwwnc.cdc.gov/EID/article/24/10/18-0018-T1.htm). These results unexpectedly suggested that the causative agent of tuberculosis in this elephant was *M. caprae*. The regions of difference analysis suggested that EPDC01 belonged to the Allgäu type of *M. caprae* found in red deer (*Cervus elaphus*) (*11*). However, when we used kSNP3 (*12*), a kmer-based method, to compare SNPs from the entire genome of EPDC01 to previously published Allgäu and Lechtal types of *M. caprae* and other MTBC species, the results showed this isolate was not closely related to either Allgäu or Lechtal types (Figure; online Technical Appendix Figure, https://wwwnc.cdc.gov/EID/article/24/10/18-0018-Techapp1.pdf) (*13*).

The isolate was susceptible to isoniazid, rifampin, ethambutol, and levofloxacin according to the broth microdilution method (BrothMIC MTB-1; Kyokuto Pharmaceutical, Inc, Tokyo, Japan). It also was susceptible to pyrazinamide using Bactec MGIT 960 PZA kit (Becton Dickinson).

The infected elephant initially weighed 2,400 kg; isoniazid (4.5–7 mg/kg), pyrazinamide (31–33 mg/kg),

Figure. Phylogenetic tree of isolate EPDC01 from a captive Borneo elephant with *Mycobacterium caprae* infection, Japan, 2016, and 8 *Mycobacterium caprae* strains (Allgäu and Lechtal types) from a report by Broeckl et al. (*13*). Short reads of *M. caprae* strains were assembled by CLC Genomics Workbench version 9.5.1 (https://www.qiagenbioinformatics.com/solutions/functional-genomics/?gclid=EAIaIQobChMIvvGL3L7T2wIVTSOBCh2FAAKtEAAYASAAEgKLWvD_BwE) before analysis. Core single-nucleotide polymorphisms of all 13 strains, including reference *M. tuberculosis* complex strains (*M. bovis*, AF2122/97 [GenBank accession no. NC_002945.4]: *M. orygis*, 112400015 [NZ_APKD00000000.1]: *M. pinnipedii*, BAA-688 [MWXB00000000.1]: *M. microti*, strain 12 [CP010333.1]: and M. mungi, BM22813 [NZ_LXTB00000000.1]), were determined and used for tree construction based on neighbor-joining by kSNP3 (12). A tree including all 61 strains described by Broeckl et al. (*13*) is shown in the online Technical Appendix Figure (https://wwwnc.cdc.gov/EID/article/24/10/18-0018-Techapp1.pdf). Scale bar indicates nucleotide substitutions per site.
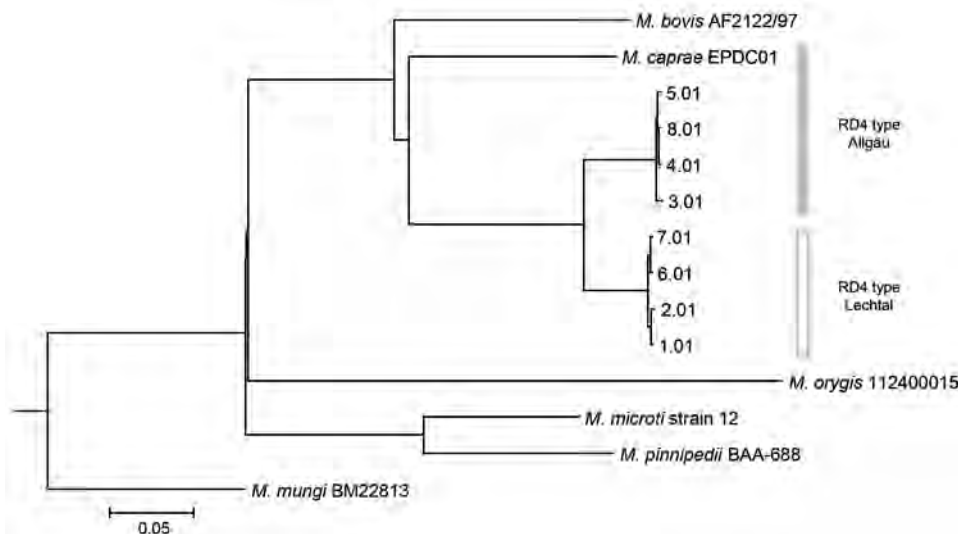
and levofloxacin (11 mg/kg) were administered rectally, once a day. When weighing on a scale was not possible, the elephant's weight was estimated using the chest girth method. After 1 month of treatment, the vaginal discharge disappeared, and the elephant's sputum culture became negative after 2 months. After 6 months, the multidrug treatment was interrupted for 3 weeks because of severe gastrointestinal disturbance and hepatic dysfunction. Rectal administration of isoniazid and pyrazinamide was resumed for an additional 3 months after recovery from adverse effects. Follow-up trunk wash samples were culture negative, but *M. caprae* was isolated from a sputum sample collected from the chin in February 2017. This new isolate was resistant to isoniazid. The drug regimen was then changed to oral rifampin (10 mg/kg) and rectal ethambutol (30 mg/kg), levofloxacin (10 mg/kg), and pyrazinamide (30 mg/kg). Under the modified treatment, the recurrence symptoms disappeared, and the routine sputum cultures became negative.

We also sequenced the recurrent isoniazid-resistant isolate (EPDC02) using a MiSeq and detected a mutation in *katG* where Ser-315 was replaced by 113 Thr (S315T). No mutations were detected in other representative drug resistance–related genes, such as *rpoB* (rifampin); *rrn*, *gidB*, and *rpsL* (streptomycin); *embABC* (ethambutol); *pncAC* (pyrazinamide); and *gyrAB* (quinolone). The pairwise distance between the initial and relapse isolates (EPDC01 and EPDC02) involved at least 7 single-nucleotide variants found in coding regions (Table 2).

For serologic monitoring of treatment, we tested archived serum samples collected before and during treatment using the DPP assay. Although a sample in November 2003 was reactive on CFP10/ESAT-6 but not on MPB83, at the time of culture-based tuberculosis diagnosis (February 2016), the reaction to CFP10/ESAT-6 was more intense, and the complete band of MPB83 appeared. The intensity to 2 test lines gradually decreased during the initial treatment (September 2016) and disease recrudescence (February 2017). The modified 18-month course of treatment is scheduled to end in October 2018.

Employees at the zoo were assessed for tuberculosis based on symptoms, radiographs, and serology using the QuantiFERON-TB Gold test (QIAGEN, Tokyo, Japan); none had active tuberculosis. Clinical examination, culture, PCR, and tuberculin skin test were used to evaluate as many primates and hoofstock as possible in the collection, and no tuberculosis-positive animals were identified.

Conclusions

A better understanding of tuberculosis in elephants is crucial to improve medical management and reduce risk of transmission to other animals and humans. During the initial treatment of the elephant reported here, treatment was interrupted for 3 weeks because of adverse effects. Reducing the dose of isoniazid was the probable cause of the acquired isoniazid resistance. When treating tuberculosis in elephants, the benefits and adverse effects should be

Table 2. Single nucleotide polymorphism differences between isolates EPDC01 and EPDC02 from a captive Borneo elephant with *Mycobacterium caprae* infection, Japan, 2016*

Genomic position	Gene	Mutation	Amino acid change	Description of function
1,338,135	*Rv1194c*	G → frameshift	Gln127 → frameshift	Unknown
1,445,272	*Rv1290A*	C → T	Ala72 → Val	Unknown
2,155,168	*katG*	C → T	Ser315 → Asn	Catalase; isoniazid resistance
2,577,556	*Rv2306A*	G → A	Gly150 → Glu	Unknown
3,200,585	*Rv2891*	T → G	Leu107 → Arg	Unknown
3,777,062	*Rv3365c*	C → A	Gly147 → Val	Unknown
4,298,329	*pks2*	G → A	Pro426 → Leu	Lipid metabolism
4,345,372	*Rv3869*	G → C	Ala112 → Pro	Unknown

*Excluded paralogue genes, which are the descendants of an ancestral gene and underwent a duplication event.

weighed carefully. The DPP provides an indirect measure of infection and disease status (*6*). In this elephant, declining DPP reactivity was thought to indicate a response to therapy; however, more sensitive biomarkers to monitor therapeutic response are needed.

Previously, epidemiologic observations of elephant tuberculosis by IS*6110* restriction fragment-length polymorphism have been based on evidence of local zoonotic risk for transmission to humans or of an epizootic reservoir for transmission to elephants or other animal species (goats and rhinoceros) (*1,14*). Recently, *M. tuberculosis* strains in 2 captive elephants in a small traveling circus harbored 3 nucleotide changes, according to whole-genome sequencing (*15*). *M. tuberculosis* has been isolated from Asian elephants among regions in southern Asia (*3,4*). Although the transmission routes have not been defined, our result and those of previous reports indicate that MTBC species may be spilling over into elephants.

Our finding emphasizes the need to identify the species of MTBC when tuberculosis is diagnosed in elephants. Although corroborating epidemiologic evidence of transmission has not been discovered, genomic data of the *M. caprae* isolates has been registered in the open database (BioProject ID PRJDB6469; BioSample ID SAMD00098240 for EPDC01, SAMD00098241 for EPDC02). Accumulation of genomic data of clinical isolates is expected to be helpful for future comparative studies.

About the Author

Ms. Yoshida is a microbiology researcher involved in the Clinical Research Center, National Hospital Organization Kinki-chuo Chest Medical Center, and the Graduate School of Biomedical Sciences, Nagasaki University in Japan. Her research interests include the examination of mycobacterial agents, including those from elephants with tuberculosis.

References

1. Murphree R, Warkentin JV, Dunn JR, Schaffner W, Jones TF. Elephant-to-human transmission of tuberculosis, 2009. Emerg Infect Dis. 2011;17:366–71. http://dx.doi.org/10.3201/eid1703.101668
2. Chandranaik BM, Shivashankar BP, Umashankar KS, Nandini P, Giridhar P, Byregowda SM, et al. *Mycobacterium tuberculosis* infection in free-roaming wild Asian elephant. Emerg Infect Dis. 2017;23:555–7. http://dx.doi.org/10.3201/eid2303.161439
3. Obanda V, Poghon J, Yongo M, Mulei I, Ngotho M, Waititu K, et al. First reported case of fatal tuberculosis in a wild African elephant with past human–wildlife contact. Epidemiol Infect. 2013;141:1476–80. http://dx.doi.org/10.1017/S0950268813000022
4. Zachariah A, Pandiyan J, Madhavilatha GK, Mundayoor S, Chandramohan B, Sajesh PK, et al. *Mycobacterium tuberculosis* in wild Asian elephants, southern India. Emerg Infect Dis. 2017;23:504–6. http://dx.doi.org/10.3201/eid2303.161741
5. Gagneux S, DeRiemer K, Van T, Kato-Maeda M, de Jong BC, Narayanan S, et al. Variable host-pathogen compatibility in *Mycobacterium tuberculosis*. Proc Natl Acad Sci U S A. 2006;103:2869–73. http://dx.doi.org/10.1073/pnas.0511240103
6. Lyashchenko KP, Greenwald R, Esfandiari J, Mikota S, Miller M, Moller T, et al. Field application of serodiagnostics to identify elephants with tuberculosis prior to case confirmation by culture. Clin Vaccine Immunol. 2012;19:1269–75. http://dx.doi.org/10.1128/CVI.00163-12
7. Greenwald R, Lyashchenko O, Esfandiari J, Miller M, Mikota S, Olsen JH, et al. Highly accurate antibody assays for early and rapid detection of tuberculosis in African and Asian elephants. Clin Vaccine Immunol. 2009;16:605–12. http://dx.doi.org/10.1128/CVI.00038-09
8. Clinical and Laboratory Standards Institute. Susceptibility testing of mycobacteria, nocardiae, and other aerobic actinomycetes; approved standard (M24–A2). Wayne (PA): The Institute; 2011.
9. Nagai K, Horita N, Yamamoto M, Tsukahara T, Nagakura H, Tashiro K, et al. Diagnostic test accuracy of loop-mediated isothermal amplification assay for *Mycobacterium tuberculosis*: systematic review and meta-analysis. Sci Rep. 2016;6:39090. http://dx.doi.org/10.1038/srep39090
10. Reddington K, O'Grady J, Dorai-Raj S, Niemann S, van Soolingen D, Barry T. A novel multiplex real-time PCR for the identification of mycobacteria associated with zoonotic

tuberculosis. PLoS One. 2011;6:e23481. http://dx.doi.org/10.1371/journal.pone.0023481

11. Domogalla J, Prodinger WM, Blum H, Krebs S, Gellert S, Müller M, et al. Region of difference 4 in alpine *Mycobacterium caprae* isolates indicates three variants. J Clin Microbiol. 2013;51:1381–8. http://dx.doi.org/10.1128/JCM.02966-12

12. Gardner SN, Slezak T, Hall BG. kSNP3.0: SNP detection and phylogenetic analysis of genomes without genome alignment or reference genome. Bioinformatics. 2015;31:2877–8. http://dx.doi.org/10.1093/bioinformatics/btv271

13. Broeckl S, Krebs S, Varadharajan A, Straubinger RK, Blum H, Buettner M. Investigation of intra-herd spread of *Mycobacterium caprae* in cattle by generation and use of a whole-genome sequence. Vet Res Commun. 2017;41:113–28. http://dx.doi.org/10.1007/s11259-017-9679-8

14. Oh P, Granich R, Scott J, Sun B, Joseph M, Stringfield C, et al. Human exposure following *Mycobacterium tuberculosis* infection of multiple animal species in a metropolitan zoo. Emerg Infect Dis. 2002;8:1290–3. http://dx.doi.org/10.3201/eid0811.020302

15. Simpson G, Zimmerman R, Shashkina E, Chen L, Richard M, Bradford CM, et al. *Mycobacterium tuberculosis* infection among Asian elephants in captivity. Emerg Infect Dis. 2017;23:513–6. http://dx.doi.org/10.3201/eid2303.160726

Address for correspondence: Shiomi Yoshida, Clinical Research Center, National Hospital Organization Kinki-chuo Chest Medical Center, 1180 Nagasone-cho, Kita-ku, Sakai-shi, Osaka, 591-8555, Japan; email: dustin@kch.hosp.go.jp
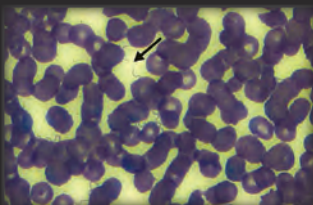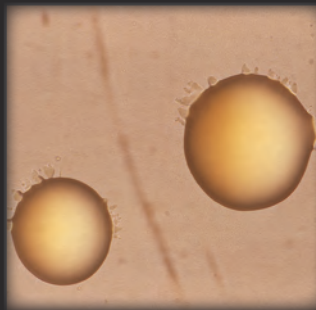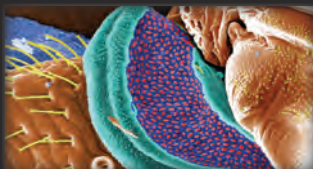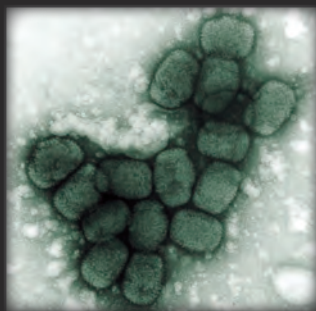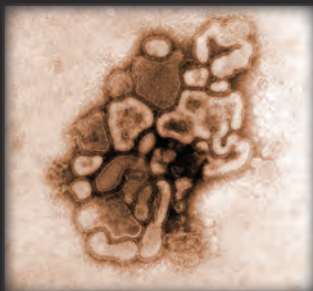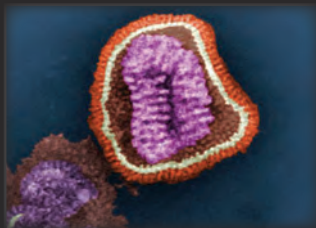
Genetic Diversity and Antimicrobial Drug Resistance of Serotype VI Group B *Streptococcus*, Canada

Alefiya Neemuchwala, Sarah Teatero, Lindsay Liang, Irene Martin, Walter Demzcuk, Allison McGeer, Nahuel Fittipaldi

Author affiliations: Public Health Ontario Laboratory, Toronto, Ontario, Canada (A. Neemuchwala, S. Teatero, L. Liang, N. Fittipaldi); National Microbiology Laboratory, Public Health Agency of Canada, Winnipeg, Manitoba, Canada (I. Martin, W. Demzcuk); University of Toronto, Toronto (A. McGeer, N. Fittipaldi); Mount Sinai Hospital, Toronto (A. McGeer)

Two genetically dissimilar sequence type 1 clades dominate the serotype VI group B *Streptococcus* population of strains causing invasive disease in Canada. Isolates of this rare serotype, recovered mainly from adult patients, were all susceptible to penicillin and vancomycin. However, we observed resistance to erythromycin and clindamycin.

Serotype VI group B *Streptococcus* (GBS), which is common in Japan (prevalence rates 16%–40%) and has recently emerged in Malaysia and Taiwan, remains rare in Europe and North America (*1–4*). However, invasive serotype VI infections have been noticed in Alberta and Ontario, Canada (*5,6*), and unpublished surveillance data for Canada (National Microbiology Laboratory, https://www.canada.ca/en/public-health/services/publications/drugs-health-products/national-laboratory-surveillance-invasive-streptococcal-disease-canada-annual-summary-2015.html) show low frequency (1.2%–4.1%) but sustained isolation of this GBS serotype in recent years. Here, we characterize a collection of 26 invasive serotype VI GBS strains recovered by passive surveillance in central Canada during 2010–2014 (online Technical Appendix 1, https://wwwnc.cdc.gov/EID/article/24/10/17-1711-Techapp1.xlsx). Two isolates came from early onset disease (patients age 0–6 days) and 1 from late-onset disease (patients age 7–90 days). Twenty-two isolates came from adult patients (9 age 18–60 years and 13 age >60 years, a distribution similar to that reported for adult patients with serotype V or serotype IV invasive disease in Canada [*5,6*]). Patient age was not available for 1 isolate.

We sequenced the genomes of all isolates using Illumina technology (Illumina, San Diego, CA, USA; National Center for Biotechnology Information BioProject PRJNA420560) and performed in silico multilocus sequence typing. Isolates belonged to sequence types (STs) ST889 (n = 1), ST297 (n = 1), ST14 (n = 2), and ST1 (n = 22) (online Technical Appendix 1). ST297, ST14, and ST1 are members of clonal complex (CC) 1; most serotype IV and V isolates responsible for adult disease in Canada also belong to CC1 (*5–7*). However, genome-wide, single-nucleotide polymorphism (SNP)–based phylogenetic analysis showed that CC1 isolates of these 3 serotypes are genetically dissimilar (online Technical Appendix 2 Figure 1, https://wwwnc.cdc.gov/EID/article/24/10/17-1711-Techapp2.pdf; genome-wide SNPs were identified relative to the genome of GBS-M002, a serotype VI isolate from Taiwan [GenBank accession no. CP013908.1]). Antimicrobial drug resistance among serotype VI isolates was, overall, similar to that described among serotype IV and V isolates causing adult invasive disease in Canada (*5,8*) (MICs for penicillin, erythromycin, clindamycin, tetracycline, and vancomycin were determined using the agar dilution method or Etest according to Clinical and Laboratory Standards Institute guidelines [*9*]). All serotype VI isolates were susceptible to penicillin and vancomycin (online Technical Appendix 1). Resistance to erythromycin was found in 10 (38%) invasive isolates, resistance to clindamycin in 9 (35%), and resistance to tetracycline in 8 (31%) (online Technical Appendix 1). All lincosamide- and macrolide-resistant strains possessed gene *ermB*; 1 isolate had genes *mefA* and *msrD*. Genes *tetS*, *tetM*, and *tetO* were associated with observed resistance to tetracycline (online Technical Appendix 1).

Most (n = 22) ST1 isolates in our collection had a pilus island (PI) profile consisting of PI-1 containing the recently described PI-1 backbone protein subunit BP-1b (*10*) (BP1b-PI-1), in combination with PI-2a (online Technical Appendix 1). One ST1 isolate (NGBS1605) possessed the traditional PI-1 and PI-2a (online Technical Appendix 1). The ST14 isolates had BP1b-PI-1 and PI-2b. The ST889 isolate possessed only PI-2a (online Technical Appendix 1). We found differences among isolates in genes encoding α-like proteins (Alps): the ST297 isolate and most ST1 strains had gene *bca* encoding α-C protein. ST1 isolates NGBS543 and NGBS1605 possessed gene *alp3*, encoding Alp3. The ST14 and ST889 isolates possessed gene *alp1*, encoding Alp1 (or epsilon) protein (online Technical Appendix 1).

We next examined the extent of genetic diversity among the numerically dominant group of serotype VI ST1 organisms. For comparative purposes, genome data for 3 additional serotype VI strains were included (French strain CCH330, SRA accession no. ERX298473; Malaysian strain PR06, GenBank accession no. AOSD00000000.1; and 1 temporally matched serotype VI isolate recovered from a colonized pregnant woman in Canada; online Technical Appendix 1). Recombination was the main driver of genetic diversity among serotype VI ST1 organisms. Most (n = 16)

ST1 isolates clustered closely with Malaysia strain PR06 (online Technical Appendix 2 Figure 2). This clade (arbitrarily named the Malaysian clade) included most ST1 isolates with resistance to erythromycin and clindamycin. Recombination in a region of ≈200 kbp containing the genes encoding the 2-component virulence regulator CsrRS differentiated the Malaysian clade from a second clade formed by 5 Canadian isolates and the French and Taiwanese ST1 isolates (arbitrarily named the Taiwanese clade) (online Technical Appendix 2 Figure 2). Recombination also explains the aforementioned differences in Alp- and pilus subunit–encoding genes among serotype VI ST1 strains. Isolates NGBS543 and NGBS1605 differed from other ST1 isolates by recombination in a region spanning 107 and 89 kbp, respectively, containing Alp-encoding genes. These 2 isolates also differed between themselves by recombination in the PI-1 locus (online Technical Appendix 2 Figure 2).

Global travel and migration are known contributors to the emergence of bacterial clones in new geographies (11). Serotype VI GBS infections have emerged in Malaysia and Taiwan (3,4). The population of serotype VI GBS isolates in Canada is dominated by 2 ST1 clades, each closely related genetically to the Malaysian or Taiwanese isolates. Although it is tempting to speculate that these 2 ST1 genotypes were introduced into Canada from overseas, the speculation cannot be fully supported by our current limited dataset. Continued monitoring for serotype VI GBS infections is warranted.

About the Author
Ms. Neemuchwala is a research associate at Public Health Ontario in Toronto, Ontario, Canada. Her research interests include the molecular epidemiology of pathogenic streptococci.

References
1. Le Doare K, Heath PT. An overview of global GBS epidemiology. Vaccine. 2013;31(Suppl 4):D7–12. http://dx.doi.org/10.1016/j.vaccine.2013.01.009
2. Morozumi M, Wajima T, Takata M, Iwata S, Ubukata K. Molecular characteristics of group B Streptococci isolated from adults with invasive infections in Japan. J Clin Microbiol. 2016;54:2695–700. http://dx.doi.org/10.1128/JCM.01183-16
3. Eskandarian N, Ismail Z, Neela V, van Belkum A, Desa MN, Amin Nordin S. Antimicrobial susceptibility profiles, serotype distribution and virulence determinants among invasive, non-invasive and colonizing Streptococcus agalactiae (group B Streptococcus) from Malaysian patients. Eur J Clin Microbiol Infect Dis. 2015;34:579–84. http://dx.doi.org/10.1007/s10096-014-2265-x
4. Lin HC, Chen CJ, Chiang KH, Yen TY, Ho CM, Hwang KP, et al. Clonal dissemination of invasive and colonizing clonal complex 1 of serotype VI group B Streptococcus in central Taiwan. J Microbiol Immunol Infect. 2016;49:902–9. http://dx.doi.org/10.1016/j.jmii.2014.11.002
5. Alhhazmi A, Hurteau D, Tyrrell GJ. Epidemiology of invasive group B streptococcal disease in Alberta, Canada, from 2003 to 2013. J Clin Microbiol. 2016;54:1774–81. http://dx.doi.org/10.1128/JCM.00355-16
6. Teatero S, McGeer A, Low DE, Li A, Demczuk W, Martin I, et al. Characterization of invasive group B Streptococcus strains from the greater Toronto area, Canada. J Clin Microbiol. 2014;52:1441–7. http://dx.doi.org/10.1128/JCM.03554-13
7. Flores AR, Galloway-Peña J, Sahasrabhojane P, Saldaña M, Yao H, Su X, et al. Sequence type 1 group B Streptococcus, an emerging cause of invasive disease in adults, evolves by small genetic changes. Proc Natl Acad Sci U S A. 2015;112:6431–6. http://dx.doi.org/10.1073/pnas.1504725112
8. Teatero S, Athey TB, Van Caeseele P, Horsman G, Alexander DC, Melano RG, et al. Emergence of serotype IV group B Streptococcus adult invasive disease in Manitoba and Saskatchewan, Canada, is driven by clonal sequence type 459 strains. J Clin Microbiol. 2015;53:2919–26. http://dx.doi.org/10.1128/JCM.01128-15
9. Clinical and Laboratory Standards Institute. Performance standards for antimicrobial susceptibility testing. 25th informational supplement (M100–S23). Wayne (PA): The Institute; 2015.
10. Teatero S, Neemuchwala A, Yang K, Gomes J, Athey TBT, Martin I, et al. Genetic evidence for a novel variant of the pilus island 1 backbone protein in group B Streptococcus. J Med Microbiol. 2017;66:1409–15. http://dx.doi.org/10.1099/jmm.0.000588
11. Morens DM, Fauci AS. Emerging infectious diseases: threats to human health and global stability. PLoS Pathog. 2013;9:e1003467. http://dx.doi.org/10.1371/journal.ppat.1003467

Address for correspondence: Nahuel Fittipaldi, Public Health Ontario Laboratory, 661 University Ave, Ste 17-100, Toronto, ON M5G 1M1, Canada; email: nahuel.fittipaldi@oahpp.ca

Psychrobacter sanguinis Wound Infection Associated with Marine Environment Exposure, Washington, USA

Jesse Bonwitt, Michael Tran, Angela Droz, Anna Gonzalez, William A. Glover

Author affiliations: Centers for Disease Control and Prevention, Atlanta, Georgia, USA (J. Bonwitt); Durham University, Durham, England (J. Bonwitt); Washington State Department of Health, Shoreline, Washington, USA (J. Bonwitt, M. Tran, W.A. Glover); Harrison Medical Center, Bainbridge Island, Washington, USA (A. Droz); Kitsap Public Health District, Bremerton, Washington, USA (A. Gonzalez)

We report a 26-year-old man with *Psychrobacter sanguinis* cellulitis of a wound sustained during ocean fishing in Washington, USA, in 2017. *Psychrobacter* spp. are opportunistic pathogens found in a wide range of environments. Clinicians should be aware of *Psychrobacter* spp. and perform 16S rRNA sequencing if this pathogen is suspected.

In February 2017, a 26-year-old man sought treatment at an urgent care facility (Harrison Medical Center, Bainbridge Island, Washington, USA) for a hand laceration and reported tingling in his fingers, hand, and forearm. The laceration was a healing 6-cm diagonal cut across the dorsum of the hand with surrounding erythema and cellulitis without active bleeding. Vital signs (blood pressure, pulse, respiration, and temperature) were within reference ranges. The patient reported that his wound occurred while he was cutting squid bait when he was ocean fishing for crabs in Puget Sound (Pacific Ocean), Washington, USA. The squid bait was purchased frozen from an independent fishing retail store. The patient did not report any other pertinent medical history (e.g., immunosuppression). We cleaned and dressed his wound, administered tetanus vaccine (Adacel; Sanofi Pasteur Inc., Swiftwater, Pennsylvania, USA) prophylactically, and treated him as an outpatient with oral cephalexin and topical bacitracin zinc. He fully recovered.

We submitted a wound swab sample to the hospital laboratory for bacterial culture. The cultures yielded rare colonies of coagulase-negative *Staphylococcus* spp. and light growth of a gram-negative rod. In a subsequent attempt to identify the unknown gram-negative rod by VITEK 2 (bioMérieux Inc., Durham, NC, USA), the results suggested *Brucella* spp. The isolate was sent to Washington State Public Health Laboratories (Shoreline, Washington, USA) for confirmatory testing, but the isolate tested negative for *Brucella* spp. by PCR. No leftover squid bait was available for sampling. Gram staining of the isolate revealed gram-negative coccobacilli arranged in pairs with rare cells that retained crystal violet stain. When culturing at 35°C was performed, medium-sized, convex, sticky, nonhemolytic colonies formed on blood agar and pinpoint colonies with pitting on chocolate agar. Colonies were catalase, oxidase, and urease positive. The isolate could not be identified by matrix-assisted laser desorption/ionization mass spectrometry (MALDI Biotyper CA System, research-use-only version 4.1.8; Bruker Daltonics Inc., MA, USA). Sequencing of 16S rRNA performed by the Centers for Disease Control and Prevention (Atlanta, Georgia, USA) identified the bacterium as *Psychrobacter sanguinis* (GenBank accession no. MH178035).

We performed antimicrobial susceptibility testing under aerobic conditions at 35°C using disk diffusion testing. Despite the absence of standardized break points for *Psychrobacter* spp., the large zone sizes indicated that the isolate was susceptible to cefazolin, cefepime, cefoxitin, ceftriaxone, ciprofloxacin, meropenem, penicillin, and tetracycline. The isolate tested negative for β-lactamase.

Psychrobacter are psychrotrophic (i.e., cold tolerant), gram-negative bacteria of the family *Moraxellaceae* (*1*). *Psychrobacter* spp. have been isolated from marine species (crustaceans, fish, and marine mammals); marine environments (seabed and seaweed); food products (seafood, cheese, and meat); storks; pig digestive tracts; and lamb lungs (https://www.ncbi.nlm.nih.gov/Taxonomy/Browser/wwwtax.cgi). *Psychrobacter* spp. might also be a component of the human microbiota; studies have demonstrated the presence of *P. arenosus*, *P. faecalis*, *P. phenylpyruvicus*, and *P. pulmonis* in the human gut (*2*).

Only a subset of *Psychrobacter* spp. are considered medically relevant opportunistic pathogens on the basis of a limited number of published case reports (*1,3*). Clinical manifestations depend on the infection site and include bacteremia (*4,5*), meningitis (*6,7*), surgical wound infection (*8*), and ocular infection (*9*). Of these cases, only 1 was associated with exposure to a marine environment; in that case, the patient experienced *P. phenylpyruvicus* bacteremia after consuming a raw geoduck clam that was possibly imported from the Pacific Northwest (*5*).

P. sanguinis was reported as a new species in 2012, after retrospective isolation from the blood of 4 patients in New York, USA (*10*). *P. sanguinis* infection was subsequently reported in a patient with meningitis in France (*7*), and an organism closely related to *P. sanguinis* (98% identity of 16S rRNA) was reported in a patient with meningitis in Mexico (*6*). One of these patients acquired the infection nosocomially, but the source of the infections could not be determined, and exposure to marine environments was not reported for either case. Both patients were treated with antimicrobial drugs; 1 patient fully recovered, and the other died from complications, including septic shock. *P. sanguinis* has previously been described as broadly susceptible (*7*); however, *Psychrobacter* spp. have displayed penicillin resistance (*1*).

We describe a case of *P. sanguinis* infection in a healthy person after wound exposure to squid bait and seawater of the Pacific Northwest Coast. The source of the infection could not be determined, but isolation of *Psychrobacter* spp. from a wide range of environments suggests the infection could have occurred from exposure to the marine environment. Contamination of the wound by human gut microbiota cannot be excluded but is unlikely, given that only 2 types of bacteria were isolated from the wound. The wound displayed cellulitis, a presentation consistent with infection by an opportunistic pathogen; this finding, therefore, expands the clinical spectrum of *P. sanguinis* infection. Clinicians and laboratorians should be aware of the opportunistic potential of *Psychrobacter* spp. and the limitations of commercial identification systems for confirming these agents.

Acknowledgments

We thank the staffs of the Microbiology Department of the Harrison Medical Center and the Special Bacteriology Reference Laboratory of the US Centers for Disease Control and Prevention.

About the Author

Dr. Bonwitt is a veterinarian and Epidemic Intelligence Service officer in the Division of Scientific Education and Professional Development, Center for Surveillance, Epidemiology and Laboratory Services, Office of Public Health Scientific Services, Centers for Disease Control and Prevention, Atlanta, Georgia, USA, assigned to the Washington State Department of Health. His research interests are zoonotic and emerging infectious diseases and qualitative research at the animal–human interface.

References

1. Vaneechoutte M, Dijkshoorn L, Nemec A, Kämpfer P, Wauters G. *Acinetobacter*, *Chryseobacterium*, *Moraxella*, and other nonfermentative gram-negative rods. In: Jorgensen JH, Pfaller MA, Carroll KC, Funke G, Landry ML, Richter SS, et al., editors. Manual of clinical microbiology. 11th ed. Washington: AMS Press; 2015. p. 813–37.
2. Lagier J-C, Khelaifia S, Alou MT, Ndongo S, Dione N, Hugon P, et al. Culture of previously uncultured members of the human gut microbiota by culturomics. Nat Microbiol. 2016;1:16203. http://dx.doi.org/10.1038/nmicrobiol.2016.203
3. Deschaght P, Janssens M, Vaneechoutte M, Wauters G. *Psychrobacter* isolates of human origin, other than *Psychrobacter phenylpyruvicus*, are predominantly *Psychrobacter faecalis* and *Psychrobacter pulmonis*, with emended description of *P. faecalis*. Int J Syst Evol Microbiol. 2012;62:671–4. http://dx.doi.org/10.1099/ijs.0.032631-0
4. Caspar Y, Recule C, Pouzol P, Lafeuillade B, Mallaret MR, Maurin M, et al. *Psychrobacter arenosus* bacteremia after blood transfusion, France. Emerg Infect Dis. 2013;19:1118–20. http://dx.doi.org/10.3201/eid1907.121599
5. Leung WK, Chow VC, Chan MC, Ling JM, Sung JJ. *Psychrobacter* bacteraemia in a cirrhotic patient after the consumption of raw geoduck clam. J Infect. 2006;52:e169–71. http://dx.doi.org/ 10.1016/j.jinf.2005.08.031
6. Ortiz-Alcántara JM, Segura-Candelas JM, Garcés-Ayala F, Gonzalez-Durán E, Rodríguez-Castillo A, Alcántara-Pérez P, et al. Fatal *Psychrobacter* sp. infection in a pediatric patient with meningitis identified by metagenomic next-generation sequencing in cerebrospinal fluid. Arch Microbiol. 2016;198:129–35. http://dx.doi.org/10.1007/s00203-015-1168-2
7. Le Guern R, Wallet F, Vega E, Courcol RJ, Loïez C. *Psychrobacter sanguinis*: an unusual bacterium for nosocomial meningitis. J Clin Microbiol. 2014;52:3475–7. http://dx.doi.org/10.1128/JCM.01197-14
8. Stepanović S, Vuković D, Bedora-Faure M, K'ouas G, Djukić S, Svabić-Vlahović M, et al. Surgical wound infection associated with *Psychrobacter phenylpyruvicus*-like organism. Diagn Microbiol Infect Dis. 2007;57:217–9. http://dx.doi.org/10.1016/j.diagmicrobio.2006.08.002
9. Gini GA. Ocular infection caused by *Psychrobacter immobilis* acquired in the hospital. J Clin Microbiol. 1990;28:400–1.
10. Wirth SE, Ayala-del-Río HL, Cole JA, Kohlerschmidt DJ, Musser KA, Sepúlveda-Torres LC, et al. *Psychrobacter sanguinis*

sp. nov., recovered from four clinical specimens over a 4-year period. Int J Syst Evol Microbiol. 2012;62:49–54. http://dx.doi.org/10.1099/ijs.0.029058-0

Diagnosis of *Haemophilus influenzae* Pneumonia by Nanopore 16S Amplicon Sequencing of Sputum

Jangsup Moon,[1] Yoonhyuk Jang,[1] Narae Kim, Wan Beom Park, Kyung-Il Park, Soon-Tae Lee, Keun-Hwa Jung, Manho Kim, Sang Kun Lee, Kon Chu

Author affiliations: Seoul National University Hospital, Seoul, South Korea (J. Moon, Y. Jang, N. Kim, W.B. Park, S.-T. Lee, K.-H. Jung, M. Kim, S.K. Lee, K. Chu); Seoul National University Hospital Healthcare System Gangnam Center, Seoul (K.-I. Park)

We used deep sequencing of the 16S rRNA gene from sputum to identify *Haemophilus influenzae* in a patient with community-acquired pneumonia. This method may be more effective than conventional diagnostic tests in pneumonia patients because of its speed and sensitivity.

Pathogen identification in patients with community-acquired pneumonia primarily relies on culture-based techniques (*1,2*). Sequencing-based approaches for pathogen identification are being applied to pneumonia patients (*3*). MinION (Oxford Nanopore Technologies, Oxford, UK), a nanopore sequencer, is gaining attention in metagenomics research because of its capability for long-read sequencing and real-time analysis, along with its small size (*4,5*). Recently, the first use of MinION for real-time metagenomic sequencing of bronchoalveolar lavage (BAL) specimens in pneumonia patients was reported (*6*). We report successfully detecting a respiratory pathogen by deep sequencing of 16S amplicons of sputum using MinION.

[1]These authors contributed equally to this article.

A 77-year-old man with end-stage renal disease and asthma was hospitalized in June 2017 because of hypoxic respiratory failure. Dyspnea developed 4 days before admission, and sputum production and rhinorrhea increased significantly. Crackles were present in both lungs, and tachypnea was noted. Chest computed tomography scan revealed multiple nodular lesions and branching opacities in both lungs (Figure, panel A). Leukocytosis was absent, but C-reactive protein and procalcitonin were elevated (46.41 mg/dL [reference 0–0.5 mg/dL] and 32.03 ng/mL [reference 0–0.5 ng/mL], respectively). Results of extensive diagnostic testing performed on sputum, including Gram staining, bacterial culture, acid-fast bacilli testing, and PCR for 16 respiratory viruses and tuberculosis/nontuberculous mycobacteria, were negative. After 2 weeks of empiric antimicrobial treatment with ceftazidime and ciprofloxacin, the patient recovered to baseline status.

We retrospectively performed 16S amplicon sequencing with MinION. We extracted genomic DNA (Genomic DNA Mini Kit, Invitrogen, Carlsbad, CA, USA) from sputum obtained by oropharyngeal suction after a single empiric administration of an antimicrobial drug (cefuroxime, 500 mg). We generated the sequencing libraries using a rapid 16S amplicon sequencing kit (SQK-RAS201). After 30 cycles of PCR using universal 16S primers (27F and 1492R) included in the kit, we attached sequencing adaptors. A total of 470,231 reads were generated during the 5-hour sequencing time. We analyzed the reads using the EPI2ME 16S BLAST workflow (https://blast.ncbi.nlm.nih.gov/Blast.cgi); 122,722 reads aligned with 1 of the bacterial 16S rRNA gene sequences with ≥80% accuracy. Of these reads, 119,943 (98.1%) were aligned with the genus *Haemophilus* and 115,068 (94.11%) were aligned with *Haemophilus influenzae* (Figure, panels B, C). We obtained similar results by analyzing the subgroups of reads generated during the first 10 minutes and during the first hour (Figure, panel C). Because the overwhelming majority of the reads were aligned with *H. influenzae* versus other oral commensal bacteria, we regarded *H. influenzae* as the pathogen. Repeated nanopore sequencing using
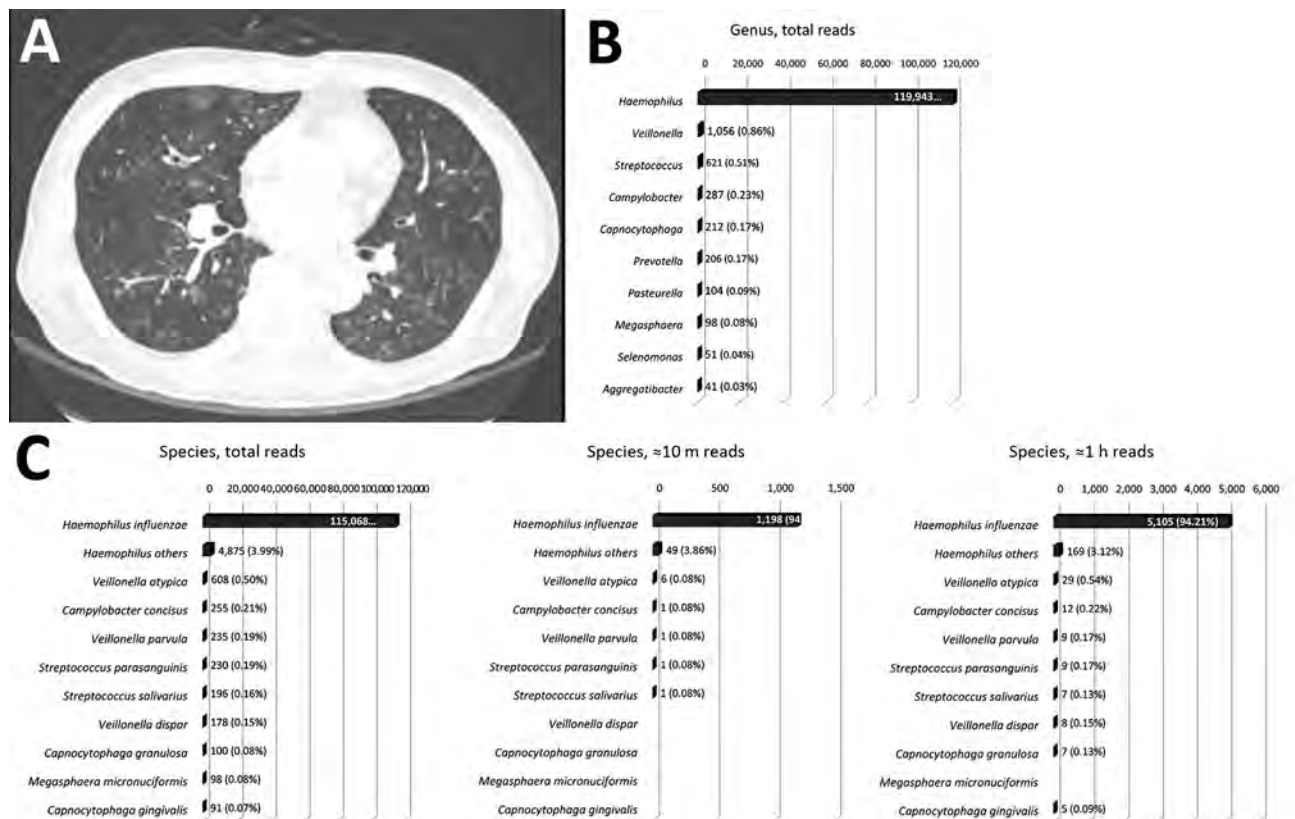
Figure. Chest computed tomography scan and sequencing of the 16S amplicon in a 77-year-old man with end-stage renal disease and asthma. A) Hypoxic respiratory failure with bilateral infiltrates are visible on chest computed tomography scan. B) Sequencing of the 16S amplicon performed on sputum using the MinION sequencer (Oxford Nanopore Technologies, Oxford, UK). Sequencing for 5 h generated 470,231 reads. A total of 122,272 reads were aligned with 1 of the bacterial 16S rRNA gene sequences, and most reads (119,943 [98.1%]) were aligned with genus *Haemophilus*. C) Of the 122,272 aligned reads, nearly all (115,068 [94.11%]) were aligned with the species *H. influenzae* (left). The number of reads aligned with *H. influenzae* was >100-fold larger than those aligned with other oral commensal bacteria. Similar results were obtained from the subgroup analyses of reads generated during the first hour (middle) and during the first 10 min (right).

different workflow and additional quantitative PCR confirmed the results (online Technical Appendix, https://wwwnc.cdc.gov/EID/article/24/10/18-0234-Techapp1.pdf).

We identified the pneumonia pathogen in this patient by deep sequencing of 16S amplicons from sputum using MinION. The reads aligned to *H. influenzae* were >100-fold more abundant than reads aligned with other commensal bacteria, reflecting the significant proliferation of *H. influenzae* in the patient's respiratory tract. *H. influenzae* is an opportunistic pathogen of the respiratory tract that becomes pathogenic only when other risk factors are present (*7*). *H. influenzae* infection is most effectively treated with intravenous third-generation cephalosporins, whereas resistance to β-lactam antimicrobial drugs is prevalent (*8*).

We suggest deep sequencing of the 16S rRNA gene from sputum as a new method of detecting respiratory pathogens. Although expectorated sputum is the most readily available specimen, the specimen must transverse the upper airways, which are colonized with multiple bacteria; thus, criteria for acceptable sputum are widely used (*9*). Otherwise, quantitative cultures of BAL specimens are used; these specimens are less affected by upper airway commensals, but BAL is largely restricted to nosocomial or ventilator-associated pneumonia (*10*). Respiratory pathogens can be identified directly from sputum by comparing the relative ratio of reads aligned with each bacteria, without the prerequisite of microscopic examination or bronchoscopy.

Nanopore sequencing of 16S amplicons enables rapid pathogen identification in pneumonia patients. With the MinION sequencer, generated reads can be analyzed in real time, which makes this approach more promising (*4*,*6*). Tentative point-of-care diagnosis by nanopore 16S sequencing and confirmation of the result by standard culture methods would be a feasible approach. In the case we report, we performed sequencing for 5 hours; moreover, the subgroup analyses of reads generated for the first hour and for the first 10 minutes produced similar results, indicating that a relatively short sequencing time would be sufficient for pathogen identification. We estimate that the turnaround time for MinION 16S sequencing can be reduced to <8 hours.

The 16S amplicon sequencing–based diagnostic approach can be more sensitive than conventional tests and would be particularly useful for identifying unculturable bacteria or detecting bacteria in specimens collected after exposure to antimicrobial drugs. Therefore, this method might enable detection of pathogens that were not detected by conventional tests (*3*), as demonstrated by the case we report.

Nanopore 16S amplicon sequencing from sputum can be more effective than conventional diagnostic tests in pneumonia patients because of its speed and sensitivity. However, further studies with more cases are needed to establish reliable diagnostic criteria for respiratory pathogens based on the relative read abundance compared with commensal bacteria.

About the Author

Dr. Moon is an assistant professor at the Seoul National University Hospital. His primary research interests include metagenomics analysis for pathogen identification from clinical samples. Dr. Jang is a resident at the Seoul National University Hospital. His primary research interests include encephalitis.

References

1. Jain S, Self WH, Wunderink RG, Fakhran S, Balk R, Bramley AM, et al.; CDC EPIC Study Team. Community-acquired pneumonia requiring hospitalization among US adults. N Engl J Med. 2015;373:415–27. http://dx.doi.org/10.1056/NEJMoa1500245
2. Holter JC, Müller F, Bjørang O, Samdal HH, Marthinsen JB, Jenum PA, et al. Etiology of community-acquired pneumonia and diagnostic yields of microbiological methods: a 3-year prospective study in Norway. BMC Infect Dis. 2015;15:64. http://dx.doi.org/10.1186/s12879-015-0803-5
3. Dickson RP, Erb-Downward JR, Prescott HC, Martinez FJ, Curtis JL, Lama VN, et al. Analysis of culture-dependent versus culture-independent techniques for identification of bacteria in clinically obtained bronchoalveolar lavage fluid. J Clin Microbiol. 2014;52:3605–13. http://dx.doi.org/10.1128/JCM.01028-14
4. Quick J, Loman NJ, Duraffour S, Simpson JT, Severi E, Cowley L, et al. Real-time, portable genome sequencing for Ebola surveillance. Nature. 2016;530:228–32. http://dx.doi.org/10.1038/nature16996
5. Moon J, Kim N, Lee HS, Shin H-R, Lee S-T, Jung K-H, et al. *Campylobacter fetus* meningitis confirmed by a 16S rRNA gene analysis using the MinION nanopore sequencer, South Korea, 2016. Emerg Microbes Infect. 2017;6:e94. http://dx.doi.org/10.1038/emi.2017.81
6. Pendleton KM, Erb-Downward JR, Bao Y, Branton WR, Falkowski NR, Newton DW, et al. Rapid pathogen identification in bacterial pneumonia using real-time metagenomics. Am J Respir Crit Care Med. 2017;196:1610–2. http://dx.doi.org/10.1164/rccm.201703-0537LE
7. Agrawal A, Murphy TF. *Haemophilus influenzae* infections in the *H. influenzae* type b conjugate vaccine era. J Clin Microbiol. 2011;49:3728–32. http://dx.doi.org/10.1128/JCM.05476-11
8. Tristram S, Jacobs MR, Appelbaum PC. Antimicrobial resistance in *Haemophilus influenzae*. Clin Microbiol Rev. 2007;20:368–89. http://dx.doi.org/10.1128/CMR.00040-06
9. Bartlett JG. Diagnostic tests for agents of community-acquired pneumonia. Clin Infect Dis. 2011;52(Suppl 4):S296–304. http://dx.doi.org/10.1093/cid/cir045
10. Bartlett JG. Diagnostic test for etiologic agents of community-acquired pneumonia. Infect Dis Clin North Am. 2004;18:809–27. http://dx.doi.org/10.1016/j.idc.2004.08.002

Address for correspondence: Kon Chu, Seoul National University Hospital, Department of Neurology, 101 Daehak-ro, Jongno-gu, Seoul 110-744, South Korea; email: stemcell.snu@gmail.com

Revisiting Influenza Vaccination Exemption

Margaret Ryan, Laurie Duran, Rachel Lee, Sengkham Wu

Author affiliations: University of California San Diego School of Medicine, San Diego, California, USA (M. Ryan); Defense Health Agency Immunization Healthcare Branch, San Diego (M. Ryan, L. Duran); Naval Medical Center, San Diego (M. Ryan, L. Duran, R. Lee, S. Wu)

Serious adverse events after immunizations are rare. We review the case of a man who, 50 years earlier, experienced a serious adverse neurologic event 2 weeks after receiving influenza vaccine. He had received no subsequent seasonal influenza vaccinations, but after the risks and benefits were considered, he was vaccinated without adverse event that season.

Neurologic adverse events following immunization (AEFIs), such as encephalitis or acute disseminated encephalomyelitis (ADEM), developing after influenza vaccination have been observed but are rare. It is challenging to determine the causal relationship between an influenza vaccination and an AEFI. A 2011 review by the Institute of Medicine found epidemiologic evidence to be insufficient and mechanistic evidence to be weak for establishing a causal association between influenza vaccination and encephalitis or ADEM (1). A more recent review of serious AEFIs found that 4 cases of ADEM had possible causal association with vaccination for the 2009 pandemic influenza A(H1N1) virus (2).

We examined 1 example of an AEFI in a patient who was subsequently issued a medical exemption from future vaccinations. The patient's original AEFI was documented in 1969 (3). Meningoencephalitis developed in the patient, a 29-year-old member of the US military, ≈2 weeks after receiving seasonal influenza vaccine. After a brief hospitalization and supportive care, he recovered without sequelae. The patient was given a medical exemption from subsequent influenza vaccinations for the remainder of his time in the military. For the next 48 years, he declined nearly all vaccinations. (In 2011, the patient did receive 1 dose of a vaccine unrelated to influenza.)

In September 2017, at 77 years of age, the patient expressed concern to his primary care physician about his level of protection against infections because he was considering moving to an assisted living facility. After discussing risks and benefits with his healthcare providers, he agreed to receive pneumococcal conjugate vaccine 13 in October 2017, followed ≈1 month later by seasonal influenza vaccine (ccIIV4; Flucelvax; Seqirus, Summit, NJ, USA). He reported feeling well over the subsequent 3 months of follow-up and anticipates that in the fall of 2018 he will receive pneumococcal polysaccharide vaccine 23 and seasonal influenza vaccine.

The influenza vaccine that this patient received in 1969 was a bivalent product that included A2/Aichi/2/68 and B/Massachusetts/3/66 antigens cultured in embryonated chicken eggs (4). It is unclear how the 1969 vaccine compares with modern-era influenza vaccines in terms of rates of rare AEFIs and how medical experts assessed causality after the AEFI that resulted in the patient's exemption from all future influenza vaccinations, nearly 50 years ago. However, AEFI causality assessments have become more rigorous over time, under United States and World Health Organization guidelines (5,6).

When deciding whether to continue vaccinating a patient who has experienced a serious neurologic AEFI, all available information should be considered, including the licensing of the vaccine and, in the United States, the Centers for Disease Control and Prevention/Advisory Committee on Immunization Practices' General Best Practice Guidelines for Immunization (7). The risk for new or recurrent neurologic events after subsequent vaccination is unknown.

More cases of encephalitis and ADEM are associated with virus infection than with vaccination. However, recurrence of such events is rare, even after repeated virus infections. Because of this rarity, when relapse of ADEM occurs in adults, it is more likely to be diagnosed as multiple sclerosis than as an independent recurrence of ADEM (8).

Providers may be challenged to determine if, when, and how to administer vaccines to a patient who has had a serious AEFI. Although it may seem easiest and safest to permanently exempt persons from further vaccination, doing so may inappropriately deprive them of disease protection because factors relevant to risk and benefit change over time (9). We propose that vaccine exemptions should be revisited regularly, regardless of how long they have been in effect.

Acknowledgment

About the Author

Dr. Ryan is currently the medical director of the Pacific Region Office of the Defense Health Agency Immunization Healthcare Branch and an adjunct professor at the University of California San Diego School of Medicine. Many of her research publications focus on infectious diseases of military importance.

References

1. Committee to Review Adverse Effects of Vaccines; Institute of Medicine. Stratton K, Ford A, Rusch E, Clayton EW, et al., editors. Adverse effects of vaccines: evidence and causality. Washington: National Academies Press; 2011. p. 293–308.
2. Williams SE, Pahud BA, Vellozzi C, Donofrio PD, Dekker CL, Halsey N, et al. Causality assessment of serious neurologic adverse events following 2009 H1N1 vaccination. Vaccine. 2011;29:8302–8. http://dx.doi.org/10.1016/j.vaccine.2011.08.093
3. Rosenberg GA. Meningoencephalitis following an influenza vaccination. N Engl J Med. 1970;283:1209. http://dx.doi.org/10.1056/NEJM197011262832208
4. Centers for Disease Control. Influenza vaccine: recommendations of the Public Health Service Advisory Committee on Immunization Practices. MMWR Morb Mortal Wkly Rep. 1970;19:327.
5. Halsey NA, Edwards KM, Dekker CL, Klein NP, Baxter R, Larussa P, et al.; Causality Working Group of the Clinical Immunization Safety Assessment Network. Algorithm to assess causality after individual adverse events following immunizations. Vaccine. 2012;30:5791–8. http://dx.doi.org/10.1016/j.vaccine.2012.04.005
6. Tozzi AE, Asturias EJ, Balakrishnan MR, Halsey NA, Law B, Zuber PL. Assessment of causality of individual adverse events following immunization (AEFI): a WHO tool for global use. Vaccine. 2013;31:5041–6. http://dx.doi.org/10.1016/j.vaccine.2013.08.087
7. Kroger AT, Duchin J, Vázquez M. General Best Practice Guidelines for Immunization. Best practices guidance of the Advisory Committee on Immunization Practices (ACIP) [cited 16 Apr 2018]. https://www.cdc.gov/vaccines/hcp/acip-recs/general-recs/index.html
8. Koelman DL, Chahin S, Mar SS, Venkatesan A, Hoganson GM, Yeshokumar AK, et al. Acute disseminated encephalomyelitis in 228 patients: a retrospective, multicenter US study. Neurology. 2016;86:2085–93. http://dx.doi.org/10.1212/WNL.0000000000002723
9. Poland GA, Fleming DM, Treanor JJ, Maraskovsky E, Luke TC, Ball EM, et al. New wisdom to defy an old enemy: summary from a scientific symposium at the 4th Influenza Vaccines for the World (IVW) 2012 Congress, 11 October, Valencia, Spain. Vaccine. 2013;31(Suppl 1):A1–20. http://dx.doi.org/10.1016/j.vaccine.2013.02.033

Address for correspondence: Margaret Ryan, Defense Health Agency Immunization Healthcare Branch, Pacific Region Office at Naval Medical Center San Diego, Bldg 6, Rm 4V-7C1, San Diego, CA 92134, USA; email: margaret.a.ryan6.civ@mail.mil

Fatal *Cronobacter sakazakii* Sequence Type 494 Meningitis in a Newborn, Brazil

Cláudia Elizabeth Volpe Chaves,[1] Marcelo Luiz Lima Brandão,[1] Mara Luci Gonçalves Galiz Lacerda, Caroline Aparecida Barbosa Coelho Rocha, Sandra Maria do Valle Leone de Oliveira, Tânia Cristina Parpinelli, Luiza Vasconcellos, Stephen James Forsythe, Anamaria Mello Miranda Paniago

Author affiliations: National Institute of Quality Control in Health of Oswaldo Cruz Foundation, Rio de Janeiro, Brazil (C.E.V. Chaves, M.L.L. Brandão, L. Vasconcellos); Federal University of Mato Grosso do Sul, Mato Grosso do Sul, Brazil (C.E.V. Chaves, S.M. do Valle Leone de Oliveira, A.M.M. Paniago); Regional Hospital of Mato Grosso do Sul, Mato Grosso do Sul (M.L.G. Galiz Lacerda, C.A.B. Coelho Rocha, T.C. Parpinelli); foodmicrobe.com, Adams Hill, Nottingham, UK (S.J. Forsythe)

We describe a case of infection with *Cronobacter sakazakii* sequence type 494 causing bacteremia and meningitis in a hospitalized late premature infant in Brazil. We conducted microbiological analyses on samples of powdered infant formula from the same batch as formula ingested by the infant but could not identify the source of contamination.

In September 2017, a healthy boy was born at 35 weeks' gestation in Brazil. The newborn was fed breast milk and reconstituted powdered infant formula (PIF) while in the hospital. On postnatal day 4, he began sleeping more than usual and experienced hypoactivity, pallor, jaundice, seizures, metabolic acidosis, and finally respiratory insufficiency, necessitating mechanical ventilation and empiric treatment with cefepime and ampicillin. We obtained 2 blood cultures on postnatal day 4 that yielded *Cronobacter* spp. with resistance to cephalothin and cefoxitin, intermediate resistance to nitrofurantoin, and susceptibility to other antimicrobial drugs, including cefepime and ampicillin. A transfontanel ultrasound on postnatal day 6 showed grade 2 periintraventricular hemorrhage with hypoxic-ischemic lesions. Subsequent computed tomography and nuclear magnetic resonance (NMR) imaging revealed biparietal cerebral abscess (Figure). Culture of the cerebral abscess on postnatal day 33 yielded *Cronobacter* spp. that had the same pattern of antimicrobial drug susceptibility as that found in blood isolates. Because of the
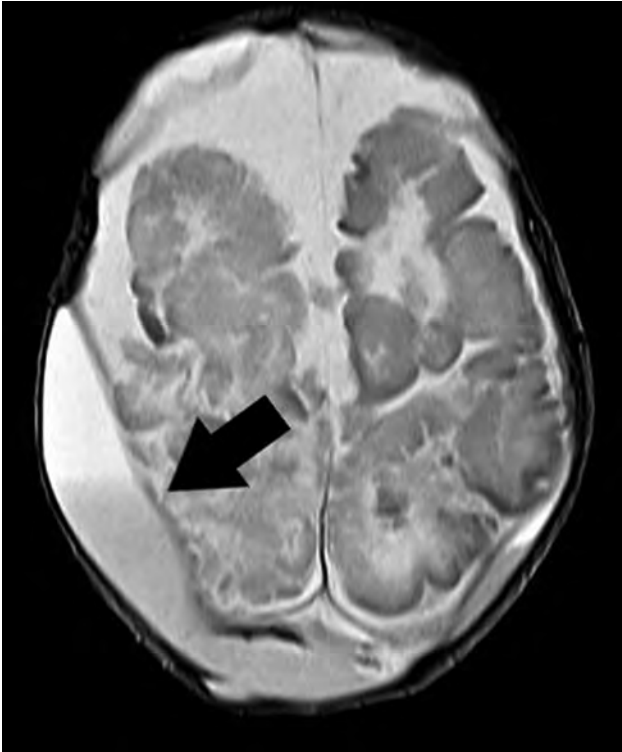
Figure. Brain nuclear magnetic resonance image of a newborn with *Cronobacter sakazakii* sequence type 494 meningitis, Brazil. Extradural collections are visible in both parietal regions. Arrow indicates the more pronounced extradural collection, measuring ≈1.8 cm, in the right parietal region.

patient's progressive clinical deterioration, we changed the antimicrobial therapy to meropenem on postnatal day 10; however, the infant failed to improve, and he died on postnatal day 46.

The mother's pregnancy was uncomplicated except for a urinary tract infection (UTI), for which she received cephalexin, in the third trimester. She experienced another UTI caused by *Enterococcus faecalis* and endometritis shortly after giving birth and underwent endometrial curettage and received ampicillin/sulbactam. We did not identify *Cronobacter* spp. in the urine or endometrial curettage material.

We were unable to analyze a sample from PIF container, the contents of which had been used. Because contaminated PIF from opened cans has been identified as the vehicle in nearly all infant *Cronobacter* infections in the past decade for which a source has been found (*1*), this lack of testing is probably the most significant limitation of this investigation. Subsequently, we sent an unopened can of the PIF from the same lot consumed by the newborn to Nacional Institute of Quality Control in Health from Oswaldo Cruz Foundation (INCQS/Fiocruz), a public laboratory in the Brazilian System of Sanitary Surveillance, where the PIF was analyzed in accordance with 2 standard procedures (*2,3*). Neither method recovered *Cronobacter*.

According to the hospital's standard procedure, all PIF was reconstituted with potable water that was heated >70°C, cooled, and used immediately. However, we could not trace the total time between the reconstitution of the PIF, the time it was maintained during cooling, and the subsequent feeding to the newborn, because the hospital does not have procedures for recording this process.

Ten newborns, 6 of whom were preterm infants, had been fed from the same lot of PIF. We followed the infants clinically during their hospital stay, and none showed signs or symptoms of *Cronobacter* infection.

We did not obtain swab specimens for surveillance. We collected environmental samples from the newborn's location after birth and from formula preparation equipment for microbiological tests in the hospital approximately 3 weeks after illness onset. However, several cleaning and disinfection procedures had been performed, limiting our chances to detect the pathogen in these samples. We collected 1 rectal swab from the newborn brother of the patient on postnatal day 4. We streaked samples onto the surface of ChromID CPS agar (bioMérieux, Rio de Janeiro, Brazil), and test results were negative for *Cronobacter*. However, this method is not specific for *Cronobacter* isolation.

Contaminated PIF and expressed breast milk have been epidemiologically linked with *Cronobacter* infections in neonates (*1,4*), and cases in Brazil have been reported in the literature (*5,6*). The magnitude of *Cronobacter* disease in Brazil is unclear, partly because it is not a compulsory notifiable disease. The most recent reported cases occurred in 2013, when *C. malonaticus* sequence types (ST) 394 and ST440 were responsible for bacteremia in 3 neonates, and the source of contamination was not identified (*5,7*).

In our study, the analyzed PIF did not show *Cronobacter* contamination. In addition, the method of PIF preparation used in the hospital (using water >70°C) would probably inactivate any *Cronobacter* present in the PIF. Because we analyzed only 1 sample, it is possible that we did not detect *Cronobacter* because contamination was not homogeneous across the lot or was below the limit of detection for our methods. We recommend the use of sterile liquid infant formulas in the hospital for patients in neonatal intensive care units unless there is no suitable alternative.

We used the *Cronobacter* MLST Database (http://pubmlst.org/cronobacter) to perform multilocus sequence typing on the 3 *Cronobacter* isolates we detected (*8*). We identified the strains as *C. sakazakii* ST494, an ST which is not in any of the recognized *C. sakazakii* clonal complex (CC) pathovars, such as *C. sakazakii* CC4, which is strongly associated with neonatal meningitis (*9*).

Cronobacter bacteria can cause severe meningitis, resulting in brain abscess formation. Virulence studies of *C. sakazakii* ST494 strains are needed to elucidate their pathogenicity and to compare with *C. sakazakii* CC4 strains.

Acknowledgments

About the Author

Ms. Volpe is an infectious diseases specialist and PhD student in infectious diseases at the Federal University of Mato Grosso do Sul, Brazil, with research interests in hospital infectious disease control.

References

1. Friedemann M. Epidemiology of invasive neonatal *Cronobacter* (*Enterobacter sakazakii*) infections. Eur J Clin Microbiol Infect Dis. 2009;28:1297–304. http://dx.doi.org/10.1007/s10096-009-0779-4
2. International Organization for Standardization, Microbiology of the food chain—horizontal method for the detection of *Cronobacter* spp. ISO 22964:2017. Geneva: The Organization; 2017.
3. Chen Y, Lampel K, Hammack T. *Cronobacter*. In: Bacteriological analytical manual. 8th ed. Revision A, 1998. Rockville (MD): US Department of Health and Human Services, Food and Drug Administration; 2012 [cited 2018 Aug 20]. https://www.fda.gov/Food/FoodScienceResearch/LaboratoryMethods/ucm289378.htm
4. McMullan R, Menon V, Beukers AG, Jensen SO, van Hal SJ, Davis R. *Cronobacter sakazakii* infection from expressed breast milk, Australia. Emerg Infect Dis. 2018;24:393–4. http://dx.doi.org/10.3201/eid2402.171411
5. Brandão MLL, Umeda NS, Carvalho KR, Filippis I. Investigation of an outbreak caused by *Cronobacter malonaticus* in a maternity hospital in Teresina, Piauí: characterization and typing by pulsed field gel electrophoresis [in Portuguese]. Vig Sanit Debate. 2015;3:91–6.
6. Barreira ER, Souza ER, Gois DC, Freitas PF, Fernandes JC. *Enterobacter sakazakii* meningitis in a newborn infant: case report [in Portuguese]. Pediatria (São Paulo). 2003;25:65–70.
7. Umeda NS, de Filippis I, Forsythe SJ, Brandão MLL. Phenotypic characterization of *Cronobacter* spp. strains isolated from foods and clinical specimens in Brazil. Food Res Int. 2017;102:61–7. http://dx.doi.org/10.1016/j.foodres.2017.09.083
8. Forsythe SJ, Dickins B, Jolley KA. *Cronobacter*, the emergent bacterial pathogen *Enterobacter sakazakii* comes of age; MLST and whole genome sequence analysis. BMC Genomics. 2014;15:1121. http://dx.doi.org/10.1186/1471-2164-15-1121
9. Hariri S, Joseph S, Forsythe SJ. *Cronobacter sakazakii* ST4 strains and neonatal meningitis, United States. Emerg Infect Dis. 2013;19:175–7. http://dx.doi.org/10.3201/eid1901.120649

Address for correspondence: Marcelo Luiz Lima Brandão, INCQS/Fiocruz–Immunology, Av. Brasil, 4365 Manguinhos, Rio de Janeiro, RJ, CEP 21040-900, Brazil; email: marcelo.brandao@incqs.fiocruz.br

Introduction of Eurasian-Origin Influenza A(H8N4) Virus into North America by Migratory Birds

Andrew M. Ramey, Andrew B. Reeves, Tyrone Donnelly, Rebecca L. Poulson, David E. Stallknecht

Author affiliations: US Geological Survey Alaska Science Center, Anchorage, Alaska, USA (A.M. Ramey, A.B. Reeves, T. Donnelly); University of Georgia, Athens, Georgia, USA (R.L. Poulson, D.E. Stallknecht)

We identified a Eurasian-origin influenza A(H8N4) virus in North America by sampling wild birds in western Alaska, USA. Evidence for repeated introductions of influenza A viruses into North America by migratory birds suggests that intercontinental dispersal might not be exceedingly rare and that our understanding of viral establishment is incomplete.

Research of and surveillance for influenza A viruses in wild birds inhabiting western Alaska have consistently provided support for the exchange of viruses between East Asia and North America via Beringia (*1,2*). Sampling of wild birds inhabiting Izembek National Wildlife Refuge (NWR) and surrounding areas in Alaska (≈55°N, 163°W) conducted during 2011–2015 has been used in recent research to identify the dispersal of influenza A(H9N2) viruses among China, South Korea, and Alaska (*3*); provide inference about the evolutionary pathways of economically important foreign-origin poultry pathogens introduced into North America (*4*); and identify sampling efficiencies for optimizing the detection of evidence for intercontinental virus exchange (*5*).

During September–October 2016, we collected 541 combined oral-pharyngeal and cloacal swab samples from hunter-harvested waterfowl (*Anseriformes* spp.) and 401 environmental fecal samples from monospecific flocks of either emperor geese (*Chen canagica*) or glaucous-winged gulls (*Larus glaucescens*) within and around Izembek NWR. Samples were deposited into viral transport media, placed in dry shippers charged with liquid nitrogen within 24 h, shipped, and stored frozen at –80°C before laboratory analysis. We screened samples for the influenza A virus matrix gene and subjected them to virus isolation; resultant isolates were genomically sequenced in accordance with previously reported methods (*5*). A total of 116 samples tested positive for the matrix gene, and 38 isolates were recovered of the following combined subtypes: H1N2, H3N2, H3N2/N6 (mixed infection), H3N8, H4N6, H5N2, H6N2, H7N3,

H8N4, and H12N2. We selected the single H8N4 isolate, A/northern pintail/Alaska/UGAI16-3997/2016(H8N4) (GenBank accession nos. MG976689–96), for genomic characterization as part of this investigation.

We queried sequence information for the complete coding region of each gene segment of A/northern pintail/Alaska/UGAI16-3997/2016(H8N4) against the GenBank database to identify strains sharing ≥99% nt identity. We then reconstructed maximum-likelihood phylogenetic trees for each gene segment in MEGA 7.0.21 (https://www.megasoftware.net/) by incorporating sequence information for representative reference sequences from avian-origin influenza A virus isolates from Eurasia and North America using the general time–reversible plus invariant sites (G+I) model with 1,000 bootstrap replications.

Gene segments for A/northern pintail/Alaska/UGAI16-3997/2016(H8N4), isolated from a sample collected from a hunter-harvested duck on September 6, 2016, shared ≥99% nt identity to those of ≥1 isolates recovered from wild and domestic birds sampled in East Asia during 2006–2016 (online Technical Appendix Table, https://wwwnc.cdc.gov/EID/article/24/10/18-0447-Techap1.pdf). This isolate also shared ≥99% nt identity with 1–4 isolates recovered from wild bird samples collected at Izembek NWR during 2012–2015 at the polymerase acidic and polymerase basic 2 gene segments (online Technical Appendix Table). A/northern pintail/Alaska/UGAI16–3997/2016(H8N4) did not, however, share ≥99% nt identity at all 8 gene segments with any other influenza A virus isolate for which genomic information was available, indicating that this H8N4 isolate might
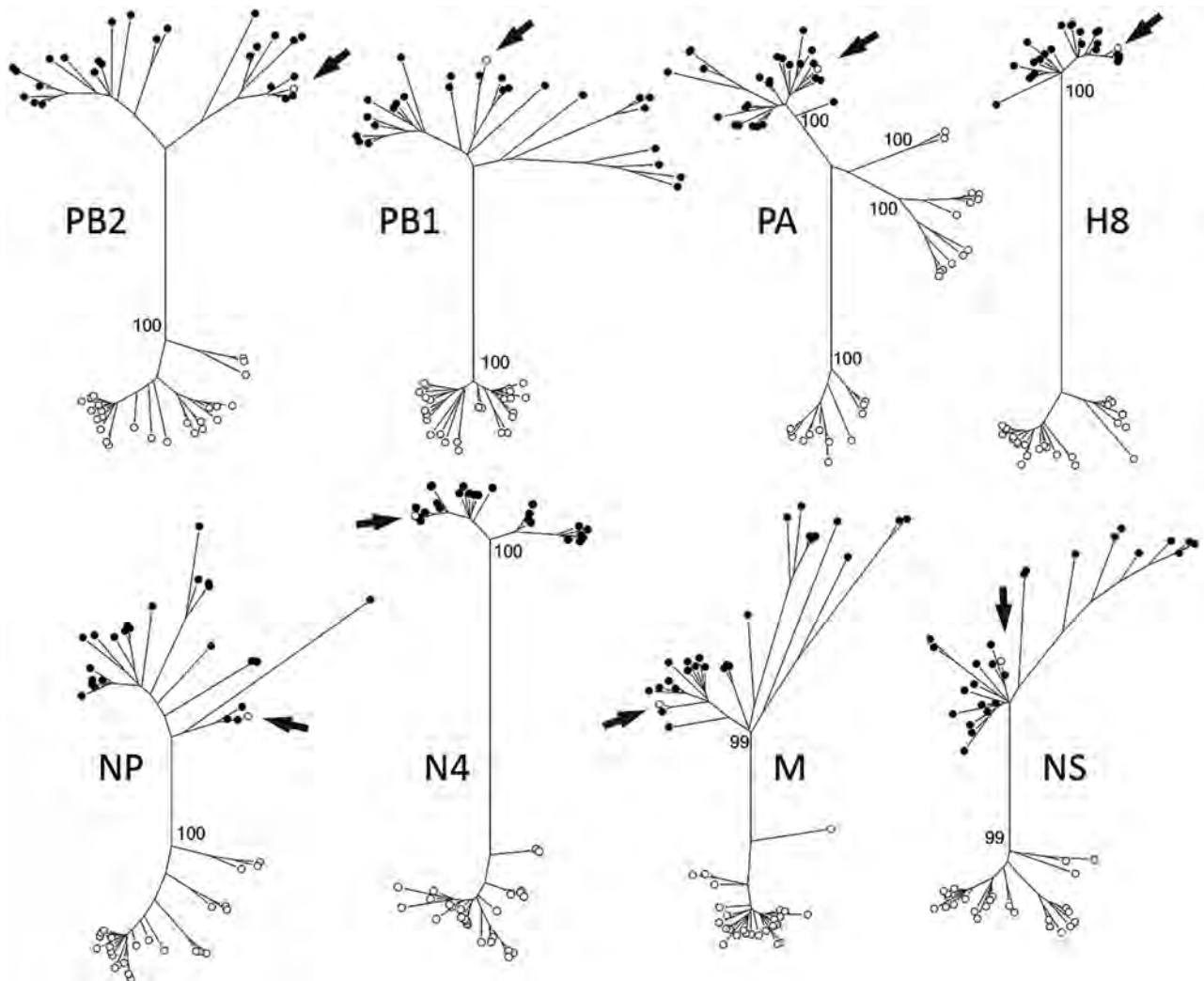
Figure. Maximum-likelihood phylogenetic trees showing inferred relationships among nucleotide sequences for the complete coding regions of gene segments for influenza A virus strain A/northern pintail/Alaska/UGAI16–3997/2016(H8N4) (white circle indicated with an arrow) and reference sequences from viruses isolated from birds in Eurasia (black circles) and North America (white circles). Bootstrap support values for continentally affiliated clades are shown. Phylogenetic trees with complete strain names as tip labels are provided in the online Technical Appendix Figure (https://wwwnc.cdc.gov/EID/article/24/10/18-0447-Techap1.pdf). H, hemagglutinin; M, matrix; N, neuraminidase; NP, nucleoprotein; NS, nonstructural; PA, polymerase acidic; PB, polymerase basic.

represent a previously unidentified or unreported genome constellation (online Technical Appendix Table).

Phylogenetic analyses strongly supported structuring of tree topologies into major clades by continental affiliation of reference sequences (bootstrap values ≥99; online Technical Appendix Figure). Sequence information for all 8 gene segments of A/northern pintail/Alaska/UGAI16-3997/2016(H8N4) clustered within clades composed of reference sequences for influenza A viruses originating from samples collected in Eurasia (Figure; online Technical Appendix Figure). Therefore, phylogenetic analyses provided support for Eurasian ancestry of this genomic constellation. We inferred our results to provide evidence for the introduction of this foreign-origin H8N4 virus into North America by migratory birds given previous support for intercontinental viral dispersal derived through genetic characterization of avian influenza A viruses originating from western Alaska (1–3,5), the intercontinental migratory tendencies of northern pintails (6,7) and other species inhabiting Izembek NWR at the time of sampling (8), the paucity of domestic poultry in this region, and the proximity of Izembek NWR to East Asia.

During 2010–2016, research and surveillance for influenza A viruses in wild birds inhabiting North America have provided evidence for the intercontinental dispersal of the following 4 viral genome constellations between Eurasia and North America: H16N3 (9), H9N2 (3), highly pathogenic clade 2.3.4.4 H5N8 (10), and H8N4 (this study). Four reports of independent purported intercontinental dispersal events for influenza A viruses via migratory birds during 7 years of sampling do not disprove the paradigm of restricted viral dispersal between Eurasia and North America. However, repeated detections of these viruses crossing the Bering Strait (3,10; this study) suggest that viral dispersal between East Asia and North America might not be exceedingly rare. Thus, a lack of selective advantage for comparatively rare foreign-origin influenza A viruses, purifying selection for endemic viruses, or both might be important mechanisms regulating the establishment of these viruses within the wild bird reservoir. Therefore, additional research directed toward understanding selection pressures regulating the establishment of these viruses might provide useful inference for informing surveillance and response activities for economically costly or potentially pandemic foreign-origin viruses in wild birds inhabiting North America.

Acknowledgments

About the Author

Dr. Ramey is a research scientist at the US Geological Survey Alaska Science Center, Anchorage, Alaska. His primary research interests include the maintenance and dispersal of infectious agents by wildlife.

References

1. Ramey AM, Pearce JM, Flint PL, Ip HS, Derksen DV, Franson JC, et al. Intercontinental reassortment and genomic variation of low pathogenic avian influenza viruses isolated from northern pintails (Anas acuta) in Alaska: examining the evidence through space and time. Virology. 2010;401:179–89. http://dx.doi.org/10.1016/j.virol.2010.02.006
2. Reeves AB, Pearce JM, Ramey AM, Ely CR, Schmutz JA, Flint PL, et al. Genomic analysis of avian influenza viruses from waterfowl in western Alaska, USA. J Wildl Dis. 2013;49:600–10. http://dx.doi.org/10.7589/2012-04-108
3. Ramey AM, Reeves AB, Sonsthagen SA, TeSlaa JL, Nashold S, Donnelly T, et al. Dispersal of H9N2 influenza A viruses between East Asia and North America by wild birds. Virology. 2015;482:79–83. http://dx.doi.org/10.1016/j.virol.2015.03.028
4. Ramey AM, Reeves AB, TeSlaa JL, Nashold S, Donnelly T, Bahl J, et al. Evidence for common ancestry among viruses isolated from wild birds in Beringia and highly pathogenic intercontinental reassortant H5N1 and H5N2 influenza A viruses. Infect Genet Evol. 2016;40:176–85. http://dx.doi.org/10.1016/j.meegid.2016.02.035
5. Reeves AB, Hall JS, Poulson RL, Donnelly T, Stallknecht DE, Ramey AM. Influenza A virus recovery, diversity, and intercontinental exchange: a multi-year assessment of wild bird sampling at Izembek National Wildlife Refuge, Alaska. PLoS One. 2018;13:e0195327. http://dx.doi.org/10.1371/journal.pone.0195327
6. Miller MR, Takekawa JY, Fleskes JP, Orthmeyer DL, Casazza ML, Perry WM. Spring migration of northern pintails from California's Central Valley wintering area tracked with satellite telemetry: routes, timing, and destinations. Canadian Journal of Zoology. 2005;83:1314–32. http://dx.doi.org/10.1139/z05-125
7. Hupp JW, Yamaguchi N, Flint PL, Pearce JM, Tokita K, Shimada T, et al. Variation in spring migration routes and breeding distribution of northern pintails Anas acuta that winter in Japan. J Avian Biol. 2011;42:289–300. http://dx.doi.org/10.1111/j.1600-048X.2011.05320.x
8. Hupp JW, Schmutz JA, Ely CR, Syroechkovskiy EE Jr, Kondratyev AV, Eldridge WD, et al. Moult migration of emperor geese Chen canagica between Alaska and Russia. J Avian Biol. 2007;38:462–70. http://dx.doi.org/10.1111/j.0908-8857.2007.03969.x
9. Huang Y, Wille M, Benkaroun J, Munro H, Bond AL, Fifield DA, et al. Perpetuation and reassortment of gull influenza A viruses in Atlantic North America. Virology. 2014;456-457:353–63. http://dx.doi.org/10.1016/j.virol.2014.04.009
10. Lee DH, Torchetti MK, Winker K, Ip HS, Song CS, Swayne DE. Intercontinental spread of Asian-origin H5N8 to North America through Beringia by migratory birds. J Virol. 2015;89:6521–4. http://dx.doi.org/10.1128/JVI.00728-15

New Reassortant Clade 2.3.4.4b Avian Influenza A(H5N6) Virus in Wild Birds, South Korea, 2017–18

Jung-Hoon Kwon,[1] Sol Jeong,[1] Dong-Hun Lee, David E. Swayne, Yu-jin Kim, Sun-hak Lee, Jin-Yong Noh, Tseren-Ochir Erdene-Ochir, Jei-Hyun Jeong, Chang-Seon Song

Author affiliations: Konkuk University, Seoul, South Korea (J.-H. Kwon, S. Jeong, Y.-J. Kim, S.-H. Lee, J.-Y. Noh, T.-O. Erdene-Ochir, J.-H. Jeong, C.-S. Song); US Department of Agriculture, Athens, Georgia, USA (D.-H. Lee, D.E. Swayne)

We isolated new reassortant avian influenza A(H5N6) viruses from feces of wild waterfowl in South Korea during 2017–18. Phylogenetic analysis suggested that reassortment occurred between clade 2.3.4.4b H5N8 and Eurasian low pathogenicity avian influenza viruses circulating in wild birds. Dissemination to South Korea during the 2017 fall migratory season followed.

Clade 2.3.4.4 H5 highly pathogenic avian influenza viruses (HPAIVs) have evolved by reassortment with different neuraminidase (NA) and internal genes of prevailing low pathogenicity avian influenza viruses (LPAIVs) and other HPAIVs to generate new genotypes and further evolved into genetic subgroups A–D since 2014 (1). Among these, subgroups A and B viruses were disseminated over vast geographic regions by migratory wild birds (2,3). Subgroup B influenza A(H5N8) viruses were detected in Qinghai Lake, China, and Uvs-Nuur Lake, Russia, during May–June 2016 (Qinghai/Uvs-like), followed by the identification of reassortant viruses in multiple Eurasian countries (4–6). Recently, subgroup B H5N6 viruses were isolated from birds in Greece during February 2017 and England, Germany, the Netherlands, Japan, and Taiwan during winter 2017–18 (7,8).

During December 2017–January 2018 in South Korea, we isolated 6 H5N6 HPAIVs from 231 fecal samples of wild birds collected from the banks of the Cheongmi-cheon River (37°06′56.9″N, 127°25′18.3″E) and 34 from 222 fecal samples collected from the banks of the Gokgyo-cheon River (36°45′12.3′N, 127°07′12.7′E) (online Technical Appendix 1, https://wwwnc.cdc.gov/EID/article/24/10/18-0461-Techapp1.pdf). These wild bird habitats are wintering sites of migratory waterfowl, including mallard (*Anas platyrhynchos*), spot-billed duck (*Anas poecilorhyncha*), Mandarin duck (*Aix galericulata*), and common teal (*Anas crecca*). The Gokgyo-cheon River is a major habitat site for Mandarin ducks, and numerous HPAIVs were detected in fecal samples from Mandarin ducks during 2011, 2015, and 2016 (9). We identified avian influenza virus–positive fecal samples from 38 Mandarin ducks and 2 mallards, based on DNA barcoding technique (10). We performed full-length genome sequencing and comparative phylogenetic analysis on 19 of the 40 isolates (online Technical Appendix 1; online Technical Appendix 2, https://wwwnc.cdc.gov/EID/article/24/10/18-0461-Techapp2.xlsx).

All H5N6 isolates shared high nucleotide sequence identities in all 8 gene segments (99.58%–100%) and were identified as HPAIVs based on the presence of multiple basic amino acids at the HA proteolytic cleavage site (PLREKRRKR/G). Searches of the GISAID (https://www.gisaid.org) and BLAST (https://blast.ncbi.nlm.nih.gov/Blast.cgi) databases indicated that all 8 genomes had the highest nucleotide identity with A/Great_Black-backed_Gull/Netherlands/1/2017 (Netherlands/1) clade 2.3.4.4 subgroup B H5N6 strain from December 2017 (99.17%–99.79%), rather than subgroup B H5N6 viruses from Japan and Taiwan collected during December 2017 (97.18%–99.27%).

In phylogenetic analysis, we identified 2 genotypes of subgroup B H5N6 viruses (online Technical Appendix 1 Figures 1, 2): genotypes B.N6.1 and B.N6.2. The genotype B.N6.1 viruses were identified from South Korea, Japan, Taiwan, Greece, and the Netherlands (Netherlands/1 strain), and the genotype B.N6.2 viruses were detected from England, Germany, and the Netherlands. For genotype B.N6.1, all genes except NA clustered with H5N8 HPAIV of previously reported genotypes, H5N8-NL cluster I in the Netherlands (6), Ger-11-16 in Germany (5), and Duck/Poland/82a/16-like in Italy (4). The NA gene clustered with LPAIVs circulating in wild birds in Eurasia and separated into 2 clusters, suggesting the potential for >2 independent reassortment events between H5N8 virus and unidentified wild bird origin N6 segments. Consistent clustering of South Korea isolates with the Netherlands/1 strain in maximum-likelihood (ML) phylogenies for each gene supported by high ML bootstrap values (86–100) suggests their close relationship. The genotype B.N6.2 viruses

Table. Time to most recent common ancestor for each gene segment of genotype B.N6.1 influenza A(H5N6) viruses isolated in South Korea, December 2017–January 2018*

Gene	South Korea isolates, node 1		South Korea and Europe isolates, node 2		South Korea, Europe, Japan, Taiwan, and Greece isolates, node 3	
	Mean	95% HPD	Mean	95% HPD	Mean	95% HPD
PB2	2017 Sep	2017 Jul–Oct	2017 May	2016 Dec–2017 Sep	2016 Mar	2015 Oct–2016 Jun
PB1	2017 Sep	2017 Jul–Oct	2017 May	2017 Feb–Aug	2016 Jul	2016 May–Aug
PA	2017 Sep	2017 Aug–Oct	2017 Jul	2017 Apr–Sep	2016 Oct	2016 Jul–Dec
HA	2017 Sep	2017 Jul–Oct	2017 May	2017 Feb–Jul	2016 Mar	2015 Dec–2016 May
NP	2017 Jul	2017 Apr–Sep	2017 Mar	2016 Nov–2017 Jun	2016 Jan	2015 Jul–2016 May
NA	2017 Jul	2017 Mar–Sep	2017 Feb	2016 Jul–2017 Jul	2015 Sep	2014 Aug–2016 Aug
M	2017 Aug	2017 May–Oct	2017 May	2017 Jan–Aug	2016 Mar	2016 Jan–May
NS	2017 Jul	2017 Apr–Oct	2017 Mar	2016 Nov–2017 Jun	2016 Feb	2015 Oct–2016 Jun

*Nodes of the temporally structured maximum clade credibility phylogenetic tree (online Technical Appendix Figure 4, https://wwwnc.cdc.gov/EID/article/24/10/18-0461-Techapp1.pdf). HA, hemagglutinin; HPD, highest posterior density; M, matrix; NA, neuraminidase; NP, nucleoprotein; NS, nonstructural; PA, polymerase acidic; PB, polymerase basic.

had different polymerase basic 2 (PB2) and polymerase acidic (PA) genes from genotype B.N6.1. The polymerase basic 2 gene probably originated from other LPAIVs, and a polymerase acidic gene originated from H5N8-NL cluster II genotype (6,7). The phylogenetic network and ML analysis suggest that H5N6 viruses have evolved from subgroup B H5N8 viruses into 3 independent pathways, detected in Greece, Europe/South Korea, and Japan/Taiwan (online Technical Appendix 1, Figures 2,3).

The time of most recent common ancestry (tMRCA) for each gene of genotype B.N6.1 H5N6 viruses isolated during winter 2017–18 in Eurasia, except for the NA gene, ranged from January 2016 to October 2016, suggesting that genotype B.N6.1 viruses diverged during the previous year. The tMRCA of the NA gene was September 2015 (95% highest posterior density August 2014–August 2016). The tMRCA of the NA gene has wide 95% highest posterior density range because only a few recent N6 genes of LPAIVs were available in databases for analysis. The tMRCA for each gene of H5N6 HPAIVs identified in South Korea ranged from July through September 2017, suggesting that ancestors of these viruses emerged among wild birds during or after summer 2017, possibly at the breeding and molting sites in the Palearctic region (Table; online Technical Appendix Figure 4). Detection of H5N6 HPAIV from fecal samples of wild birds in South Korea during the 2017–18 wintering season and our phylogenetic analysis suggest that the viruses had moved through wild birds during the fall migration season.

On the basis of our data and migratory pattern of birds, we estimate that H5N6 viruses possibly descended from H5N8 viruses circulating during 2016–17, reaching breeding regions of wild birds during early 2017, followed by dissemination into Europe and East Asia during the fall migration. Enhanced surveillance in wild birds is needed for early detection of new introductions of HPAIV and to trace the transmission route of HPAIV.

About the Author

Mr. Kwon is a PhD candidate at Konkuk University, Seoul, South Korea. His primary research interest is the epidemiology of HPAIVs in wild birds. Ms. Jeong is a PhD candidate at Konkuk University, Seoul. Her primary research interest is the epidemiology of viruses in wild birds.

References

1. Sonnberg S, Webby RJ, Webster RG. Natural history of highly pathogenic avian influenza H5N1. Virus Res. 2013;178:63–77. http://dx.doi.org/10.1016/j.virusres.2013.05.009
2. Lee DH, Bertran K, Kwon JH, Swayne DE. Evolution, global spread, and pathogenicity of highly pathogenic avian influenza H5Nx clade 2.3.4.4. J Vet Sci. 2017;18(S1):269–80. http://dx.doi.org/10.4142/jvs.2017.18.S1.269
3. Global Consortium for H5N8 and Related Influenza Viruses. Role for migratory wild birds in the global spread of avian influenza H5N8. Science. 2016;354:213–7. http://dx.doi.org/10.1126/science.aaf8852
4. Fusaro A, Monne I, Mulatti P, Zecchin B, Bonfanti L, Ormelli S, et al. Genetic diversity of highly pathogenic avian influenza A(H5N8/H5N5) viruses in Italy, 2016–17. Emerg Infect Dis. 2017;23:1543–7. http://dx.doi.org/10.3201/eid2309.170539
5. Pohlmann A, Starick E, Grund C, Höper D, Strebelow G, Globig A, et al. Swarm incursions of reassortants of highly pathogenic avian influenza virus strains H5N8 and H5N5, clade 2.3.4.4b, Germany, winter 2016/17. Sci Rep. 2018;8:15. http://dx.doi.org/10.1038/s41598-017-16936-8
6. Beerens N, Heutink R, Bergervoet SA, Harders F, Bossers A, Koch G. Multiple reassorted viruses as cause of highly pathogenic avian influenza A(H5N8) virus epidemic, the Netherlands, 2016. Emerg Infect Dis. 2017;23:1974–81. http://dx.doi.org/10.3201/eid2312.171062
7. Beerens N, Koch G, Heutink R, Harders F, Vries DPE, Ho C, et al. Novel highly pathogenic avian influenza A(H5N6) virus in the Netherlands, December 2017. Emerg Infect Dis. 2018; 24:770–3. http://dx.doi.org/10.3201/eid2404.172124
8. Liu YP, Lee DH, Chen LH, Lin YJ, Li WC, Hu SC, et al. Detection of reassortant H5N6 clade 2.3.4.4 highly pathogenic avian influenza virus in a black-faced spoonbill (*Platalea minor*) found dead, Taiwan, 2017. Infect Genet Evol. 2018;62:275–8. http://dx.doi.org/10.1016/j.meegid.2018.04.026
9. Kwon JH, Lee DH, Swayne DE, Noh JY, Yuk SS, Erdene-Ochir TO, et al. Reassortant clade 2.3.4.4 avian influenza A(H5N6) virus in a wild Mandarin duck, South Korea, 2016. Emerg Infect Dis. 2017;23:822–6. http://dx.doi.org/10.3201/eid2305.161905

10. Lee DH, Lee HJ, Lee YJ, Kang HM, Jeong OM, Kim MC, et al. DNA barcoding techniques for avian influenza virus surveillance in migratory bird habitats. J Wildl Dis. 2010;46:649–54. http://dx.doi.org/10.7589/0090-3558-46.2.649

Address for correspondence: Chang-Seon Song, Avian Disease Laboratory, College of Veterinary Medicine, Konkuk University, 1 Hwayang-dong, Gwangjin-gu, Seoul, 143-701, South Korea; email: songcs@konkuk.ac.kr

Clinical Isolation and Identification of *Haematospirillum jordaniae*

Gregory Hovan, Andrew Hollinger

Author affiliations: Delaware Public Health Laboratory, Smyrna, Delaware, USA (G. Hovan); Regional Hospital, Delaware[1] (A. Hollinger)

A clinical case study involving a man (35–49 years of age) with wounds to his lower right extremity. An isolate was sent to the Delaware Public Health Laboratory for confirmatory testing by genetic analysis of the 16S gene. Testing identified the isolate as a novel genus and species, *Haematospirillum jordaniae*.

The Centers for Disease Control and Prevention (CDC) recently recognized a human pathogen, *Haematospirillum jordaniae*, as a new bacterial genus and species (*1*). *H. jordaniae* is a gram-negative, spiral-shaped aerobe in the family *Rhodospirillaceae* (*1*). Before the pathogen's identification, this organism was isolated 14 times from 10 different states. These organisms were received by CDC's Special Bacteriology Reference Laboratory, Division of High-Consequence Pathogens and Pathology, National Center for Emerging and Zoonotic Infectious Diseases, over the course of 10 years (February 2003–October 2012) before the initial publication. Here we report the clinical identification of *H. jordaniae*, a potential emerging infectious pathogen, by the Delaware Public Health Laboratory (DPHL) and describe possible routes of infection.

[1]Location redacted for patient confidentiality.

A man (35–49 years of age) sought care at a hospital emergency department in September 2016 with worsening pain, redness, and swelling of the right lower extremity, which had an open wound on the right shin. The patient stated that he had finished a project cutting stones 3 weeks earlier where the water and stone chips were hitting his right leg. The patient ignored swelling, erythema, and fever he experienced around the same period when the stonecutting occurred and decided not to seek medical intervention until he was no longer able to ignore the symptoms.

The patient was found to have cellulitis of the right leg and sepsis, and he was admitted to the hospital for treatment. On the same day, he was started on intravenous clindamycin, and blood cultures were collected. The infectious disease physician discontinued clindamycin and placed the patient on vancomycin, ciprofloxacin, and aztreonam because of concern for potential infection with *Pseudomonas*, *Aeromonas*, or methicillin-resistant *Staphylococcus aureus*. Growth was observed in both sets of aerobic bottles, the first after 2 days, 15 hours, and the second after 4 days, 18 hours. Blood cultures grew gram-negative bacilli, leading the infectious disease physician to remove vancomycin but continue with ciprofloxacin and aztreonam. The patient improved before identification of the pathogen and was discharged on oral ciprofloxacin.

Gram stain of the organism revealed small, curved, gram-negative bacilli, resembling *Campylobacter*. Subcultures from the bottles did not grow aerobically until 48 hours after incubation on sheep's blood agar and chocolate agar. The organisms did not grow on MacConkey agar or when incubated anaerobically on blood agar. Although it was suspected that the organism might be a *Campylobacter* species, it did not grow in a microaerophilic environment. Biochemical testing revealed the organism as oxidase-positive, indole-negative, catalase-positive, and urease-negative (using urea agar). The isolate was sent to the DPHL for identification.

DPHL received a grown isolate from the submitting hospital 8 days after the patient's admission. The organism was cultured in the same manner as described previously; phenotypic tests were consistent with the findings of the submitting hospital. Initial identification was performed at DPHL, but the pathogen could not be determined because the organism was not part of the instrument's stored database.

The isolate's DNA was extracted and amplified by using general methods described in numerous publications. The sample generated an 845-bp portion of the 16S region. The assembled sequence was uploaded to open-source rRNA databases for comparison, including GenBank BLAST (https://blast.ncbi.nlm.nih.gov/Blast.cgi), the Ribosomal Database Project (https://rdp.cme.msu.edu/), and MicrobeNet (https://microbenet.cdc.gov). Samples most closely matched to *Novispirillum itersonii* strain

LMG_4337^T (92.3% identity). On the basis of Clinical Laboratory Standards Institute guidelines (2), this similarity indicated a possible novel species.

The DPHL Microbiology Department's laboratory manager sent the organism to CDC's Special Bacteriology Reference Laboratory. Results identified the organism as *H. jordaniae*. Upon review of MicrobeNet at a later date, the organism was found to match *H. jordaniae* H5569_con^T by 98.9%.

H. jordaniae is a common environmental microbe, but it was implicated in this clinical case in a man in Delaware. The patient had symptoms characteristic of other pathogenic bacterial illnesses. Concern exists that slow-growing, gram-negative rods identified in blood culture could be potential bioterrorism agents. Humrighouse et al. (1) described how *Francisella tularensis* infection was suspected in 2 clinical cases that were actually *H. jordaniae* infections.

Humrighouse et al. (1) proposed the name *H. jordaniae* on the basis of an isolate received in 2010. Previously, 14 organisms identified at CDC were isolated from blood taken from men 39–78 years of age with symptoms including swelling of the lower extremities (2 patients), septicemia (3 patients), and bacteremia (1 patient). The symptoms of the patient we report mirrored those symptoms.

This discovery is important because it demonstrates that organisms conceived to be environmental in nature and suspected to have limited clinical implications are emerging as human pathogens. The ability to identify bacteria by sequencing (in this case, sequencing of the 16S rRNA gene) was necessary to identify *H. jordaniae* because clinical information on this pathogen is still limited.

About the Authors

Mr. Hovan manages the Clinical Microbiology Department at the Delaware Division of Public Health Laboratory. His primary research interests are genomics and bioinformatics as they relate to public health.

Mr. Hollinger is lead technologist of a microbiology laboratory in a Delaware community hospital. His primary research interests are antibiotic resistance, molecular diagnostics in infectious disease, blood and tissue parasitic infections, and mycobacterial infections.

References

1. Humrighouse BW, Emery BD, Kelly AJ, Metcalfe MG, Mbizo J, McQuiston JR. *Haematospirillum jordaniae* gen. nov., sp. nov., isolated from human blood samples. Antonie van Leeuwenhoek. 2016;109:493–500. http://dx.doi.org/10.1007/s10482-016-0654-0
2. Clinical and Laboratory Standards Institute. Interpretive criteria for identification of bacteria and fungi by DNA target sequencing. Approved guideline (MM18-A). Wayne (PA): The Institute; 2008.

Address for correspondence: Gregory Hovan, Delaware Division of Public Health Laboratory, 30 Sunnyside Rd, Dover, DE 19903, USA; email: gregory.hovan@state.de.us

Molecular Typing and Antifungal Susceptibility of *Candida viswanathii*, India

Shamanth A. Shankarnarayan, Shivaprakash M. Rudramurthy, Arunaloke Chakrabarti, Dipika Shaw, Saikat Paul, Nandini Sethuraman, Harsimran Kaur, Anup K. Ghosh

Author affiliations: Postgraduate Institute of Medical Education and Research, Chandigarh, India (S.A. Shankarnarayan, S.M. Rudramurthy, A. Chakrabarti, D. Shaw, S. Paul, H. Kaur, A.K. Ghosh); Apollo Hospitals Enterprise, Chennai, India (N. Sethuraman)

We report invasive candidiasis caused by *Candida viswanathii* over 2 time periods during 2013–2015 in a tertiary care hospital in Chandigarh, India. Molecular typing revealed multiple clusters of the isolates. We detected high MICs for fluconazole in the second time period.

Invasive candidiasis is a life-threatening infection caused by various *Candida* species. Although *C. albicans* has been the predominant species causing invasive candidiasis, non-albicans *Candida* (NAC) species have emerged globally (1). *C. viswanathii*, a pathogen first isolated from the cerebrospinal fluid of a patient in 1959 (2), is rarely encountered, and only 17 cases have been reported worldwide (3). This agent has been isolated sporadically from animal and environmental sources (4–6).

We report on 23 cases of invasive candidiasis caused by *C. viswanathii* at a tertiary care center in Chandigarh, India, involving 7 case-patients during December 2013–April 2014

Table. In vitro antifungal susceptibility data of *Candida viswanathii* isolates from a tertiary care hospital in Chandigarh, India

Isolate	Antifungal agent	MIC, µg/mL			
		Range	MIC $_{50}$	MIC $_{90}$	Geometric mean
C. viswanathii 2013–2014, n = 7	Amphotericin B	0.03–0.25	0.25	0.25	0.16
	Itraconazole	0.03–0.5	0.125	0.25	0.09
	Fluconazole	0.125–1	1	1	0.41
	Voriconazole	0.03–0.5	0.5	0.5	0.14
	Micafungin	0.125	0.125	0.125	0.125
	Caspofungin	0.5	0.5	0.5	0.5
	Anidulafungin	0.5–1	0.5	1	0.67
	Posaconazole	0.0312–0.0625	0.0312	0.0625	0.03
C. viswanathii 2015, n = 16	Amphotericin B	0.06–0.25	0.125	0.25	0.14
	Itraconazole	0.03–1	0.25	0.25	0.12
	Fluconazole	0.5–64	64	64	29.34
	Voriconazole	0.03–8	1	2	0.76
	Micafungin	0.125	0.125	0.125	0.12
	Caspofungin	0.125–1	0.5	0.5	0.40
	Anidulafungin	0.125–1	0.5	1	0.52
	Posaconazole	0.0321–0.5	0.25	0.25	0.17

and 16 case-patients during December 2014–April 2015. In the first time period, all isolates were from blood, whereas in the second time period, the agent was isolated from pus (n = 5), blood (n = 5), cerebrospinal fluid (n = 3), and lung nodule, lung aspirate, and iliac fluid (n = 1 each).

Of the 23 patients, 16 were men and 7 were women. Six (26%) patients had neutropenia, and 18 (90%) had tuberculosis, pancreatitis, or chronic kidney disease. Eight (34.7%) patients acquired the infection after surgery. Twelve patients used indwelling devices: 3 (15%) had a central venous catheter, 4 (20%) an endotracheal tube, 3 (15%) a drainage catheter, and 2 (10%) a urinary catheter.

We screened the hospital environment and the hands of healthcare workers for a possible source of *C. viswanathii* infection during the second time period. We could not isolate *C. viswanathii* from any of those samples from a total of 46 workers and 57 different environmental sites.

Conventional methods failed to differentiate *C. viswanathii* and *C. tropicalis*. *C. viswanathii* assimilated sucrose and cellobiose but failed to assimilate trehalose and raffinose. *C. tropicalis* has a variable assimilation pattern for these sugars.

To identify the isolates, we performed matrix-assisted laser desorption/ionization time-of-flight mass spectroscopy using MALDI-TOF MS, version 3 (Bruker Daltonik GmbH, Bremen, Germany) and sequenced the D1/D2 region of a large subunit of ribosomal DNA (*7,8*). Because we could not identify *C. viswanathii* using the MALDI-TOF MS version 3 database, we updated the database in-house by adding sequence-proved isolates of *C. viswanathii*. We identified the isolates with a log score of >1.8 by using the modified database. The rDNA sequence of the isolates showed 100% similarity with the type strain of *C. viswanathii* ATCC 22981 (GenBank accession no. NG_054835.1) except for 1 isolate (99% similarity with type strain, accession no. MF682371). The molecular phylogenetic analysis revealed that 1 isolate (B-30815) had

1 nucleotide substitution (T to C), which was 1 of the 5 substitutions we observed in *C. pseudoviswanathii* while comparing it with *C. viswanathii* (*9*).

Amplified fragment-length polymorphism revealed a similarity coefficient of ≥90% of the isolates (online Technical Appendix Figure, https://wwwnc.cdc.gov/EID/article/24/10/18-0801-Techapp1.pdf) (*7*). The isolates from the first time period formed 2 clusters (clusters A and B); 1 isolate from the second period was also in cluster B. Isolates of the second time period had 3 major clusters (clusters C, D, and E) and had higher MICs for fluconazole.

We performed antifungal susceptibility testing for amphotericin B, fluconazole, itraconazole, voriconazole, posaconazole, caspofungin, anidulafungin, and micafungin by the microbroth dilution method recommended by the Clinical and Laboratory Standards Institute (*10*). After incubating the plates for 24 h at 37°C, we took a visual reading to determine the MICs. The isolates of the second time period had higher MICs (MIC$_{50}$ 64 µg/mL, MIC$_{90}$ 64 µg/mL) for fluconazole compared with the isolates of the first period (MIC$_{50}$ 1 µg/mL, MIC$_{90}$ 1 µg/mL). We also recorded higher MICs (MIC$_{50}$ 1 µg/mL, MIC$_{90}$ 2 µg/mL) for voriconazole for the isolates of the second period (Table).

In conclusion, our study showed multiple clusters of *C. viswanathii* causing invasive infections in patients with neutropenia and chronic diseases at a single healthcare center in India. We could not trace the source of the agent. Conventional identification methods could not differentiate the isolates from those of *C. tropicalis*. The high MICs for fluconazole among the isolates from the second time period also raise concerns about possible antifungal resistance.

About the Author

Mr. Shankarnarayan is a PhD student in the Department of Medical Microbiology, PGIMER, Chandigarh, India. His doctoral focus is on evaluating the dynamics of invasive *Candida* infections among hospitalized patients.

References

1. Chakrabarti A, Sood P, Rudramurthy SM, Chen S, Kaur H, Capoor M, et al. Incidence, characteristics and outcome of ICU-acquired candidemia in India. Intensive Care Med. 2015;41:285–95. http://dx.doi.org/10.1007/s00134-014-3603-2

2. Viswanathan R, Randhawa HS. *Candida viswanathii* sp. novo isolated from a case of meningitis. Sci Cult. 1959;25:86–7.

3. Randhawa HS, Mishra SK, Damodaran VN, Prakash A, Chowdhary A, Khan ZU. Pathogenicity of *Candida viswanathii* for normal and cortisone-treated mice. J Mycol Med. 2015; 25:287–92.

4. Soni P, Prasad GS, Banerjee UC. Optimization of physicochemical parameters for the enhancement of carbonyl reductase production by *Candida viswanathii*. Bioprocess Biosyst Eng. 2006;29:149–56. http://dx.doi.org/10.1007/s00449-006-0066-z

5. Soni P, Singh M, Kamble AL, Banerjee UC. Response surface optimization of the critical medium components for carbonyl reductase production by *Candida viswanathii* MTCC 5158. Bioresour Technol. 2007;98:829–33. http://dx.doi.org/ 10.1016/j.biortech.2006.03.008

6. Junior JS, Mariano AP, De Angelis DDF. Biodegradation of biodiesel/diesel blends by *Candida viswanathii*. Afr J Biotechnol. 2009;8:2774–8.

7. Chakrabarti A, Rudramurthy SM, Kale P, Hariprasath P, Dhaliwal M, Singhi S, et al. Epidemiological study of a large cluster of fungaemia cases due to *Kodamaea ohmeri* in an Indian tertiary care centre. Clin Microbiol Infect. 2014;20:O83–9.

8. Ghosh AK, Paul S, Sood P, Rudramurthy SM, Rajbanshi A, Jillwin TJ, et al. Matrix-assisted laser desorption ionization time-of-flight mass spectrometry for the rapid identification of yeasts causing bloodstream infections. Clin Microbiol Infect. 2015;21:372–8.

9. Ren YC, Xu LL, Zhang L, Hui FL. *Candida baotianmanensis* sp. nov. and *Candida pseudoviswanathii* sp. nov., two ascosporic yeast species isolated from the gut of beetles. Int J Syst Evol Microbiol. 2015;65:3580–5. PubMed http://dx.doi.org/10.1099/ijsem.0.000460

10. Clinical Laboratory Standards Institute. Reference method for broth dilution antifungal susceptibility testing of yeasts, 3rd edition, approved standard (M27–A3). Wayne (PA): The Institute; 2008.

Address for correspondence: Anup K. Ghosh, Postgraduate Institute of Medical Education and Research, Medical Microbiology, 2nd Fl, Sector-12, Chandigarh, India; email: ak_ghosh3@rediffmail.com, anupkg3@gmail.com

Community-Acquired *Staphylococcus argenteus* Sequence Type 2250 Bone and Joint Infection, France, 2017

Josselin Rigaill, Florence Grattard, Sylvain Grange, Fabien Forest, Elie Haddad, Anne Carricajo, Anne Tristan, Frederic Laurent, Elisabeth Botelho-Nevers, Paul O. Verhoeven

Author affiliations: University Hospital of Saint-Etienne, Saint-Etienne, France (J. Rigaill, F. Grattard, S. Grange, F. Forest, E. Haddad, A. Carricajo, E. Botelho-Nevers, P.O. Verhoeven); Jean Monnet University, Saint-Etienne (J. Rigaill, F. Grattard, A. Carricajo, E. Botelho-Nevers, P.O. Verhoeven); International Centre for Infectiology Research, Lyon, France (A. Tristan, F. Laurent); French National Reference Centre for Staphylococci, Lyon (A.Tristan, F. Laurent)

We report a rare case of *Staphylococcus argenteus* bone and joint infection in a 9-year-old boy in France. His finger arthritis was complicated by osteitis 5 weeks later, which resulted in a secondary intervention. This case indicates the virulence of *S. argenteus*, an emerging pathogen whose clinical effects are poorly described.

Staphylococcus argenteus (formerly *S. aureus* clonal complex 75) is an emerging species in the *S. aureus* complex (*1*). Several studies reported sporadic cases of *S. argenteus* infections mainly in Asia, Oceania, and the Pacific Islands (*2*) but rarely in Europe (*3*). We report the clinical characteristics of a community-acquired bone and joint infection with *S. argenteus* in a child living in France.

At the end of July 2017, a 9-year-old boy with no unusual medical history or previous local trauma was hospitalized because of acute signs of infection of the third finger on his right hand. He was first seen in a local hospital and given an initial diagnosis of cellulitis (arthritis). Two days later, he was admitted to the emergency pediatric ward of a tertiary care hospital where a surgical joint exploration was performed and confirmed the diagnosis of arthritis associated with an abscess of the extensor tendon sheath (Table).

Surgical microbiological samples cultured on blood agar plates (aerobic conditions at 37°C for 24 h) grew a strain that was identified by matrix-assisted laser desorption/ionization time-of-flight mass spectrometry (Microflex LT, Bruker, France) as having log scores ranging from 1.39 to

1.87 (corresponding to *S. aureus*, *S. simiae*, or *S. epidermidis*). These scores were lower than those required for reliable identification of species (2.3) or genus (2.1) levels. Antimicrobial drug susceptibility testing (Vitek2; bioMérieux, Marcy l'Etoile, France) identified resistance to penicillin G.

Because there was no initial reliable identification of this strain, we performed molecular tests. The strain was negative for *nuc*, *lukS*-PV, *mec*A, *mec*C, *tst*-1, and *spa* genes. The V3 region sequence of the gene coding for 16S rRNA showed 100% identity with that for *S. aureus*.

Table. Clinical characteristics and timeline for patient with community-acquired *Staphylococcus argenteus* sequence type 2250 bone and joint infection, France, 2017*

Characteristic	Jul 30	Aug 2	Aug 8	Sep 5	Nov 2
Hospital	Local	Tertiary care	Tertiary care	Tertiary care	Tertiary care
Clinical features	Pain in third finger of right hand	Fever (temperature 38.6°C); pain and functional impotence in flexion of finger	Poor tolerance of antimicrobial drugs	Fever (temperature 38.4°C); pain in finger	Stiffness in finger; no pain
Signs at physical examination	Inflammatory edema of finger; no inoculation lesion	Phlegmon of finger: inflammatory skin; edema on second phalanx	ND	Misalignment of second phalanx	No signs of infection
Laboratory findings					
Leukocytes, ×10⁹ cells/L†	20	7.2	ND	11.6	7.2
C-reactive protein, mg/L‡	58	17.7	ND	ND	0.3
Microbiological	Culture of infection site not performed (no pus); blood culture not performed	Surgical samples: neutrophils and gram-positive cocci (identified as *S. argenteus*); blood cultures sterile	ND	Surgical samples: few neutrophils and negative gram staining results; culture remained sterile after 10 d; negative 16S rDNA PCR result; blood cultures not performed	ND
Radiologic findings	Not performed	Radiograph of hand: no signs of osteitis	ND	MRI of hand: osteitis	ND
Histologic findings			ND	Chronic osteitis	ND
Diagnosis considered	Cellulitis of finger	Arthritis of second phalanx; abscess of extensor tendon sheath	ND		ND
Treatment					
Antimicrobial drugs	AMX (1,000 mg/d) and CLA (125 mg/d)	CFZ (2,200 mg/d) and GEN (400 mg/d) for 2 d; AMX (2,000 mg/d), CLA (250 mg/d), RIF (600 mg/d) for 6 wk	Stop AMX and CLA; FUS (1.5 g/d) and RIF (600 mg/d) for 5 wk	Sep 8: CLI (900 mg/d) and OFX (400 mg/d) for 6 wk	ND
Surgery		Surgical joint lavage and débridement for massive purulent abscess that reached the extensor tendon and joint capsule of second phalanx; no articular cartilage lesion	ND	Surgical lavage and realignment of phalanxes with implantation of external fixator on Sep 8	ND
Outcome	Discharged	Improvement at discharge on Aug 4; patient seen on Aug 6, 8, 10, and 12	Good outcome	Discharged on Sep 11; patient seen on Sep 13, 15, and 22, and Oct 6; external fixator removed on Oct 6	Good outcome and functional rehabilitation; patient seen on Dec 27 and had similar findings

*AMX, amoxicillin; CFZ, cefazolin; CLA, clavulanic acid; CLI, clindamycin; FUS, fusidic acid; GEN, gentamicin; MRI, magnetic resonance imaging; ND, not determined; OFX, ofloxacin; RIF, rifampin.
†Reference range 4.5–13.5 × 10⁹ cells/L.
‡Reference value <5 mg/L.

Microarray analysis (*S. aureus* Genotyping Kit 2.0; Alere Technologies GmbH, Jena, Germany) assigned this strain to the clonal complex 2250/2277 of one of the main clusters of *S. argenteus* (*2,4*). The patient was discharged and received an oral antimicrobial regimen for 6 weeks; healing was closely monitored (Table).

Five weeks later, the patient was hospitalized because of recurrent signs of infection (Table). Magnetic resonance imaging of the right hand showed osteitis (online Technical Appendix Figure, panel A, https://wwwnc.cdc.gov/EID/article/23/10/18-0727-Techapp1.pdf). A second surgical procedure was performed (Table). Cultures of surgical samples remained sterile after 10 days and a 16S rDNA PCR result was negative. Histologic analysis showed chronic osteitis (online Technical Appendix Figure, panel B). An oral drug regimen, including clindamycin and ofloxacin for 6 weeks, was prescribed. Long-term outcome was good (Table), despite persistence of stiffness in the finger.

This rare case of osteomyelitis caused by *S. argenteus* highlights the difficulties in correctly identifying this species. As with *S. schweitzeri, S. argenteus* is an emergent species that has been described as part of the *S. aureus* species complex (*5*). *S. argenteus* was first described in 2002 as a CC75/sequence type T1223 clone of *S. aureus* in Aboriginal communities in Australia (*6*). This species was named *S. argenteus* in 2011 because of its lack of staphyloxanthin production (*1*). Most studies reported prevalence rates for *S. argenteus* among strain collections of 0.16%–18.6% according to geographic distribution, with a clear predominance in Asia and the West Pacific region (*1,5–7*) and a rare description in Europe (*3*).

In our case, no epidemiologic link to Asia or the West Pacific region was observed. The clinical spectrum of infections with *S. argenteus* remains poorly described, but varies from asymptomatic nasal carriage (*8*) to community-acquired infections, including skin and soft tissue infections (*1,6*), bacteremia (*1,9*), and foodborne illness (*8*). Apart from 2 cases of bacteremia reported by Dupieux et al. (*9*), clinical data for *S. argenteus* infections have been poorly detailed (online Technical Appendix Figure). To the best of our knowledge, only 1 case of osteomyelitis has been reported (*7*).

Previous cases and the case we report indicate that *S. argenteus* could be responsible for invasive infections that are difficult to manage. *S. argenteus* was initially considered to be less virulent than *S. aureus* on the basis of a study in Australia, which reported that this species was associated mainly with skin and soft tissue infections and rarely with bacteremia (3/220 cases) (*1*). However, a comparative study of 311 cases of *S. argenteus* and *S. aureus* sepsis in Thailand showed a similar outcome after 28 days (*10*). Moreover, virulence factors,

such as Panton-Valentine leucocidin and enterotoxins, have been described in *S. argenteus* isolates (*4,8–10*). In contrast to reports from Aboriginal communities in Australia (*6*) and remote populations in the West Pacific region (online Technical Appendix Table), resistance to methicillin was not detected in strains from the case-patients in this study.

In contrast to *S. aureus*, the effect of carriage of *S. argenteus* has not been studied. For our case-patient, screening for *S. argenteus* nasal carriage was not performed. However, a recent study of foodborne illness outbreaks reported the ability of this bacterium to spread in the environment and colonize food handlers (*8*).

S. argenteus is an emerging species for which its clinical spectrum remains poorly described. Further studies are needed to better address the global prevalence and clinical role of this bacterium, including its potential effects in chronic human infections.

About the Author

Dr. Rigaill is a microbiology fellow at the University Hospital of Saint-Etienne, Saint-Etienne, France. His primary research interest is identifying the determinants of *S. aureus* carriage.

References

1. Tong SY, Sharma-Kuinkel BK, Thaden JT, Whitney AR, Yang S-J, Mishra NN, et al. Virulence of endemic nonpigmented northern Australian *Staphylococcus aureus* clone (clonal complex 75, *S. argenteus*) is not augmented by staphyloxanthin. J Infect Dis. 2013;208:520–7. http://dx.doi.org/10.1093/infdis/jit173
2. Moradigaravand D, Jamrozy D, Mostowy R, Anderson A, Nickerson EK, Thaipadungpanit J, et al. Evolution of the *Staphylococcus argenteus* ST2250 clone in northeastern Thailand is linked with the acquisition of livestock-associated staphylococcal genes. MBio. 2017;8:e00802–17. http://dx.doi.org/10.1128/mBio.00802-17
3. Argudín MA, Dodémont M, Vandendriessche S, Rottiers S, Tribes C, Roisin S, et al. Low occurrence of the new species *Staphylococcus argenteus* in a *Staphylococcus aureus* collection of human isolates from Belgium. Eur J Clin Microbiol Infect Dis. 2016;35:1017–22. http://dx.doi.org/10.1007/s10096-016-2632-x

4. Wakabayashi Y, Umeda K, Yonogi S, Nakamura H, Yamamoto K, Kumeda Y, et al. Staphylococcal food poisoning caused by *Staphylococcus argenteus* harboring staphylococcal enterotoxin genes. Int J Food Microbiol. 2018;265:23–9. http://dx.doi.org/10.1016/j.ijfoodmicro.2017.10.022

5. Tong SY, Schaumburg F, Ellington MJ, Corander J, Pichon B, Leendertz F, et al. Novel staphylococcal species that form part of a *Staphylococcus aureus*-related complex: the non-pigmented *Staphylococcus argenteus* sp. nov. and the non-human primate-associated *Staphylococcus schweitzeri* sp. nov. Int J Syst Evol Microbiol. 2015;65:15–22. http://dx.doi.org/10.1099/ijs.0.062752-0

6. McDonald M, Dougall A, Holt D, Huygens F, Oppedisano F, Giffard PM, et al. Use of a single-nucleotide polymorphism genotyping system to demonstrate the unique epidemiology of methicillin-resistant *Staphylococcus aureus* in remote aboriginal communities. J Clin Microbiol. 2006;44:3720–7. http://dx.doi.org/10.1128/JCM.00836-06

7. Thaipadungpanit J, Amornchai P, Nickerson EK, Wongsuvan G, Wuthiekanun V, Limmathurotsakul D, et al. Clinical and molecular epidemiology of *Staphylococcus argenteus* infections in Thailand. J Clin Microbiol. 2015;53:1005–8. http://dx.doi.org/10.1128/JCM.03049-14

8. Aung MS, San T, Aye MM, Mya S, Maw WW, Zan KN, et al. Prevalence and genetic characteristics of *Staphylococcus aureus* and *Staphylococcus argenteus* isolates harboring Panton-Valentine leukocidin, enterotoxins, and TSST-1 genes from food handlers in Myanmar. Toxins (Basel). 2017;9:E241. http://dx.doi.org/10.3390/toxins9080241

9. Dupieux C, Blondé R, Bouchiat C, Meugnier H, Bes M, Laurent S, et al. Community-acquired infections due to *Staphylococcus argenteus* lineage isolates harbouring the Panton-Valentine leucocidin, France, 2014. Euro Surveill. 2015;20:21154. http://dx.doi.org/10.2807/1560-7917.ES2015.20.23.21154

10. Chantratita N, Wikraiphat C, Tandhavanant S, Wongsuvan G, Ariyaprasert P, Suntornsut P, et al. Comparison of community-onset *Staphylococcus argenteus* and *Staphylococcus aureus* sepsis in Thailand: a prospective multicentre observational study. Clin Microbiol Infect. 2016;22:458.e11–9. http://dx.doi.org/10.1016/j.cmi.2016.01.008

Address for correspondence: Elisabeth Botelho-Nevers, Infectious Diseases Department, University Hospital of Saint-Etienne, Av Albert Raimond, 42055 Saint-Etienne CEDEX 02, France; email: elisabeth.botelho-nevers@univ-st-etienne.fr

Circulation of Influenza A(H5N8) Virus, Saudi Arabia

Hussain Al-Ghadeer,[1] Daniel K.W. Chu,[1]
Ehab A. Rihan, Ehab M. Abd-Allah, Haogao Gu,
Alex W.H. Chin, Ibrahim A. Qasim, Ali Aldoweriej,
Sanad S. Alharbi, Marshad A. Al-Aqil,
Ali Al-Sahaf, Salah S. Abdel Rahman,
Ali H. Aljassem, Ali Abdul-Al, Mohammed R. Aljasir,
Yousef M.O. Alhammad, Samy Kasem,
Malik Peiris, Ahmed Z.S.A. Zaki, Leo L.M. Poon

Author affiliations: Ministry of Environment, Water, and Agriculture, Riyadh, Saudi Arabia (H. Al-Ghadeer, E.A. Rihan, E.M. Abd-Allah, I.A. Qasim, A. Aldoweriej, S.S. Alharbi, M.A. Al-Aqil, A. Al-Sahaf, S.S. Abdel Rahman, A.H. Aljassem, A. Abdul-Al, M.R. Aljasir, Y.M.O. Alhammad, S. Kasem, A.Z.S.A. Zaki); University of Hong Kong, Hong Kong (D.K.W. Chu, H. Gu, A.W.H. Chin, M. Peiris, L.L.M. Poon); Kafr El-Sheikh University, Kafr El-Sheikh, Egypt (S. Kasem)

Highly pathogenic avian influenza A(H5N8) viruses have been detected in several continents. However, limited viral sequence data are available from countries in the Middle East. We report full-genome analyses of highly pathogenic H5N8 viruses recently detected in different provinces in Saudi Arabia.

On December 19, 2017, a high number of dead birds from various species was reported in a live bird market in Riyadh, Saudi Arabia, by the Department of Animal Resources Services, Ministry of Environment, Water, and Agriculture. Oropharyngeal and cloacal swab samples were collected from affected birds and investigated for highly pathogenic avian influenza (HPAI) viruses in Riyadh Veterinary Diagnostic Laboratory using reverse transcription PCR (RT-PCR) (1). These tests detected HPAI A(H5N8) virus. After this index outbreak, HPAI was reported in adjacent provinces. Surveillance studies were performed in all provinces ($\geq$1 major poultry market and 10 backyard farms per province) to estimate disease prevalence. As of May 2018, a total of 7,273 birds had been investigated; 805 were positive for H5N8, which was detected in 7 provinces (Riyadh, Eastern, Al-Qasim, Makkah, Al-Madinah, Asir, and Jizan). The highest number of positive results was reported in Riyadh (693 samples), in which different commercial poultry farms (22 farms for laying hens, 2 for broiler breeders, and 1 for quail) were affected. A contingency plan, based on a stamping-out policy, was implemented to control the disease. More than 8.8 million birds were depopulated.

[1]These authors contributed equally to this article.

Positive clinical specimens (N = 14) collected from different settings, different provinces, different avian species or a combination were sent to a World Health Organization H5 reference laboratory in Hong Kong for confirmation. All samples tested positive for membrane protein (M) and hemagglutinin (HA) subtype H5 genes by RT-PCR (online Technical Appendix Table 1, https://wwwnc.cdc.gov/EID/article/24/10/18-0846-Techapp.pdf). Samples that had a cycle threshold value <29 in the M gene assay also tested positive for N8 by RT-PCR. Ten of these samples were positive for virus isolation in embryonated chicken eggs and were associated with death of the chicken embryos by day 3 postinoculation.

We amplified viral RNA extracted from the clinical specimens and virus isolates using a multisegment RT-PCR approach for full-genome amplification (2). We subjected the RT-PCR products to next-generation sequencing on an Illumina MiSeq (PE300) platform (Illumina, San Diego, CA, USA). We edited the deduced consensus sequences (average sequence coverage >10,000×) using BioEdit (https://www.mbio.ncsu.edu/BioEdit/bioedit.html) and analyzed them phylogenetically using MEGA7 (https://www.megasoftware.net) (GISAID accession nos. for reference sequences, EPI1215422–EPI1215461, EPI1215137–EPI1215184; http://platform.gisaid.org).

The deduced sequences revealed that H5N8 viruses (n = 11) from different sites in Saudi Arabia are almost identical (sequence identity >99.7%), indicating a common origin for this outbreak. Phylogenetic analyses of HA sequences showed that they belong to clade 2.3.4.4 group B (Figure) (3). Polymerase acidic protein (PA), HA, nucleoprotein (NP), neuraminidase (NA), M, and nonstructural protein (NS) segments were genetically similar to those derived from recent group B H5N8 viruses (online Technical Appendix Table 2, Figure 1). No genetic markers associated with mammalian host adaptation, α2,6 receptor-binding specificity, or antimicrobial drug resistance were detected (data not shown) (4). The gene constellation of PA, HA, NP, NA, M, and NS segments of these H5N8 viruses is similar to those of some H5N8 viruses detected in wild migratory birds from different geographic areas (e.g., A/Anser_cygnoides/Hubei/FW44/2016 and A/green-winged teal/Egypt/877/2016) (4,5). The polymerase basic protein (PB) 1 and 2 segments of these viruses are similar to those of HPAI H5N5 viruses detected in the Far East (e.g., A/environment/Kamchatka/18/2016) and Europe (e.g., A/swan/Germany-SN/R10645/2016) (online Technical Appendix Figure 1). H5N5 viruses of this lineage were previously proposed to be reassortants of an H5N8 virus (6), with the PB1 and PB2 segments derived from an H10 virus (A/duck/Mongolia/245/2015-like virus) and the PA, HA, M, and NS segments derived from a H5N8 virus. Our results agree with previous observations that H5N8 viruses of this lineage continue to evolve and reassort with other influenza virus subtypes in migratory bird populations (7,8).

The studied samples were collected from multiple avian species in different settings from 3 provinces (online Technical Appendix Table 1). Of 986 samples from poultry holding sites, 182 (18.5%) tested positive for H5N8 virus. The transmission pathway of H5N8 virus in Saudi Arabia is being investigated. Molecular dating analyses suggest that the most recent common ancestor of these H5N8 viruses emerged in this country in September 2017 (online Technical Appendix Figure 2). The potential roles of wild birds, backyard poultry practices, poultry trading, and other human activities in dissemination of these viruses are yet to be determined. However, our results suggest wide circulation of H5N8 viruses caused by a single introduction.

Recently, outbreaks of H5N8 viruses were reported in the Middle East (Israel, Iran, Iraq, and Kuwait) (1). However, with the exception of a few HA sequences (n = 12), no other H5N8 viral sequences from this region are available in major sequence databases, which has hampered the investigation of H5N8 viruses in this region. Multiple introductions of H5N8 viruses with different gene constellations have been reported in Egypt (9,10), but their genetic relationship to H5N8 viruses detected in other countries in the Middle East is not clear. Further surveillance using full-genome analyses is urgently needed to identify major risk factors for HPAI H5N8 viruses in the Middle East.
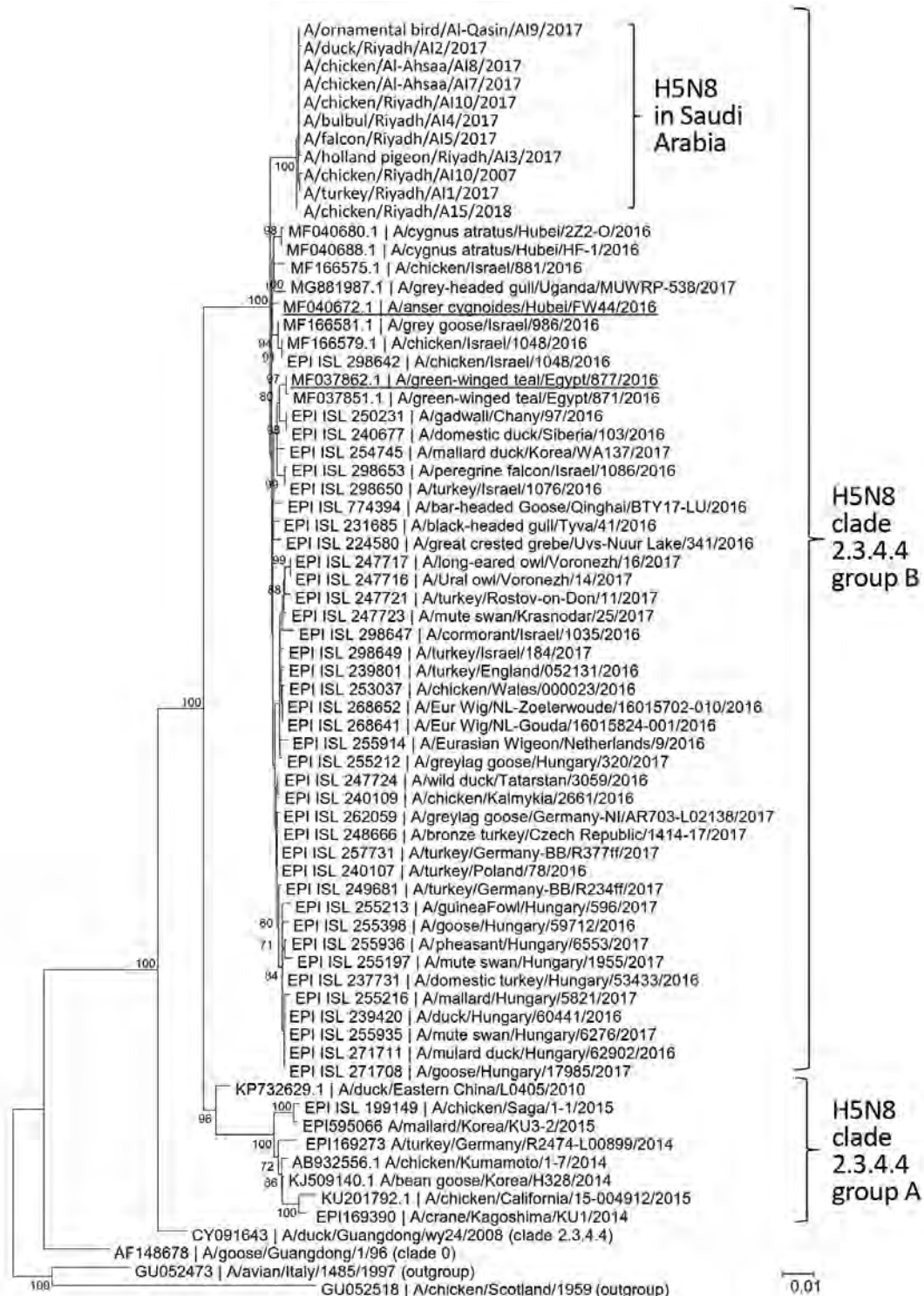
About the Author

Dr. Al-Ghadeer is a virologist at Riyadh Veterinary Diagnostic Laboratory, Ministry of Environment, Water, and Agriculture, Riyadh, Saudi Arabia. His main research interest is molecular diagnosis of viral diseases and viral genome sequencing.

Figure. Phylogenetic analysis of hemagglutinin sequences of influenza A(H5N8) viruses detected in oropharyngeal and cloacal swab samples from birds in Saudi Arabia. Aligned sequences were analyzed in MEGA7 (http://www.megasoftware.net). We constructed the phylogenetic tree using the neighbor-joining method. Representative viral sequences and viral sequences that are highly similar to those reported in this study were included in the analysis. H5N8 viruses reported in this study are labeled. Bootstrap values ≥60% are shown. Representative viruses sharing a similar gene constellation as the H5N8 viruses found in Saudi Arabia are underlined (see text for details). Virus isolate numbers (EPI ISL) in GISAID (http://platform.gisaid.org) or gene accession numbers in GenBank for corresponding viral sequences are provided. Scale bar indicates estimated genetic distance.

References

1. World Organisation for Animal Health. Update on avian influenza in animals (types H5 and H7) [cited 2018 May 19]. http://www.oie.int/en/animal-health-in-the-world/update-on-avian-influenza/
2. Zhou B, Donnelly ME, Scholes DT, St. George K, Hatta M, Kawaoka Y, et al. Single-reaction genomic amplification accelerates sequencing and vaccine production for classical and swine origin human influenza A viruses. J Virol. 2009;83:10309–13. http://dx.doi.org/10.1128/JVI.01109-09
3. El-Shesheny R, Barman S, Feeroz MM, Hasan MK, Jones-Engel L, Franks J, et al. Genesis of influenza A(H5N8) viruses. Emerg Infect Dis. 2017;23:1368–71. http://dx.doi.org/10.3201/eid2308.170143
4. Ma L, Jin T, Wang H, Liu H, Wang R, Li Y, et al. Two reassortant types of highly pathogenic H5N8 avian influenza virus from wild birds in Central China in 2016. Emerg Microbes Infect. 2018;7:14. http://dx.doi.org/10.1038/s41426-017-0012-y
5. Kandeil A, Kayed A, Moatasim Y, Webby RJ, McKenzie PP, Kayali G, et al. Genetic characterization of highly pathogenic avian influenza A H5N8 viruses isolated from wild birds in Egypt. J Gen Virol. 2017;98:1573–86. http://dx.doi.org/10.1099/jgv.0.000847
6. Fusaro A, Monne I, Mulatti P, Zecchin B, Bonfanti L, Ormelli S, et al. Genetic diversity of highly pathogenic avian influenza A(H5N8/H5N5) viruses in Italy, 2016-17. Emerg Infect Dis. 2017;23:1543–7. http://dx.doi.org/10.3201/eid2309.170539
7. Pohlmann A, Starick E, Grund C, Höper D, Strebelow G, Globig A, et al. Swarm incursions of reassortants of highly pathogenic avian influenza virus strains H5N8 and H5N5, clade 2.3.4.4b, Germany, winter 2016/17. Sci Rep. 2018;8:15. http://dx.doi.org/10.1038/s41598-017-16936-8
8. Global Consortium for H5N8 and Related Influenza Viruses. Role for migratory wild birds in the global spread of avian influenza H5N8. Science. 2016;354:213–7. http://dx.doi.org/10.1126/science.aaf8852
9. Salaheldin AH, El-Hamid HSA, Elbestawy AR, Veits J, Hafez HM, Mettenleiter TC, et al. Multiple introductions of influenza A(H5N8) virus into poultry, Egypt, 2017. Emerg Infect Dis. 2018;24:943–6. http://dx.doi.org/10.3201/eid2405.171935
10. Yehia N, Naguib MM, Li R, Hagag N, El-Husseiny M, Mosaad Z, et al. Multiple introductions of reassorted highly pathogenic avian influenza viruses (H5N8) clade 2.3.4.4b causing outbreaks in wild birds and poultry in Egypt. Infect Genet Evol. 2018;58:56–65. http://dx.doi.org/10.1016/j.meegid.2017.12.011

Address for correspondence: Leo L.M. Poon, the University of Hong Kong School of Public Health, LKS Faculty of Medicine, 5/F William MW Mong Block, Bldg 21, Sassoon Road, Hong Kong, China; email: llmpoon@hku.hk; or Hussain Al-Ghadeer, Riyadh Veterinary Diagnostic Laboratory, General Administration of Laboratories, Ministry of Environment, Water, and Agriculture, Riyadh 11454, Saudi Arabia; email: E23315@mewa.gov.sa

Severe Respiratory Illness Outbreak Associated with Human Coronavirus NL63 in a Long-Term Care Facility

Julie Hand, Erica Billig Rose, Andrea Salinas, Xiaoyan Lu, Senthilkumar K. Sakthivel, Eileen Schneider, John T. Watson

Author affiliations: Louisiana Department of Health, Baton Rouge, Louisiana, USA (J. Hand, A. Salinas); Centers for Disease Control and Prevention, Atlanta, Georgia, USA (E.B. Rose, X. Lu, S.K. Sakthivel, E. Schneider, J.T. Watson)

We describe an outbreak of severe respiratory illness associated with human coronavirus NL63 in a long-term care facility in Louisiana in November 2017. Six of 20 case-patients were hospitalized with pneumonia, and 3 of 20 died. Clinicians should consider human coronavirus NL63 for patients in similar settings with respiratory disease.

Human coronaviruses (HCoVs) OC43, 229E, NL63, and HKU1 are frequently associated with upper respiratory tract infection but can also cause lower respiratory tract infections (LRTIs), such as pneumonia or bronchitis. Transmission of these viruses primarily occurs through respiratory droplets and indirect contact with secretions from infected persons. Signs and symptoms of illness often include runny nose, headache, cough, sore throat, and fever. LRTI occurs less frequently, but young children, older adults, and persons who are immunosuppressed appear to be at higher risk for these types of infections (*1–3*).

A wide range of respiratory viruses are known to circulate in long-term care facilities (LTCFs) and contribute to respiratory illness in the residents who live in them (*4*). Although outbreaks of HCoV-OC43 have been described among elderly populations in long-term care settings (*5*), outbreaks of severe respiratory illness associated with HCoV-NL63 have not, to our knowledge, been documented in LTCF settings.

On November 15, 2017, the Louisiana Department of Health (Baton Rouge, Louisiana, USA) was notified of a possible outbreak of severe respiratory illness by a representative of an LTCF that provides nursing home care and short-term rehabilitation services to 130 residents. At the time of notification, the facility reported 11 residents with chest radiograph–confirmed pneumonia. For this investigation, we defined a case-patient as any LTCF resident with respiratory tract symptoms of new onset in November 2017, and we considered LRTI diagnoses that were based

Table. Signs and symptoms reported by case-patients with severe respiratory illness during outbreak associated with human coronavirus NL63 in long-term care facility, by hospitalization status, Louisiana, USA, November 1–18, 2017

Sign or symptom	No. (%) case-patients with severe respiratory illness, N = 20	Case-patients with lower respiratory tract infection, no. (%)		
		Total, n = 16	Hospitalized, n = 6	Nonhospitalized, n = 10
Cough	19 (95)	15 (94)	5 (83)	10 (100)
Chest congestion	13 (65)	9 (56)	1 (17)	8 (80)
Shortness of breath	5 (25)	4 (25)	3 (50)	1 (10)
Wheezing	3 (15)	3 (19)	3 (50)	0
Fever*	3 (15)	3 (19)	1 (17)	2 (20)
Altered mental status	2 (10)	2 (13)	2 (33)	0
*Fever as recorded in patient medical charts.				

on clinical or radiologic evidence. During November 1–18, a total of 20 case-patients (60% male) of a median age of 82 (range 66–96) years were identified. The number of cases of respiratory illness peaked in mid-November. The most common symptoms were cough (95%) and chest congestion (65%). Shortness of breath, wheezing, fever, and altered mental status were also reported (Table). Sixteen (80%) case-patients had abnormal findings on chest radiograph; pneumonia was noted in 14. All case-patients had concurrent medical conditions; the most common were heart disease (70%, 14/20), dementia (65%, 13/20), hypertension (40%, 8/20), diabetes (35%, 7/20), and lung disease (35%, 7/20). Six (30%) case-patients required hospitalization; all had chest radiograph–confirmed pneumonia. Hospitalized LRTI case-patients demonstrated shortness of breath (50% vs. 10%), wheezing (50% vs. 0%), and altered mental status (33% vs. 0%) more frequently than did nonhospitalized LRTI case-patients (Table).

We performed molecular diagnostic viral testing on nasopharyngeal specimens from 13 case-patients by real-time PCR at the Louisiana State Public Health Laboratory (Baton Rouge, Louisiana, USA) and the Centers for Disease Control and Prevention (Atlanta, Georgia, USA). Of the 13 available specimens, HCoV-NL63 was detected in 7 (54%); rhinovirus was co-detected in 2 specimens. Of the 6 specimens negative for HCoV-NL63, 1 was positive for rhinovirus, and 1 was positive for parainfluenza virus 1. For the 6 case-patients hospitalized with pneumonia, median length of hospital stay was 4 (range 1–5) days; none of these case-patients were mechanically ventilated or admitted to the intensive care unit. Nasopharyngeal specimens were available from 2 of the hospitalized case-patients, and HCoV-NL63 was detected in both. HCoV-NL63 respiratory infection was considered a contributory cause in the deaths of 3 case-patients (1 hospitalized and 2 nonhospitalized) that occurred 10–36 days after illness onset. The concurrent medical conditions of those who died included dementia, cardiovascular disease, cancer, multiple sclerosis, Parkinson disease, diabetes mellitus, hypertension, asthma, and chronic kidney disease.

Infection control measures, including adherence to standard and droplet precautions for symptomatic residents, reviewing hand and personal hygiene policies, and enhanced environmental cleaning, were implemented in the LTCF on November 15. All residents were monitored daily for the onset of respiratory symptoms. The case-patients resided in rooms throughout the facility. However, residents often shared rooms, walked throughout the facility, and spent much of their time in shared areas (e.g., gym, dining rooms, and recreational rooms). Because all case-patients had visited the gym at the facility for recreation or physical therapy before becoming ill, environmental cleaning of this area was performed. No new cases among residents were identified after November 18, 2017, and no facility staff members reported respiratory symptoms during this outbreak.

The use of molecular diagnostics and respiratory virus panels has become more common, enabling specific HCoVs to be more easily identified. In the United States, HCoV respiratory infections commonly occur in the fall and winter, and annual variations are noted in patterns of circulation of individual HCoVs (6). At the time of this outbreak, national surveillance data from the National Respiratory and Enteric Virus Surveillance System indicated that HCoV-NL63 was the predominant circulating HCoV type.

This outbreak demonstrates that HCoV-NL63 can be associated with severe respiratory illness in LTCF residents. Clinicians and public health practitioners should consider HCoV-NL63 in patients with similar clinical presentations in these settings.

About the Author

Ms. Hand is an epidemiologist manager at the Louisiana Department of Health, Infectious Disease Epidemiology Section, Baton Rouge, Louisiana, USA. Her primary research focus is influenza and other viral respiratory diseases.

References

1. Lee J, Storch GA. Characterization of human coronavirus OC43 and human coronavirus NL63 infections among hospitalized children <5 years of age. Pediatr Infect Dis J. 2014;33:814–20. http://dx.doi.org/10.1097/INF.0000000000000292
2. Walsh EE, Shin JH, Falsey AR. Clinical impact of human coronaviruses 229E and OC43 infection in diverse adult

populations. J Infect Dis. 2013;208:1634–42. http://dx.doi.org/10.1093/infdis/jit393

3. Englund J, Feuchtinger T, Ljungman P. Viral infections in immunocompromised patients. Biol Blood Marrow Transplant. 2011;17(Suppl):S2–5. http://dx.doi.org/10.1016/ j.bbmt.2010.11.008

4. Falsey AR, Dallal GE, Formica MA, Andolina GG, Hamer DH, Leka LL, et al. Long-term care facilities: a cornucopia of viral pathogens. J Am Geriatr Soc. 2008;56:1281–5. http://dx.doi.org/10.1111/j.1532-5415.2008.01775.x

5. Birch CJ, Clothier HJ, Seccull A, Tran T, Catton MC, Lambert SB, et al. Human coronavirus OC43 causes influenza-like illness in residents and staff of aged-care facilities in Melbourne, Australia. Epidemiol Infect. 2005;133:273–7. http://dx.doi.org/10.1017/S0950268804003346

6. Killerby ME, Biggs HM, Haynes A, Dahl RM, Mustaquim D, Gerber SI, et al. Human coronavirus circulation in the United States 2014–2017. J Clin Virol. 2018;101:52–6. http://dx.doi.org/10.1016/j.jcv.2018.01.019

Address for correspondence: John T. Watson, Centers for Disease Control and Prevention, 1600 Clifton Rd NE, Mailstop A34, Atlanta, GA 30329-4027, USA; email: acq4@cdc.gov

LETTER

External Quality Assessment for Zika Virus Molecular Diagnostic Testing, Brazil

Sally A. Baylis, Johannes Blümel

Author affiliation: Paul-Ehrlich-Institut, Langen, Germany

To the Editor: Fischer et al. described an external quality assessment exercise for laboratories in Brazil that perform molecular testing for Zika virus and the development of an armored RNA control material (1). Armored RNAs are RNA transcripts synthesized by in vitro transcription; they are encapsulated in a bacteriophage protein coat and are nuclease resistant. In addition to the external quality assessment samples, laboratories were sent vials of the World Health Organization (WHO) International Standard (IS) for Zika virus, which was prepared by using heat-inactivated virus (2). Concentrations of WHO ISs are defined in IUs, in this case referring to the viral load, and, because of limitations on number of vials prepared in each batch, they are intended for calibrating secondary standards, including calibrators and run controls in IU facilitating comparison of assays (http://apps.who.int/medicinedocs/documents/s23325en/s23325en.pdf). Secondary standards, such as armored RNAs, traceable in IU (in accordance with ISO 17511:2003), are important complementary reagents to WHO ISs. However, the study by Fischer et al. was missing the calibration of the armored RNA in IU, which is essential for traceability.

Because of packaging limitations of the protein coat, armored RNAs contain only partial genome sequences, compared with live or inactivated virus preparations such as the WHO ISs, which contain full-length genomes. Consequently, armored RNAs are restricted to controlling only certain assays. However, it may be easier to import armored RNAs into countries where disease outbreaks are occurring because they are noninfectious and have not been derived from either viremic plasma or cell culture–derived virus that has undergone heat inactivation.

Inactivation protocols of viral stock materials must be validated on a case-by-case basis. Certain viruses, such as Zika virus, are heat labile (3), whereas viruses such as alphaviruses are much more heat resistant, although there is a wide variation in susceptibility to heat inactivation between different members of the genus (4,5). The availability of controls, such as armored RNAs, is essential to ensure consistent assay performance on a daily basis and maintain stocks of WHO IS samples for calibration.

References

1. Fischer C, Pedroso C, Mendrone A Jr, Bispo de Filippis AM, Vallinoto AC, Ribeiro BM, et al. External quality assessment for Zika virus molecular diagnostic testing, Brazil. Emerg Infect Dis. 2018;24:888–92. http://dx.doi.org/10.3201/eid2405.171747

2. Baylis SA, Hanschmann KO, Schnierle BS, Trösemeier JH, Blümel J; Zika Virus Collaborative Study Group. Harmonization of nucleic acid testing for Zika virus: development of the 1st World Health Organization International Standard. Transfusion. 2017;57:748–61. http://dx.doi.org/10.1111/trf.14026

3. Blümel J, Musso D, Teitz S, Miyabayashi T, Boller K, Schnierle BS, et al. Inactivation and removal of Zika virus during manufacture of plasma-derived medicinal products. Transfusion. 2017;57:790–6. http://dx.doi.org/10.1111/trf.13873

4. Park SL, Huang YJ, Hsu WW, Hettenbach SM, Higgs S, Vanlandingham DL. Virus-specific thermostability and heat inactivation profiles of alphaviruses. J Virol Methods. 2016;234:152–5. http://dx.doi.org/10.1016/j.jviromet.2016.04.004

5. Huang YJ, Hsu WW, Higgs S, Vanlandingham DL. Temperature tolerance and inactivation of chikungunya virus. Vector Borne Zoonotic Dis. 2015;15:674–7. http://dx.doi.org/10.1089/vbz.2015.1795
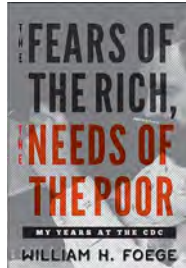
Address for correspondence: Sally A. Baylis, Paul-Ehrlich-Institut, Paul-Ehrlich-Strasse 51-59, Langen, D-63225, Germany; email: Sally.Baylis@pei.de

The Fears of the Rich, the Needs of the Poor: My Years at the CDC

To say that William Foege's life has been inspirational is an understatement. It has encompassed literal life-and-death adventures, often intertwined with efforts to prevent and control some of the most destructive infectious diseases of the past half century. By recounting his time as an officer in the Epidemic Intelligence Service, his public health experiences in war zones, and his service as director of the Centers for Disease Control, Dr. Foege provides a front-row seat from which to watch the field of public health progress.

The Fears of the Rich, the Needs of the Poor: My Years at the CDC is well organized chronologically, with contextual information clearly documented. Foege recounts many momentous CDC adventures and introduces the reader to numerous CDC contemporaries. However, although the title may be captivating, it does not reflect the focus of the book well. Many of Foege's assignments involved underserved and poverty-stricken populations, and he occasionally touches on the effects of wealth and class on the health of these populations, but the book is primarily about his experiences at CDC. That being said, in stating his "three essentials for good public health programs," Foege does say: "The first is the conviction that the basis for public health is to achieve health equity; therefore, the bottom line is social justice in health."

This book was written with a public health audience in mind but would be a fascinating read for anyone with an interest in public health. Foege's distinct colloquial voice and dry humor personalize the book, bringing his work to life. Foege provides a first-hand account of the recent history of humanity's struggles with infectious diseases across the world, including progress made in the field of public health over the decades of his career. By sharing real stories of infectious diseases that devastated populations and how Foege and his colleagues grew into the leaders that helped bring these epidemics under control, the book provides guidance and inspiration for current and future public health workforces. Although public health can be a thankless profession, through this memoir Foege reminds us how indispensable the field is for our world's future.

Loren Robinson, Cjloe Vinoya-Chung

DOI: https://doi.org/10.3201/eid2410.180687

Author affiliation: Commonwealth of Pennsylvania—Health, Health Promotion and Disease Prevention, West Harrisburg, Pennsylvania, USA

Address for correspondence: Cjloe Vinoya-Chung, Commonwealth of Pennsylvania—Health, Health Promotion and Disease Prevention, 625 Forster St H&W, 8th Fl, West Harrisburg, PA 17120, USA; email: cvinoya@pa.gov

John Singer Sargent (1856–1925), *Interior of a Hospital Tent*, **1918.** Watercolour over pencil on paper; 16 in × 21 in/39 cm × 53 cm. Imperial War Museums, © IWM ART 1611, Lambeth Road London SE1 6HZ

Concurrent Conflicts—the Great War and the 1918 Influenza Pandemic

Terence Chorba and Byron Breedlove

The generation that endured through what was perhaps the most devastating epidemic ever—the great influenza pandemic of 1918—is now gone. The influenza strain of that pandemic infected about 500 million people, one third of the world's population, with extraordinarily high pathogenicity and virulence. The result was staggering mortality: an estimated 20 to 100 million lives were lost worldwide. The estimate of deaths of Americans attributable to influenza in that pandemic is 675,000, the majority of which were among those from ages 20 through 40 years. During World War I, the "Great War," three influenza-associated mortality waves occurred in northern Europe, beginning in early summer of 1918 and extending over the course of a year; influenza accounted for more fatalities than military engagement. The highest point of combined influenza and pneumonia mortality occurred in October 1918. At the time, the pandemic strain became known as "the Spanish flu," so called because neutral Spain lacked war censors and was the first country to report on the pandemic publicly; however, the geographic origin of the causative organism remains an enigma.

Author affiliation: Centers for Disease Control and Prevention, Atlanta, Georgia, USA

Among that generation was the artist John Singer Sargent, who was born in Florence in 1856 and raised principally in France, the child of two Americans: an eye doctor turned medical illustrator father, and an amateur artist mother. Home-schooled and trained at the École des Beaux-Arts in Paris, he enjoyed a storied career, principally as a portraitist. In early summer 1918, late in his renowned career when living in England, Sargent was invited back to France on commission by British Prime Minister Lloyd George, Field Marshal Douglas Haig, and the British Department of Information, War Memorials Committee, to depict the Anglo-American effort in the war.

During late September, while preparing sketches for his iconic painting *Gassed* in a military camp near Roisel (in Péronne, France), Sargent fell ill with influenza. Sargent was cared for and convalesced in a hospital tent in France. He wrote that he lay there, "with the accompaniment of groans of wounded, and the chokings and coughing of gassed men, which was a nightmare. It always seemed strange on opening one's eyes to see the level cots and the dimly lit long tent looking so calm, when one was dozing in pandemonium."

Sargent's hospital experience inspired the image featured on this month's cover, *Interior of a Hospital Tent*. This watercolor depicts the interior of a hospital tent with military cots arrayed in file on the side, covered with blankets in a mix of red (contagious cases) and brown (convalescing or noninfluenza cases), two colors that must have dominated the entire war hospital environment. The scene is actually one of tranquility, a respite from the chaos and carnage of war. In one bed, a soldier lies reading, his head bolstered by pillows; in another, a soldier sleeps on his side with an open tent flap behind him, his bed bathed in light from the world of the healthy. Beyond them, there are three or four more cots with soldiers reclining in varying amounts of darkness and light. Above all, in varying shades of military brown, is a great propped tent canopy.

Sargent remained hospitalized for a week, but unlike so many of the much younger soldiers, he recovered and returned to his task of documenting what he saw. At the outset of his journey through France in July 1918, he had written that the best material for his commission would be to see "a big road encumbered with troop and traffic… combining English and Americans." By mid-October in northern France, Sargent had had his fill of war. He wrote, "I have wasted lots of time going to the front trenches. There is nothing to paint there—it is ugly, meagre, and cramped…. I have seen what I wanted, roads crammed with troops on the march. It is the finest spectacle that war affords…"

By the end of October, Sargent returned to Britain to complete the several works for which he had been commissioned. What he had seen firsthand and documented from his experiences in the conflict were the amplification mechanisms for infectious disease transmission that war provides: crowding, migration, and poor ventilation and sanitation. Because there were no vaccines available with proven safety and efficacy to protect against influenza and no antibiotics to treat secondary bacterial infections from influenza or wounds, there were few public health measures available to counter the spread and devastation of the pandemic.

Whether the great pandemic tipped the balance of power toward the cause of the Allies, such that surrender came in November 1918, remains a matter of debate. The theory that one conflict had a significant impact on the outcome of the other is supported by data published from archives in Austria (Price-Smith 2008), which indicate that waves of morbidity and mortality from influenza were experienced both to a larger extent and earlier among the Central Powers (Germany, Austria-Hungary, the Ottoman Empire, and Bulgaria) than among the Allies. Unfortunately, the pandemic was not limited in its geographic reach, and through 1920, it exerted a tremendous toll on morbidity and mortality and created economic and social burdens, both elsewhere in Europe and throughout the Americas, Africa, Asia, Australia, and the Pacific.

Bibliography

1. Barry JM. The great influenza: the epic story of the deadliest plague in history. New York: Penguin; 2004.
2. Bristow NK. American pandemic: the lost worlds of the 1918 epidemic. New York: Oxford University Press; 2012.
3. Centers for Disease Control and Prevention. History of 1918 flu pandemic [cited 2018 Jun 18]. https://www.cdc.gov/flu/pandemic-resources/1918-commemoration/1918-pandemic-history.htm
4. Charteris E. John Sargent. Sevenoaks (UK): Pickle Partners Publishing; 2016.
5. Fairbrother T. John Singer Sargent; New York: Harry N. Abrams; 1994.
6. Fisher JE. Envisioning disease, gender, and war: women's narratives of the 1918 influenza pandemic. New York: Palgrave Macmillan; 2012.
7. Olson S. John Singer Sargent: his portrait; New York: St. Martin's Press; 1986.
8. Philips H, Killingray D, editors. The Spanish influenza pandemic of 1918–19: new perspectives. New York: Routledge; 2003.
9. Price-Smith AT. Contagion and chaos. Cambridge (MA): MIT Press; 2008.
10. Taubenberger JK, Morens DM. 1918 influenza: the mother of all pandemics. Emerg Infect Dis. 2006;12:15–22. http://dx.doi.org/10.3201/eid1209.05-0979

EMERGING INFECTIOUS DISEASES®

Upcoming Issue

- *Cryptococcus gattii* Complex Infections in HIV-Infected Patients, Southeastern United States

- *Rickettsia typhi* as Cause of Fatal Encephalitic Typhus in Hospitalized Patients, Germany, 1940–1944

- Detection of Tickborne Relapsing Fever Spirochete, Austin, Texas, USA

- Effects of Pneumococcal Conjugate Vaccine on Genotypic Penicillin Resistance and Serotype Changes, Japan, 2010–2017

- Hantavirus Pulmonary Syndrome—25th Anniversary of the Four Corners Outbreak

- Human Infections with *Rickettsia japonica*, China, 2015

- Fatal Case of Diphtheria and Risk for Reemergence, Singapore

- Mitigation of Influenza B Epidemic with School Closures, Hong Kong, China, 2018

- Characterization of *Burkholderia thailandensis* Isolated from an Infected Wound

- *Ehrlichia* Infections, North Carolina, USA, 2016

- Timing the Origin of *Cryptococcus gattii* sensu stricto, Southeastern United States

- Japanese Spotted Fever Endemic in China

- Molecular Characterization of African Swine Fever Virus, China, 2018

- Racial/Ethnic Disparities in Antimicrobial Drug Use, United States, 2014–2015

- Enterovirus D68 Surveillance in St. Louis, Missouri, USA, 2016

- Novel Multidrug-Resistant *Cronobacter sakazakii* Causing Meningitis in Neonate, China, 2015

- Norovirus Gastroenteritis among Hospitalized Patients, Germany, 2007–2012

- Evaluation of Co-feeding Transmission of *Rickettsia rickettsii* among *Amblyomma aureolatum* Ticks Exposed to Guinea Pigs Susceptible or Immune to *R. rickettsii*

**Complete list of articles in the November issue at
http://www.cdc.gov/eid/upcoming.htm**

Upcoming Infectious Disease Activities

October 1–3, 2018
International Conference on Migration Health
Sponsored by the International Society of Travel Medicine
Rome, Italy
http://www.istm.org/ICMH2018

October 3–7, 2018
ID Week
San Francisco, CA, USA
http://www.idweek.org/

October 14–18, 2018
Keystone Symposia Conference
Hong Kong, China
www.keystonesymposia.org/18S2

October 28–30, 2018
International Society for Vaccines
2018 Annual Congress
Atlanta, GA, USA
www.ISVCongress.org

October 28–November 1, 2018
ASTMH
American Society of Tropical Medicine and Hygiene
New Orleans, LA, USA
http://www.astmh.org/

October 31—November 4, 2018
11th International Respiratory Syncytial Virus Symposium
Asheville, NC, USA
http://rsvsymposium.com/

November 9–12, 2018
ProMED
International Society for Infectious Diseases
7th International Meeting on Emerging Diseases and Surveillance
Vienna, Austria
http://imed.isid.org/index.shtml

April 16–18, 2019
International Conference on One Health Antimicrobial Resistance
Amsterdam, the Netherlands
https://www.escmid.org/ICOHAR2019/

Announcements
Email announcements to EIDEditor (eideditor@cdc.gov). Include the event's date, location, sponsoring organization, and a website. Some events may appear only on EID's website, depending on their dates.

Earning CME Credit

To obtain credit, you should first read the journal article. After reading the article, you should be able to answer the following, related, multiple-choice questions. To complete the questions (with a minimum 75% passing score) and earn continuing medical education (CME) credit, please go to http://www.medscape.org/journal/eid. Credit cannot be obtained for tests completed on paper, although you may use the worksheet below to keep a record of your answers.

You must be a registered user on http://www.medscape.org. If you are not registered on http://www.medscape.org, please click on the "Register" link on the right hand side of the website.

Only one answer is correct for each question. Once you successfully answer all post-test questions, you will be able to view and/or print your certificate. For questions regarding this activity, contact the accredited provider, CME@medscape.net. For technical assistance, contact CME@medscape.net. American Medical Association's Physician's Recognition Award (AMA PRA) credits are accepted in the US as evidence of participation in CME activities. For further information on this award, please go to https://www.ama-assn.org. The AMA has determined that physicians not licensed in the US who participate in this CME activity are eligible for AMA PRA Category 1 Credits™. Through agreements that the AMA has made with agencies in some countries, AMA PRA credit may be acceptable as evidence of participation in CME activities. If you are not licensed in the US, please complete the questions online, print the AMA PRA CME credit certificate, and present it to your national medical association for review.

Article Title
Human Pegivirus in Patients with Encephalitis of Unclear Etiology, Poland

CME Questions

1. Your patient is a 39-year-old man with encephalitis of unclear etiology. According to the case series by Bukowska-Ośko and colleagues, which of the following statements about evidence for HPgV infection in the CNS among patients with encephalitis of unclear etiology is correct?

A. 5′ UTR HPgV RNA was detected in serum in 4 of 96 patients with encephalitis of unclear origin, and 3 of these patients were also positive in CSF
B. Two patients were co-infected with other pathogenic viruses
C. The presence of viral RNA in CSF proved that this was the cause of encephalitis
D. HPgV-infected patients were clinically distinct from the other patients

2. According to the case series by Bukowska-Ośko and colleagues, which of the following statements about HPgV sequences in CSF compared with those circulating in serum is correct?

A. Single-strand conformation polymorphism (SSCP) showed no differences between the serum and CSF-derived viral sequences
B. Two unique amino acid E2 region changes in CSF vs serum variants were serine changed to phenylalanine at aa postion 508, and proline to leucine at position 572 in another patient
C. Amino acid E2 region changes in CSF vs serum variants were both within regions predicted to contain T-cell epitopes
D. Phylogenetic comparison of 5′ UTR and E2 sequences showed sequences interspersed between different patients

3. According to the case series by Bukowska-Ośko and colleagues, which of the following statements about clinical implications of evidence for HPgV infection in the CNS among patients with encephalitis of unclear etiology would be correct?

A. The study proves that HPgV infection in the CNS causes encephalitis
B. Liver is the major site of HPgV replication
C. The primary target of HPgV infection may be a progenitor hematopoietic stem cell, allowing a route for CNS access
D. 5′ UTR and E2 region sequence differences between CSF and serum compartments are not biologically meaningful

Earning CME Credit

To obtain credit, you should first read the journal article. After reading the article, you should be able to answer the following, related, multiple-choice questions. To complete the questions (with a minimum 75% passing score) and earn continuing medical education (CME) credit, please go to http://www.medscape.org/journal/eid. Credit cannot be obtained for tests completed on paper, although you may use the worksheet below to keep a record of your answers.

You must be a registered user on http://www.medscape.org. If you are not registered on http://www.medscape.org, please click on the "Register" link on the right hand side of the website.

Only one answer is correct for each question. Once you successfully answer all post-test questions, you will be able to view and/or print your certificate. For questions regarding this activity, contact the accredited provider, CME@medscape.net. For technical assistance, contact CME@medscape.net. American Medical Association's Physician's Recognition Award (AMA PRA) credits are accepted in the US as evidence of participation in CME activities. For further information on this award, please go to https://www.ama-assn.org. The AMA has determined that physicians not licensed in the US who participate in this CME activity are eligible for AMA PRA Category 1 Credits™. Through agreements that the AMA has made with agencies in some countries, AMA PRA credit may be acceptable as evidence of participation in CME activities. If you are not licensed in the US, please complete the questions online, print the AMA PRA CME credit certificate, and present it to your national medical association for review.

Article Title
Influenza Transmission Dynamics in Urban Households, Managua, Nicaragua, 2012–2014

CME Questions

1. Your patient is a 5-year-old boy with influenza, living in a low-income urban household with 2 parents and 2 siblings. According to the case-ascertained study by Gordon and colleagues, which of the following statements about overall risk for influenza infection in household contacts, mean serial interval for within-household transmission, and transmissibility of different strains in low-income urban households in Managua, Nicaragua, is correct?

A. Overall risk for influenza infection was 5.7% in household contacts of index cases
B. Mean serial interval for within-household transmission was 6 days
C. Higher transmissibility of influenza B than influenza A overall was explained by higher transmissibility of influenza B among children
D. Nearly half of index cases were treated with oseltamivir

2. According to the case-ascertained study by Gordon and colleagues, which of the following statements about risk factors for transmission of influenza virus within low-income urban households in Managua, Nicaragua, is correct?

A. Children were more susceptible to influenza A and B than adults, presumably caused by lower levels of preexisting immunity and contact patterns
B. Oseltamivir treatment significantly reduced the risk for influenza transmissibility

C. Influenza A(H1N1) was significantly more infective than influenza A(H3N2) or B
D. Household contacts with index cases having >4 household contacts had approximately 30% to 40% higher risk for infection

3. According to the case-ascertained study by Gordon and colleagues, which of the following statements about clinical implications of findings regarding the transmission of influenza virus in low-income urban households in Managua, Nicaragua, is correct?

A. Study findings are generalizable to persons with influenza regardless of receipt of medical care
B. Study findings are generalizable to adults with influenza
C. The study proves the efficacy of interventions designed to reduce influenza transmission to household contacts of index cases
D. Only 5% of household contacts were vaccinated against influenza, so the study was underpowered to detect vaccine effectiveness

Summary of Authors' Instructions

Authors' Instructions. For a complete list of EID's manuscript guidelines, see the author resource page: http://wwwnc.cdc.gov/eid/page/author-resource-center.

Manuscript Submission. To submit a manuscript, access Manuscript Central from the Emerging Infectious Diseases web page (www.cdc.gov/eid). Include a cover letter indicating the proposed category of the article (e.g., Research, Dispatch), verifying the word and reference counts, and confirming that the final manuscript has been seen and approved by all authors. Complete provided Authors Checklist.

Manuscript Preparation. For word processing, use MS Word. Set the document to show continuous line numbers. List the following information in this order: title page, article summary line, keywords, abstract, text, acknowledgments, biographical sketch, references, tables, and figure legends. Appendix materials and figures should be in separate files.

Title Page. Give complete information about each author (i.e., full name, graduate degree(s), affiliation, and the name of the institution in which the work was done). Clearly identify the corresponding author and provide that author's mailing address (include phone number, fax number, and email address). Include separate word counts for abstract and text.

Keywords. Use terms as listed in the National Library of Medicine Medical Subject Headings index (www.ncbi.nlm.nih.gov/mesh).

Text. Double-space everything, including the title page, abstract, references, tables, and figure legends. Indent paragraphs; leave no extra space between paragraphs. After a period, leave only one space before beginning the next sentence. Use 12-point Times New Roman font and format with ragged right margins (left align). Italicize (rather than underline) scientific names when needed.

Biographical Sketch. Include a short biographical sketch of the first author—both authors if only two. Include affiliations and the author's primary research interests.

References. Follow Uniform Requirements (www.icmje.org/index.html). Do not use endnotes for references. Place reference numbers in parentheses, not superscripts. Number citations in order of appearance (including in text, figures, and tables). Cite personal communications, unpublished data, and manuscripts in preparation or submitted for publication in parentheses in text. Consult List of Journals Indexed in Index Medicus for accepted journal abbreviations; if a journal is not listed, spell out the journal title. List the first six authors followed by "et al." Do not cite references in the abstract.

Tables. Provide tables within the manuscript file, not as separate files. Use the MS Word table tool, no columns, tabs, spaces, or other programs. Footnote any use of boldface. Tables should be no wider than 17 cm. Condense or divide larger tables. Extensive tables may be made available online only.

Figures. Submit editable figures as separate files (e.g., Microsoft Excel, PowerPoint). Photographs should be submitted as high-resolution (600 dpi) .tif or .jpg files. Do not embed figures in the manuscript file. Use Arial 10 pt. or 12 pt. font for lettering so that figures, symbols, lettering, and numbering can remain legible when reduced to print size. Place figure keys within the figure. Figure legends should be placed at the end of the manuscript file.

Videos. Submit as AVI, MOV, MPG, MPEG, or WMV. Videos should not exceed 5 minutes and should include an audio description and complete captioning. If audio is not available, provide a description of the action in the video as a separate Word file. Published or copyrighted material (e.g., music) is discouraged and must be accompanied by written release. If video is part of a manuscript, files must be uploaded with manuscript submission. When uploading, choose "Video" file. Include a brief video legend in the manuscript file.

Types of Articles

Perspectives. Articles should not exceed 3,500 words and 50 references. Use of subheadings in the main body of the text is recommended. Photographs and illustrations are encouraged. Provide a short abstract (150 words), 1-sentence summary, and biographical sketch. Articles should provide insightful analysis and commentary about new and reemerging infectious diseases and related issues. Perspectives may address factors known to influence the emergence of diseases, including microbial adaptation and change, human demographics and behavior, technology and industry, economic development and land use, international travel and commerce, and the breakdown of public health measures.

Synopses. Articles should not exceed 3,500 words in the main body of the text or include more than 50 references. Use of subheadings in the main body of the text is recommended. Photographs and illustrations are encouraged. Provide a short abstract (not to exceed 150 words), a 1-line summary of the conclusions, and a brief biographical sketch of first author or of both authors if only 2 authors. This section comprises case series papers and concise reviews of infectious diseases or closely related topics. Preference is given to reviews of new and emerging diseases; however, timely updates of other diseases or topics are also welcome. If detailed methods are included, a separate section on experimental procedures should immediately follow the body of the text.

Research. Articles should not exceed 3,500 words and 50 references. Use of subheadings in the main body of the text is recommended. Photographs and illustrations are encouraged. Provide a short abstract (150 words), 1-sentence summary, and biographical sketch. Report laboratory and epidemiologic results within a public health perspective. Explain the value of the research in public health terms and place the findings in a larger perspective (i.e., "Here is what we found, and here is what the findings mean").

Policy and Historical Reviews. Articles should not exceed 3,500 words and 50 references. Use of subheadings in the main body of the text is recommended. Photographs and illustrations are encouraged. Provide a short abstract (150 words), 1-sentence summary, and biographical sketch. Articles in this section include public health policy or historical reports that are based on research and analysis of emerging disease issues.

Dispatches. Articles should be no more than 1,200 words and need not be divided into sections. If subheadings are used, they should be general, e.g., "The Study" and "Conclusions." Provide a brief abstract (50 words); references (not to exceed 15); figures or illustrations (not to exceed 2); tables (not to exceed 2); and biographical sketch. Dispatches are updates on infectious disease trends and research that include descriptions of new methods for detecting, characterizing, or subtyping new or reemerging pathogens. Developments in antimicrobial drugs, vaccines, or infectious disease prevention or elimination programs are appropriate. Case reports are also welcome.

Research Letters Reporting Cases, Outbreaks, or Original Research. EID publishes letters that report cases, outbreaks, or original research as Research Letters. Authors should provide a short abstract (50-word maximum), references (not to exceed 10), and a short biographical sketch. These letters should not exceed 800 words in the main body of the text and may include either 1 figure or 1 table. Do not divide Research Letters into sections.

Letters Commenting on Articles. Letters commenting on articles should contain a maximum of 300 words and 5 references; they are more likely to be published if submitted within 4 weeks of the original article's publication.

Commentaries. Thoughtful discussions (500–1,000 words) of current topics. Commentaries may contain references (not to exceed 15) but no abstract, figures, or tables. Include biographical sketch.

Another Dimension. Thoughtful essays, short stories, or poems on philosophical issues related to science, medical practice, and human health. Topics may include science and the human condition, the unanticipated side of epidemic investigations, or how people perceive and cope with infection and illness. This section is intended to evoke compassion for human suffering and to expand the science reader's literary scope. Manuscripts are selected for publication as much for their content (the experiences they describe) as for their literary merit. Include biographical sketch.

Books, Other Media. Reviews (250–500 words) of new books or other media on emerging disease issues are welcome. Title, author(s), publisher, number of pages, and other pertinent details should be included.

Conference Summaries. Summaries of emerging infectious disease conference activities (500–1,000 words) are published online only. They should be submitted no later than 6 months after the conference and focus on content rather than process. Provide illustrations, references, and links to full reports of conference activities.

Online Reports. Reports on consensus group meetings, workshops, and other activities in which suggestions for diagnostic, treatment, or reporting methods related to infectious disease topics are formulated may be published online only. These should not exceed 3,500 words and should be authored by the group. We do not publish official guidelines or policy recommendations.

Photo Quiz. The photo quiz (1,200 words) highlights a person who made notable contributions to public health and medicine. Provide a photo of the subject, a brief clue to the person's identity, and five possible answers, followed by an essay describing the person's life and his or her significance to public health, science, and infectious disease.

Etymologia. Etymologia (100 words, 5 references). We welcome thoroughly researched derivations of emerging disease terms. Historical and other context could be included.

Announcements. We welcome brief announcements of timely events of interest to our readers. Announcements may be posted online only, depending on the event date. Email to eideditor@cdc.gov.

EMERGING INFECTIOUS DISEASES

Pages 1785–1972

John Singer Sargent (1856–1925), *Interior of a Hospital Tent*, **1918**. Watercolour over pencil on paper; 16 in × 21 in/39 cm × 53 cm. Imperial War Museums, © IWM ART 1611, Lambeth Road London SE1 6HZ